Université du Québec
Institut National de la Recherche Scientifique
Centre Armand-Frappier - Santé Biotechnologie

APPLICATION DU CONCEPT DE LA BIOPSIE LIQUIDE CHEZ DES ESPECES MARINES AFIN D'EVALUER L'ETAT DE SANTE DES ECOSYSTEMES MARINS ET COTIERS

Par
Sophia Ferchiou, M.Sc.

Thèse présentée pour l'obtention du grade de
Philosophiae doctor (Ph.D.)
en biologie

Jury d'évaluation

Président du jury et examinateur interne	Philippe Constant, Ph.D. INRS- Centre Armand-Frappier - Santé Biotechnologie
Examinateur externe	Frédérique Le Roux, Ph.D. Université de Montréal
Examinateur externe	Paul George, Ph.D. Université Laval
Co-directeur de recherche	Stéphane Betoulle, Ph.D. Université de Reims Champagne-Ardenne
Directeur de recherche	Yves St-Pierre, Ph.D. INRS- Centre Armand-Frappier - Santé Biotechnologie

« Le changement n'apporte pas toujours la croissance, mais il n'y a pas de croissance sans changement. »

- Roy T. Bennett

Remerciements

Je tiens d’abord à remercier chaleureusement mon directeur de recherche, Yves St-Pierre, pour son mentorat durant mon doctorat. Ta guidance m’a permis de grandir, tant professionnellement que personnellement. Merci pour ton soutien, ta confiance et surtout, ta patience d’ange. Tu m’as donné une liberté précieuse, tout en restant le phare dans le brouillard de ma recherche, ce qui m’a permis de surpasser même mes propres espérances.

Un grand merci à ma famille pour leur soutien infaillible tout au long de mes aventures académiques. Votre encouragement et votre motivation à me pousser toujours plus loin ont été inestimables. Vous avez toujours souligné l’importance de la curiosité et de l'apprentissage comme les fondations d’une vie enrichie — et vous aviez raison !

Merci à mon copain, Luc, pour son écoute, son amour et son incroyable talent pour me faire rire même lors des jours sombres. Ta capacité à m’encourager à poursuivre mes rêves tout en restant les pieds sur terre est purement magique. Grâce à toi, j'ai trouvé l'équilibre parfait entre ma passion pour la recherche et ma vie personnelle.

Un merci très spécial à France pour son aide précieuse et ses conseils à toute heure. Merci de m'avoir patiemment introduite aux mystères de la biologie moléculaire et de m'avoir guidée à travers ses nombreux labyrinthes techniques. L’aventure doctorale aurait été bien plus grise sans ta présence colorée. Merci pour tout !

Une pensée particulière pour Marlène Fortier, dont l'engagement, la disponibilité constante et la bonne humeur ont éclairé nos journées.

Un gros merci à mes (anciennes) collègues et amies, Camille, Fanny, Rita, Lina, Noémie, et Amira. Travailler avec vous a été un véritable plaisir. Les fous rires dans le bureau et nos débats scientifiques endiablés vont sérieusement me manquer.

Je tiens aussi à remercier mon co-directeur de recherche, Stéphane Betoulle, ainsi qu'à tous nos collaborateurs, Samuel Turgeon, Anne-Laure Ferchaud et Thierry Boulinier, pour avoir enrichi cette aventure par leurs contributions précieuses. Un grand merci également à tout le personnel de l'IPEV, et en particulier à l'équipe de Yann Le Meur, pour leur support logistique inestimable durant notre mission aux îles de Kerguelen, ainsi qu'à l'équipe de conservation du parc marin du Saguenay-Saint-Laurent pour leur assistance lors de nos multiples échantillonnages. Je remercie chaleureusement l'équipe de Jacques Labonne pour leur aide précieuse et leurs conseils avisés. Un grand merci également à nos collègues Richard Villemur et Frédéric Veyrier pour leurs nombreux conseils et leur soutien. Je suis reconnaissant à toute l'équipe de Martin Smith et de Pedro Oliveira pour m'avoir permis de me familiariser avec la plateforme Nanopore, y compris les protocoles de préparation de librairies et les méthodes bio-informatiques. Enfin, merci à tous les membres du jury d'évaluation pour avoir accepté d'évaluer ma thèse.

Liste des publications scientifiques

Total: 7 **1ère auteure (5):** 4 publiées, 1 soumis

Ferchiou, S., Caza, F., Sinha, K., Sauvageau, J. and St-Pierre, Y. (2024). Assessing marine ecosystem health using multi-omic analysis of blue mussel liquid biopsies: A case study within a national marine park. *Chemosphere*, Aug 1;362:142714..

Caza F, **Ferchiou S**, Danion M, Paris S, Barjhoux I, David E, Lambert J, Kestemont P, Cosio C and St-Pierre Y. (2024) Effects of tebuconazole on the microbiome of rainbow trout (Oncorhynchus mykiss): implications for fish health and ecological consequences (soumis à *Chemosphere*).

Ferchiou S, Caza F, Villemur R, Betoulle S and St-Pierre Y. (2024) From shells to sequences: A proof-of-concept study for on-site analysis of hemolymphatic circulating cell-free DNA from sentinel mussels using Nanopore technology, *Sci. Total Environ.*, Jul 15;934:172969.

Fronton F, **Ferchiou S**, Caza F, Villemur R, Robert D and St-Pierre Y. (2023) Insights into the circulating microbiome of Atlantic and Greenland halibut populations: the role of species-specific and environmental factors, *Sci Rep.* Apr 12;13(1):5971.

Ferchiou S, Caza F, Villemur R, Labonne J and St-Pierre Y. (2023) Skin and Blood Microbial Signatures of Sedentary and Migratory Trout (Salmo trutta) of the Kerguelen Islands, *Fishes.* Mar 24;8(4):174.

Ferchiou S, Caza F, de Boissel PG, Villemur R and St-Pierre Y. (2022) Applying the concept of liquid biopsy to monitor the microbial biodiversity of marine coastal ecosystems, *ISME Comm.* Jul 27;2(1):61.

Ferchiou S, Caza F, Villemur R, Betoulle S and St-Pierre Y. (2022) Species-and site-specific circulating bacterial DNA in Subantarctic sentinel mussels Aulacomya atra and Mytilus platensis, *Sci Rep.* Jun 10;12(1):9547.

Liste des communications scientifiques

Présentations orales

Total : 7 / **Prix :** 5 / **Internationale:** 1

Ferchiou S, Caza F, Carpentier C, Turgeon S, Villemur R, Corbeil J, Prunier J, Archambault P et St-Pierre Y. (2024) Evaluer l'état de santé des milieux marins et côtiers une moule à la fois : Exemple d'application dans une aire marine protégée, *Journées scientifiques de l'INRS,* Québec, Qc, Canada **(Meilleure présentation orale)**

Ferchiou S, Caza F, Falardeau-Côté M, Carpentier C, Turgeon S, Villemur R, Corbeil J, Archambault P et St-Pierre Y. (2023) De l'Arctique à la Côte-Nord : Évaluation des milieux marins et côtiers en appliquant le concept de biopsie liquide chez la moule bleue (*Mytilus spp.*), *Rencontre scientifique- Sentinelle Nord,* Québec, Qc, Canada

Ferchiou S, Caza F, Turgeon S, Corbeil J, Carpentier C, Villemur R et St-Pierre Y. (2023) Utilisation de la biopsie liquide chez la moule (*Mytilus spp.*) pour évaluer l'état de santé des écosystèmes marins et côtiers. *Congrès Armand-Frappier,* Saint-Sauveur, Qc, Canada **(Meilleure présentation orale)**

Ferchiou S, Caza F, Turgeon S, Corbeil J, Carpentier C, Villemur R et St-Pierre Y. (2023) Combinaison du concept de biopsie liquide et d'une approche multi-omique chez la moule bleue (*Mytilus spp.*) pour évaluer l'état de santé des écosystèmes marins côtiers : Exemple d'application au Parc marin du Saguenay-Saint-Laurent. *Colloque Conjoint en écotoxicologie (EcotoQ/ECOBIM)*, Québec, Qc, Canada **(Prix du public)**

Ferchiou S, Caza F, Villemur R, Betoulle S and St-Pierre Y. (2022) Using liquid biopsies in sentinel mussels for monitoring biodiversity in marine ecosystems. Artic Circle Assembly – Mon Projet Nordique (finaliste), Reykjavík, Islande.

Ferchiou S, Caza F, Villemur R, Betoulle S et St-Pierre Y. (2022) Combiner le concept de biopsie liquide chez les moules bleues et la technologie de séquençage Nanopore® pour l'évaluation de l'impact des changements climatiques et de la pollution sur les écosystèmes marins côtiers. *Colloque Conjoint en écotoxicologie (EcotoQ/Chapitre Saint-Laurent),* Québec, Qc, Canada **(Meilleure présentation orale)**

Ferchiou S, Caza F, Villemur R, Betoulle S et St-Pierre Y. (2021) Étude du microbiome bactérien chez la moule comme indicateur de l'état de santé des écosystèmes marins et côtiers en régions polaires. *Congrès de Bactériologie intégrative: Symbiose – Pathogenèse (BiSP),* Montréal, Qc, Canada **(Meilleure présentation orale)**

Présentations par affiche

Total : 2 / **Internationale:** 1

Ferchiou S, Caza F, Carpentier C, Turgeon S, Villemur R, Corbeil J and St-Pierre Y. (2024) Combining liquid biopsy with a multi-omic approach in blue mussels (*Mytilus spp*.): The next wave in marine ecosystem health diagnostics, *ISME19,* Cape Town, South Africa

Ferchiou S, Caza F, Falardeau-Côté M, Archambault P, Corbeil J, Turgeon S, Villemur R et St-Pierre Y. (2023) Utilisation de la biopsie liquide chez la moule pour surveiller la biodiversité et la santé des écosystèmes marins, côtiers et polaires, *Journées Nordiques-INQ,* Trois-Rvières, Qc, Canada

Communications non révisées par des pairs

Total : 2

Ferchiou S, Caza F and St-Pierre Y. (2023) Liquid biopsy in sentinel mussels, *protocols.io.* https://dx.doi.org/10.17504/protocols.io.81wgb6z9olpk/v2

Ferchiou S, Del Valle C, Betoulle S, Caza F et St-Pierre Y. (2020) Protocole pour extraction et conservation de l'ADN de l'hémolymphe de moules. *Comité de production cinématographique - INRS.* https://www.youtube.com/watch?v=8DZaBoW3ogQ

Résumé

Les changements climatiques et la pollution exercent une pression significative sur les écosystèmes marins côtiers, nécessitant des méthodes de surveillance efficaces. Les bivalves, utilisés comme espèces sentinelles, sont cruciaux dans cette démarche mais se heurtent à des limites liées à l'utilisation de biomarqueurs conventionnels, notamment en termes de sensibilité et de capacité prédictive. Pour surmonter ces défis, notre équipe cherche à exploiter le potentiel de la biopsie liquide, un concept en émergence dans le développement en oncologie basé sur l'analyse de l'ADN relâché dans la circulation sanguine par les cellules tumorales. L'analyse de l'ADN libre circulant (ccfDNA) permet ainsi de distinguer l'ADN de l'hôte (ADN du soi) de celui provenant de l'environnement (ADN du non-soi). Notre hypothèse suggère que l'application de ce concept chez la moule nous permettra d'obtenir une compréhension plus fine des interactions écologiques et des réponses biologiques aux stress environnementaux.

L'objectif général de ce projet visait à appliquer la biopsie liquide aux organismes marins afin d'évaluer l'état de santé des écosystèmes marins, avec une attention particulière portée aux régions polaires, particulièrement vulnérables aux changements climatiques et à la propagation de pathogènes.

Nos résultats ont démontré que les signatures microbiennes observées chez les moules varient de manière interspécifique et spatiale et sont influencées par les conditions environnementales et l'exposition à la pollution. Nous avons aussi montré que le ccfDNA hémolymphatique, adapté pour le séquençage Nanopore, permet une évaluation efficace de la biodiversité locale, ainsi que la détection d'agents microbiens et parasitaires qui pourraient être pathogènes, tant pour les moules que pour d'autres espèces animales et végétales présentes dans l'environnement. L'utilisation de techniques de séquençage avancées, telles que le séquençage aléatoire *shotgun* et la technologie Nanopore, a facilité l'identification de pathogènes potentielles et l'exploration de la diversité virale, surmontant les limites des approches métagénomiques conventionnelles.

Enfin, en intégrant une approche multi-omique, nous avons pu mettre en évidence des perturbations dans le métabolisme énergétique et mitochondrial des moules, indicatives de stress environnementaux et anthropiques affectant leur habitat.

En conclusion, notre étude a pu démontrer que l'utilisation de la biopsie liquide ouvre des perspectives pour l'étude des modifications épigénétiques induites par des facteurs anthropiques et environnementaux, offrant ainsi une approche intégrée pour mesurer la biodiversité et détecter les espèces invasives sans recourir au *metabarcoding*. L'intégration de l'analyse multi-omique des biomarqueurs circulants à partir d'échantillons de sang ou d'hémolymphe récoltés chez des organismes sentinelles comme la moule promet de révolutionner la surveillance environnementale, offrant des outils de diagnostic précis, sensibles et pratiques pour la protection des écosystèmes marins côtiers.

Mots-clés : Changements climatiques, biopsie liquide, analyse multi-omique, moule bleue, biomarqueurs

Abstract

Climate change and pollution exert significant pressure on coastal marine ecosystems, necessitating effective monitoring methods. Bivalves, used as sentinel species, are crucial in this endeavor but face limitations related to the use of conventional biomarkers, particularly in terms of sensitivity and predictive capacity. To overcome these challenges, our team seeks to leverage the potential of liquid biopsy, an emerging concept in oncology development based on the analysis of DNA released into the bloodstream by tumor cells. The analysis of circulating cell-free DNA (ccfDNA) thus allows us to distinguish host DNA (self-DNA) from environmental DNA (non-self DNA). Our hypothesis suggested that applying this concept to mussels will enable a more nuanced understanding of ecological interactions and biological responses to environmental stressors.

The overall objective of this project was to apply liquid biopsy to marine organisms to assess the health of marine ecosystems, with particular attention to polar regions, which are highly vulnerable to climate change and the spread of pathogens.

Our results showed that the microbial signatures observed in mussels vary interspecifically and spatially, and are influenced by environmental conditions and exposure to pollution. We have also demonstrated that hemolymphatic ccfDNA, suited for Nanopore sequencing, enables an effective evaluation of local biodiversity and the detection of microbial and parasitic agents that could be pathogenic not only for mussels but also for other animal and plant species present in the environment. The use of advanced sequencing techniques, such as random shotgun sequencing and Nanopore technology, has facilitated the identification of potential pathogens and the exploration of viral diversity, overcoming the limitations of traditional metagenomic approaches. By integrating a multi-omic approach, we have highlighted disturbances in the energy and mitochondrial metabolism of mussels, indicative of environmental and anthropogenic stress affecting their habitat.

In conclusion, our study has demonstrated that the use of liquid biopsy opens up new perspectives for studying epigenetic modifications induced by anthropogenic and environmental factors, thus offering an integrated approach for measuring biodiversity and detecting invasive species without resorting to metabarcoding. The integration of multi-omic analysis of circulating biomarkers from blood or hemolymph samples collected from sentinel organisms like the mussel promises to revolutionize environmental monitoring, providing precise, sensitive, and practical diagnostic tools for the protection of coastal marine ecosystems.

Keywords: Climate change, liquid biopsy, multi-omic analysis, blue mussel, biomarkers

Table des matières

Liste des figures

Chapitre 1

Chapitre 2

Chapitre 3

Chapitre 4

Chapitre 5

Chapitre 6

Liste des tableaux

Chapitre 1

Chapitre 3

Chapitre 4

Chapitre 5

Liste des annexes

Liste des abréviations

A. atra	*Aulacomya atra*
ADNe	ADN environnemental
ADNmt	ADN mitochondrial
AMP	Aire marine protégée
ASV	*Amplicon sequence variants*
BEST	*Biomarkers, EndpointS, and other Tools*
CC	*Climate change*
ccfDNA	ADN libre circulant
CH_4	Méthane
circARN	ARN circulaire
cmDNA	*Circulating microbiome DNA*
CNV	Variation du nombre de copies
CO_2	Dioxyde de carbone
COG	*Clusters of orthologous groups*
CTC	Cellule tumorale circulante
ctDNA	ADN tumoral circulant
dd-ccfDNA	ADN circulant dérivé du donneur
ddPCR	PCR digitale en gouttelettes
DPNI	Dépistage prénatal non invasif
eDNA	*Environmental DNA*
eLBiom	*Environmental liquid biopsy in marine ecology*
FAO	Organisation des nations unies pour l'alimentation et l'agriculture
FDA	*Food and Drug Administration*
GES	Gaz à effet de serre
IPEV	Institut Polaire Français Paul-Émile Victor
KEGG	*Kyoto Encyclopedia of Genes and Genomes*
LEfSe	*Linear discriminant analysis effect size*
LB	*Liquid biopsy*
lncARN	ARN long non-codant
M. platensis	*Mytilus platensis*
M. mytilus	*Mytilus mytilus*
MAG	Metagenome-assembled genome
mcfDNA	ccfDNA d'origine microbienne
miARN	MicroARN
mtDNA	*Mitochondrial DNA*
N_2O	Oxyde nitreux
NCLDV	*Nucleocytoplasmic large DNA virus*
NGS	Séquençage de nouvelle génération
NIH	*National Institutes of Health*
ONT	*Oxford Nanopore Technologies*

PAM	Peptides antimicrobiens
PCoA	*Principal Coordinate Analysis*
PERMANOVA	*Multivariate analysis of variance with permutation*
PLP	*Perlucin-like protein*
ROS	Espèce réactive de l'oxygène
SNP	Polymorphisme mononucléotidique
SOB	*Sulphur-oxidizing bacteria*
Wnt	*Wingless-related integration site*

Chapitre 1

Introduction générale

1. L'impact des changements climatiques sur les milieux marins : Le rôle essentiel des espèces sentinelles

Les changements climatiques désignent les variations moyennes de la température sur des périodes allant de quelques années à plusieurs décennies [1]. Ces fluctuations, qu'elles soient régionales ou globales, découlent de facteurs naturels — tels que les variations de l'activité volcanique, les changements orbitaux de la Terre et les fluctuations de l'émission solaire — et de facteurs anthropiques [2, 3]. Depuis le début du XXe siècle, l'activité humaine a induit un forçage climatique important via l'émission de gaz à effet de serre (GES) comme le dioxyde de carbone (CO_2), le méthane (CH_4) et l'oxyde nitreux (N_2O) [3]. Ces GES piègent une partie du rayonnement infrarouge émis par la Terre, contribuant ainsi au réchauffement climatique. Ce phénomène est amplifié par des rétroactions positives, comme la fonte du pergélisol qui libère de grandes quantités de CO_2 et de CH_4 dans l'atmosphère [1, 3, 4]. En conséquence, une augmentation notable de la température de la surface terrestre et marine a été enregistrée depuis les années 1990 (**Figure 1**), et sans intervention significative, les modèles prévoient une hausse moyenne de la température globale de 2°C d'ici 2050 [1, 5].

1.1 Changements climatiques du milieu marin

Les milieux marins, confrontés au réchauffement et à une acidification croissante, ainsi qu'à une élévation du niveau de la mer et à des événements météorologiques de plus en plus extrêmes, subissent des impacts considérables (**Figure 2**) [1]. Ces changements perturbent la dynamique des courants marins profonds et, par extension, la circulation océanique mondiale. Les écosystèmes polaires, particulièrement sensibles en raison de leur climat frigide, de leur dépendance à la glace de mer et de leur biodiversité endémique, sont parmi les plus menacés [6, 7]. L'océan, en tant que puits de carbone, absorbe une quantité substantielle de CO_2 atmosphérique, mais cette absorption accrue rend les eaux plus acides, particulièrement dans les régions froides. La disparition des glaces et la perte de biodiversité dans ces zones sont susceptibles de déclencher des réactions en chaîne à travers les écosystèmes marins, perturbant les cycles biologiques et la résilience des espèces [7, 8].

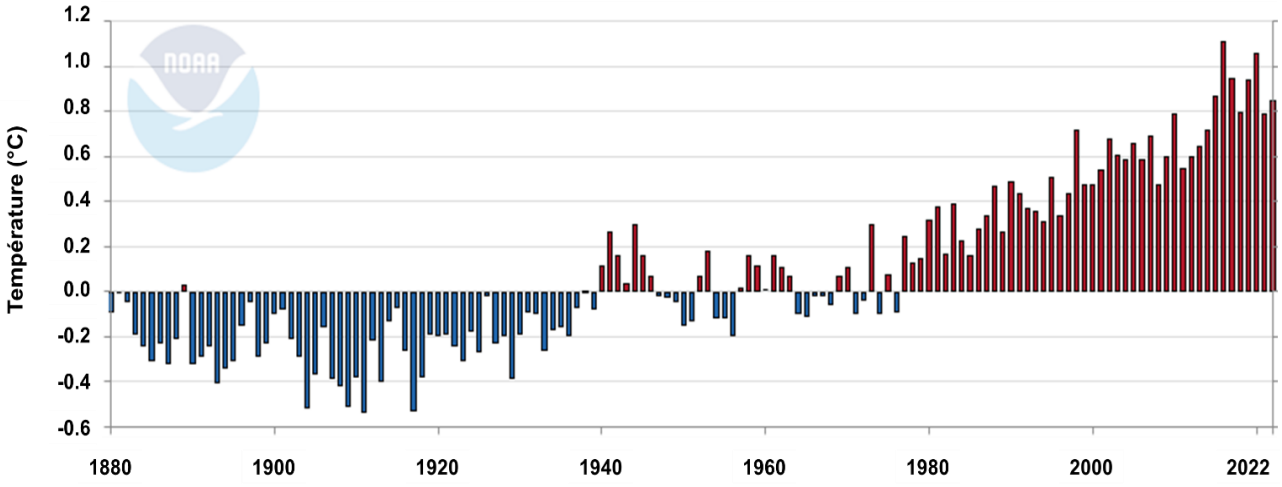

Figure 1. Anomalies de températures de surface marines et terrestres mondiales comparées à la moyenne du 20e siècle chaque mois de mars de 1880 à 2022. Les mois de mars plus froids que la moyenne sont colorés en bleu ; les mois de mars plus chauds que la moyenne sont colorés en rouge. Modifiée de NOAA Climate.gov (NOAA, 2023).

1.2 Les menaces sur les espèces marines

L'intensification des changements climatiques exerce une pression croissante sur la biologie marine à divers niveaux organisationnels [9-11]. L'augmentation de la température des eaux perturbe non seulement les habitats existants, mais redistribue également les niches écologiques des espèces, permettant ainsi à des espèces invasives et à des agents pathogènes de s'implanter [7, 12, 13]. L'acidification océanique, résultant de l'absorption accrue de CO_2, compromet des processus fondamentaux comme la calcification, essentielle à la survie des coraux et des mollusques [7, 14, 15]. L'acidité accrue des eaux favorise la dissolution de composés calciques tels que l'aragonite, indispensable à l'intégrité structurelle de nombreux organismes marins.

Parallèlement, l'élévation du niveau de la mer et les tempêtes plus fréquentes et plus violentes provoquent une érosion côtière accélérée, mettant ainsi en danger des écosystèmes côtiers vitaux comme les mangroves et les herbiers marins, qui jouent un rôle clé dans le cycle de vie de nombreuses espèces marines [16, 17].

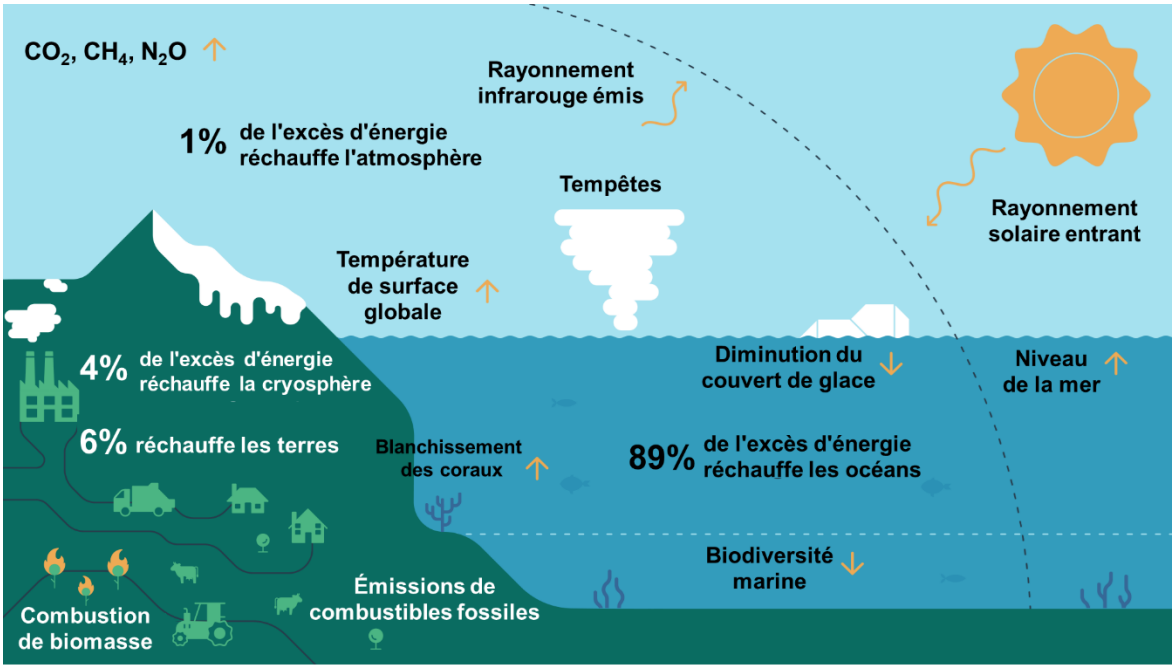

Figure 2. Schéma illustrant la distribution du réchauffement climatique à travers les différentes composantes de la Terre et de ses principales conséquences sur l'environnement. Modifiée de EU Copernicus Marine Service information et de Von Schuckmann *et al.* (2022).

Ces perturbations climatiques génèrent un stress direct et indirect sur les espèces marines, induisant par exemple un affaiblissement de leur système immunitaire, particulièrement chez les organismes ectothermes [13, 14, 18]. Un tel stress peut entraîner une dysbiose, c'est-à-dire un déséquilibre du microbiote, parfois accompagnée d'une augmentation des bactéries pathogènes [19]. Par exemple, des études révèlent une corrélation entre le réchauffement climatique et la propagation des bactéries du genre *Vibrio*, qui sont responsables d'infections chez les organismes marins et représentent également un risque pour la santé humaine [7, 20]. De plus, une étude de Lesser *et al.* (2019) a mis en lumière une corrélation possible entre les changements climatiques et l'augmentation des cas de leucémies chez les bivalves, en lien avec le rétrotransposon *Steamer*. Ce cancer, transmissible horizontalement, compromet gravement la santé des populations de bivalves, causant des déclins significatifs, en particulier sur les côtes de l'Atlantique et du Pacifique [21-23].

Ces impacts écologiques entraînent des répercussions importantes non seulement sur les écosystèmes marins, mais aussi sur les communautés humaines qui en dépendent. Des initiatives de recherche sont donc cruciales pour évaluer l'étendue des impacts environnementaux et anthropiques sur les écosystèmes marins et d'identifier les espèces sentinelles qui peuvent servir d'indicateurs précoces de ces changements perturbateurs.

1.3 Avancés et défis des programmes de surveillance marine

La création d'aires marines protégées (AMP) et de réserves marines est cruciale pour la conservation des écosystèmes marins et pour la préservation de leurs valeurs écologiques, sociales, économiques et culturelles. L'archipel de Kerguelen, situé dans les îles subantarctiques près du front polaire sud de l'océan Indien, illustre parfaitement ce concept. Stratégiquement positionné à la convergence de trois fronts océaniques et doté de vastes plateaux continentaux, l'archipel est un épicentre de productivité dans un océan relativement pauvre, soutenant un réseau trophique riche et diversifié [24]. En raison de son isolement par rapport aux activités humaines, l'archipel de Kerguelen offre un cadre unique pour la recherche scientifique, en particulier pour le suivi à long terme des populations d'oiseaux et de mammifères marins, ainsi que pour l'étude des impacts des changements globaux. En tant que l'un des derniers refuges de naturalité mondiale préservant l'intégrité de son patrimoine naturel, l'archipel revêt une grande importance pour les efforts de conservation à l'échelle globale [24]. Face à la vulnérabilité de ces milieux aux changements climatiques, l'Institut Polaire Français Paul-Émile Victor (IPEV) a initié le programme *Proteker* en 2011. Ce programme multidisciplinaire vise à surveiller la biodiversité et à renforcer la protection des écosystèmes marins de cette région isolée [25].

Un autre exemple notable est le parc marin du Saguenay-Saint-Laurent au Québec, qui couvre 1 245 km^2 de territoire marin [26]. Ce parc abrite des écosystèmes diversifiés avec plus de 2 000 espèces animales et végétales, ainsi que des mammifères marins tels que le rorqual bleu et le béluga du Saint-Laurent, des espèces considérées en situation précaire [27]. Cette AMP favorise non seulement la conservation, mais elle encourage également l'utilisation éducative, récréative et scientifique de l'écosystème de manière

durable et respectueuse, jouant un rôle essentiel dans la protection et la valorisation de la biodiversité marine.

L'efficacité de ces AMP repose sur une surveillance régulière, essentielle pour assurer la stabilité ou l'amélioration de la santé des écosystèmes concernés. Dans ce contexte, l'implantation de divers programmes de suivi, s'appuyant sur l'utilisation de bioindicateurs, est essentielle tant au niveau national qu'international. Ces programmes permettent une gestion durable des milieux marins et assurent une évaluation continue de leur état de santé.

Parmi eux, le *National Seabird Program*, créé en 2001 par le *NOAA Fisheries National Seabird Program*, et le programme *Mussel Watch*, fondé en 1975, sont des exemples phares de l'utilisation de bioindicateurs pour évaluer la santé des milieux marins [28, 29]. Le premier programme repose sur les oiseaux marins pour détecter les variations écologiques, tandis que le second utilise les bivalves pour suivre la qualité des eaux marines et côtières. Ces initiatives mesurent des biomarqueurs variés — concentrations de métaux lourds, présence de contaminants organiques persistants comme les pesticides, les hydrocarbures aromatiques polycycliques et les retardateurs de flamme — et évaluent les perturbations organiques à l'aide d'indicateurs génétiques, biochimiques, métaboliques et histologiques, tout en les contextualisant avec des paramètres abiotiques tels que le pH, la température, et la salinité.

Cependant, ces méthodologies traditionnelles présentent des limites, notamment en ce qui concerne la caractérisation de la structure génétique des populations et la détection des espèces rares ou élusives [30]. Pour pallier ces contraintes, des programmes récents exploitant l'ADN environnemental (ADNe), tels que OBIS-SEAMAP et Tara Oceans, inaugurés en 2002 et 2009 respectivement, ont été initiés [31]. Ces nouvelles initiatives permettent une évaluation plus complète de la biodiversité marine, apportant des précisions sur la présence et la distribution étendue d'espèces, y compris celles qui échappent aux méthodes conventionnelles de collecte [32, 33] (**Figure 3**). L'ADNe fournit également des données importantes sur les populations et le sexe des organismes

étudiés [34]. Le potentiel de l'ADNe à conserver les données biologiques sur le long terme vient transformer les efforts de conservation marine, en fournissant une vision holistique et évolutionnaire sur la santé des écosystèmes marins, ainsi que des AMP [35]. La récupération de l'ADNe présente un potentiel pour les recherches paléoécologiques et archéologiques, permettant de retracer l'écologie et l'évolution des communautés biologiques à travers des échantillons sédimentaires millénaires [33].

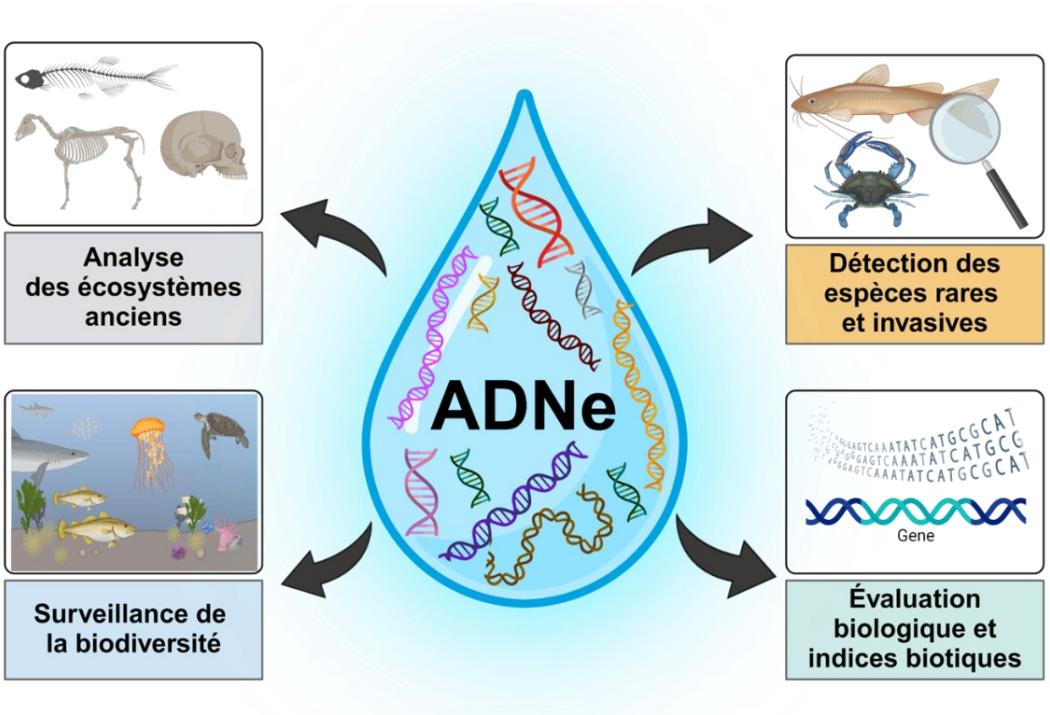

Figure 3. Les applications potentielles de l'ADN environnemental (eDNA) dans les écosystèmes aquatiques qui incluent la détection d'espèces rares et invasives, la surveillance de la biodiversité, l'analyse des écosystèmes anciens, ainsi que l'évaluation et biologique basée sur l'ADN extrait d'échantillons environnementaux. Adaptée de Pawlowski *et al.* (2020) et de Ruppert *et al.* (2019).

Néanmoins, il convient de souligner que l'analyse de l'ADNe peut être logistiquement complexe et coûteux, particulièrement pour la détection de taxons rares. Les erreurs de séquençage, le biais de séquençage préférentiel et d'autres facteurs techniques peuvent entraver l'interprétation des données [36]. Les conditions environnementales telles que la température, l'humidité, et la présence de contaminants peuvent également affecter la qualité et la quantité de l'ADN récupéré, compromettant ainsi la fiabilité des résultats [37, 38]. Cette sensibilité des échantillons d'ADNe aux conditions de transport et d'entreposage vient aussi complexifier leur gestion. De plus, la contamination externe et les mélanges d'ADN posent des défis supplémentaires dans l'analyse de l'ADNe [39, 40].

Par ailleurs, bien que les techniques moléculaires permettent une détection rapide des espèces cibles ou une caractérisation approfondie de la biodiversité à partir de petits échantillons, elles nécessitent des investissements significatifs en temps et en ressources analytiques [36]. Des méthodes émergentes de séquençage exempt de PCR, telles que le séquençage aléatoire de type *shotgun*, l'enrichissement mitochondrial et l'enrichissement génique, sont prometteuses, mais demeurent peu adoptées pour l'analyse de l'ADNe qui favorise plutôt les approches de *metabarcoding* en raison de leur coût élevé et des ressources substantielles requises pour le séquençage et l'analyse [36]. Ces techniques nécessitent aussi des traitements en laboratoire plus approfondis, ce qui augmente encore les coûts associés à ces analyses.

Les programmes de recherche utilisant l'ADNe et les programmes de surveillance traditionnels se distinguent par leur méthode d'échantillonnage, le type d'information qu'ils fournissent, leurs applications et leurs limites (**Tableau 1**). La combinaison des techniques de surveillance conventionnelles avec l'approche innovante de l'ADNe constitue un outil indispensable, non seulement pour évaluer l'impact anthropique sur les écosystèmes marins, mais aussi pour guider les politiques de gestion et de conservation des ressources maritimes.

Tableau 1 : Principales différences entre les programmes de recherche utilisant l'ADN environnemental (ADNe) et les programmes de surveillance traditionnels.

	Programmes de surveillance traditionnels	Programmes de surveillance avec l'ADN environnemental
Méthodes d'échantillonnage	Observation directe des espèces ou collecte des échantillons spécifiques.	Collecte des échantillons d'eau, d'air ou de sol et analyse de l'ADN présent.
Type d'informations	Informations sur des espèces spécifiques et sur l'impact des activités humaines.	Informations sur les écosystèmes aquatiques ou difficiles d'accès, sur la biodiversité, y compris les espèces rares ou difficiles à observer et sur l'impact des activités humaines
Limites	Méthodes moins sensibles à la détection de certaines espèces, peuvent être coûteuses et chronophages.	Technologie en développement, nécessité d'équipements et de procédures spécialisés, complexité de l'analyse, contamination possible de l'ADN, influence des conditions environnementales, gestion du transport et de l'entreposage des échantillons.
Impact sur l'environnement	Peuvent être perturbateurs pour les écosystèmes, surtout s'il y a capture ou manipulation d'espèces.	Minimalement invasifs.

1.4 Espèces sentinelles des milieux marins

La surveillance des écosystèmes marins, face aux pressions environnementales et anthropiques croissantes, s'appuie sur des programmes de recherche dédiés à l'étude des espèces sentinelles. Les espèces sentinelles agissent comme un baromètre des changements écologiques, révélant soit la détérioration soit l'amélioration de l'état d'un écosystème [41, 42]. Elles reflètent également les effets cumulatifs de ces polluants sur un système biologique vivant. De plus, certains polluants peuvent s'accumuler dans les organismes vivants à des niveaux beaucoup plus élevés que dans l'environnement immédiat. Dans le contexte de biomarqueurs prédictifs et sensibles, on note également qu'elles peuvent montrer des réponses biologiques (comme des changements dans les taux de reproduction ou dans le comportement) qui signalent des problèmes avant que des niveaux dangereux de pollution soient atteints. Dans le cadre de ce projet, une espèce sentinelle est caractérisée par 1) sa sensibilité aux perturbations, 2) son rôle

crucial dans l'écosystème, et 3) sa capacité à fournir des données concrètes sur la santé environnementale à l'aide de biomarqueurs spécifiques.

Dans les milieux marins, les oiseaux marins, les poissons pélagiques, ainsi que les mammifères marins sont souvent désignés comme sentinelles en raison de leur sensibilité aux changements environnementaux, leur large répartition géographique, leur facilité d'observation et leur rôle important dans les écosystèmes [43]. Le suivi de l'accumulation de contaminants chez ces espèces, tels que les retardateurs de flammes, pesticides et métaux lourds, permet d'évaluer l'ampleur de la pollution marine [44, 45].

Les bivalves, tels que les moules et les myes, sont également privilégiés en tant qu'indicateurs d'intégrité des écosystèmes côtiers [42, 46]. Leur présence quasi ubiquitaire, leur nature sessile, ainsi que leur capacité de filtration en font des bio-accumulateurs efficaces de xénobiotiques et d'autres polluants biologiques et chimiques, ce qui en fait d'excellents modèles pour l'écotoxicologie. Par ailleurs, la sensibilité de leur système immunitaire aux changements environnementaux, tels que la température, la salinité et l'acidification des océans, en fait des indicateurs sensibles de l'état de santé de leur habitat [18, 47, 48]. Au-delà de la surveillance de la pollution marine, l'étude des bivalves offre des informations sur la complexité et la résilience des écosystèmes marins, enrichissant notre compréhension des mécanismes d'adaptation et de survie des communautés marines face aux défis écologiques.

2. La moule bleue

La moule bleue (*Mytilus edulis*) [49], ou moule commune, est l'espèce sentinelle la plus étudiée et la plus utilisée pour le suivi de l'état de santé des écosystèmes marins côtiers. Elle représente l'espèce phare du genre *Mytilus*. Elle partage ce genre avec d'autres espèces étroitement apparentées, telles que *Mytilus galloprovincialis* [50], *Mytilus trossulus* [51], *Mytilus californianus* [52] ou encore *Mytilus platensis* [53]. Ces espèces présentent des similitudes marquées et peuvent s'hybrider, complexifiant ainsi leur classification [54, 55].

2.1 Anatomie et physiologie

La moule se caractérise par sa coquille bivalve, constituée de deux valves symétriques unies par un ligament élastique. Cette coquille est formée d'une couche externe calcaire robuste et d'une couche interne nacrée, riche en aragonite [56]. L'intérieur abrite des organes vitaux recouverts par le manteau, responsable de la sécrétion de la coquille [57]. Le système nerveux est dispersé en plusieurs ganglions, optimisant la réponse sensorielle [58]. Le pied est un organe musculaire, soutenu par des filaments de byssus, qui assure l'adhérence au substrat [59]. Les muscles adducteurs permettent la fermeture de la coquille pour protéger l'organisme contre les prédateurs [57, 60].

Sur le plan reproductif, la moule bleue est caractérisée par un système dioïque, où la ponte et la fécondation se déroulent dans la colonne d'eau [61]. Après la fécondation, les larves planctoniques se développent, puis se fixent au substrat, entamant leur métamorphose en moules adultes. Des études ont également mis en évidence des phénomènes d'hermaphrodisme pouvant être simultané – production de gamètes mâles et femelles par le même individu – ou séquentiel – capacité de changer de sexe au cours de la vie [62]. Ceci vient souligner la complexité et la flexibilité des stratégies reproductives de cet organisme.

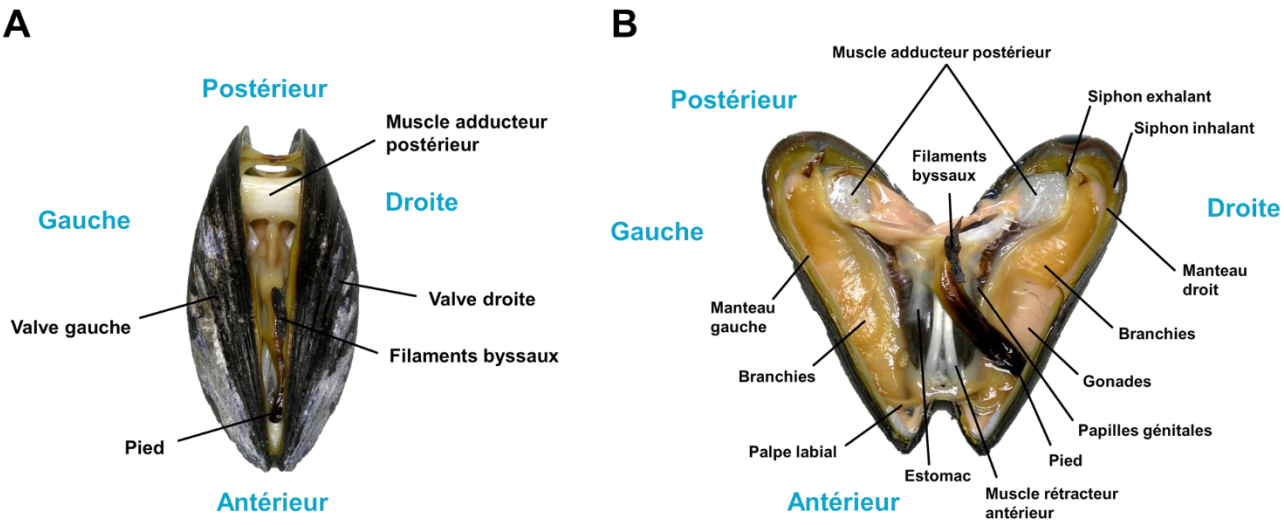

Figure 4. Anatomie générale de la moule bleue. A) Vue latérale de la moule et B) une vue ventrale après la découpe des muscles adducteurs et l'ouverture forcée des valves. Modifiée de Delahaut *et al.* (2012) et de Zenz (2006).

La moule bleue est également un organisme filtreur efficace. Sa capacité à filtrer l'eau varie en fonction de plusieurs facteurs tels que la taille, la disponibilité de nourriture, la qualité de l'eau et son état de santé, avec une capacité estimée entre 1,8 et 2,4 litres d'eau par heure [63, 64]. Ses branchies se composent de filaments délicats couverts de cils vibratiles [65]. Ces cils génèrent un courant d'eau qui passe à travers les branchies, facilitant ainsi l'aspiration de l'eau par le siphon inhalant [63, 65]. Une fois dans les branchies, l'eau est filtrée, permettant l'extraction de l'oxygène et la capture de particules organiques, ainsi que de bactéries. L'eau filtrée est par la suite rejetée via le siphon exhalant. Les particules alimentaires capturées sont alors acheminées vers le système digestif, constitué d'une bouche, d'un œsophage, d'un estomac, d'un intestin et d'une glande digestive, où elles seront ingérées et métabolisées [57].

Le système circulatoire de la moule est semi-ouvert, où l'hémolymphe, transportée par le cœur, circule librement parmi les tissus, facilitant le transfert de l'oxygène, des nutriments et des déchets [66]. Les hémocytes, cellules immunitaires présentes dans l'hémolymphe, forment la première ligne de défense immunologique de la moule [67].

Les hémocytes se classent en deux catégories principales : les granulocytes et les hyalinocytes (**Figure 5**) [66, 68]. Les granulocytes, qui constituent la majorité des cellules immunitaires chez la moule, se classent en deux catégories principales : les éosinophiles et les basophiles. Les éosinophiles ont une activité plus élevée dans la phagocytose et l'activité oxydative que les basophiles suggérant une plus grande réactivité sur le plan immunitaire. Les basophiles sont impliqués dans les interactions dynamiques entre les hémocytes et dans la constitution des noyaux d'agrégation [69]. Les hyalinocytes, bien que moins actifs dans la phagocytose et la production des espèces réactives de l'oxygène (ROS), contribuent significativement à la défense immunitaire en produisant des protéines associées à la voie de signalisation Wnt (*Wingless-related integration site*). Cette fonction est particulièrement essentielle dans les contextes infectieux, où ces cellules jouent un rôle adaptatif face aux parasites et manifestent une plus grande sensibilité aux dommages génotoxiques. Ces mécanismes diversifiés illustrent les différentes stratégies du système immunitaire inné des moules bleues dans la défense contre les infections et les maladies.

	Hyalinocytes	Granulocytes	
		Éosinophiles	Basophiles
			
Granules	Peu ou pas	Nombreuses (0.5-1.5 µm)	Nombreuses (0.2-0.3 µm)
Diamètre de la cellule	4-9 µm	7-12 µm	7-10 µm
Phagocytose	+	+++	++
ROS production	+	+++	++
Apoptose	+	+++	+++
Principales voies immunitaires	Voie de signalisation Wnt	Voies MAPK, Ras et NF-κβ	Voies MAPK, Ras et NF-κβ

Figure 5. Principaux hémocytes chez la moule bleue (*Mytilus spp.*) et leurs caractéristiques. Adaptée de De la Ballina *et al.* (2022) et de Cheng (1984).

2.2 Rôle dans les écosystèmes marins côtiers

La moule assume des fonctions écologiques et économiques cruciales au sein des écosystèmes côtiers marins (**Figure 6**). Agissant en tant que bio-ingénieurs, ces mollusques influencent de manière significative la structure et la fonction des habitats marins [70, 71]. Par l'excrétion de bio-dépôts, composés de fèces et de pseudofèces (particules alimentaires non-digérées), les moules enrichissent les sédiments en nutriments essentiels tels que l'azote, le phosphore et la silice [72]. Cette augmentation en nutriments bénéficie aux détritivores et à d'autres organismes benthiques qui constituent une ressource alimentaire clé pour une variété d'espèces marines [73].

En outre, les moules contribuent à la stabilité des fonds marins et à la lutte contre l'érosion [74]. En s'accrochant fermement aux substrats et en formant des agrégats denses, elles modèrent l'impact physique des vagues, protégeant ainsi les littoraux de l'érosion en dissipant l'énergie des vagues et en réduisant le transport de sédiments. Les structures complexes créées par les bancs de moules offrent également des niches écologiques pour une diversité d'espèces, incluant algues, invertébrés et poissons. Les coquilles des

moules, qu'elles soient vides ou non, servent de support pour une multitude d'organismes filtreurs et non-filtreurs.

La capacité de la moule bleue à filtrer les nutriments et la matière organique de l'eau joue un rôle prépondérant dans la clarification de l'eau, augmentant ainsi la pénétration de la lumière et favorisant la prolifération de végétaux et de bactéries phototrophes [71]. Ce processus transforme les habitats aquatiques en systèmes riches et productifs, améliorant la qualité de l'eau, augmentant la biodiversité et soutenant la productivité des zones côtières.

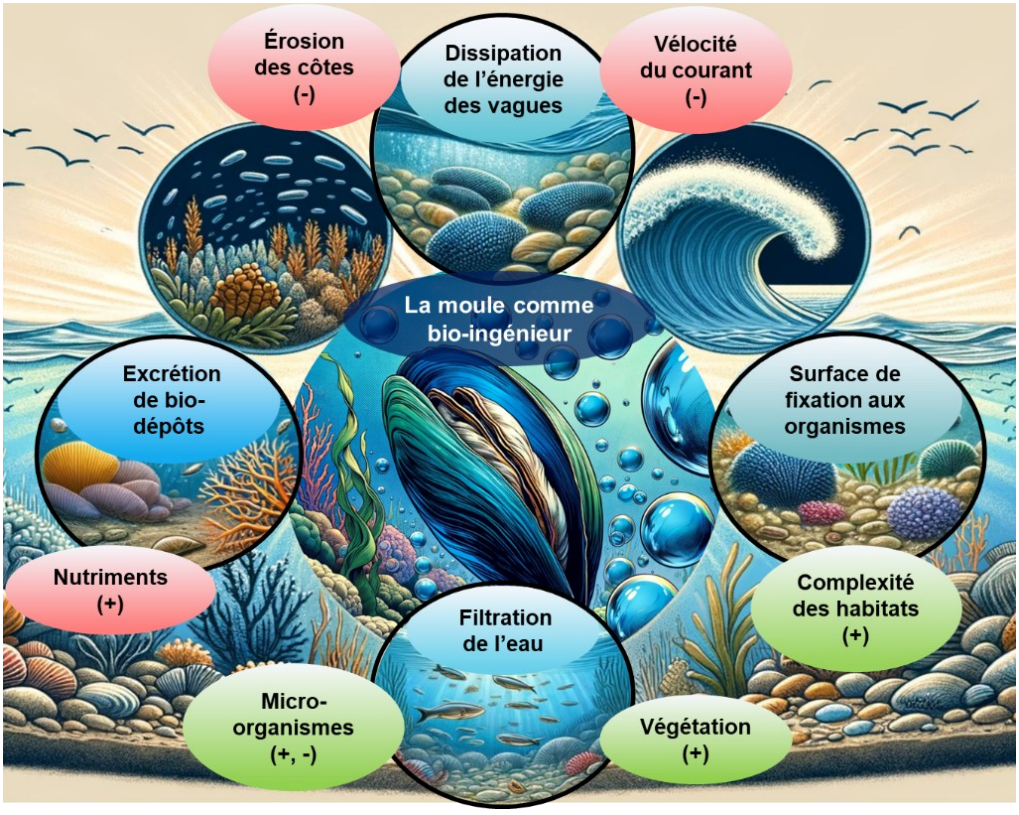

Figure 6. Le rôle de la moule comme bio-ingénieur dans les écosystèmes marins et côtiers. Les bulles vertes et rouges représentent les principaux effets biotiques et abiotiques respectivement. Image générée avec l'aide de l'intelligence artificielle.

2.3 Rôle dans la diète

La moule occupe une position cruciale au sein de la chaîne alimentaire marine, établissant un pont entre les producteurs primaires, tels que les microalgues et les particules organiques, et les consommateurs de niveau supérieur, incluant de nombreux carnivores marins [75, 76]. Sa présence est vitale pour le transfert d'énergie et de nutriments à travers l'écosystème, servant de ressource alimentaire pour une variété d'espèces, notamment les poissons de fond, les étoiles de mer, les crabes et les oiseaux marins (**Figure 7**).

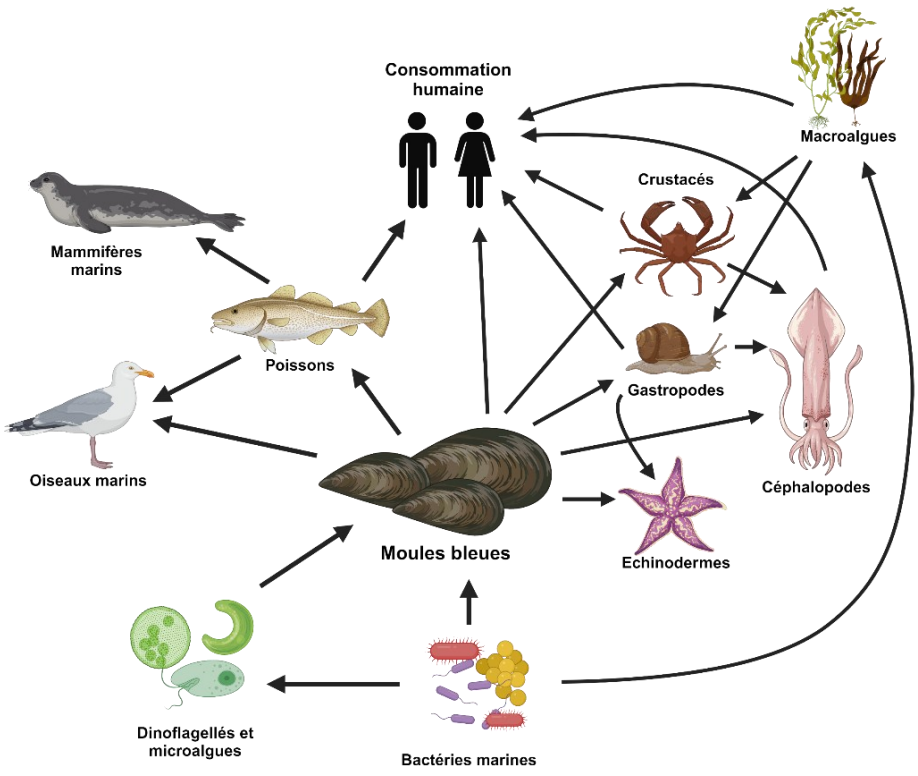

Figure 7. Réseau alimentaire marin généralisé avec des liens représentant les liens trophiques. Modifiée de Llewellyn *et al.* (2006).

Dans le secteur halieutique, les bivalves jouent également un rôle économique non négligeable. Selon les données de l'organisation des nations unies pour l'alimentation et l'agriculture (FAO), les bivalves constituent environ 15 % de la production aquacole

mondiale, représentant plus de 17 millions de tonnes annuellement [77]. La famille des *Mytilidae*, incluant la moule bleue, figurent parmi les espèces les plus cultivées.

Au-delà de leur importance économique, les bivalves occupent une place significative dans les régimes alimentaires traditionnels des communautés inuites de l'Arctique [78]. Les études analysant les contenus en lipides et contaminants des bivalves consommés par ces communautés sont rares et ponctuelles, mais elles soulignent l'importance de surveiller ces aspects pour la santé publique, particulièrement avec l'impact actuel et prévu du changement climatique sur les pathogènes entériques dans l'Arctique canadien. [79-81].

Les fluctuations dans les populations de moules peuvent avoir des répercussions significatives sur la chaîne alimentaire, affectant directement la croissance et la survie des espèces dépendantes. Elles jouent un rôle de premier plan dans la régulation des populations d'algues, le transfert d'énergie et le maintien de l'équilibre écologique. La moule bleue s'érige donc en acteur indispensable de la santé et de la diversité des écosystèmes marins côtiers, soulignant l'importance de sa conservation pour l'équilibre écologique et le bien-être économique des communautés côtières.

2.4 Rôle dans les études fondamentales

Les bivalves, y compris les moules, sont au cœur de recherches fondamentales dans divers champs de recherche, notamment en immunologie [82] (**Figure 8**). Ces organismes servent de modèles précieux pour l'étude de l'immunité innée, particulièrement en ce qui concerne les mécanismes de défense des muqueuses [83-85]. Chez les vertébrés et les invertébrés, l'adhésion des pathogènes aux surfaces muqueuses constitue souvent le prélude à l'infection.

En filtrant l'eau, les bivalves exposent leurs branchies et autres organes palliaux, tels que le manteau et les palpes labiaux, aux agents pathogènes aquatiques, faisant de la cavité palliale un point d'entrée et une barrière essentielle contre les agents pathogènes [86, 87]. Le mucus qui recouvre les surfaces palliales et les hémocytes présents jouent un rôle crucial dans l'immunité et l'homéostasie [82, 85]. Outre son rôle de barrière physique,

le mucus est riche en molécules actives dans les interactions hôte-microbe, incluant des lectines spécifiques au galactose et au mannose, des protéines à domaine C1q, et des agents antimicrobiens comme la défensine et le lysozyme [83].

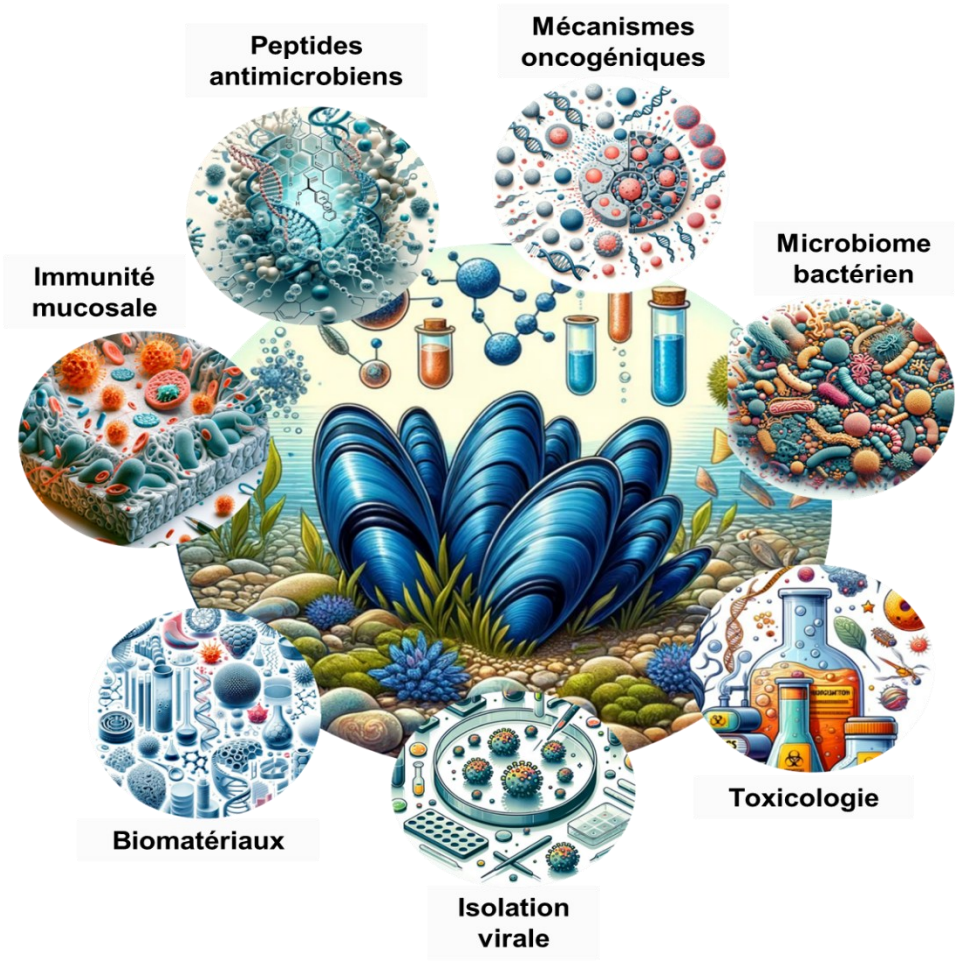

Figure 8. Les bivalves comme modèles pertinents pour la santé humaine. Les bivalves servent de modèles directs pour des enjeux de santé humaine tels que l'immunité mucosale, la régulation du microbiome ou encore la production de peptides antimicrobiens. En tant que filtreurs, les bivalves jouent un rôle dans la détoxification lors des proliférations d'algues toxiques et peuvent accumuler virus et microplastiques. La biominéralisation de leur coquille présente des similitudes avec la formation osseuse et l'étude de cancers contagieux chez ces organismes éclaire certains processus oncogènes. Image générée avec l'aide de l'intelligence artificielle.

L'expression de certaines de ces protéines est influencée par des facteurs environnementaux. Par exemple, une augmentation des niveaux de lectines dans le mucus a été observée chez les huîtres et les moules soumises à des défis bactériens [88, 89]. L'étude de la diversité fonctionnelle des molécules immunitaires associées aux muqueuses chez les bivalves offre une opportunité unique d'explorer les interactions complexes entre microorganismes mutualistes, commensaux et pathogènes et de mieux comprendre les mécanismes de défense innée essentiels à la santé animale.

Parallèlement, en lien avec le système immunitaire inné des bivalves, les peptides antimicrobiens (PAM) se révèlent être une alternative prometteuse aux antibiotiques conventionnels dans le traitement des maladies humaines et animales [90-93]. Malgré leur large spectre d'action contre les souches bactériennes pathogènes résistantes aux antibiotiques traditionnels, peu de PAM ont atteint les phases II et III des essais cliniques, principalement à cause des variations environnementales affectant leur efficacité, comme le pH, la méconnaissance de leur mécanisme d'action et leur courte demi-vie in vivo diminuant potentiellement leur efficacité en tant qu'antibiotiques [82, 94].

En plus des PAM, le système immunitaire des bivalves produit d'autres substances aux promesses biotechnologiques importantes, notamment les cytokines [82, 93]. Ces petites glycoprotéines, essentielles pour une réponse immunitaire rapide et efficace même à faible concentration, présentent un grand potentiel d'applications biotechnologiques, marquant l'importance des bivalves dans la recherche avancée pour la santé humaine et la sécurité alimentaire.

En outre, d'autres applications biotechnologiques s'inspirent des protéines modifiées issues des mollusques telles que la ziconotide, un peptide dérivé de l'escargot cône et commercialisé sous le nom de Prialt comme médicament pour la thérapie de la douleur chronique, une "colle médicale" inspirée des protéines adhésives byssales des moules ou encore des lectines artificielles se liant aux cellules cancéreuses des bivalves qui pourraient trouver une application en tant qu'outils diagnostiques ou thérapeutiques [82, 95-97].

Les bivalves se distinguent également comme modèles pour l'analyse de l'écologie et de l'évolution des interactions hôte-microbe [82, 98, 99]. Le microbiome peut moduler la réponse immunitaire de l'hôte et influencer les manifestations des maladies. La dysbiose, particulièrement en milieu marin et en aquaculture, est souvent liée à des épisodes accrus de mortalité et de pathologies [100]. En tant que filtres naturels, les bivalves jouent un rôle important dans la régulation des pathogènes aquatiques, soit en réduisant leur concentration dans l'eau, soit en les concentrant dans leurs tissus, où certains peuvent survivre et parfois proliférer [101]. De plus, leur association avec une variété de micro-organismes symbiotiques joue un rôle clé dans leur aptitude à résister aux contaminants biologiques et chimiques, minimisant ainsi l'accumulation de substances nocives dans leurs organes [82]. Ainsi, la présence d'une communauté microbienne diversifiée et bien adaptée est vitale pour leur bien-être et leur permet de s'ajuster aux changements de leur environnement. Ces capacités font des bivalves un modèle d'étude pour comprendre les interactions microbiennes fondamentales, surtout dans le cadre de la résilience aux changements environnementaux, de la santé humaine et de la sécurité alimentaire.

Par ailleurs, les bivalves s'avèrent être des modèles de recherche particulièrement pertinents pour approfondir notre compréhension des réponses immunitaires associées à l'exposition aux toxines [82, 102]. Les bivalves présentent une tolérance notable aux phycotoxines, ayant la capacité d'accumuler ces substances en grande quantité. Lorsque les toxines ne sont pas rapidement éliminées en tant que pseudofèces, elles s'accumulent dans la glande digestive, où elles compromettent le système immunitaire en provoquant inflammation et dysfonction immunitaire, avec un impact direct sur les hémocytes [103, 104]. Cependant, la capacité des bivalves à bioaccumuler ces toxines tout en résistant à leurs effets sublétaux démontre leur valeur en tant que modèles pour l'analyse du métabolisme des toxines [82]. Cette résilience comprend la capacité de modifier et de détoxifier les toxines, les transformant en molécules moins nocives via des processus chimiques et enzymatiques complexes [105]. Les bivalves constituent des outils potentiels pour le développement de bioindicateurs ou de marqueurs cellulaires destinés à la surveillance de l'environnement et à la sécurité alimentaire.

Les bivalves se révèlent être des sujets d'étude pertinents dans la recherche oncologique, notamment en raison de la néoplasie disséminée. Cette affection, analogue à la leucémie, se caractérise par une propagation cancéreuse à travers l'hémolymphe et les tissus des bivalves, entraînant la mort de l'organisme [106]. Observée chez au moins 15 espèces de bivalves, cette maladie se caractérise par une prolifération cellulaire d'origine probablement hématocytaire [22, 82, 107]. De manière notable, chez certaines espèces telles que *Mya arenaria*, *Mytilus trossulus*, *Cerastoderma edule* et *Polititapes aureus*, le cancer a été identifié comme clonal et transmissible horizontalement, agissant comme une allogreffe naturelle qui se transmet d'un individu à l'autre [22, 108]. Cette transmission horizontale de cellules cancéreuses représente un phénomène rare et le premier documenté chez des organismes marins, qui jusqu'alors avait été observé uniquement chez les diables de Tasmanie et les chiens [109]. Ces cancers transmissibles horizontalement illustrent des cas de métastases où le cancer non seulement survit à son hôte, mais continue aussi d'évoluer en infectant de nouveaux hôtes. La néoplasie transmissible chez les bivalves constitue ainsi un modèle de recherche innovant pour examiner des aspects cruciaux de l'oncogenèse, comme l'évolution du cancer, la métastase et l'influence des éléments transposables sur le développement tumoral, tout en explorant les stratégies de défense de l'hôte contre la propagation du cancer [82, 110]. De plus, il a été observé que sous stress thermique, les hémocytes infectés circulant chez les moules peuvent quitter l'hémolymphe, être expulsés dans l'eau de mer, et ensuite être capturés par d'autres bivalves. Cette observation illustre une dimension supplémentaire de la dynamique de la maladie, mettant en lumière la propagation interindividuelle des pathogènes au sein de populations de bivalves [110]. Cette transmission entre individus véhiculée par les hémocytes renforce l'intérêt pour les mécanismes biologiques complexes chez les bivalves.

En plus de leur intérêt dans les études d'immunologie et de toxicologie, les bivalves jouent un rôle significatif dans d'autres secteurs de la recherche médicale, notamment dans l'étude des processus biologiques fondamentaux. La formation de l'exosquelette des bivalves, par exemple, est un sujet d'étude pertinent en recherche médicale, servant de modèle pour la formation et la réparation osseuses [82]. Ce processus implique des cellules épithéliales spécialisées situées à la surface dorsale du manteau, responsables

de la sécrétion du fluide extrapalléal composé de protéines, polysaccharides, glycoprotéines et lipides [111]. La diversité de la complexité et des motifs de la coquille fait des bivalves un organisme modèle idéal pour étudier l'évolution de la biominéralisation et pour l'utilisation de la couche interne nacrée de la coquille comme biomatériau pour des applications orthopédiques.

2.5 Biomarqueurs traditionnels

Outre leur importance dans la recherche fondamentale, les moules jouent un rôle crucial en tant qu'espèces sentinelles dans la surveillance des milieux aquatiques [46, 112, 113]. En utilisant des biomarqueurs spécifiques, les moules permettent de détecter rapidement les menaces potentielles et de répondre efficacement, contribuant ainsi à la préservation de l'intégrité écologique et au développement de stratégies de conservation adaptées.

Les biomarqueurs en écologie moléculaire jouent un rôle fondamental dans la compréhension des réponses biologiques des organismes face à leur environnement, notamment en ce qui concerne l'exposition aux polluants [114]. La classification des biomarqueurs varie en fonction du contexte d'application, des objectifs de recherche et des techniques d'analyse utilisées. Par exemple, dans le domaine de la recherche biomédicale, le cadre des *Biomarkers, EndpointS, and other Tools* (BEST), élaboré par la *Food and Drug Administration* (FDA) et les *National Institutes of Health* (NIH), identifie sept catégories distinctes de biomarqueurs (**Figure 9**). Ces catégories facilitent une compréhension plus structurée et ciblée des indicateurs biologiques pertinents pour les évaluations cliniques et les interventions thérapeutiques.

En écologie environnementale, notamment chez les études sur la moule, on distingue trois types principaux de biomarqueurs: les biomarqueurs d'exposition, qui indiquent la présence ou la concentration d'un contaminant, de son métabolite ou de son produit d'interaction dans l'organisme ou son environnement; les biomarqueurs d'effet, indiquant les répercussions biochimiques ou physiologiques résultant de l'exposition à un agent de stress environnemental; et les biomarqueurs de susceptibilité, qui identifient la vulnérabilité spécifique d'un organisme face à un contaminant ou un xénobiotique [115, 116].

Figure 9. Les sept catégories de biomarqueurs dans la recherche clinique. Classification des biomarqueurs en fonction de leur principale application clinique et de leurs objectifs. Adaptée de Division of Pharmacy Professional Development et García-Gutiérrez *et al.* (2020).

Les biomarqueurs d'exposition, principalement analysés par des méthodes biochimiques, permettent la détection de contaminants métalliques tels que le cadmium et le mercure, qui nuisent au système nerveux et au développement des moules [117, 118]. Ces biomarqueurs permettent également d'identifier d'autres substances toxiques, comme les hydrocarbures aromatiques polycycliques et les perturbateurs endocriniens, ainsi que leurs métabolites, susceptibles de s'accumuler dans la chaîne alimentaire [119]. Bien que leur mesure soit relativement simple, ces biomarqueurs ne fournissent pas d'informations sur les effets réels des contaminants sur les organismes et peuvent être influencés par d'autres facteurs, tels que le métabolisme des moules [119, 120].

Les biomarqueurs d'effet, quant à eux, fournissent des indications sur les changements biochimiques ou physiologiques qui surviennent suite à l'exposition à des polluants [116]. Ceci inclut les modifications dans l'activité enzymatique, telles que celles de l'acétylcholinestérase ou du cytochrome P450, ainsi que l'augmentation des marqueurs de stress oxydatif, qui peuvent indiquer une exposition à des neurotoxines ou à des substances génératrices de radicaux libres [121, 122]. Les anomalies morphologiques et les dommages à l'ADN peuvent également servir d'indicateurs d'exposition à des agents génotoxiques [116, 122].

Les biomarqueurs de susceptibilité offrent un aperçu sur l'influence de la génétique individuelle, notamment à travers des polymorphismes génétiques spécifiques, et leur interaction avec l'exposition aux xénobiotiques, jouant un rôle déterminant dans les facteurs de risque liés à différentes pathologies [116]. Des études antérieures ont révélé que l'exposition des moules à des métaux lourds peut entraîner un polymorphisme des allozymes [123, 124]. Toutefois, il est important de noter que la diversité allélique au sein des populations de moules peut être affectée par une multitude de facteurs biotiques et abiotiques environnementaux [123].

Bien que les biomarqueurs d'effet et de susceptibilité soient sensibles et pertinents pour évaluer divers types de stress environnementaux, leur utilisation est limitée par la difficulté à obtenir une image complète de l'état de santé des moules et de leur écosystème [125]. Les variations interindividuelles et l'influence de facteurs non polluants nécessitent l'analyse de nombreux échantillons pour obtenir des résultats significatifs [119, 125]. Cette complexité souligne l'importance de développer et de valider de nouveaux biomarqueurs plus spécifiques et sensibles, capables de fournir des indications précises sur l'impact environnemental et d'améliorer notre capacité à protéger les écosystèmes marins [116, 126].

2.6 Les nouveaux biomarqueurs

Les progrès dans le domaine biomédical, notamment en matière de développement de biomarqueurs sensibles et prédictifs, inspirent l'établissement de nouveaux biomarqueurs en écologie [127-129]. Comparativement aux biomarqueurs traditionnels, l'utilisation de ces nouveaux biomarqueurs dans un contexte multi-omique en écologie peut apporter une perspective enrichie sur l'impact des contaminants sur les moules et leur environnement (**Tableau 2**) [128, 130]. L'intégration d'analyses génomiques, épigénétiques, transcriptomiques, protéomiques, et métabolomiques permet une exploration approfondie des mécanismes moléculaires et de leurs actions spécifiques, conduisant à une détection plus précoce et sensible des effets néfastes liés à l'exposition aux polluants [126, 130, 131].

Tableau 2: Principales différences entre les biomarqueurs traditionnels et les nouveaux biomarqueurs.

	Biomarqueurs traditionnels	Nouveaux biomarqueurs
Type de biomarqueurs	Mesures de bioaccumulation de polluants organiques et inorganiques, des enzymes de détoxication, des niveaux de stress oxydatif, des anomalies morphologiques et des indicateurs de dommages à l'ADN	Profils d'expression génique, modifications épigénétiques, séquences d'ADN, d'ARN, de protéines et/ou de métabolites spécifiques.
Techniques d'analyses	Méthodes biochimiques et physiologiques classiques (ex: spectrophotométrie, tests enzymatiques).	Séquençage de nouvelle génération (NGS), analyses transcriptomiques, protéomiques et/ou métabolomique.
Avantages	• Méthodes standardisées pour leur mesure; • Protocoles et équipements accessibles; • Utilisation plus viable dans des projets avec des budgets limités; • Informations directes sur certains types de stress environnementaux.	• Grande spécificité pour des stress environnementaux et détection possible à des niveaux très bas de contaminants; • Informations sur les effets des polluants, les mécanismes de toxicité et la santé générale de l'organisme; • Potentiel de découverte de nouveaux biomarqueurs de stress environnemental.
Limites	• Spécifiques à un type particulier de polluant; • Détection des effets des polluants qu'à des concentrations relativement élevées; • Influencées par des facteurs abiotiques et biotiques • Ne fournissent pas une image complète des impacts biologiques ou des mécanismes d'action spécifiques.	• Grande quantité de données complexes à analyser; • Équipements spécialisés; • Compétences en bio-informatique; • Limitation de la comparabilité des résultats entre différentes études par la non-standardisation de certaines méthodes.

Par exemple, l'étude du transcriptome, en tant que biomarqueur émergent, permet une analyse approfondie de l'expression génique et d'identifier des voies de signalisation et de processus biologiques affectés par les contaminants [132, 133]. Cette approche contribue à l'identification de gènes exprimés de manière différentielle, facilitant le ciblage de nouveaux biomarqueurs pour l'exposition et la toxicité. Les microARN (miARN), qui sont de courtes séquences d'ARN impliquées dans la régulation génique, constituent un autre exemple de nouveau biomarqueur. Leur modulation en réponse à différents stress environnementaux les identifie comme des indicateurs utiles des effets des contaminants sur les organismes [134, 135].

Par ailleurs, l'analyse de la méthylation de l'ADN constitue une nouvelle méthode d'intérêt. Les modifications dans la méthylation de l'ADN ou des histones, qui influencent l'expression des gènes et les fonctions cellulaires sans modifier la séquence d'ADN, sont considérées comme des indicateurs précoces de stress environnemental [136, 137]. Historiquement, l'étude de la méthylation de l'ADN présentait des défis dus à la complexité des méthodes requises qui impliquaient souvent des traitements chimiques de l'ADN pour détecter ces modifications [138]. Cependant, avec l'émergence et l'amélioration des technologies de séquençage de nouvelle génération (NGS), l'analyse de la méthylation de l'ADN est devenue plus accessible. Le séquençage par NGS peut révéler des motifs de méthylation à travers le génome entier avec une précision au niveau de chaque base [138]. En outre, l'utilisation de la technologie de séquençage Nanopore représente un progrès notable dans les méthodes d'analyse de la méthylation de l'ADN [139]. Cette technologie permet l'observation en temps réel des modifications de méthylation sur les cytosines en position 5' et les adénines, facilitant une détection rapide et efficace des réponses cellulaires aux contaminants [137, 139].

Malgré leur potentiel pour améliorer la spécificité, la sensibilité et la compréhension des mécanismes moléculaires dans les réactions des organismes, l'utilisation de nouveaux biomarqueurs est parfois contrainte par des coûts élevés de séquençage et une complexité dans l'interprétation des données [140, 141]. Ces limitations rendent les biomarqueurs traditionnels plus appropriés pour certains projets, notamment ceux avec des restrictions budgétaires ou des analyses plus ciblées. Le choix entre l'emploi de

biomarqueurs traditionnels ou de nouvelles approches doit être déterminé par les objectifs spécifiques de la recherche, les ressources disponibles et le type d'informations visées. Il est important de noter que le développement et l'amélioration des biomarqueurs constituent un effort en continu [142, 143]. L'intégration de biomarqueurs innovants enrichit notre compréhension des effets des contaminants sur les écosystèmes marins et leurs indicateurs biologiques, ce qui soutient la prise de décisions éclairées pour la préservation des milieux aquatiques. Cette progression vers l'utilisation de nouveaux biomarqueurs facilite une surveillance environnementale plus complète, contribuant efficacement à la gestion et à la protection des écosystèmes marins.

2.7 Défis actuels de l'usage des moules comme bioindicateurs

Bien que les moules soient largement utilisées pour la surveillance environnementale des milieux aquatiques, leur application rencontre plusieurs défis notables. La variabilité génétique et physiologique, tant au sein d'une espèce qu'entre différentes espèces, peut affecter leur réactivité aux contaminants [122]. Cette diversité biologique exige une standardisation des méthodes d'échantillonnage et d'analyse afin de garantir la comparabilité des données obtenues [46]. En outre, malgré la capacité des moules à bioaccumuler des contaminants, l'établissement d'une corrélation directe entre l'exposition aux contaminants et les effets sur leur santé nécessite souvent des études complémentaires [46]. Les facteurs environnementaux abiotiques, tels que la température et le pH, ainsi que les facteurs biotiques, comme la disponibilité des nutriments, peuvent influencer les réponses biologiques des moules, rendant l'interprétation des données de biomarqueurs plus complexe [144]. De plus, la collecte, le transport et l'analyse des échantillons de moules représentent des processus coûteux et logistiquement exigeants, surtout pour les zones reculées ou difficiles d'accès telles que les régions polaires [145]. Enfin, la dépendance aux biomarqueurs traditionnels limite souvent l'identification précise des causes sous-jacentes des modifications observées sans le recours à des analyses supplémentaires [125]. L'adoption de normes uniformes pour la collecte, la conservation et l'analyse des échantillons, notamment pour les nouveaux biomarqueurs, est cruciale pour assurer la fiabilité et la comparabilité des résultats [125, 144]. Pour adresser ces enjeux, les chercheurs s'emploient à développer

de nouvelles méthodes et à affiner les protocoles existants, dans le but d'améliorer la précision et l'efficacité de la surveillance environnementale par l'utilisation des moules.

Transitionnant de l'écologie à la médecine, l'amélioration des techniques de surveillance et de diagnostic est également une priorité dans le domaine médical, où des avancées majeures sont réalisées pour minimiser l'invasivité et maximiser la précision et l'efficacité du diagnostic.

3. La biopsie liquide

La biopsie liquide est une avancée majeure dans le domaine du diagnostic médical, offrant une approche non invasive pour la détection et l'analyse de biomarqueurs tumoraux, ainsi que d'autres données génétiques essentielles à partir de fluides corporels, avec une prédominance pour le sang [146-148]. Cette technique contraste avec les biopsies tissulaires traditionnelles, qui, bien qu'essentielles pour obtenir des informations génétiques et histopathologiques sur les tumeurs, sont plus invasives et ne permettent pas de suivi continu [148, 149]. Les biopsies liquides, en revanche, permettent une évaluation rapide et régulière du stade et de la progression du cancer, favorisant l'ajustement des traitements personnalisés et améliorant ainsi potentiellement les chances de survie des patients. Leur caractère répétable facilite le suivi dynamique de l'évolution de la maladie, représentant une amélioration notable en termes de risque, coût et facilité d’exécution (**Figure 10**) [147-149].

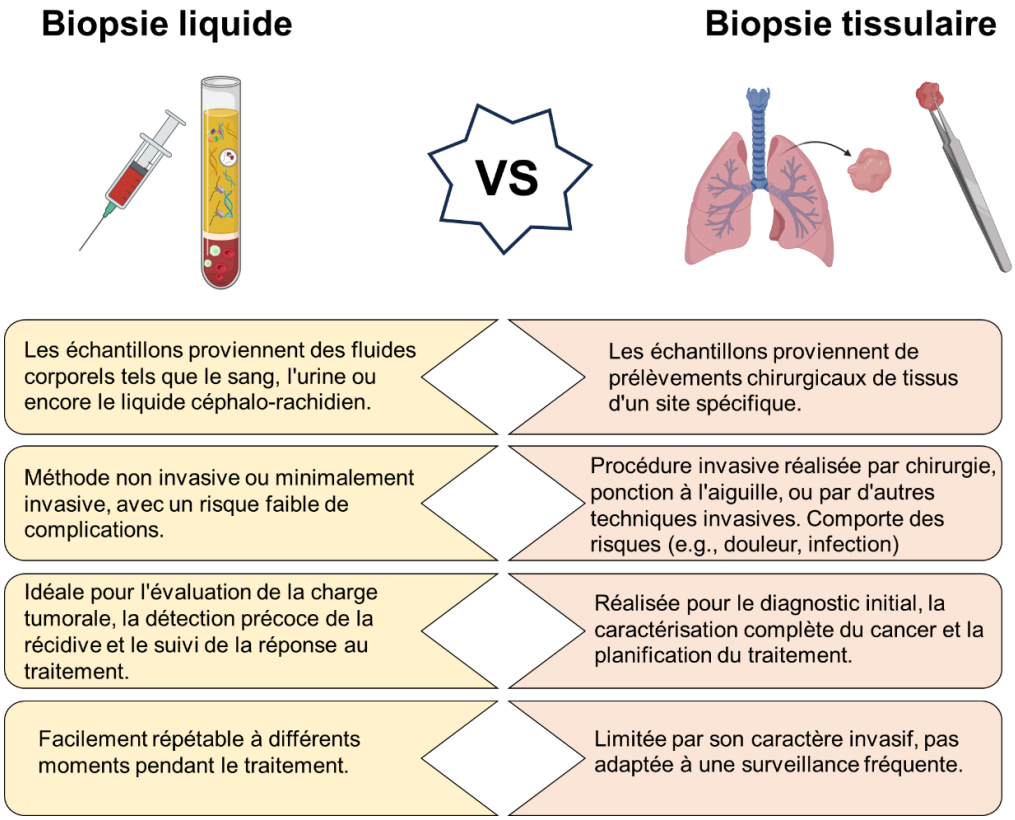

Figure 10. Comparaison entre la biopsie liquide et la biopsie traditionnelle des tissus en oncologie. Adaptée de Adhit *et al.* (2023).

3.1 Émergence et évolution de la biopsie liquide

La biopsie liquide repose sur l'identification de divers composants biologiques présents dans les fluides corporels tels que le sang, l'urine ou le liquide céphalo-rachidien, pour détecter et surveiller des pathologies. Ces composants incluent principalement l'ADN libre circulant (ccfDNA), qui est de l'ADN extracellulaire résultant de la nécrose ou de l'apoptose cellulaire et de la sécrétion de vésicules extracellulaires. Un autre composant essentiel est l'ADN tumoral circulant (ctDNA), de l'ADN spécifique aux tumeurs provenant directement des cellules cancéreuses. D'autres composants, tels que l'ARN circulant, les cellules tumorales circulantes (CTC) et les exosomes, sont également détectés et jouent un rôle clé dans l'évaluation de l'état et de la progression des cancers (**Figure 11**) [146, 148-150].

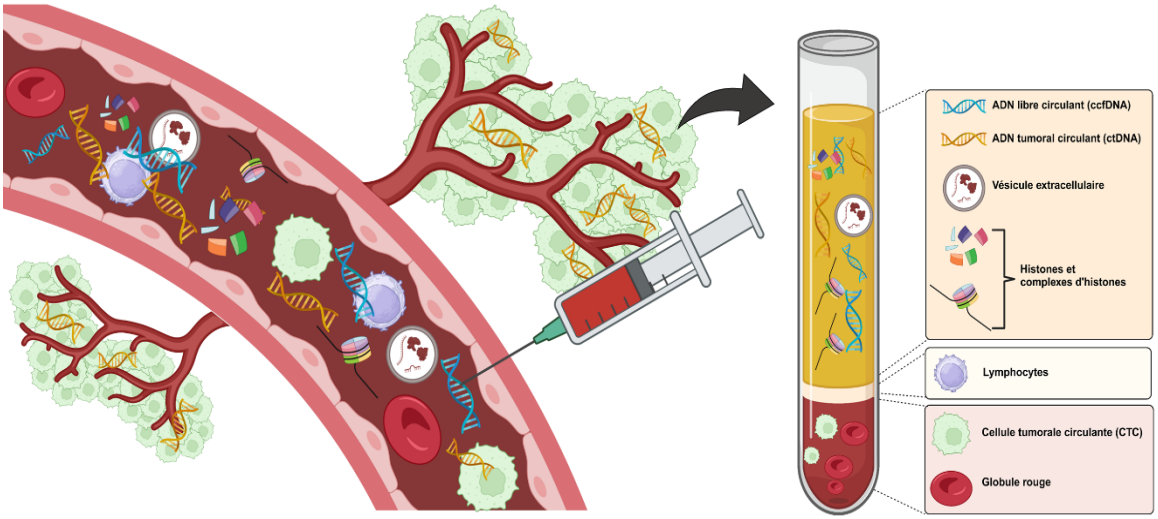

Figure 11. Schéma représentant les principaux composants de la biopsie liquide à partir du sang. La biopsie liquide prélevée à partir du sang périphérique contient différents matériaux associés aux tumeurs tels que les cellules tumorales (CTC), de l'ADN tumoral circulant (ctDNA), des exosomes, ainsi que des histones libres et des complexes d'histones comme biomarqueurs. L'entrée des CTC dans la circulation sanguine se fait via la tumeur primaire et/ou de lésions métastatiques. L'ADN libre circulant (ccfDNA) est relâché dans le sang par les cellules saines. De telles fractions peuvent être isolées et analysées pour les aberrations spécifiques aux tumeurs aux niveaux génomique, transcriptomique, protéomique et métabolomique. Adaptée de Tsoneva *et al.* (2023).

L'intérêt pour le diagnostic à partir de matériel génétique circulant remonte à 1869, lorsque Thomas Ashworth a observé pour la première fois des CTC chez un patient métastatique, suggérant une dissémination du cancer via le flux sanguin [151, 152]. Ce n'est qu'en 1948 que les scientifiques ont commencé à détecter et quantifier l'ADN libre circulant (ccfDNA) dans le sang chez des individus sains et malades [153]. En 1966, l'identification de niveaux élevés de ccfDNA chez des patients atteints de lupus a été rapportée, et dans les années 1980, cet ADN a été détecté chez des patients oncologiques [154, 155]. À cette époque, la distinction entre le ccfDNA provenant de cellules tumorales et celui de cellules saines n'était pas encore possible. En 1994, une avancée majeure a permis de détecter des changements génétiques et mutationnels spécifiques des tumeurs à partir du ccfDNA, établissant ainsi le concept de l'ADN tumoral circulant (ctDNA) [156].

Introduite officiellement en 2010, le concept de "biopsie liquide" a rapidement été adoptée en recherche et pratique clinique, stimulée par des progrès technologiques [157]. Ces avancées ont rendu possible la détection précise du ctDNA et d'autres biomarqueurs dans le sang, ouvrant la voie au dépistage précoce des cancers, à la surveillance thérapeutique, à l'identification de résistances aux traitements et à la gestion des récidives tumorales [148, 158]. De nos jours, la biopsie liquide est également utilisée pour détecter diverses lésions tissulaires et pour réaliser des analyses métagénomiques, incluant l'identification de l'ADN de divers agents pathogènes, enrichissant ainsi considérablement ses capacités diagnostiques [158-162].

3.2 Applications dans le domaine médical

La biopsie liquide représente un progrès significatif dans le diagnostic et la gestion de diverses pathologies infectieuses et oncologiques [158, 163].

Le ccfDNA, principalement d'origine endogène mais également exogène, s'impose comme un biomarqueur essentiel pour le dépistage rapide et non invasif dans plusieurs domaines cliniques, tels que le dépistage prénatal, la gestion des transplantations et la prise en charge oncologique [162].

3.2.1 Applications initiales

La biopsie liquide a marqué un tournant en oncologie en offrant des outils précieux pour la détection précoce du cancer, l'identification précise du stade tumoral et le suivi rigoureux des patients atteints de cancers localisés [157]. Évoluant au-delà de ces applications initiales, cette technique s’est élargie pour inclure la prédiction de la progression métastatique chez les patients à un stade avancé, l'évaluation de l'efficacité des traitements et le suivi de la maladie résiduelle minimale, indiquant la présence d'un cancer persistant après traitement [157, 158, 164].

Le ccfDNA, un des principaux composants analysés lors d'une biopsie liquide, est majoritairement formé de fragments d'environ 166 paires de bases, taille correspondant à celle d'un fragment d'ADN associé à un nucléosome [146, 165]. Chez les patients

cancéreux, une fraction mineure du ccfDNA, le ctDNA, est issue des cellules tumorales et est principalement libéré lors de l'apoptose, avec des fragments plus courts comparativement au ccfDNA non tumoral [146, 162, 165, 166]. L'isolement et l'analyse du ctDNA fournissent des informations cruciales sur l'évolution du cancer, les cibles thérapeutiques potentielles, les mécanismes de résistance aux traitements et facilitent également la détection précoce des cancers (**Figure 12**) [148, 157, 163, 164]. Ces processus sont renforcés par des technologies avancées, telles que la PCR digitale en gouttelettes (ddPCR) et la technologie NGS, qui améliorent notre capacité à détecter et caractériser les mutations dans le ctDNA [146]. Cependant, la faible concentration de ctDNA chez les individus asymptomatiques et la présence de variations génétiques dans les tissus normaux posent des défis significatifs pour l'interprétation des résultats. [163, 167].

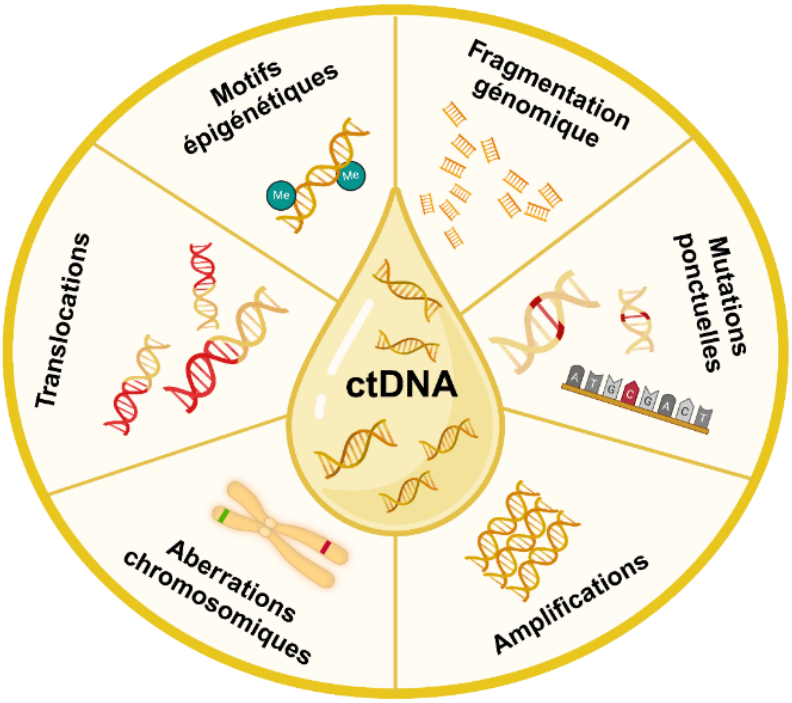

Figure 12. Isolation et exemples d'analyse de l'ADN tumoral circulant (ctDNA) à partir de la biopsie liquide. Cette figure illustre l'isolation du ctDNA, localisé dans le plasma à partir d'un unique échantillon sanguin. La technique fragmentomique du ccfDNA analyse la distribution de la taille des fragments pour distinguer spécifiquement le ctDNA du reste du ccfDNA. La détection et la quantification du ctDNA repose sur diverses méthodes génomiques visant à identifier des anomalies génétiques telles que des mutations ponctuelles et des réarrangements génétiques, tandis que les motifs épigénétiques sont quantifiés via le séquençage. Adaptée de Alix-Panabières et Pantel (2021).

comparativement aux individus sains, servent également d'indicateurs utiles de la charge tumorale [166]. Cependant, l'interprétation des niveaux de ccfDNA peut être complexifiée par des variables biologiques telles que l'élimination partielle du ccfDNA via l'urine ou les effets de l'état de santé général du patient, qui peut fluctuer en raison de l'exercice ou d'infections bactériennes ou virales [167, 168]. De plus, les étapes pré-analytiques, telles que le prélèvement et la manipulation des échantillons, peuvent introduire des altérations chimiques et contaminer les échantillons avec de l'ADN génomique provenant des leucocytes, affectant ainsi l'intégrité du ccfDNA [167, 169, 170].

Les analyses de méthylation du ccfDNA et du ctDNA ouvrent de nouvelles perspectives pour le dépistage précoce du cancer, en offrant une haute sensibilité et spécificité [163, 167]. Néanmoins, l'usage du bisulfite dans l'analyse de la méthylation du ccfDNA introduit certains biais, incluant des déséquilibres en GC, des dommages à l'ADN, des biais d'amplification par PCR ou encore des artefacts d'alignement [171]. L'émergence du séquençage natif de l'ADN par la plateforme Oxford Nanopore Technologies (ONT) permet des résultats de méthylation de résolution comparable au séquençage bisulfite sans les contraintes de dégradation ou de perte de matériel [171]. La plateforme ONT se distingue également par son coût initial modéré, sa portabilité et sa capacité de séquençage en temps réel, simplifiant le traitement des échantillons et éliminant le besoin d'une amplification complexe par PCR [172]. Bien que l'analyse de la méthylation du ccfDNA offre une nouvelle voie prometteuse pour la détection précoce du cancer, elle présente certains défis. Parmi ceux-ci, la faible incidence de certaines pathologies et les risques liés aux procédures diagnostiques, en particulier pour les gliomes, représentent des obstacles notables [165, 167]. Par ailleurs, les analyses de méthylation génomique ne fournissent pas d'informations sur la localisation précise de la tumeur et les marqueurs épigénétiques tendent à être moins stables à travers les divisions cellulaires [167]. Ces considérations ajoutent une complexité à l'adoption du dépistage précoce basé sur la méthylation.

En plus des défis liés à l'analyse des biomarqueurs, la bancarisation et l'archivage des échantillons biologiques à long terme deviennent cruciaux, notamment pour garantir

l'intégrité du matériel génétique sur de longues périodes. Inspirées par les techniques forensiques, les cartes FTA® (Whatman FTA) jouent un rôle essentiel dans cette conservation [173-176]. Ces cartes, conçues avec une matrice de cellulose imprégnée de réactifs chimiques, permettent la lyse des cellules et la stabilisation des acides aminés et des nucléotides à température ambiante sur de longues périodes [176]. Elles simplifient la collecte, le stockage, et l'analyse des biomarqueurs tumoraux, facilitant ainsi l'acquisition de données essentielles [174].

Malgré ces avancées, des défis persistent dans l'application du ctDNA pour le dépistage précoce du cancer, principalement en raison de sa sensibilité limitée face à la diversité des aberrations génomiques des tumeurs solides [163]. Sans une connaissance précise de la composition génétique de la tumeur, les tests de ctDNA doivent cibler un large éventail d'aberrations génomiques courantes dans les cancers, nécessitant des méthodes extrêmement sensibles pour détecter de faibles quantités de ctDNA dans le sang. Actuellement, des tests multianalytes, y compris ceux basés sur la méthylation du ctDNA, sont en développement pour adresser cette sensibilité et permettre une détection précoce de divers types de cancer [163, 177].

Au-delà du ctDNA, les biomarqueurs tels que les CTC, les vésicules extracellulaires, les microARN et les protéines sont aussi comme des éléments clés pour enrichir l'analyse de la biopsie liquide (**Figure 13**) [148, 178, 179]. Les CTC permettent une analyse directe des cellules cancéreuses, fournissant des informations sur la biologie tumorale et la résistance aux traitements, et ont prouvé leur importance dans le diagnostic précoce de divers cancers [158, 163]. Les vésicules extracellulaires, incluant les exosomes, se composent de bicouches lipidiques renfermant protéines, ARN, et ADN issus de cellules saines ou malignes, offrant un miroir fidèle de l'état physiologique ou pathologique [158]. Des microARN spécifiques, présents dans les fluides corporels, ont été reliés aux processus de diagnostic, de pronostic et de suivi de l'efficacité thérapeutique dans le contexte oncologique [180]. En parallèle, l'analyse des protéines circulantes, y compris des antigènes spécifiques au cancer, des métabolites et des plaquettes influencées par les tumeurs permettraient aussi de caractériser le microenvironnement tumoral [158].

L'intégration des données issues des CTC, ctDNA, vésicules extracellulaires, microARN, protéines et autres composés présents dans les biofluides offre plusieurs avantages et promet une représentation moléculaire en temps réel et plus complète de l'hétérogénéité tumorale [181, 182]. Néanmoins, une standardisation rigoureuse et une validation des méthodes analytiques sont essentielles avant l'intégration de ces approches émergentes dans la pratique clinique courante pour le dépistage précoce du cancer [158, 182].

Ces différentes applications illustrent la polyvalence croissante de la biopsie liquide, ouvrant la porte à des utilisations étendues au-delà de l'oncologie.

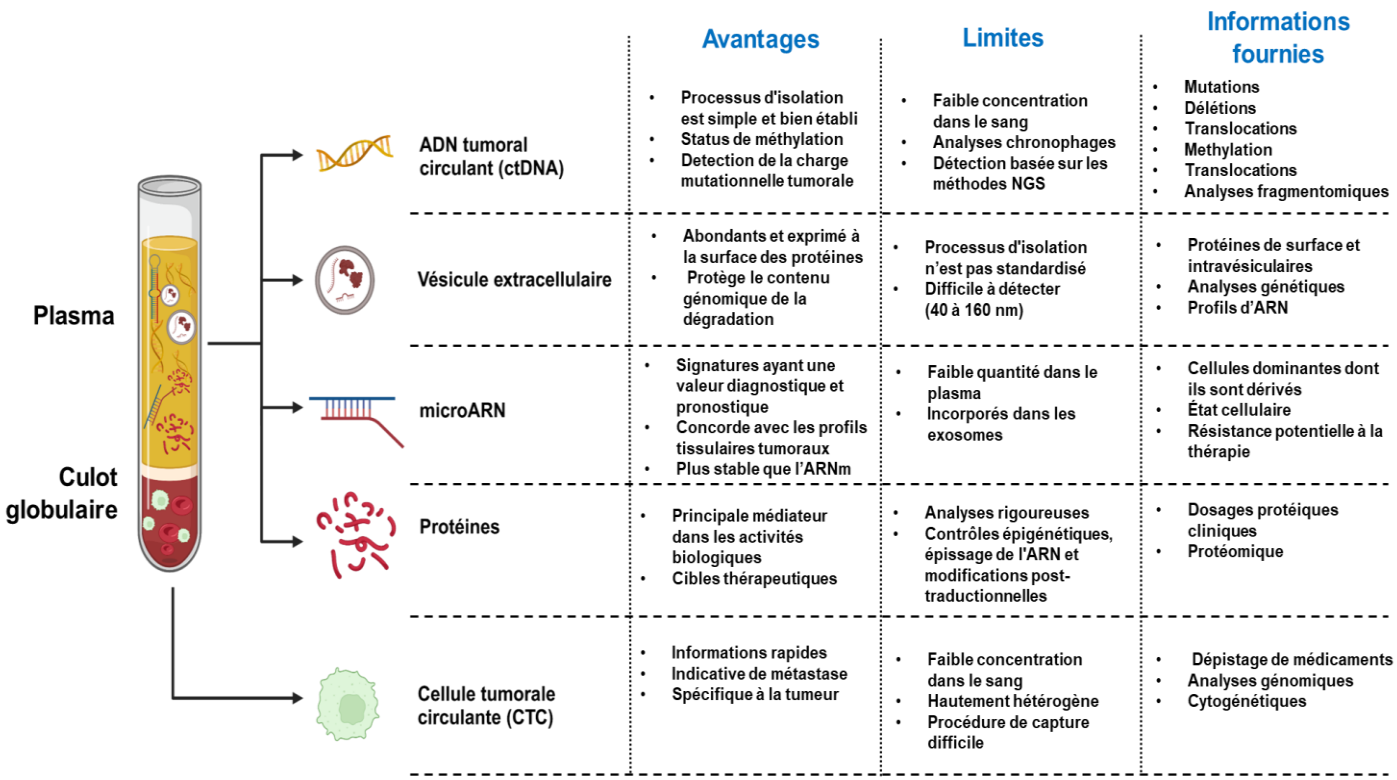

Figure 13. Exemples de composants circulants isolés via biopsie liquide et leurs implications en contexte clinique. Illustration de différents analytes sanguins récupérés par biopsie liquide. Chaque analyte présente des avantages spécifiques, ainsi que des limitations dans son application au diagnostic, au suivi et à la gestion thérapeutique des maladies tumorales. Adapté de Armakolas *et al.* (2023).

3.2.2 Applications focussées sur l'ADN du non-soi

Le ccfDNA représente une source précieuse d'informations sur la physiologie cellulaire et les désordres tissulaires, permettant le diagnostic et la surveillance en continu. Outre son origine endogène (ADN du soi), le ccfDNA peut également être dérivé de sources exogènes (ADN du non-soi) comme l'ADN de tissus fœtaux, microbien, viral, ainsi que de cellules souches transplantées et de greffes d'organes solides (**Figure 14**) [159, 183, 184].

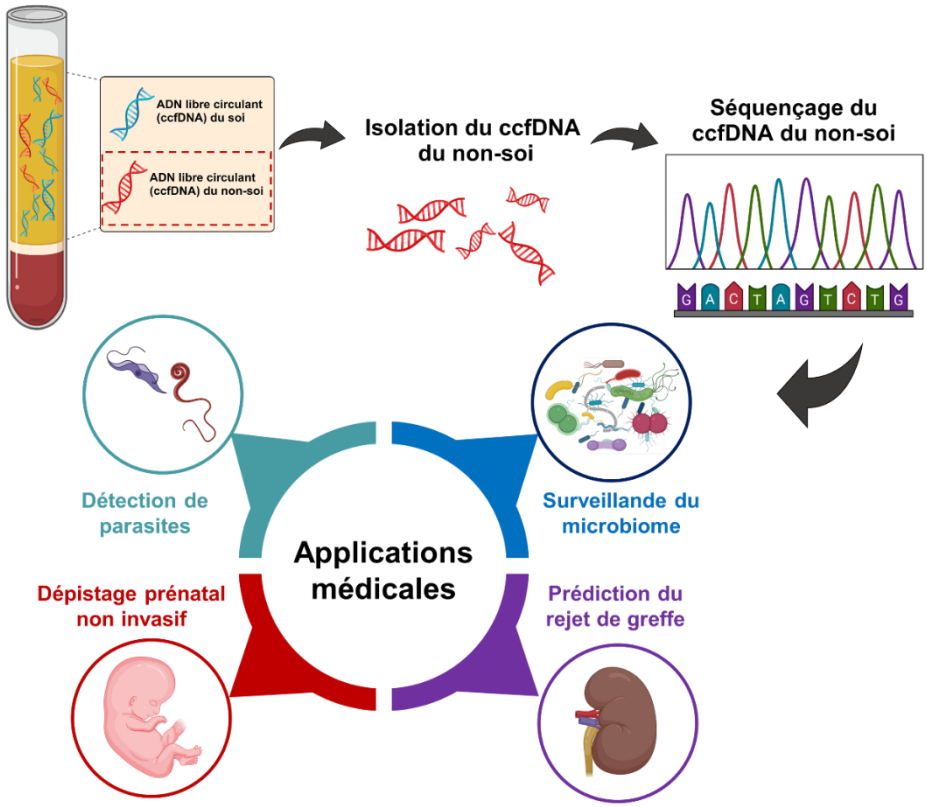

Figure 14. Exemples d'applications médicales de l'ADN du non-soi détecté dans le ccfDNA plasmatique. L'ADN du non-soi incluant l'ADN fœtal, microbien, viral ou issu de transplantations d'organes solides, peut être extrait du plasma et analysé par séquençage de nouvelle génération (NGS). Cette approche offre des avantages significatifs pour la détection précoce de diverses pathologies et infections, la surveillance des complications post-transplantation, l'amélioration du dépistage prénatal non invasif ou encore l'ajustement des stratégies thérapeutiques.

En obstétrique, le dépistage prénatal non invasif (DPNI) via l'analyse de ccfDNA dans le plasma maternel est devenu de plus en plus une pratique standard pour identifier les anomalies chromosomiques fœtales chez des personnes à risque, s'étendant des trisomies communes aux aneuploïdies des chromosomes sexuels et aux microdélétions [185]. L'évolution vers l'analyse génomique complète a élargi la détection aux trisomies rares et aux variations du nombre de copies (CNV), malgré des défis persistants dans l'identification de CNV de petite taille. Cependant, l'interprétation des résultats du DPNI doit tenir compte des limitations biologiques, comme la provenance principalement placentaire du ccfDNA maternel, qui peut ne pas refléter fidèlement le génome fœtal. Les tests de ccfDNA nécessitent donc des confirmations diagnostiques pour un diagnostic définitif [185, 186]. La fiabilité variable de la détection de certaines conditions l'importance des tests diagnostiques complémentaires. L'émergence du séquençage à molécule unique et de l'analyse de la méthylation de l'ADN sans conversion offrent un potentiel d'amélioration dans la détection précoce des anomalies et dans d'autres domaines comme l'oncologie [187].

Dans le domaine des transplantations d'organes solides, l'ADN circulant dérivé du donneur (dd-ccfDNA) se révèle aussi être un biomarqueur non invasif prometteur pour la détection précoce des dommages d'allogreffe [162]. Les limites de l'histopathologie, notamment sa variabilité et sa faible sensibilité, soulignent l'importance d'approches plus précises et quantitatives comme la biopsie liquide. Cette dernière offre une méthode non invasive pour surveiller l'état de l'allogreffe et adapter le traitement de manière proactive, avec des études indiquant une normalisation post-transplantation des niveaux de ccfDNA [162]. Les techniques actuelles, incluant la PCR multiplexe et le séquençage par NGS, ciblent des polymorphismes mononucléotidiques (SNP) pour détecter efficacement le dd-ccfDNA sans nécessiter les génotypes du donneur ou du receveur [188]. Le séquençage aléatoire *shotgun* permet également la détection des infections post-transplantation, soulignant la prévalence des pathogènes viraux, bactériens et fongiques [162]. La validation clinique de ces méthodes reste cruciale pour leur adoption en pratique clinique.

D’autre part, la vision traditionnelle des fluides biologiques humains comme étant des environnements stériles a été révisée avec l'identification du ccfDNA d'origine microbienne (mcfDNA) dans la circulation sanguine [159, 189-191]. Deux mécanismes principaux contribuent à sa présence : la translocation microbienne, où bactéries et virus franchissent les barrières épithéliales, et l'invasion opportuniste de la circulation sanguine par des pathogènes à la suite de dommages physiques ou infectieux, entraînant des bactériémies ou virémies [159, 192-194]. L'identification de ces fragments microbiens par séquençage offre un moyen avancé de diagnostiquer les infections. L'importance du mcfDNA comme outil de diagnostic précoce pour des conditions telles que les infections fongiques, la tuberculose et la septicémie est désormais reconnue, jouant un rôle essentiel dans le suivi et le traitement des infections [159, 195-197]. Bien que constituant une minorité de l'ADN total dans le plasma (~1%), la détection de ces fragments infimes est essentielle pour un diagnostic précis et fiable des infections [198]. Le processus complet, de la préparation de l'échantillon au laboratoire jusqu'aux résultats, peut être achevé rapidement (2-3 jours), fournissant des données cliniquement pertinentes pour le traitement efficace des patients [184]. L’analyse du mcfDNA par séquençage montre une sensibilité et une spécificité élevées pour l'identification des agents pathogènes, surpassant la culture et d'autres méthodes microbiologiques conventionnelles [159, 184].

Cependant, l'intégration du séquençage métagénomique du mcfDNA dans les laboratoires de microbiologie clinique est limitée par des coûts élevés d'équipement et de réactifs, ainsi que par la complexité du traitement analytique [199]. Les étapes pré-analytiques, la prévention de la contamination et les compétences spécialisées requises représentent des défis supplémentaires [159]. De plus, la capacité de cette méthode à détecter les pathogènes viraux à ARN reste limitée, demandant des approches diagnostiques alternatives pour certaines infections virales suspectées [184]. Malgré ces obstacles, l'analyse du mcfDNA a le potentiel de transformer le diagnostic des maladies infectieuses, offrant un diagnostic plus rapide et plus précis que les méthodes conventionnelles et facilitant une gestion clinique plus efficace [184]. La combinaison du mcfDNA avec des techniques diagnostiques traditionnelles peut augmenter significativement le rendement diagnostique, surtout pour les infections critiques comme la pneumonie aiguë sévère et la septicémie [195, 197, 200]. Des recherches

supplémentaires sont nécessaires pour optimiser son utilisation clinique, définir le meilleur intégration dans les protocoles diagnostiques existants, et évaluer son application aux côtés d'autres méthodes de diagnostic des maladies infectieuses.

L'utilisation du ccfDNA du non-soi dans le diagnostic clinique, en analysant ses origines et les marqueurs épigénétiques, par exemple, ouvre des voies innovantes pour la surveillance post-transplantation, le dépistage prénatal et le diagnostic des infections microbiennes [159, 162, 184, 187]. L'utilisation de la biopsie liquide se positionne à l'avant-garde des innovations susceptibles de transformer le suivi de la santé, en facilitant la détection précoce des maladies et en optimisant l'efficacité des traitements. Pour intégrer pleinement ces progrès dans la pratique clinique, la poursuite de la recherche et une validation clinique approfondie sont essentielles, afin de surmonter les défis techniques et biologiques.

3.2.3 L'intégration d'approches multi-omiques

L'analyse multi-omique des biomarqueurs circulants, incluant le ccfDNA, mais aussi le transcriptome circulant ou encore les profils épigénétiques, propose une approche intégrée robuste [201, 202]. Elle marque une nouvelle ère dans le concept de biopsie liquide qui peut désormais se définir comme l'ensemble des composantes d'un fluide, comme le sang. Les données génomiques, épigénomiques, transcriptomiques, protéomiques, glycomiques ou encore métabolomiques offrent des perspectives uniques pour la détection, le suivi et le traitement des désordres physiologiques et pathologiques (**Figure 15**) [201, 203].

La génomique explore les variations génétiques, y compris les mutations ponctuelles, les variations du nombre de copies et les réarrangements chromosomiques présents dans le ctDNA [163, 204]. L'analyse génomique du ccfDNA permet de mieux comprendre les mécanismes de développement de diverses maladies, notamment le cancer, le diabète, et les maladies cardiovasculaires [205-207]. Cette discipline ouvre la voie à des stratégies innovantes en matière de diagnostic, de traitement, et de prévention. Par ailleurs, les altérations somatiques générant des modifications protéiques, en corrélation avec les

mutations du ccfDNA, peuvent améliorer la précision diagnostique pour certaines formes de cancer, offrant ainsi des perspectives prometteuses pour la médecine personnalisée [201]. L'épigénétique examine les changements réversibles dans l'expression des gènes qui surviennent sans modifications de la séquence d'ADN elle-même, offrant des

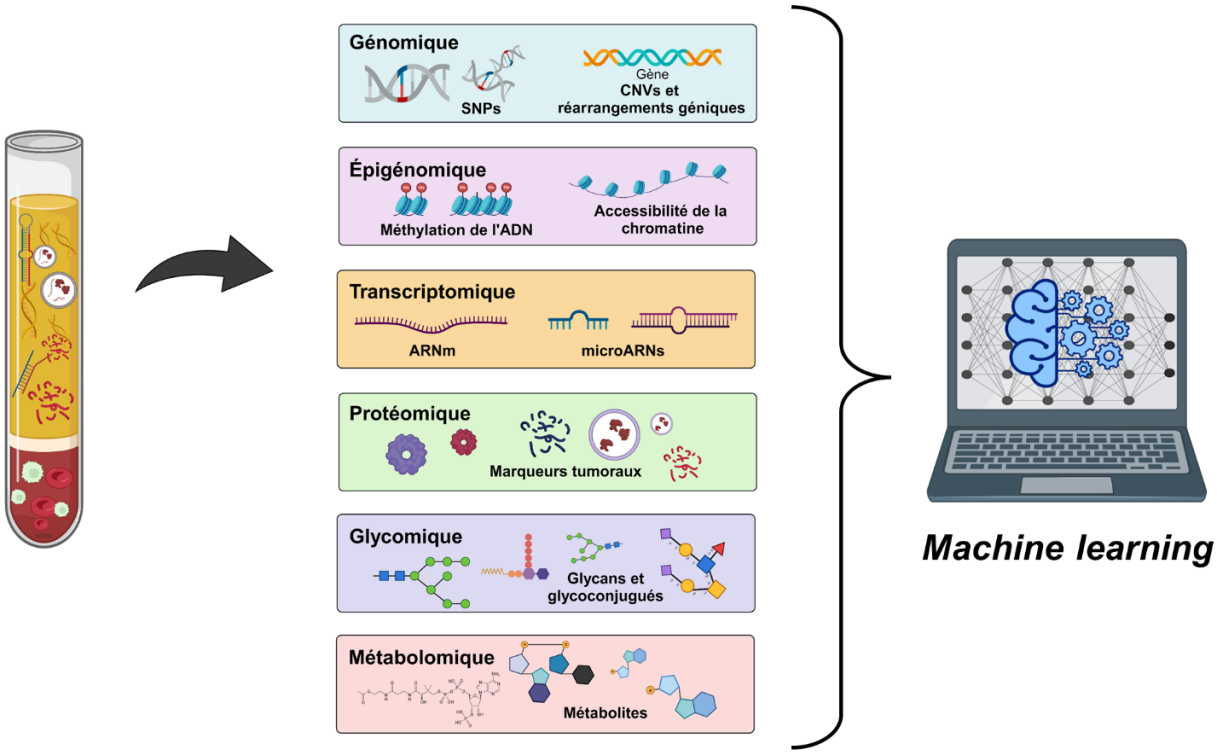

Figure 15. Intégration d'une approche multi-omique dans la biopsie liquide pour une analyse complète. Cette stratégie combine l'analyse d'une variété d'analytes, provenant de divers fluides biologiques tels que le sang, et intègre des données génomiques, épigénomiques, transcriptomiques, protéomiques, glycomiques ou encore métabolomiques, enrichissant la compréhension des états physiologiques et pathologiques. Cette compilation d'informations peut ensuite venir enrichir et entraîner les modèles de l'intelligence artificielle afin d'identifier des motifs complexes, facilitant la détection précoce, le suivi et la personnalisation des interventions thérapeutiques. Adaptée de Di Sario *et al.* (2023).

perspectives cruciales pour le diagnostic et le traitement personnalisés des maladies [201, 208]. Parmi les modifications épigénétiques, la méthylation de l'ADN et les modifications des histones, peuvent moduler l'expression génique et être associés à diverses pathologies [207-209].

Des altérations dans les motifs de méthylation du ccfDNA, qui se manifestent fréquemment aux premières phases de la tumorigenèse – notamment au niveau des îlots CpG des gènes suppresseurs de tumeurs – jouent un rôle clé dans l'initiation et la progression de divers cancers [209, 210]. Il a également été observé que des altérations épigénétiques spécifiques sur le ccfDNA long permettent de distinguer plus aisément le ccfDNA d'origine fœtale de celui d'origine maternelle [187]. L'exploitation de ces signatures épigénétiques permet d'élucider les processus pathologiques et de développer des outils de diagnostic plus précis et plus personnalisés [209].

La transcriptomique permet d'explorer l'ARN circulant, fournissant des informations précieuses sur les niveaux d'expression génique et les processus moléculaires en cours de différents tissus [211]. Cette approche est essentielle pour identifier les gènes actifs ou réprimés dans le ccfDNA et pour mieux comprendre leur rôle dans le développement et la progression de certaines pathologies [208, 211]. De plus, les changements notables observés dans les ARNm et dans les ARN non codants, tels que les miARN, les ARN long non-codant (lncARN) et les ARN circulaire (circARN), enrichit notre compréhension de la manière dont l'expression génique est régulée épigénétiquement [201, 211]. Les lncARN, en particulier, jouent un rôle important dans la modulation de l'expression et de la stabilité des miARN et des ARNm, offrant ainsi des perspectives nouvelles pour la recherche sur les mécanismes de régulation génétique et leur impact sur la pathogenèse des maladies [201, 208].

La glycomique consiste à étudier la structure et la fonction des glycanes, des glycolipides et des glycoprotéines comme les protéoglycanes [212, 213]. Les glycanes et les glycoconjugués jouent des rôles essentiels dans de nombreux processus biologiques, tels que la communication cellulaire, la reconnaissance immunitaire, le repliement des protéines et la modulation de la fonction des protéines [214, 215]. Leur structure et leur

composition peuvent varier considérablement, et leurs altérations ont été associées à de nombreuses maladies, notamment le cancer, les maladies auto-immunes et les maladies infectieuses [201, 213]. En outre, la glycomique englobe également l'étude des gènes responsables de la synthèse des glycanes, tels que les glycosyltransférases, offrant ainsi une compréhension plus complète des mécanismes moléculaires régissant ces structures complexes et leur impact sur la santé et la maladie [216].

La métabolomique se concentre sur l'analyse des petits métabolites moléculaires (de moins de 1,5 kDa) présents dans divers fluides corporels [217, 218]. Ces métabolites peuvent changer de manière dynamique en réponse à des conditions pathologiques telles que les maladies hépatiques ou les cancers gastro-intestinaux [201, 217, 219]. La présence d'une tumeur, par exemple, peut induire des modifications globales dans le métabolisme de l'organisme, en ajustant l'utilisation de certaines sources d'énergie pour satisfaire les besoins accrus de la tumeur [218]. Le métabolome permet une compréhension plus approfondie des perturbations métaboliques associées aux pathologies.

En résumé, l'adoption d'approches multi-omiques promet une détection plus précise et sensible, particulièrement aux stades précoces de maladies spécifiques. Ces méthodes pourraient grandement améliorer notre capacité à diagnostiquer et à suivre l'évolution des pathologies, marquant un progrès notable dans les diagnostics cliniques [201, 202, 217]. De surcroît, l'intégration de données multi-omiques via des techniques d'apprentissage automatique (e.i. *machine learning*) est en train de révolutionner la biopsie liquide, améliorant la précision et la robustesse des diagnostics grâce à des méthodes telles que l'apprentissage par ensemble, qui consolident les résultats de multiples modèles pour optimiser les diagnostics cliniques [202, 203].

Cette expansion des capacités de la biopsie liquide, initialement conçue pour les applications humaines, trouve également des utilisations prometteuses dans le domaine vétérinaire.

3.2.4 Applications autres que chez l'humain

Au-delà de son application chez l'humain, l'étude du ccfDNA s'étend depuis peu sur diverses espèces animales [220-222]. Bien que la recherche sur le ccfDNA chez les animaux ne soit pas aussi avancée que celle réalisée chez les humains, l'intérêt pour son potentiel en tant que biomarqueur et son utilité pour l'exploration de la physiopathologie dans le règne animal, particulièrement chez les animaux domestiques dont le chien, est en hausse [220]. Le ccfDNA commence d'ailleurs à être reconnu comme un indicateur pertinent en médecine vétérinaire pour le suivi de la réaction aux traitements et de l'évolution des pathologies cancéreuses chez les animaux souffrant de tumeurs [223, 224]. L'application du ccfDNA en médecine vétérinaire s'est même étendue notamment pour le dépistage prénatal non invasif en utilisant le ccfDNA provenant du fœtus animal [225]. Cependant, l'utilisation de cette méthode nécessite une optimisation et une validation supplémentaires. Elle requiert la détermination précise de l'âge gestationnel optimal pour la collecte efficace de l'ADN circulant, l'identification des méthodes adéquates de prélèvement et de stockage des échantillons, ainsi que le choix du type d'échantillon (par exemple, sang entier, plasma ou sérum) et des techniques d'isolement et d'analyse pour une quantification précise de l'ADN circulant libre [221, 225]. Néanmoins, ces défis ne compromettent pas la viabilité de l'application routinière du dépistage prénatal non invasif chez les animaux [225]. L'intégration méthodique des progrès technologiques pourrait améliorer la sensibilité et la précision des tests au fil du temps. L'adoption du dépistage prénatal non invasif chez les animaux a le potentiel d'améliorer significativement la gestion des programmes d'élevage, tant domestiques que sauvages. Par ailleurs, l'intérêt pour l'étude du microbiome sanguin s'est accru en médecine vétérinaire [226]. La composition des communautés bactériennes varie avec l'âge et l'environnement de l'animal. L'analyse du mcfDNA chez les animaux domestiques ou d'élevage, tels que chiens, chats, bovins ou poulets, offre un moyen rapide et précis de détecter les dysbioses et les infections pathogènes [226-230]. Les modifications du microbiome sanguin peuvent favoriser l'apparition de maladies [227, 231]. Les progrès en métagénomique permettent de décrire des écosystèmes dynamiques qui peuvent être altérés par des maladies, perturbant l'équilibre entre l'hôte et son microbiote. Une compréhension approfondie des variations dans les communautés microbiennes pourrait

conduire à une surveillance plus efficace et rapide des animaux d'élevage, ayant un impact notable non seulement sur leur bien-être, mais aussi sur des considérations socio-économiques [232].

3.2.5 Nécessité de développer la biopsie liquide en écologie marine

Alors que la biopsie liquide se développe rapidement dans le domaine de la médecine humain et vétérinaire [224], il devient évident que cette technologie pourrait apporter des bénéfices significatifs en écologie marine. Cependant, l'application de cette technique aux organismes aquatiques, tels que les poissons et les bivalves, demeure largement inexplorée, soulignant la nécessité d'adapter et de développer des méthodes spécifiques pour dans ce domaine. L'écologie marine présente des défis uniques qui nécessitent des ajustements techniques particuliers. Les organismes aquatiques évoluent dans des environnements extrêmement divers, complexifiant l'application directe des techniques de biopsie liquide conçues initialement pour les mammifères terrestres. De plus, les interactions complexes entre les organismes marins et leur environnement, soumis à des conditions variables, ajoutent un niveau supplémentaire de complexité à l'interprétation des résultats obtenus par ces méthodes.

Il est essentiel de développer des protocoles spécifiques pour la collecte, le traitement et l'analyse du ccfDNA et du mcfDNA chez les espèces marines. Cela inclut l'optimisation des méthodes de prélèvement d'échantillons tels que l'hémolymphe, le sang ou le mucus, ainsi que l'adaptation des techniques d’extraction et de séquençage aux particularités de ces échantillons. Certaines études ont démontré la faisabilité d’étudier le mcfDNA chez moule à partir de l’hémolymphe prélevée dans le muscle adducteur [233-235]. La collecte et l’analyse du ccfDNA et du mcfDNA chez les poissons et les moules, à partir du sang et de l’hémolymphe respectivement, permettraient de développer des biomarqueurs de stress environnemental et de santé, offrant une approche non invasive pour évaluer l'état des populations dans des environnements variés.

4. Problématique du projet de recherche

Les changements climatiques représentent un défi majeur pour les écosystèmes marins, notamment dans les régions polaires. Ces zones, extrêmement sensibles aux variations environnementales, subissent des impacts profonds qui menacent leur intégrité et leur biodiversité. Il existe un besoin crucial de développer des biomarqueurs sensibles et prédictifs pour évaluer avec précision ces impacts sur ces écosystèmes fragiles. Les bivalves, en raison de leur large répartition, leur capacité de filtration et de bioaccumulation, se révèlent être des bioindicateurs pertinents pour la surveillance des milieux aquatiques. Néanmoins, les méthodes traditionnelles de surveillance font face à des défis logistiques considérables, notamment les difficultés d'échantillonnage dans des régions isolées et les coûts élevés associés au maintien de conditions de conservation adéquates, comme la chaîne de froid.

Dans ce contexte, l'application de la biopsie liquide, traditionnellement utilisée en médecine, est une stratégie potentiellement prometteuse pour surmonter ces obstacles, permettant le développement de biomarqueurs sensibles et prédictifs. Cette méthode non invasive permet l'analyse rapide de l'ADN circulant libre (ccfDNA) qui inclut à la fois l'ADN de l'hôte et celui provenant d'autres organismes présents dans l'écosystème. Chez les moules, l'ADN du soi, libéré dans l'hémolymphe, offrirait un aperçu des réponses génomiques aux stress environnementaux ou anthropiques. Parallèlement, l'ADN du non-soi, acquis par filtration, révèlerait des informations sur les éléments biotiques externes affectant l'organisme. Ce projet propose d'adapter la biopsie liquide pour les organismes marins, particulièrement dans les écosystèmes polaires où l'adaptabilité est limitée et où le réchauffement climatique pourrait accélérer la prolifération de pathogènes. Cette approche pourrait améliorer la caractérisation de la diversité pathogénique et la détection des variations épigénétiques, offrant ainsi de nouvelles perspectives sur la santé des écosystèmes marins. Les échantillons génétiques prélevés peuvent être conservés sur des cartes FTA, facilitant l'utilisation de technologies avancées de séquençage telles que le *shotgun sequencing* et le séquençage Nanopore. Cette méthode améliore également la gestion des défis logistiques associés à la conservation, au transport, et au stockage des échantillons sur le terrain. L'approche multi-omique, intégrant des analyses du microbiome bactérien, du virome, du transcriptome, du

glycome et du méthylome, viendrait enrichir notre compréhension des variations spatio-temporelles des composants biologiques, renforçant notre capacité à évaluer et surveiller la santé des écosystèmes côtiers. L'intégration de ces technologies dans les études écologiques promet pourrait potentiellement permettre une surveillance plus précise et prédictive, essentielle pour la préservation des milieux marins face aux pressions environnementales et anthropiques. La biopsie liquide ouvre ainsi la voie au développement de nouveaux biomarqueurs en écologie marine et à la mise en place de programmes de surveillance à long terme, notamment face au changement climatique et à l'élévation des températures océaniques.

5. Hypothèse et objectifs du projet de thèse

Hypothèse : L'hypothèse du projet de recherche propose que l'application du concept de biopsies liquides chez espèce sentinelle comme la moule puisse être utilisée pour établir des biomarqueurs sensibles et prédictifs permettant d'évaluer la santé des écosystèmes marins côtiers, d'anticiper les impacts des changements climatiques sur ces milieux et leurs organismes, ainsi que de surveiller l'évolution de la biodiversité marine.

But de l'étude : L'objectif général du projet est d'appliquer le concept de la biopsie liquide sur des espèces marines afin d'évaluer l'état de santé des écosystèmes marins.

Objectifs de l'étude :

1. Appliquer le concept de biopsie liquide pour analyser le microbiome bactérien circulant chez différentes espèces marines.
2. Caractériser le ccfDNA hémolymphatique de la moule.
3. Intégrer les approches multi-omiques au concept de la biopsie liquide.

Ce projet permettra, à long terme, de mettre en place des outils rapides et efficaces afin de mesurer l'impact du changement climatique sur les écosystèmes marins polaires et côtiers.

Chapitre 2

ADN bactérien circulant spécifique aux espèces et aux sites chez les moules sentinelles subantarctiques *Aulacomya atra* et *Mytilus platensis*

Article publié: *Scientific Reports* 2022, 12(1):9547

Résumé

Les impacts des changements climatiques sont particulièrement sévères dans les régions polaires où l'augmentation des températures et la réduction de la couverture de glace marine menacent l'intégrité écologique des écosystèmes côtiers marins. En raison de leur large distribution et de leur importance écologique, les moules sont actuellement utilisées comme organismes sentinelles dans les programmes de surveillance des écosystèmes côtiers à travers le monde. Dans cette étude, nous avons exploité le concept de biopsie liquide combiné à une méthode d'échantillonnage logistiquement pratique pour étudier le microbiome bactérien hémolymphatique chez deux espèces de moules (*Aulacomya atra* et *Mytilus platensis*) dans les îles de Kerguelen, un archipel volcanique subantarctique isolé. Nous avons découvert que les signatures du microbiome circulant des deux espèces diffèrent significativement bien qu'elles partagent les mêmes moulières. Nous avons également constaté que le microbiome diffère significativement entre les sites d'échantillonnage, souvent en corrélation avec les particularités de l'écosystème. Les modèles prédictifs ont également révélé que les deux espèces possèdent des microbiomes fonctionnels distincts et que le microbiome circulant d'*Aulacomya atra* était plus sensible aux changements induits par un stress thermique aigu que celui de *Mytilus platensis*. Dans l'ensemble, notre étude suggère que la définition du microbiome circulant est un outil utile pour évaluer l'état de santé des écosystèmes marins et pour mieux comprendre les interactions entre les espèces sentinelles et leur habitat,

Contribution des auteurs

Yves St-Pierre, France Caza, Stéphane Betoulle et moi avons conçu l'étude. France et moi avons mené toutes les expériences et j'ai également effectué toutes les analyses bio-informatiques et statistiques de cet article. Tous les auteurs ont pris part à l'interprétation des données et à leur évaluation critique. Le manuscrit a été rédigé par France, Yves et moi, bénéficiant des contributions et de l'approbation de tous les auteurs à chaque étape du processus.

scientific reports

OPEN

Species- and site-specific circulating bacterial DNA in Subantarctic sentinel mussels *Aulacomya atra* and *Mytilus platensis*

Sophia Ferchiou[1], France Caza[1], Richard Villemur[1], Stéphane Betoulle[2] & Yves St-Pierre[1]✉

Impacts of climate changes are particularly severe in polar regions where warmer temperatures and reductions in sea-ice covers threaten the ecological integrity of marine coastal ecosystems. Because of their wide distribution and their ecological importance, mussels are currently used as sentinel organisms in monitoring programs of coastal ecosystems around the world. In the present study, we exploited the concept of liquid biopsy combined to a logistically friendly sampling method to study the hemolymphatic bacterial microbiome in two mussel species (*Aulacomya atra* and *Mytilus platensis*) in Kerguelen Islands, a remote Subantarctic volcanic archipelago. We found that the circulating microbiome signatures of both species differ significantly even though their share the same mussel beds. We also found that the microbiome differs significantly between sampling sites, often correlating with the particularity of the ecosystem. Predictive models also revealed that both species have distinct functional microbiota, and that the circulating microbiome of *Aulacomya atra* was more sensitive to changes induced by acute thermal stress when compared to *Mytilus platensis*. Taken together, our study suggests that defining circulating microbiome is a useful tool to assess the health status of marine ecosystems and to better understand the interactions between the sentinel species and their habitat.

Abbreviations

A. atra	*Aulacomya atra*
M. platensis	*Mytilus platensis*
cmDNA	Circulating microbiome DNA, biodiversity
PCoA	Principal Coordinate Analysis
ASVs	Amplicon sequence variants
PERMANOVA	Multivariate analysis of variance with permutation
LEfSe	Linear discriminant analysis effect size
SOB	Sulphur-oxidizing bacteria

Climate changes are known to alter biodiversity at a global scale[1,2]. This is particularly true for Subantarctic regions, which have undergone significant changes in recent years due to global warming[3–5]. Sea surface temperatures in the Western Antarctic Peninsula have increased by ~ 1 °C since the industrial revolution and is expected to accelerate with the constant augmentation of global CO_2 concentrations, as suggested by predictive models[6,7]. The consequences of the global warming include alterations of the interactions between hosts and their associated microbiomes (*i.e.*, assemblages of microorganisms)[8–10]. Such dysbiosis could not only affect marine ecosystems per se, but also favors the emergence and proliferation of opportunistic pathogens[11,12]. Emerging infectious disease outbreaks in marine ecosystems would not only impact directly on the host populations but can also lead to mass mortalities of keystone species[9,13]. This is particularly true for sedentary and filtrating marine organisms such as mussels and oysters that are more prone to frequent, episodic mortality events during

[1]INRS-Centre Armand-Frappier Santé Technologie, 531 Boul. des Prairies, Laval, QC H7V 1B7, Canada. [2]UMR-I 02 SEBIO Stress environnementaux et Biosurveillance des milieux aquatiques, Université Reims Champagne-Ardenne, Campus Moulin de la Housse, 51687 Reims, France. ✉email: yves.st-pierre@inrs.ca

heat waves in summer[14–16]. Moreover, bivalves, which play a central role in an ecosystem integrity, are the most widely used sentinel species to monitor coastal marine environments as they are sedentary and have high filtering capacities leading to accumulation of pathogens and pollutants[17,18]. Their high filtering activity links them to their surrounding environment. Many marine mussel-based biomarkers have thus been developed over the years for monitoring environmental quality and for assessing environmental variations, particularly in remote areas such as polar regions[17,19,20].

The development of ethical (non-lethal) and logistically friendly sampling methods combined with the concept of liquid biopsy offers, however, a new window of opportunity to develop highly sensitive and predictable biomarkers[21]. Liquid biopsy, combined with high throughput DNA sequencing of circulating plasmatic DNA fragments, is commonly used in the biomedical field for decision-making in patients with cancer[22]. More recently, it has also been shown to be a useful mean to measure the presence of DNA fragments of non-self origin even in absence of overt diseases[23]. This has led to a novel concept, the "circulating microbiome DNA" (cmDNA)[24]. In contrast to tissue-specific microbiome analysis, characterization of the cmDNA allows to obtain a signature that reflects bacterial populations derived from classical niches (such as the gut, skin, oral cavity, etc.). This is also true in sentinel species, such as bivalves, which hemolymphatic cmDNA contains a rich and diverse microbiome and can be used as biomarkers to reflect host fitness and health status[25–29]. In fact, characterization of microbiomes in general has become an important tool to measure the impact of environmental and anthropogenic stressors in health and resilience of marine coastal ecosystems[29]. For example, in the case of *M. galloprovincialis*, in vivo exposure to polystyrene nanoplastics significantly affects different hemolymph immune parameters and a shift the ciruclating microbiome[27].

The coastal marine ecosystems of the Subantarctic Islands of Kerguelen (49°26′S, 69°50′E) are inhabited by two mussel species: the Subantarctic population of blue mussels, *Mytilus platensis* (*M. platensis*), and the ribbed mussel *Aulacomya atra* (*A. atra*). The isolated archipelago of Kerguelen is part of an oceanic submerged plateau that was built 35 million years ago following continuous volcanic activity. This archipelago is home to a maritime nature reserve classified as a UNESCO World Heritage Site since 2019. It is also a central hub for research on marine biodiversity in the Southern Ocean[30]. Recent observations indicate that Kerguelen Plateau is also characterized by the submarine gas emission that may represents active volcanic activity associated with cold seeps and hydrothermal vents[31]. This makes Kerguelen a unique site to measure the impact of climate changes on marine coastal habitats. In the present work, we report our findings of the first study of the hemolymphatic circulating microbiome collected in the two mussel species that inhabit mixed mussel beds located at different sites of the Kerguelen Islands.

Results

Species-dependent variations in bacterial communities. A total of 150 samples of *M. platensis* (all from the intertidal zone) and *A. atra* (intertidal and subtidal) were analyzed. For each sample, the cmDNA was profiled by sequencing the 16S rRNA gene amplicons of the V3–V4 hypervariable region. A total of 6,489,570 paired-end sequences passed quality filtering (43,264 ± 27,652 per sample). Amplicon sequence variants (ASVs) were generated from 21,389 high-quality reads. Overall, the relative abundance of bacterial phyla in both mussel species were dominated by *Proteobacteria* (56.0% and 41.6% for *A. atra* and *M. platensis* respectively), *Bacteroidetes* (14.8% and 14.2% respectively), and *Parcubacteria* (7.2% and 8.3% respectively), which accounted for more than 60% of all reads (Fig. 1). This composition is consistent with a recent metagenomic study showing that bacteria enriched in seawater in polar regions were mostly *Proteobacteria*, *Actinobacteria*, *Bacteroidetes* and *Parcubacteria*[32]. Multivariate analysis (PERMANOVA) on a weighted UniFrac showed, however, that the global composition of the microbiome was significantly different between *A. atra* and *M. platensis* (weighted UniFrac PERMANOVA, $F_{(1, 154)} = 5.02$, $p < 0.001$). A case in point at the phylum level is the presence of *Acidobacteria* (4%), *Chloroflexi* (4%), *Spirochaetes* (2%), *Tenericutes* (3%), and *Verrucomicrobia* (3%) in *M. platensis* but not in *A. atra*. In contrast, *Fusobacteria* (4%) were more abundant in *A. atra* in the intertidal zone. This phylum is commonly found in marine sediment environments but has been reported to constitute the major phylum in oil-contaminated anaerobic niche of seawater following the deep-water horizon oil spill and other marine reservoirs[33,34]. Interestingly, the highest abundance of *Fusobacteria* was detected at Port-aux-Français, the capital settlement of Kerguelen Islands and the only site with active port activity (Supplementary Figure S1). Furthermore, no significant differences in the composition of the microbiome were found in *A. atra* between subtidal and intertidal zones (weighted UniFrac PERMANOVA, $F(1, 88) = 1.49$, $p = 0.103$)).

Site-dependent beta diversity analysis. We next examined spatial variations in the cmDNA profiles of both mussel species. For this, we collected samples from 16 sites, including 5 mixed mussel beds (Port-aux-Français, Port-Couvreux, Île Haute, Île Haute-Baie des Bergers, and Anse-aux-Écueils) and 5 subtidal sites where samples of *A. atra* were collected (Fig. 2). To compare β-diversity between sampling sites, principal coordinate analysis (PCoA) based on the weighted UniFrac distance was carried out for both species (Fig. 3). Multivariate analysis revealed a significant separation of samples according to sampling sites. An ADONIS on weighted UniFrac analysis showed a significant difference according to sampling sites ($p < 0.001$) for both species. For *M. platensis*, distances to group centroids were significantly different (Permutest, $F_{(10, 55)} = 4.83$, $p = 0.002$) in samples collected at Anse de Saint-Malo and Anse Sablonneuse (Fig. 3A). In the case of A. *atra*, the betadisper analysis highlights four distinct microbial sites where the community structure was significantly higher (Permutest, $F_{(13, 75)} = 3.32$, $p = 0.002$); Port-Couvreux (intertidal), Îlot Channer (intertidal), Anse-aux-Écueils (intertidal) and Anse-du-Halage (subtidal) showed a strong separation with other sites.

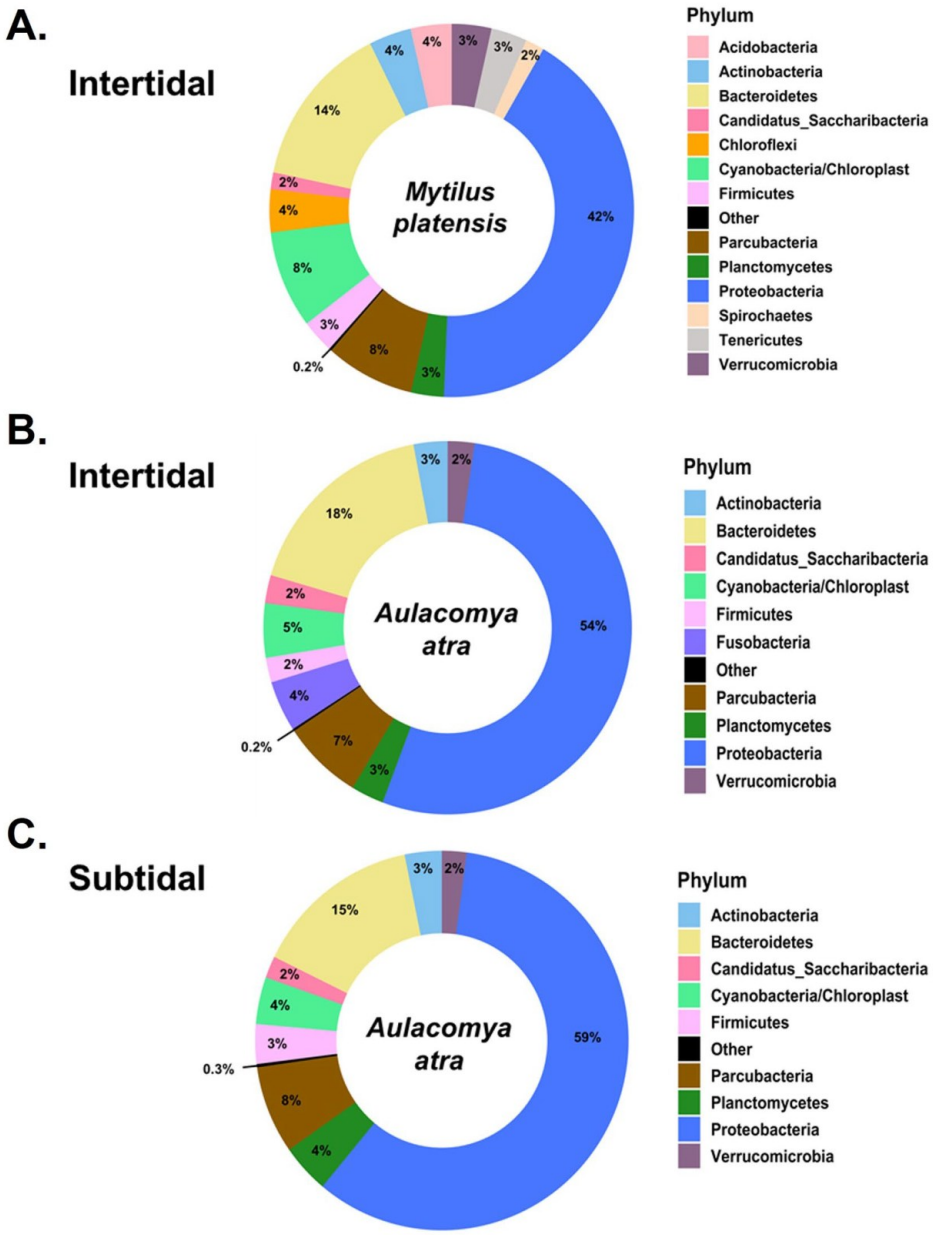

Figure 1. Phylum-level analysis of hemolymphatic bacterial DNA. (**A**) *M. platensis* and (**B**) *A. atra* collected in intertidal zones. (**C**) of *A. atra* collected in subtidal zones. Phylum with a relative abundance of ≤ 1.5% are represented as "Other".

Site-dependent alpha diversity analysis. We next compared the alpha diversity for each site using three diversity indices including richness, Shannon index, and Pielou's evenness. Globally, we found no significant differences in the cmDNA for both mussel species collected during two successive campaigns at Kerguelen (2017 and 2018) (Supplementary Figure S2). A comparative analysis of the alpha diversity according to sites revealed, however, significant differences between sites for both species (Fig. 4). In the case of *M. platensis*, the richness estimator showed a significant variation ($\chi^2 = 18.977$, $p = 0.0401$, $df = 10$). The lowest richness value was observed at Anse Sablonneuse (65.7 ± 9.9), a mussel bed occurring in mid to lower shore sand. In the case of *A. atra*, richness estimator ($\chi^2 = 38.779$, $p < 0.001$), Shannon index ($\chi^2 = 37.996$, $p < 0.001$) and Pielou's evenness

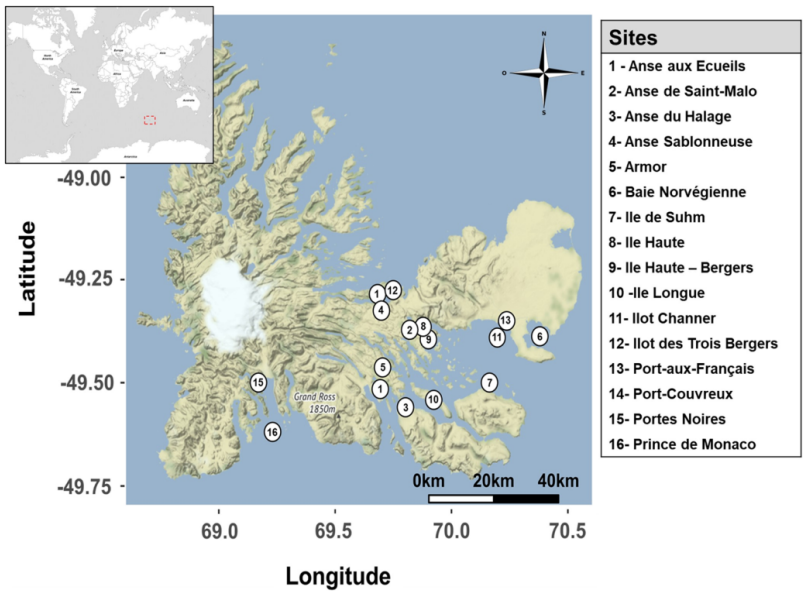

Figure 2. Map of the French Subantarctic Kerguelen Islands showing the sampling sites. The map was generated with the ggmap package in R programming language (R version 4.0.3, R Core Team[88]).

($\chi^2 = 36.647$, $p < 0.001$) varied greatly between sites for both intertidal and subtidal zones. Lowest alpha diversity indices in *A. atra* sites were observed at Port-Couvreux (intertidal) and Île Longue (subtidal).

Site-dependent variations at the genus level. Differences between sites for both species were further documented at the genus level, focusing first on the top 30 genus, which represent 32% of all genera. Among the notable findings, we found strong abundance of *Pseudoalteromonas* and *Psychromonas* in *M. platensis* collected at the Anse Sablonneuse (Fig. 5). The cmDNA of *M. platensis*, but not *A. atra*, collected in the intertidal zone of the Îlot Channer, an islet formed of basaltic rocks surrounded by a belt of large brown algae (*Durvillea* and *Macrocystis*), was dominated by *Aquabacterium*, a common bacteria found within kelps[35]. In the case of *A. atra*, we found a relative abundance of *Sphingomonas* at several sites, including Port-Couvreux, Ile Longue, Île du Suhm and Portes-Noires which accounted for 31.5–57.7% of total reads (Supplementary Table S1). This genus dominance could be attributed to the significant occurrence of kelp (*Macrocystis pyrifera*) at these sampling sites. This is in agreement with Florez et al.[36] who reported that epiphytic bacterial communities in macroalgae are associated with *Sphingomonadales*/*Sphingomonas* are known to degrade alginate as carbon source[37,38]. It was also worth noting that *A. atra* collected at the intertidal zone of the fjord of Portes Noires showed quite a unique abundance of *Acidovorax, of* which several species are phytopathogenic, and *Parvularcula,* compared to any other sites or to *M. platensis*. Interestingly, abundance of *Vibrio* was higher in *A. atra* in both intertidal and subtidal mussels of Port-aux-Français.

The differences between sites were further studied at the genus level by focusing this time on the phyla that differed between both species. The most significant difference between *M. platensis* and *A. atra* was observed at Port-Couvreux (Supplementary Figure S3). We also found that bacterial DNA from the genus *Kistimonas*, a member of the *Hahellacae* family of *Proteobacteria*, was not detected in *A. atra* at any site but was present in *M. platensis* at Port-Couvreux, Île Haute, Île Haute-Baie du Berger, and Anse-aux-Écueils. Bacterial DNA from the genus *Sulforimonas* was also commonly found in *M. platensis* at several sites but rarely in *A. atra*. Overall, these results showed that both mussel species have distinct circulating microbiome profiles that vary according to the geographic locations of the mussel beds. Given the fact that season changes may play a major role in shaping bacterial community structure in bivalves, further investigations are needed to compare seasonal variability in the microbiome between both mussel species[39,40].

Environmental microbiota can also be influenced by anthropogenic sources. This could explain why the relative abundance of bacteria of the *Vibrio* genus were more abundant at Port-aux-Français (in both intertidal and subtidal zones) in *A. atra* than at other sampling sites (Supplementary Table S1). LEfSe analysis indeed revealed that *Vibrio* was the top genus-level biomarkers that distinguished Port-aux-Français from all other sites (Supplementary Table S2). This finding is consistent with a previous study showing that anthropogenic impacts are higher at Port-aux-Français when compared to other sites[41]. In Mediterranean Sea, the proliferation of opportunistic pathogens affiliated to *Vibrio spp.* is suspected to be a major factor in disease outbreaks in bivalve species[42,43]. Moreover, *Vibrio spp.* encompasses a variety of pathogens whose presence within bivalve tissues and interactions

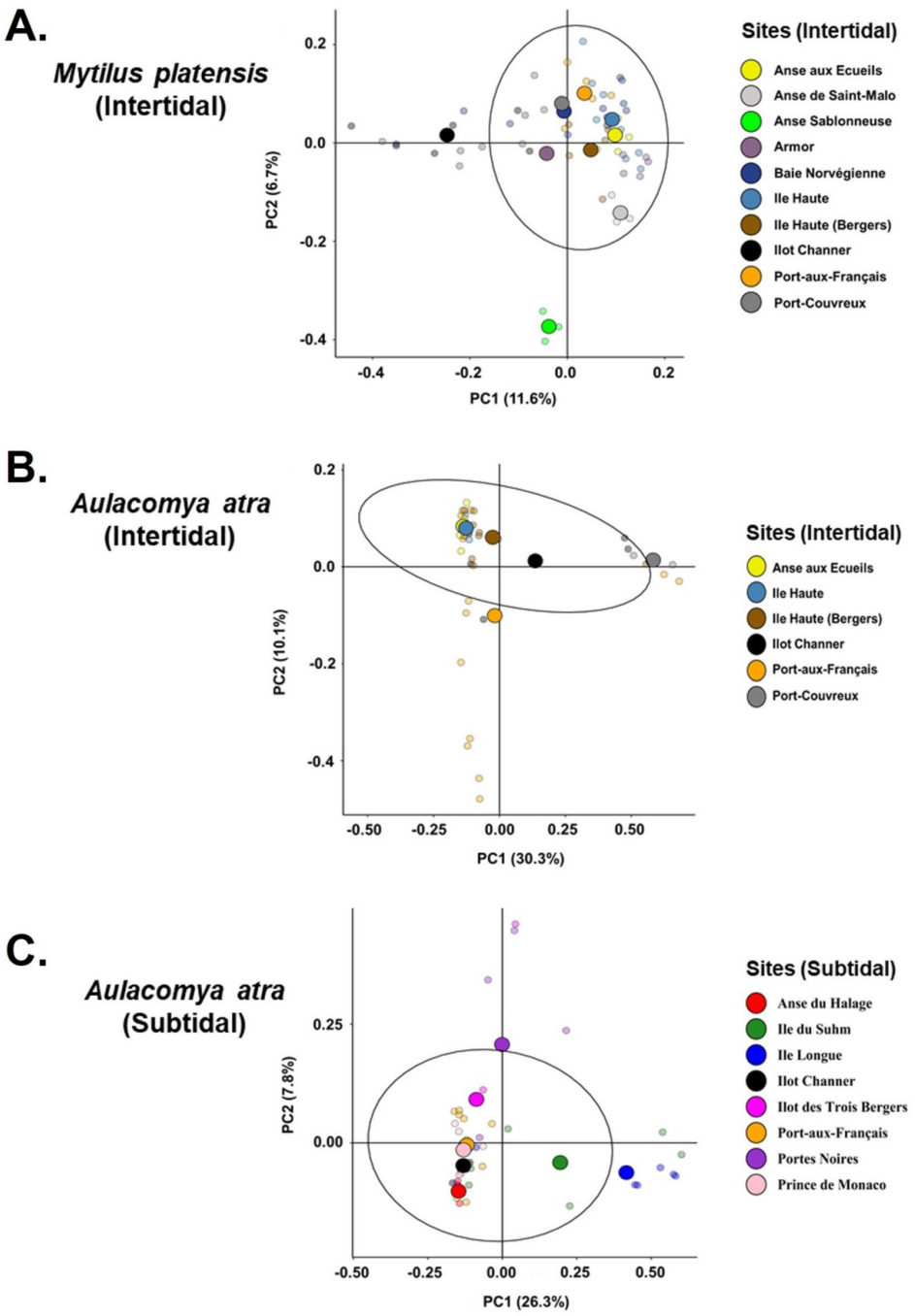

Figure 3. Principal Coordinates Analysis (PCoA) of bacterial DNA bacterial communities at different sites. Weighted UniFrac-based of in samples collected in *M. platensis* (**A**), *A. atra* in intertidal (**B**) and subtidal (**C**) zones. Centroids for each site are illustrated by larger circles. Black ellipses represent 90% confidence interval.

with their immune system are well documented[44]. Taken together, our results indicate that hemolymph cmDNA profiles reflect the local environment and the impacts of anthropogenic stressors.

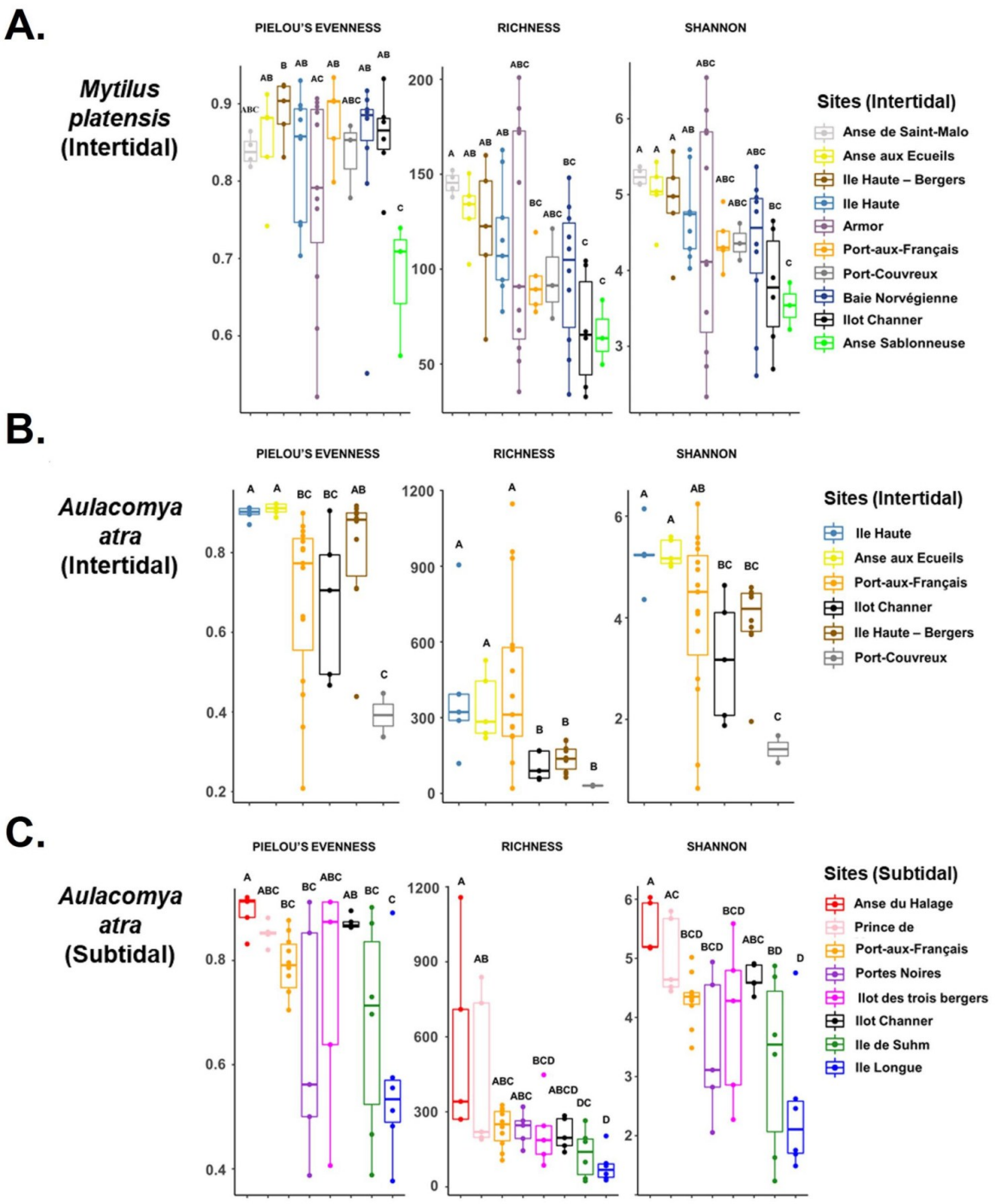

Figure 4. Alpha diversity analysis. Box plots of alpha diversity of (**A**) *M. platensis* collected in intertidal zone and *A. atra* in intertidal (**B**) and subtidal (**C**) zones. Species evenness observed richness and Shannon diversity indexes were calculated for each site. Significant *p* values ($p < 0.05$) were obtained using permutation test as a non-parametric test following by a post-hoc pairwise comparisons.

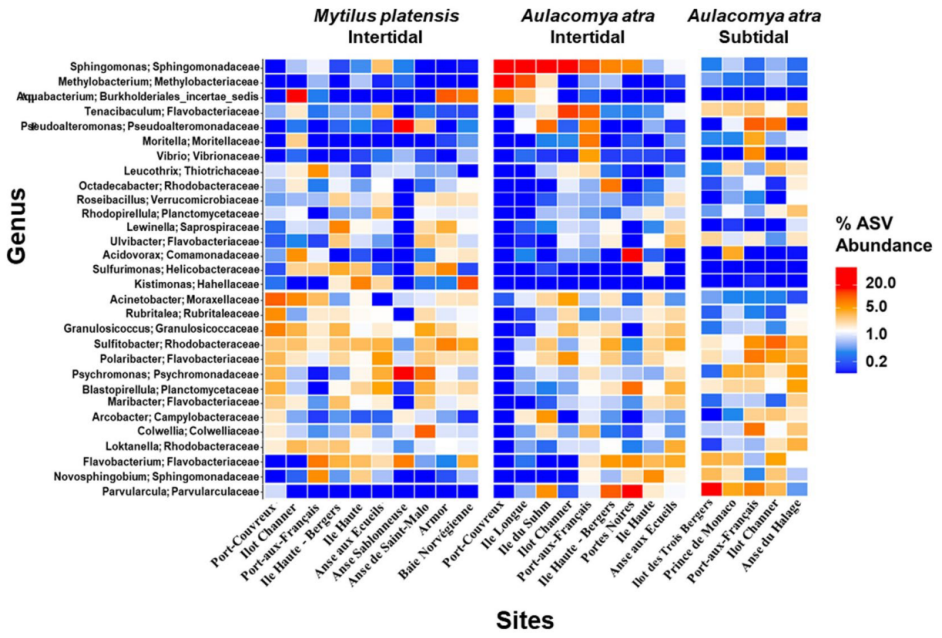

Figure 5. Heatmaps showing relative abundance (%) of the top 30 bacterial genera of hemolymphatic microbiota between in both mussel species. Red colors indicate higher abundance and blue colors indicate lower abundances.

Functional analysis of the cmDNA. Predictive functional analysis from 16 s rRNA profiling is becoming a common tool to link the abundance of specific taxa with metabolic profiles[45–47]. To further explore the distinctive traits that distinguish the circulating microbiome of mussels at different sites, we studied its functional content predicted from the KEGG database using Piphillin tool. Our findings confirmed that the bacterial pathways varied significantly between *A. atra* and *M. platensis* and between sites (Fig. 6). A case in point is the abundance of the pathways involved in xenobiotics degradation, carbohydrate metabolism and amino acid metabolism in the hemolymph of *A. atra* at Port-Couvreux.

Effect of thermal stress on cmDNA. Environmental conditions, particularly temperature, are known to affect the hemolymphatic microbiome in many marine invertebrates[26,48,49]. In fact, alteration of microbiota by thermal stress can induce mortality in some organisms[50]. To determine whether the circulating microbiome of both species was modulated equally to thermal stress, both mussel species was subjected to an acute thermal stress under laboratory conditions. Our results showed that *Pseudoalteromonas spp.*, a bacterial genus found in the bacterioplankton in Antarctica[51], was the most abundant genus obtained in both mussel specimens and its abundance increased significantly ($p < 0.001$) in both mussels exposed at a higher temperature (30 °C) (Fig. 7A, Supplementary Table S3). A significant increase in *Cobetia*, a facultative psychrotrophic bacteria that can grow at temperature ranging from 0 to 40 °C[52], was also seen in *A. atra* but not in *M. platensis*. A Venn diagram showed that the hemolymphatic cmDNA in *A. atra* harbored 3–4 times more genera that that of *M. platensis*, suggesting a higher diversity (Fig. 7B). The higher diversity found in *A. atra* was confirmed upon analysis of richness and Shannon indices (Fig. 7C). Taken together, these results suggest that both mussel species react differently to thermal stress, consistent with results reported in an experimental model of acute thermal stress[21].

Discussion

In the present work, using hemolymphatic liquid biopsies, we compared the cmDNA of two mussel species that cohabit the coastal ecosystems of Kerguelen. More specifically, we found that: 1) The cmDNA bacterial profiles of both species differ significantly; 2) differences were site-dependent; 3) both species had distinct functional microbiota, and 4) the circulating bacterial microbiome of *A. atra* was more sensitive to changes induced by an experimental model of thermal stress. Overall, this study shows that both mussel species of Kerguelen Islands have distinctive bacterial cmDNA signatures that can be used for long term monitoring of the impact of climate changes on marine coastal ecosystems. We also show that defining the bacterial cmDNA signature in sentinel species is compatible with a minimally invasive, ethical and logistically friendly sampling method adapted for research in remote regions such as Kerguelen Islands.

Our study has revealed that hemolymphatic bacterial DNA in mussels are species-specific, even though both mussel species co-habit intimately in mussel beds of Kerguelen. These results suggest the existence of a selective

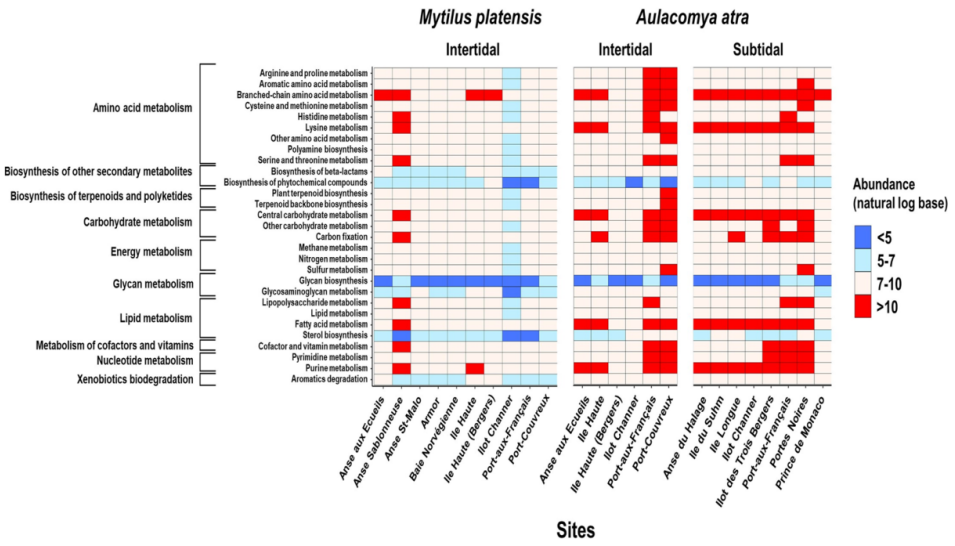

Figure 6. Predictive functional analysis. Heatmaps based on the main KEGG pathways predicted at the different sampling sites. Relative abundance (natural logarithm base) of metabolic pathways based on 16S rRNA data is shown for both mussel species. Enrichments correspond to the positive values (red color) while depletions correspond to negative values (blue).

bacterial retention between the two mussel species. Similar conclusions have been reported recently by Weingarten et al.[53] who studied the gut microbiota of four different freshwater *Unionidae* mussels. Several non-exclusive hypotheses can be formulated to explain these findings. First, this could be related to intrinsic characteristics of filtration between species[54]. For instance, *M. platensis* is characterized by longer labial palps allowing to capture and reject finer material in comparison with other bivalves and have higher filtration rates than *A. atra*[55,56]. It has also been suggested that the circulating microbiome is not just dependent of particles ingestion but may be impacted by the interactions between environmental microbiota and host gills for selectively retaining certain taxa. Indeed, it has been demonstrated that ctenidia (*i.e.,* paired gills) are responsible for particle sorting such as plankton, organic detritus and bacteria. Some studies have shown that picoplankton (0.2–2 µm) represents a significant contribution to the mussel diet and their ingestion was found to be cleared at higher rates than bacteria (~0.6 µm in size) by *M. platensis*[57–59]. This suggests that factors other than size affect capture of particles by ctenidia of bivalves, such as availability of the seston, might come into play. Marine aggregates (1–500 µm) may also contribute to enhance the uptake of picoplankton and bacteria[60,61]. Particle selection and ingestion in filter-feeding bivalves may thus depend on differential morphology of the ctenidia[54,62]. Particle discrimination can also be influenced by interactions between chemical constituents of the cohesive mucous of pallial organs and surface carbohydrates of captured particles[59,63]. Differences between microbiota in bivalves can also be modulated by the mucosal immunity[64–66]. Bivalve pallial mucus contains agglutinins that can interact with several bacterial species. It may also depends to immune humoral factors, such as antimicrobial peptides, that play a central role in defense, most notably in the extrapallial compartment where enriched nutrients such as proteins and polysaccharides that promote microbial proliferation[67]. Another immune mechanism that may explain the differential microbiome signature is the selective killing of bacteria bacteriophages[65]. For instance, two phages isolated in Pacific oyster larvae provide a non–host-derived immunity against pathogenic *V. coralliilyticus*[68]. Bacteriophage adherence to bivalve mucosal surfaces is central in this symbiotic relationship. Clearly, further comparative studies between *M. platensis* and *A. atra* are required to address this question.

Our data highlights that cmDNA bacterial profiles are site-specific and may provide critical information on the surrounding marine ecosystems. A good example is the presence sulfur-oxidizing bacteria (SOB) (e.g., *Sulfitobacter spp.* and *Sulfurimonas spp.*), which represent a significant part in hemolymph microbiota in both mussel species collected at different sites (Supplementary Table S1). SOB represent a large part of microbial communities in marine surface sediments where they play a key role in element cycling[69,70]. Coastal ecosystems around the Kerguelen islands are characterized by high wind speeds and strong tidal currents causing sediment dispersion along the coast[71–73]. In addition to symbionts, the region around the Kerguelen Plateau is characterized by the presence of cold seeps and hydrothermal vents emitting chemical-rich fluids[31]. It is likely that symbiotic SOB are present in the gills of the two mussels and contribute to provide organic carbon as energy source to the host by consuming sulfide from the Subantarctic vents. Another example of how the circulating microbiome can provide clues on local environmental conditions is the detection of DNA derived from thermophilic bacteria, such as *Geobacillus spp.* and *Thermomonas spp.*, which were found in *A. atra* collected at Îlot-des-Trois-Bergers and Prince-de-Monaco (Supplementary Table S1). Both sites are located near geothermally heated habitats[74]. High abundance of kelps could also modulate the circulating microbiome signature. The coastlines of Kerguelen Islands are occupied by highly productive giant kelp beds forming undersea forests in hard bottom. Giving the

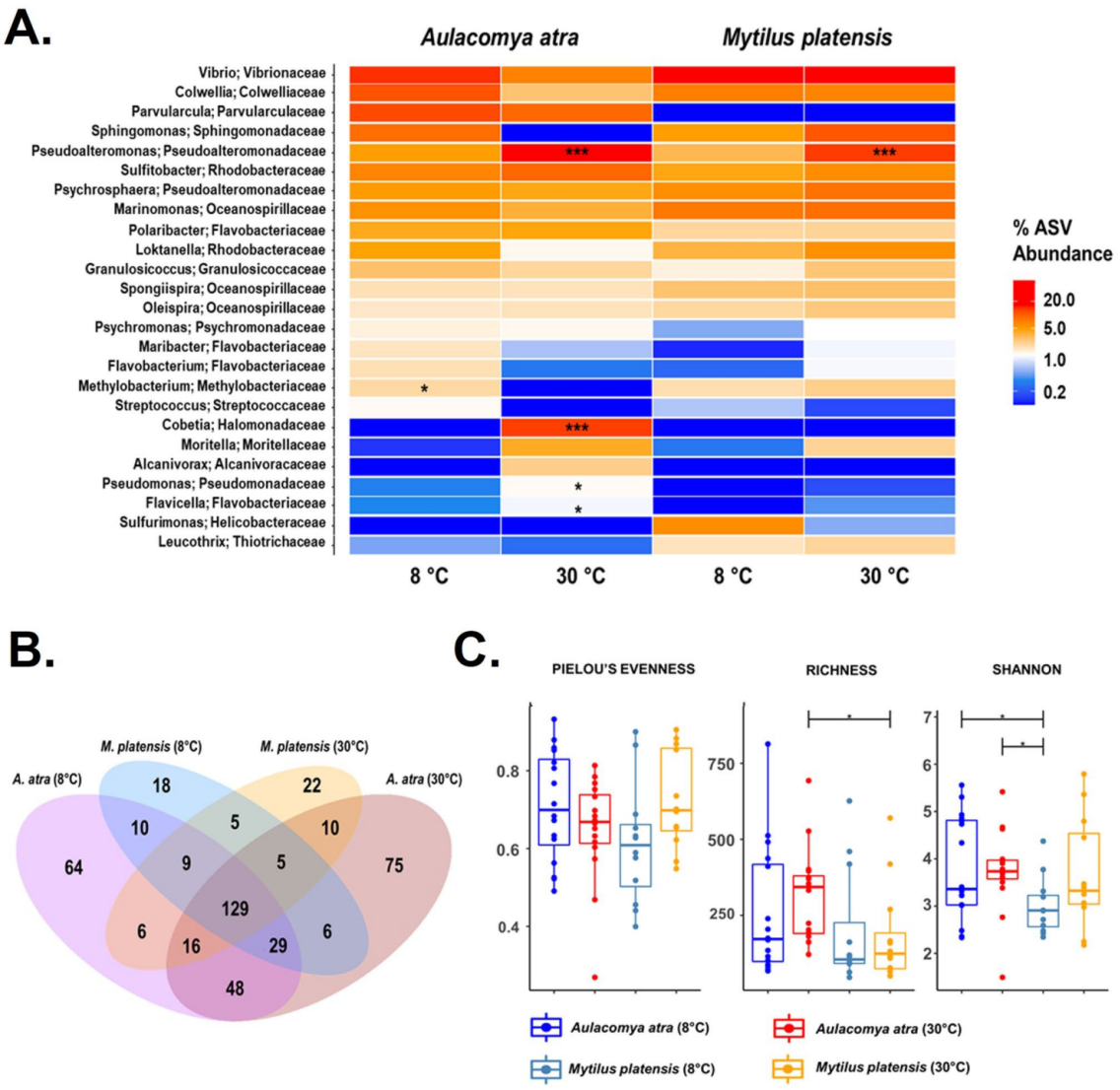

Figure 7. Changes in bacterial cmDNA profiles in mussels following an acute thermal stress. (**A**) Heatmap outlining the presence and the relative abundance (%) of the top 30 bacterial genera of at different temperatures. The data were generated from 8 345 ASVs. Red colors indicate higher abundance and blue colors indicate lower abundances. Stars indicate taxa that were significantly different from four groups, as determined by LDA Effect Size analysis. (**B**) A Venn diagram showing the number of unique and shared bacterial genera in both species at 8 °C and 30 °C. (**C**) Alpha diversity of *A. atra* and *M. platensis* hemolymphatic cmDNA at 8 °C and 30 °C. Species evenness, observed richness and Shannon diversity indexes were calculated for each group. Note: $*0.01 < p \leq 0.05$; $**0.001 < p \leq 0.01$; $***p \leq 0.001$.

fact that numerous strains of the genus *Sphingomonas* can decompose algal polysaccharides and be a dominant bacterium from a marine oligotrophic environment[38,75], it is therefore not surprising to find a great abundance of this genus at sampling sites characterized by kelp forests. Taken together, these results illustrate the potential of defining the circulating microbiome signature in mussels for long-term monitoring of environmental changes occurring in coastal marine ecosystems.

Intertidal mussels are exposed to sea surface and air temperature variations reflecting the solar exposition, the wind speed, the sea level pressure, humidity index and the dual tides in Kerguelen[76–78]. In 2018, according to the PROTEKER's registries from their temperature loggers at Îlot Channer site at a depth of 5 m, the temperature varied from 2.7 to 9.5 °C, where *A. atra* is found[79]. The situation is of course quite different in the intertidal zones where temperature changes is subjected to high variations within a single day and between tides. Considering the growth rate of some bacteria, it is logical to expect a microbiome shift after a thermal stress as we did observe in

our experimental model of thermal stress. Such effect of thermal stress on the cmDNA has been documented in the past for bivalves[26,40,48]. However, this effect was more pronounced in *A. atra* when compared to *M. platensis*, as shown by the significant increase of the bacteria of the *Cobetia* genus in *A. atra*. These bacteria can grow at temperature up to 40 °C[52]. In addition, it is also important to pinpoint that the microbiome signature in mussels will also be affected by seasonal variations.

Overall, our data with the circulating microbiome suggests that *A. atra* is more sensitive to thermal stress when compared to *M. platensis*. These results are consistent with previous studies comparing the hemolymphatic component of both species in response to thermal stress[80]. Whether such this plays a role in its progressive disappearance for the profit of *Mytilus spp.* in many marine ecosystems is unclear now[81]. Clearly, monitoring of mixed beds may represent a unique opportunity to study the effect of climate change on marine coastal ecosystems in the Southern hemisphere, a particularly sensitive region to climate change.

Materials and methods

Sample collection. *A. atra* and *M. platensis* specimens (55–70 mm length) were collected at 16 sites of the French sub-Antarctic Kerguelen Islands during the 2017 and 2018 Summer campaigns (Fig. 2). Liquid biopsy samples were collected from samples collected in both intertidal or subtidal (~ 5 m depth) zones and immediately processed (within an hour) on site as previously described[21]. Briefly, intravalvular liquid was removed with the tip of a knife and hemolymph withdrawn from the adductor muscle using a syringe fitted with a 21-gauge needle. Samples were immediately transferred into 1.5 mL sterile Eppendorf tube and centrifuged on site for 3 min at 3000×*g* at ambient temperature using a portable, battery-operated TOMY Multi Spin centrifuge (TOMY, Japan). Samples were pooled to eliminate individual differences and to minimize small-scale variability[25,82]. After centrifugation, cell pellets were dispersed gently and a 50 µL aliquot was applied on individual discs of Whatman 903™ FTA® cards (Sigma-Aldrich, Oakville, ON, Canada). After a 30 min drying period at ambient temperature, individual cards were kept in zip-sealed sampling plastic bags containing one small desiccant. Ethanol was used to disinfect handling equipment, and gloves were always worn during the procedure to prevent contamination from human hands.

Thermal stress experiments. Adult specimens of *M. platensis* and *A. atra* were collected on the intertidal rocky shores of Port-aux-Français (49°21′4.682″ S, 70°13′22.496″ E) at Kerguelen Islands in November and December 2018. Mussels were transported to laboratory within the hour and immediately transferred in a temperature-controlled (8 °C) aerated aquarium containing filtered recirculating seawater maintained on a 12 h:12 h light/dark cycle for at least 24 h. Mussels were placed in a 30 °C seawater recipient for 90 min. This acute stress model is commonly used in other studies to investigate the effect of temperature stress between mussels congeners[80,83–85]. Controls included mussels incubated for the same period of time at 8 °C. After 90 min, hemolymph samples were immediately processed as described above and 70 µL of hemolymph was spotted on FTA cards kept in sample bags with a desiccant.

Preprocessing and sequencing. Individual discs were cut from the FTA cards using a sterile 5.0 mm single round hole punch and total DNA isolated using the QIAamp DNA Investigator Kit (Qiagen, Hilden, Germany) according to the manufacturer's protocol. Quantification of DNA was carried out in duplicate using Quant-iT™ PicoGreen® dsDNA detection kit (Molecular Probes, Eugene OR). Amplification of the 16S ribosomal RNA (rRNA) gene amplifications and 16S gene amplicon sequencing for all DNA samples were performed at Centre d'expertise et de services Génome Québec (Montréal, QC, Canada) using the universal primers 341F (5'-CCTACGGGNGGCWGCAG-3') and 805R (5'-GACTACHVGGGTATCTAATCC-3')[86]. Sequence libraries were prepared by Génome Québec with TruSeq® DNA Library Prep Kit (Illumina, San Diego, CA, USA) and quantified using KAPA Library Quantification Kit for Illumina platforms (Kapa Biosystems). Paired-end sequences were generated on a MiSeq platform PE300 (Illumina Corporation, San Diego, CA, USA) with the MiSeq Reagent Kit v3 600 cycles (Illumina, San Diego, CA, USA).

Bioinformatic analysis. Illumina sequence data (FASTQ files) were received as output from Génome Québec. For each primer pair dataset, reads from the raw sequencing data were trimmed using *Cutadapt* (version 2.8) tool implemented in Unix Shell (version 4.4.19; Ubuntu version 18.04). For data pre-processing, the DADA2 pipeline (version 1.16.0; Callahan et al.[87]) was used to generate 16S rRNA (V3-V4) amplicon sequence variants (ASVs). Briefly, forward and reverse reads were trimmed, filtered and truncated based on their quality scores. The error model was calculated for forward and reverse reads. After denoising and merging, chimeric sequences (bimeras) were removed from the datasets by following the consensus method as implemented in DADA2. All subsequent analyses were performed within the R environment (R version 4.0.3, R Core Team[88]). The final table obtained consisted of a tabulation of number of occurrences of non-chimeric ASVs in each sample. Taxonomy assignments of representative ASVs were performed using the naïve Bayesian classifier method with the latest RDP 16 database. Sequences (4.8% of reads) attributed to Archaea or unclassified at phylum level were removed from the dataset. Raw datasets analyzed during the current study are publicly available on NCBI Sequence Read Archive (PRJNA773369).

Statistical analysis. Bacterial community analysis were performed in the R environment using the *phyloseq*, *microbiomeSeq, microbiomeMarker* and *vegan* packages[89–92]. Alpha diversity indices, including the Shannon index, Pielou's evenness and richness estimator, were calculated using Wilcoxon/Kruskal–Wallis test between groups. Beta diversity between sample groups was determined based on the UniFrac distance and visualized by principal coordinates analysis (PCoA). Heatmaps were performed based on the relative abundance and

constructed with the 30 most abundant genera. Bacterial biota composition differences among sites were studied using multivariate analysis of variance with permutation (PERMANOVA) with 9999 permutations. Permutation multivariate analysis of dispersion (PERMDISP) was also conducted with the function betadisper and permutest in order to test for homogeneity of multivariate dispersions (i.e., deviations from centroids) among sampling sites. The linear discriminant analysis (LDA) identifies the effect size (LEfSe) with which these taxa differentiate the samples. The threshold on the logarithmic score of LDA analysis was set to 2.0. Comparative metagenomic functional composition was predicted from the latest Kyoto Encyclopedia of Genes and Genomes (KEGG) database[93] using a recently developed online tool Piphillin (http://secondgenome.com/Piphillin)[45,94]. The differential abundance analysis of gene abundance data was completed with the online tool MicrobiomeAnalyst[95].

Received: 25 October 2021; Accepted: 29 April 2022
Published online: 10 June 2022

References

1. Brondizio, E. S., Settele, J., Díaz, S. & Ngo, H. T. (eds.) *Global Assessment Report on Biodiversity and Ecosystem Services of the Intergovernmental Science–Policy Platform on Biodiversity and Ecosystem Services* (IPBES Secretariat, 2019).
2. Weiskopf, S. R. *et al.* Climate change effects on biodiversity, ecosystems, ecosystem services, and natural resource management in the United States. *Sci. Total Environ.* **733**, 137782. https://doi.org/10.1016/j.scitotenv.2020.137782 (2020).
3. Turner, J. & Marshall, G. J. *Climate Change in the Polar Regions* (Cambridge University Press, 2011).
4. Meredith, M. *et al.* Polar Regions. Chapter 3, *IPCC Special Report on the Ocean and Cryosphere in a Changing Climate.* https://www.ipcc.ch/srocc/chapter/chapter-3-2/ *(2019).*
5. Rignot, E. *et al.* Four decades of Antarctic Ice Sheet mass balance from 1979–2017. *Proc. Natl. Acad. Sci. USA* **116**, 1095–1103. https://doi.org/10.1073/pnas.1812883116 (2019).
6. Siegert, M. *et al.* The Antarctic Peninsula under a 1.5°C global warming scenario. *Front. Environ. Sci.* **7**, 102. https://doi.org/10.3389/fenvs.2019.00102 (2019).
7. Iz, H. B. Is the global sea surface temperature rise accelerating?. *Geod. Geodyn.* **9**, 432–438. https://doi.org/10.1016/j.geog.2018.04.002 (2018).
8. Qiu, Z. *et al.* Future climate change is predicted to affect the microbiome and condition of habitat-forming kelp. *Proc. R. Soc. B.* **286**, 20181887. https://doi.org/10.1098/rspb.2018.1887 (2019).
9. Burge, C. A., Kim, C. J., Lyles, J. M. & Harvell, C. D. Special issue Oceans and Humans Health: The ecology of marine opportunists. *Microb. Ecol.* **65**, 869–879. https://doi.org/10.1007/s00248-013-0190-7 (2013).
10. Cavicchioli, R. *et al.* Scientists' warning to humanity: Microorganisms and climate change. *Nat. Rev. Microbiol.* **17**, 569–586. https://doi.org/10.1038/s41579-019-0222-5 (2019).
11. Harvell, C. D. *et al.* Emerging marine diseases–climate links and anthropogenic factors. *Science* **285**, 1505–1510. https://doi.org/10.1126/science.285.5433.1505 (1999).
12. Egan, S. & Gardiner, M. Microbial dysbiosis: Rethinking disease in marine ecosystems. *Front. Microbiol.* **7**, 991. https://doi.org/10.3389/fmicb.2016.00991 (2016).
13. Wilkins, L. G. E. *et al.* Host-associated microbiomes drive structure and function of marine ecosystems. *PLoS Biol.* **17**, e3000533. https://doi.org/10.1371/journal.pbio.3000533 (2019).
14. Seuront, L., Nicastro, K. R., Zardi, G. I. & Goberville, E. Decreased thermal tolerance under recurrent heat stress conditions explains summer mass mortality of the blue mussel Mytilus edulis. *Sci. Rep.* **9**, 17498. https://doi.org/10.1038/s41598-019-53580-w (2019).
15. Tsuchiya, M. Mass mortality in a population of the mussel *Mytilus edulis* L. caused by high temperature on rocky shores. *J. Exp. Mar. Biol. Ecol.* **66**, 101–111. https://doi.org/10.1016/0022-0981(83)90032-1 (1983).
16. Malham, S. K. *et al.* Summer mortality of the Pacific oyster, *Crassostrea gigas*, in the Irish Sea: The influence of temperature and nutrients on health and survival. *Aquaculture* **287**, 128–138. https://doi.org/10.1016/j.aquaculture.2008.10.006 (2009).
17. Beyer, J. *et al.* Blue mussels (*Mytilus edulis* spp.) as sentinel organisms in coastal pollution monitoring: A review. *Mar. Environ. Res.* **130**, 338–365. https://doi.org/10.1016/j.marenvres.2017.07.024 (2017).
18. Ladeiro, M. P. *et al.* Mussel as a tool to define continental watershed quality. In *Organismal and Molecular Malacology* (ed Ray, S.), IntechOpen. https://doi.org/10.5772/67995 (2017).
19. Bonacci, S. *et al.* Esterase activities in the bivalve mollusc *Adamussium colbecki* as a biomarker for pollution monitoring in the Antarctic marine environment. *Mar. Pollut. Bull.* **49**, 445–455. https://doi.org/10.1016/j.marpolbul.2004.02.033 (2004).
20. Storhaug, E. *et al.* Seasonal and spatial variations in biomarker baseline levels within Arctic populations of mussels (Mytilus spp.). *Sci. Total Environ.* **656**, 921–936. https://doi.org/10.1016/j.scitotenv.2018.11.397 (2019).
21. Caza, F. *et al.* Liquid biopsies for omics-based analysis in sentinel mussels. *PLoS ONE* **14**, e0223525. https://doi.org/10.1371/journal.pone.0225359 (2019).
22. Ignatiadis, M., Sledge, G. W. & Jeffrey, S. S. Liquid biopsy enters the clinic - implementation issues and future challenges. *Nat. Rev. Clin. Oncol.* **18**, 297–312. https://doi.org/10.1038/s41571-020-00457-x (2021).
23. Kowarsky, M. *et al.* Numerous uncharacterized and highly divergent microbes which colonize humans are revealed by circulating cell-free DNA. *Proc. Natl. Acad. Sci. USA* **114**, 9623–9628. https://doi.org/10.1073/pnas.1707009114 (2017).
24. Chen, H. *et al.* Circulating microbiome DNA: An emerging paradigm for cancer liquid biopsy. *Cancer Lett.* **521**, 82–87. https://doi.org/10.1016/j.canlet.2021.08.036 (2021).
25. Lokmer, A. *et al.* Spatial and temporal dynamics of Pacific oyster hemolymph microbiota across multiple scales. *Front. Microbiol.* **7**, 1367. https://doi.org/10.3389/fmicb.2016.01367 (2016).
26. Lokmer, A. & Wegner, M. K. Hemolymph microbiome of Pacific oysters in response to temperature, temperature stress and infection. *ISME J.* **9**, 670–682. https://doi.org/10.1038/ismej.2014.160 (2015).
27. Auguste, M. *et al.* Exposure to TiO2 nanoparticles induces shifts in the microbiota composition of Mytilus galloprovincialis hemolymph. *Sci. Total Environ.* **670**, 129–137. https://doi.org/10.1016/j.scitotenv.2019.03.133 (2019).
28. Vezzulli, L. *et al.* Climate influence on Vibrio and associated human diseases during the past half-century in the coastal North Atlantic. *Proc. Natl. Acad. Sci. USA* **113**, E5062–E5071. https://doi.org/10.1073/pnas.1609157113 (2016).
29. Musella, M. *et al.* Tissue-scale microbiota of the Mediterranean mussel (*Mytilus galloprovincialis*) and its relationship with the environment. *Sci. Total Environ.* **717**, 137209. https://doi.org/10.1016/j.scitotenv.2020.137209 (2020).
30. Féral, J.-P. *et al.* PROTEKER: Implementation of a submarine observatory at the Kerguelen islands (Southern Ocean). *Underw. Technol.* **34**, 3–10. https://doi.org/10.3723/ut.34.003 (2016).
31. Spain, E. A. *et al.* Shallow seafloor gas emissions near Heard and McDonald Islands on the Kerguelen Plateau, southern Indian Ocean. *Earth Space Sci.* **7**, e2019EA000695. https://doi.org/10.1029/2019EA000695 (2020).

32. Cao, S. *et al.* Structure and function of the Arctic and Antarctic marine microbiota as revealed by metagenomics. *Microbiome.* **8**, 47. https://doi.org/10.1186/s40168-020-00826-9 (2020).
33. Wang, L.-Y. *et al.* Comparison of bacterial community in aqueous and oil phases of water-flooded petroleum reservoirs using pyrosequencing and clone library approaches. *Appl. Microbiol. Biotechnol.* **98**, 4209–4221. https://doi.org/10.1007/s00253-013-5472-y (2014).
34. Gutierrez, T., Berry, D., Teske, A. & Aitken, M. D. Enrichment of Fusobacteria in sea surface oil slicks from the Deepwater Horizon oil spill. *Microorganisms.* **4**, 24. https://doi.org/10.3390/microorganisms4030024 (2016).
35. Michelou, V. K., Caporaso, J. G., Knight, R. & Palumbi, S. R. The ecology of microbial communities associated with *Macrocystis pyrifera*. *PLoS ONE* **8**, e67480. https://doi.org/10.1371/annotation/48e29578-a073-42e7-bca4-2f96a5998374 (2013).
36. Florez, J. Z. *et al.* Structure of the epiphytic bacterial communities of *Macrocystis pyrifera* in localities with contrasting nitrogen concentrations and temperature. *Algal Res.* **44**, 101706. https://doi.org/10.1016/j.algal.2019.101706 (2019).
37. Minich, J. J. *et al.* Elevated temperature drives kelp microbiome dysbiosis, while elevated carbon dioxide induces water microbiome disruption. *PLoS ONE* **13**, e0192772. https://doi.org/10.1371/journal.pone.0192772 (2018).
38. Lin, J. D., Lemay, M. A. & Parfrey, L. W. Diverse bacteria utilize alginate within the microbiome of the giant kelp *Macrocystis pyrifera*. *Front. Microbiol.* **9**, 1914. https://doi.org/10.3389/fmicb.2018.01914 (2018).
39. Pierce, M. L. & Ward, J. E. Microbial ecology of the Bivalvia, with an emphasis on the family Ostreidae. *J. Shellfish Res.* **37**, 793–806. https://doi.org/10.2983/035.037.0410 (2018).
40. Pierce, M. L. & Ward, J. E. Gut Microbiomes of the Eastern Oyster (*Crassostrea virginica*) and the Blue Mussel (*Mytilus edulis*): Temporal variation and the influence of marine aggregate-associated microbial communities. *mSphere.* **4**, e00730-19. https://doi.org/10.1128/mSphere.00730-19 (2019).
41. Delille, D. & Gleizon, F. Distribution of enteric bacteria in Antarctic seawater surrounding the Port-aux-Francais permanent station (Kerguelen Island). *Mar. Pollut. Bull.* **46**, 1179–1183. https://doi.org/10.1016/S0025-326X(03)00164-4 (2003).
42. Nguyen, T. V. & Alfaro, A. C. Metabolomics investigation of summer mortality in New Zealand Greenshell mussels (*Perna canaliculus*). *Fish Shellfish Immunol.* **106**, 783–791. https://doi.org/10.1016/j.fsi.2020.08.022 (2020).
43. Vezzulli, L. *et al.* Comparative 16SrDNA gene-based microbiota profiles of the Pacific oyster (*Crassostrea gigas*) and the Mediterranean Mussel (*Mytilus galloprovincialis*) from a shellfish farm (Ligurian Sea, Italy). *Microb. Ecol.* **75**, 495–504. https://doi.org/10.1007/s00248-017-1051-6 (2018).
44. Romalde, J. L., Diéguez, A. L., Lasa, A. & Balboa, S. New Vibrio species associated to molluscan microbiota: A review. *Front. Microbiol.* **4**, 413. https://doi.org/10.3389/fmicb.2013.00413 (2014).
45. Narayan, N. R. *et al.* Piphillin predicts metagenomic composition and dynamics from DADA2-corrected 16S rDNA sequences. *BMC Genom.* **21**, 56. https://doi.org/10.1186/s12864-019-6427-1 (2020).
46. Peng, W. *et al.* Integrated 16S rRNA sequencing, metagenomics, and metabolomics to characterize gut microbial composition, function, and fecal metabolic phenotype in non-obese type 2 diabetic Goto-Kakizaki rats. *Front. Microbiol.* **10**, 3141. https://doi.org/10.3389/fmicb.2019.03141 (2020).
47. Koner, S. *et al.* Assessment of carbon substrate catabolism pattern and functional metabolic pathway for microbiota of limestone caves. *Microorganisms* **9**, 1789. https://doi.org/10.21203/rs.3.rs-549787/v1 (2021).
48. Li, Y. F. *et al.* Temperature elevation and *Vibrio cyclitrophicus* infection reduce the diversity of haemolymph microbiome of the mussel *Mytilus coruscus*. *Sci. Rep.* **9**, 16391. https://doi.org/10.1038/s41598-019-52752-y (2019).
49. Scanes, E. *et al.* Climate change alters the haemolymph microbiome of oysters. *Mar. Pollut. Bull.* **164**, 111991. https://doi.org/10.1016/j.marpolbul.2021.111991 (2021).
50. Hylander, B. L. & Repasky, E. A. Temperature as a modulator of the gut microbiome: What are the implications and opportunities for thermal medicine?. *Int. J. Hyperth.* **36**, 83–89. https://doi.org/10.1080/02656736.2019.1647356 (2019).
51. Lo Giudice, A. *et al.* Marine bacterioplankton diversity and community composition in an antarctic coastal environment. *Microb. Ecol.* **63**, 210–223. https://doi.org/10.1007/s00248-011-9904-x (2012).
52. Yumoto, I. *et al.* Temperature and nutrient availability control growth rate and fatty acid composition of facultatively psychrophilic Cobetia marina strain L-2. *Arch. Microbiol.* **181**, 345–351. https://doi.org/10.1007/s00203-004-0662-8 (2004).
53. Weingarten, E. A., Atkinson, C. L. & Jackson, C. R. The gut microbiome of freshwater Unionidae mussels is determined by host species and is selectively retained from filtered seston. *PLoS ONE* **14**, e0224796. https://doi.org/10.1371/journal.pone.0224796 (2019).
54. Rosa, M., Ward, J. E. & Shumway, S. E. Selective capture and ingestion of particles by suspension-feeding bivalve molluscs: A review. *J. Shellfish Res.* **37**, 727–746. https://doi.org/10.2983/035.037.0405 (2018).
55. Griffiths, C. L. & King, J. A. Some relationships between size, food availability and energy balance in the ribbed mussel *Aulacomya ater*. *Mar. Biol.* **51**, 141–149. https://doi.org/10.1007/BF00555193 (1979).
56. Riisgård, H. U. Filtration rate and growth in the blue mussel, *Mytilus edulis* Linneaus, 1758: Dependence on algal concentration. *J. Shellfish Res.* **10**, 29–36 (1991).
57. Sonier, R. *et al.* Picophytoplankton contribution to *Mytilus edulis* growth in an intensive culture environment. *Mar. Biol.* **163**, 73. https://doi.org/10.1007/s00227-016-2845-7 (2016).
58. Jacobs, P., Troost, K., Riegman, R. & Van der Meer, J. Length-and weight-dependent clearance rates of juvenile mussels (*Mytilus edulis*) on various planktonic prey items. *Helgol. Mar. Res.* **69**, 101–112. https://doi.org/10.1007/s10152-014-0419-y (2015).
59. Ward, J. E. & Shumway, S. E. Separating the grain from the chaff: Particle selection in suspension- and deposit-feeding bivalves. *J. Exp. Mar.* **300**, 83–130. https://doi.org/10.1016/j.jembe.2004.03.002 (2004).
60. Waite, A. M., Safi, K. A., Hall, J. A. & Nodder, S. D. Mass sedimentation of picoplankton embedded in organic aggregates. *Limnol. Oceanogr.* **45**, 87–97. https://doi.org/10.4319/lo.2000.45.1.0087 (2000).
61. Ward, J. E. & Kach, D. J. Marine aggregates facilitate ingestion of nanoparticles by suspension-feeding bivalves. *Mar. Environ. Res.* **68**, 137–142. https://doi.org/10.1016/j.marenvres.2009.05.002 (2009).
62. Ward, J. E. Biodynamics of suspension-feeding in adult bivalve molluscs: Particle capture, processing, and fate. *Invertebr. Biol.* **115**, 218–231. https://doi.org/10.2307/3226932 (1996).
63. Rosa, M. *et al.* Physicochemical surface properties of microalgae and their combined effects on particle selection by suspension-feeding bivalve molluscs. *J. Exp. Mar.* **486**, 59–68. https://doi.org/10.1016/j.jembe.2016.09.007 (2017).
64. Allam, B. & Espinosa, E. P. Bivalve immunity and response to infections: Are we looking at the right place?. *Fish Shellfish Immunol.* **53**, 4–12. https://doi.org/10.1016/j.fsi.2016.03.037 (2016).
65. Barr, J. J. *et al.* Bacteriophage adhering to mucus provide a non-host-derived immunity. *Proc. Natl. Acad. Sci. USA* **110**, 10771–10776. https://doi.org/10.1073/pnas.1305923110 (2013).
66. Allam, B. & Espinosa, E. P. Mucosal immunity in mollusks. In *Mucosal Health in Aquaculture* (eds Beck, B. H. & Peatman, E.) 325–370 (Academic Press, 2015).
67. Huang, J. *et al.* Hemocytes in the extrapallial space of *Pinctada fucata* are involved in immunity and biomineralization. *Sci. Rep.* **8**, 4657. https://doi.org/10.1038/s41598-018-22961-y (2018).
68. Kim, H. J. *et al.* Isolation and characterization of two bacteriophages and their preventive effects against pathogenic *Vibrio coralliilyticus* causing mortality of Pacific oyster (*Crassostrea gigas*) larvae. *Microorganisms.* **8**, 926. https://doi.org/10.3390/microorganisms8060926 (2020).

69. Ihara, H. *et al.* Sulfur-oxidizing bacteria mediate microbial community succession and element cycling in launched marine sediment. *Front. Microbiol.* **8**, 152. https://doi.org/10.3389/fmicb.2017.00152 (2017).
70. Jørgensen, B. B. & Nelson, D. C. Sulfide oxidation in marine sediments: Geochemistry meets microbiology. *Geol. S. Am. S.* **379**, 63–81. https://doi.org/10.1130/0-8137-2379-5.63 (2004).
71. Zhou, M. *et al.* Surface currents and upwelling in Kerguelen Plateau regions. *Biogeosci. Discuss.* **11**, 6845–6876. https://doi.org/10.5194/bgd-11-6845-2014 (2014).
72. Gille, S. T., Carranza, M. M., Cambra, R. & Morrow, R. Wind-induced upwelling in the Kerguelen Plateau region. *Biogeosciences* **11**, 6389–6400. https://doi.org/10.5194/bg-11-6389-2014 (2014).
73. Park, Y. H., Roquet, F., Durand, I. & Fuda, J. L. Large-scale circulation over and around the Northern Kerguelen Plateau. *Deep Sea Res.* **II**(55), 566–581. https://doi.org/10.1016/j.dsr2.2007.12.030 (2008).
74. Renac, C. *et al.* Hydrothermal fluid interaction in basaltic lava units, Kerguelen Archipelago (SW Indian Ocean). *Eur. J.* **22**, 215–234. https://doi.org/10.1127/0935-1221/2009/0022-1993 (2010).
75. Vancanneyt, M. *et al. Sphingomonas alaskensis* sp. nov., a dominant bacterium from a marine oligotrophic environment. *Int. J. Syst. Evol.* **51**, 73–79. https://doi.org/10.1099/00207713-51-1-73 (2001).
76. Helmuth, B. S. & Hofmann, G. E. Microhabitats, thermal heterogeneity, and patterns of physiological stress in the rocky intertidal zone. *Biol. Bull.* **201**, 374–384. https://doi.org/10.2307/1543615 (2001).
77. Testut, L., Wöppelmann, G., Simon, B. & Téchiné, P. The sea level at Port-aux-Français, Kerguelen Island, from 1949 to the present. *Ocean Dyn.* **56**, 464–472. https://doi.org/10.1007/s10236-005-0056-8 (2006).
78. Pohl, B. *et al.* Recent climate variability around the Kerguelen Islands (Southern Ocean) seen through weather regimes. *J. Appl. Meteorol. Climatol.* **60**, 711–731. https://doi.org/10.1175/JAMC-D-20-0255.1 (2021).
79. PROTEKER. *Ilôt Channer (Passe Royale)—Sea water temperature at 5 and 13 m depth (T°C) daily average 2014–2019.* https://www.proteker.net/swt-ilot-channer-passe-royale/ (2021).
80. Caza, F. *et al.* Comparative analysis of hemocyte properties from *Mytilus edulis* desolationis and *Aulacomya ater* in the Kerguelen Islands. *Mar. Environ. Res.* **110**, 174–182. https://doi.org/10.1016/j.marenvres.2015.09.003 (2015).
81. Caza, F., Cledon, M. & St-Pierre, Y. Biomonitoring climate change and pollution in marine ecosystems: A review on Aulacomya ater. *J. Mar. Biol.* **2016**, 7183813. https://doi.org/10.1155/2016/7183813 (2016).
82. Rey-Campos, M. *et al.* High individual variability in the transcriptomic response of Mediterranean mussels to Vibrio reveals the involvement of myticins in tissue injury. *Sci. Rep.* **9**, 3569. https://doi.org/10.1038/s41598-019-39870-3 (2019).
83. Caza, F. *et al.* Hemocytes released in seawater act as Trojan horses for spreading of bacterial infections in mussels. *Sci. Rep.* **10**, 19696. https://doi.org/10.1038/s41598-020-76677-z (2020).
84. Yao, C. L. & Somero, G. N. Thermal stress and cellular signaling processes in hemocytes of native (*Mytilus californianus*) and invasive (*M. galloprovincialis*) mussels: Cell cycle regulation and DNA repair. *Comp. Biochem. Physiol.* **165**, 159–168. https://doi.org/10.1016/j.cbpa.2013.02.024 (2013).
85. Lockwood, B. L., Sanders, J. G. & Somero, G. N. Transcriptomic responses to heat stress in invasive and native blue mussels (genus Mytilus): Molecular correlates of invasive success. *J. Exp. Biol.* **213**, 3548–3558. https://doi.org/10.1242/jeb.046094 (2010).
86. Klindworth, A. *et al.* Evaluation of general 16S ribosomal RNA gene PCR primers for classical and next-generation sequencing-based diversity studies. *Nucleic Acids Res.* **41**, e1. https://doi.org/10.1093/nar/gks808 (2013).
87. Callahan, B. J. *et al.* DADA2: High-resolution sample inference from Illumina amplicon data. *Nat. Methods.* **13**, 581–583. https://doi.org/10.1038/nmeth.3869 (2016).
88. R Core Team. *R: A Language and Environment for Statistical Computing* (R Foundation for Statistical Computing, 2021).
89. McMurdie, P. J. & Holmes, S. phyloseq: An R package for reproducible interactive analysis and graphics of microbiome census data. *PLoS ONE* **8**, e61217. https://doi.org/10.1371/journal.pone.0061217 (2013).
90. Oksanen, J. & Blanchet, F. G. *Vegan: Community Ecology Package*. 2. 3-0 (2015).
91. Ssekagiri, A., Sloan, W. & Ijaz, U. Z. microbiomeSeq: an R package for analysis of microbial communities in an environmental context, In *ISCB Africa ASBCB Conference* (Kumasi, Ghana, 2017).
92. Cao, Y. *Microbiome marker: Microbiome Biomarker Analysis Toolkit*. R package version 0.99.0 (2020). https://github.com/yiluheihei/microbiomeMarker. Accessed March 2022.
93. Kanehisa, M. *et al.* KEGG for integration and interpretation of large-scale molecular data sets. *Nucleic Acids Res.* **40**, D109–D114. https://doi.org/10.1093/nar/gkr988 (2012).
94. Iwai, S. *et al.* Piphillin: Improved prediction of metagenomic content by direct inference from human microbiomes. *PLoS ONE* **11**, e0166104. https://doi.org/10.1371/journal.pone.0166104 (2016).
95. Dhariwal, A. *et al.* MicrobiomeAnalyst: A web-based tool for comprehensive statistical, visual and meta-analysis of microbiome data. *Nucleic Acids Res.* **45**, W180–W188. https://doi.org/10.1093/nar/gkx295 (2017).

Acknowledgements

This research was performed at Kerguelen with the logistic support of the French Polar Institute Paul-Emile-Victor (IPEV). The authors would like to thank all the personnel from the IPEV and the Terres Australes et Antarctiques Françaises (TAAF) for their help and hospitality during our stays. The authors would also like to thank Jean-Pierre Féral and Thomas Saucède and the PROTEKER team for their expert advice and technical support. The author would also like to thank Ms. Marlène Fortier for her excellent technical help. This work was funded in part by the National Science and Engineering Research Council of Canada (YSP) (Grant No. RGPIN-2019-06607) and the IPEV (YSP and SB).

Author contributions

F.C., S.F., S.B. and Y.S.P. conceived the study. All authors were responsible for interpretation of data and critical appraisal. All authors executed experiments and/or contributed to the experimental design and/or analyses of the results. F.C., S.F, and Y.S.P. drafted the manuscript with input from all authors at all stages.

Competing interests

The authors declare no competing interests.

Additional information

Supplementary Information The online version contains supplementary material available at https://doi.org/10.1038/s41598-022-13774-1.

Correspondence and requests for materials should be addressed to Y.S.-P.

Supplementary material

Species- and site-specific circulating bacterial DNA in Subantarctic sentinel mussels *Aulacomya atra* and *Mytilus platensis*

Sophia Ferchiou[1], France Caza[1], Richard Villemur[1], Stéphane Betoulle[2], and Yves St-Pierre[1].

1) INRS-Centre Armand-Frappier Santé Technologie, 531 Boul. des Prairies, Laval, QC, Canada, H7V 1B7

2) Université Reims Champagne-Ardenne, UMR-I 02 SEBIO Stress environnementaux et Biosurveillance des milieux aquatiques, Campus Moulin de la Housse, 51687 Reims, France.

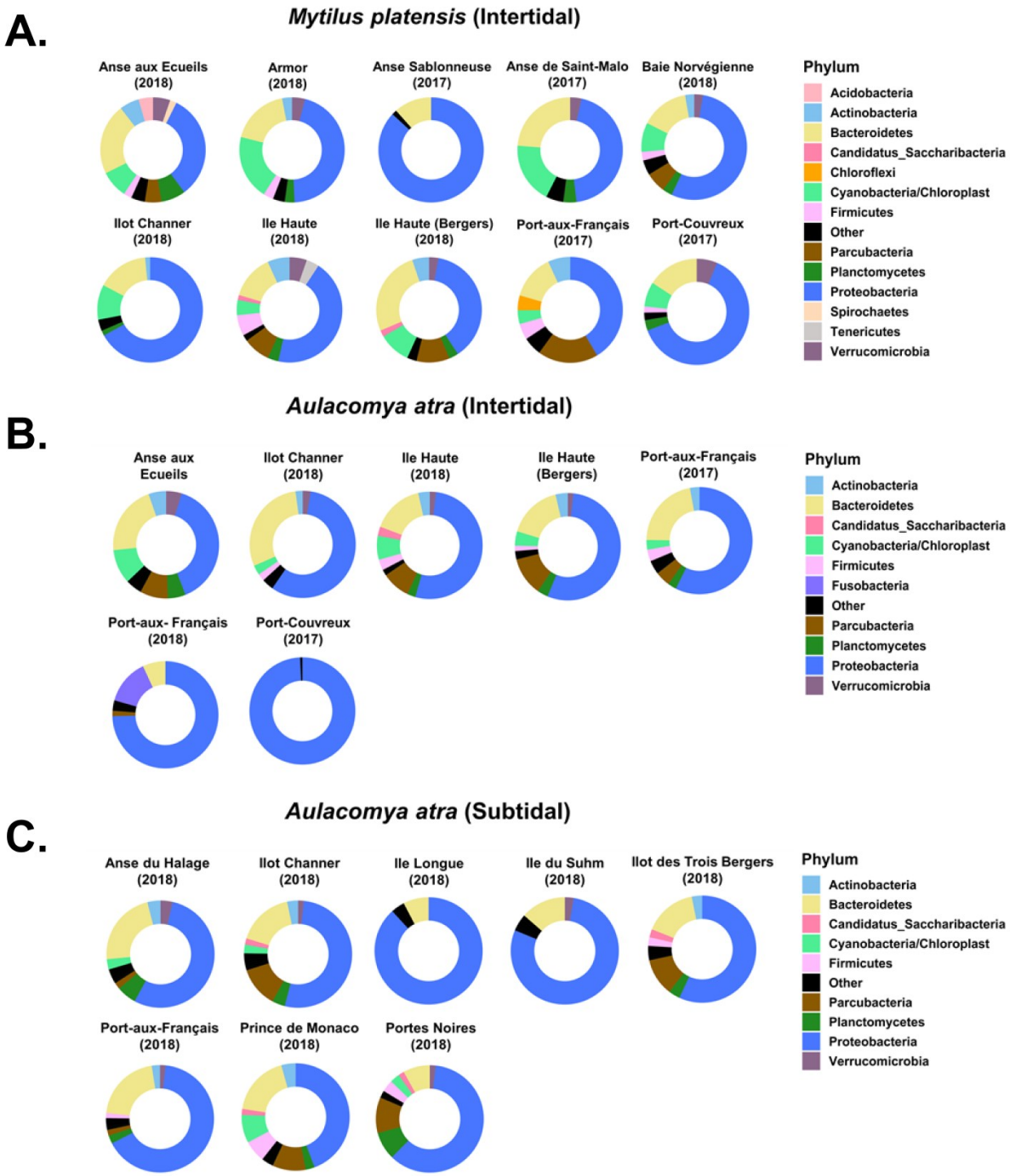

Supp. Figure S1: Pie charts summarizing the phylum-level microbiota composition of the hemolymph of *Mytilus platensis* and *Aulacomya atra* in intertidal sites (A-B) and (C) of *Aulacomya atra* in subtidal sites during 2017 and 2018. Phylum with a relative abundance of ≤ 1.5% are represented as "Other".

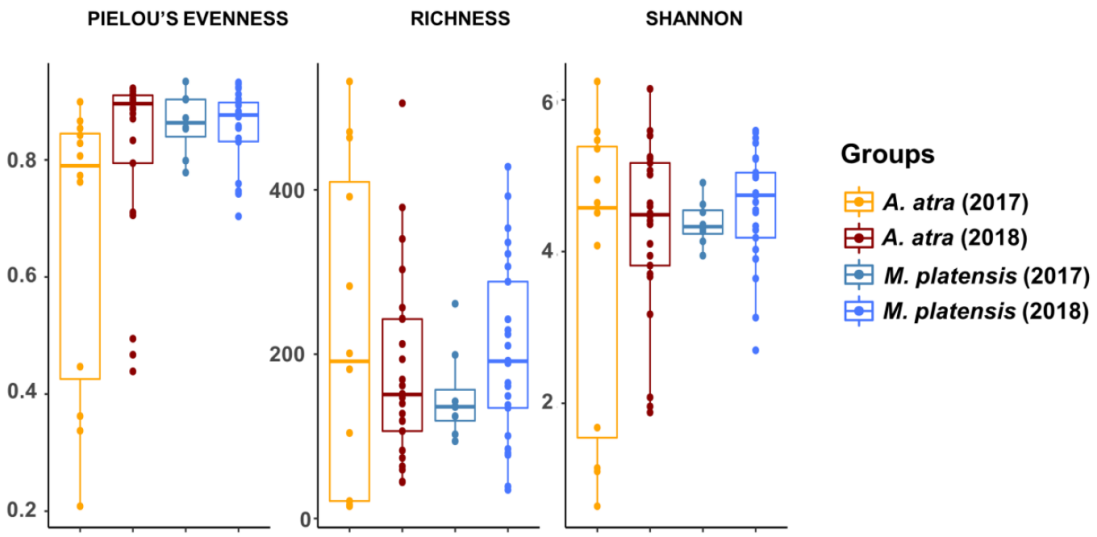

Supp. Figure S2: Box plots of alpha diversity of *Aulacomya atra* and *Mytilus platensis* hemolymph microbiota in mixed mussel beds in 2017 and 2018. Species evenness, observed richness and Shannon diversity indexes were calculated for each groups. No significant differences ($p < 0.05$) were observed between groups.

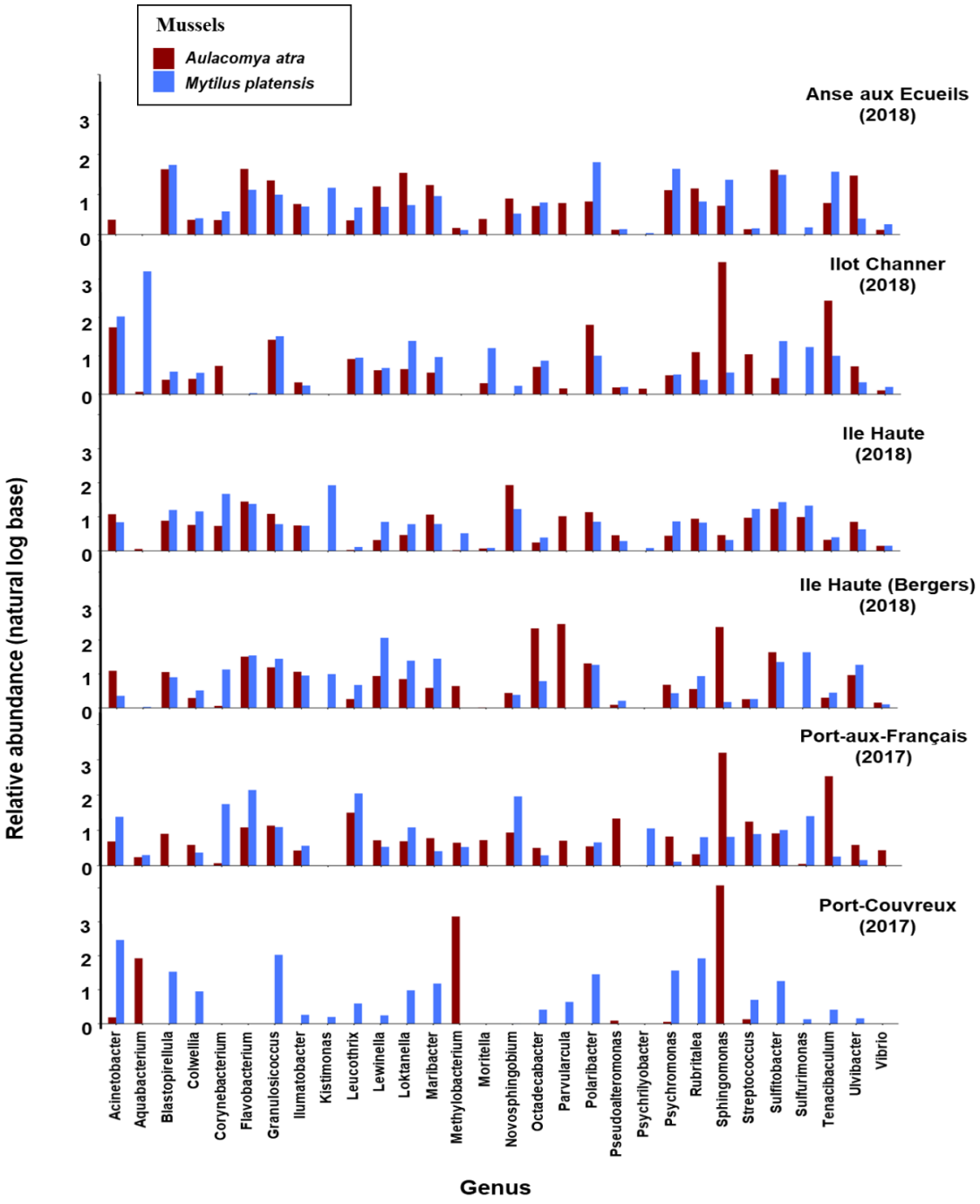

Supp. Figure 3: Bar graphs showing the relative abundance (natural logarithm base) of the top 30 bacterial genera of circulating microbiota in mixed mussel beds. All samples were collected in 2017 and 2018. Red color represents *Aulacomya atra* and blue color represents *Mytilus platensis* specimens.

Chapitre 3

Application du concept de biopsie liquide pour surveiller la biodiversité microbienne des écosystèmes côtiers marins

Article publié: *ISME Communications* 2022, 2(1):61

Résumé

La biopsie liquide (BL) est un concept qui gagne rapidement du terrain dans le domaine biomédical. Ce concept repose en grande partie sur la détection de fragments d'ADN libre circulant (ccfDNA) qui sont principalement libérés sous forme de petits fragments suite à la mort cellulaire dans divers tissus. Un petit pourcentage de ces fragments provient de tissus ou d'organismes étrangers (ADN du non-soi). Dans ce travail, nous avons appliqué ce concept aux moules, une espèce sentinelle connue pour sa grande capacité de filtration de l'eau de mer. Nous avons exploité la capacité des moules à agir comme des filtres naturels pour capturer des fragments d'ADN environnemental de différentes origines afin de fournir des informations sur la biodiversité des écosystèmes marins et côtiers. Nos résultats ont montré que l'hémolymphe des moules contient des fragments d'ADN dont la taille varie considérablement, allant de 1 à 5 kb. Le séquençage aléatoire *shotgun* a révélé qu'une quantité significative de fragments d'ADN avait une origine microbienne. Parmi ceux-ci, nous avons trouvé des fragments d'ADN provenant de bactéries, d'archées et de virus, y compris des virus connus pour infecter une variété d'hôtes qui peuplent couramment les écosystèmes marins et côtiers. En somme, notre étude démontre que l'application du concept de BL aux moules offre une source de connaissances riche et encore inexplorée concernant la biodiversité microbienne d'un écosystème marin et côtier.

Contribution des auteurs

Yves St-Pierre, France Caza, Philippine Granger Joly de Boissel et moi avons conçu l'étude. France et moi avons mené toutes les expériences et nous avons également effectué toutes les analyses bio-informatiques et statistiques de cet article. Tous les auteurs ont pris part à l'interprétation des données et à leur évaluation critique. Le manuscrit a été rédigé par France, Yves et moi, bénéficiant des contributions et de l'approbation de tous les auteurs à chaque étape du processus.

ISME

www.nature.com/ismecomms

ARTICLE OPEN

Applying the concept of liquid biopsy to monitor the microbial biodiversity of marine coastal ecosystems

Sophia Ferchiou[1,2], France Caza[1,2], Philippine Granger Joly de Boissel[1], Richard Villemur[1] and Yves St-Pierre[1]✉

Liquid biopsy (LB) is a concept that is rapidly gaining ground in the biomedical field. Its concept is largely based on the detection of circulating cell-free DNA (ccfDNA) fragments that are mostly released as small fragments following cell death in various tissues. A small percentage of these fragments are from foreign (nonself) tissues or organisms. In the present work, we applied this concept to mussels, a sentinel species known for its high filtration capacity of seawater. We exploited the capacity of mussels to be used as natural filters to capture environmental DNA fragments of different origins to provide information on the biodiversity of marine coastal ecosystems. Our results showed that hemolymph of mussels contains DNA fragments that varied considerably in size, ranging from 1 to 5 kb. Shotgun sequencing revealed that a significant amount of DNA fragments had a nonself microbial origin. Among these, we found DNA fragments derived from bacteria, archaea, and viruses, including viruses known to infect a variety of hosts that commonly populate coastal marine ecosystems. Taken together, our study shows that the concept of LB applied to mussels provides a rich and yet unexplored source of knowledge regarding the microbial biodiversity of a marine coastal ecosystem.

ISME Communications; https://doi.org/10.1038/s43705-022-00145-0

INTRODUCTION

Climate change (CC) impacts on the biodiversity of marine ecosystems are a rapidly evolving field of research. Global warming not only induces important physiological stress but also pushes the evolutionary limit of thermal tolerance of marine organisms, affecting the habitat of several species and pushing them to find more favorable conditions [1, 2]. In addition to its impact on the biodiversity of metazoans, CC also disrupts the delicate balance of host-microbe interactions. Such microbial dysbiosis is a major threat to marine ecosystems as it makes marine life more susceptible to infectious pathogens [3, 4]. CC is believed to play an important role in mass mortality events, a major concern for the management of marine ecosystems worldwide [5, 6]. This is an important issue given the economic, ecological, and nutritional impacts of many marine species. This is particularly true for bivalves found in polar regions where the effects of CC are more immediate and severe [6, 7]. In fact, bivalves, such as *Mytilus* spp., have been extensively used for monitoring the impact of CC in marine ecosystems. Not surprisingly, a relatively large number of biomarkers have been developed to monitor their health status, often using a two-tier approach that includes functional biomarkers based on enzymatic activities or cellular functions, such as cell viability and phagocytic activity [8]. These approaches also include measuring concentrations of specific stress indicators that accumulate in their soft tissues following uptake of high amounts of seawater. However, the high filtering capacities and the semi-open circulatory system of bivalves offer an opportunity to develop novel hemolymphatic biomarkers that exploit the concept of liquid biopsy (LB), a simple and minimally invasive approach used by clinicians for patient management based on a simple sample of blood [9, 10]. Although several types of circulating molecules can be detected in human LB, the concept is largely based on DNA sequencing analysis of circulating cell-free DNA (ccfDNA) fragments in plasma. In fact, the existence of DNA circulating in human plasma has been known since the middle of the 20th century [11], but it is only in recent years that the advent of high-throughput sequencing methods has led to clinical diagnostics based on ccfDNA. The presence of these circulating DNA fragments results in part from a passive release of genomic DNA (nuclear and mitochondrial) following cell death. In healthy individuals, the concentration of ccfDNA is normally low (<10 ng/mL) but can be increased by 5–10 times in patients suffering from various pathologies or subjected to stress, resulting in tissue damage. The size of ccfDNA fragments varies considerably but generally range from 150 to 200 bp [12]. Analysis of ccfDNA of *self-origin*, i.e., derived from host normal or transformed cells can be used to detect genetic and epigenetic alterations present in nuclear and/or mitochondrial genomes, thereby helping clinicians choose among specific molecularly targeted therapies [13]. However, ccfDNA can be derived from a *nonself* origin, such as ccfDNA derived from fetal cells during pregnancy or from transplanted organs [14–17]. ccfDNA is also an important source of information for detecting the presence of nucleic acids from infectious agents (*nonself*), thus making it possible to noninvasively detect a wide range of infections that are not identified by blood culture, avoiding invasive biopsy of infected tissues [18]. Recent studies have indeed

[1]INRS-Centre Armand-Frappier Santé Biotechnologie, Laval, Québec H7V 1B7, Canada. [2]These authors contributed equally: Sophia Ferchiou, France Caza.
✉email: yves.st-pierre@inrs.ca

Received: 12 January 2022 Revised: 28 June 2022 Accepted: 8 July 2022
Published online: 27 July 2022

shown that human blood contains a rich source of information for the identification of viral and bacterial pathogens and that ~1% of ccfDNA found in human plasma has a nonself origin [19]. These studies suggest that it is possible to assess the biodiversity of the circulating microbiome of an organism from the analysis of ccfDNA. Until very recently, however, this concept has exclusively been applied and studied in humans and, to a lesser extent, to other vertebrates [20, 21].

In the present work, we have taken advantage of the potential of LB to analyze the ccfDNA of *Aulacomya atra*, a southern species of mussels commonly found in the sub-Antarctic Kerguelen Archipelago, a group of islands located at the top of a large plateau that was built by volcanic eruptions 35 million years ago. Using an in vitro experimental system, we found that DNA fragments present in seawater are rapidly taken up by mussels and gain access to the hemolymphatic compartments. Shotgun sequencing showed that hemolymphatic ccfDNA of mussels contains DNA fragments of both self and nonself origin and included symbiotic bacteria as well as DNA fragments derived from biological communities that are typical of cold volcanic marine coastal ecosystems. Hemolymphatic ccfDNA also contained viral sequences derived from viruses with distinct host ranges. We also found DNA fragments derived from metazoans, such as bony fish, anemones, algae, and insects. Taken together, our study demonstrates that the concept of LB can be successfully applied to marine invertebrates to access a rich genomic reservoir within a marine ecosystem.

MATERIALS AND METHODS

Mussel collection

Adult specimens (55–70 mm length) of *Mytilus platensis* (*M. platensis*) and *Aulacomya atra* (*A. atra*) were collected on the intertidal rocky shore of Port-aux-Français (049°21.235S, 070°13.490E) at Kerguelen Islands in December 2018. Other adult blue mussels (*Mytilus spp.*) were obtained from a commercial supplier (PEI Mussel King Inc., Prince Edward Islands, Canada) and placed in a temperature-controlled (4 °C) aerated tank containing 10–20 L of 32‰ artificial saline water (Reef Crystal artificial marine salt, Instant Ocean, VA, USA). For each experiment, individual shell lengths and weights were measured.

Circulating cell-free DNA extraction

A free and open access protocol for the procedure is available online (https://doi.org/10.17504/protocols.io.81wgb6z9olpk/v1). Briefly, hemolymphatic LBs were collected from the abductor muscle as described [22]. The hemolymph was clarified by centrifugation at 1200 × *g* for 3 min, and the supernatant was frozen (−20 °C) until use. To isolate and purify ccfDNA, samples (1.5–2.0 mL) were thawed and processed using the NucleoSnap cfDNA kit (Macherey-Nagel, Bethlehen, PA) according to the manufacturer's instructions. The ccfDNA was stored at −80 °C until further analysis. In some experiments, ccfDNA was extracted and purified using the QIAamp DNA Investigator Kit (QIAGEN, Toronto, ON, Canada). Purified DNA was quantified by standard PicoGreen assay. The fragment distribution of the extracted ccfDNA was analyzed by capillary electrophoresis with an Agilent 2100 Bioanalyzer (Agilent Technologies Inc., Santa Clara, CA) using a High Sensitivity DNA kit. The assay was performed according to the manufacturer's instructions using 1 µL of ccfDNA sample.

Sequence analysis pipeline

To sequence the hemolymphatic ccfDNA fragments, shotgun libraries were prepared by Génome Québec (Montreal, Quebec, Canada) using the Illumina DNA Mix set for Illumina MiSeq PE75. Standard adapters (BioO) were used. Raw data files are available on the NCBI Sequence Read Archive (SRR8924808 and SRR8924809). Basic read quality was assessed using FastQC [23]. The adapters and low-quality reads were trimmed with Trimmomatic [24]. The paired-end shotgun reads were merged into longer single reads with FLASH with a minimum overlap of 20 bp to avoid mismatches [25]. Merged reads were annotated with BLASTN using a bivalve NCBI Taxonomy database (*e* value < $1e^{-3}$ and 90% homology), and masking of low-complexity sequences was performed using DUST [26]. Reads were divided into two groups: those that were related to bivalve sequences (here named *self* reads) and those not (*nonself* reads). Both groups were assembled separately with MEGAHIT to generate contigs [27]. In parallel, the taxonomic distribution of microbiome nonself reads was classified with Kraken2 [28] and represented graphically with a Krona pie chart on Galaxy [29, 30]. Optimal kmers were determined from our preliminary experiments as kmers-59. Self contigs were then identified by alignment with BLASTN (bivalve NCBI database, *e* value < $1e^{-10}$ and 60% homology) for a final annotation. In parallel, nonself group contigs were annotated with BLASTN (nt NCBI database, *e* value < $1e^{-10}$ and 60% homology). BLASTX was also conducted on nonself contigs using the nr and RefSeq protein NCBI databases (*e* value < $1e^{-10}$ and 60% homology). A pool of BLASTN and BLASTX from nonself contigs represented the final set of contigs (see supplementary file).

PCR amplification

The primers used for PCR are listed in Table S1. Taq DNA polymerase (Bio Basic Canada, Markham, ON) was used to amplify ccfDNA targeted genes. The following reaction conditions were employed: denaturation at 95 °C for 3 min; 35 cycles of 95 °C for 1 min, the prescribed annealing temperature for 1 min and elongation at 72 °C for 1 min; and a final 72 °C for 10 min. PCR products were separated by electrophoresis in agarose gels (1.5%) containing SYBR™ Safe DNA Gel Stain (Invitrogen, Burlington, ON, Canada) at 95 V.

DNA uptake by mussels

Mussels (*Mytilus* spp.) were acclimated in 500 mL of oxygenated seawater (32 PSU) at 4 °C for 24 h. Plasmidic DNA containing an insert encoding the cDNA sequence of the human galectin-7 gene (NCBI Accession number L07769) was added to the tank at a final concentration of 190 pg/µL. Controls included mussels incubated under the same conditions without the addition of DNA. A third control tank contained DNA without mussels. To track the quality of DNA in seawater, samples (20 µL; triplicates) of seawater were withdrawn from each tank at the indicated times. To track plasmid DNA in mussels, LBs were collected at the indicated times and analyzed by qPCR and ddPCR. Given the high salt levels in seawater, the aliquots were diluted in PCR quality water (1:10) before all PCR analyses.

Digital droplet PCR

Digital droplet PCR (ddPCR) was performed using the QX200 BioRad (Mississaugua, ON, Canada) protocol. Optimal temperatures were established using temperature curves (Table S1). Droplets were generated with a QX200 droplet generator (BioRad). ddPCR was performed as follows: 95 °C for 5 min; 50 cycles of 95 °C for 30 s and the indicated annealing temperature for 1 min and 72 °C for 30 s; 4 °C for 5 min; and 90 °C for 5 min. Droplet number and positive reactions (copies/µL) were measured with a QX200 droplet reader (BioRad). Samples with fewer than 10,000 droplets were rejected. No template control was carried out on each run of ddPCR.

Real-time qPCR

qPCR was performed using Rotor-Gene® 3000 (Corbett Research, Sydney, Australia) with *LGALS7*-specific primers. All qPCRs were performed in 20 µL with the QuantiFast SYBR Green PCR Kit (QIAGEN). The qPCRs were initiated with a 15-min incubation at 95 °C followed by 40 cycles of 95 °C for 10 s and 60 °C for 60 s with a single acquisition. A melting curve was generated at the end of the qPCR using 95 °C for 5 s, 65 °C for 60 s and 97 °C with continuous acquisition. Each qPCR was performed in triplicate, and no template controls were included.

RESULTS

Uptake of DNA by mussels

Because mussels are known for their high filtration rate capacity, we first studied whether they can filter and retain DNA fragments present in seawater. We were also interested in whether these fragments accumulate in their semi-open hemolymphatic system. We addressed this issue experimentally by tracking the fate of soluble DNA fragments added to aquariums containing blue mussels. To facilitate the tracking of the DNA fragments, we used foreign (nonself) plasmid DNA containing the human galectin-7 gene. Tracking of plasmidic DNA fragments in seawater and mussels was followed by ddPCR. Our results showed that although

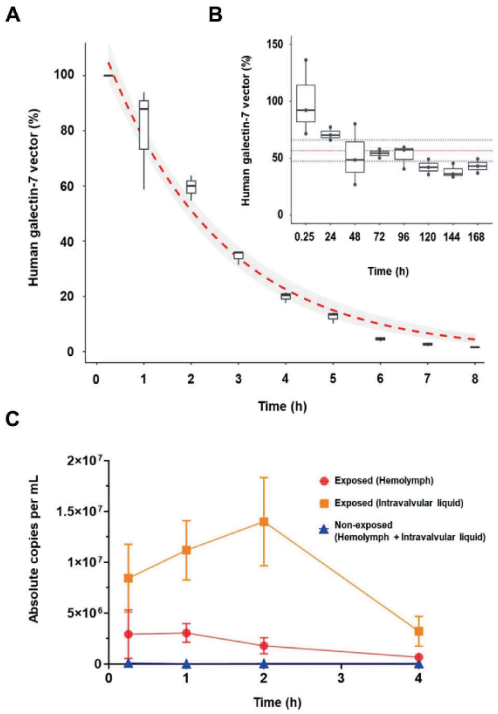

Fig. 1 Experimental accumulation of nonself in mussels. Relative concentration of plasmidic DNA in seawater in presence (**A**) or absence (**B**) of mussels as measured by ddPCR. In **A**, the results are expressed as percentages and the limits of the box represent the 75th and 25th percentiles. A fitted logarithmic curve is represented in red with a gray shade area that represents the 95% confidence interval. In **B**, the red line indicates the mean value and blue lines represent the 95% confidence interval of the concentrations. **C** Accumulation of the plasmidic DNA in the hemolymph and intravalvular fluid of mussels at different time post-addition of plasmidic DNA. The results are shown as absolute number of copies/mL detected (±SE).

the amount of DNA fragments remained relatively stable over time (up to 7 days) in seawater in the absence of mussels, the levels almost completely disappeared within 8 h in the presence of mussels (Fig. 1a, b). Exogenous DNA fragments were readily detectable within 15 min in both intravalvular fluids and hemolymph (Fig. 1c). These fragments were still detected up to 4 h postexposure. Such filtering activity for DNA fragments is comparable to that reported for filtration of bacteria and algae [31]. These results suggest that mussels can filter and accumulate exogenous DNA in their fluidic compartments.

Hemolymphatic ccfDNA in mussels

We next studied the origin of ccfDNA in mussels collected in a mussel bed at Kerguelen Islands, a remote group of islands with limited anthropogenic impact. For this purpose, hemolymphatic ccfDNA from mussels was isolated and purified using methods that are commonly employed for purification of human ccfDNA [32, 33]. We found that the mean hemolymphatic ccfDNA concentrations in mussels were in the range of low micrograms per mL of hemolymph (see Table S2, supplementary information). Such a range of concentrations is significantly greater than that found in healthy humans (low nanograms per mL); however, ccfDNA levels in cancer patients can reach several micrograms per mL in rare cases [34, 35]. Analysis of the size distribution of hemolymphatic ccfDNA showed that these fragments varied considerably in size, ranging from 1000 bp to 5000 bp (Fig. 2). Similar results were obtained using the silica-based QIAamp Investigator kit, a method commonly used in forensic science to rapidly isolate and purify genomic DNA from samples at low DNA concentrations, including ccfDNA [36].

Shotgun sequencing of hemolymphatic ccfDNA

In humans and primates, ~1% of ccfDNA has a nonself origin [21, 37]. Given the semi-open circulatory system of bivalves, the microorganism-rich seawater, and the size profile of mussel ccfDNA, we hypothesized that hemolymphatic ccfDNA of mussels is likely to contain a rich and diverse reservoir of microbial DNA. To test this hypothesis, we performed shotgun sequencing of hemolymphatic ccfDNA of *Aulacomya atra* specimens collected at Kerguelen Islands, generating more than 10 million reads, of which 97.6% passed quality control. Reads were then classified based on self and nonself origins using BLASTN and the NCBI bivalve database (Fig. S1, supplementary information).

ccfDNA of self-origin

In humans, both nuclear and mitochondrial DNA can be released in circulation [38]. In the present study, however, it was not possible to characterize in detail the nuclear genomic DNA of mussels given that the genome of *A. atra* has not yet been sequenced and reported. However, we were able to identify a number of ccfDNA fragments of self-origin using bivalve libraries (Fig. S2, supplementary information). We also confirmed the presence of DNA fragments of self-origin using targeted PCR amplification of those *A. atra* genes that have been sequenced (Fig. 3). Similarly, given that the mitochondrial genome of *A. atra* was available in public databases, it was possible to find evidence of mitochondrial ccfDNA fragments in the hemolymph of *A. atra*. The presence of mitochondrial DNA fragments was confirmed by PCR amplification (Fig. 3).

Bacterial microbiome analysis of ccfDNA using Kraken2

Given the rich microbial content of marine seawater, we initially focused on the characterization of hemolymphatic microbial DNA sequences. For this, we used two distinct strategies. The first strategy employed Kraken2, an algorithm-based sequence classification program, which allows identification of microbial sequences with an accuracy comparable to BLAST and other tools [28]. Greater than 6719 reads were identified to be of bacterial origin, whereas 124 and 64 were of archaeal and viral origins, respectively (Fig. 4). The most prevalent bacterial DNA fragments originated from *Firmicutes* (46%), *Proteobacteria* (27%), and *Bacteroides* (17%) (Fig. 4a). This distribution was consistent with previous microbiome studies in marine blue mussels [39, 40]. *Gammaproteobacteria* were the dominant class of *Proteobacteria* (44%) and included many *Vibrionales* (Fig. 4b). The presence of DNA fragments of the *Vibrio* genus in hemolymphatic ccfDNA of *A. atra* was confirmed by ddPCR (Fig. 4c) [41]. To obtain more information on the bacterial origin of ccfDNA, a complementary approach was used (Figure S2, supplementary information). In this case, reads that overlapped were assembled as paired-end reads and were classified as of self (bivalves) or nonself origin using BLASTN and an *e* value of $1e^{-3}$ and a cutoff with >90% homology. Because the genome of *A. atra* has not yet been sequenced, we used a de novo assembly strategy with the MEGAHIT next-generation sequencing (NGS) assembler. A total of 147 188 contigs were identified as being of nonself (bivalve) origin. These contigs were then blasted using BLASTN and BLASTX using an *e* value of $1e^{-10}$. This strategy allowed us to identify 482 non-bivalve fragments present within the ccfDNA of *A. atra*. Greater than half (57%) of these DNA fragments were of bacterial origin with a

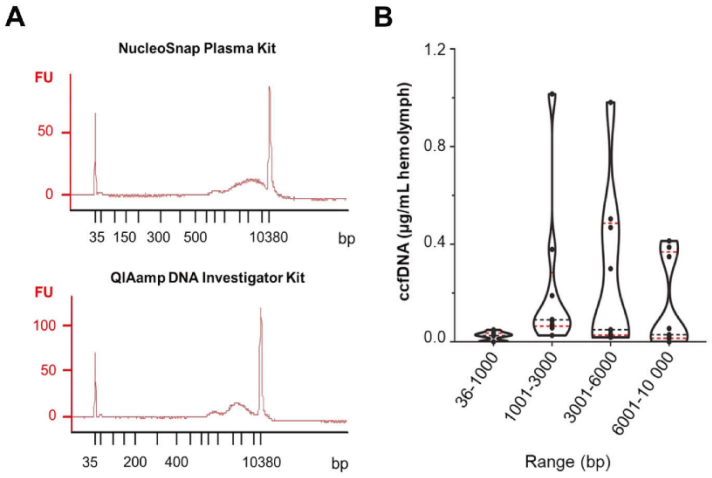

Fig. 2 Fragment size distribution of hemolymphatic ccfDNA in mussels. A Representative electropherograms of the hemolymphatic ccfDNA of *Mytilus sp.* extracted with NucleoSnap Plasma Kit (above) and QIAamp DNA Investigator Kit. **B** Violin plots showing the distribution of the hemolymphatic ccfDNA concentrations (±SE) in mussels. Black and red lines represent the median and the first and third quartiles respectively.

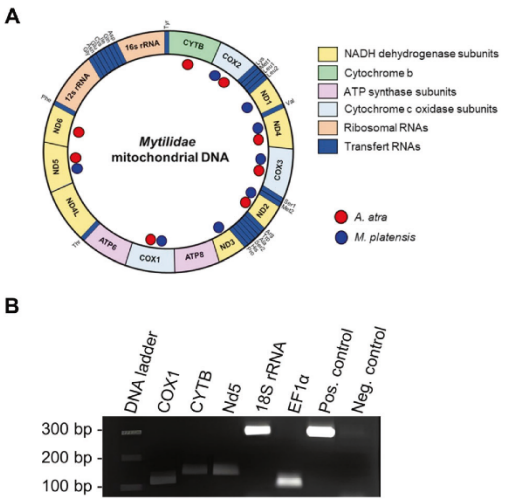

Fig. 3 Validation of DNA fragments of self-origin. A Presence of different mitochondrial genes in the hemolymph of *A. atra* (red points – Accession: SRX5705969) and *M. platensis* (blue points – Accession: SRX5705968) amplified by PCR. Figure was adapted from Breton *et al.*, 2011 **B** Amplifications of hemolymph supernatant from *A. atra* stored on FTA papers. PCR amplifications of HKG 18S rRNA, Elongation factor 1α (EF1α) and mitochondrial genes Cytochrome b (CYTB), Cytochrome c oxidase subunit 1 (COX1), and NADH dehydrogenase subunit 5 (Nd5) were carried out with a 3 mm punch directly added into the PCR tube containing the PCR mix.

majority from gill symbionts that included thiotrophic symbionts and from *Solemya velum* gill symbionts (Fig. 5).

Archeal microbiome

Kraken2 analysis also showed that ccfDNA from mussels contained DNA fragments derived from Archaea, including from *Euryarchaeota* (65%), *Crenarchaeota* (24%), and *Thaurmarcheota* (11%) (Fig. 6a). The presence of DNA fragments derived from *Euryarchaeota* and *Crenarchaeota*, which have previously been found in the microbe assemblage of *Mytilus californicus*, may not be surprising [42]. Although *Euryarchaeota* have been commonly associated with extreme environments, it is now recognized that both *Euryarcheota* and *Crenarcheota* are among the most abundant prokaryotes in oceanic low-temperature environments [43, 44]. The presence of methanothopic microorganisms in mussels is not unexpected given recent reports of widespread methane seeps escaping from the seafloor of the Kerguelen Plateau [45] and the potential microbial methane production observed in coastal areas of Kerguelen Islands [46].

Circulating virome

Our attention was then turned to reads derived from DNA viruses. To our knowledge, this is the first untargeted study of the viral content in mussels. As expected, we found DNA fragments derived from bacteriophages (*Caudovirales*) (Fig. 6b). However, the most prevalent viral DNA originated from the phylum *Nucleocytoviricota*, which is also known as nucleocytoplasmic large DNA viruses (NCLDVs) and harbors the largest genomes among any viruses. Among this phylum, a majority of DNA sequences were derived from *Mimiviridae* (58%) and *Poxviridae* (21%), the natural hosts of which include vertebrates and arthropods, and a lesser extent of these DNA sequences were derived from *Phycodnaviridae*, which are known to infect marine eukaryotic algae. Sequences from *Pandoravirus*, a genus of giant virus with the largest genome size of any known viral genus, were also obtained. Interestingly, the range of hosts known to be infected by viruses that we identified through sequencing of hemolymphatic ccfDNA was relatively large (Figure S3, supplementary information). It includes viruses known to infect insects, such as *Baculoviridae* and *Iridoviridae*, as well as those known to infect amoebae, algae, and vertebrates. We also found sequences that matched genomic sequences of *Pithovirus sibericum*. Pithoviruses (aka "Zombie viruses") were first isolated from a 30,000-year-old permafrost layer in Siberia [47]. Our findings are thus consistent with a previous report showing that modern species of these viruses have not gone all extinct [48], and these viruses may be found in distant subarctic marine ecosystems.

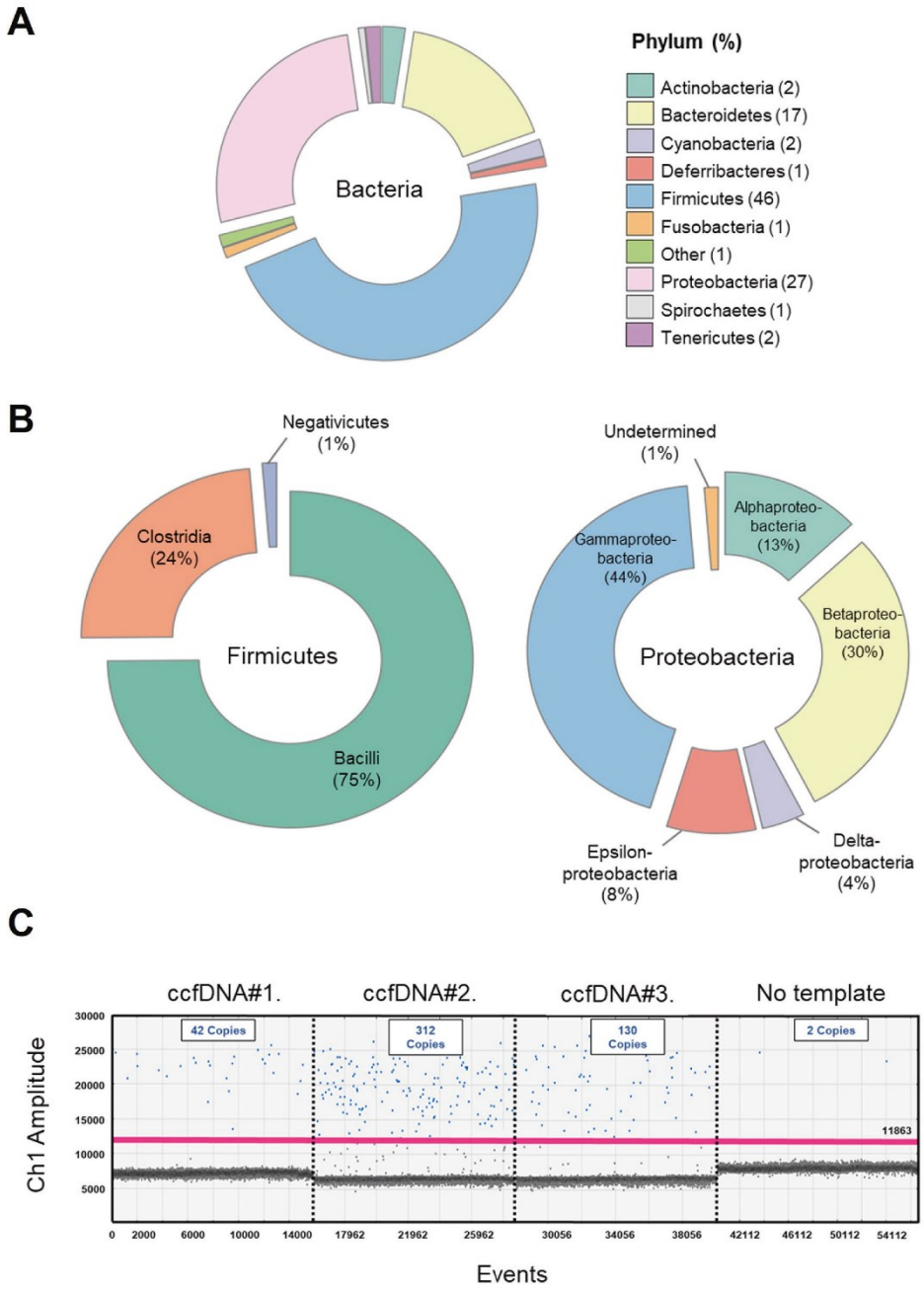

Fig. 4 ccfDNA of bacterial origin. A Relative abundance at the phylum-level. **B** Microbial diversity of the two top phyla (Firmicutes and Proteobacteria). **C** Representative ddPCR amplification of *Vibrio* spp. 16S rRNA gene fragment (blue color) in three hemolymphs of *A. atra*.

Detection of metazoan-derived nonself ccfDNA sequences

We finally examined whether we could find DNA fragments originating from other metazoans. A total of 482 nonself contigs were identified using BLASTN and BLASTX performed with nt, nr and RefSeq libraries (genomes and proteins). Our results showed that metazoan nonself ccfDNA fragments were dominated by DNA from bony fish (Fig. 5). DNA fragments from insects and other species were also found. A relatively large percentage of DNA

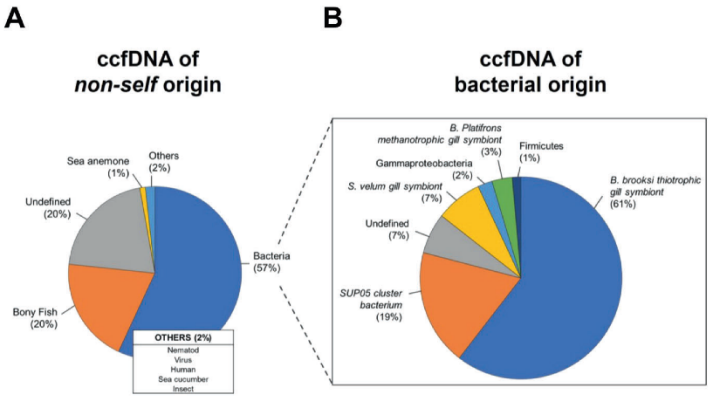

Fig. 5 ccfDNA of various origins as identified using BLASTN and BLASTX. A total of 482 assembled contigs were analyzed. **A** Overall taxonomic distribution profile of metagenomic contig annotation (prokaryotes and eukaryotes). **B** Detailed distribution of bacterial DNA fragments identified using BLASTN and BLASTX.

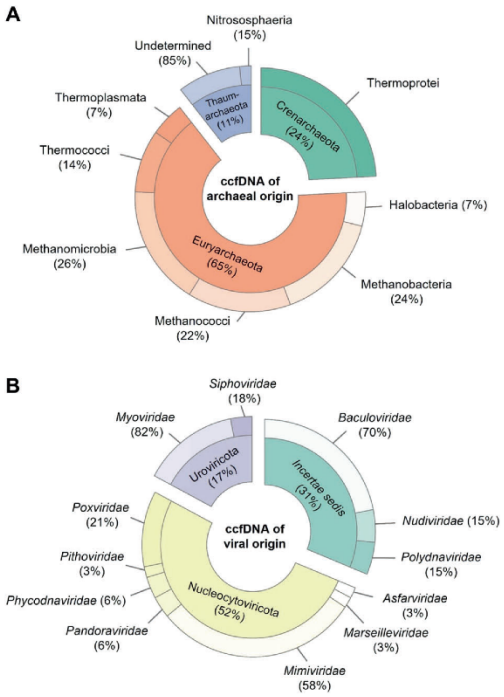

Fig. 6 ccfDNA fragments of archaeal and viral origins. Classification of nonself reads using the Kraken taxonomic classification system.

fragments were not identified possibly because a large number of marine species are underrepresented in genomic databases compared to terrestrial species [49].

DISCUSSION

In the present work, we applied the concept of LB to mussels, arguing that shotgun sequencing of hemolymphatic ccfDNA could provide insights into the constituents of a marine coastal ecosystem. More specifically, we showed that 1) the hemolymph of mussels contains a relatively high concentration (at the microgram level) of relatively large (~1–5 kb) circulating DNA fragments; 2) these DNA fragments are of both a self and nonself origin; 3) among the nonself origins of these DNA fragments, we found bacterial, archaeal and viral DNA as well as DNA from other metazoans; and 4) the accumulation of these hemolymphatic nonself ccfDNA fragments in the hemolymph is rapid and favored by the intrinsic filtration activity of mussels. Taken together, our study shows that the concept of LB, which has mostly been applied in the biomedical field to date, encodes a rich and yet unexplored source of knowledge that could be used to better understand the interactions between sentinel species and their environment.

In addition to primates, isolation of ccfDNA has been reported in mammals, including mice, dogs, cats, and horses [50–52]. To our knowledge, however, our study is the first to report the detection and sequencing of ccfDNA of a marine species with an open circulatory system. This anatomical feature and the filtering capacity of mussels probably explains, at least in part, the distinct size profile of circulating DNA fragments when compared to other species. In humans, most DNA fragments that circulate into the bloodstream are small fragments ranging between 150 and 200 bp with a maximum peak at 167 bp [34, 53]. A smaller but significant proportion of DNA fragments falls between 300 and 500 bp, and ~5% of DNA fragments are longer than 900 bp [54]. This size distribution is explained by the fact that the major source of ccfDNA in plasma originates from cell death, either due to apoptosis or following necrosis of circulating hematopoietic cells in healthy individuals or tumor cell apoptosis in cancer patients (referred to as circulating tumor DNA, ctDNA). The size distribution of hemolymphatic ccfDNA we found in mussels, which ranges from 1000 to 5000 bp, suggests that the ccfDNA of mussels has a different origin. This is a logical hypothesis given that mussels have a semi-open vascular system and live in a marine aquatic environment that contains high concentrations of genomic DNA derived from microorganisms. In fact, our laboratory experiments using foreign DNA suggest that mussels accumulate DNA fragments present in seawater, at least for several hours after which they are either degraded, and/or released, and/or stored in different tissues following cellular uptake. Using the intravalvular compartment would reduce the ccfDNA from self origin, but also from nonself origin considering the rarity of (prokaryotic and eukaryotic) cells. Considering the importance of innate immunity in bivalves and the high numbers of circulating phagocytes, we

further hypothesize that even nonself ccfDNA is enriched by the circulating phagocytes which accumulate foreign DNA upon phagocytosis of microorganisms and/or cell debris. Taken together, our findings suggest that hemolymphatic ccfDNA in bivalves are a unique reservoir of molecular information and reinforces their status as sentinel species.

Our data showed that sequencing and analysis of bacterial-derived hemolymphatic ccfDNA fragments can provide critical information on the bacterial flora of the host and bacteria present in the surrounding marine ecosystem. The shotgun sequencing approach revealed sequences from the gill symbiont bacteria of *A. atra* that would otherwise have been missed if the common 16S rRNA identification method was employed partly due to a bias in the reference library. In fact, our data using LB collected from *M. platensis* in the same mussel bed at Kerguelen showed that both mussel species had a similar composition of their gill-associated bacterial symbiont (Figure S4, supplementary information). Such similarity for both genetically distinct mussels possibly reflects the composition of the bacterial community in the cold, sulfidic and volcanic sediment of Kerguelen [55–58]. A higher proportion of sulfur-reducing microorganisms is well described in bioturbated coastal zones [59], such as the coast of Port-aux-Français, where mussels were collected. Another possibility is that the mussel symbiont flora can be influenced by horizontal transmission [60, 61]. More studies will be required to determine the correlation between the marine environment, the ocean floor surface and the mussel symbiotic bacterial composition. These studies are currently underway.

The length and concentration of hemolymphatic ccfDNA, the ease of its purification and its high quality that allows for rapid shotgun sequencing are among the many benefits of using ccfDNA of mussels to assess the biodiversity of marine coastal ecosystems. This approach is particularly effective for characterizing viral communities (virome) within a given ecosystem [62, 63]. In contrast to bacteria, archaea and eukaryotes, viral genomes do not harbor phylogenetically conserved genes, such as the 16S sequences. Our findings, showed that liquid biopsies from sentinel species like mussels can be used to identify a relatively large number of ccfDNA fragments of viruses known to infect hosts which commonly populate coastal marine ecosystems. This included viruses known to infect protists, arthropods, insects, plants, and bacterial viruses (i.e., bacteriophages). A similar distribution was found when we studied the virome of hemolymphatic ccfDNA of blue mussels (*M. platensis*) collected in the same mussel beds at Kerguelen (Table S2, supplementary information). Shotgun sequencing of ccfDNA is indeed a new approach that has gained momentum for studying the virome in humans or other species [21, 37, 64]. This approach is particularly useful for studying dsDNA viruses because not a single gene is conserved in all dsDNA viruses, which represent the most diverse and expansive Baltimore classes of viruses [65]. Although most of these viruses remain unclassified and likely include viruses in completely uncharted parts of the virus world [66], we found that the virome of both mussel *A. atra* and *M. platensis* species and the host range were similar between both species (see Fig. S3, supplementary information). Such similarity is not surprising, as it likely reflects the lack of selectivity during the uptake of DNA present in the surrounding environment. Future studies using purified RNA are currently needed to characterize the RNA virome.

In our study, we used a very stringent pipeline that was adapted from the work of Kowarsky and colleagues [37] who used a two-step removal of self ccfDNA before and after the assembly on its merged reads and contigs, thereby generating a large proportion of unmapped reads. Accordingly, we cannot rule out that a proportion of these unmapped reads can still be of self origin, most notably as we do not have a reference genome for this mussel species. We also used this pipeline because we were concerned by chimeras formed between self and nonself reads and the length of the reads generated by the Illumina MiSeq PE75s. Another reason for the large proportion of unmapped reads is that a large proportion of marine microorganisms, especially in such a remote area as Kerguelen, has not yet been annotated. We used the Illumina MiSeq PE75, assuming that the ccfDNA length fragments would be similar to human ccfDNA. For future studies, given our results showing that hemolymphatic ccfDNA has longer reads than that of humans and/or mammals, we would recommend sequencing platforms that are more adapted to longer ccfDNA fragments. This practice would greatly facilitate the identification of a higher number of reads, allowing deeper analyses. Obtaining a complete sequence of the nuclear genome of *A. atra*, which is not currently available, would also greatly facilitates the distinction between ccfDNA of self and nonself origin. Considering that our study was focused on the feasibility of applying the concept of liquid biopsy to mussels, we are hopeful that as future studies exploit this concept, new tools and pipelines will be developed to improve that potential of this method to study the microbial biodiversity of marine ecosystems.

As a noninvasive clinical biomarker, elevated levels of human plasmatic ccfDNA have been associated with several diseases, tissue damage and stress conditions [67–69]. This increase is attributed to the release of DNA fragments of self-origin upon tissue damage. We examined this issue using acute thermal stress where mussels were exposed for a short period of time at 30 °C. We performed this assay with three different species of mussels in three independent experiments. We did not however detect any variations in the ccfDNA levels following acute thermal stress (see Fig. S5, supplementary information). This finding is likely explained, at least in part, to the fact that mussels have a semi-open circulatory system and accumulate large concentrations of nonself DNA given their high filtering activity. Alternatively, mussels, such as many invertebrates, may be more tolerant to stress-induced tissue damage, limiting the release of ccfDNA in their hemolymph [70, 71].

To date, DNA analysis of biodiversity in aquatic ecosystems has mostly centered on environmental DNA (eDNA) metabarcoding. This approach, however, is often limited in terms of biodiversity analysis when using primers. The use of shotgun sequencing bypasses the PCR limitations and a biased selection of primer sets. In a sense, our approach is thus closer to the more recently used high-throughput eDNA shotgun sequencing methods that enable direct sequencing of fragmented DNA and analysis of basically all living organisms [72, 73]. However, there are a number of fundamental issues that distinguish LB from standard eDNA approaches. Of course, the major difference between eDNA and LB is the use of a natural filtering host. The use of marine species, such as sponges and bivalves (*Dresseina* spp.), as natural filter to study eDNA has been reported [74, 75]. The study on *Dreissena*, however, used tissular biopsy from which DNA was extracted. Analysis of ccfDNA from LB does not require tissular biopsy and specialized and occasionally costly equipment and logistics associated with eDNA or tissular biopsies. In fact, we have recently reported that ccfDNA from LB can be stored and analyzed on FTA support, bypassing the need for maintaining a cold chain, a major issue for studies in remote regions [76]. Extraction of ccfDNA from liquid biopsies is also simple and provides high-quality DNA for shotgun sequencing and PCR analysis. This is a major advantage considering some of the technical limitations associated with eDNA analysis [77]. The simplicity and low cost of the sampling method is also particularly well adapted for long-term monitoring surveillance programs. Another well-known feature of bivalves, in addition to their high filtering capacity, is the chemical mucopolysaccharidic composition of their mucus, which favors the uptake of viruses [78, 79]. This makes bivalves an ideal natural filter to characterize the biodiversity of a given aquatic ecosystem and the impacts of CC. Although the presence of DNA fragments from the host can be viewed as a limit to the approach compared to eDNA, the cost associated by the presence of such self ccfDNA is offset by the wealth of information that can be simultaneously obtained to study on the health status of

the host. This includes the presence of viral sequences integrated in the host genome of the host. This is particularly important in the case of mussels given the existence of horizontally-transmitted leukemogenic retroviruses in bivalves [80, 81]. Another advantage of LB compared to eDNA is that it exploits the phagocytic activity of hemolymphatic circulating hemocytes which engulfed microorganisms (and their genome). Phagocytosis is the most fundamental role for hemocytes in bivalves [82]. Finally, the approach takes advantage of the high filtration capacity of mussels (which pumps an average of 1.5 L/h of seawater) and the bi-diurnal cycles, both of which increases the mixing of different layers of seawater columns, thereby allowing the capture of heterogenous eDNA [83, 84]. Analysis of ccfDNA from mussels is thus an interesting avenue considering their nutritional, economic and ecological impact. In a manner similar to the analysis of LB collected in humans, the approach further opens up the possibility of measuring genetic and epigenetic alterations of the host's DNA in response to xenobiotics. For example, it is possible to envisage third-generation sequencing technologies to perform genome-wide analysis of methylation in ccfDNA of self-origin using nanopore sequencing. This process should be facilitated by the fact that the length of ccfDNA fragments of mussels is ideally compatible with long-read sequencing platforms that enable genome-wide analysis of DNA methylation from a single sequencing run without the need for chemical conversion [85, 86]. This is an interesting possibility because DNA methylation patterns have been shown to reflect responses to environmental stress and persist for many generations. It could thus provide valuable information on potential mechanisms regulating responses following exposure to climate change or pollutants [87]. The use of LB, however, is not without limitations. Needless to say, it requires the presence of sentinel species in the ecosystem. As mentioned above, the use of LB to assess the biodiversity of a given ecosystem also requires a stringent bioinformatic pipeline to take into account the presence of DNA fragments of self-origin. The other major challenge is the availability of reference genomes from marine species. Hopefully, initiatives, such as the marine mammal genome project and the recently established Fish10k project [88], will facilitate such analysis in the future. The application of the LB concept to marine filtering organisms is also compatible with recent advances in sequencing technologies, rendering it fully suited for the development of multiomics biomarkers to provide important information on the health status of marine habitats in response to environmental stress.

DATA AVAILABILITY

Genome sequencing data have been deposited in the NCBI Sequence Read Archive https://www.ncbi.nlm.nih.gov/sra/SRR8924808 under the Bioprojects SRR8924808.

REFERENCES

1. Brierley AS, Kingsford MJ. Impacts of climate change on marine organisms and ecosystems. Curr Biol. 2009;19:R602–R614.
2. Gissi E, Manea E, Mazaris AD, Fraschetti S, Almpanidou V, Bevilacqua S, et al. A review of the combined effects of climate change and other local human stressors on the marine environment. Sci Total Environ. 2021;755:142564.
3. Carella F, Antuofermo E, Farina S, Salati F, Mandas D, Prado P, et al. In the wake of the ongoing mass mortality events: co-occurrence of Mycobacterium, Haplosporidium and other pathogens in Pinna nobilis collected in Italy and Spain (Mediterranean Sea). Front Mar Sci. 2020;7:48.
4. Seuront L, Nicastro KR, Zardi GI, Goberville E. Decreased thermal tolerance under recurrent heat stress conditions explains summer mass mortality of the blue mussel Mytilus edulis. Sci Rep. 2019;9:17498.
5. Fey SB, Siepielski AM, Nussle S, Cervantes-Yoshida K, Hwan JL, Huber ER, et al. Recent shifts in the occurrence, cause, and magnitude of animal mass mortality events. Proc Natl Acad Sci USA. 2015;112:1083–8.
6. Scarpa F, Sanna D, Azzena I, Mugetti D, Cerruti F, Hosseini S, et al. Multiple non-species-specific pathogens possibly triggered the mass mortality in Pinna nobilis. Life. 2020;10:238.
7. Bradley M, Kutz SJ, Jenkins E, O'Hara TM. The potential impact of climate change on infectious diseases of Arctic fauna. Int J Circumpolar Health. 2005;64:468–77.
8. Beyer J, Green NW, Brooks S, Allan IJ, Ruus A, Gomes T, et al. Blue mussels (Mytilus edulis spp.) as sentinel organisms in coastal pollution monitoring: a review. Mar Environ Res. 2017;130:338–65.
9. Siravegna G, Marsoni S, Siena S, Bardelli A. Integrating liquid biopsies into the management of cancer. Nat Rev Clin Oncol. 2017;14:531–48.
10. Wan JCM, Massie C, Garcia-Corbacho J, Mouliere F, Brenton JD, Caldas C, et al. Liquid biopsies come of age: towards implementation of circulating tumour DNA. Nat Rev Cancer. 2017;17:223–38.
11. Mandel P, Metais P. Nuclear acids in human blood plasma. Comptes Rendus Séances Soc Biol Filiales. 1948;142:241–3.
12. Bronkhorst AJ, Ungerer V, Holdenrieder S. The emerging role of cell-free DNA as a molecular marker for cancer management. Biomol Detect Quantif. 2019;17:100087.
13. Ignatiadis M, Sledge GW, Jeffrey SS. Liquid biopsy enters the clinic - implementation issues and future challenges. Nat Rev Clin Oncol. 2021;18:297–312.
14. Lo YM, Corbetta N, Chamberlain PF, Rai V, Sargent IL, Redman CW, et al. Presence of fetal DNA in maternal plasma and serum. Lancet. 1997;350:485–7.
15. Moufarrej MN, Wong RJ, Shaw GM, Stevenson DK, Quake SR. Investigating pregnancy and its complications using circulating cell-free RNA in women's blood during gestation. Front Pediatr. 2020;8:605219.
16. Oellerich M, Sherwood K, Keown P, Schutz E, Beck J, Stegbauer J, et al. Liquid biopsies: donor-derived cell-free DNA for the detection of kidney allograft injury. Nat Rev Nephrol. 2021;17:591–603.
17. Wong FC, Lo YM. Prenatal diagnosis innovation: genome sequencing of maternal plasma. Annu Rev Med. 2016;67:419–32.
18. Gu W, Deng X, Lee M, Sucu YD, Arevalo S, Stryke D, et al. Rapid pathogen detection by metagenomic next-generation sequencing of infected body fluids. Nat Med. 2021;27:115–24.
19. Huang YF, Chen YJ, Fan TC, Chang NC, Chen YJ, Midha MK, et al. Analysis of microbial sequences in plasma cell-free DNA for early-onset breast cancer patients and healthy females. BMC Med Genom. 2018;11:16.
20. Goggs R, Jeffery U, LeVine DN, Li RHL. Neutrophil-extracellular traps, cell-free DNA, and immunothrombosis in companion animals: a review. Vet Pathol. 2020;57:6–23.
21. Kowarsky M, De Vlaminck I, Okamoto J, Neff NF, LeBreton M, Nwobegabay J, et al. Cell-free DNA reveals potential zoonotic reservoirs in non-human primates. BioRxiv. 2018;481093.
22. Caza F, Bernet E, Veyrier FJ, Betoulle S, St-Pierre Y. Hemocytes released in seawater act as Trojan horses for spreading of bacterial infections in mussels. Sci Rep. 2020;10:19696.
23. Andrew S. FastQC: a quality control tool for high throughput sequence data. 2010. http://www.bioinformatics.babraham.ac.uk/projects/fastqc.
24. Bolger AM, Lohse M, Usadel B. Trimmomatic: a flexible trimmer for Illumina sequence data. Bioinformatics. 2014;30:2114–20.
25. Magoč T, Salzberg SL. FLASH: fast length adjustment of short reads to improve genome assemblies. Bioinformatics. 2011;27:2957–63.
26. Morgulis A, Gertz EM, Schäffer AA, Agarwala R. A fast and symmetric DUST implementation to mask low-complexity DNA sequences. Comput Biol. 2006;13:1028–40.
27. Li D, Liu CM, Luo R, Sadakane K, Lam TW. MEGAHIT: an ultra-fast single-node solution for large and complex metagenomics assembly via succinct de Bruijn graph. Bioinformatics. 2015;31:1674–6.
28. Wood DE, Salzberg SL. Kraken: ultrafast metagenomic sequence classification using exact alignments. Genome Biol. 2014;15:R46.
29. Cuccuru G, Orsini M, Pinna A, Sbardellati A, Soranzo N, Travaglione A, et al. Orione, a web-based framework for NGS analysis in microbiology. Bioinformatics. 2014;30:1928–9.
30. Ondov BD, Bergman NH, Phillippy AM. Interactive metagenomic visualization in a Web browser. BMC Bioinform. 2011;12:385.
31. Lüskow F, Riisgård H. In situ filtration rates of blue mussels (Mytilus edulis) measured by an open-top chamber method. OJMS. 2018;8:395–406.
32. Szpechcinski A, Struniawska R, Zaleska J, Chabowski M, Orlowski T, Roszkowski K, et al. Evaluation of fluorescence-based methods for total vs. amplifiable DNA quantification in plasma of lung cancer patients. J Physiol Pharmacol. 2008;59:675–81.
33. Tissot C, Toffart AC, Villar S, Souquet PJ, Merle P, Moro-Sibilot D, et al. Circulating free DNA concentration is an independent prognostic biomarker in lung cancer. Eur Respir J. 2015;46:1773–80.
34. Kustanovich A, Schwartz R, Peretz T, Grinshpun A. Life and death of circulating cell-free DNA. Cancer Biol Ther. 2019;20:1057–67.
35. Prouteau A, Denis JA, De Fornel P, Cadieu E, Derrien T, Kergal C, et al. Circulating tumor DNA is detectable in canine histiocytic sarcoma, oral malignant melanoma, and multicentric lymphoma. Sci Rep. 2021;11:877.

36. Vandewoestyne M, Van Hoofstat D, Franssen A, Van Nieuwerburgh F, Deforce D. Presence and potential of cell free DNA in different types of forensic samples. For Sci Int Genet. 2013;7:316–20.
37. Kowarsky M, Camunas-Soler J, Kertesz M, De Vlaminck I, Koh W, Pan W, et al. Numerous uncharacterized and highly divergent microbes which colonize humans are revealed by circulating cell-free DNA. Proc Natl Acad Sci USA. 2017;114:9623–8.
38. Meddeb R, Dache ZAA, Thezenas S, Otandault A, Tanos R, Pastor B, et al. Quantifying circulating cell-free DNA in humans. Sci Rep. 2019;9:5220.
39. Li YF, Yang N, Liang X, Yoshida A, Osatomi K, Power D, et al. Elevated seawater temperatures decrease microbial diversity in the gut of Mytilus coruscus. Front Physiol. 2018;9:839.
40. Musella M, Wathsala R, Tavella T, Rampelli S, Barone M, Palladino G, et al. Tissue-scale microbiota of the Mediterranean mussel (Mytilus galloprovincialis) and its relationship with the environment. Sci Total Environ. 2020;717:137209.
41. Thompson JR, Randa MA, Marcelino LA, Tomita-Mitchell A, Lim E, Polz MF. Diversity and dynamics of a north atlantic coastal Vibrio community. Appl Environ Microbiol. 2004;70:4103–10.
42. Pfister CA, Meyer F, Antonopoulos DA. Metagenomic profiling of a microbial assemblage associated with the California mussel: a node in networks of carbon and nitrogen cycling. PLoS One. 2010;5:e10518.
43. Galand PE, Casamayor EO, Kirchman DL, Potvin M, Lovejoy C. Unique archaeal assemblages in the Arctic Ocean unveiled by massively parallel tag sequencing. ISME J. 2009;3:860–9.
44. Korzhenkov AA, Toshchakov SV, Bargiela R, Gibbard H, Ferrer M, Teplyuk AV, et al. Archaea dominate the microbial community in an ecosystem with low-to-moderate temperature and extreme acidity. Microbiome. 2019;7:11.
45. Spain EA, Johnson SC, Hutton B, Whittaker JM, Lucieer V, Watson SJ, et al. Shallow seafloor gas emissions near Heard and McDonald Islands on the Kerguelen Plateau, southern Indian Ocean. Earth Space Sci. 2020;7:e2019EA000695.
46. Farías L, Florez-Leiva L, Besoain V, Sarthou G, Fernández C. Dissolved greenhouse gases (nitrous oxide and methane) associated with the naturally iron-fertilized Kerguelen region (KEOPS 2 cruise) in the Southern Ocean. Biogeosciences. 2015;12:1925–40.
47. Legendre M, Bartoli J, Shmakova L, Jeudy S, Labadie K, Adrait A, et al. Thirty-thousand-year-old distant relative of giant icosahedral DNA viruses with a pandoravirus morphology. Proc Natl Acad Sci USA. 2014;111:4274–9.
48. Levasseur A, Andreani J, Delerce J, Bou Khalil J, Robert C, La Scola B, et al. Comparison of a modern and fossil pithovirus reveals its genetic conservation and evolution. Genome Biol Evol. 2016;8:2333–9.
49. Kelley JL, Brown AP, Therkildsen NO, Foote AD. The life aquatic: advances in marine vertebrate genomics. Nat Rev Genet. 2016;17:523–34.
50. Colmer SF, Luethy D, Abraham M, Stefanovski D, Hurcombe SD. Utility of cell-free DNA concentrations and illness severity scores to predict survival in critically ill neonatal foals. PLoS One. 2021;16:e0242635.
51. Rushton JG, Ertl R, Klein D, Tichy A, Nell B. Circulating cell-free DNA does not harbour a diagnostic benefit in cats with feline diffuse iris melanomas. J Feline Med Surg. 2019;21:124–32.
52. Tagawa M, Shimbo G, Inokuma H, Miyahara K. Quantification of plasma cell-free DNA levels in dogs with various tumors. J Vet Diagn Investig. 2019;31:836–43.
53. Shi J, Zhang R, Li J, Zhang R. Size profile of cell-free DNA: a beacon guiding the practice and innovation of clinical testing. Theranostics. 2020;10:4737–48.
54. Fernando MR, Jiang C, Krzyzanowski GD, Ryan WL. Analysis of human blood plasma cell-free DNA fragment size distribution using EvaGreen chemistry based droplet digital PCR assays. Clin Chim Acta. 2018;483:39–47.
55. Findlay AJ. Microbial impact on polysulfide dynamics in the environment. FEMS Microbiol Lett. 2016;363:fnw103.
56. Jørgensen BB, Findlay AJ, Pellerin A. The biogeochemical sulfur cycle of marine sediments. Front Microbiol. 2019;10:849.
57. Teske A, Brinkhoff T, Muyzer G, Moser DP, Rethmeier J, Jannasch HW. Diversity of thiosulfate-oxidizing bacteria from marine sediments and hydrothermal vents. Appl Environ Microbiol. 2000;66:3125–33.
58. Zhang X, Du Z, Zheng R, Luan Z, Qi F, Cheng K, et al. Development of a new deep-sea hybrid Raman insertion probe and its application to the geochemistry of hydrothermal vent and cold seep fluids. Deep Sea Res Part I Oceanogr Res Pap. 2017;123:1–12.
59. Egger M, Riedinger N, Mogollón JM, Jørgensen BB. Global diffusive fluxes of methane in marine sediments. Nat Geosci. 2018;11:421–5.
60. Ansorge R, Romano S, Sayavedra L, Kupczok A, Tegetmeyer HE, Dubilier N, et al. Functional diversity enables multiple symbiont strains to coexist in deep-sea mussels. Nat Microbiol. 2019;4:2487–97.
61. Russell SL, Pepper-Tunick E, Svedberg J, Byrne A, Ruelas Castillo J, Vollmers C, et al. Horizontal transmission and recombination maintain forever young bacterial symbiont genomes. PLoS Genet. 2020;16:e1008935.
62. Angly FE, Felts B, Breitbart M, Salamon P, Edwards RA, Carlson C, et al. The marine viromes of four oceanic regions. PLoS Biol. 2006;4:e368.
63. Li Z, Pan D, Wei G, Pi W, Zhang C, Wang JH, et al. Deep sea sediments associated with cold seeps are a subsurface reservoir of viral diversity. ISME J. 2021;15:2366–78.
64. Thongsripong P, Chandler JA, Kittayapong P, Wilcox BA, Kapan DD, Bennett SN. Metagenomic shotgun sequencing reveals host species as an important driver of virome composition in mosquitoes. Sci Rep. 2021;11:8448.
65. Koonin EV, Krupovic M, Agol VI. The Baltimore classification of viruses 50 years later: how does it stand in the light of virus evolution? Microbiol Mol Biol Rev. 2021;85:e0005321.
66. Koonin EV, Dolja VV, Krupovic M, Varsani A, Wolf YI, Yutin N, et al. Global organization and proposed megataxonomy of the virus world. Microbiol Mol Biol Rev. 2020;84:e00061–19.
67. Breitbach S, Tug S, Simon P. Circulating cell-free DNA: an up-coming molecular marker in exercise physiology. Sports Med. 2012;42:565–86.
68. Preissner KT, Herwald H. Extracellular nucleic acids in immunity and cardiovascular responses: between alert and disease. Thromb Haemost. 2017;117:1272–82.
69. Schwarzenbach H. Circulating nucleic acids as biomarkers in breast cancer. Breast Cancer Res. 2013;15:211.
70. Murphy DJ. Freezing resistance in intertidal invertebrates. Annu Rev Physiol. 1983;45:289–99.
71. Robledo JAF, Yadavalli R, Allam B, Espinosa EP, Gerdol M, Greco S, et al. From the raw bar to the bench: bivalves as models for human health. Dev Comp Immunol. 2019;92:260–82.
72. Cowart DA, Murphy KR, Cheng CC. Metagenomic sequencing of environmental DNA reveals marine faunal assemblages from the West Antarctic Peninsula. Mar Genom. 2018;37:148–60.
73. Parducci L, Bennett KD, Ficetola GF, Alsos IG, Suyama Y, Wood JR, et al. Ancient plant DNA in lake sediments. New Phytol. 2017;214:924–42.
74. Mariani S, Baillie C, Giuliano C, Riesgo A. Sponges as natural environmental DNA samplers. Curr Biol. 2019;29:R401–R402.
75. Weber S, Brink L, Wörner M, Künzel S, Veith M, Teubner D, et al. Molecular diet analysis in zebra and quagga mussels (Dreissena spp.) and an assessment of the utility of aquatic filter feeders as biological eDNA filters. BioRxiv. 2021; 432951.
76. Caza F, Joly de Boissel PG, Villemur R, Betoulle S, St-Pierre Y. Liquid biopsies for omics-based analysis in sentinel mussels. Plos One. 2019;14:e0223525.
77. Hunter ME, Ferrante JA, Meigs-Friend G, Ulmer A. Improving eDNA yield and inhibitor reduction through increased water volumes and multi-filter isolation techniques. Sci Rep. 2019;9:5259.
78. Burkhardt W III, Calci KR. Selective accumulation may account for shellfish-associated viral illness. Appl Environ Microbiol. 2000;66:1375–8.
79. Di Girolamo R, Liston J, Matches J. Ionic bonding, the mechanism of viral uptake by shellfish mucus. Appl Environ Microbiol. 1977;33:19–25.
80. Metzger MJ, Reinisch C, Sherry J, Goff SP. Horizontal transmission of clonal cancer cells causes leukemia in soft-shell clams. Cell. 2015;161:255–63.
81. Metzger MJ, Villalba A, Carballal MJ, Iglesias D, Sherry J, Reinisch C, et al. Widespread transmission of independent cancer lineages within multiple bivalve species. Nature. 2016;534:705–9.
82. Canesi L, Gallo G, Gavioli M, Pruzzo C. Bacteria–hemocyte interactions and phagocytosis in marine bivalves. Microsc Res Tech. 2002;57:469–76.
83. Andruszkiewicz EA, Koseff JR, Fringer OB, Ouellette NT, Lowe AB, Edwards CA, et al. Modeling environmental DNA transport in the coastal ocean using Lagrangian particle tracking. Front Mar Sci. 2019;6:477.
84. Wood ZT, Lacoursière-Roussel A, LeBlanc F, Trudel M, Kinnison MT, Garry McBrine C, et al. Spatial heterogeneity of eDNA transport improves stream assessment of threatened salmon presence, abundance, and location. Front Ecol Evol. 2021;9:650717.
85. Rand AC, Jain M, Eizenga JM, Musselman-Brown A, Olsen HE, Akeson M, et al. Mapping DNA methylation with high-throughput nanopore sequencing. Nat Methods. 2017;14:411–3.
86. Simpson JT, Workman RE, Zuzarte PC, David M, Dursi LJ, Timp W. Detecting DNA cytosine methylation using nanopore sequencing. Nat Methods. 2017;14:407–10.
87. Cavalli G, Heard E. Advances in epigenetics link genetics to the environment and disease. Nature. 2019;571:489–99.
88. Fan G, Song Y, Yang L, Huang X, Zhang S, Zhang M, et al. Initial data release and announcement of the 10,000 Fish Genomes Project (Fish10K). Gigascience. 2020;9:giaa080.

ACKNOWLEDGEMENTS

A part of this research project has been performed at Port-aux-Français Station (Kerguelen Islands) with the logistic support of the French Polar Institute Paul-Emile-Victor (IPEV). The authors would like to thank Dr. Stéphane Betoulle (SB) who provided us with the opportunity to do research at Kerguelen and for providing

constructive and insightful discussion and invaluable comments during this project. The authors would also like to thank all the personnel from the IPEV and the Terres Australes et Antarctiques Françaises (TAAF) for their help and hospitality during our stay in the Kerguelen archipelago. The author would also like to thank Ms. Marlène Fortier for her excellent technical help. This work was funded in part by the National Science and Engineering Research Council of Canada (YSP) and IPEV (YSP and SB).

AUTHOR CONTRIBUTIONS

SF, FC, PGJB and YSP conceived the study. All authors were responsible for interpretation of data and critical appraisal. All authors executed experiments and/or contributed to the experimental design and/or analyses of the results. SF, FC, and YSP drafted the manuscript with input from all authors. All authors discussed the results and implications and commented on the manuscript at all stages.

COMPETING INTERESTS

The authors declare no competing interests.

ADDITIONAL INFORMATION

Supplementary information The online version contains supplementary material available at https://doi.org/10.1038/s43705-022-00145-0.

Correspondence and requests for materials should be addressed to Yves St-Pierre.

Applying the concept of liquid biopsy to monitor the microbial biodiversity of marine coastal ecosystems

Supplementary information

Sophia Ferchiou*, France Caza*, Philippine Granger Joly de Boissel, Richard Villemur and Yves St-Pierre

INRS-Centre Armand-Frappier Santé Biotechnologie, Laval, Québec, Canada, H7V 1B7.

* : These authors contributed equally to this work.

Corresponding Author : Yves St-Pierre, INRS-Centre Armand-Frappier Santé Biotechnologie, 531 Boul. Des Prairies, Laval, Québec, Canada, H7V 1B7.
E-mail: yves.st-pierre@inrs.ca

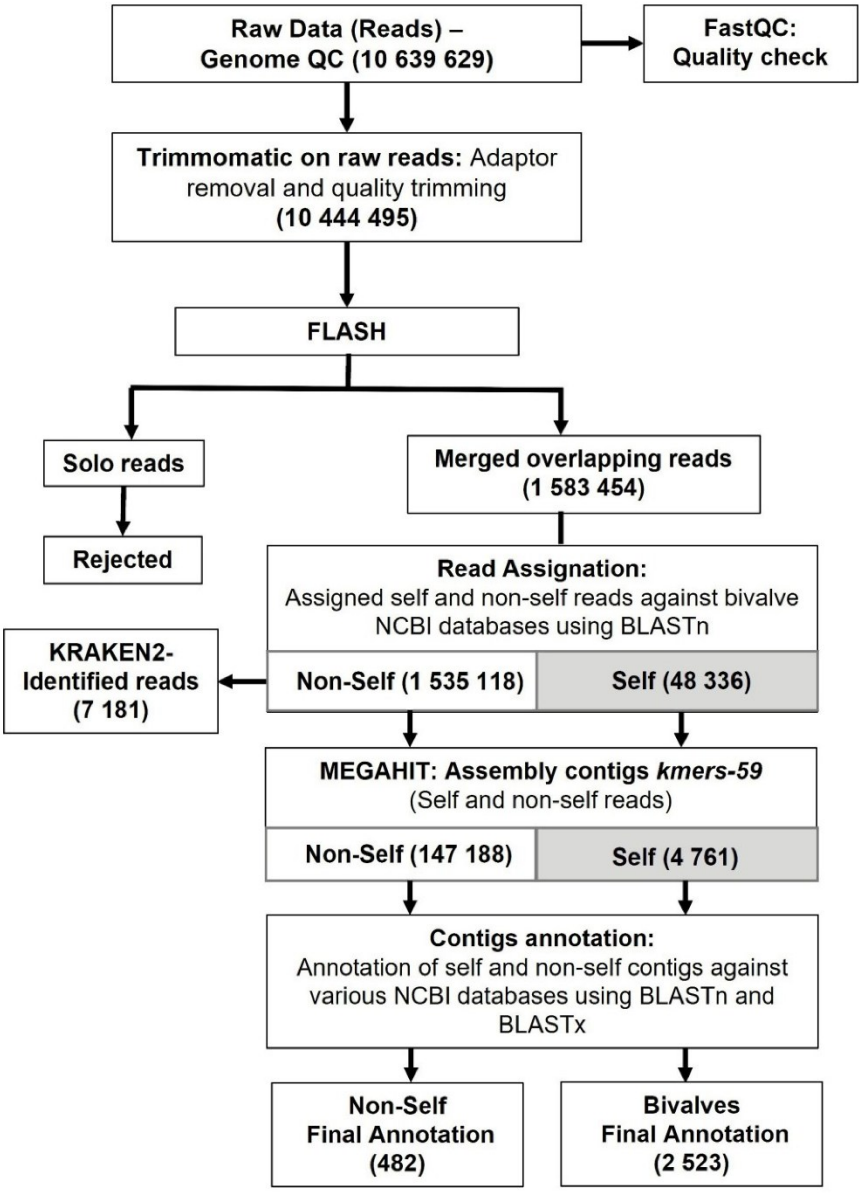

Supp Figure 1. Workflow of bioinformatic analysis of the ccfDNA shotgun sequencing data. Raw data quality was assessed with FastQC . Reads were trimmed with Trimmomatic and merged with FLASH tools. Overlapping reads were then assigned against bivalve databases using BLASTn. Both self and non-self reads were assembled with MEGAHIT. Final contig annotations were obtained using BLASTn and BLASTx with various NCBI databases.

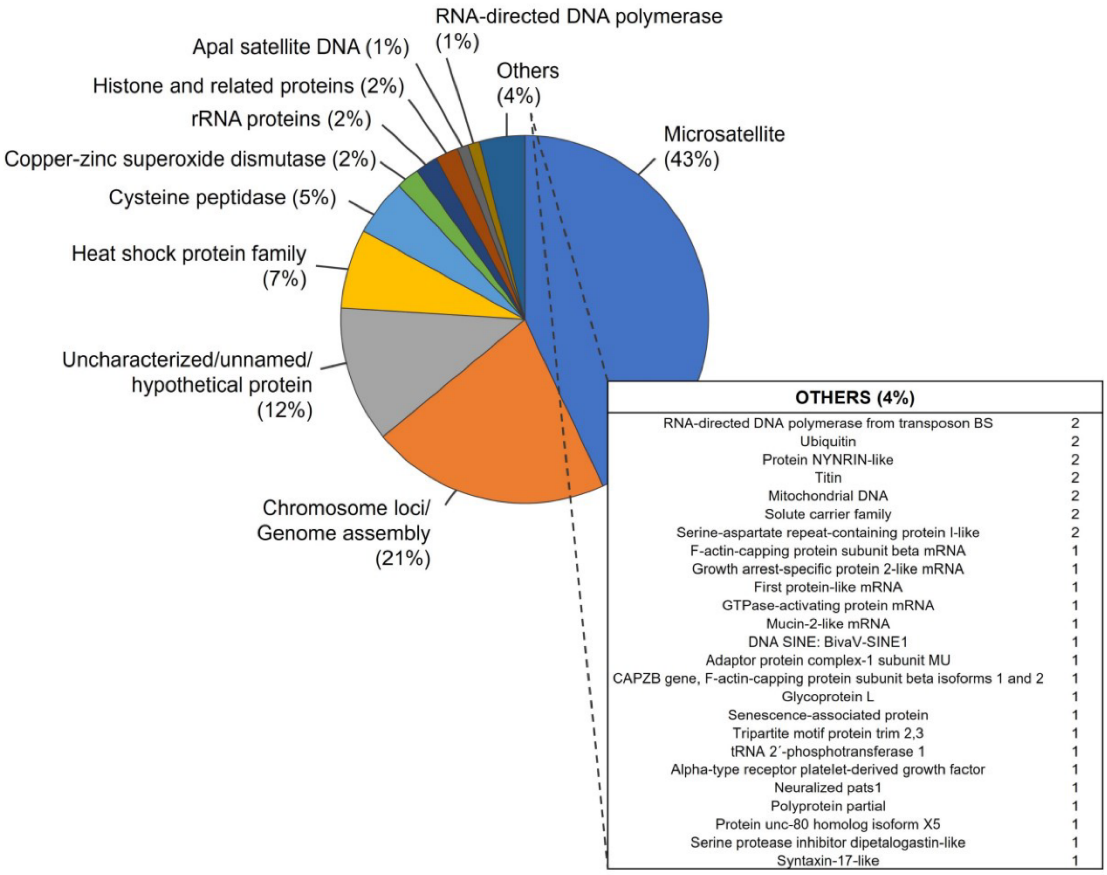

OTHERS (4%)	
RNA-directed DNA polymerase from transposon BS	2
Ubiquitin	2
Protein NYNRIN-like	2
Titin	2
Mitochondrial DNA	2
Solute carrier family	2
Serine-aspartate repeat-containing protein I-like	2
F-actin-capping protein subunit beta mRNA	1
Growth arrest-specific protein 2-like mRNA	1
First protein-like mRNA	1
GTPase-activating protein mRNA	1
Mucin-2-like mRNA	1
DNA SINE: BivaV-SINE1	1
Adaptor protein complex-1 subunit MU	1
CAPZB gene, F-actin-capping protein subunit beta isoforms 1 and 2	1
Glycoprotein L	1
Senescence-associated protein	1
Tripartite motif protein trim 2,3	1
tRNA 2´-phosphotransferase 1	1
Alpha-type receptor platelet-derived growth factor	1
Neuralized pats1	1
Polyprotein partial	1
Protein unc-80 homolog isoform X5	1
Serine protease inhibitor dipetalogastin-like	1
Syntaxin-17-like	1

Supp Figure 2. Detection of DNA fragments of self-origin. Annotation of self assembled contigs (n=580) using BLASTn and BLASTx performed with the Bivalvia libraries (genomes and proteins).

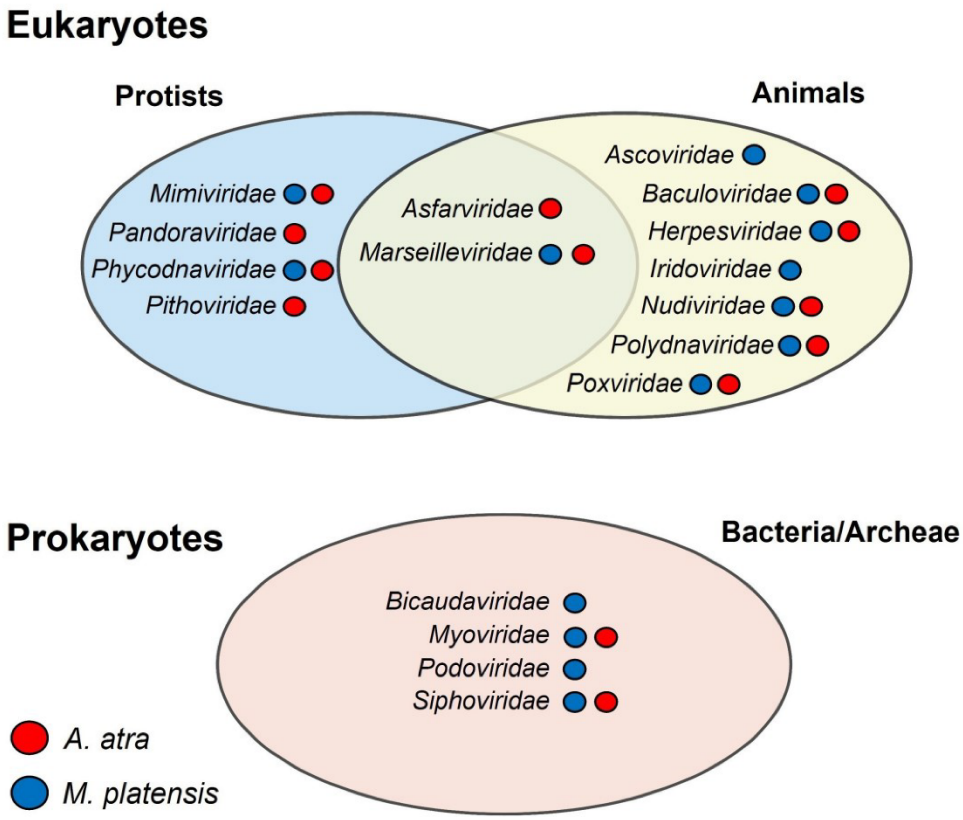

Supp Figure 3. Families of viruses identified in non-self reads for *A. atra* and *M. platensis.* Venn diagram analysis illustrating the the hosts of families of viruses identified and the overlap between *A. atra* (red points) and *M. platensis* (blue points).

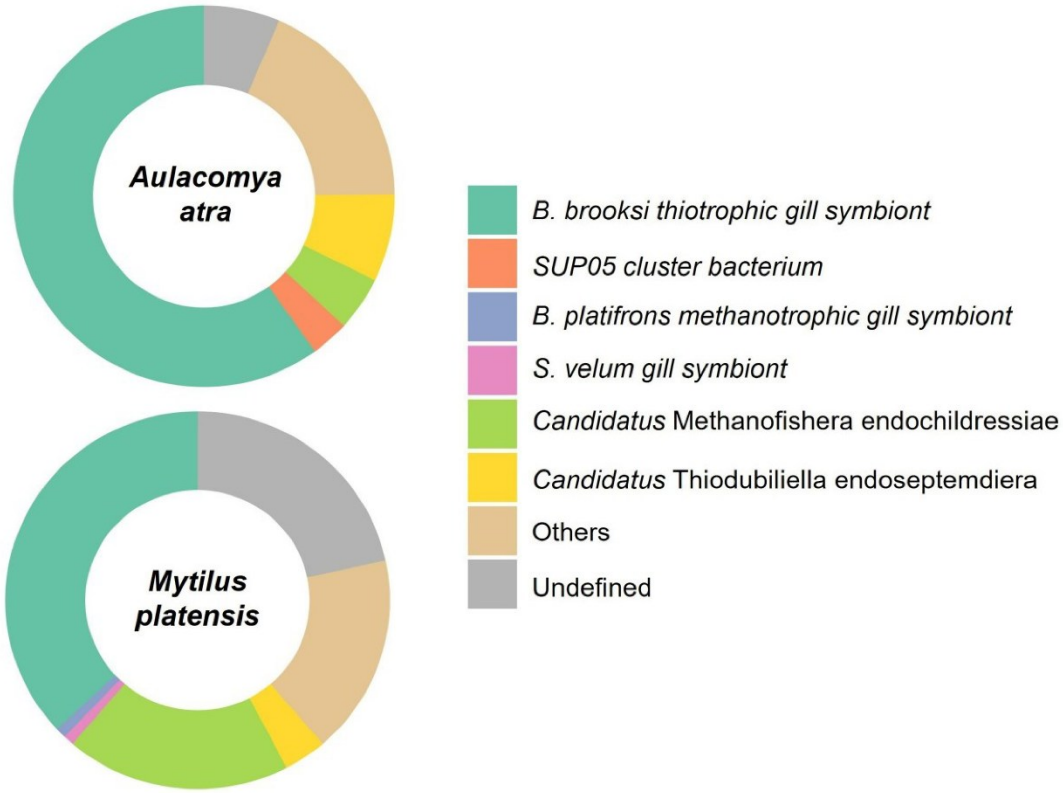

Supp Figure 4. Pie charts showing the composition of the gill-associated bacteria for *A. atra* and *M. platensis*.

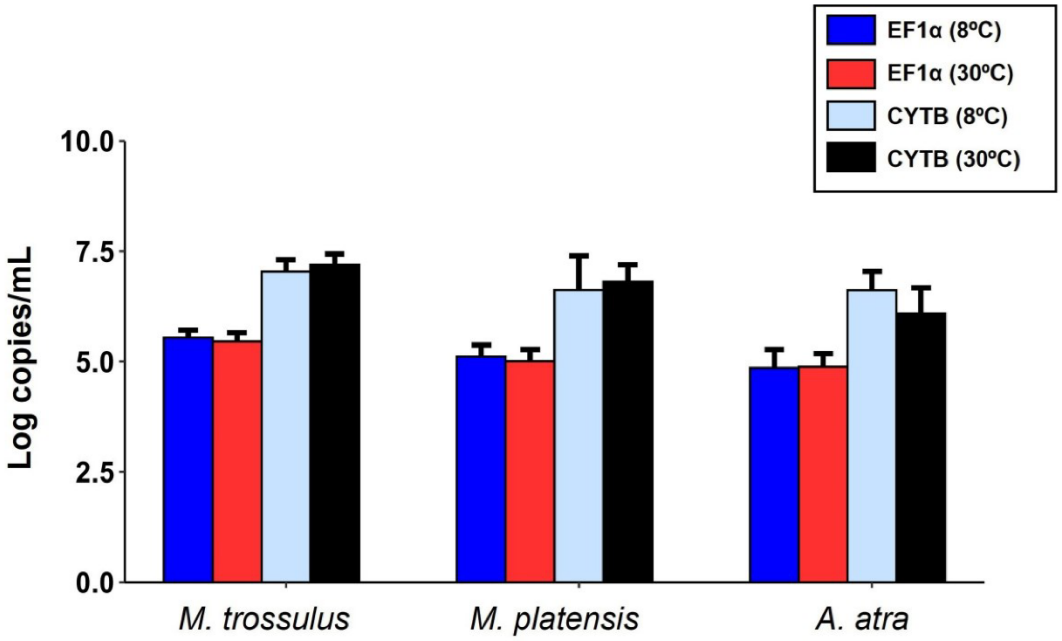

Supp Figure 5. Thermal stress: measure of *EF1α* and CYTB gene levels in ccfDNA of three different *Mythilidae*. Ten mussels of each group (*M.trossulus, M. platensis* and *A. atra)* were placed in sea water at 30°C for 90 minutes or 8°*C* (control group). Hemolymphs were stored on FTA papers and ccfDNA extractions were carried with QIAamp DNA Investigator Kit for *M. platensis* and *A. atra.* Hemolymphs of *M. trossulus* were frozen and extracted with NucleoSnap DNA Plasma Kit. Measures of *EF!a and CYTB genes* by ddPCR amplifications are reported as copies per ml of hemolymph.

Supplementary Table 1. Primers used for different experiments.

Species Target	Gene Target	Primer Name	Primer Sequence (5′ to 3′)	Fragment Size (bp)	Ta† (°C)
Droplet digital PCR					
Mytilus edulis (AY580270.1)	*EF1α*	EF1α835F	CACCACGAGTCTCTCCCAGA	105	53.4 to 63
		EF1α939R	GCTGTCACCACAGACCATTCC		
Mytilus chilensis (KT966847.1)	*CYTB-MC*	Cbmt3828F	GTAGCTTACCTTGGACGGGC	152	51 to 59
		Cbmt3696R	CGGCTAGGGTTGTACTGGTG		
Vibrio spp. (AJ316181.1)	*Vib16S*	Vib550F	GGCGTAAAGCGCATGCAGGT	113	51.9 to 62.3
		Vib663R	GAAATTCTACCCCCCTCTACAG		
Homo sapiens (NM_001042507.4)	*LGALS7*	GAL7HS45F	CAAGTCCTCACTGCCCGAG	188	51.0 to 62.3
		GAL7HS233R	GAGCCTTGCTCCTTGCTGTT		
Standard PCR					
Aulacomya atra (*N/A)	*CYTB-AA*	CbmtAAF	TTAGCTCTGCTTTGCTCGGT	145	60
		CbmtAAR	TCCCAATTCAGGTCAACCCT		
Mytilus edulis (L33448.1)	*18SrRNA*	18SrRNA79F	TAGTGAAACCGCGAATGGCT	296	60
		18SrRNA374R	CCCGTTACCCGTTACAACCA		
Aulacomya atra (Accession : *N/A)	*COX1*	COX1AAF	TACACAGTCCATCCGGTCCC	120	60
		COX1AAR	TCCTGATATGATTTTTCCCCGGT		
Aulacomya atra (*N/A)	*Nd5*	Nd674F	GTTCATTCCCAACATTCGCACA	141	60
		Nd799R	TGTATTTCGGTTGGCTTTCCAC		
Mytilus edulis (AY580270.1)	*EF1α*	EF1α835F	CACCACGAGTCTCTCCCAGA	105	60
		EF1α939R	GCTGTCACCACAGACCATTCC		
Homo sapiens (NM_001042507.4)	*LGALS7*	GAL7HS45F	CAAGTCCTCACTGCCCGAG	188	60
		GAL7HS233R	GAGCCTTGCTCCTTGCTGTT		

*N/A Primers were designed based on the sequence obtained from reads assemblies. PCR amplicons were further obtained and sequenced to validate the presence of mitochondrial DNA.

† Annealing temperature

Supp Table 2. Comparison of ccfDNA extraction methods in hemolymph of *Mythylidae* using two different kits. ccfDNA was extracted from frozen hemolymph or from supernatant spotted on FTA cards using a 5mm punch. NucleoSnap cfDNA kit (Macherey-Nagel, Germany) was used on thawed hemolymph whereas QIAamp DNA Investigator kit (QIAGEN Inc., Canada) could be used dually on both thawed hemolymph or hemolymph preserved on FTA cards.

Species	Extraction kit	n	Punch (mm) or hemolymph (µL)	Concentration (µg) per mL of hemolymph	SDV
M. edulis spp.	Nucleosnap cfDNA	17	1 500 µL	2.67	0.90
M. platensis	QIAamp DNA Investigator	9	5 mm	0.73	0.24
A. atra	QIAamp DNA Investigator	10	5 mm	0.99	0.39
M. edulis spp.	QIAamp DNA Investigator	10	70 µL	7.10	2.03

Supp Table 3. Summary of Kraken2 analysis of non-self reads for *A. atra* and *M. platensis*

Reads	Non-self reads (*A. atra*)	Non-self reads (*M. platensis*)
Unclassified reads	**1 558 305**	**1 067 732**
Classified reads :	**7 181**	**3 893**
Bacteria	6 719	3 656
Virus	64	57
Archaea	124	96
Unassigned	274	84

Chapitre 4

Des coquilles aux séquences : une étude de preuve de concept pour l'analyse sur site de l'ADN libre circulant hémolymphatique provenant de moules sentinelles utilisant la technologie Nanopore

Article publié: *Sci. Total Environ.* 2024, 934:172969

Résumé

Les moules bleues sont souvent abondantes et largement réparties dans les écosystèmes marins côtiers des régions polaires. En raison de leur distribution étendue, de leur importance écologique et de leur mode de vie sédentaire, les bivalves sont considérés comme des indicateurs appropriés de la santé et des changements des écosystèmes. Le suivi de la dynamique des populations de moules bleues peut fournir des informations sur la biodiversité globale, les interactions entre espèces et le fonctionnement des écosystèmes. Dans ce travail, nous avons combiné le concept de biopsie liquide (BL), un concept émergent en médecine basé sur le séquençage de l'ADN libre circulant (ccfDNA), avec la plateforme Oxford Nanopore Technologies (ONT) utilisant un laboratoire portable dans une région éloignée. Nos résultats démontrent que cette plateforme est idéalement adaptée pour le séquençage de fragments de ccfDNA hémolymphatiques chez les moules bleues. Le pourcentage d'ADN non-soi représentait plus de 50 % du ccfDNA dans certains sites d'échantillonnage, permettant l'acquisition rapide d'une vue d'ensemble de la biodiversité d'un écosystème marin côtier. Ces fragments provenaient de virus, bactéries, plantes, arthropodes, algues et de multiples chordés. Outre l'ADN non-soi, nous avons aussi analysé les fragments d'ADN provenant des 14 chromosomes des moules bleues, ainsi que ceux issus des génomes mitochondriaux. Les analyses entre divers sites d'échantillonnage ont montré que la biodiversité variait significativement au sein des micro-habitats. Notre travail montre que la plateforme ONT est bien adaptée pour la BL chez les moules bleues sentinelles dans des conditions éloignées et difficiles, permettant d'accélérer le travail de terrain pour les stratégies de conservation et la gestion des ressources dans divers contextes.

Contribution des auteurs

Yves St-Pierre, France Caza, Stéphane Betoulle et moi avons décidé du plan expérimental. France Caza et moi avons réalisé l'ensemble des expériences de cet article et participé à chacune d'entre elles. J'ai également effectué les différentes analyses bio-informatiques et biostatistiques. Le manuscrit a été rédigé par Yves, France et moi, bénéficiant des contributions et de l'approbation de tous les auteurs à chaque étape du processus.

Science of the Total Environment 934 (2024) 172969

Contents lists available at ScienceDirect

Science of the Total Environment

journal homepage: www.elsevier.com/locate/scitotenv

From shells to sequences: A proof-of-concept study for on-site analysis of hemolymphatic circulating cell-free DNA from sentinel mussels using Nanopore technology

Sophia Ferchiou [a], France Caza [a], Richard Villemur [a], Stéphane Betoulle [b], Yves St-Pierre [a,*]

[a] INRS-Centre Armand-Frappier Santé Technologie, 531 Boul. des Prairies, Laval, QC H7V 1B7, Canada
[b] Université Reims Champagne-Ardenne, UMR-I 02 SEBIO Stress environnementaux et Biosurveillance des milieux aquatiques, Campus Moulin de la Housse, 51687 Reims, France

HIGHLIGHTS

- Analysis of the ccfDNA of sentinel mussels from monitoring marine ecosystems.
- Up to 50 % of hemolymphatic ccfDNA has a non-self origin.
- Non-self ccfDNA derives from viruses, bacteria, algae, and vertebrates.
- The ccfDNA from liquid biopsies is ideally suited to long-read sequencing.
- The ONT platform is ideally suited for ccfDNA analysis in remote areas

GRAPHICAL ABSTRACT

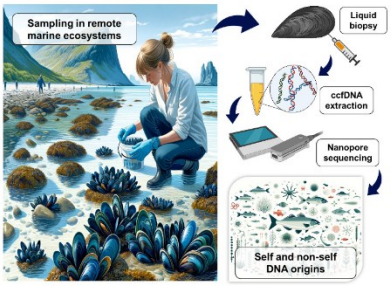

ARTICLE INFO

Editor: Warish Ahmed

Keywords:
Climate change
Liquid biopsy
Mussels
Biodiversity
Self/non-self DNA

ABSTRACT

Blue mussels are often abundant and widely distributed in polar marine coastal ecosystems. Because of their wide distribution, ecological importance, and relatively stationary lifestyle, bivalves have long been considered suitable indicators of ecosystem health and changes. Monitoring the population dynamics of blue mussels can provide information on the overall biodiversity, species interactions, and ecosystem functioning. In the present work, we combined the concept of liquid biopsy (LB), an emerging concept in medicine based on the sequencing of free circulating DNA, with the Oxford Nanopore Technologies (ONT) platform using a portable laboratory in a remote area. Our results demonstrate that this platform is ideally suited for sequencing hemolymphatic circulating cell-free DNA (ccfDNA) fragments found in blue mussels. The percentage of non-self ccfDNA accounted for >50 % of ccfDNA at certain sampling Sites, allowing the quick, on-site acquisition of a global view of the biodiversity of a coastal marine ecosystem. These ccfDNA fragments originated from viruses, bacteria, plants, arthropods, algae, and multiple Chordata. Aside from non-self ccfDNA, we found DNA fragments from all 14 blue mussel chromosomes, as well as those originating from the mitochondrial genomes. However, the distribution of nuclear and mitochondrial DNA was significantly different between Sites. Similarly, analyses between various sampling Sites showed that the biodiversity varied significantly within microhabitats. Our work shows that the

* Corresponding author at: NRS-Centre Armand-Frappier Santé Technologie, 531 Boul. des Prairies, Laval, Québec H7V 1B7, Canada.
E-mail address: yves.st-pierre@inrs.ca (Y. St-Pierre).

https://doi.org/10.1016/j.scitotenv.2024.172969
Received 8 December 2023; Received in revised form 30 April 2024; Accepted 1 May 2024
Available online 15 May 2024

ONT platform is well-suited for LB in sentinel blue mussels in remote and challenging conditions, enabling faster fieldwork for conservation strategies and resource management in diverse settings.

Abbreviations

M. platensis	*Mytilus platensis*
ccfDNA	circulating cell-free DNA
LB	liquid biopsy
cmDNA	circulating microbial DNA
mtDNA	DNA
ONT	Oxford Nanopore Technologies
PCoA	principal coordinate analysis
ASVs	amplicon sequence variants
PERMANOVA	multivariate analysis of variance with permutation
LEfSe	Linear discriminant analysis Effect Size

1. Introduction

Climate change and pollution profoundly impact coastal marine ecosystems, threatening the diversity and delicate balance that supports all life forms. This is particularly accentuated in intertidal marine species inhabiting coastal ecosystems in polar regions (Duncan et al., 2022; Frémont et al., 2022; Gissi et al., 2021). Climate change, marked by global warming, ocean acidification, and extreme weather events, poses risks such as habitat loss, altered community structures, and physiological impacts on intertidal organisms. In the case of anthropogenic threats, including pollution from runoff, it contributes to toxicity and biodiversity reduction (Bashir et al., 2020; Landrigan et al., 2020; James et al., 2023). Any changes in these ecosystems can have a variety of impacts on marine ecosystems, including on the interactions between symbiotic or pathogenic microbes and the hosts they colonize, increasing the vulnerability of marine species to infectious pathogens (Hernroth and Baden, 2018; Zgouridou et al., 2022). As a result, considerable efforts are dedicated to implementing real-time, cost-effective, long-term surveillance and monitoring programs to understand better the changes driven by anthropogenic activities.

Dense mussel beds, particularly those of the blue mussel (*Mytilus* spp.), are crucial components of coastal ecosystems around the world. As ecosystem engineers, they significantly enhance biodiversity and contribute to the structural complexity of their habitats (Borthagaray and Carranza, 2007). Known for their high filtering capacity, mussels improve water quality by removing pollutants and pathogens, and their excretions furnish nutrients that support other marine life forms, enriching the overall productivity of the ecosystem (Sousa et al., 2009; van Broekhoven et al., 2015). Additionally, the complex physical structures of mussel beds provide habitats for a diverse range of marine organisms, thus boosting local biodiversity (Lintas and Seed, 1994). Mussels also serve as sentinel species due to their sensitive response to environmental changes, making them excellent biological indicators for monitoring marine pollution and the effects of climate change (Beyer et al., 2017; Martínez-Gómez et al., 2017; Westerbom et al., 2019; Provenza et al., 2022). However, field-based monitoring programs in remote areas face logistical challenges, notwithstanding the substantial risks and costs of transporting and storing samples. These challenges are particularly accentuated for monitoring marine ecosystems in polar regions, where the effects of climate change are most felt (Le Bohec et al., 2013; Meredith et al., 2019).

Genomics is crucial in enhancing our understanding of how marine ecosystems respond to climate change. It provides valuable insights into the genetic basis of adaptation, phenotypic plasticity, and species' responses to changing environmental conditions, aiding conservation and management efforts in marine ecosystems (Bernatchez et al., 2023). Genomic tools can help assess the genetic diversity of marine species and populations, which is essential for understanding species' adaptive potential and ability to respond to changing environmental conditions. Integrating genomic data with information on gene expression (transcriptomics) and epigenetic modifications (epigenomics) makes it possible to identify the molecular mechanisms underlying phenotypic responses to climate change stressors in marine organisms. The integration of genomic, environmental, and modeling data not only provides a more nuanced understanding of how species might shift geographically but also offers insights into the mechanisms of adaptation and survival under climate change (Chen et al., 2022).

One of the most promising and predictive genomic tools that has recently emerged is the liquid biopsy (LB) concept. This minimally invasive approach has recently gained acceptance in the biomedical field (Poulet et al., 2019). This concept is based on plasma-derived circulating cell-free DNA (ccfDNA) analysis. Although the existence of ccfDNA was established >70 years ago, it is only with the recent development of high throughput DNA sequencing technologies that the potential of this approach has been recognized for monitoring disease progression and response to treatment. The kinetics of ccfDNA release in peripheral blood results from a complex interplay between apoptosis, necrosis, and cellular senescence (Lo et al., 2021; Rostami et al., 2020). Host-derived ccfDNA originates mainly from the nucleus and, to a lesser extent, from mitochondria (ccf-mtDNA). Initially focusing on the analysis of genomic DNA fragments released by tumor cells (Wan et al., 2017), LB is now used in various clinical settings, allowing to obtain a wide range of information to assess the health status of patients with different clinical conditions, including cardiovascular, neurodegenerative, and inflammatory diseases (Alix-Panabières and Pantel, 2021; Ignatiadis et al., 2021).

Apart from providing information obtained from the analysis of DNA fragments released from the host's tissues (referred to here as "self-DNA"), LB can also be used to analyze DNA of "non-self" origin, most notably during pregnancy or transplantation (Ngo et al., 2018; Oellerich et al., 2021). Recent studies have also revealed that human blood contains approximately 1 % of ccfDNA comes from microbial organisms, allowing non-invasive detection of a wide range of bacterial, viral, fungal and parasitic infections, avoiding biopsy of infected tissues (Han et al., 2020; Kowarsky et al., 2017). Studies on the circulating microbiome, often achieved by sequencing the variable *V3* and *V4* regions of the bacterial 16S rRNA gene or by metagenomic approaches, are now common in humans for detecting pathogens, dysbiosis or specific microbiome profiles associated with the onset or progression of disease or the response of a patient to a particular treatment (Blauwkamp et al., 2019; Gopalakrishnan et al., 2018). We and others have recently applied this concept using blood or plasma samples collected from animals, including marine species (Auguste et al., 2024; Ferchiou et al., 2023; Fronton et al., 2023; Lokmer and Mathias Wegner, 2015; Townsend et al., 2021). Sequencing of ccfDNA is also ideally suited to detect the presence of viral genomes, as viruses release their genetic material into the bloodstream. By sequencing the ccfDNA and analyzing the sequencing data, it is possible to identify and characterize viral genomes (Kowarsky et al., 2017).

Illumina sequencing is the most common method for analyzing ccfDNA in clinical settings. This method is well adapted for sequencing short DNA fragments in human blood. Indeed, ccfDNA fragments from vertebrates have a size distribution ranging between 40 and 220 bp, with a ladder pattern with a major peak at approximately 166 bp, which corresponds to single nucleosomal DNA fragments that are protected

from DNA degradation, in contrast to open strand of DNA (An et al., 2019; Favaro et al., 2022; Keller et al., 2021; Kustanovich et al., 2019; Snyder et al., 2016; Werner et al., 2022). Similarly, most mitochondrial ccfDNA fragments are relatively short, ranging from a few dozen to a few hundred base pairs in length (Peng et al., 2023; Zhang et al., 2016). In invertebrates, such as mussels, hemolymphatic ccfDNA fragments are significantly longer, ranging from 1000 to 5000 bp (Ferchiou et al., 2022a, 2022b). This suggests that the ccfDNA of mussels has a different origin, a logical hypothesis given that mussels have a semi-open vascular system and live in an aquatic environment containing high concentrations of genomic DNA derived from microorganisms and metazoans. Theoretically, the length of hemolymphatic ccfDNA in mussels is thus ideally suited for long-read sequencing technologies. Longer reads can span repetitive regions, structural variants, and genomic regions with high heterozygosity, providing a more complete picture of the genetic information present in ccfDNA. Long-read sequencing can also be advantageous for identifying DNA of unknown origin, including bacterial and viral DNA, or in scenarios where the reference genome is not available or incomplete. Long-read sequencing can further provide advantages when using bioinformatic pipelines to identify the origin of DNA fragments. In some cases, such as the Oxford Nanopore Technology (ONT), it can also provide real-time data acquisition, allowing researchers to monitor sequencing progress and make adjustments during the sequencing run. Nanopore sequencers, such as the MinION device, are portable and relatively compact, making them suitable for fieldwork in challenging environments like polar marine ecosystems. This portability greatly facilitates the study of cfDNA in remote areas with limited access to laboratory facilities. It also provides relatively fast turnaround times compared to other sequencing technologies, allowing researchers to obtain preliminary results and make informed decisions promptly.

In the present work, we have evaluated the feasibility of utilizing Oxford Nanopore Technologies to analyze liquid biopsies obtained from *Mytilus platensis* (*M. platensis*) mussels inhabiting a remote subantarctic marine ecosystem.

2. Materials and methods

2.1. Sampling of liquid biopsies

Adult specimens (>70 mm length) of *M. platensis* were collected in November 2021 at three rocky microhabitats of an intertidal mussel bed located on the shore of Base Armor (−49°.27.9858 S, 69°.43.7138 E), located on the central plateau of the main island of the Kerguelen Archipelago (Fig. 1). The microhabitats, characterized by semi-diurnal tides, were chosen according to their specific physicochemical conditions. Site 1, located directly in the area where the freshwater of Armor Lake flows into the marine waters of the Gulf of Morbihan in Hurley Bay, exhibited physicochemical parameters similar to that of freshwater in the Armor Lake spillway. Site 2 represented a higher saline water environment at the wharf's end. Site 3, located in a small creek, displayed intermediate physicochemical features between Sites 1 and 2. Mussels were collected at low tide. The hemolymph was immediately extracted from the adductor mussel with a sterile 21-gauge needle. A total of 10 pools, each containing approximately 3–4 mussels per pool (~1.5 mL each), were collected per Site and immediately centrifuged for 3 min at 6000 rpm using a battery-operated mini-centrifuge (TOMY Multi Spin Centrifuge, Japan). Supernatants were transferred into a 1.5 mL sterile Eppendorf tube and kept on ice until ccfDNA extraction. After centrifugation, cell pellets were resuspended in a volume of 50 μL, homogenized and dispersed on individual discs of Whatman 903™ FTA® cards (Sigma-Aldrich, Oakville, ON, Canada). After a 30-min drying period at ambient temperature, individual cards were kept in zip-sealed sampling plastic bags containing one small desiccant. All physicochemical properties, including conductivity, pH and temperature, were measured with portable multiparameter devices (Milwaukee Models MW102 pH/temperature meters and MW301 EC meter, Milwaukee, USA).

2.2. Circulating cell-free DNA extraction and library preparation

All experiments, including sample processing and DNA analysis, were conducted in field conditions. Hemolymph samples were clarified with a second centrifugation for 3 min at 6000 rpm at ambient temperature and transferred into a sterile 1.5 mL Eppendorf tube. According to the manufacturer's instructions, hemolymphatic ccfDNA was isolated using the QIAamp DNA Investigator Kit (Qiagen, Hilden, Germany). Purified DNA was quantified using the Qubit™ dsDNA HS assay kit protocol (ThermoFisher Scientific, Cleveland, OH, USA) as described by the manufacturer's instructions. Whole genome amplification was conducted using the REPLI-g UltraFast Mini Kit (Qiagen, Hilden, Germany) according to the manufacturer's recommendations. This allowed us to achieve uniform amplification of long DNA strands with minimal sequence bias (Ahsanuddin et al., 2017). Notably, REPLI-g is compatible with Nanopore technology, making it well-suited for untargeted long-read sequencing using the Rapid sequencing kit. The PCR-free library preparation approach is also advantageous for DNA sequencing in remote areas such as the Kerguelen Islands. Sequencing ccfDNA libraries for Oxford Nanopore Technologies were prepared using the Rapid sequencing gDNA - whole genome amplification kit (SQK-RAD004, ONT, Oxford, UK), following the manufacturer's instructions. Each ccfDNA library per Site was prepared in triplicate and loaded onto R9.4.1 flow cells (ONT, Oxford, UK), and the sequencing was performed using ONT MinION™ portable sequencing devices (i.e. Mk 1B and Mk1C). As there was no Internet connection, the Mk1B sequencing device was run offline with MinKNOW™ software v21.06.0, a base-calling program provided by ONT. MinKNOW™ software v22.08.4 was used on the Mk1C sequencing device. We also used Guppy v5.0.11 to conduct the fast base-calling model with a quality score threshold ≥9. We prepared more ccfDNA libraries for Site 2 based on the best-performing sequencing data. The total sequencing run time was 13 h for Site 1, 30 h for Site 2 and 7 h for Site 3 (Table 1). Raw data files from ccfDNA sequencing libraries are available on NCBI Sequence Read Archive (PRJNA954899).

2.3. Bioinformatic analysis

Cutadapt (v3.5) (Marcel, 2011) was used for trimming sequencing adapters (5′-GTTTTCGCATTTATCGTGAAACGCTTTCGCGTTTTTCGTGCG-TCAGTTCA-3′ and 3′-CAAAAGCGTAAATAGCACTTTGCGAAAGCGCAAAAAGCACGCA-GTCAAGTCGT-5′) and short sequences (≤500 bp) from the raw sequencing data. An initial taxonomic assignment was carried out on trimmed reads aligned against the NCBI bivalve database (NCBI taxid 6544) using the basic local alignment search tool BLAST+ (v2.12.0) with an *e-value* ≤ 1e−3 and at least 80 % of homology. Non-self reads were identified as the remaining reads not related to bivalves. Verifications of taxonomic profiles of non-self reads were obtained using alignment with BLASTn and BLASTx using nt and nr NCBI databases, respectively, as the most accurate libraries. We manually curated the analysis and established rigorous parameters to prevent false positives, including setting the *e-value* at ≤1e−50 and a query length of ≥500 bp. However, we finally kept only the BLASTn analyses as we found that results using BLASTn alignment generated higher accuracy and fewer duplicates than BLASTx. BLASTn allows for a more straightforward and faster comparison, which is crucial for maintaining the integrity and specificity of our findings. We also tested classification methods, such as Kraken2 (Wood et al., 2019) with the Standard library compiled using the RefSeq database (downloaded on May 17, 2021) or Metamaps (Dilthey et al., 2019). We found that K-mer-based methods were not highly effective in classifying DNA fragments of non-self origin, generating an unsatisfactory number of false positives. We estimated that <0.01 % of the total reads were of human origin. As we used the REPLI-g kit, we excluded all phi29 bacteriophage sequences from our

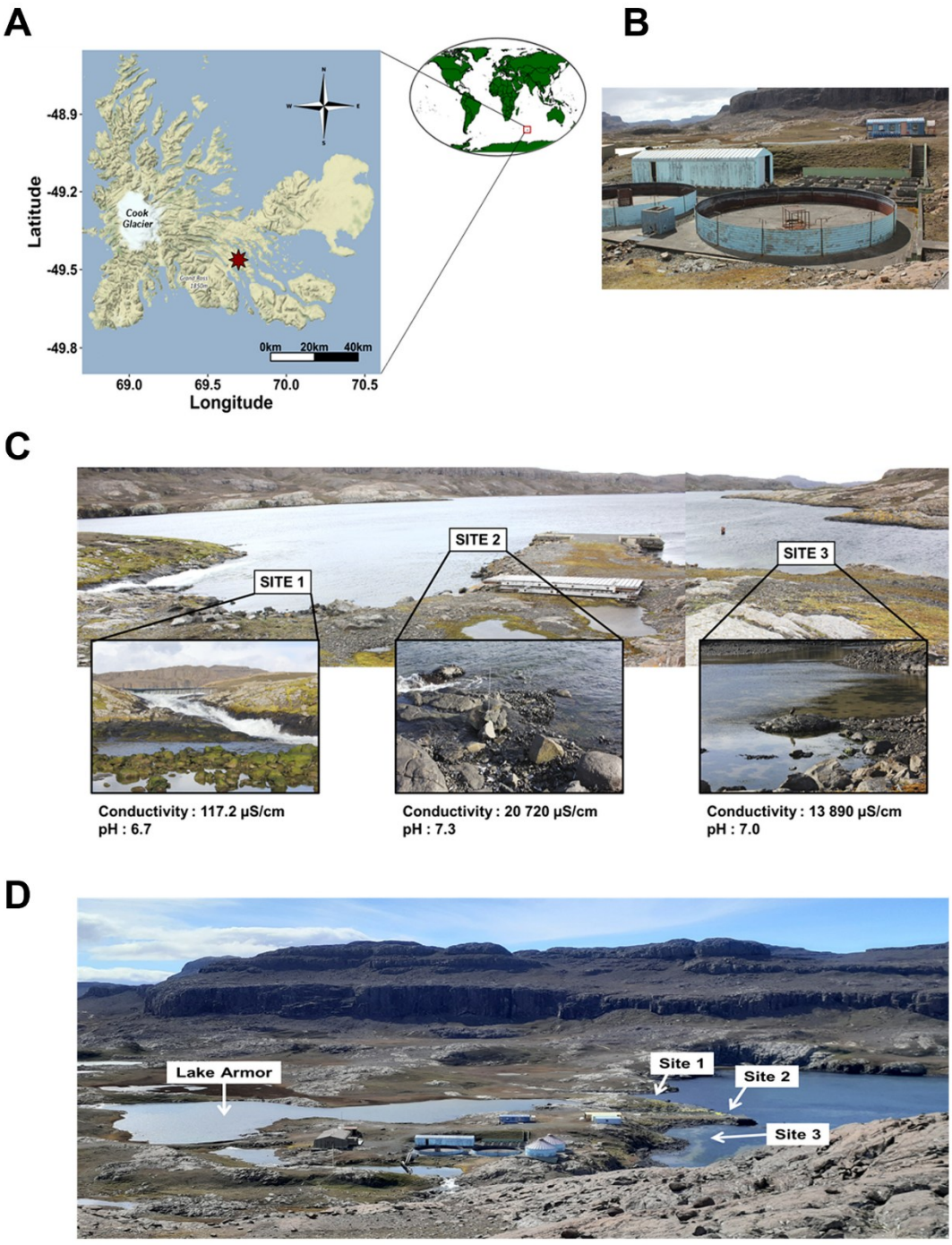

Fig. 1. Sampling locations. (A) Location of Armor Site (red star) in Kerguelen Islands, French Southern and Antarctic Lands. The map was created with *ggmap* (v3.0.2), *ggplot2*(v3.4.2) and *mapdata* (v2.3.0) R packages (v4.2.3) (Becker et al., 2022; Kahle and Wickham, 2013; R Core Team, 2023). (B) Remains of the *Aquasaumon Armor* farming station. (C) Positioning of the three microhabitats characterized by distinct physicochemical properties. (D) Distant view of the Armor Site showing microhabitats and Lake Armor.

Table 1
Sequencing statistics for MinION runs with circulating cell-free DNA samples from *M. platensis* collected at three sampling Sites. The quality score (Q) threshold was set ≥9.

Sites	*n*	Run time	DNA input (ng)	Throughput (Mbp)	Reads (number)	Average reads length (bp)	N50
Site 1 (runoff)	3	13 h32	472–800	1050.8	708,910	851 (39–116,323)	1535
Site 2 (sea water)	8	30 h06	800–1282	4508.7	968,048	2676 (50–116,743)	5017
Site 3 (brackish water)	3	7 h19	800–1623	926.0	116,985	2866 (79–80,967)	5662
Total	14	50 h57	472–1623	6485.5	1,793,943	1967	4196

analysis to ensure the accuracy and reliability of our results. Virus identifications were also compared with Virsorter2 (v2.2.3) (Guo et al., 2021), a pipeline allowing the detection of a wide array of DNA and RNA viral genomes while filtering out any low-quality viral sequences using CheckV (v0.7.0 9) (Nayfach et al., 2021). Final viral sequences were annotated using the DRAMv tool (v1.2.0) (Shaffer et al., 2020).

2.4. 16S rRNA data processing

To perform a comprehensive understanding of cmDNA, we sequenced the 16S rRNA (V3-V4) gene from DNA extracted from hemolymphatic cell pellets (with six samples per micro-habitat) following the method described by Caza et al. (2019). Specifically, our 16S rRNA analyses were conducted on hemocyte pellets collected on FTA cards in a metropolitan region. This method offers significant advantages for field studies, particularly in challenging environments, as it eliminates the need for maintaining a cold chain. Briefly, individual discs were cut from the FTA cards using a sterile 5.0 mm single round hole punch. According to the manufacturer's protocol, total DNA was isolated using the QIAamp DNA Investigator Kit (Qiagen, Hilden, Germany). DNA was quantified in duplicate using the Qubit dsDNA HS Assay Kit (ThermoFisher Scientific, Cleveland, OH, USA). Amplification of the 16S ribosomal RNA (rRNA) genes and 16S gene amplicon sequencing were performed at the Centre d'Expertise et de Services Génome Québec (Montreal, QC, Canada) using the universal primers 341F (5′-CCTACGGGNGGCWGCAG-3′) and 805R (5′-GACTACHVGGGTATCTAATCC-3′) targeting the V3–V4 hypervariable regions (Klindworth et al., 2013). The CS1 (ACACTGACGACATGGTTCTACA) and CS2 (TACGGTAGCAGAGACTTGGTCT) tags were used as Illumina adapters and sample-identification barcodes. Negative controls were included during the amplification step and the library preparation. Libraries were quantified using the Quant-iT PicoGreen dsDNA Assay Kit (ThermoFisher Scientific, Carlsbad, CA, USA) and the Kapa Illumina GA with Revised Primers-SYBR Fast Universal kit (Kapa Biosystems Inc., MA). Paired-end sequences were generated on a MiSeq platform PE300 (Illumina Corporation, San Diego, CA, USA) with the MiSeq Reagent Kit v3 600 cycles (Illumina). For data pre-processing, the DADA2 pipeline (v1.16.0) (Callahan et al., 2016) was used to generate 16S rRNA (V3-V4) amplicon sequence variants (ASVs) as described in Ferchiou et al., 2023. The raw data files are publicly available on the NCBI Sequence Read Archive (PRJNA954899).

2.5. Statistical analysis

All statistical analyses were performed within the R environment (v4.2.3) (R Core Team, 2023). The ccfDNA data were analyzed using the Kruskal-Wallis followed by pairwise Mann-Whitney tests for continuous variables, while the Chi-square test was used for categorical variables. For 16S rRNA amplicons, the alpha-diversity index was calculated using the *phyloseq* (v1.42.0) (McMurdie and Holmes, 2013) R package, where the average values of each group were compared using Wilcoxon rank sum tests. Microbiota composition differences among groups were determined using multivariate analysis of variance with permutation (PERMANOVA) as implemented in the R package *vegan* (v.1.42.0) (Oksanen et al., 2015) with 9999 permutations to test for differences in unweighted UniFrac distance. Differences in beta diversity were also visualized with principal coordinates analysis (PCoA) plots. Linear discriminant analysis (LDA) identified the effect size (LEfSe) that differentiates the samples among these taxa with a threshold on the logarithmic score of the LDA analysis set to 3.0. LEfSe analysis was performed using the *lefser* R package (v1.12.1) (Khleborodova, 2023). *False-discovery rate* (*FDR*) methods were used to correct for multiple comparisons (Benjamini and Hochberg, 1995). FDR correction is a post-hoc test that controls for the proportion of false positives among all significant results. It is a less conservative test than the Bonferroni correction and Tukey's HSD test, making it more powerful (Midway et al., 2020).

3. Results

3.1. Logistics and sampling Sites

The study was conducted at the Kerguelen Islands, more precisely at a remote research Site called Armor. This isolated archipelago of Kerguelen is part of an oceanic submerged plateau located near the boundary of the Indian Ocean and the Southern Ocean (Fig. 1A). The Armor Site stands as a reminder of the unsuccessful *Aquasaumon Armor* farming station, where countless salmonids were introduced decades ago into the fjord-like Lake Armor and its tributaries (Davaine et al., 1997; Duhamel and Williams, 2011) (Fig. 1B). A relatively large mussel bed borders the shore around a small pier. In this mussel bed, three Sites were selected based on their different physicochemical characteristics. The salinity and pH of Site 1 are typical to runoff water from Armor Lake. In contrast, the salinity and pH found at Sites 2 and 3 are more consistent with seawater and brackish water but physically separated by the pier (Fig. 1C). The mussel bed where mussels were collected is characterized by semi-diurnal tides and located within a relatively short distance of the infrastructures (Fig. 1D). The entire study, including purification of DNA, preparation of libraries and DNA sequencing, was conducted in one of the abandoned infrastructures with no internet connection and electrical power from a battery powered by a portable gas generator. A clean and sealed lab environment was prepared to minimize contamination (Fig. S1). Overall, we sequenced 1,793,943 reads (Qscore ≥ 9), representing approximately 6.5 Gbp throughout 50 h of sequencing (Table 1). More than 30 h of sequencing were devoted to Site 2 to measure the platform's stability in a non-optimal environment. We also sequenced the ccfDNA of mussels collected from two adjacent Sites (Sites 1 and 3) for comparative analysis. After trimming, the average lengths of the hemolymphatic ccfDNA reads were 2676 and 2866 bp for mussels collected at Sites 2 and 3, respectively (Table 1). For Site 1, the average length of the ccfDNA fragments was 851 bp.

3.2. Analysis of ccfDNA of self and non-self origin

For our analysis, reads were first divided into two groups: those originating from *Mytilus* spp. sequences (self) and those of foreign origin (non-self). Out of the 1,265,585 trimmed reads obtained, 694,449 and 571,136 were assigned as from a self and non-self origin, respectively (Table 2). The highest percentages of reads of non-self origin were found at Sites 2 (53 %) and 3 (59 %). In contrast, only 9 % of reads found in Site 1 were from a non-self origin (Fig. 2A). The average read length varied between 850 and approximately 2800 reads, with smaller reads in Site 1,

Table 2
Reads of self and non-self origins (≥500 bp).

Sites	Trimmed reads	Self reads	Non-self reads	Average length (bp): Self	Average length (bp): Non-self
Site 1 (runoff)	337,362	306,915	30,447	1523 (500–46,351)	1266 (500–116,323)
Site 2 (sea water)	834,975	349,347	485,628	2814 (500–116,743)	3731 (500–72,983)
Site 3 (brackish water)	93,248	38,187	55,061	2663 (500–54,065)	4116 (500–80,967)
Total	1,265,585	694,449	571,136	2235	3623

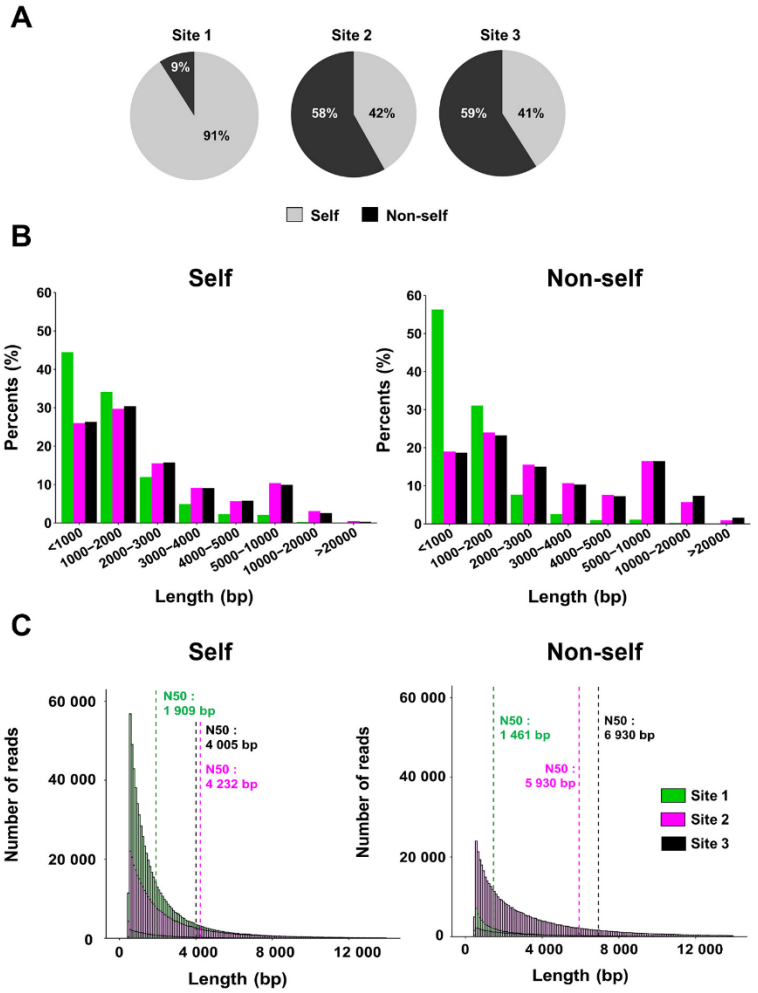

Fig. 2. Distribution of hemolymphatic DNA fragments of self and non-self origins. (A) Pie charts showing the proportion of self and non-self DNA fragments. (B) Sequence length distributions of self (left) and non-self (right) reads. The results are expressed as percentages (%). (C) Histograms showing the length distribution of self (left) and non-self (right) reads with dashed lines representing N50 values. The results are expressed as the absolute number of reads.

independently of their origin (Fig. 2B and C). We found that prokaryotes, particularly bacteria, were dominant (73–89 %) for all sampling Sites, followed by viruses (3–24 %) and eukaryotes (1–7 %) (Fig. 3A). These data are consistent with the rich microbial content of marine seawater, known to contain $>10^5$–10^6 bacteria per mL (Whitman et al., 1998). The length of the non-self DNA fragments varied little depending on the origin. However, we found statistically significant differences between the prokaryote fragments versus those from viral and eukaryotic genomes (Fig. 3B). The eukaryotic diversity was mainly composed of Chordata for all three Sites (Fig. 3C). Greater than half of this phylum was found at Site 3 (78 %), followed by Site 1 (62 %) and Site 2 (54 %). Overall, the results showed that the origin of the non-self ccfDNA varies considerably between microhabitats of a mussel bed.

3.3. Circulating bacterial DNA analysis

There are several ways to analyze the circulating bacterial microbiome. Generally, it is often analyzed from cell pellets by amplifying the

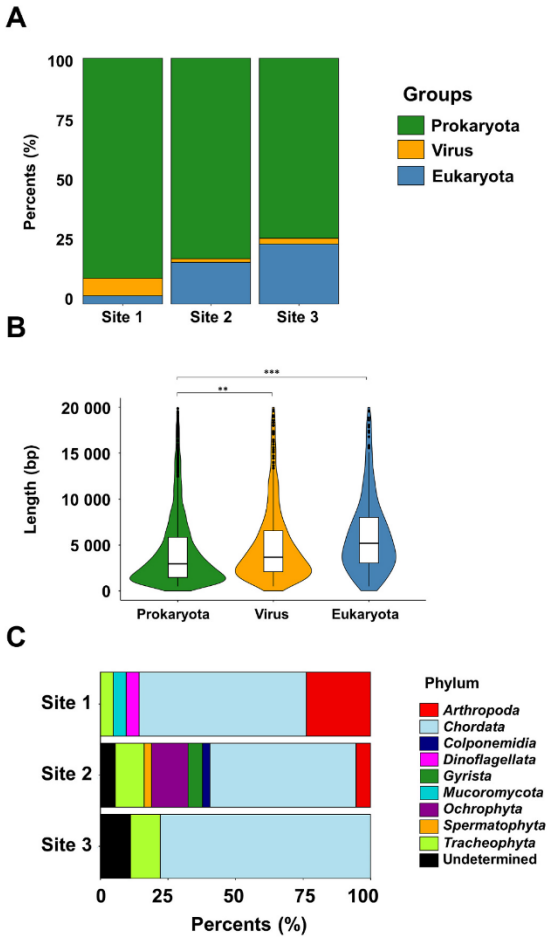

Fig. 3. Origin of non-self ccfDNA fragments. (A) Stacked bar plots of the relative abundance of prokaryotic (green), eukaryotic (blue), and virus (yellow) reads based on BLASTn hit to the NCBI nt database. The results are expressed as percentages (%). (B) Visualization (violin plot overlaid a box plot) of the read lengths of prokaryotic (green), viral (yellow) and eukaryotic (blue) non-self fragments. (C) Stacked bar plots representing phylum-level analysis of non-self eukaryotic DNA. The results are expressed as percentages (%). Note: ***$p \leq 0.001$.

V3-V4 region of the gene coding for 16S ribosomal RNA, common to all bacteria. We thus compared the signature of the circulating microbiome identified through ccfDNA sequencing with that obtained from hemocyte pellets. We hypothesized that these two signatures would have notable differences because a large proportion of blue mussel hemocytes are very active in bacterial opsonization, thus containing a pool of bacterial DNA different from that of ccfDNA. In the case of the bacterial ccfDNA, we found that *Escherichia*, *Sphingomonas*, and *Candidatus Pelagibacter* were the dominant genera for all three Sites (Fig. 4A). The presence of *Shigella* was more important in Site 1 when compared to Sites 2 and 3, which had a higher abundance of *Streptomyces*. Six samples per micro-habitat were analyzed for the 16S rRNA (V3-V4) gene sequencing on hemolymphatic cell pellets. 3045 ASVs were generated from 323,514 sequences passing quality filtering (8810 ± 3176 per sample). Overall, we found the relative abundance of genera mainly was composed of *Lewinella* (24 %, 6 %, and 11 % for Site 1, Site 2, and Site 3, respectively), *Sulfitobacter* (6 %, 7 %, and 7 %, respectively), *Kistimonas* (2 %, 5 % and 7 % respectively), *Granulosicoccus* (4 %, 5 % and 4 % respectively), and *Sulfurimonas* (4 %, 5 % and 3 % respectively) (Fig. 4B). This is in agreement with the dominance of *Pseudomonata* and *Bacteroidota*, which accounted for >65 % of the composition of all Sites (Fig. S2). We did not detect the presence of *Escherichia*, *Candidatus Pelagibacter*, or *Shigella* genera in 16S rRNA gene analysis as we did in the ccfDNA study. A closer look at the microbiome profile obtained using both methods indicated that between 26 % and 45 % of the genera detected in the ccfDNA were also seen in the cell pellets by the 16S method (Fig. 4C). The genera *Granulosicoccus*, *Lewinella*, *Sulfitobacter*, *Sulfurimonas*, and *Yoonia* were the only ones found at all three Sites using both methods. These results are consistent with a previous 16S study showing that *Granulosicoccus*, *Lewinella*, *Sulfitobacter*, and *Sulfurimonas* were the most abundant genera in intertidal blue mussels at Armor in 2018 (Ferchiou et al., 2022a, 2022b). A linear discriminant analysis (LDA) effect size (*LefSe*) analysis revealed that *Lewinella*, along with *Octadecabacter*, *Psychrobacter*, and *Lacihabitans*, were the top genera that distinguished Site 1 from Sites 2 and 3 (Fig. 5A). We did not, however, detected any statistically significant differences between Sites in the diversity indices, including richness ($\chi^2 = 2.21, p \geq 0.05$, df = 2), Shannon ($\chi^2 = 2.31, p \geq 0.05$) and Simpson ($\chi^2 = 2.34, p \geq 0.05$) indexes (Fig. 5B). Comparative analysis of the β-diversity between Sites using the principal coordinate analysis (PCoA) based on unweighted UniFrac distance revealed significant differences among Sites ($F_{(15, 2)} = 1.32$, $p \leq 0.001$) (Fig. 5C). Microbial community structures differed significantly between all Sites using pairwise comparisons ($p \leq 0.05$). Together, these results demonstrate that the bacterial DNA profiles found in the hemolymph as ccfDNA differ significantly from those obtained from the cell pellet. Our results further showed that, regardless of the method used, the circulating bacterial microbiome signatures differ between Sites.

3.4. Circulating virome analysis

We then paid particular attention to ccfDNA of viral origin. To do this, we used two different strategies. First, we employed a BLAST alignment strategy with a reference library of known viruses, such as NCBI Viral Genomes database, using a high stringency cut-off (*e* value < 1e−50). Our results showed that bacteriophages dominated Site 1. In contrast, ccfDNA from non-phage was more abundant at Sites 2 and 3 (Fig. 6A). Among the latter, the viral community was mainly composed of single-stranded DNA (ssDNA) viruses (Fig. 6B). At Site 1, the relative abundance of ssDNA viruses was comparable to that of double-stranded (dsDNA) viruses, consistent with the dominance of *Caudoviricetes* and *Malgrandaviricetes* (dsDNA and ssDNA viruses respectively) (Fig. 6C). By comparison, the presence of non-phage viruses at Sites 2 and 3 was attributed to the presence of DNA fragments originating from *Arfiviricetes* and *Megaviricetes*.

Due to the need for universal gene annotations, using read aligner tools to identify viral sequences in environmental metagenomics data is challenging. This is why, as a second strategy, we used VirSorter2 as a complementary multi-classifier strategy. This tool exploits hallmark genes to identify viruses only distantly related to RefSeq genomes (Guo et al., 2021). Using this strategy, we identified the presence of ccfDNA fragments of non-phage origin at Site 1 that were associated with *Arfiviricetes* and, to a lesser extent, with *Faserviricetes* (Fig. 6A, C). In contrast, the repertoire of viral sequences at Sites 2 and 3 was similar using both strategies. At the family level, ccfDNA fragments from *Circoviridae* were found at all Sites (Fig. 6D). Interestingly, Site 1 exhibited a greater diversity than Site 3, despite the latter having a higher number of non-self sequences. These data are consistent with previous findings showing that estuarine environmental factors may impact marine viral abundance (Chen et al., 2019; Jasna et al., 2019; Sun et al., 2021).

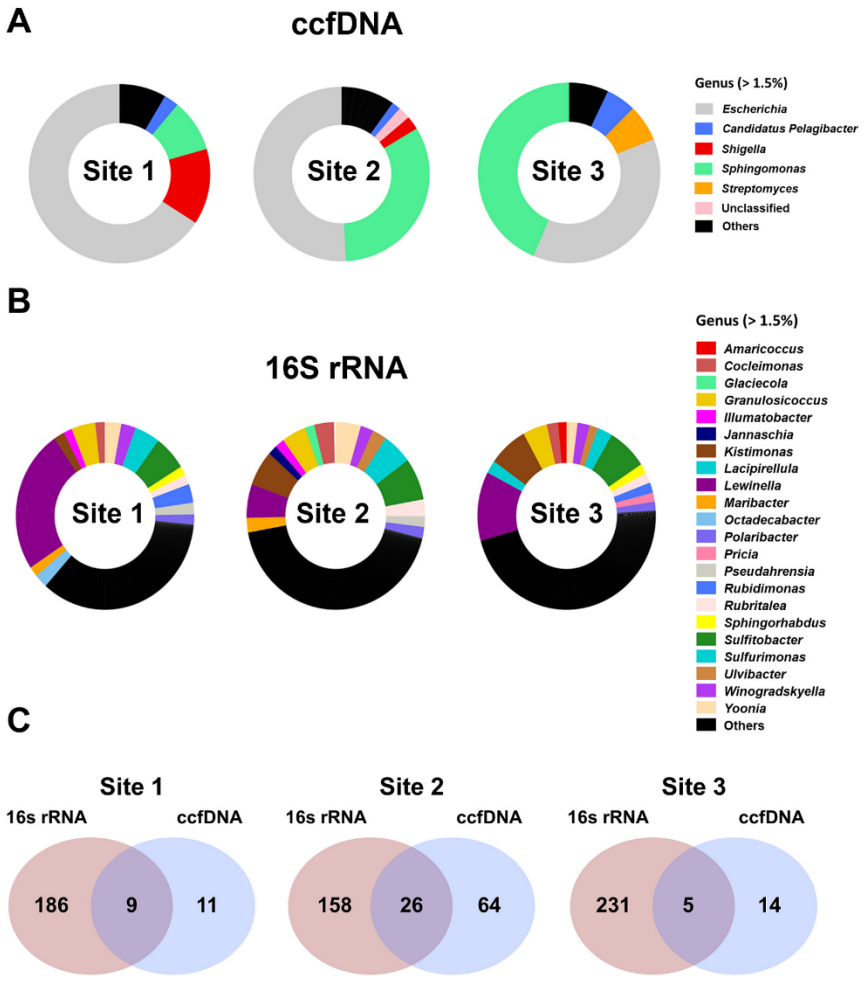

Fig. 4. Hemolymphatic circulating microbiome. (A) Relative abundances at the genus level of bacterial ccfDNA. (B) 16S rRNA analysis on hemolymphatic cell pellets. A genus with a relative abundance of ≤1.5 % is represented as "Other". (C) Venn diagrams showing the number of unique and shared genera in both ccfDNA and 16S rRNA analysis.

3.5. Self (*M. platensis*) origin

Next, we investigated the ccfDNA of self-origin, focusing on the distribution patterns of nuclear and mitochondrial DNA. We found ccfDNA from all 14 chromosomes and ccfDNA of mitochondrial origin. However, nuclear and mitochondrial DNA distribution significantly differed between Sites ($\chi^2 = 26.22, p \leq 0.001$), particularly between Site 1 and Sites 2 and 3. The relative abundance of ccfDNA fragments derived from chromosomes 3 and 6 was higher in Site 1 (26 % and 16 %, respectively) compared to Sites 2 (7 % and 8 %, respectively) and 3 (6 % and 6 %, respectively) (Fig. 7A). In contrast, the percentage of mitochondrial DNA was similar (approximately 0.2 %) for all three Sites. Analysis of the length of ccfDNA originating from each chromosome and mitochondrial DNA showed chromosomal and mitochondrial ccfDNA fragments from Site 1 were significantly shorter, ranging from 1325 bp to 1887 bp, than those from Sites 2 and 3 (ranging from 2608 bp and 2225 bp) (Fig. 7B). When we examined the distribution of the mitochondrial genes, we found that ccfDNA derived from *MT-ND4* gene was the most prevalent, especially in the case of Site 1 (36 %), in comparison to Site 2 (23 %) and Site 3 (22 %) (Fig. 7C).

4. Discussion

In the present work, we sought to determine the feasibility of using Nanopore technology for the sequencing of hemolymphatic ccfDNA of the blue mussels and, at the same time, evaluate the potential for nanopore-based sequencing for on-site analysis in a remote location representative of a polar environment. Overall, our results demonstrate that this technological platform is well suited for ccfDNA sequencing in remote areas and ideally suited for sequencing long hemolymphatic ccfDNA fragments found in blue mussels. Our findings further showed that studies of the hemolymphatic ccfDNA of blue mussels provide a rich source of information on the prevalence and abundance of bacterial and viral genomes present in the host and its surrounding environment, allowing the detection of a wide range of viruses with the potential to infect the host or other organisms present in the marine ecosystem. From a more fundamental point of view, our results also demonstrate that the circulating mussel microbiome comprises two distinct compartments,

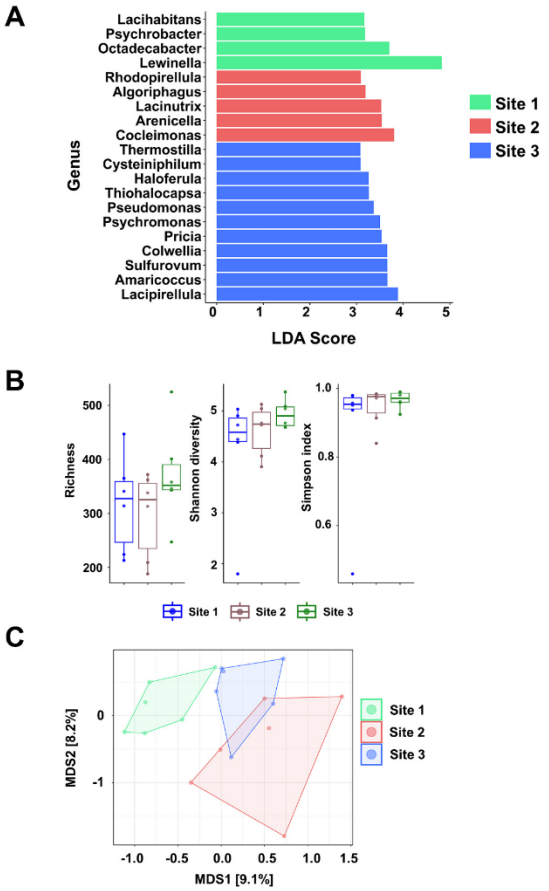

Fig. 5. Beta-diversity and alpha-diversity of circulating microbial DNA among microhabitats. (A) Discriminant genera as determined by analysis of the ccfDNA and using the 16S rRNA sequencing. The logarithmic score of the LDA analysis was set to 3. (B) Alpha diversity of circulating microbiome as determined following analysis of the ccfDNA and 16S rRNA sequencing. Observed richness, Shannon diversity and Simpson indexes were calculated for each group. No significant differences were observed between microhabitats. (C) Principal Coordinates Analysis (PCoA) of bacterial DNA bacterial communities in both analyses. Unweighted UniFrac-based of Site 1 (green), Site 2 (red) and Site 3 (blue) samples.

the first being defined by the analysis of free genomic DNA fragments circulating in the hemolymph. In contrast, the second is determined by DNA bacterial genomics present in the cellular fraction of the hemolymph. Finally, we show that the information contained in the ccfDNA collected from the blue mussel, including self- and non-self ccfDNA, is impacted by its immediate environment, which is a definite advantage for better assessing the complexity of the microhabitats within mussel beds, which offer refuge, feeding grounds, and nursery areas for various species.

The use of LB in marine ecology can be compared to analysis using environmental DNA (eDNA) up to a certain point. We instead consider both methods complementary to each other, as they provide valuable insights into the health status of an ecosystem and its biodiversity (Fig. 8). Analysis of ccfDNA, however, is better suited for providing information on the impact of environmental stressors on a given host. This includes genetic and epigenetic changes in the nuclear and mitochondrial genomes. It can also detect the presence of foreign (non-self) DNA fragments integrated into the host genome. A case in point is the integration of retroviral elements (such as proviruses) in the host genome. This is an important issue in marine ecology, given the existence of horizontally transmitted retroviral elements in bivalves (Metzger et al., 2015; Metzger et al., 2016). The results of our study also indicate that LB is better suited for long-read sequencing platforms, such as ONT. This is a non-neglectable advantage considering the logistically-friendly Nanopore sequencing platform. Generally, eDNA fragments are relatively short compared to the intact DNA from an organism's genome. This is because DNA released into the environment can undergo degradation processes, such as enzymatic degradation and physical decay, resulting in DNA molecule fragmentation over time. Factors such as water temperature, UV exposure, and the presence of microbial communities can influence the rate of DNA degradation and, consequently, the average fragment length (Grzyb and Frączek, 2012; Jo et al., 2019; Mauvisseau et al., 2022). These factors are attenuated in the case of hemolymphatic ccfDNA present in mussels. Another fundamental difference between eDNA and ccfDNA collected from the mussel is this hypothesis is supported by our results demonstrating that ccfDNA is defined by its microhabitat, as shown by our differences between the three Sites. Although the distance between these three Sites is only a few meters (< 10 m), our results indicate a marked difference in biodiversity at the eukaryotic and prokaryotic levels. These results are consistent with our recent studies in controlled conditions, which demonstrated that the turnover of hemolymphatic ccfDNA is very rapid (<2–3 h) (Ferchiou et al., 2022a, 2022b). eDNA is more suitable for monitoring biodiversity over large geographical areas. However, future experiments comparing eDNA and ccfDNA samples in natural and experimental settings will be needed to understand better how these multi-omics approaches can provide a more comprehensive overview of biodiversity, ecological interactions, and environmental stress responses in various aquatic ecosystems.

LB represents a ground-breaking, non-invasive approach to medical diagnostics, with a primary focus on detecting tumor biomarkers and analyzing crucial genetic data derived from various body fluids, particularly blood. Originally pioneered in the field of oncology, LB has revolutionized cancer detection, staging, and monitoring, thereby eliminating the necessity for invasive tissue biopsies in localized cancer patients. Nowadays, it is also being increasingly used in other medical fields to study DNA fragments with a non-self-origin. For example, in the case of the detection of genetic anomalies in the fetus, thus reducing the risks incurred during amniocentesis or detecting the rejection of allogeneic grafts. Thanks to the availability of sequencing data generated by the numerous studies and clinical trials aimed at validating this clinical application, several research teams have studied the presence of DNA fragments of non-human origin. The most recent studies have shown that approximately 1 % of ccfDNA in humans comes from various microorganisms, notably viruses (Eldem et al., 2023; Kowarsky et al., 2017; Linthorst et al., 2023). In the mussel, our results demonstrate that the percentage of ccfDNA of non-self origin is significantly higher than that found in humans. This difference is not surprising given that bivalves have a semi-open vascular system and that the concentration of viruses in seawater and freshwater varies between 10^6 and 10^9 viruses per mL, which is ten times higher than the concentration of bacteria (Maranger and Bird, 1995). Yet, we know very little about the aquatic virome of coastal marine ecosystems and their interaction with their host. Identifying DNA of viral origin in seawater through bioinformatic sequencing data analysis is still challenging. Here, we used the VirSorter2 classifier as a complementary tool to BLASTn alignment analysis to detect viral sequences from our datasets. VirSorter2 offers higher specificity in predicting the presence of ssDNA, dsDNA and RNA viruses within the viral communities (Guo et al., 2021). On the one hand, our data indicated the presence of double-stranded DNA viruses at all Sites, including *Caudoviricetes*, with Site 1 showing a higher prevalence, consistent with the abundance of tailed bacteriophages in freshwater

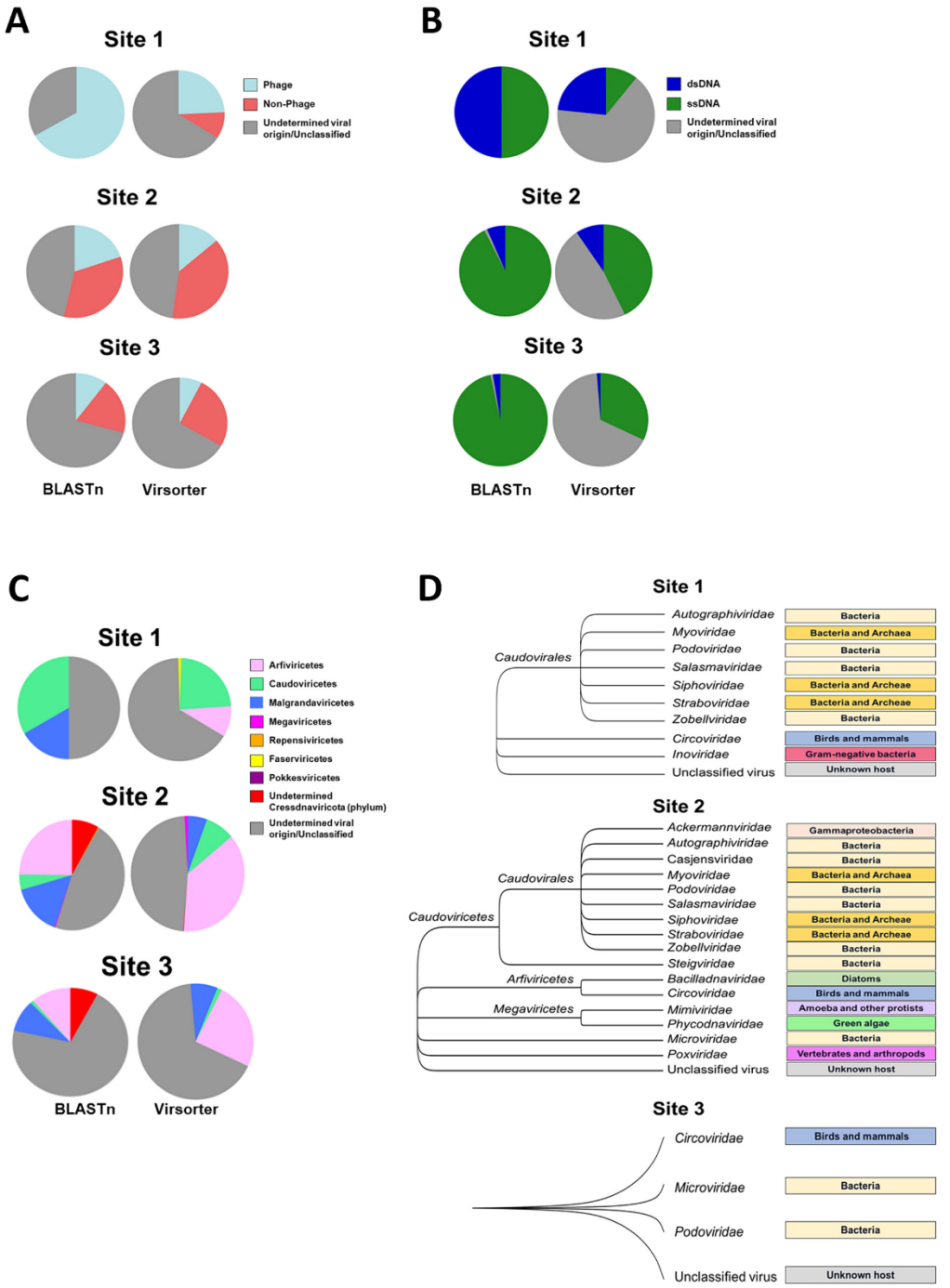

Fig. 6. Hemolymphatic ccfDNA fragments of viral origin. Comparisons of (A) bacteriophage sequences, (B) viral DNA structures and (C) virus classes found in each Site using BLASTn (left) and Virsorter2 (right). (D) Phylogenetic tree of virus families and their hosts based on VirSorter2 annotation tool.

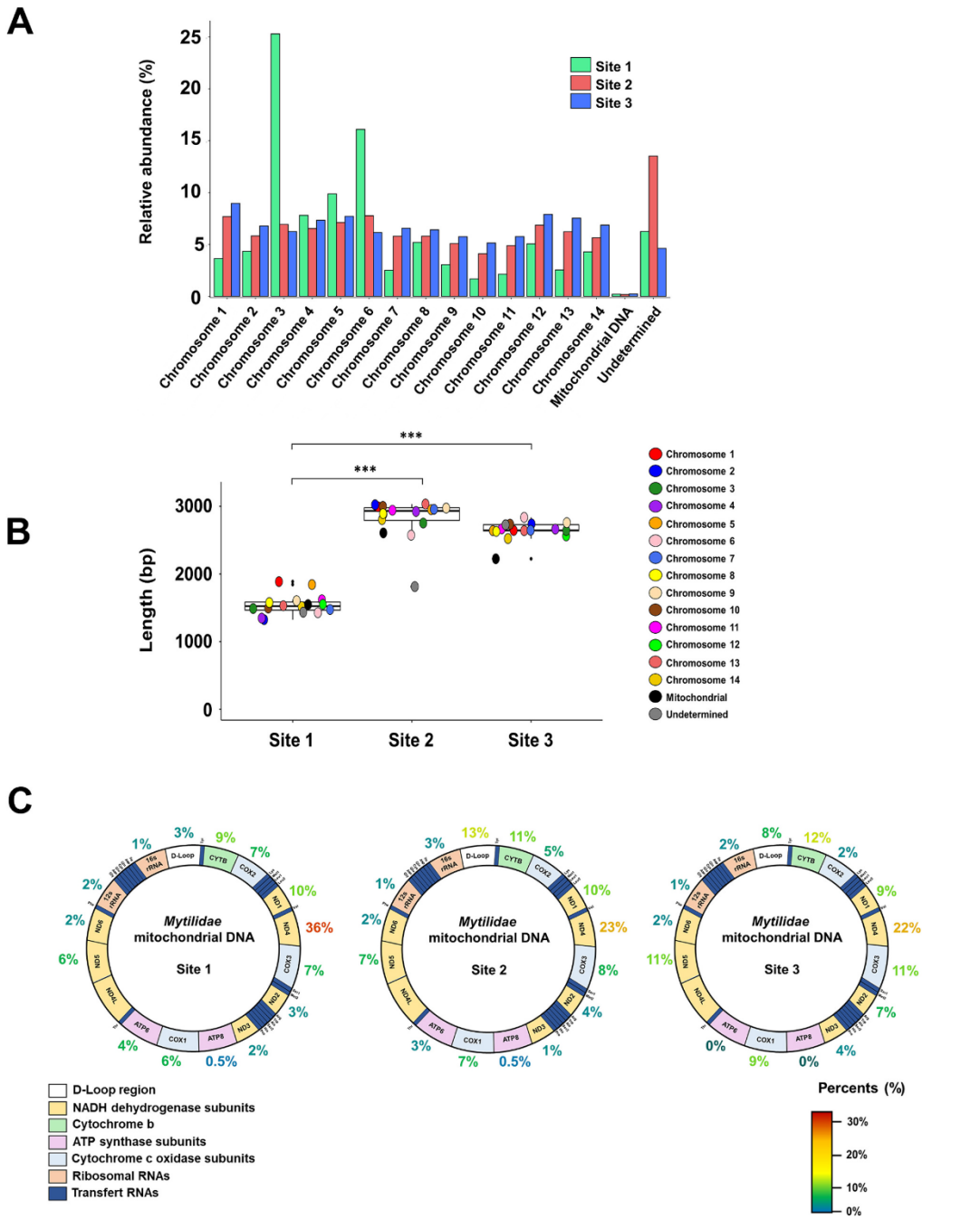

Fig. 7. Hemolymphatic ccfDNA fragments of host's origin. (A) Bar plots of the distribution patterns representing the relative abundances of both nuclear and mitochondrial DNA in Site 1 (green), Site 2 (red) and Site 3 (blue). (B) Box plot showing the length of both chromosomal and mitochondrial ccfDNA fragments. (C) Mitochondrial maps of blue mussels showing the relative abundances of different mitochondrial genes detected in all three microhabitats. Note: ***$p \leq 0.001$.

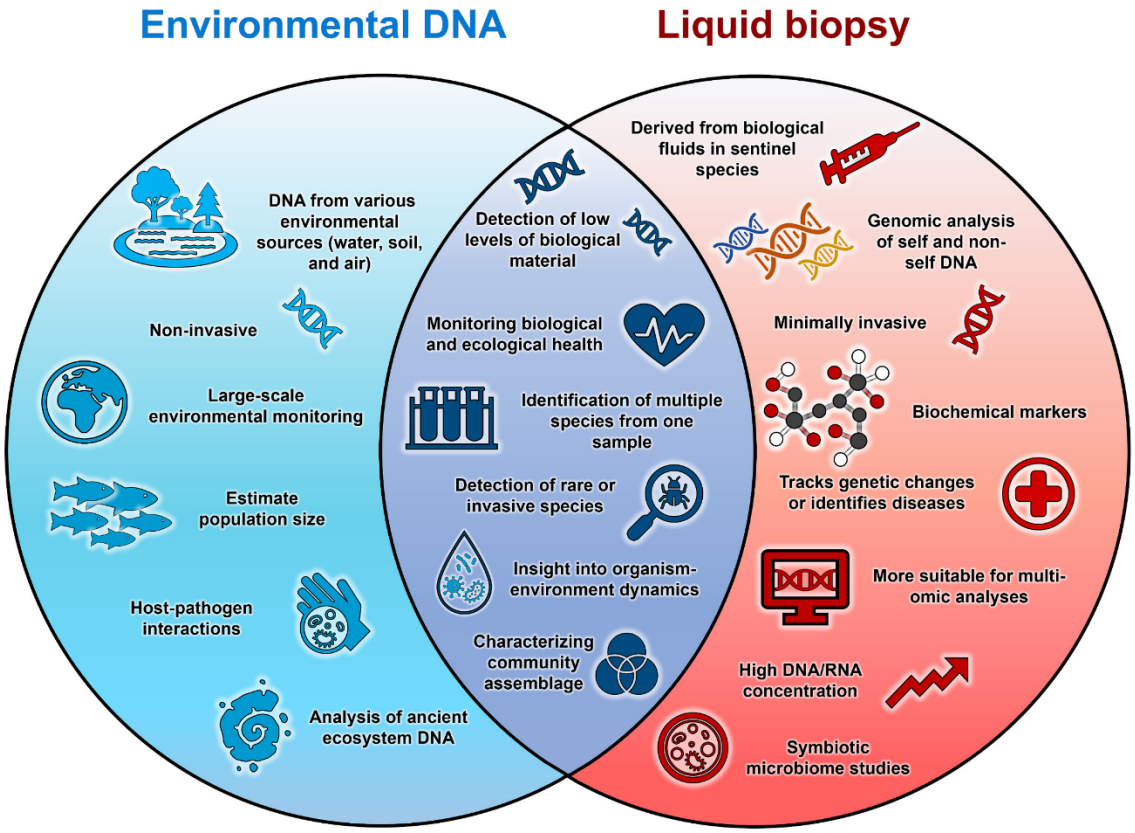

Fig. 8. Comparative Analysis of eDNA and Liquid Biopsies in Marine Biology: Similarities and Distinctions.

viral communities (Palermo et al., 2021; Roux et al., 2012). On the other hand, the major single-stranded DNA virus family detected in all Sites was *Circoviridae*, a family of viruses with a host range that includes birds and mammals. Our data are thus consistent with previous studies reported that viromes analyzed in freshwater and polar seawater are dominated by bacteriophages (e.g., *Caudoviricetes*) and circoviruses (López-Bueno et al., 2009; Roux et al., 2012; Yu et al., 2018). Furthermore, caudoviruses, phydnaviruses, and mimiviruses have been reported to be predominant in open Antarctic soil (Zablocki et al., 2014). We hypothesize that estuarine ecological dynamics could explain the relatively low viral diversity observed at Site 3. Wei and colleagues have reported that environmental factor changes caused by mixing freshwater and seawater, including salinity, significantly decrease the viral production and decay rates (Wei et al., 2019). However, we must remain cautious about these conclusions. Although we were able to identify a relatively high number of viral sequences (2643 sequences) with our pipeline, a high abundance of undetermined or unclassified were found, consistent with the challenging task of identifying viral sequences in marine ecosystems (Culley, 2013; Marx, 2022). Viruses exhibit high genetic diversity and often lack conserved genes across different viral families, making identifying viral sequences solely based on known reference sequences challenging. Moreover, eDNA extracted from seawater may contain fragmented and partial viral DNA sequences. This can complicate the assembly and analysis of complete viral genomes or specific viral genes. Matching and annotating the detected viral sequences using existing resources explain, at least in part, the challenging task of identifying viruses in marine ecosystems. Integrating LB with long-read sequencing and developing predictive tools will significantly enhance the characterization of the "circulating virome" in sentinel species, potentially revealing viral integration in the host genome, such as retroviruses. This approach not only expands our understanding of viral presence but also offers insights into genetic anomalies that could be crucial for monitoring and managing marine ecosystems. In our study, we paid particular attention to the circulating microbiome (cmDNA). Changes in the composition of the cmDNA hold potential as promising biomarkers, allowing the detection of dysbiosis in response to environmental factors or potential pathogens (Liu et al., 2022; Sobhani et al., 2019). Here, we have, for the first time, compared signatures derived from ccfDNA to those obtained by standard PCR-based methods applied to DNA isolated from hemocytes. Phagocytosis by mussel hemocytes is a vital defense mechanism against bacterial pathogens and contributes to the clearance of potential threats in the mussel's body (Canesi et al., 2002; Caza et al., 2020). Overall, our findings suggest that combining both analyses allows to get a more complete picture of the bacterial flora of the host and bacteria present in the surrounding marine ecosystem. This hypothesis is supported by our data showing that bacterial DNA that was dominant in ccfDNA, most notably from *E. coli*, *Shigella* spp., and *Streptomyces*, was not detected in cell pellets. This is consistent with James and colleagues' research, which reported a higher presence of ccfDNA from *E. coli* DNA in human plasma but not in the gut microbiome (James et al., 2022). We hypothesize that the high prevalence of enterobacterial DNA in the hemolymph of mussels (at the three Sites) is related to the wastewater from the nearby Armor station. This possibility is consistent with a previous study by Stark and colleagues

showing that untreated sewage in the Antarctic environment does disseminate non-native microorganisms such as *Enterobacteriaceae* (Stark et al., 2016). Our data showing a prevalence of ccfDNA originating from aerobic or facultative anaerobic bacterial genera such as *Lewinella*, *Escherichia*, *Shigella*, or *Sphingomonas* is consistent with the dominance of aerobic marine microorganisms in the gills and hemolymph, as previously reported (Musella et al., 2020). This could explain why we have hardly detected (2 reads out of millions of reads) any obligated anaerobic archaea in our microbiomes (Offre et al., 2013). Our results are also consistent with previous studies showing that the circulating microbiome depends not just on particle ingestion but also on the interactions between environmental microbiota and host gills (Sonier et al., 2016; Ward and Shumway, 2004). Finally, our data revealed that the core circulating microbiome of intertidal blue mussels remains stable over the years. In a previous study conducted in 2018 at the same Site, we showed that *Granulosicoccus*, *Lewinella*, *Sulfitobacter*, and *Sulfurimonas* were the most abundant bacterial genera (Ferchiou et al., 2022a, 2022b). Overall, this study is one of the rare, if not the first, study that combines the 16S rRNA gene analysis on circulating hemocytes and ccfDNA bacterial signature for a more comprehensive understanding of the circulating bacterial microbiome.

As discussed above, one of the key advantages of LB is the ability to analyze the self-DNA, which includes both mitochondrial circular DNA (mtDNA) and the nuclear chromosomal DNA. In humans, although mtDNA represents <1 % of total cellular DNA, its detection within ccfDNA is being increasingly used as a qualitative and quantitative biomarker in neurodegenerative diseases, diabetes, cancer, and aging (Leuthner and Meyer, 2021; Malik and Czajka, 2013; Schirrmacher, 2020; Wallace, 2010). Furthermore, growing evidence highlights that mitochondrial dysfunction is a hallmark of environmental alterations (Duarte-Hospital et al., 2022). Our study confirms data from previous reports on the existence of circulating cell-free mtDNA in bivalves, paving the way to use mtDNA as a biomarker to gain insight into their health status (Ferchiou et al., 2022a, 2022b). Our results indicated that although the concentration of circulating mtDNA was similar in all three Sites, we found a higher frequency in Site 1 (36 % versus 23 and 22 % in Sites 2 and 3, respectively) of DNA fragments derived from the *MT-ND4* gene, which encodes the NADH-ubiquinone oxidoreductase chain 4 (ND4) protein, a subunit of the NADH dehydrogenase (ubiquinone). We hypothesize that the *MT-ND4* gene is more resistant to degradation. Whether this is linked to its methylation status is possible, as environmental factors modulate the methylation status of genomic DNA. Indeed, mtDNA gene expression and compaction are regulated by the mitochondrial transcription factor A (TFAM), a member of the high mobility group proteins essential for maintaining mtDNA (Alam et al., 2003). The binding of TFAM to DNA is increased on hypermethylated genes, forming a tight TFAM-DNA complex that might be more resistant to DNA degradation as compared to hypomethylated mtDNA regions (Stoccoro and Coppedè, 2021; Yue et al., 2022). This would explain the results of Tomanek and colleagues, who found a disruption of protein homeostasis in blue mussels during hyposaline conditions with a decline in proteins associated with NADH activity (Tomanek, 2012). Surprisingly, we also observed an overrepresentation of ccfDNA related to chromosomes 3 and 6 in Site 1, suggesting that environmental conditions at Site 1 also impact the distribution of ccfDNA fragments from the nuclear chromosomal DNA, consistent with the redistribution of nuclear heterochromatin. Redistribution of heterochromatin is often associated with senescence, individual fitness, and phenotypic evolution (An et al., 2023). Whether this is related to epigenetic changes, which regulate the chromatin architecture, is a real possibility, as DNA methylation, for example, is known to be highly sensitive to environmental conditions (Coppedè, 2023; Margueron and Reinberg, 2010; Peng and Karpen, 2008). Additional research is needed to address this issue. This study could take advantage of the Oxford Nanopore Technology, which facilitates the analysis of DNA methylation from long fragments and the physical properties of ccfDNA in mussels. Our findings showing that ccfDNA fragments in mussels of Site 1 are shorter than those at other Sites add to the hypothesis that environmental conditions impact both mitochondrial and nuclear genomic DNA and reflect on the ccfDNA signatures. This could also be attributed, at least in part, to the fact that DNA preservation rates tend to be lower in freshwater environments, as higher salinity levels, ionic content, and pH values have been shown to promote DNA preservation and minimize degradation (Collins et al., 2018). One of the most plausible explanations is that shorter ccfDNA fragments at Site 1 are related to increased DNase activity. Such DNAse activity is likely to originate from bacteria's secretion of extracellular DNAse. The secretion of DNAse is part of the bacterial machinery that is essential for the breakdown of organic matter to generate low molecular weight compounds for bacterial uptake. Many phyla harbor gene-encoding DNAses, including Proteobacteria and Firmicutes, two dominant phyla in aquatic environments (Al-Wahaibi et al., 2019). Several lines of evidence support this hypothesis. Firstly, previous studies have shown that blue mussels have higher DNase I activity at lower pH levels (Bihari et al., 2007). Secondly, microcosm and mesocosm experiments have shown that lower pH promotes environmental DNA degradation (Seymour et al., 2018; Strickler et al., 2015). Thirdly, DNAse activity is optimal in hypotonic conditions. Adding salt reduces activity (Pan and Lazarus, 1997; Prince et al., 1998). Finally, an alternative and non-exclusive hypothesis is related to epigenetic changes induced by the environment. This hypothesis is supported by previous studies showing that DNA methylation, for example, is highly sensitive to environmental conditions (Coppedè, 2023; Margueron and Reinberg, 2010; Peng and Karpen, 2008). This hypothesis is also supported by our data showing that the number and origin of fragments differ considerably between the host chromosomes. Further investigations are needed to address this issue adequately.

In summary, we have used the Oxford Nanopore Technologies to study the self- and non-self origins of the hemolymphatic ccfDNA of mussels, including the metavirome and ccfDNA fragments derived from prokaryotes and eukaryotes present in the coastal marine ecosystem. We have further combined this approach with standard 16S rRNA sequencing of the hemolymph cell component to characterize mussels' circulating microbiome. We have studied how environmental factors quantitatively and qualitatively affect the hemolymphatic non-self ccfDNA and ccfDNA derived from mitochondrial and nuclear genomes. Exploring seasonal shifts in self and non-self ccfDNA could provide valuable information on the response of sentinel mussels to climate change in coastal marine ecosystems.

Supplementary data to this article can be found online at https://doi.org/10.1016/j.scitotenv.2024.172969.

Funding information

This work was partly funded by the National Science and Engineering Research Council of Canada (Grant No. x-2019-06607, YSP), Fonds de recherche du Québec - Nature and Technology (SF), Ecotoq (SF and YSP) and IPEV (Project # 1245, SB and YSP).

CRediT authorship contribution statement

Sophia Ferchiou: Writing – review & editing, Writing – original draft, Investigation, Formal analysis, Data curation, Conceptualization. **France Caza:** Writing – review & editing, Supervision, Funding acquisition, Conceptualization. **Richard Villemur:** Writing – original draft, Conceptualization. **Stéphane Betoulle:** Writing – review & editing, Supervision, Funding acquisition, Conceptualization. **Yves St-Pierre:** Writing – review & editing, Writing – original draft, Supervision, Project administration, Investigation, Funding acquisition, Conceptualization.

Declaration of competing interest

The authors declare the following financial interests/personal

relationships which may be considered as potential competing interests: Yves St-Pierre reports financial support was provided by INRS Armand-Frappier Santé Biotechnologie Research Centre. If there are other authors, they declare that they have no known competing financial interests or personal relationships that could have appeared to influence the work reported in this paper.

Data availability

Metagenome sequencing data have been deposited in the NCBI Sequence Read Archive under the Bioprojects PRJNA954899.

Acknowledgements

This research project has been performed at the Armor Site (Kerguelen Islands) with the logistic support of the French Polar Institute Paul-Emile-Victor (IPEV). The authors would like to thank Dr. Stéphane Betoulle (SB), who provided us with the opportunity to do research at Kerguelen, and for his valuable contribution and support during this project. The authors would also like to thank all the personnel from the IPEV and the Terres Australes et Antarctiques Françaises (TAAF) for their help and hospitality during our stay in the Kerguelen archipelago. The author would also like to thank Ms. Marlène Fortier for her excellent technical help.

References

Ahsanuddin, S., Afshinnekoo, E., Gandara, J., Hakyemezoğlu, M., Bezdan, D., Minot, S., Greenfield, N., Mason, C.E., 2017. Assessment of REPLI-g multiple displacement whole genome amplification (WGA) techniques for metagenomic applications. J. Biomol. Tech. 28, 46. https://doi.org/10.7171/jbt.17-2801-008.

Alam, T.I., Kanki, T., Muta, T., Ukaji, K., Abe, Y., Nakayama, H., Takio, K., Hamasaki, N., Kang, D., 2003. Human mitochondrial DNA is packaged with TFAM. Nucleic Acids Res. 31, 1640–1645. https://doi.org/10.1093/nar/gkg251.

Alix-Panabières, C., Pantel, K., 2021. Liquid biopsy: from discovery to clinical application. Cancer Discov. 11, 858–873. https://doi.org/10.1158/2159-8290.CD-20-1311.

Al-Wahaibi, A.S., Lapinska, E., Rajarajan, N., Dobretsov, S., Upstill-Goddard, R., Burgess, J.G., 2019. Secretion of DNases by marine bacteria: a culture based and bioinformatics approach. Front. Microbiol. 10, 969. https://doi.org/10.3389/fmicb.2019. 00969.

An, Q., Hu, Y., Li, Q., Chen, X., Huang, J., Pellegrini, M., Zhou, X.J., Rettig, M., Fan, G., 2019. The size of cell-free mitochondrial DNA in blood is inversely correlated with tumor burden in cancer patients. Precis. Clin. Med. 2, 131–139. https://doi.org/10.1093/pcmedi/pbz014.

An, Y., Zhao, X., Zhang, Z., Xia, Z., Yang, M., Ma, L., Zhao, Y., Xu, G., Du, S., Wu, X., Zhang, S., Hong, X., Jin, X., Sun, K., 2023. DNA methylation analysis explores the molecular basis of plasma cell-free DNA fragmentation. Nat. Commun. 14, 287. https://doi.org/10.1038/s41467-023-35959-6.

Auguste, M., Leonessi, M., Balbi, T., Doni, L., Oliveri, C., Vezzulli, L., Canesi, L., 2024. Seasonal fluctuations of hemolymph microbiota and immune parameters in Mytilus galloprovincialis farmed at La Spezia, Italy. Aquaculture 578, 740028. https://doi.org/10.1016/j.aquaculture.2023.740028.

Bashir, I., Lone, F.A., Bhat, R.A., Mir, S.A., Dar, Z.A., Dar, S.A., 2020. Concerns and threats of contamination on aquatic ecosystems. In: Bioremediation and Biotechnology, Sustainable Approaches to Pollution Degradation. Springer, Berlin, Germany, pp. 1–26. https://doi.org/10.1007/978-3-030-35691-0_1.

Becker, R.A., Wilks, A.R., Brownrigg, R., 2022. mapdata: Extra Map Databases. R package version 2.3.0. https://CRAN.R-project.org/package=mapdata2018.

Benjamini, Y., Hochberg, Y., 1995. Controlling the false discovery rate: a practical and powerful approach to multiple testing. J. R. Stat. Soc. Series B. Stat. Methodol. 57, 289–300. https://doi.org/10.1111/j.2517-6161.1995.tb02031.x.

Bernatchez, L., Ferchaud, A.L., Berger, C.S., Venney, C.J., Xuereb, A., 2023. Genomics for monitoring and understanding species responses to global climate change. Nat. Rev. Genet. 1–19. https://doi.org/10.1038/s41576-023-00657-y.

Beyer, J., Green, N.W., Brooks, S., Allan, I.J., Ruus, A., Gomes, T., Bråte, I.L.N., Schøyen, M., 2017. Blue mussels (Mytilus edulis spp.) as sentinel organisms in coastal pollution monitoring: A review. Mar. Environ. Res. 130, 338–365. https://doi.org/10.1016/j.marenvres.2017.07.024.

Bihari, N., Fafandel, M., Perić, L., 2007. Tissue distribution of neutral deoxyribo-nuclease (DNase) activity in the mussel *Mytilus galloprovincialis*. Comp. Biochem. Physiol. B Biochem. Mol. Biol. 147, 550–556. https://doi.org/10.1016/j.cbpb.2007.03.008.

Blauwkamp, T.A., Thair, S., Rosen, M.J., Blair, L., Lindner, M.S., Vilfan, I.D., Kawli, T., Christians, F.C., Venkatasubrahmanyam, S., Wall, G.D., Cheung, A., 2019. Analytical and clinical validation of a microbial cell-free DNA sequencing test for infectious disease. Nat. Microbiol. 4, 663–674. https://doi.org/10.1038/s41564-018-0349-6.

Borthagaray, A.I., Carranza, A., 2007. Mussels as ecosystem engineers: their contribution to species richness in a rocky littoral community. Acta Oecol. 31, 243–250. https://doi.org/10.1016/j.actao.2006.10.008.

Callahan, B.J., McMurdie, P.J., Rosen, M.J., Han, A.W., Johnson, A.J.A., Holmes, S.P., 2016. DADA2: high-resolution sample inference from Illumina amplicon data. Nat. Methods 13, 581–583. https://doi.org/10.1038/nmeth.3869.

Canesi, L., Gallo, G., Gavioli, M., Pruzzo, C., 2002. Bacteria-hemocyte interactions and phagocytosis in marine bivalves. Microsc. Res. Tech. 57, 469–476. https://doi.org/10.1002/jemt.10100.

Caza, F., de Boissel, P.G.J., Villemur, R., Betoulle, S., St-Pierre, Y., 2019. Liquid biopsies for omics-based analysis in sentinel mussels. PloS One 14, e0223525. https://doi.org/10.1371/journal.pone.0223525.

Caza, F., Bernet, E., Veyrier, F.J., Betoulle, S., St-Pierre, Y., 2020. Hemocytes released in seawater act as Trojan horses for spreading of bacterial infections in mussels. Sci. Rep. 10, 19696. https://doi.org/10.1038/s41598-020-76677-z.

Chen, X., Wei, W., Wang, J., Li, H., Sun, J., Ma, R., Jiao, N., Zhang, R., 2019. Tide driven microbial dynamics through virus-host interactions in the estuarine ecosystem. Water Res. 160, 118–129. https://doi.org/10.1016/j.watres.2019.05.051.

Chen, Y., Jiang, Z., Fan, P., Ericson, P.G., Song, G., Luo, X., Lei, F., Qu, Y., 2022. The combination of genomic offset and niche modelling provides insights into climate change-driven vulnerability. Nat. Commun. 13, 4821. https://doi.org/10.1038/s41467-022-32546-z.

Collins, R.A., Wangensteen, O.S., O'Gorman, E.J., Mariani, S., Sims, D.W., Genner, M.J., 2018. Persistence of environmental DNA in marine systems. Commun. Biol. 1, 185. https://doi.org/10.1038/s42003-018-0192-6.

Coppedè, F., 2023. Genes and the environment in cancer: focus on environmentally induced DNA methylation changes. Cancers 15, 1019. https://doi.org/10.3390/cancers1504 1019.

Culley, A.I., 2013. Insight into the unknown marine virus majority. Proc. Natl. Acad. Sci. U. S. A. 110, 12166–12167. https://doi.org/10.1073/pnas.1310671110.

Davaine, P., Beall, E., Guerri, O., Caraguel, J.M., 1997. Salmonid introductions into virgin ecosystems (Kerguelen Islands, Subantarctic): stakes, results, prospects. Bull. fr. pêche piscic. 344, 93–110. https://doi.org/10.1051/kmae:1997013.

Dilthey, A.T., Jain, C., Koren, S., Phillippy, A.M., 2019. Strain-level metagenomic assignment and compositional estimation for long reads with MetaMaps. Nat. Commun. 10, 3066. https://doi.org/10.1038/s41467-019-10934-2.

Duarte-Hospital, C., Tête, A., Brial, F., Benoit, L., Koual, M., Tomkiewicz, C., Kim, M.J., Blanc, E.B., Coumoul, X., Bortoli, S., 2022. Mitochondrial dysfunction as a hallmark of environmental injury. Cells 11, 110. https://doi.org/10.3390/cells11010110.

Duhamel, G., Williams, R., 2011. History of whaling, sealing, fishery and aquaculture trials in the area of the Kerguelen Plateau. In: The Kerguelen Plateau: marine ecosystem and fisheries. Société française d'ichtyologie, Paris, pp. 15–28. https://doi.org/10.13140/2.1.2059.7446.

Duncan, A., Barry, K., Daum, C., Eloe-Fadrosh, E., Roux, S., Schmidt, K., Tringe, S.G., Valentin, K.U., Varghese, N., Salamov, A., Grigoriev, I.V., Leggett, R.M., Moulton, V., Mock, T., 2022. Metagenome-assembled genomes of phytoplankton microbiomes from the Arctic and Atlantic Oceans. Microbiome 10, 67. https://doi.org/10.1186/s40168-022-01254-7.

Eldem, V., Kuralay, S.C., Özdoğan, G., Özçelik, G.H., Aydın, D., Çakmak, G., Gürler, M.Ö., Çay, S.B., Çınar, Y.U., Dikmen, F., Yusuf, I., 2023. Comprehensive analysis of circulating viral DNA in maternal plasma at population-scale using low-pass whole-genome sequencing. Genomics 115, 110556. https://doi.org/10.1016/j.ygeno. 2022.110556.

Favaro, P.F., Stewart, S.D., McDonald, B.R., Cawley, J., Contente-Cuomo, T., Wong, S., Hendricks, W.P., Trent, J.M., Khanna, C., Murtaza, M., 2022. Feasibility of circulating tumor DNA analysis in dogs with naturally occurring malignant and benign splenic lesions. Sci. Rep. 12, 6337. https://doi.org/10.1038/s41598-022-09716-6.

Ferchiou, S., Caza, F., de Boissel, P.G.J., Villemur, R., St-Pierre, Y., 2022a. Applying the concept of liquid biopsy to monitor the microbial biodiversity of marine coastal ecosystems. ISME Commun. 2, 61. https://doi.org/10.1038/s43705-022-00145-0.

Ferchiou, S., Caza, F., Villemur, R., Betoulle, S., St-Pierre, Y., 2022b. Species- and site-specific circulating bacterial DNA in Subantarctic sentinel mussels *Aulacomya atra* and *Mytilus platensis*. Sci. Rep. 12, 9547. https://doi.org/10.1038/s41598-022-13774-1.

Ferchiou, S., Caza, F., Villemur, R., Labonne, J., St-Pierre, Y., 2023. Skin and blood microbial signatures of sedentary and migratory trout (*Salmo trutta*) of the Kerguelen Islands. Fishes 8, 174. https://doi.org/10.3390/fishes8040174.

Frémont, P., Gehlen, M., Vrac, M., Leconte, J., Delmont, T.O., Wincker, P., Iudicone, D., Jaillon, O., 2022. Restructuring of plankton genomic biogeography in the surface ocean under climate change. Nat. Clim. Chang. 12, 393–401. https://doi.org/10.1038/s41558-022-01314-8.

Fronton, F., Ferchiou, S., Caza, F., Villemur, R., Robert, D., St-Pierre, Y., 2023. Insights into the circulating microbiome of Atlantic and Greenland halibut populations: the role of species-specific and environmental factors. Sci. Rep. 13, 5971. https://doi.org/10.1038/s41598-023-32690-6.

Gissi, E., Manea, E., Mazaris, A.D., Fraschetti, S., Almpanidou, V., Bevilacqua, S., Coll, M., Guarnieri, G., Lloret-Lloret, E., Pascual, M., Petza, D., Rilov, G., Schonwald, M., Stelzenmüller, V., Katsanevakis, S., 2021. A review of the combined effects of climate change and other local human stressors on the marine environment. Sci. Total Environ. 755, 142564 https://doi.org/10.1016/j.scitotenv.2020.142564.

Gopalakrishnan, V., Helmink, B.A., Spencer, C.N., Reuben, A., Wargo, J.A., 2018. The influence of the gut microbiome on cancer, immunity, and cancer immuno-therapy. Cancer Cell 33, 570–580. https://doi.org/10.1016/j.ccell.2018.03.015.

Grzyb, J., Frączek, K., 2012. Activity of phosphohydrolytic enzymes in waters. Ecol. Chem. Eng. A 19, 583–589.
Guo, J., Bolduc, B., Zayed, A.A., Varsani, A., Dominguez-Huerta, G., Delmont, T.O., Pratama, A.A., Gazitúa, M.C., Vik, D., Sullivan, M.B., Roux, S., 2021. VirSorter2: a multi-classifier, expert-guided approach to detect diverse DNA and RNA viruses. Microbiome 9, 1–13. https://doi.org/10.1186/s40168-020-00990-y.
Han, D., Li, R., Shi, J., Tan, P., Zhang, R., Li, J., 2020. Liquid biopsy for infectious diseases: A focus on microbial cell-free DNA sequencing. Theranostics 10, 5501–5513. https://doi.org/10.7150/thno.45554.
Hernroth, B.E., Baden, S.P., 2018. Alteration of host-pathogen interactions in the wake of climate change – increasing risk for shellfish associated infections? Environ. Res. 161, 425–438. https://doi.org/10.1016/j.envres.2017.11.032.
Ignatiadis, M., Sledge, G.W., Jeffrey, S.S., 2021. Liquid biopsy enters the clinic — implementation issues and future challenges. Nat. Rev. Clin. Oncol. 18, 297–312. https://doi.org/10.1038/s41571-020-00457-x.
James, W.A., Ogunrinde, E., Wan, Z., Kamen, D.L., Oates, J., Gilkeson, G.S., Jiang, W., 2022. A distinct plasma microbiome but not gut microbiome in patients with systemic lupus erythematosus compared to healthy individuals. J. Rheumatol. 49, 592–597. https://doi.org/10.3899/jrheum.210952.
James, R.K., Keyzer, L.M., van de Velde, S.J., Herman, P.M., van Katwijk, M.M., Bouma, T.J., 2023. Climate change mitigation by coral reefs and seagrass beds at risk: how global change compromises coastal ecosystem services. Sci. Total Environ. 857, 159576 https://doi.org/10.1016/j.scitotenv.2022.159576.
Jasna, V., Parvathi, A., VK, A., Aparna, S., Dayana, M., AJ, A., NV, M., 2019. Factors determining variations in viral abundance and viral production in a tropical estuary influenced by monsoonal cycles. Reg. Stud. Mar. Sci. 28, 100589 https://doi.org/10.1016/j.rsma.2019.100589.
Jo, T., Murakami, H., Yamamoto, S., Masuda, R., Minamoto, T., 2019. Effect of water temperature and fish biomass on environmental DNA shedding, degradation, and size distribution. Ecol. Evol. 9, 1135–1146. https://doi.org/10.1002/ece3.4802.
Kahle, D., Wickham, H., 2013. ggmap: spatial visualization with ggplot2. R J. 5, 144–161. https://doi.org/10.32614/RJ-2013-014.
Keller, L., Belloum, Y., Wikman, H., Pantel, K., 2021. Clinical relevance of blood-based ctDNA analysis: mutation detection and beyond. Br. J. Cancer 124, 345–358. https://doi.org/10.1038/s41416-020-01047-5.
Khleborodova, A., 2023. lefser: R Implementation of the LEfSE Method for Microbiome Biomarker Discovery. R package version 1.12.1. https://github.com/waldronlab/lefser.
Klindworth, A., Pruesse, E., Schweer, T., Peplies, J., Quast, C., Horn, M., Glöckner, F.O., 2013. Evaluation of general 16S ribosomal RNA gene PCR primers for classical and next-generation sequencing-based diversity studies. Nucleic Acids Res. 41, e1 https://doi.org/10.1093/nar/gks808.
Kowarsky, M., Camunas-Soler, J., Kertesz, M., Vlaminck, I. De, Koh, W., Pan, W., Martin, L., Neff, N.F., Okamoto, J., Wong, R.J., Kharbanda, S., El-Sayed, Y., Blumenfeld, Y., Stevenson, D.K., Shaw, G.M., Wolfe, N.D., Quake, S.R., 2017. Numerous uncharacterized and highly divergent microbes which colonize humans are revealed by circulating cell-free DNA. Proc. Natl. Acad. Sci. U. S. A. 114, 9623–9628. https://doi.org/10.1073/pnas.1707009114.
Kustanovich, A., Schwarttz, R., Peretz, T., Grinshpun, A., 2019. Life and death of circulating cell-free DNA. Cancer Biol. Ther. 20 (8), 1057–1067. https://doi.org/10.1080/15384047.2019.1598759. Aug 3.
Landrigan, P.J., Stegeman, J.J., Fleming, L.E., Allemand, D., Anderson, D.M., Backer, L. C., et al., 2020. Human health and ocean pollution. Ann. Glob. Health 86, 151. https://doi.org/10.5334/aogh.2831.
Le Bohec, C., Whittington, J.D., Le Maho, Y., 2013. Polar monitoring: seabirds as sentinels of marine ecosystems. In: Adaptation and Evolution in Marine Environments, vol. 2. Springer, Berlin, Heidelberg, pp. 205–230.
Leuthner, T.C., Meyer, J.N., 2021. Mitochondrial DNA mutagenesis: feature of and biomarker for environmental exposures and aging. Curr. Environ. Health Rep. 8, 294–308. https://doi.org/10.1007/s40572-021-00329-1.
Lintas, C., Seed, R., 1994. Spatial variation in the fauna associated with Mytilus edulis on a wave-exposed rocky shore. J. Moll. Stud. 60, 165–174. https://doi.org/10.1093/mollus/60.2.165.
Linthorst, J., Baksi, M.M., Welkers, M.R., Sistermans, E.A., 2023. The cell-free DNA virome of 108,349 Dutch pregnant women. Prenat. Diagn. 43, 448–456. https://doi.org/10.1002/pd.6143.
Liu, Y., Xiao, F., Zhang, R., Zhang, X., 2022. Alterations of plasma microbiome: A potentially new perspective to the dysbiosis in systemic lupus erythematosus? J. Rheumatol. 49, 549–551. https://doi.org/10.3899/jrheum.220023.
Lo, Y.M.D., Han, D.S.C., Jiang, P., Chiu, R.W.K., 2021. Epigenetics, fragmentomics, and topology of cell-free DNA in liquid biopsies. Science 372, eaaw3616. https://doi.org/10.1126/science.aaw3616.
Lokmer, A., Mathias Wegner, K., 2015. Hemolymph microbiome of Pacific oysters in response to temperature, temperature stress and infection. ISME J. 9, 670–682. https://doi.org/10.1038/ismej.2014.160.
López-Bueno, A., Tamames, J., Velázquez, D., Moya, A., Quesada, A., Alcamí, A., 2009. High diversity of the viral community from an Antarctic lake. Science 326, 858–861. https://doi.org/10.1126/science.1179287.
Malik, A.N., Czajka, A., 2013. Is mitochondrial DNA content a potential biomarker of mitochondrial dysfunction? Mitochondrion 13, 481–492. https://doi.org/10.1016/j.mito.2012.10.011.
Maranger, R., Bird, D.F., 1995. Viral abundance in aquatic systems: a comparison between marine and fresh waters. Mar. Ecol. Prog. Ser. 121, 217–226. https://doi.org/10.3354/meps121217.
Marcel, M., 2011. Cutadapt removes adapter sequences from high-throughput sequencing reads, EMB net. EMBnet J. 17, 10–12. https://doi.org/10.14806/ej.17.1.200.
Margueron, R., Reinberg, D., 2010. Chromatin structure and the inheritance of epigenetic information. Nat. Rev. Genet. 11, 285–296. https://doi.org/10.1038/nrg2752.
Martínez-Gómez, C., Robinson, C.D., Burgeot, T., Gubbins, M., Halldorsson, H.P., Albentosa, M., Bignell, J.P., Hylland, K., Vethaak, A.D., 2017. Biomarkers of general stress in mussels as common indicators for marine biomonitoring programmes in Europe: the ICON experience. Mar. Environ. Res. 124, 70–80. https://doi.org/10.1016/j.marenvres.2015.10.012.
Marx, V., 2022. Why the ocean virome matters. Nat. Methods 19, 924–927. https://doi.org/10.1038/s41592-022-01567-3.
Mauvisseau, Q., Harper, L.R., Sander, M., Hanner, R.H., Kleyer, H., Deiner, K., 2022. The multiple states of environmental DNA and what is known about their persistence in aquatic environments. Environ. Sci. Technol. 56, 5322–5333. https://doi.org/10.1021/acs.est.1c07638.
McMurdie, P.J., Holmes, S., 2013. Phyloseq: An R package for reproducible interactive analysis and graphics of microbiome census data. PloS One 8, e61217. https://doi.org/10.1371/journal.pone.0061217.
Meredith, M., Sommerkorn, M., Cassotta, S., Derksen, C., Ekaykin, A., Hollowed, A.B., Kofinas, G., Mackintosh, A., Melbourne-Thomas, J., Muelbert, M.M.C., Ottersen, G., Pritchard, H., Schuur, E.A.G., 2019. Polar regions. Chapter 3. In: IPCC Special Report on the Ocean and Cryosphere in a Changing Climate. https://www.ipcc.ch/srocc/chapter/chapter-3-2/.
Metzger, M.J., Reinisch, C., Sherry, J., Goff, S.P., 2015. Horizontal transmission of clonal cancer cells causes leukemia in soft-shell clams. Cell 161, 255–263. https://doi.org/10.1016/j.cell.2015.02.042.
Metzger, M.J., Villalba, A., Carballal, M.J., Iglesias, D., Sherry, J., Reinisch, C., Muttray, A.F., Baldwin, S.A., Goff, S.P., 2016. Widespread transmission of independent cancer lineages within multiple bivalve species. Nature 534, 705–709. https://doi.org/10.1038/nature18599.
Midway, S., Robertson, M., Flinn, S., Kaller, M., 2020. Comparing multiple comparisons: practical guidance for choosing the best multiple comparisons test. PeerJ 8, e10387. https://doi.org/10.7717/peerj.10387.
Musella, M., Wathsala, R., Tavella, T., Rampelli, S., Barone, M., Palladino, G., Biagi, E., Brigidi, P., Turroni, S., Franzellitti, S., Candela, M., 2020. Tissue-scale microbiota of the Mediterranean mussel (*Mytilus galloprovincialis*) and its relationship with the environment. Sci. Total Environ. 717, 137209 https://doi.org/10.1016/j.scitotenv.2020.137209.
Nayfach, S., Camargo, A.P., Schulz, F., Eloe-Fadrosh, E., Roux, S., Kyrpides, N.C., 2021. CheckV assesses the quality and completeness of metagenome-assembled viral genomes. Nat. Biotechnol. 39, 578–585. https://doi.org/10.1038/s41587-020-00774-7.
Ngo, T.T., Moufarrej, M.N., Rasmussen, M.L.H., Camunas-Soler, J., Pan, W., Okamoto, J., Neff, N.F., Liu, K., Wong, R.J., Downes, K., Tibshirani, R., 2018. Noninvasive blood tests for fetal development predict gestational age and preterm delivery. Science 360, 1133–1136. https://doi.org/10.1126/science.aar3819.
Oellerich, M., Sherwood, K., Keown, P., Schütz, E., Beck, J., Stegbauer, J., Rump, L.C., Walson, P.D., 2021. Liquid biopsies: donor-derived cell-free DNA for the detection of kidney allograft injury. Nat. Rev. Nephrol. 17, 591–603. https://doi.org/10.1038/s41581-021-00428-0.
Offre, P., Spang, A., Schleper, C., 2013. Archaea in biogeochemical cycles. Annu. Rev. Microbiol. 67, 437–457. https://doi.org/10.1146/annurev-micro-092412-155614.
Oksanen, J., Blanchet, F., Kindt, R., Legendre, P., Minchin, P., O'Hara, R., Simpson, G., Solymos, P., Stevens, M., Wagner, H.J.W.A.C., 2015. Vegan: Community Ecology Package. R Package Vegan, vers. 2.2-1, 3. Worl. Agro. Cent., pp. 7–81
Palermo, C.N., Shea, D.W., Short, S.M., 2021. Analysis of different size fractions provides a more complete perspective of viral diversity in a freshwater embayment. Appl. Environ. Microbiol. 87, 1–15. https://doi.org/10.1128/AEM.00197-21.
Pan, C.Q., Lazarus, R.A., 1997. Engineering hyperactive variants of human deoxyribonuclease I by altering its functional mechanism. Biochemistry 36, 6624–6632. https://doi.org/10.1021/bi962960x.
Peng, J.C., Karpen, G.H., 2008. Epigenetic regulation of heterochromatic DNA stability. Curr. Opin. Genet. Dev. 18, 204–211. https://doi.org/10.1016/j.gde.2008.01.021.
Peng, F., Wang, S., Feng, Z., Zhou, K., Zhang, H., Guo, X., Xing, J., Liu, Y., 2023. Circulating cell-free mtDNA as a new biomarker for cancer detection and management. Cancer Biol. Med. https://doi.org/10.20892/j.issn.2095-3941.2023.0280.
Poulet, G., Massias, J., Taly, V., 2019. Liquid biopsy: general concepts. Acta Cytol. 63, 449–455. https://doi.org/10.1159/000499337.
Prince, W.S., Baker, D.L., Dodge, A.H., Ahmed, A.E., Chestnut, R.W., Sinicropi, D.V., 1998. Pharmacodynamics of recombinant human DNase I in serum. Clin. Exp. Immunol. 113, 289–296. https://doi.org/10.1046/j.1365-2249.1998.00647.x.
Provenza, F., Rampih, D., Pignattelli, S., Pastorino, P., Barceló, D., Prearo, M., Specchiulli, A., Renzi, M., 2022. Mussel watch program for microplastics in the Mediterranean sea: identification of biomarkers of exposure using *Mytilus galloprovincialis*. Ecol. Indic. 142, 109212 https://doi.org/10.1016/j.ecolind.2022.109212.
R Core Team, 2023. R: A Language and Environment for Statistical Computing. R Foundation for Statistical Computing.
Rostami, A., Lambie, M., Yu, C.W., Stambolic, V., Waldron, J.N., Bratman, S.V., 2020. Senescence, necrosis, and apoptosis govern circulating cell-free DNA release kinetics. Cell Rep. 31, 107830 https://doi.org/10.1016/j.celrep.2020.107830.
Roux, S., Enault, F., Robin, A., Ravet, V., Personnic, S., Theil, S., Colombet, J., Sime-Ngando, T., Debroas, D., 2012. Assessing the diversity and specificity of two

freshwater viral communities through metagenomics. PloS One 7, e33641. https://doi.org/10.1371/journal.pone.0033641.
Schirrmacher, V., 2020. Mitochondria at work: new insights into regulation and dysregulation of cellular energy supply and metabolism. Biomedicines 8, 1–38. https://doi.org/10.3390/biomedicines8110526.
Seymour, M., Durance, I., Cosby, B.J., Ransom-Jones, E., Deiner, K., Ormerod, S.J., Colbourne, J.K., Wilgar, G., Carvalho, G.R., De Bruyn, M., Edwards, F., 2018. Acidity promotes degradation of multi-species environmental DNA in lotic mesocosms. Commun. Biol. 1, 4. https://doi.org/10.1038/s42003-017-0005-3.
Shaffer, M., Borton, M.A., McGivern, B.B., Zayed, A.A., Rosa, S.L. La, Solden, L.M., Liu, P., Narrowe, A.B., Rodríguez-Ramos, J., Bolduc, B., Gazitúa, M.C., Daly, R.A., Smith, G.J., Vik, D.R., Pope, P.B., Sullivan, M.B., Roux, S., Wrighton, K.C., 2020. DRAM for distilling microbial metabolism to automate the curation of microbiome function. Nucleic Acids Res. 48, 8883–8900. https://doi.org/10.1093/nar/gkaa621.
Snyder, M.W., Kircher, M., Hill, A.J., Daza, R.M., Shendure, J., 2016. Cell-free DNA comprises an in vivo nucleosome footprint that informs its tissues-of-origin. Cell 164, 57–68. https://doi.org/10.1016/j.cell.2015.11.050.
Sobhani, I., Bergsten, E., Couffin, S., Amiot, A., Nebbad, B., Barau, C., de'Angelis, N., Rabot, S., Canoui-Poitrine, F., Mestivier, D., Pédron, T., Khazaie, K., Sansonetti, P.J., 2019. Colorectal cancer-associated microbiota contributes to oncogenic epigenetic signatures. Proc. Natl. Acad. Sci. U. S. A. 116, 24285–24295. https://doi.org/10.1073/pnas.1912129116.
Sonier, R., Filgueira, R., Guyondet, T., Tremblay, R., Olivier, F., Meziane, T., Starr, M., LeBlanc, A.R., Comeau, L.A., 2016. Picophytoplankton contribution to *Mytilus edulis* growth in an intensive culture environment. Mar. Biol. 163, 1–15. https://doi.org/10.1007/s00227-016-2845-7.
Sousa, R., Gutiérrez, J.L., Aldridge, D.C., 2009. Non-indigenous invasive bivalves as ecosystem engineers. Biol. Invasions 11, 2367–2385. https://doi.org/10.1007/s10530-009-9422-7.
Stark, J.S., Corbett, P.A., Dunshea, G., Johnstone, G., King, C., Mondon, J.A., Power, M. L., Samuel, A., Snape, I., Riddle, M., 2016. The environmental impact of sewage and wastewater outfalls in Antarctica: an example from Davis station, East Antarctica. Water Res. 105, 602–614. https://doi.org/10.1016/j.watres.2016.09.026.
Stoccoro, A., Coppedè, F., 2021. Mitochondrial DNA methylation and human diseases. Int. J. Mol. Sci. 22, 4594. https://doi.org/10.3390/ijms22094594.
Strickler, K.M., Fremier, A.K., Goldberg, C.S., 2015. Quantifying effects of UV-B, temperature, and pH on eDNA degradation in aquatic microcosms. Biol. Conserv. 183, 85–92. https://doi.org/10.1016/j.biocon.2014.11.038.
Sun, M., Zhan, Y., Marsan, D., Páez-Espino, D., Cai, L., Chen, F., 2021. Uncultivated viral populations dominate estuarine viromes on the spatiotemporal scale. mSystems 6, e01020-20. https://doi.org/10.1128/msystems.01020-20.
Tomanek, L., 2012. Environmental proteomics of the mussel *Mytilus*: implications for tolerance to stress and change in limits of biogeographic ranges in response to climate change. Integr. Comp. Biol. 52, 648–664. https://doi.org/10.1093/icb/ics114.
Townsend, K.S., Johnson, P.J., LaCarrubba, A.M., Martin, L.M., Ericsson, A.C., 2021. Exodontia associated bacteremia in horses characterized by next generation sequencing. Sci. Rep. 11, 6314. https://doi.org/10.1038/s41598-021-85484-z.
van Broekhoven, W., Jansen, H., Verdegem, M., Struyf, E., Troost, K., Lindeboom, H., et al., 2015. Nutrient regeneration from feces and pseudofeces of mussel Mytilus edulis spat. Mar. Ecol. Prog. 534, 107–120. https://doi.org/10.3354/meps11402.
Wallace, D.C., 2010. Mitochondrial DNA mutations in disease and aging. Environ. Mol. Mutagen. 51, 440–450. https://doi.org/10.1002/em.20586.
Wan, J.C., Massie, C., Garcia-Corbacho, J., Mouliere, F., Brenton, J.D., Caldas, C., Pacey, S., Baird, R., Rosenfeld, N., 2017. Liquid biopsies come of age: towards implementation of circulating tumour DNA. Nat. Rev. Cancer 17, 223–238. https://doi.org/10.1038/nrc.2017.7.
Ward, J.E., Shumway, S.E., 2004. Separating the grain from the chaff: particle selection in suspension- and deposit-feeding bivalves. J. Exp. Mar. Bio. Ecol. 300, 83–130. https://doi.org/10.1016/j.jembe.2004.03.002.
Wei, W., Wang, N., Cai, L., Zhang, C., Jiao, N., Zhang, R., 2019. Impacts of freshwater and seawater mixing on the production and decay of virioplankton in a subtropical estuary. Microb. Ecol. 78, 843–854. https://doi.org/10.1007/s00248-019-01362-2.
Werner, B., Warton, K., Ford, C.E., 2022. Endogenous cell-free DNA in fetal bovine serum introduces artifacts to in vitro cell-free DNA models. BioTechniques 73, 219–226. https://doi.org/10.2144/btn-2022-0040.
Westerbom, M., Mustonen, O., Jaatinen, K., Kilpi, M., Norkko, A., 2019. Population dynamics at the range margin: implications of climate change on sublittoral blue mussels (*Mytilus trossulus*). Front. Mar. Sci. 6, 292. https://doi.org/10.3389/fmars.2019.00292.
Whitman, W.B., Coleman, D.C., Wiebe, W.J., 1998. Perspective prokaryotes: the unseen majority. Proc. Natl. Acad. Sci. U. S. A. 95, 6578–6583. https://doi.org/10.1073/pnas. 95.12.6578.
Wood, D.E., Lu, J., Langmead, B., 2019. Improved metagenomic analysis with Kraken 2. Genome Biol. 20, 257. https://doi.org/10.1186/s13059-019-1891-0.
Yu, D.T., Han, L.L., Zhang, L.M., He, J.Z., 2018. Diversity and distribution characteristics of viruses in soils of a marine-terrestrial ecotone in East China. Microb. Ecol. 75, 375–386. https://doi.org/10.1007/s00248-017-1049-0.
Yue, Y., Ren, L., Zhang, C., Miao, K., Tan, K., Yang, Q., Hu, Y., Xi, G., Luo, G., Yang, M., Zhang, J., Hou, Z., An, L., Tian, J., Roberts, R., 2022. Mitochondrial genome undergoes de novo DNA methylation that protects mtDNA against oxidative damage during the peri-implantation window. Proc. Natl. Acad. Sci. U. S. A. 119, e2201168119 https://doi.org/10.1073/pnas.
Zablocki, O., van Zyl, L., Adriaenssens, E.M., Rubagotti, E., Tuffin, M., Cary, S.C., Cowan, D., 2014. High-level diversity of tailed phages, eukaryote-associated viruses, and virophage-like elements in the metaviromes of antarctic soils. Appl. Environ. Microbiol. 80, 6879–6887. https://doi.org/10.1128/AEM.01525-14.
Zgouridou, A., Tripidaki, E., Giantsis, I.A., Theodorou, J.A., Kalaitzidou, M., Raitsos, D. E., Lattos, A., Mavropoulou, A.M., Sofianos, S., Karagiannis, D., Chaligiannis, I., Anestis, A., Papadakis, N., Feidantsis, K., Mintza, D., Staikou, A., Michaelidis, B., 2022. The current situation and potential effects of climate change on the microbial load of marine bivalves of the Greek coastlines: an integrative review. Environ. Microbiol. 24, 1012–1034. https://doi.org/10.1111/1462-2920.15765.
Zhang, R., Nakahira, K., Guo, X., Choi, A.M., Gu, Z., 2016. Very short mitochondrial DNA fragments and heteroplasmy in human plasma. Sci. Rep. 6, 36097.

From shells to sequences:
A proof-of-concept study for on-site analysis of hemolymphatic circulating cell-free DNA from sentinel mussels using Nanopore technology

Sophia Ferchiou[1], France Caza[1], Richard Villemur[1], Stéphane Betoulle[2], and Yves St-Pierre[1]

1) INRS-Centre Armand-Frappier Santé Technologie, 531 Boul. des Prairies, Laval, QC, Canada, H7V 1B7

2) Université Reims Champagne-Ardenne, UMR-I 02 SEBIO Stress environnementaux et Biosurveillance des milieux aquatiques, Campus Moulin de la Housse, 51687 Reims, France

Supplementary Table and Figures

Supplementary Figure 1: Logistics of study conduct. (**A**) An overview of the abandoned Armor Site. (**B**) A closer view of Armor. The arrow indicates where the portable lab was installed. (**C-E**) A view of the sealed lab.

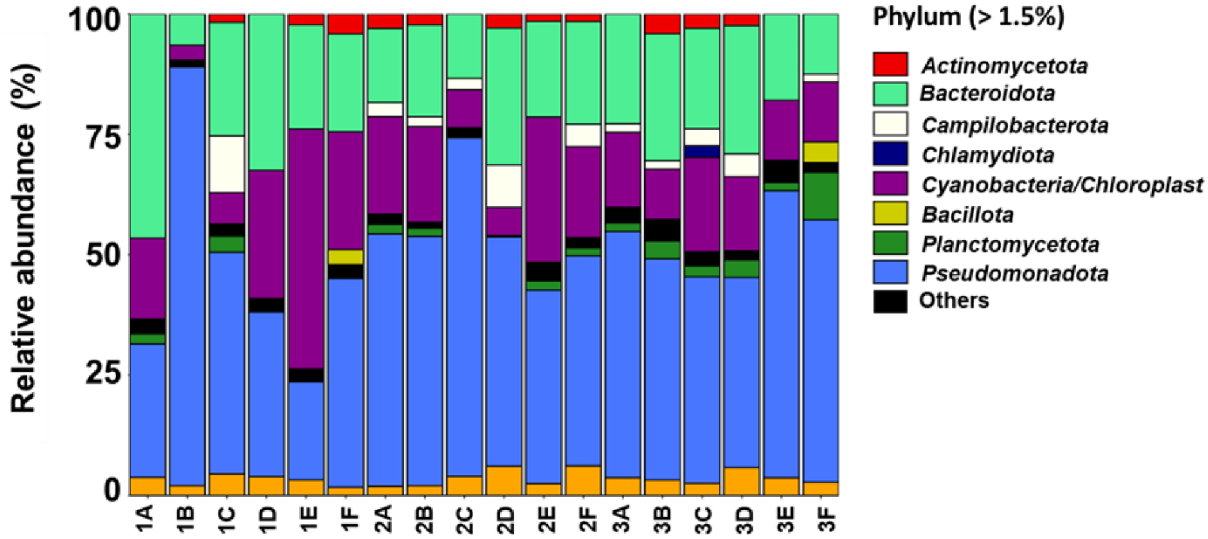

Figure S2. Phylum-level from 16S rRNA analysis in all samples. Phylum with a relative abundance of ≤ 1.5% are represented as "Other".

Chapitre 5

Évaluation de la santé des écosystèmes marins par une analyse multi-omique à partir de biopsies liquides chez les moules bleues : une étude de cas dans un parc marin national

Article publié: *Chemosphere. 2024 Aug 1;362:142714.*

Résumé

Les écosystèmes marins sont confrontés à des menaces croissantes provenant de nombreux facteurs de stress environnementaux, nécessitant une compréhension plus approfondie de leur impact sur la biodiversité et la santé des organismes sentinelles. Dans cette étude, nous avons réalisé une analyse multi-omique spatio-temporelle à l'aide des échantillons de biopsies liquides collectés chez des moules bleues (*Mytilus spp.*) dans différents écosystèmes marins d'un parc national. Nous avons exploré les profils épigénétiques, transcriptomiques, glycomiques, protéomiques et microbiens pour mieux comprendre l'interaction complexe entre la biodiversité de l'écosystème et la réponse biologique des moules à leur environnement. Notre analyse a révélé des fluctuations temporelles dans l'alpha-diversité du microbiome circulant associées aux activités humaines. L'analyse de l'ADN libre circulant (ccfDNA) hémolymphatique a fourni des informations sur la biodiversité et la présence de pathogènes potentiels. L'analyse épigénétique a révélé de nombreux sites d'hypo-méthylation au sein de l'ADN mitochondrial (ADNmt). Les analyses transcriptomiques et glycomiques comparatives ont mis en évidence des différences dans les voies métaboliques et les gènes associés aux fonctions immunitaires et de réparation de tissus. Cette étude démontre le potentiel de l'analyse multi-omique de la biopsie liquide chez les sentinelles pour offrir une vue holistique des impacts environnementaux des activités humaines sur les écosystèmes marins côtiers. Dans l'ensemble, cette approche a le potentiel d'améliorer l'efficacité et l'efficience des divers efforts de conservation, conduisant à une prise de décision plus éclairée et à une meilleure surveillance pour la conservation de la biodiversité et des écosystèmes.

Contribution des auteurs

Yves St-Pierre, France Caza et moi avons conçu le plan expérimental. France et moi avons mené l'ensemble des expériences concernant le microbiome, le transcriptome, l'épigénome et une partie des analyses du glycome. Kumardip Sinha a été responsable des expériences sur le protéome et a également travaillé sur une autre portion du glycome. J'ai pour ma part réalisé les différentes analyses bio-informatiques et biostatistiques. Le manuscrit a été rédigé par Yves et moi, avec les contributions et l'approbation de tous les auteurs à chaque étape du processus.

Chemosphere 362 (2024) 142714

Contents lists available at ScienceDirect

Chemosphere

journal homepage: www.elsevier.com/locate/chemosphere

Assessing marine ecosystem health using multi-omic analysis of blue mussel liquid biopsies: A case study within a national marine park

Sophia Ferchiou [a], France Caza [a], Kumardip Sinha [b], Janelle Sauvageau [b], Yves St-Pierre [a,*]

[a] INRS-Center Armand-Frappier Santé Technologie, 531 Boul. des Prairies, Laval, QC, Canada, H7V 1B7
[b] Human Health Therapeutics, National Research Council, 100 Sussex Dr., K1N 5A2, Ottawa, Ontario, Canada

HIGHLIGHTS

- Multi-omic analysis of mussels in a National Park.
- Application of the liquid biopsy concept to sentinel species.
- Links human activity to biodiversity changes.
- Provides insights for improved conservation.

GRAPHICAL ABSTRACT

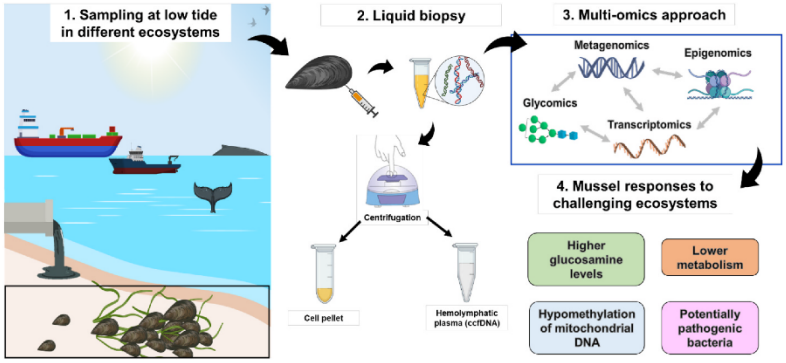

ARTICLE INFO

Handling editor: Prof Willie Peijnenburg

Keywords:
Climate change
Liquid biopsy
Mussels
Multi-omics
National marine park
Microbiome

ABSTRACT

Marine ecosystems are under escalating threats from myriad environmental stressors, necessitating a deeper understanding of their impact on biodiversity and the health of sentinel organisms. In this study, we carried out a spatiotemporal multi-omic analysis of liquid biopsies collected from mussels (Mytilus spp.) in marine ecosystems of a national park. We delved into the epigenomic, transcriptomic, glycomic, proteomic, and microbiomic profiles to unravel the intricate interplay between ecosystem biodiversity and mussels' biological response to their environments. Our analysis revealed temporal fluctuations in the alpha diversity of the circulating microbiome associated with human activities. Analysis of the hemolymphatic circulating cell-free DNA (ccfDNA) provided information on the biodiversity and the presence of potential pathogens. Epigenomic analysis revealed widespread hypomethylation sites within the mitochondrial (mtDNA). Comparative transcriptomic and glycomic analyses highlighted differences in metabolic pathways and genes associated with immune and wound healing functions. This study demonstrates the potential of multi-omic analysis of liquid biopsy in sentinel to provide a holistic view of human activities' environmental impacts on marine coastal ecosystems. Overall, this approach

* Corresponding author. INRS-Centre Armand-Frappier Santé Technologie, 531 Boul. Des Prairies, Laval, Québec, Canada, H7V 1B7.
E-mail address: yves.st-pierre@inrs.ca (Y. St-Pierre).

https://doi.org/10.1016/j.chemosphere.2024.142714
Received 9 April 2024; Received in revised form 25 June 2024; Accepted 26 June 2024
Available online 29 June 2024

has the potential to enhance the effectiveness and efficiency of various conservation efforts, leading to more informed decision-making and better outcomes for biodiversity and ecosystem conservation.

Abbreviations

ccfDNA	circulating cell-free DNA
cmDNA	circulating microbiome DNA
eDNA	environmental DNA
mtDNA	mitochondrial DNA
MAG	metagenome-assembled genome
PLP	perlucin-like protein
PCoA	principal coordinate analysis
ASVs	amplicon sequence variants
PERMANOVA	multivariate analysis of variance with permutation
LEfSe	Linear discriminant analysis Effect Size
KEGG	Kyoto Encyclopedia of Genes and Genomes
COG	Clusters of orthologous groups

1. Introduction

Climate change and pollution significantly affect coastal marine environments. The combined impact of human activities on these ecosystems is severe and multifaceted, leading to biodiversity loss through species extinctions, reduced population sizes, disrupted food webs, and altered energy flow within ecosystems (Gissi et al., 2021; O'Hara et al., 2021; Prakash, 2021; Muruganandam et al., 2023). Effective management policies are thus crucial to protecting vulnerable habitats, maintaining biodiversity, and enhancing the resilience of coastal ecosystems from the threats of climate change and pollution. Bivalves, serving as sentinel species, which are organisms that act as a barometer of ecological changes, play a critical role in monitoring these areas (Berthet, 2013; Beyer et al., 2017). Effectively monitoring and managing marine ecosystems using bivalves requires significant resources and expertise, most notably in terms of logistical perspective because specialized equipment is often needed to gather data effectively, making monitoring programs expensive. Many biomarkers developed for bivalves, especially those based on tissue biopsies, target specific cellular or tissue functions (Viarengo et al., 2007; Beyer et al., 2017). Despite their relevance in indicating the health status of the host, their sensitivity and predictive value remain limited (Lam, 2009). Moreover, they are not well-suited for assessing the broader impacts of human activities on biodiversity, which is often achieved through traditional methods such as direct observations or environmental DNA analysis (Bernatchez et al., 2024). An ideal approach would involve a logistically friendly predictive method that identifies potential threats and risks to ecosystems before they cause significant damage, enabling proactive management strategies. Such an approach can serve as an early warning system, enabling managers to take preventative actions before issues become critical.

One possibility would be to adapt the concept of liquid biopsy, originally developed in oncology, where detection is crucial for preventing disease onset, selecting the most effective treatment, and monitoring treatment success (Siravegna et al., 2017; Heitzer et al., 2019). A liquid biopsy involves collecting and analyzing bodily fluids, such as blood (or hemolymph for invertebrates) and is less invasive than traditional methods requiring tissue samples. The use of this approach now extends well beyond oncology. It can not only be used in other areas of medicine but also in marine biology as a way to early detect physiological disturbances underlying the development of diseases or exposure to environmental stress, allowing for earlier intervention and mitigation strategies (Caza et al., 2019; Sharma et al., 2019; Ferchiou et al., 2022a; Moufarrej et al., 2022). We hypothesize that liquid biopsy collected in sentinel species can be a valuable approach for developing predictive biomarkers and understanding the impact of pollution on marine coastal ecosystems. Analyzing the molecular content of the liquid biopsy, such as circulating cell-free DNA (ccfDNA), can help identify molecular biomarkers that indicate exposure to specific pollutants or the overall health status of the organism. We have previously shown, for example, that the hemolymphatic ccfDNA of mussels contains DNA fragments that vary considerably in size, ranging from 1 to 5 kb, and that a significant amount of DNA fragments had a nonself microbial origin (Caza et al., 2019; Ferchiou et al., 2022a). Ideally, from a single drop of hemolymph, it would be desirable to obtain not only information on the biodiversity but also early signs of perturbations, the host's response, and multi-levels of biological information.

In this work, we conducted a proof-of-concept study for a multi-omics approach using the blue mussel as a sentinel species to gain valuable insights into the overall health and quality of the coastal marine ecosystems found in a National park for which protection of marine ecosystems in response to climate change and human activities is a major concern. For this, we employed a diverse set of omics analyses, including 16S rRNA for microbiome profiling and ccfDNA to distinguish nonself-from self-DNA, transcriptomics, proteomics and methylomics for these two studied sites. This integrated strategy offers comprehensive insights into the blue mussel's biological and environmental interactions, illustrating the potential of multi-omics in marine ecology research.

2. Materials and methods

2.1. Location and characteristics of the study site

The study was conducted in in Saguenay-St-Lawrence Marine Park (SSLMP), a national marine conservation area located in Eastern Canada in Quebec and renowned for its rich biodiversity across multiple marine habitats. However, the area faces significant pressure from various human activities, particularly seasonal tourist activities. Five sites were selected for our study between Fall 2019 and Fall 2020. Among these, three sites exhibit sandy environments, while the remaining two sites feature rocky environments (Fig. 1). Notably, the Cap-de-Bon-Désir site (48° 16′ 14″ N; 69° 28′ 01″ W) was chosen as a reference site because of the absence of direct pollution sources. Conversely, the Baie-Sainte-Catherine (48° 07′ 00″ N; 69° 43′ 17″ W), Pointe-Rouge (48° 08′ 08″ N; 69° 42′ 03″ W), Moulin-à-Baude (48° 09′ 26″ N; 69° 39′ 44″ W), and Pointe-à-John (48° 13′ 57″ N; 69° 32′ 47″ W) sites are recognized as polluted (e.g., dissolved nutrients inputs, fecal contamination, trace metals) due to their exposure to boat traffic, marina activities, and the discharge of domestic and agricultural effluents (Lemaire and Pelletier, 2013, 2018). In addition, several neighboring municipalities, including Bergeronnes, either lack adequate wastewater treatment infrastructure or have none at all, giving rise to significant environmental concerns (Lemaire and Pelletier, 2013; Demers-Lemay, 2019). Specifically, Bergeronnes discharges wastewater directly into the Grandes-Bergeronnes River, leading to increased concentrations of trace metals and microbial pathogens, particularly at Pointe-à-John (Lemaire and Pelletier, 2013). Moreover, the Moulin-à-Baude Bay receives water from rivers like the Moulin-à-Baude, which collects agricultural runoff from upstream communities. This runoff contaminates the bay with pollutants such as fecal coliforms, orthophosphates, and nitrogen oxides (Comité ZIP, 2005; Lemaire and Pelletier, 2013).

3. Sample collection

Adult specimens of blue mussels (*Mytilus* spp.) were collected from the intertidal zone, with approximately 40–50 individuals gathered per site between 2019 and 2022. Hemolymph was withdrawn from the adductor muscle using a syringe fitted with a 21-gauge needle, as described by Ferchiou et al. (2022b). Each sample contained hemolymph from approximately 3-4 mussels pooled together (~1.5 mL each) and was immediately centrifuged for 3 min at 6200 rpm (TOMY Multi Spin Centrifuge, Japan). After centrifugation, cell pellets, containing bacteria and hemocytes, the circulating cells in bivalves, were resuspended, and 50 μL aliquots were applied to individual discs of Whatman 903™ FTA® cards (Sigma-Aldrich, Oakville, ON, Canada). These cards, made with a chemically treated cellulose matrix, stabilize amino acids and nucleotides at room temperature for long-term storage and are ideally suited for the analysis of liquid biopsies (Caza et al., 2019). Based on various factors (see Results), we decided to analyze ccfDNA from two specific sites. Supernatants containing ccfDNA were frozen and stored at −20 °C until further use. Five supernatant samples per site were collected only during the Fall of 2020 and 2022 at the two studied sites: Moulin-à-Baude and Cap-de-Bon-Désir. Cell pellets were also frozen during that period for additional analysis, including transcriptomics and methylomics.

3.1. DNA extraction

Total DNA was isolated, as described by Ferchiou et al. (2023). Briefly, 5 mm punched discs from the FTA® cards were directly used for DNA extraction using the QIAamp DNA Investigator Kit (Qiagen, Germany) according to the manufacturer's instructions. Meanwhile, according to the manufacturer's recommendations, ccfDNA was isolated from supernatant samples and purified using the NucleoSnap cfDNA kit

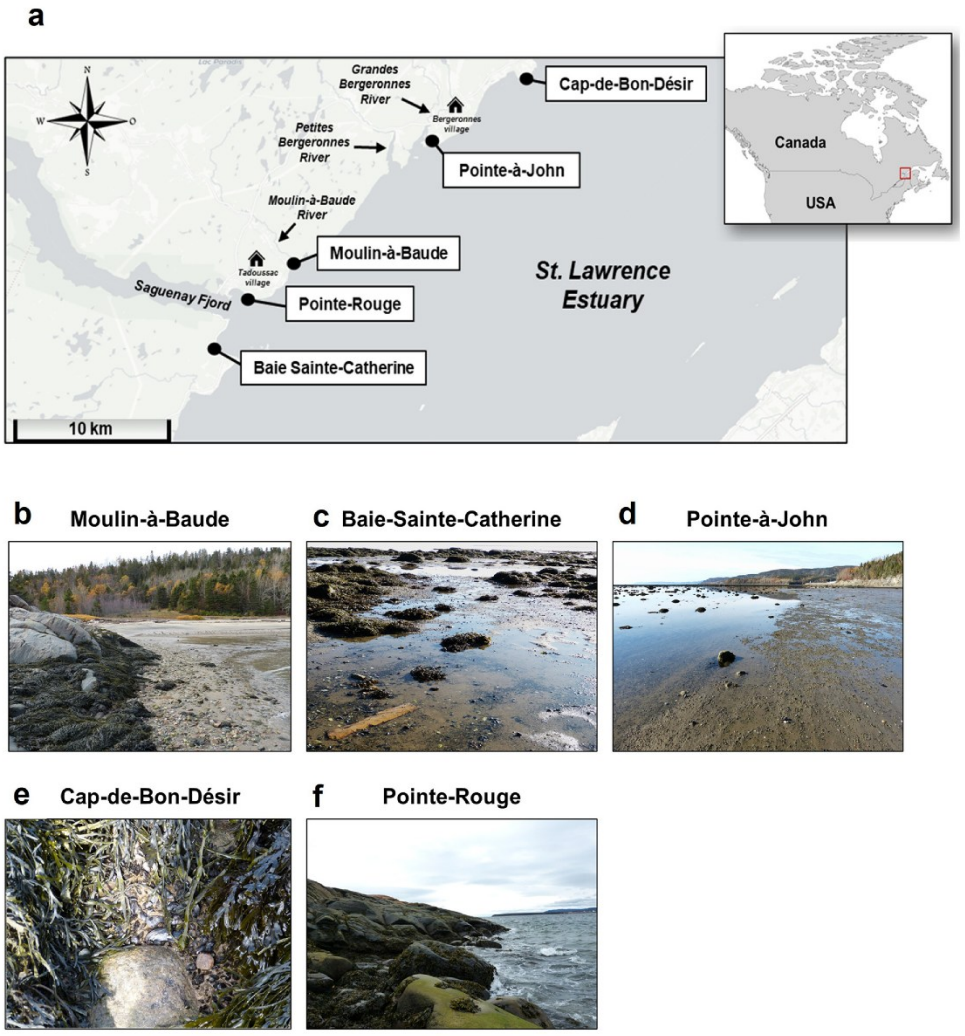

Fig. 1. Study area. (a) Map showing the five *Mytilus* spp. intertidal sampling sites. (b–f) Intertidal sampling sites in Saguenay-St. Lawrence Marine Park, photographed at low tide. Moulin-à-Baude, Baie-Sainte-Catherine, and Pointe-à-John are characterized by sandy, wave-exposed beaches, while Cap-de-Bon-Désir and Pointe-Rouge are rocky shores where mussels are covered by sand and seaweed.

(Macherey-Nagel, Germany). Purified DNA was quantified using a Qubit™ dsDNA HS assay kit (Invitrogen, Carlsbad, CA, USA).

3.2. 16S rRNA and shotgun sequencing

Amplifications of V3–V4 regions of the 16S rRNA gene and sequencing (16S rRNA) for all total DNA samples from cell pellets were performed at Genome Quebec (Montreal, Canada) using the universal primers 341F (5′-CCTACGGGNGGCWGCAG-3′) and 805R (5′-GACTACHVGGGTATCTAATCC-3′) (Klindworth et al., 2013). Sequence libraries were prepared by Genome Quebec with a DNA Library Preparation Kit for Illumina. Paired-end sequences were generated using the MiSeq platform PE300 (Illumina, San Diego, CA, USA) with the 600-cycle MiSeq Reagent Kit v3 (Illumina, CA, USA). For shotgun sequencing of hemolymphatic ccfDNA, libraries were prepared by Genome Quebec for Illumina NovaSeq 6000 S4 PE150 with the NovaSeq 6000 S4 Reagent kit v1.5 (Illumina, CA, USA). IDT dual-index adaptors were used. Raw 16S and shotgun metagenomic DNA data files are available on the NCBI Sequence Read Archive (PRJNA915419 and PRJNA754391).

3.3. Analysis of 16S-based microbial taxonomic data

Illumina sequence data (FASTQ files) were received as output from Genome Quebec. Cutadapt v4.2 was used as a tool in the Unix Shell v5.1.16 (Ubuntu version 22.04) environment for trimming primers from the raw sequencing data. For data pre-processing, the DADA2 v1.16.0 pipeline (Callahan et al., 2016) was used to generate 16S rRNA (V3–V4) non-chimeric amplicon sequence variants (ASVs) for all samples. The latest RDP 18 database was used for taxonomy assignments of representative ASVs (Wang et al., 2007). All statistical analyses were performed in R v4.2.3 (R Core Team, 2023). Alpha diversity indices (Shannon index, Pielou's evenness and richness estimator) were calculated using phyloseq and microbiomeSeq packages and pairwise permutation tests were performed to obtain significant p-values ($p < 0.05$) (McMurdie and Holmes, 2013; Ssekagiri et al., 2017). Significant microbial composition differences among groups were determined using multivariate analysis of variance with permutation (PERMANOVA) with 9999 permutations followed by pairwise permutation tests. To explore the taxonomic differences across seasons and sites, we employed linear discriminant analysis (LDA) effect size (LEfSe) utilizing the microbiomeMarker package (Cao et al., 2022). The threshold on the logarithmic score (log10) of the LDA analysis was set to 3.0. We analyzed unique and shared AVSs among groups using Venn diagrams with the ggVennDiagram package (Gao et al., 2021). Pie charts and histogram plots were generated using the R package ggplot2 (Wickham, 2016).

3.4. Circulating cell-free DNA analysis

The quality of raw ccfDNA reads was analyzed using FastQC v0.11.9 (Andrew, 2010). The adapters and low-quality reads were trimmed with Trimmomatic v0.39 (Bolger et al., 2014). The paired-end shotgun reads were merged using FLASH v1.2.11 (Magoč and Salzberg, 2011). We selected a minimum overlap of 20 bp and a mismatch ratio of 0.25 as parameters. Self-merged reads were identified with BLASTN v2.14.1 using the bivalves NCBI taxonomy database (e-value $< 1e{-}3$). Nonself-reads were identified as reads not related to bivalves. Self and nonself-reads were assembled separately using MEGAHIT v1.2.9 to generate contigs for each site (Li et al., 2015). N50 for both sites was evaluated using the assemblyStatics tool (Challis, 2017). Nonself-contigs (>300 bp) were then identified by alignment with BLASTN and BLASTX using nt and nr NCBI databases (e-value $< 1e{-}40$). BLASTN and BLASTX results were pooled for each site as final sets. All statistical analyses were performed in R v4.2.3. Metagenome-assembled genomes (MAGs) were reconstructed from metagenomic assemblies using the Anvi'o platform, which facilitates analysis and visualization of 'omics data (Eren et al., 2021). Contigs were processed to identify open reading frames with Prodigal v2.6.3 (Hyatt et al., 2010), followed by annotation using HMMER v3.2.1 (Eddy, 2011) for single-copy core genes in bacteria and archaea. Genome assembly coverage was determined using Bowtie2 v2.3.5.1 (Langmead and Salzberg, 2012), and SAM files produced were converted to BAM format with Samtools v1.15.1 (Li et al., 2009). Coverage and detection statistics were generated with Anvi'o profiles, which were then merged using the Anvi-merge tool. MAGs were initially binned with CONCOCT v1.1.0 (Alneberg et al., 2014).

3.5. RNA extraction and RNA-seq

Five samples per site were used to perform the transcriptomics analysis. Total RNA was extracted from frozen cell pellets, resuspended in 750 μL of TRIzol® and mixed by inversion with 200 μL of chloroform. After phase separation, the RNA-containing aqueous phase was carefully transferred and mixed with 400 μL of isopropanol to precipitate the RNA. The resulting RNA pellets were washed with 75% ethanol and then dissolved by incubation for 15 min at 55 °C with agitation at 700 rpm in 30 μL of PCR-grade water. Subsequent purification was performed using the RNeasy Plus Mini Kit (Qiagen, Germany), with the final RNA eluted in 30 μL of PCR-grade water. Quantification of RNA was carried out using a Qubit 1.0 fluorometer with the Qubit™ RNA HS assay kit (Invitrogen, Carlsbad, CA, USA), and RNA quality was assessed via the NanoDrop 2000/2000C spectrophotometer (Thermo Fisher Scientific, Waltham, MA, United States). Purified total RNA was forwarded to Genome Quebec (Montreal, QC, Canada). The mRNA library preparation was performed using an NEB stranded library preparation kit for Illumina®, followed by sequencing on an Illumina NovaSeq 6000 platform with the NovaSeq 6000 S4 reagent kit (Illumina, CA, USA), generating 100 bp paired-end reads. Raw data files are available on the NCBI Sequence Read Archive (PRJNA1070309).

3.6. RNA-seq and glycomic profiles analysis

Sequence quality was evaluated using FastQC. Before de novo assembly, Trimmomatic was employed to trim adapters and remove low-quality reads. The transcriptome assembly was then conducted with Trinity, and the overall assembly quality was assessed using TrinityStats.pl. Gene abundance in each sample was estimated using the RSEM tool (RNA-Seq by Expectation-Maximization) (Li and Dewey, 2011). Long open reading frames (ORFs) within the transcripts were identified using the TransDecoder v5.5.0 tool, facilitating the generation of protein sequences for the predicted coding regions (Haas, 2023). Transcript identification was performed running BLAST against nucleotide and protein sequences with an e-value threshold of 1e-50. Predicted protein sequences underwent HMMER searches against the Pfam database for functional annotation (Eddy, 2011). To gain a deeper understanding of the biological differences between mussels at both sites, we conducted two functional analyses using widely utilized databases that encompass a diverse range of organisms. Specifically, further analyses were performed for clusters of orthologous groups (COG) and Kyoto Encyclopedia of Genes and Genomes (KEGG) pathways using the DIAMOND tool for the COG database and the KofamKOALA online software, respectively (Galperin et al., 2015; Aramaki et al., 2020). Differential gene expression (DGE) analysis was conducted using DESeq2 and edgeR packages from Bioconductor (Robinson et al., 2010; Love et al., 2014). Differentially expressed genes were identified based $|\log_2 FC| > 10$ and FDR <0.05. Only genes with at least 100 counts in at least 50% of the samples in one of the groups were considered in the analysis. All statistical analyses were executed in R v4.2.3. Venn diagrams were generated utilizing the ggVennDiagram package in R. Principal Component Analysis (PCA) and heatmap visualization was conducted using the Glimma and pheatmap packages, respectively (Su et al., 2017; Kolde, 2019). Identification of glycogens was performed by querying the Glycosmos database (Yamada et al., 2020).

3.7. Monosaccharide composition analysis

Whole hemolymph samples from both sites were analyzed, as reported previously, with modifications in terms of treatment before hydrolysis and dilutions. The samples (4 per site) were centrifuged at 4500 rpm for 10 min before hydrolysis and filtered through a 10 kDa MWCO filter to remove monosaccharides such as glucose, present at high concentrations and other metabolites. The supernatant (25 μL) was then subjected to TFA (5 M) in triplicates (200 μL) and heated at 100 °C for 2h. After evaporation, the hydrolysate was resuspended in HPLC-grade water (75 μL) and then diluted (1:10, v:v, for filtering) before injection also in triplicates on a High-Performance Anion-Exchange

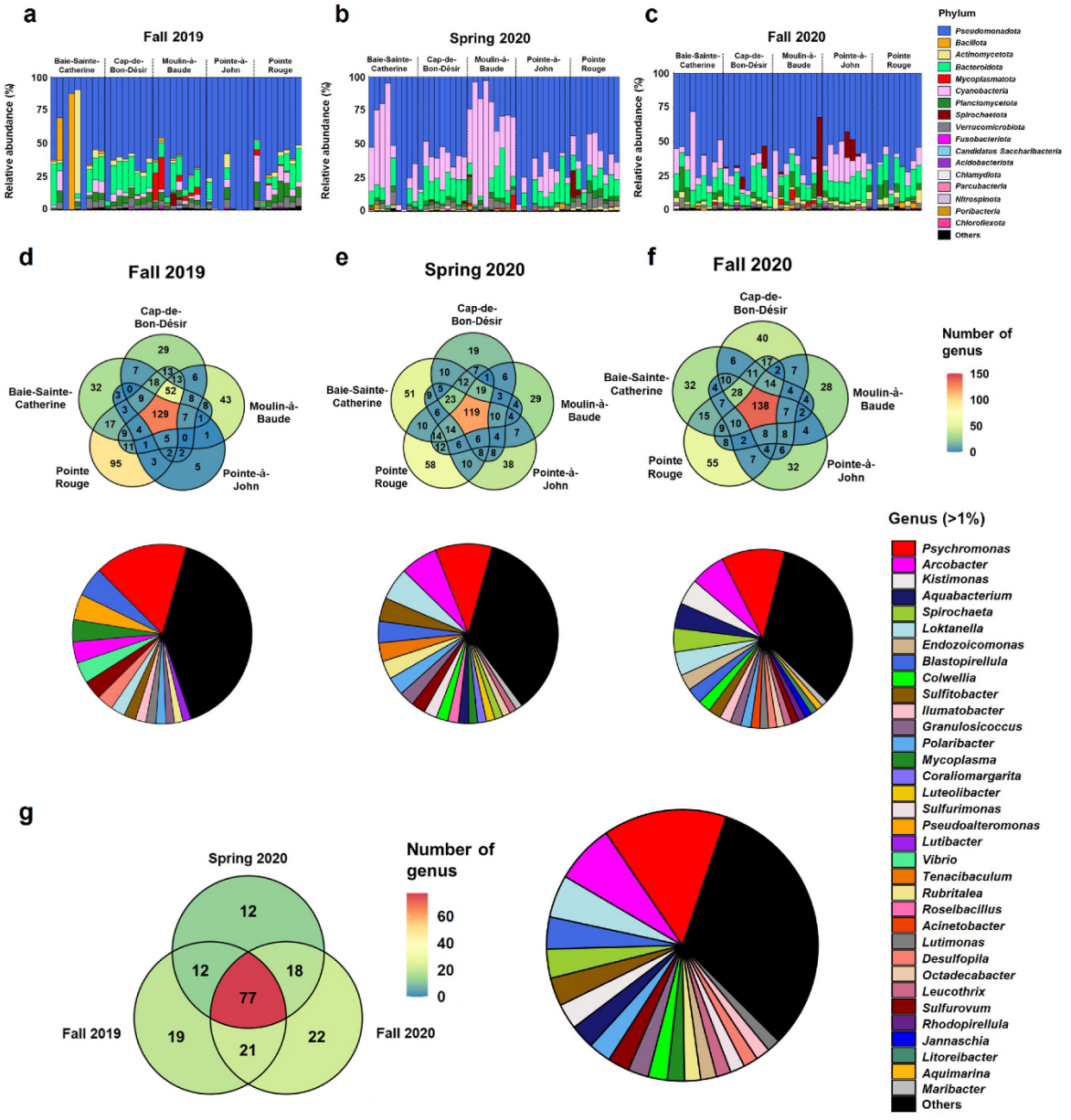

Fig. 2. Shared phylum-level and genus-level taxa across different seasons and sampling sites. Phylum-level analysis of *Mytilus* spp. collected in intertidal zones during (a) Fall 2019, (b) Spring 2020 and (c) Fall 2020. Phylum with a relative abundance of ≤1.5% is represented as "Others." Venn diagrams and pie charts show the number of unique and shared genera in *Mytilus* spp. intertidal sites during (d) Fall 2019, (e) Spring 2020 and (f) Fall 2020. (g) Venn diagram and pie chart represent the 181 'core' bacterial genera's distribution across the three seasons. Only shared genera with a relative abundance of ≥1% are represented in pie charts. Red colors indicate higher abundances, and blue colors indicate lower abundances. (For interpretation of the references to color in this figure legend, the reader is referred to the Web version of this article.)

Chromatography system coupled with a Pulsed Amperometric Detector (HPAEC-PAD) as previously described. The monosaccharides were identified from a monosaccharide standard mix (Thermo Fisher Scientific, Waltham, MA, United States) and quantified after extrapolation from a calibration curve as described by Rohrer (2021). Statistical analyses were conducted using one-way analysis of variance (ANOVA) and Tukey's post-hoc tests for parametric data. Nonparametric permutation tests were applied when data did not meet the assumptions required for ANOVA. All statistical analyses were performed in R v4.2.3.

3.8. DNA isolation and nanopore sequencing

Four samples per site were used for DNA methylation analysis. DNA was extracted from frozen cell pellets using the QIAamp DNA Investigator Kit (Qiagen, Germany) according to the manufacturer's instructions. Quality was assessed using a NanoDrop 2000/2000C spectrophotometer. Library preparations were performed with an Oxford Nanopore Ligation Sequencing Kit (ONT, SQK-LSK114) according to the manufacturer's instructions. Sequencing was carried out on the ONT Mk1C device using version 10.4.1 flowcells. Raw fast5 files are available on the NCBI Sequence Read Archive (PRJNA1070574).

3.9. Methylation analysis

DNA methylation (5 mC) and hydroxymethylation (5hmC) calls were determined using megalodon v2.5.0 with Guppy v6.0.1 models for MinION data. Reads were aligned to the *Mytilus edulis* reference genome (PEIMSO, NCBI) using minimap2 (Li, 2018). Methylation frequencies from both strands were quantified with METEORE (Yuen et al., 2021). All statistical analyses were performed in R v4.2.3. Visualisations were generated using methylartist 1.2.11 and ggplot2 R package (Cheetham et al., 2022).

4. Results

4.1. Spatiotemporal analysis of hemolymphatic circulating microbiome of mussels

Our analysis encompassed a total of 133 samples from cell pellets. Sequencing of 16S rRNA gene amplicons targeting the V3–V4 hypervariable region yielded 5 721 260 paired-end sequences that successfully passed quality filtering (an average of 43 017 $\pm$ 1163 per sample). From these high-quality reads, we generated amplicon sequence variants (ASVs) amounting to 23 625. Our findings revealed the presence of bacterial genera commonly associated with domestic wastewater, such as *Bordetella*, *Clostridium*, *Corynebacterium*, *Roseomonas*, and *Exiguobacterium*, at the Moulin-à-Baude, Pointe-Rouge, Pointe-à-John, and Baie-Sainte-Catherine sites (Table S1). Notably, we consistently detected the bacterial phylum *Mycoplasmatota* at the Moulin-à-Baude site throughout various seasons (Fig. 2a–c). This phylum is predominantly represented by *Mycoplasma* and *Tenacibaculum*, two genera known for their potential pathogenic effects on fish and humans (Fernández-Álvarez and Santos, 2018; Nowlan et al., 2020; Dawood et al., 2022). Furthermore, our analysis unveiled shared and unique microbial taxa at different locations, including a core microbiome predominantly composed of genera characteristic of marine waters. These genera included DNA derived from bacteria typically found in cold environments, such as *Colwellia*, *Psychrilyobacter*, *Psychroserpens, Glaciecola*, *Psychromonas*, *Octadecabacter*, *Polaribacter*, *Shewanella*, and *Sulfurimonas* (Fig. 2d–g). LEfSe analysis revealed that the cmDNA of mussels collected at Cap-de-Bon-Désir primarily consisted of discriminant genera integral to the core microbiome, characteristic of cold marine ecosystems, and this pattern persisted across different seasons (Fig. 3). In contrast, the cmDNA of mussels at the Moulin-à-Baude site exhibited an elevated presence of *Vibrio* and *Mycoplasma*, particularly in Fall (2019).

4.2. Differences in alpha-diversity of the circulating microbiome

Our analysis revealed notable findings regarding the diversity and richness of microbial communities at different sampling sites. The Moulin-à-Baude and Pointe-à-John sites, which are exposed to agricultural and domestic effluents, consistently exhibited the lowest levels of diversity and richness across all years and seasons (Fig. 4). Additionally, Baie-Sainte-Catherine and Pointe-à-John displayed the lowest evenness in both Fall 2019–2020 and Spring 2020. In contrast, Pointe-Rouge and Cap-de-Bon-Désir showcased the highest alpha-diversity indices during both the fall of 2019 and spring of 2020. However, an interesting shift in patterns emerged during the Fall of 2020. During this period, we observed only minor fluctuations in all alpha-diversity metrics across the sampling sites, indicating a more consistent microbial community structure across locations. This suggests a potential stabilization or convergence of microbial diversity during that particular season.

4.3. Analysis of self and nonself hemolymphatic ccfDNA

We next focused on analyzing circulating cell-free DNA (ccfDNA) at two geographically distinct sites, Moulin-à-Baude and Cap-de-Bon-Désir. This selection was based on several important factors: 1) the Cap-de-Bon-Désir site exhibited significantly higher alpha-diversity indices during both autumn 2019 and spring 2020 compared to Moulin-à-Baude.; 2) there was a substantial disparity in the bacterial composition between the two sites. The microbiome of the Cap-de-Bon-Désir site was primarily composed of core microbiome genera, which are considered integral to healthy marine ecosystems. In contrast, the Moulin-à-Baude site was characterized by a significant presence of *Vibrio*, *Mycoplasma*, and *Tenacibaculum*, highlighting potential differences in microbial community structure, and 3) both sites possess ecological importance as critical habitats for marine mammals, including harbor seals and minke whales.

We first investigated the source of ccfDNA fragments in blue mussels by conducting a categorization of all sequencing reads into two distinct groups: those aligning with *Mytilus* spp. sequences (referred to as "self)" ccfDNA and those identified as originating from external sources (nonself). For both sites, we assembled approximately 3–4 million contigs from approximately 150 million reads. Among these contigs, about 10–12% were classified as originating from nonself sources (Table 1). The majority of the nonself DNA fragments originated from viruses and bacteria, which accounted for more than 75% of all identified contigs, followed by metazoans (7–8%) and chromists (3–15%) (Fig. 5).

Among the notable differences between the two sites, we observed a significant abundance of Platyhelminthes (flatworms) and Priapulida (marine worms typically found in marine sediments) at the Moulin-à-Baudes site. Additionally, we detected DNA from *Tenacibaculum maritimum*, known to cause tenacibaculosis in marine fish, and DNA from *Dicrocoelium dendriticum*, a parasitic flatworm that infects the liver and bile ducts of various mammals (Table 2) (Raj et al., 2022; Mabrok et al., 2023). Using metagenome-assembled genomes (MAGs), we confirmed the presence of various parasitic and microbial genera at the Moulin-à-Baude site, including *Tremotoda* and *Mycoplasma* spp. (Table S2). The metazoan diversity mainly consisted of marine organisms at both sites, such as polychaete annelid worms (e.g., *Sabellidae*, *Nereididae*), sea anemones (e.g., *Actiniidae*), sea stars (e.g., *Asteriidae*), marine isopods (*Idoteidae*), and marine gastropods (e.g., *Littorinidae*, *Patellidae*). Interestingly, the Cap-de-Bon-Désir site exhibited a significant presence of brown algae DNA, including species such as *Ectocarpus siliculosus*, *Endarachne binghamiae*, and *Petalonia fascia* (Table 2). This finding aligns with the abundant macroalgal fauna observed at this site (Chabot and Rossignol, 2003). Viral DNA analysis at both sites uncovered a more varied viral community at the Moulin-à-Baude site, featuring bacterial viruses, algae viruses, and retroviruses (Figure S1). This diversity showed a distinct correlation with specific hosts, including *Vibrio phage*,

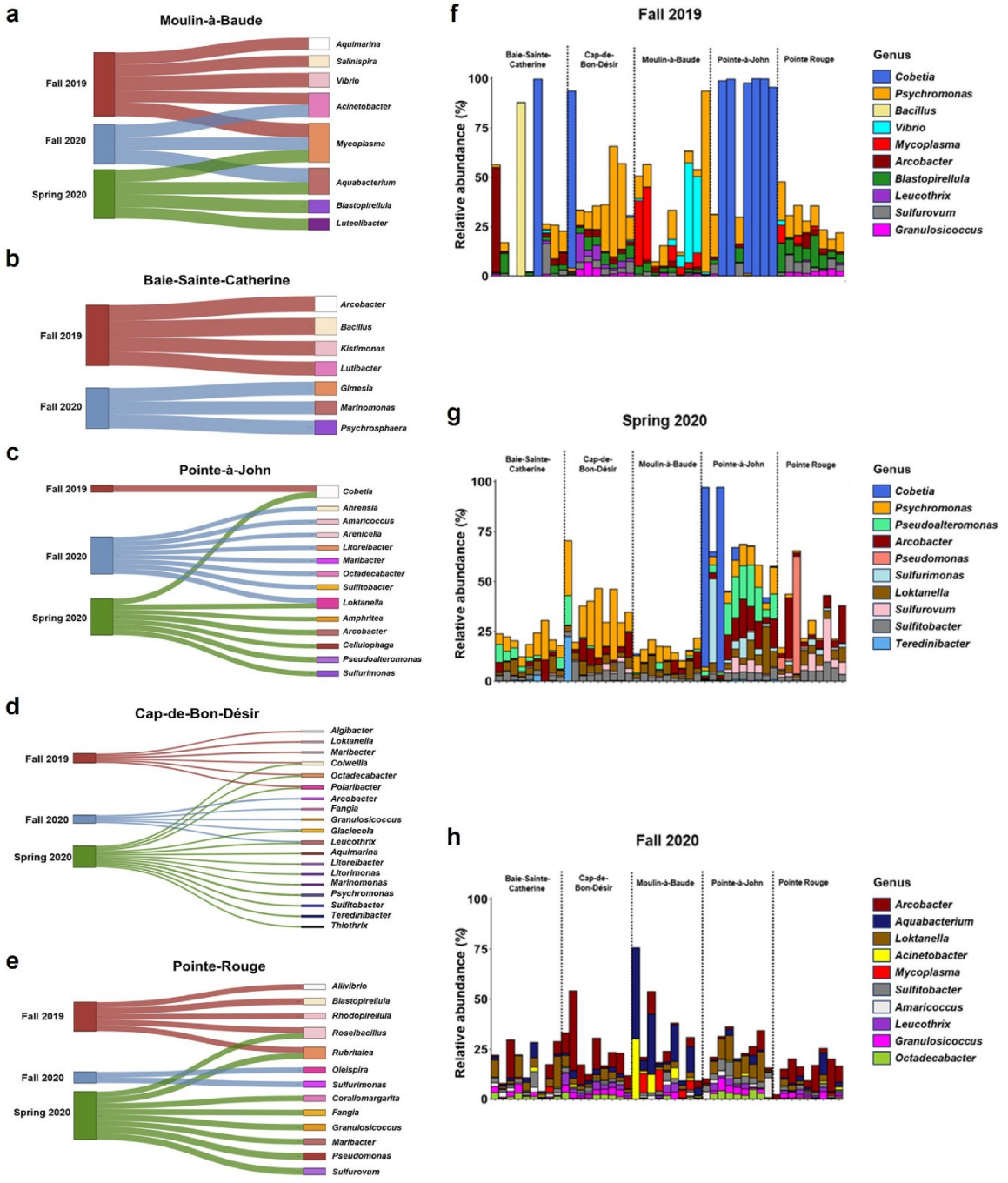

Fig. 3. Bacterial differential abundance at the genus level. (a–e) Sankey diagrams showing the discriminant genera (logarithmic discriminant analysis (LDA) score >3) in *Mytilus* spp. intertidal sites during Fall 2019 (red), Spring 2020 (green) and Fall 2020 (blue). (f–h) Bar plots showing the proportions of the discriminant genera among sampling sites across different seasons. (For interpretation of the references to color in this figure legend, the reader is referred to the Web version of this article.)

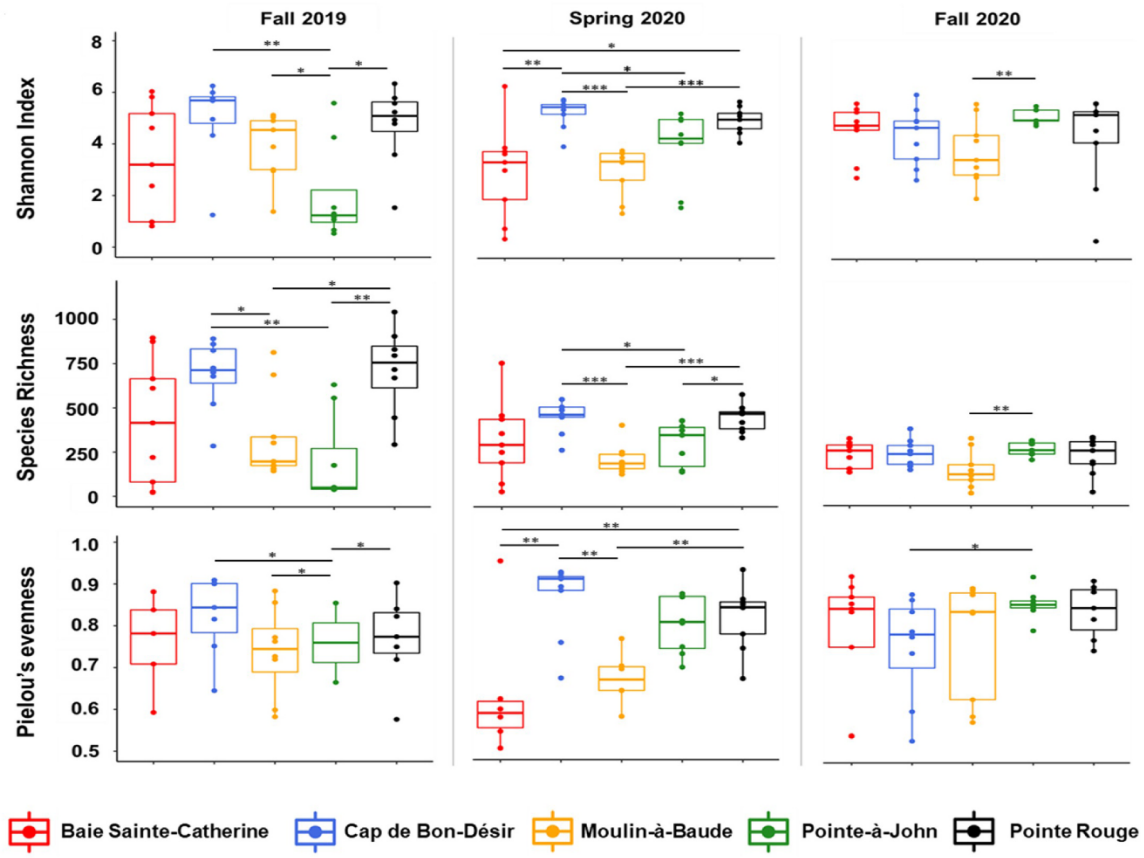

Fig. 4. Alpha diversity analysis of hemolymphatic bacterial DNA. Box plots for (a) Shannon diversity, (b) observed richness and (c) species evenness indexes were calculated for each *Mytilus* spp. intertidal sampling site during Fall 2019, Spring 2020 and Fall 2020. A dashed line separates each seasonal group. Significant p-values ($p < 0.05$) were obtained using a permutation test as a non-parametric test following post-hoc pairwise comparisons. Note: * $0.01 < p \leq 0.05$, ** $0.001 < p \leq 0.01$, *** $p \leq 0.001$.

Table 1
Self and nonself origin of hemolymphatic ccfDNA.

Sites	n	Reads (Self)	Reads (Nonself)	Contigs (Self)	Contigs (Nonself)	Percentages (Nonself)
Moulin-à-Baude	5	106 517 051	27 705 760	3 266 468	384 825	11.8%
Cap-de- Bon-Désir	5	143 948 371	26 026 324	3 696 621	447 595	12.1%

Tenacibaculum phage, and viruses associated with brown algae (Table 2).

4.4. Site-dependent variations in transcriptional and epigenetic responses

4.4.1. Differential gene expression analysis

We next performed a transcriptomic analysis on blue mussels from two sites, using hemocyte pellets. Due to the lack of annotated genomes for this species, we employed de novo assembly to identify the transcripts with a setting at a minimum of 100 reads per transcript. Using this approach, we were able to identify a total of 17 686 transcripts, averaging about 37 million reads per sample (Fig. S2). By annotating these transcripts with various public databases, we determined that the vast majority (over 99%) corresponded to the blue mussel species (Fig. S3a). Over 60% of the transcripts were successfully annotated (Figs. S3b–c). Principal Component Analysis (PCA) demonstrated significant gene expression profiles in the circulating transcriptome of mussels at the two sites (Fig. 6a). Mussels at Cap-de-Bon-Désir site showed a ten-fold increase in transcripts compared to mussels from Moulin-à-Baude site (Fig. 6b). Hierarchical cluster analysis using the expression data of the 50 genes from both sites revealed two distinct clusters with similar changes in expression across different samples. (Fig. 6c). Several genes that were upregulated in hemocytes of mussels sampled at Moulin-à-Baude, such as animal haem peroxidase, p53 DNA binding domain, and chaperonin 10 kd subunit are associated with environmental stressors while others, like triosephosphate isomerase and cytochrome *c* oxydase subunit VIIc, are associated with nutrient availability (Follis et al., 2014; Sirokmány and Geiszt, 2019). We also noted an increased expression of genes such as NADH dehydrogenase and ATP synthase, normally indicative of a higher metabolism in hemocytes of mussels collected at Cap-de-Bon-Désir. In independent

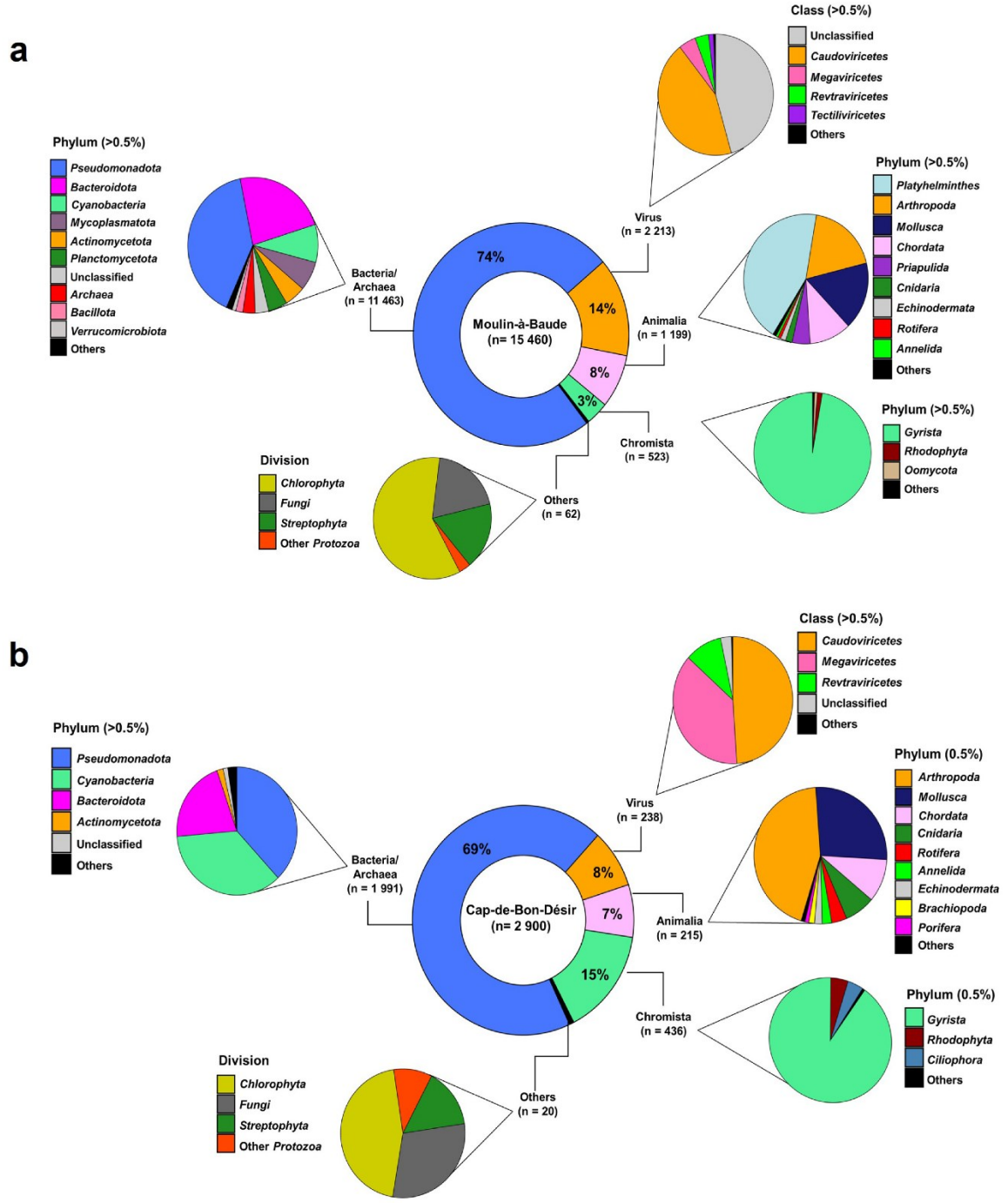

Fig. 5. Nonself DNA contig compositions. A total of (a) 15 460 assembled contigs were analyzed for Moulin-à-Baude, and (b) 2900 assembled contigs were analyzed for Cap-de-Bon-Désir. Taxonomic distribution profiles of metagenomic contig identification from hemolymphatic ccfDNA were characterized using BLASTN and BLASTX.

Table 2
The most abundant non-self of the hemolymphatic ccfDNA (Top 4 species for each category are shown).

Categories	Sites	Species (top 4)	(%)
Bacteria	Moulin-à-Baude	*Mycoplasmatales bacterium*	**6.2**
		Flavobacteriales bacterium	**5.5**
		Phycisphaerae bacterium	**2.9**
		Alteromonadales bacterium	**2.6**
	Cap-de-Bon-Désir	*Pleurocapsa minor*	**5.6**
		Waterburya agarophytonicola	**3.6**
		Acidiferrobacterales bacterium	**2.6**
		Polaribacter sp.	**2.0**
Virus	Moulin-à-Baude	*Vibrio phage*	**14.3**
		Prokaryotic dsDNA virus sp.	**13.3**
		Caudovirales phage	**8.3**
		Retrovirus Mytilus edulis	**4.9**
	Cap-de-Bon-Désir	*Ectocarpus siliculosus virus*	**33.6**
		Vibrio phage	**24.4**
		Tenacibaculum phage	**19.3**
		Retrovirus Mytilus edulis	**9.2**
Animalia	Moulin-à-Baude	*Dicrocoelium dendriticum* (lancet liver fluke)	**14.5**
		Patellidae (sea snail family)	**9.1**
		Idotea baltica (isopod)	**7.4**
		Priapulus spp. (cactus worm)	**4.7**
	Cap-de-Bon-Désir	*Idotea baltica* (isopod)	**31.2**
		Lottia spp. (limpet)	**10.2**
		Littorina spp. (common periwinkle)	**7.9**
		Patellidae (sea snail family)	**5.6**
Chromista	Moulin-à-Baude	*Laminariaceae* (brown algal seaweed family)	**27.9**
		Ectocarpus siliculosus (brown alga)	**10.3**
		Chordariaceae (brown algae family)	**6.3**
		Petalonia fascia (broad leaf weed)	**2.5**
	Cap-de-Bon-Désir	*Endarachne binghamiae* (brown alga)	**27.8**
		Ectocarpus siliculosus (brown alga)	**13.8**
		Petalonia fascia (broad leaf weed)	**9.4**
		Chordariaceae (brown algae family)	**6.9**

experiments, we validated by RT-PCR the higher expression, in mussels from Cap-de-Bon-Désir, of the Cytochrome *c* oxydase 1 gene, which plays a vital role in the electron transport chain and oxidative phosphorylation within mitochondria (Fig. 6d) (Ludwig et al., 2001).

4.4.2. Functional analysis and glycomic profiles

We then conducted functional analyses to better understand the biological differences between mussels at both sites. The first analysis involved the Kyoto Encyclopedia of Genes and Genomes (KEGG), which provides a comprehensive overview of cellular processes and metabolic pathways associated with various biological functions. The second analysis utilized Clusters of Orthologous Groups (COG), which classify genes with similar functions across different species, disregarding specific pathways and offering a broader perspective on gene functions. Once again, our findings demonstrated significant distinctions between the two sites. Particularly noteworthy variations were observed in cellular processes and metabolism, shedding light on the divergent molecular mechanisms underlying these biological functions. Additionally, disparities were also identified in information processing and storage, indicating dissimilarities in the genetic and molecular components responsible for these processes (Fig. 7a–b).

Glycosylation plays a multifaceted role in various cellular functions, such as the immune response and the formation and integrity of the shell. We paid special attention to glycosylation-related genes, which are referred to as glycogenes (Akase and Angata, 2019). We found that at the Cap-de-Bon-Désir site, there was >10-fold increase in the number of glycogenes compared to the other site (Fig. 7c). Among the glycogenes that were overexpressed, we found a diverse repertoire of genes, including several lectins and genes involved in glycosynthesis (Fig. 7d). We also observed a higher expression of the gene encoding the Perlucin-like protein (PLP) in mussels of Moulin-à-Baude. Differences in the hemolymphatic glycome between mussels from both sites were also observed at the biochemical level. Analysis of hemolymphatic monosaccharides by HPAEC-PAD showed statistically higher levels of glucosamine in the hemolymph of mussels of Moulin-à-Baude (Fig. 7e). Hemolymph can contain a wide range of glycosylated proteins, such as hemocyanin, coagulogen, etc. (Osaki and Kawabata, 2004; Lorenzon et al., 2011; Salazar et al., 2019). Measuring the protein concentration can provide valuable information in terms of mussel's health and condition as these proteins are critical, for example, for respiration (Lorenzon et al., 2011).

4.4.3. DNA methylation

We thus studied whether the DNA methylation status differed between mussels at both sites. Given the lack of comprehensive genomic annotations for the blue mussel, our study primarily centered on mitochondrial DNA (mtDNA), which is also known to undergo demethylation following exposure to pollutants (Sharma et al., 2019). Alignment to the mitochondrial genome (PEIMSO) resulted in a mean coverage of 143X (SD = ±52.64). Our findings indicate a widespread hypomethylation at both CpG and CpN sites within the mtDNA of mussels inhabiting the Moulin-à-Baude site (Fig. 8a–b). Significant hypomethylation of CpG sites within mitochondrial genes, including ATP6, COX1, COX2, COX3, CYTB, NAD1, NAD4, and NAD5, was observed (Fig. 8c). Approximately 56% of CpG sites in mtDNA showed methylation abnormalities, which exhibited hypomethylation in 40% of its CpG sites at Moulin-à-Baude. Furthermore, mtDNA hypomethylation was also observed across all mitochondrial genes at the Moulin-à-Baude site compared to the Cap-de-Bon-Désir site, with over 68% of CpN sites being hypomethylated, indicative of a 90% anomaly (Fig. 8d).

5. Discussion

Our study demonstrates the efficacy of multi-omics analysis of liquid biopsies collected from mussels as a powerful tool to obtain a comprehensive understanding of the biological responses of sentinel mussels to environmental stress. This holistic approach provides deeper insights into the underlying mechanisms of these impacts and has significant implications for conservation efforts, particularly in national parks and other ecologically valuable areas. By pinpointing these specific molecular alterations, we can prioritize conservation strategies and develop targeted mitigation interventions. This evidence-based approach facilitates informed decision-making, ensuring that actions align with the conservation and protection of these ecosystems.

Our study yielded a comprehensive understanding of the bacterial communities associated with coastal marine ecosystems, shedding light on specific genera and phyla present at different sites. Key outcomes included the identification of potential pollution indicators and the characterization of a core microbiome specific to healthy marine environments. Additionally, our spatiotemporal analysis of the circulating microbiome provided insights into the dynamic nature of microbial communities and their response to environmental changes. For example, we observed significant fluctuations in the alpha diversity of the microbiome during Fall 2019 and Spring 2020. However, in the Fall of 2020, we found only very minor fluctuations in alpha-diversity metrics, including richness, Shannon diversity, and evenness indices, across sites. We hypothesize that this reduced impact is attributed to decreased anthropogenic activities resulting from the COVID-19 pandemic. From March to June 2020, there was a complete closure of the park, including the cancellation of all activities and services, followed by a partial reopening from July to October. These results support the hypothesis that the interruption or reduction of human activities for a short period is sufficient to prevent fluctuations in the mussel microbiome. This hypothesis is also consistent with observations made during the COVID-19 epidemic in other marine ecosystems (Edward et al., 2021; Weng et al., 2023). However, further studies will be necessary to confirm this hypothesis.

Analysis of ccfDNA, which has gained importance in various medical

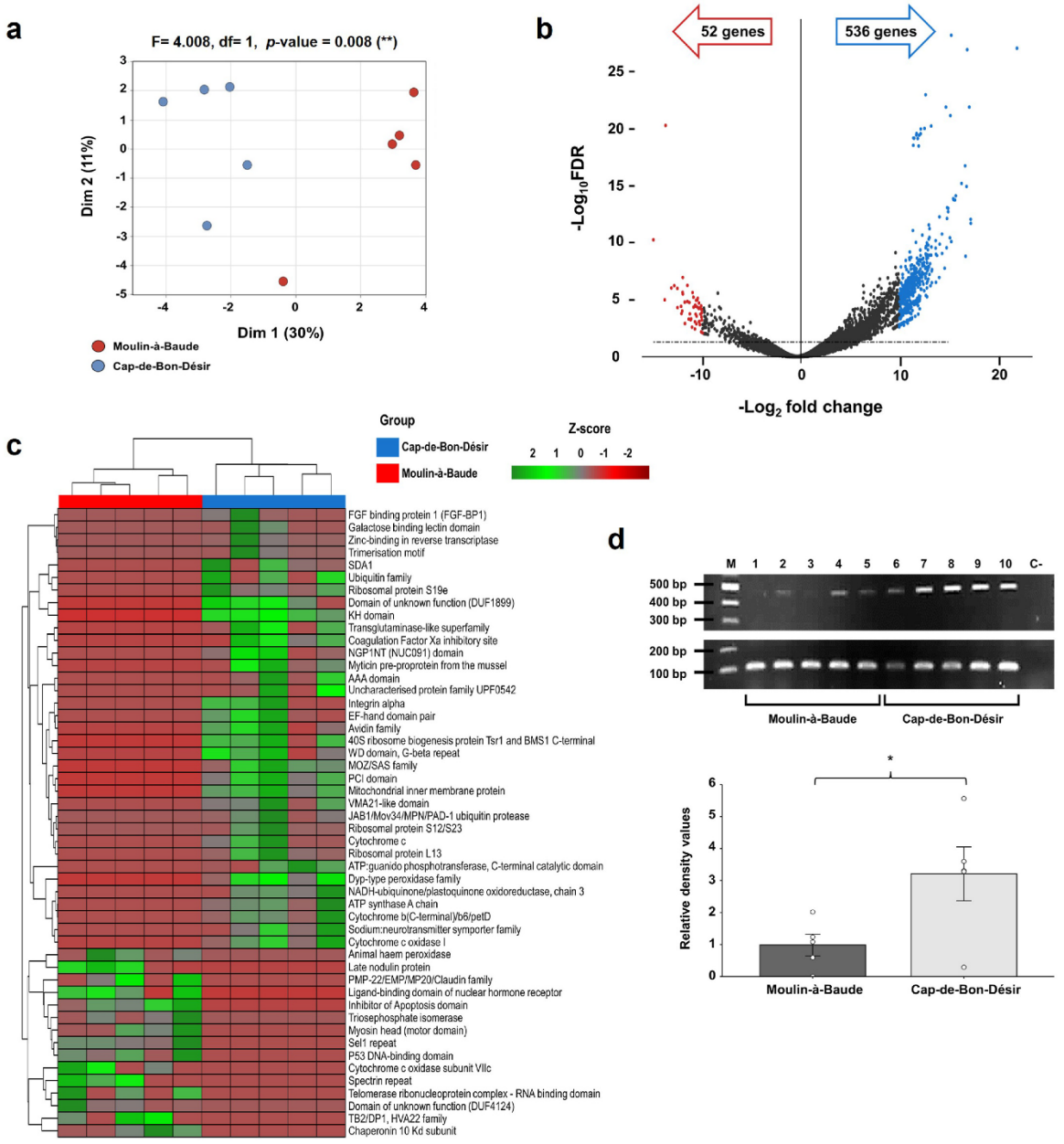

Fig. 6. RNA-Seq differential expression. (a) Multidimensional scaling (MDS) plot showing the distinct clustering of sample points. (b) The volcano plot depicts significantly differentially upregulated genes, with $\log_2$ fold-change (FC) and -$\log_{10}$ P-value (adjusted using the FDR correction method). Genes meeting criteria of FDR $\leq$0.05 and |FC| $\geq$ 10 are highlighted; red for Moulin-à-Baude, blue for Cap-de-Bon-Désir). (c) Heatmap showing gene expression levels (normalized by Z-score) of the top 50 genes that exhibit the highest differential expression. (d) Upper panel: RT-PCR analysis showing the expression of *COX1* and *EF1α* genes in *Mytilus* spp. samples from both sites. M indicates the 100-base-pair DNA ladder; lanes 1–2: Moulin-à-Baude samples; lanes 3–4: Cap-de-Bon-Désir samples; lane 5: negative control (no DNA template). Lower panel: Bar graph showing the relative expression density (mean ± SE) of the COX1 gene between samples from both sites. Statistical significance was assessed using one-way ANOVA, with results indicated by an asterisk (* $0.01 < p \leq 0.05$). (For interpretation of the references to color in this figure legend, the reader is referred to the Web version of this article.)

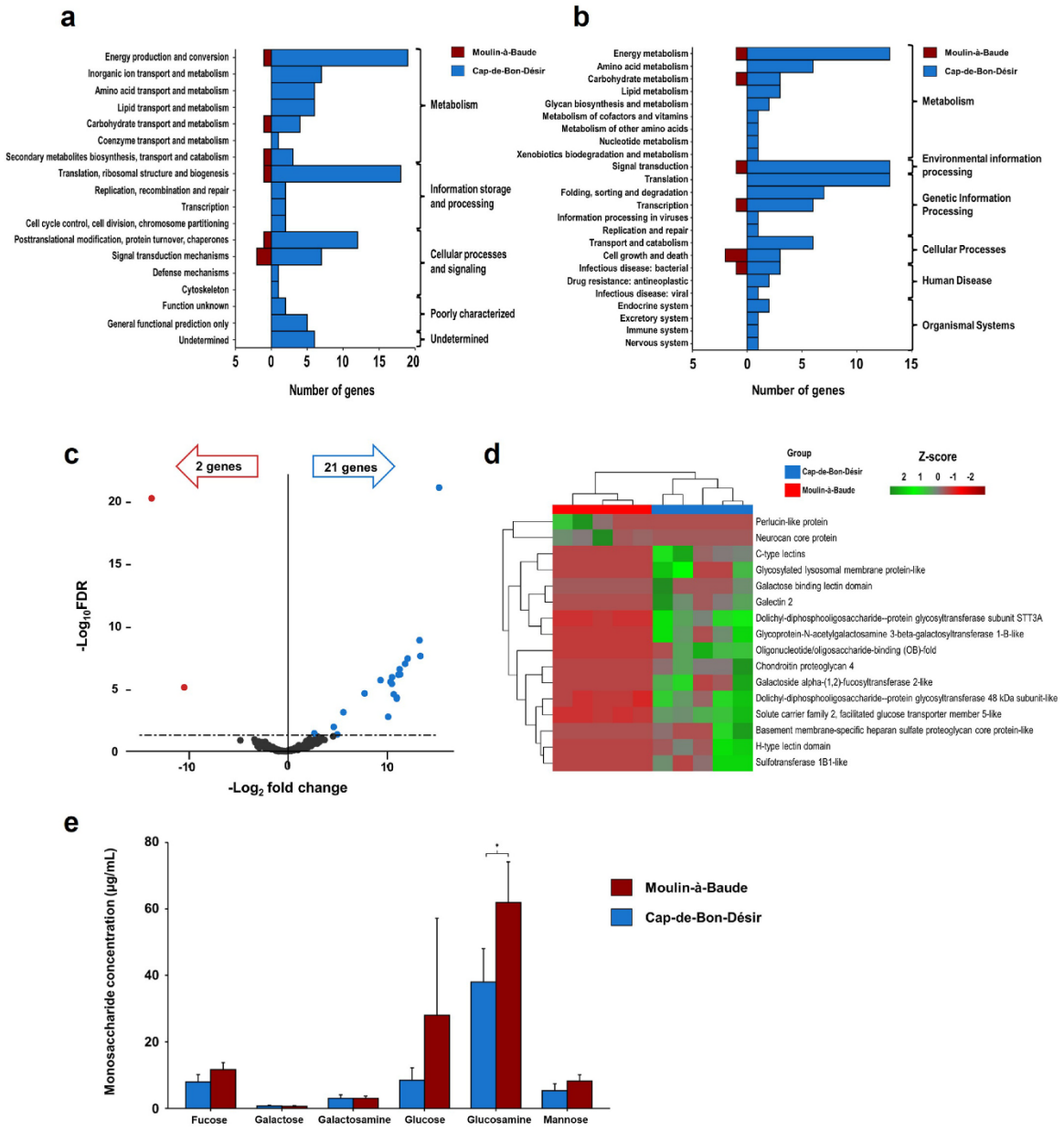

Fig. 7. COG and KEGG pathway classifications and glycomic-related gene analyses (a) Distribution of COG categories; the y-axis enumerates the most prevalent COG terms. (b) Bar plot illustrating the enriched KEGG pathways among upregulated genes at both sites. (c) Volcano plot demonstrating the relationship between $\log_2$ fold-change (FC) on the x-axis and $-\log_{10}$ of the P-value (adjusted using the FDR correction method) on the y-axis for significantly differentially upregulated glycogenes (defined by FDR ≤ 0.05 and $|FC| \geq 2$); Moulin-à-Baude (red) and Cap-de-Bon-Désir (blue), with the number of genes highlighted. (d) Heatmap, normalized by Z-score within each row, of glycomic-related genes. (e) Hemolymphatic monosaccharide. This comparison is based on glycoproteins isolated through protein hydrolysis and 10 MWCO filtration from four samples at each site. Data represent averages from three sets of triplicate injections and reactions. Samples were pooled by site for statistical analysis. Error bars represent standard deviation. * $0.01 < p \leq 0.05$). (For interpretation of the references to color in this figure legend, the reader is referred to the Web version of this article.)

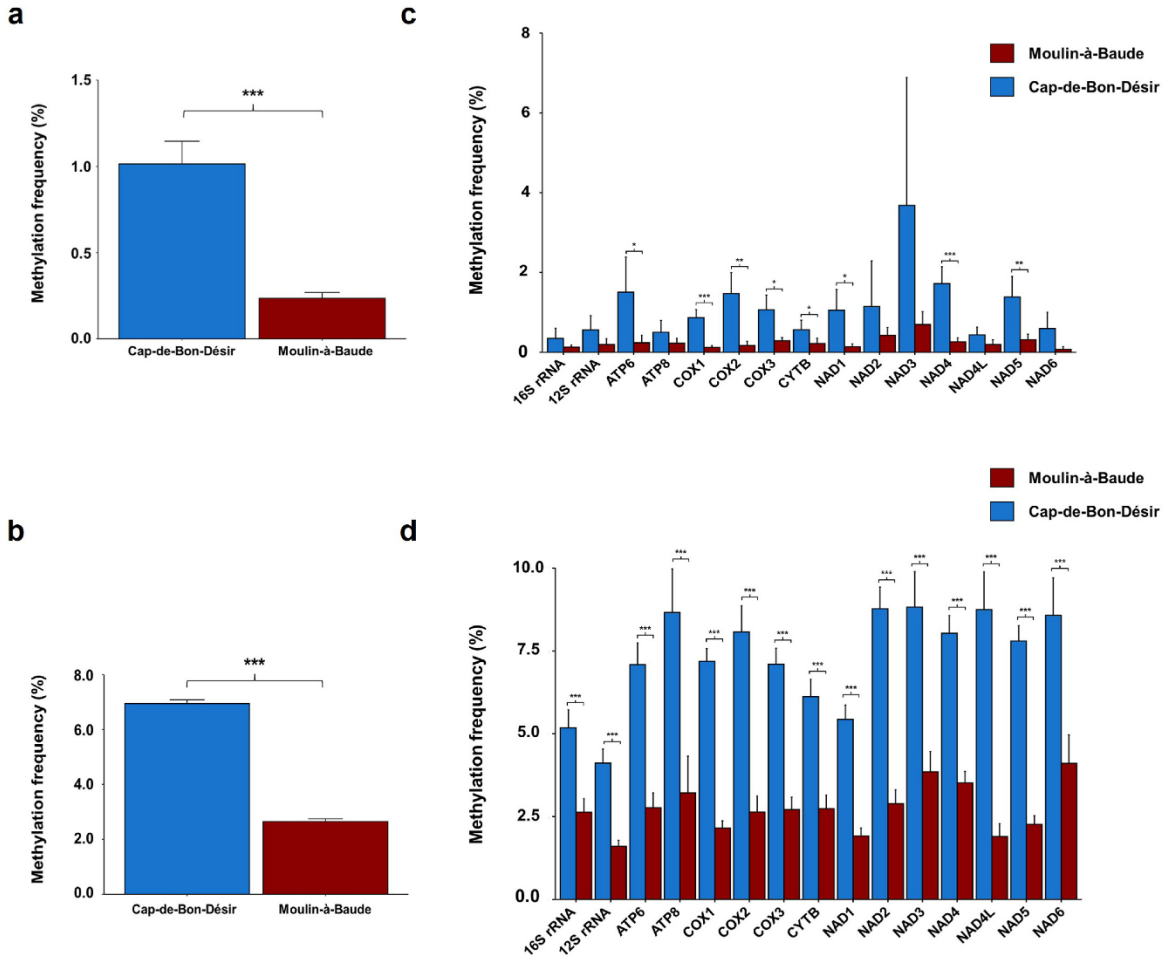

Fig. 8. Comparison of mtDNA CpG and CpN methylation. Bar graphs showing the mean (±SE) percent methylation frequency within the whole mitochondrial genome at (a) CpG sites and (b) CpN sites. Methylation levels are shown for each mitochondrial gene at (c) CpG sites and (d) CpN sites. Significant p-values ($p < 0.05$) were obtained using a permutation test as a non-parametric test following post-hoc pairwise comparisons. Note: * $0.01 < p \leq 0.05$, ** $0.001 < p \leq 0.01$, *** $p \leq 0.001$. Cap-de-Bon-Désir site is indicated in blue, and the Moulin-à-Baude in red. (For interpretation of the references to color in this figure legend, the reader is referred to the Web version of this article.)

applications, is only in its infancy in marine biology. Although bacterial DNA dominates the ccfDNA, we were able to identify DNA from other microorganisms, viruses and parasites with relative ease. This enabled us to obtain a more detailed view of the differences in the virome, bacteriome, and parasitome between Moulin-à-Baude, an ecosystem near the town of Tadoussac where water from surrounding agricultural activities flows, and Moulin-à-Baude, located more than 20 km downstream. For instance, at Moulin-à-Baude, we observed a predominant presence of DNA from *Mycoplasma* spp. or Platyhelminthes, which encompass several parasitic species capable of infecting humans and other animals. Notable examples of parasitic flatworms include blood flukes (*Schistosoma* spp.), responsible for causing schistosomiasis, and tapeworms (*Taenia* spp.), which infect the intestines of vertebrates. Yet, analysis of ccfDNA faces major limitations, particularly in the case of viruses. For example, viral genomes are generally smaller than cellular genomes, and viral ccfDNA fragments tend to be further fragmented after release from infected cells, making them even more difficult to distinguish from background noise. Most importantly, marine viral diversity remains poorly explored (Coutinho et al., 2017; Dance, 2021; Vincent and Vardi, 2023). Our data, as well as our biobank of liquid biopsies, which is facilitated by storage on FTA cards, could be revisited in the future as progress is made in the development of bioinformatics tools and databases to ensure accurate identification of all potential viral pathogens. As reference genomes and databases for marine species continue to develop, retrospective studies using the data obtained from our study will become possible, enabling the detection of rare or unknown species, among other insights.

To investigate hemocytes' response to environmental stress, we analyzed the circulating transcriptome, which represents a rich source of biomarkers in medicine (Solé et al., 2019). The concept of a "circulating transcriptome" is now, however, new in marine biology. It is well known that hemocytes are highly responsive to environmental changes and offer insights into the underlying biological processes within them (Negri et al., 2013; de Boissel et al., 2017; Châtel et al., 2018). When combined with other "omics" approaches, however, the analysis of hemocyte transcriptomes provides a deeper understanding of the

organism's response to stress. In our study, we observed distinct transcriptional activities in mussels from both Moulin-à-Baude and Cap-de-Bon-Désir sites, reflecting differences in metabolic processes. Several factors could account for the lower metabolic activity observed in the hemocytes of mussels from Moulin-à-Baude compared to those from Cap-de-Bon-Désir. Exposure to pollutants such as heavy metals, pesticides, or pharmaceuticals can disrupt cellular processes and energy production, leading to decreased metabolic activity in hemocytes. Limited food availability may also induce a state of reduced metabolic activity in mussels as an energy conservation strategy, which can affect hemocyte function (Le Guernic et al., 2015). Additionally, low oxygen levels in the water can prompt mussels to adjust their metabolism to function under oxygen-limited conditions, resulting in an overall decrease in hemocyte metabolic activity (Sun et al., 2021).

Irrespective of the cause, our findings align with our glycomics analysis. We observed an increase in the expression of PLP. This glycoprotein is known to play a role in the shell formation of mollusks (Rey-Campos et al., 2019a; Bi et al., 2020; Feng et al., 2023). It is also expressed in hemocytes, suggesting that it also plays a role in innate immune defense and pathogen recognition (Lin et al., 2013; Rey-Campos et al., 2019b). This C-type lectin was previously associated with the innate immune response in shellfish and bivalves, most notably in response to *Vibrio* spp. (Rey-Campos et al., 2019a; Bi et al., 2020; Feng et al., 2023). This upregulation of PLP expression can be attributed to factors primarily related to the mussel's response to stress or immune challenges. When mussels encounter bacterial or fungal infections, their hemocytes typically increase PLP production to combat the threat. Similarly, exposure to environmental pollutants like heavy metals, pesticides, or pharmaceuticals can also lead to elevated PLP expression. PLPs may play a role in wound healing by promoting tissue repair and inhibiting bacterial growth at the site of injury (Wang et al., 2008; Dodenhof et al., 2014). Interestingly, we also observed increased expression of neurocan in hemocytes from Moulin-à-Baude. Neurocan is a large extracellular chondroitin sulfate proteoglycan found in the nervous system and other tissues (Rauch et al., 2001). Our glyco-proteomic analysis revealed an elevated level of glucosamine in the hemolymph of mussels collected from Moulin-à-Baude, providing further evidence of the contrasting nature of the two environments. Glucosamine, found at the core of glycans and glycoproteins, is affected by various factors, such as heat and stress, which influence glycoprotein production within cells. Glucosamine plays an important role in shell repair and defense mechanisms (Canesi and Pruzzo, 2016; Agbaje et al., 2018). Because the higher glucosamine levels were only apparent after TFA hydrolysis, and after hydrolysis N-acetylglucosamine is hydrolysed into glucosamine, we hypothesized that the glucosamine we observed was most likely derived from glycoproteins constituent. This hypothesis was supported by the high protein content we observed via a protein Bicinchoninic acid assay (0.62–1.35 mg/mL) (Fig. S4). Another indication that these glycans were protein-bound was the lower migration bands observed via non-denaturing SDS-Page after PNGase cleavage of the glycoproteins (Fig. S5). Glycoproteins are involved in vital biochemical functions, including respiration and cellular response. For instance, hemocyanins, blood glycoproteins in mussels, facilitate oxygen transport (Coates and Costa-Paiva, 2020). These biochemical findings align with our genetic analysis, demonstrating the upregulation of defense-related genes and the downregulation of genes associated with energy metabolism.

What are the mechanisms underlying these observed transcriptomic/glycomic/proteomic alterations? One hypothesis relates to the DNA methylation status of genomic DNA. Changes in DNA methylation patterns are known to occur in response to various types of stress, including exposure to pathogens, pollutants, and other physicochemical factors (Meaney and Szyf, 2005; Martin and Fry, 2018; Ladd-Acosta and Fallin, 2019). Importantly, these changes in DNA methylation can sometimes be heritable, impacting mussels over the long term. In our study, we observed a clear and significant hypomethylation of the mitochondrial genome in mussels from Moulin-à-Baude. Several studies have shown that exposure to environmental stress, such as chemicals and pollutants, can induce global DNA hypomethylation (Dolinoy et al., 2007; Herbstman et al., 2013). While hypomethylation is generally associated with upregulation of gene expression, the downregulation of mitochondrial genes observed in our study suggests the involvement of alternative regulatory mechanisms. These mechanisms could include the recruitment of transcriptional repressors to mtDNA, inhibiting transcription, or feedback mechanisms from altered metabolic states that suppress mitochondrial gene expression regardless of methylation status (Hervouet et al., 2018; Shokolenko and Alexeyev, 2022). Additionally, epigenetic perturbators, such as environmental factors, drugs, or diseases, can influence the epigenetic state of mtDNA (Heijmans et al., 2008; Heyn et al., 2012; Sarkies, 2023). The proximity of the Moulin-à-Baude site to a wastewater discharge point likely exposes the blue mussels to disruptive agents like pesticides or pollutants, potentially leading to the widespread hypomethylation observed in their DNA. Interestingly, previous research has also linked hypomethylation of mtDNA with cellular senescence induced by chronic oxidative stress (Yu et al., 2017). Regardless, these results open the door to future research into the agents responsible for epigenetic changes in mussels and the use of epigenetic biomarkers to monitor the health of an ecosystem. Fortunately, the Oxford Nanopore Technology employed in our study offers several advantages that facilitate DNA methylation studies compared to traditional methods (Searle et al., 2023). This technology enables direct sequencing of native DNA in CpG and non-CpG contexts, eliminating potential biases introduced by chemical modifications and preserving the original methylation patterns. Moreover, DNA methylation analysis serves as a highly sensitive biomarker for assessing the epigenomic response to environmental stressors, including chemical pollution, temperature fluctuations, water acidification, and viral infections (Putnam et al., 2016; Zhang and Cao, 2019; Sharavanan et al., 2020). It is also worth noting that DNA methylation is just one of several epigenetic mechanisms involved in gene expression regulation. Histone modifications and non-coding RNAs are among the other mechanisms contributing to the dynamic control of gene transcription (Bure et al., 2022).

In conclusion, our study demonstrates that multi-omic analysis of liquid biopsies collected from mussels provides a powerful tool for comprehensively assessing the impact of human activities on marine coastal ecosystems. Interpreting the complex and often intertwined information from multiple omics data sets can be challenging, requiring specialized expertise and careful consideration of potential confounding factors. Leveraging the power of machine learning for data analysis, pattern recognition, and predictive modeling in the near future will help our understanding of cellular responses and potentially enable the identification of early warning signals. This knowledge can inform conservation efforts, environmental monitoring strategies, and the development of sustainable practices for the future.

Funding information

This work was partly funded by the National Science and Engineering Research Council of Canada (Grant No. x-2019-06607, YSP), Glyconet (Grant No. ID-13, YSP), Sentinelle Nord YSP) and the Institut Nordique du Québec (INQ, YSP). S.F. is supported by a scholarship from the Fonds de Recherche du Québec-Nature et Technologie (FRQNT) and the Ecotoq Research Network.

CRediT authorship contribution statement

Sophia Ferchiou: Writing – original draft, Validation, Methodology, Investigation, Formal analysis, Data curation, Conceptualization. **France Caza:** Writing – review & editing, Validation, Methodology, Investigation, Formal analysis, Data curation, Conceptualization. **Kumardip Sinha:** Writing – review & editing, Methodology, Formal analysis, Conceptualization. **Janelle Sauvageau:** Writing – review & editing, Validation, Methodology, Formal analysis, Conceptualization.

Yves St-Pierre: Writing – review & editing, Validation, Supervision, Resources, Project administration, Methodology, Investigation, Funding acquisition, Formal analysis, Conceptualization.

Declaration of competing interest

The authors declare that they have no known competing financial interests or personal relationships that could have appeared to influence the work reported in this paper.

Data availability

Data will be made available on request.

Appendix A. Supplementary data

Supplementary data to this article can be found online at https://doi.org/10.1016/j.chemosphere.2024.142714.

References

Agbaje, O.B.A., Shir, I.B., Zax, D.B., Schmidt, A., Jacob, D.E., 2018. Biomacromolecules within bivalve shells: is chitin abundant? Acta Biomater. 80, 176–187. https://doi.org/10.1016/j.actbio.2018.09.009.

Akase, S., Angata, K., 2019. Databases of glycogenes (GGDB and FlyGlycoDB). Glycoforum 22, A7. https://doi.org/10.32285/glycoforum.22A7.

Alneberg, J., Bjarnason, B.S., De Bruijn, I., Schirmer, M., Quick, J., Ijaz, U.Z., et al., 2014. Binning metagenomic contigs by coverage and composition. Nat. Methods 11, 1144–1146. https://doi.org/10.1038/nmeth.3103.

Andrew, S., 2010. FastQC: a quality control tool for high throughput sequence data. http://www.bioinformatics.babraham.ac.uk/projects/fastqc.

Aramaki, T., Blanc-Mathieu, R., Endo, H., Ohkubo, K., Kanehisa, M., Goto, S., et al., 2020. KofamKOALA: KEGG Ortholog assignment based on profile HMM and adaptive score threshold. Bioinformatics 36, 2251–2252. https://doi.org/10.1093/bioinformatics/btz859.

Bernatchez, L., Ferchaud, A.L., Berger, C.S., Venney, C.J., Xuereb, A., 2024. Genomics for monitoring and understanding species responses to global climate change. Nat. Rev. Genet. 25, 165–183. https://doi.org/10.1038/s41576-023-00657-y.

Berthet, B., 2013. Sentinel species. In: Amiard-Triquet, C., Amiard, J.C., Rainbow, P.S. (Eds.), Ecological Biomarkers: Indicators of Ecotoxicological Effects. CRC Press, Boca Raton, USA, pp. 155–186. https://doi.org/10.1201/b13036-8.

Beyer, J., Green, N.W., Brooks, S., Allan, I.J., Ruus, A., Gomes, T., et al., 2017. Blue mussels (Mytilus edulis spp.) as sentinel organisms in coastal pollution monitoring: a review. Mar. Environ. Res. 130, 338–365. https://doi.org/10.1016/j.marenvres.2017.07.024.

Bi, J., Ning, M., Xie, X., Fan, W., Huang, Y., Gu, W., et al., 2020. A typical C-type lectin, perlucin-like protein, is involved in the innate immune defense of whiteleg shrimp Litopenaeus vannamei. Fish Shellfish Immunol. 103, 293–301. https://doi.org/10.1016/j.fsi.2020.05.046.

Bolger, A.M., Lohse, M., Usadel, B., 2014. Trimmomatic: a flexible trimmer for Illumina sequence data. Bioinformatics 30, 2114–2120. https://doi.org/10.1093/bioinformatics/btu170.

Bure, I.V., Nemtsova, M.V., Kuznetsova, E.B., 2022. Histone modifications and non-coding RNAs: mutual epigenetic regulation and role in pathogenesis. Int. J. Mol. Sci. 23, 5801. https://doi.org/10.3390/ijms23105801.

Callahan, B.J., McMurdie, P.J., Rosen, M.J., Han, A.W., Johnson, A.J., Holmes, S.P., 2016. DADA2: high-resolution sample inference from Illumina amplicon data. Nat. Methods 13, 581–583. https://doi.org/10.1038/nmeth.3869.

Canesi, L., Pruzzo, C., 2016. Specificity of innate immunity in bivalves: a lesson from bacteria. In: Lessons in Immunity: from Single-Cell Organisms to Mammals. Elsevier Inc., pp. 79–91. https://doi.org/10.1016/B978-0-12-803252-7.00006-0

Cao, Y., Dong, Q., Wang, D., Zhang, P., Liu, Y., Niu, C., 2022. microbiomeMarker: an R/Bioconductor package for microbiome marker identification and visualization. Bioinformatics 38, 4027–4029. https://doi.org/10.1093/bioinformatics/btac438.

Caza, F., Joly de Boissel, P.G., Villemur, R., Betoulle, S., St-Pierre, Y., 2019. Liquid biopsies for omics-based analysis in sentinel mussels. PLoS One 14, e0223525. https://doi.org/10.1371/journal.pone.0223525.

Chabot, R., Rossignol, A., 2003. Algues et faune du littoral du Saint-Laurent maritime: Guide d'identification. In: Rimouski et Pêches et Océans Canada (Institut Maurice-Lamontagne). Mont-Joli, p. 113.

Challis, R., 2017. Rjchallis/assembly-stats 17.02. Available online at: https://zenodo.org/records/322347.

Châtel, A., Lièvre, C., Barrick, A., Bruneau, M., Mouneyrac, C., 2018. Transcriptomic approach: a promising tool for rapid screening nanomaterial-mediated toxicity in the marine bivalve Mytilus edulis—application to copper oxide nanoparticles. Comp. biochem. physiol. C., Mol. 205, 26–33. https://doi.org/10.1016/j.cbpc.2018.01.003.

Cheetham, S.W., Kindlova, M., Ewing, A.D., 2022. Methylartist: tools for visualizing modified bases from nanopore sequence data. Bioinformatics 38, 3109–3112. https://doi.org/10.1093/bioinformatics/btac292.

Coates, C.J., Costa-Paiva, E.M., 2020. Multifunctional roles of hemocyanins. In: Hoeger, U., Harris, J. (Eds.), Vertebrate and Invertebrate Respiratory Proteins, Lipoproteins and Other Body Fluid Proteins, Subcellular Biochemistry. Springer, Cham. https://doi.org/10.1007/978-3-030-41769-7_9.

Comité ZIP RNE, 2005. Caractérisation de la rivière du Moulin-à-Baude. Municipalité Régionale de Compté (MRC) de la Haute-Côte-Nord. Rapport technique. https://catalogue.ogsl.ca/dataset/ca-cioos_4e9acd74-94b2-4232-9c0e-adba202281eb?local=fr Accessed 29 June 2024.

Coutinho, F.H., Silveira, C.B., Gregoracci, G.B., Thompson, C.C., Edwards, R.A., Brussaard, C.P., et al., 2017. Marine viruses discovered via metagenomics shed light on viral strategies throughout the oceans. Nat. Commun. 8, 15955 https://doi.org/10.1038/ncomms15955.

Dance, A., 2021. The incredible diversity of viruses. Nature 595, 22–25. https://doi.org/10.1038/d41586-021-01749-7.

Dawood, A., Algharib, S.A., Zhao, G., Zhu, T., Qi, M., Delai, K., et al., 2022. Mycoplasmas as host pantropic and specific pathogens: clinical implications, gene transfer, virulence factors, and future perspectives. Front. Cell. Infect. Microbiol. 12, 855731 https://doi.org/10.3389/fcimb.2022.855731.

de Boissel, P.G.J., Fournier, M., Rodriguez-Lecompte, J.C., McKenna, P., Kibenge, F., Siah, A., 2017. Functional and molecular responses of the blue mussel Mytilus edulis' hemocytes exposed to cadmium-An in vitro model and transcriptomic approach. Fish Shellfish Immunol. 67, 575–585. https://doi.org/10.1016/j.fsi.2017.06.001.

Demers-Lemay, M., 2019. 28 municipalités de l'Est-du-Québec toujours sans traitement d'égout. Available online at: https://ici.radio-canada.ca/nouvelle/1384582/traitement-eaux-usees-fleuve-saint-laurent-pollution-egouts. (Accessed 31 January 2024).

Dodenhof, T., Dietz, F., Franken, S., Grunwald, I., Kelm, S., 2014. Splice variants of perlucin from Haliotis laevigata modulate the crystallisation of CaCO3. PLoS One 9, e97126. https://doi.org/10.1371/journal.pone.0097126.

Dolinoy, D.C., Huang, D., Jirtle, R.L., 2007. Maternal nutrient supplementation counteracts bisphenol A-induced DNA hypomethylation in early development. Proc. Natl. Acad. Sci. USA 104, 13056–13061. https://doi.org/10.1073/pnas.0703739104.

Eddy, S.R., 2011. Accelerated profile HMM searches. PLoS Comput. Biol. 7, e1002195 https://doi.org/10.1371/journal.pcbi.1002195.

Edward, J.P., Jayanthi, M., Malleshappa, H., Jeyasanta, K.I., Laju, R.L., Patterson, J., Raj, K.D., Mathews, G., Marimuthu, A.S., Grimsditch, G., 2021. COVID-19 lockdown improved the health of coastal environment and enhanced the population of reef-fish. Mar. Pollut. Bull. 165, 112124 https://doi.org/10.1016/j.marpolbul.2021.112124.

Eren, A.M., Kiefl, E., Shaiber, A., Veseli, I., Miller, S.E., Schechter, M.S., et al., 2021. Community-led, integrated, reproducible multi-omics with anvi'o. Nat. Microbiol. 6, 3–6. https://doi.org/10.1038/s41564-020-00834-3.

Feng, J., Huang, Y., Huang, M., Luo, J., Que, L., Yang, S., et al., 2023. A novel perlucin-like protein (PLP) protects Litopenaeus vannamei against Vibrio harveyi infection. Fish Shellfish Immunol. 139, 108932 https://doi.org/10.1016/j.fsi.2023.108932.

Ferchiou, S., Caza, F., Joly de Boissel, P.G., Villemur, R., St-Pierre, Y., 2022a. Applying the concept of liquid biopsy to monitor the microbial biodiversity of marine coastal ecosystems. ISME Commun 2, 61. https://doi.org/10.1038/s43705-022-00145-0.

Ferchiou, S., Caza, F., Villemur, R., Betoulle, S., St-Pierre, Y., 2022b. Species- and site-specific circulating bacterial DNA in Subantarctic sentinel mussels Aulacomya atra and Mytilus platensis. Sci. Rep. 12, 9547. https://doi.org/10.1038/s41598-022-13774-1.

Ferchiou, S., Caza, F., St-Pierre, Y., 2023. Liquid biopsy in sentinel mussels. protocols.io. https://doi.org/10.17504/protocols.io.81wgb6z9olpk/v2.

Fernández-Álvarez, C., Santos, Y., 2018. Identification and typing of fish pathogenic species of the genus Tenacibaculum. Appl. Microbiol. Biotechnol. 102, 9973–9989. https://doi.org/10.1007/s00253-018-9370-1.

Follis, A.V., Llambi, F., Ou, L., Baran, K., Green, D.R., Kriwacki, R.W., 2014. The DNA-binding domain mediates both nuclear and cytosolic functions of p53. Nat. Struct. Mol. Biol. 21, 535–543. https://doi.org/10.1038/nsmb.2829.

Galperin, M.Y., Makarova, K.S., Wolf, Y.I., Koonin, E.V., 2015. Expanded microbial genome coverage and improved protein family annotation in the COG database. Nucleic Acids Res. 43, D261–D269. https://doi.org/10.1093/nar/gku1223.

Gao, C.H., Yu, G., Cai, P., 2021. ggVennDiagram: an intuitive, easy-to-use, and highly customizable R package to generate Venn diagram. Front. Genet. 12, 706907 https://doi.org/10.3389/fgene.2021.706907.

Gissi, E., Manea, E., Mazaris, A.D., Fraschetti, S., Almpanidou, V., Bevilacqua, S., et al., 2021. A review of the combined effects of climate change and other local human stressors on the marine environment. Sci. Total Environ. 755, 142564 https://doi.org/10.1016/j.scitotenv.2020.142564.

Haas, B.J., 2023. Transdecoder v5.5.0. https://github.com/TransDecoder/TransDecoder.

Heijmans, B.T., Tobi, E.W., Stein, A.D., Putter, H., Blauw, G.J., Susser, E.S., et al., 2008. Persistent epigenetic differences associated with prenatal exposure to famine in humans. Proc. Natl. Acad. Sci. USA 105, 17046–17049. https://doi.org/10.1073/pnas.0806560l0.

Heitzer, E., Haque, I.S., Roberts, C.E., Speicher, M.R., 2019. Current and future perspectives of liquid biopsies in genomics-driven oncology. Nat. Rev. Genet. 20, 71–88. https://doi.org/10.1038/s41576-018-0071-5.

Herbstman, J.B., Wang, S., Perera, F.P., Lederman, S.A., Vishnevetsky, J., Rundle, A.G., et al., 2013. Predictors and consequences of global DNA methylation in cord blood and at three years. PLoS One 8, e72824. https://doi.org/10.1371/journal.pone.0072824.

Hervouet, E., Peixoto, P., Delage-Mourroux, R., Boyer-Guittaut, M., Cartron, P.F., 2018. Specific or not specific recruitment of DNMTs for DNA methylation, an epigenetic dilemma. Clin. Epigenetics 10, 1–18. https://doi.org/10.1186/s13148-018-0450-y.

Heyn, H., Li, N., Ferreira, H.J., Moran, S., Pisano, D.G., Gomez, A., et al., 2012. Distinct DNA methylomes of newborns and centenarians. Proc. Natl. Acad. Sci. USA 109, 10522–10527. https://doi.org/10.1073/pnas.1120658109.

Hyatt, D., Chen, G.L., LoCascio, P.F., Land, M.L., Larimer, F.W., Hauser, L.J., 2010. Prodigal: prokaryotic gene recognition and translation initiation site identification. BMC Bioinf. 11, 1–11. https://doi.org/10.1186/1471-2105-11-119.

Klindworth, A., Pruesse, E., Schweer, T., Peplies, J., Quast, C., Horn, M., et al., 2013. Evaluation of general 16S ribosomal RNA gene PCR primers for classical and next-generation sequencing-based diversity studies. Nucleic Acids Res. 41, e1 https://doi.org/10.1093/nar/gks808.

Kolde, R., 2019. Pheatmap: pretty heatmaps. https://cran.r-project.org/package=pheatmap.

Ladd-Acosta, C., Fallin, M.D., 2019. DNA methylation signatures as biomarkers of prior environmental exposures. Curr. Epidemiol. Rep. 6, 1–13. https://doi.org/10.1007/s40471-019-0178-z.

Lam, P.K., 2009. Use of biomarkers in environmental monitoring. Ocean Coast Manag. 52, 348–354. https://doi.org/10.1016/j.ocecoaman.2009.04.010.

Langmead, B., Salzberg, S.L., 2012. Fast gapped-read alignment with Bowtie 2. Nat. Methods 9, 357–359. https://doi.org/10.1038/nmeth.1923.

Le Guernic, A., Felix, C., Bigot, A., David, E., Dedourge-Geffard, O., Geffard, A., et al., 2015. Food deprivation and modulation of hemocyte activity in the zebra mussel (Dreissena polymorpha). J. Shellfish Res. 34, 423–431. https://doi.org/10.2983/035.034.0226.

Lemaire, N., Pelletier, E., 2013. Chemical and microbial contamination baseline in the saguenay–st. Lawrence marine park (Eastern Canada): concentrations and fluxes from land-based sources. Arch. Environ. Contam. Toxicol. 65, 421–433. https://doi.org/10.1007/s00244-013-9911-7.

Lemaire, N., Pelletier, E., 2018. Un modèle de risque comme outil de gestion d'une aire marine protégée : l'exemple du parc marin du Saguenay–Saint-Laurent. Nat. Can. 142, 140–156.

Li, B., Dewey, C.N., 2011. RSEM: accurate transcript quantification from RNA-Seq data with or without a reference genome. BMC Bioinf. 12, 1–16. https://doi.org/10.1186/1471-2105-12-323.

Li, D., Liu, C.M., Luo, R., Sadakane, K., Lam, T.W., 2015. MEGAHIT: an ultra-fast single-node solution for large and complex metagenomics assembly via succinct de Bruijn graph. Bioinformatics 31, 1674–1676. https://doi.org/10.1093/bioinformatics/btv033.

Li, H., 2018. Minimap2: pairwise alignment for nucleotide sequences. Bioinformatics 34, 3094–3100. https://doi.org/10.1093/bioinformatics/bty191.

Li, H., Handsaker, B., Wysoker, A., Fennell, T., Ruan, J., Homer, N., et al., 2009. The sequence alignment/map format and SAMtools. Bioinformatics 25, 2078–2079. https://doi.org/10.1093/bioinformatics/btp352.

Lin, J.Y., Ma, K.Y., Bai, Z.Y., Li, J.L., 2013. Molecular cloning and characterization of perlucin from the freshwater pearl mussel, Hyriopsis cumingii. Gene 526, 210–216. https://doi.org/10.1016/j.gene.2013.05.029.

Love, M.I., Huber, W., Anders, S., 2014. Moderated estimation of fold change and dispersion for RNA-seq data with DESeq2. Genome Biol 15, 550. https://doi.org/10.1186/s13059-014-0550-8.

Ludwig, B., Bender, E., Arnold, S., Hüttemann, M., Lee, I., Kadenbach, B., 2001. Cytochrome c oxidase and the regulation of oxidative phosphorylation. Chembiochem 2, 392–403. https://doi.org/10.1002/1439-7633(20010601)2:6<392::AID-CBIC392>3.0.CO;2-N.

Lorenzon, S., Martinis, M., Ferrero, E.A., 2011. Ecological relevance of hemolymph total protein concentration in seven unrelated crustacean species from different habitats measured predictively by a density-salinity refractometer. J. Mar. Sci 2011 7. https://doi.org/10.1155/2011/153654.

Mabrok, M., Algammal, A.M., Sivaramasamy, E., Hetta, H.F., Atwah, B., Alghamdi, S., et al., 2023. Tenacibaculosis caused by Tenacibaculum maritimum: updated knowledge of this marine bacterial fish pathogen. Front. Cell. Infect. Microbiol. 12, 1068000 https://doi.org/10.3389/fcimb.2022.1068000.

Magoč, T., Salzberg, S.L., 2011. FLASH: fast length adjustment of short reads to improve genome assemblies. Bioinformatics 27, 2957–2963. https://doi.org/10.1093/bioinformatics/btr507.

Martin, E.M., Fry, R.C., 2018. Environmental influences on the epigenome: exposure-associated DNA methylation in human populations. Annu. Rev. Public Health. 39, 309–333. https://doi.org/10.1146/annurev-publhealth-040617-014629.

McMurdie, P.J., Holmes, S., 2013. phyloseq: an R package for reproducible interactive analysis and graphics of microbiome census data. PLoS One 8, e61217. https://doi.org/10.1371/journal.pone.0061217.

Meaney, M.J., Szyf, M., 2005. Maternal care as a model for experience-dependent chromatin plasticity? Trends Neurosci 28, 456–463. https://doi.org/10.1016/j.tins.2005.07.006.

Moufarrej, M.N., Vorperian, S.K., Wong, R.J., Campos, A.A., Quaintance, C.C., Sit, R.V., et al., 2022. Early prediction of preeclampsia in pregnancy with cell-free RNA. Nature 602, 689–694. https://doi.org/10.1038/s41586-022-04410-z.

Muruganandam, M., Rajamanickam, S., Sivarethinamohan, S., Reddy, M.K., Velusamy, P., Gomathi, R., et al., 2023. Impact of climate change and anthropogenic activities on aquatic ecosystem–A review. Environ. Res. 238, 117233 https://doi.org/10.1016/j.envres.2023.117233.

Negri, P., Maggi, M., Correa-Aragunde, N., Brasesco, C., Eguaras, M., Lamattina, L., 2013. Nitric oxide participates at the first steps of Apis mellifera cellular immune activation in response to non-self recognition. Apidologie 44, 575–585. https://doi.org/10.1007/s13592-013-0207-8.

Nowlan, J.P., Lumsden, J.S., Russell, S., 2020. Advancements in characterizing Tenacibaculum infections in Canada. Pathogens 9, 1029. https://doi.org/10.3390/pathogens9121029.

O'Hara, C.C., Frazier, M., Halpern, B.S., 2021. At-risk marine biodiversity faces extensive, expanding, and intensifying human impacts. Science 372, 84–87. https://doi.org/10.1126/science.abe6731.

Osaki, T., Kawabata, S., 2004. Structure and function of coagulogen, a clottable protein in horseshoe crabs. CMLS Cell. Mol. Life Sci. 61, 1257–1265. https://doi.org/10.1007/s00018-004-3396-5.

Prakash, S., 2021. Impact of climate change on aquatic ecosystem and its biodiversity: an overview. IJBI 3. https://doi.org/10.46505/IJBI.2021.3210.

Putnam, H.M., Davidson, J.M., Gates, R.D., 2016. Ocean acidification influences host DNA methylation and phenotypic plasticity in environmentally susceptible corals. Evol. Appl. 9, 1165–1178. https://doi.org/10.1111/eva.12408.

R Core Team, 2023. R: A Language and Environment for Statistical Computing. R Foundation for Statistical Computing, Vienna, Austria.

Raj, V.S., Pandey, R.P., Singh, R.K., Mohaptara, T.M., 2022. Dicrocoeliasias. In: Parija, S. C., Chaudhury, A. (Eds.), Textbook of Parasitic Zoonoses. Microbial Zoonoses. Springer, Singapore.

Rauch, U., Feng, K., Zhou, X.H., 2001. Neurocan: a brain chondroitin sulfate proteoglycan. Cell. Mol. Life Sci. 58, 1842–1856. https://doi.org/10.1007/PL00000822.

Rey-Campos, M., Moreira, R., Valenzuela-Munoz, V., Gallardo-Escarate, C., Novoa, B., Figueras, A., 2019a. High individual variability in the transcriptomic response of Mediterranean mussels to Vibrio reveals the involvement of myticins in tissue injury. Sci. Rep. 9, 3569. https://doi.org/10.1038/s41598-019-39870-3.

Rey-Campos, M., Moreira, R., Gerdol, M., Pallavicini, A., Novoa, B., Figueras, A., 2019b. Immune tolerance in Mytilus galloprovincialis hemocytes after repeated contact with Vibrio splendidus. Front. Immunol. 10, 471443 https://doi.org/10.3389/fimmu.2019.01894.

Robinson, M.D., McCarthy, D.J., Smyth, G.K., 2010. edgeR: a Bioconductor package for differential expression analysis of digital gene expression data. Bioinformatics 26, 139–140. https://doi.org/10.1093/bioinformatics/btp616.

Rohrer, J.S., 2021. High-performance anion-exchange chromatography with pulsed amperometric detection for carbohydrate and glycoconjugate analyses. In: Carbohydrate Analysis by Modern Liquid Phase Separation Techniques. Elsevier, pp. 157–207. https://doi.org/10.1016/B978-0-12-821447-3.00002-0.

Salazar, M.L., Jiménez, J.M., Villar, J., Rivera, M., Báez, M., Manubens, A., Becker, M.I., 2019. N-Glycosylation of mollusk hemocyanins contributes to their structural stability and immunomodulatory properties in mammals. J. Biol. Chem. 294, 19546–19564. https://doi.org/10.1074/jbc.RA119.009525.

Sarkies, P., 2023. Evolution beyond DNA: epigenetic drivers for evolutionary change? BMC Biol. 21, 272. https://doi.org/10.1186/s12915-023-01770-4.

Searle, B., Müller, M., Carell, T., Kellett, A., 2023. Third-generation sequencing of epigenetic DNA. Angew. Chem. 135, e202215704 https://doi.org/10.1002/ange.202215704.

Sharavanan, V.J., Sivaramakrishnan, M., Sivarajasekar, N., Senthilrani, N., Kothandan, R., Dhakal, N., et al., 2020. Pollutants inducing epigenetic changes and diseases. Environ. Chem. Lett. 18, 325–343. https://doi.org/10.1007/s10311-019-00944-3.

Sharma, N., Pasala, M.S., Prakash, A., 2019. Mitochondrial DNA: epigenetics and environment. Environ. Mol. Mutagen. 60, 668–682. https://doi.org/10.1002/em.22319.

Shokolenko, I., Alexeyev, M., 2022. Mitochondrial DNA: consensuses and controversies. DNA 2, 131–148. https://doi.org/10.3390/dna2020010.

Siravegna, G., Marsoni, S., Siena, S., Bardelli, A., 2017. Integrating liquid biopsies into the management of cancer. Nat. Rev. Clin. Oncol. 14, 531–548. https://doi.org/10.1038/nrclinonc.2017.14.

Sirokmány, G., Geiszt, M., 2019. The relationship of NADPH oxidases and heme peroxidases: fallin'in and out. Front. Immunol. 10, 394. https://doi.org/10.3389/fimmu.2019.00394.

Solé, C., Tramonti, D., Schramm, M., Goicoechea, I., Armesto, M., Hernandez, L.I., et al., 2019. The circulating transcriptome as a source of biomarkers for melanoma. Cancers 11, 70. https://doi.org/10.3390/cancers11010070.

Ssekagiri, A., Sloan, W., Ijaz, U.Z., 2017. microbiomeSeq: an R package for analysis of microbial communities in an environmental context. Available online at: https://github.com/umerijaz/microbiomeSeq.

Su, S., Law, C.W., Ah-Cann, C., Asselin-Labat, M.L., Blewitt, M.E., Ritchie, M.E., 2017. Glimma: interactive graphics for gene expression analysis. Bioinformatics 33, 2050–2052. https://doi.org/10.1093/bioinformatics/btx094.

Sun, X., Tu, K., Li, L., Wu, B., Wu, L., Liu, Z., et al., 2021. Integrated transcriptome and metabolome analysis reveals molecular responses of the clams to acute hypoxia. Mar. Environ. Res. 168, 105317 https://doi.org/10.1016/j.marenvres.2021.105317.

Viarengo, A., Lowe, D., Bolognesi, C., Fabbri, E., Koehler, A., 2007. The use of biomarkers in biomonitoring: a 2-tier approach assessing the level of pollutant-induced stress syndrome in sentinel organisms. Comp. Biochem. Physiol. C Toxicol. Pharmacol. 146, 281–300. https://doi.org/10.1016/j.cbpc.2007.04.011.

Vincent, F., Vardi, A., 2023. Viral infection in the ocean—a journey across scales. PLoS Biol. 21, e3001966 https://doi.org/10.1371/journal.pbio.3001966.

Wang, N., Lee, Y.H., Lee, J., 2008. Recombinant perlucin nucleates the growth of calcium carbonate crystals: molecular cloning and characterization of perlucin from disk abalone, Haliotis discus discus. Comp. Biochem. Physiol. B 149, 354–361. https://doi.org/10.1016/j.cbpb.2007.10.007.

Wang, Q., Garrity, G.M., Tiedje, J.M., Cole, J.R., 2007. Naive Bayesian classifier for rapid assignment of rRNA sequences into the new bacterial taxonomy. Appl. Environ. Microbiol. 73, 5261–5267. https://doi.org/10.1128/AEM.00062-07.

Weng, K.C., Friedlander, A.M., Gajdzik, L., Goodell, W., Sparks, R.T., 2023. Decreased tourism during the COVID-19 pandemic positively affects reef fish in a high use

marine protected area. PLoS One 18 (4), e0283683. https://doi.org/10.1371/journal.pone.0283683.
Wickham, H., 2016. ggplot2: Elegant Graphics for Data Analysis. Springer, New York, USA.
Yamada, I., Shiota, M., Shinmachi, D., Ono, T., Tsuchiya, S., Hosoda, M., et al., 2020. The GlyCosmos Portal: a unified and comprehensive web resource for the glycosciences. Nat. Methods 17, 649–650. https://doi.org/10.1038/s41592-020-0879-8.
Yu, D., Du, Z., Pian, L., Li, T., Wen, X., Li, W., et al., 2017. Mitochondrial DNA hypomethylation is a biomarker associated with induced senescence in human fetal heart mesenchymal stem cells. Stem Cells Int. 2017 14–16. https://doi.org/10.1155/2017/1764549.
Yuen, Z.W.S., Srivastava, A., Daniel, R., McNevin, D., Jack, C., Eyras, E., 2021. Systematic benchmarking of tools for CpG methylation detection from nanopore sequencing. Nat. Commun. 12, 3438. https://doi.org/10.1038/s41467-021-23778-6.
Zhang, Q., Cao, X., 2019. Epigenetic regulation of the innate immune response to infection. Nat. Rev. Immunol. 19, 417–432. https://doi.org/10.1038/s41577-019-0151-6.

Supplementary Figures and Table

Assessing Marine Ecosystem Health Using Multi-Omic Analysis of Blue Mussel Liquid Biopsies: A Case Study within a National Marine Park.

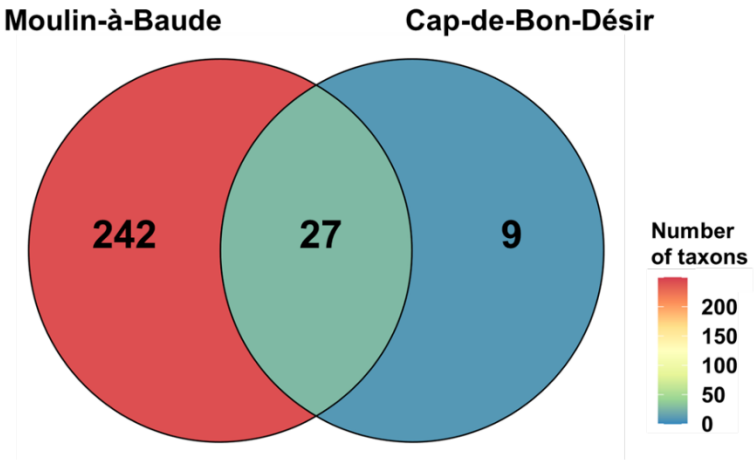

Supplementary Figure 1. Venn diagram showing the number of unique and shared contig identifications from BLAST between both sites. The overlapping region contains the number of contigs that share similar hits. Red colors indicate higher abundances and blue colors indicate lower abundances.

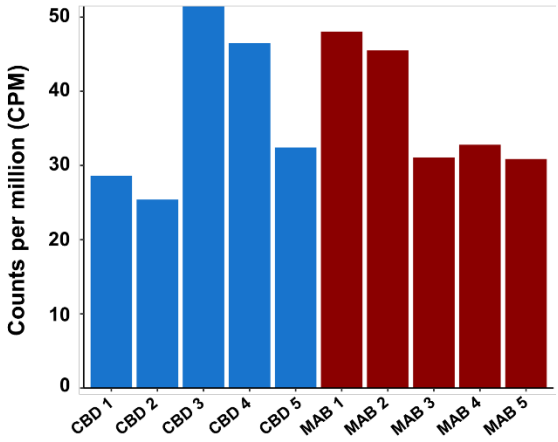

Supplementary Figure 2. Number of reads in Moulin-à-Baude and Cap-de-Bon-Désir sampling sites (FDR ≤ 0.05 and |FC| ≥ 2; red, up-regulated; blue, down-regulated). Noise threshold was greater than 100 reads.

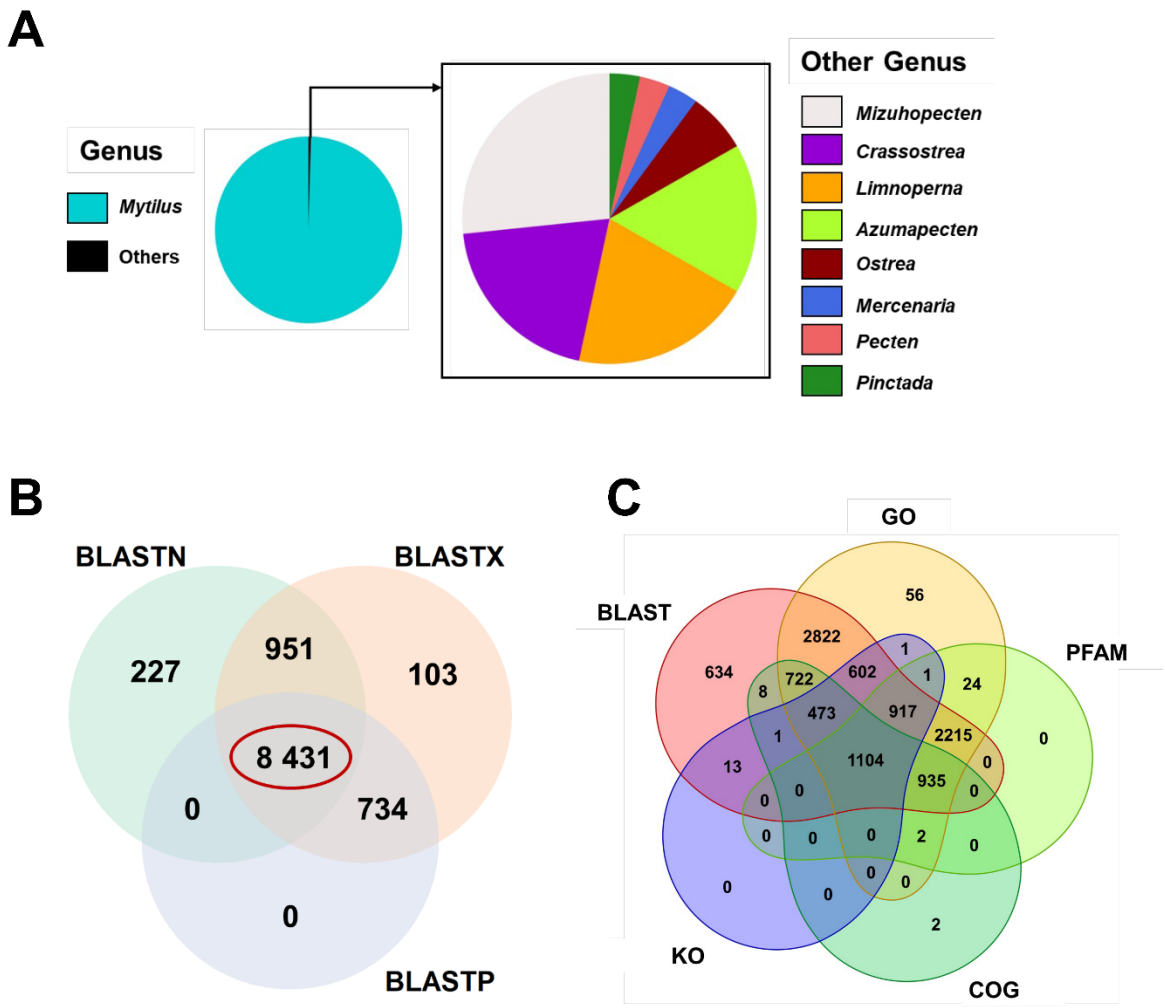

Supplementary Figure 3. Identification and annotation results of transcripts. (**A**) BLAST results against the NCBI nr and nt databases. Results showed are BLAST hits matched to Bivalvia class. (**B**) Venn diagram showing the overlap of BLAST results. (**C**) Venn diagram showing the overlap of BLAST, GO, Pfam, COG and Kegg annotations of *Mytilus spp.* transcripts.

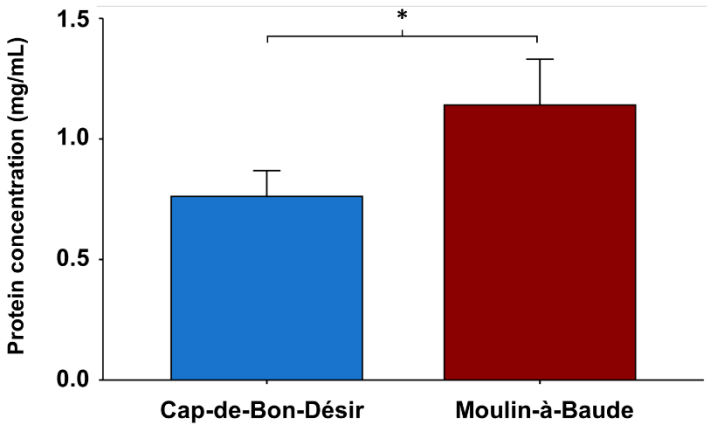

Supplementary Figure 4. Hemolymphatic protein concentrations. This bar plot illustrates the comparison of protein concentrations (mg/mL ± SD) between Cap-de-Bon-Désir (blue) and Moulin-à-Baude (red). Statistical significance was determined by Student's t-test (p = 0.019).

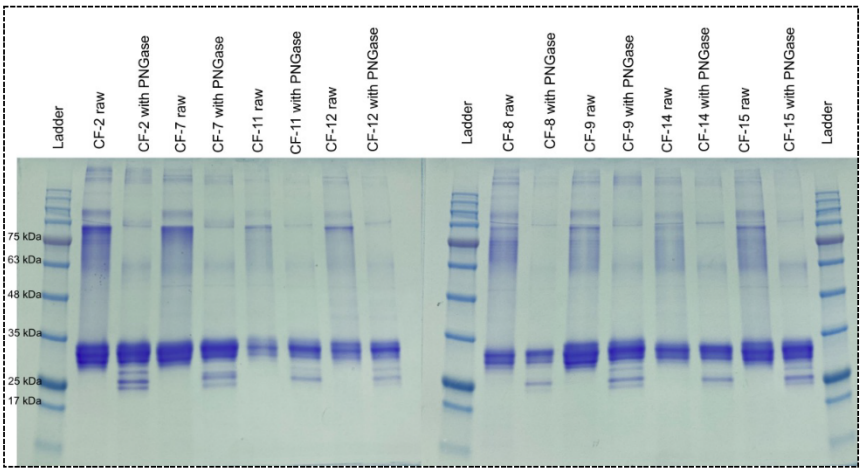

Supplementary Figure 5. Hemolymph protein samples before and after PNGase-F treatment in SDS-PAGE. Hemolymph samples were treated with PNGase F enzyme as per the Gibco™ PNGase F Glycan Cleavage Kit guidelines (Thermo Fisher Scientific, cat #A39245). The hemolymph samples were diluted with Laemmli Sample Buffer (2x Laemmli Sample Buffer, Bio-Rad, cat#1610737) and loaded onto 12% precast polyacrylamide gel (12% Mini-PROTEAN® TGX™ Precast Protein Gels, 10-well, 30 µl, Bio-Rad, cat #4561043). The gels were stained with Coomassie Brilliant Blue R-250 protein stain solution.

Supplementary Table 2. Comprehensive Taxonomic Identification Results for Nonself DNA Bins from Both Sites.

Bin_ID	Sites	Matching taxonomy (BLAST)	Number of sequences	Total length (kbp)
Bin #1	Moulin-à-Baude	*Mycoplasma spp.*	207	297
	Cap-de-Bon-Désir	*Viral sequences*	4	7
Bin #2	Moulin-à-Baude	*Tremotoda*	159	246
	Cap-de-Bon-Désir	*Phaeophyceae*	74	86
Bin #3	Moulin-à-Baude	*Phaeophyceae*	121	288
	Cap-de-Bon-Désir	*Cyanobacteria*	4	4
Bin #4	Moulin-à-Baude	Bacteriophage	38	76
	Cap-de-Bon-Désir	NA	NA	NA

Chapitre 6

Discussion

L'objectif de mon projet était d'appliquer le concept de la biopsie liquide sur des espèces marines afin d'évaluer l'état de santé des écosystèmes marins. Globalement, nous avons pu démontrer que : 1) la signature microbienne chez les moules présente des variations interspécifiques et spatiales, influencée par les conditions environnementales et l'exposition à la pollution; 2) le ccfDNA hémolymphatique de la moule a de plus longs fragments d'ADN en moyenne (> 2kbp) comparativement à ceux de l'humain (~150-200bp) et que ces longs fragments sont adaptés au *long-read sequencing* ; 3) l'intégration de méthodes multi-omiques avec la biopsie liquide enrichit notre compréhension de la santé des moules et de leur environnement.

Malgré une connaissance encore limitée sur le ccfDNA hémolymphatique, nos résultats soulignent l'importance de poursuivre le développement et l'optimisation de la biopsie liquide pour les organismes aquatiques. Initialement développée en médecine, cette méthode a été adaptée aux spécificités de divers environnements marins. Par exemple, la collecte et l'analyse du ccfDNA et du mcfDNA à partir de fluides corporels tels que l'hémolymphe, le sang et le mucus ont permis d'étendre l'application de la biopsie liquide à des espèces marines comme les moules, ainsi qu'à certaines espèces de poissons comme les truites et le flétan (**Annexe I et II**). Ces adaptations ont nécessité une phase de développement méthodologique où les protocoles existants ont été modifiés pour prendre en compte les particularités biologiques et écologiques des organismes aquatiques. Cela a inclus la mise au point de méthodes de prélèvement minimalement invasives, adaptées aux différents organismes, ainsi que l'optimisation des techniques d'extraction et de séquençage pour traiter les échantillons issus de milieux marins. Grâce à ces efforts, nous avons pu détecter des signatures moléculaires distinctives, qui constituent des outils potentiels pour une évaluation plus détaillée et précise de la santé des écosystèmes marins. Ces biomarqueurs moléculaires, identifiés dans des environnements variés, peuvent servir à prédire les impacts environnementaux et anthropiques sur les habitats marins et côtiers. En outre, l'intégration de ces méthodes dans les stratégies de surveillance permettrait une approche non invasive et continue, essentielle pour le suivi à long terme des populations marines et la détection précoce des perturbations écologiques.

Plus spécifiquement, chez la moule, nos observations montrent que : 1) le ccfDNA est principalement composé d'ADN microbien et permet de détecter la présence d'agents microbiens et parasitaires pathogènes; 2) la biopsie liquide offre une vue d'ensemble de la biodiversité du milieu aquatique, complétant ainsi les données obtenues par l'ADN environnemental et fournissant une image plus complète de la dynamique écologique; 3) les perturbations du métabolisme énergétique et mitochondrial observées chez les moules semblent être indicatives de stress environnementaux et anthropiques qui affectent leur habitat. Ces indicateurs moléculaires pourraient donc servir à prédire et à comprendre les impacts des modifications environnementales sur les organismes marins et leur écosystème, offrant des perspectives cruciales pour la gestion et la conservation des ressources marines.

Influence de l'ADN microbien circulant par des variables biotiques et abiotiques

Dans le cadre de notre étude, nous avons analysé le mcfDNA provenant du sang ou de l'hémolymphe d'organismes marins. Nos observations indiquent que le mcfDNA est influencé par plusieurs facteurs, tels que l'âge, l'espèce des organismes et la température environnementale. Nos résultats ont révélé des signatures microbiennes distinctes associées à différentes espèces marines. En outre, nous avons identifié des gènes de pathogénicité chez certaines bactéries présentes dans le sang et le mucus de truites saumonées des îles Kerguelen, un écosystème particulièrement sensible aux changements climatiques (**Annexe I**). De plus, nous avons constaté que le mcfDNA chez la truite arc-en-ciel peut être modulé par l'exposition chronique à des contaminants chimiques tels que le tébuconazole, un fongicide couramment utilisé en agriculture, sur une période de plusieurs semaines (**Annexe III**). Ces résultats soulignent l'importance du microbiome circulant dans la physiologie de l'hôte et son impact potentiel sur la santé environnementale. La haute sensibilité et spécificité des méthodes d'analyse utilisées permettent d'identifier les pathogènes potentiels, ainsi que les changements au sein du microbiome, offrant une meilleure compréhension des impacts environnementaux et anthropiques sur les organismes marins. De plus, ces analyses enrichissent les stratégies de surveillance et de gestion de la santé marine, permettant ainsi une approche plus ciblée et efficace pour protéger ces écosystèmes vulnérables. [184].

Utilisation du ccfDNA chez la moule pour étudier la biodiversité des milieux marins

Parallèlement, nous avons exploré le potentiel du ccfDNA hémolymphatique chez les moules bleues. Nous avons constaté que les fragments de ccfDNA chez la moule sont plus longs que ceux provenant d'organismes avec un système circulatoire fermé, ce qui facilite l'emploi de technologies avancées pour le séquençage de longs fragments, telle que la technologie développée par ONT (**Annexe IV**). Cette adaptation technique permet de réaliser des analyses de biodiversité directement sur le terrain, ce qui réduit le besoin de transport d'échantillons tout en améliorant la précision et la sensibilité des analyses d'ADN séquencé. Ces résultats illustrent comment l'analyse du ccfDNA hémolymphatique peut compléter les approches existantes telles que l'analyse de l'ADNe, en fournissant des informations détaillées et précises sur les espèces microbiennes, les pathogènes présents dans l'environnement marin et leurs interactions. Le ccfDNA hémolymphatique diffère de l'ADNe étant qu'elle permet une évaluation directe des impacts des stress environnementaux sur la santé globale des communautés marines, en détectant des modifications génétiques spécifiques chez les organismes, comme les mutations somatiques ou les variations épigénétiques [163, 236]. De plus, l'utilisation de la biopsie liquide offre la possibilité de recueillir des échantillons d'ADN et d'ARN de haute qualité en quantité suffisante à partir de petits volumes de fluide corporel et est particulièrement adaptée pour des analyses multi-omiques [202, 203, 237]. Les risques de contamination et les défis liés à la conservation, au transport et à l'entreposage des échantillons sur le terrain peuvent être efficacement minimisés grâce à l'utilisation de cartes FTA, qui préservent l'intégrité des échantillons [235, 238]. Cependant, l'utilisation de la biopsie liquide en écologie marine présente certains défis, notamment la sélection des espèces sentinelles adaptées et la limitation de cette méthode qui ne permet pas d'estimer la taille des populations ni d'analyser l'ADN ancien conservé dans les sédiments [33, 34].

Métabolisme des moules affecté par les stress environnementaux et anthropiques

En complément à l'analyse de l'ADN du non-soi, notre étude s'est également concentrée sur l'ADN du soi. Les bivalves, comme les moules, sont vulnérables à divers facteurs de stress qui compromettent leur physiologie, survie et capacité de reproduction. Ces stress

incluent les variations de température, la pollution chimique, l'hypoxie et l'acidification des océans [21, 122, 239]. Les polluants chimiques anthropiques, tels que les métaux lourds, les hydrocarbures et les perturbateurs endocriniens, perturbent les voies métaboliques normales, provoquant la production de radicaux libres et d'autres composés réactifs qui entraînent des dommages oxydatifs et des dysfonctionnements cellulaires [122]. De plus, l'augmentation des températures des eaux et l'eutrophisation peuvent réduire la concentration en oxygène dissous, limitant ainsi la capacité des moules à générer de l'énergie par respiration aérobie, et les forçant à adopter des mécanismes de production d'énergie alternatifs moins efficaces [239].

Notre approche multi-omique, comprenant des analyses métagénomiques, transcriptomes et glycomiques, a révélé une corrélation significative entre l'exposition des moules à des eaux usées agricoles et domestiques et une réduction de leur métabolisme. Les moules exposées à ces eaux usées montrent une présence élevée d'ADN de parasites et de microbes potentiellement pathogènes pour les métazoaires, accompagnée d'une baisse marquée de l'expression des gènes impliqués dans le métabolisme des carbohydrates, des lipides et des acides aminés. De plus, l'analyse du glycome a révélé une expression élevée des gènes associés à la perlucine, ainsi qu'une augmentation des niveaux de glucosamine, un monosaccharide. Ces composés, la perlucine et la glucosamine, jouent un rôle crucial dans la réparation de la coquille des bivalves et dans certains mécanismes de défense, soulignant leur importance dans la réponse adaptative des moules à leur environnement [240-242].

L'étude du glycome s'est avérée être un biomarqueur précieux pour évaluer la santé des moules et, par extension, celle de leur écosystème. Les glycoprotéines, impliquées dans des fonctions biochimiques vitales telles que la respiration et la réponse cellulaire, offrent des indices indispensables sur la condition physiologique des moules en réponse aux stress environnementaux [243, 244].

Rôle de la méthylation comme biomarqueur précoce

La méthylation de certains gènes est reconnue comme un biomarqueur précoce pour diverses pathologies [245, 246]. Grâce à l'utilisation de la technologie de séquençage

ONT, nous avons analysé la méthylation de l'ADN chez la moule bleue et la truite arc-en-ciel, minimisant les biais associés à l'amplification par PCR [247]. Nous avons observé que l'exposition à des contaminants, comme le tébuconazole, altère les profils de méthylation de l'ADN mitochondrial et chromosomal chez la truite (**Annexe IV**). Cette technologie a également facilité l'analyse des niveaux de méthylation sur l'ensemble des cytosines (CpN), un procédé difficilement réalisable avec les méthodes traditionnelles basées sur le bisulfite [247, 248]. L'importance de la méthylation des sites non-CpG, notamment sur l'ADN mitochondrial, est mise en évidence, soulignant leur rôle potentiel dans l'adaptation et la réponse au stress environnemental [249-251]. Une étude a d'ailleurs rapporté que la dérégulation épigénétique temporaire peut jouer un rôle crucial dans l'initiation et la progression des tumeurs dans l'organisme [252].

Cependant, l'analyse de la méthylation en écologie fait face à plusieurs défis, principalement dus à la variabilité des niveaux de méthylation, qui sont influencés par l'origine des cellules, l'âge de l'organisme et les conditions environnementales [253-255]. Une compréhension plus approfondie est nécessaire afin de mieux comprendre les motifs de méthylation conservés et de leur réflectivité entre différents types de cellules au sein d'une même espèce.

Bien que le séquençage ONT offre un haut débit, une haute résolution et la capacité de séquencer des molécules uniques, l'optimisation des protocoles pour le séquençage du ccfDNA est essentielle, surtout en raison de sa faible concentration dans le plasma sanguin [171]. La qualité de la préparation de l'échantillon, l'efficacité du processus de séquençage et les outils bio-informatiques utilisés sont autant de facteurs qui peuvent influencer l'exactitude de l'analyse de la méthylation du ccfDNA [256, 257].

Analyse *SWOT*

L'analyse *SWOT* (***S**trengths*, ***W**eaknesses*, ***O**pportunities*, *and* ***T**hreats*) résume les principaux aspects au développement de biomarqueurs basé sur le concept de la biopsie liquide chez des espèces marines (**Figure 1**). Parmi les forces, l'utilisation de la biopsie

liquide se distingue comme une méthode peu invasive et efficace pour évaluer rapidement la santé des écosystèmes marins et côtiers. Cette technique facilite également le développement de biomarqueurs sensibles, précis et prédictifs, adaptés pour des suivis de surveillance à long terme, notamment dans les régions polaires sensibles aux changements climatiques. La mise en œuvre de plateformes de surveillance renforce le développement de collaborations avec les communautés nordiques et autochtones, favorisant ainsi la recherche participative. De plus, le développement de biomarqueurs pour les milieux marins pourrait étendre leur application à des secteurs tels que la mytiliculture, qui possède une importante valeur socio-économique. Cette extension serait également bénéfique pour des entités gouvernementales, comme Parcs Canada, qui cherchent à améliorer la surveillance des milieux marins particulièrement dans les AMP. Toutefois, le projet comporte certaines limites. La faisabilité de la recherche dépend largement de la présence de bivalves dans les environnements étudiés et le coût du séquençage, ainsi que la complexité des analyses peuvent représenter des défis notables. L'accessibilité aux sites de collecte et le transport du matériel sont également problématiques dans les régions isolées. De plus, il existe un manque de connaissances approfondies sur les approches multi-omiques chez les bivalves. À long terme, la pérennité des financements pour les programmes de surveillance et le développement de nouveaux biomarqueurs demeure incertaine.

Cette analyse *SWOT* permet de souligner que le développement continu de biomarqueurs pour les milieux dépend non seulement d'une maîtrise des technologies existantes, mais également de collaborations interdisciplinaires robustes essentielles pour surmonter les obstacles et exploiter pleinement le potentiel complet des programmes de surveillance à long terme.

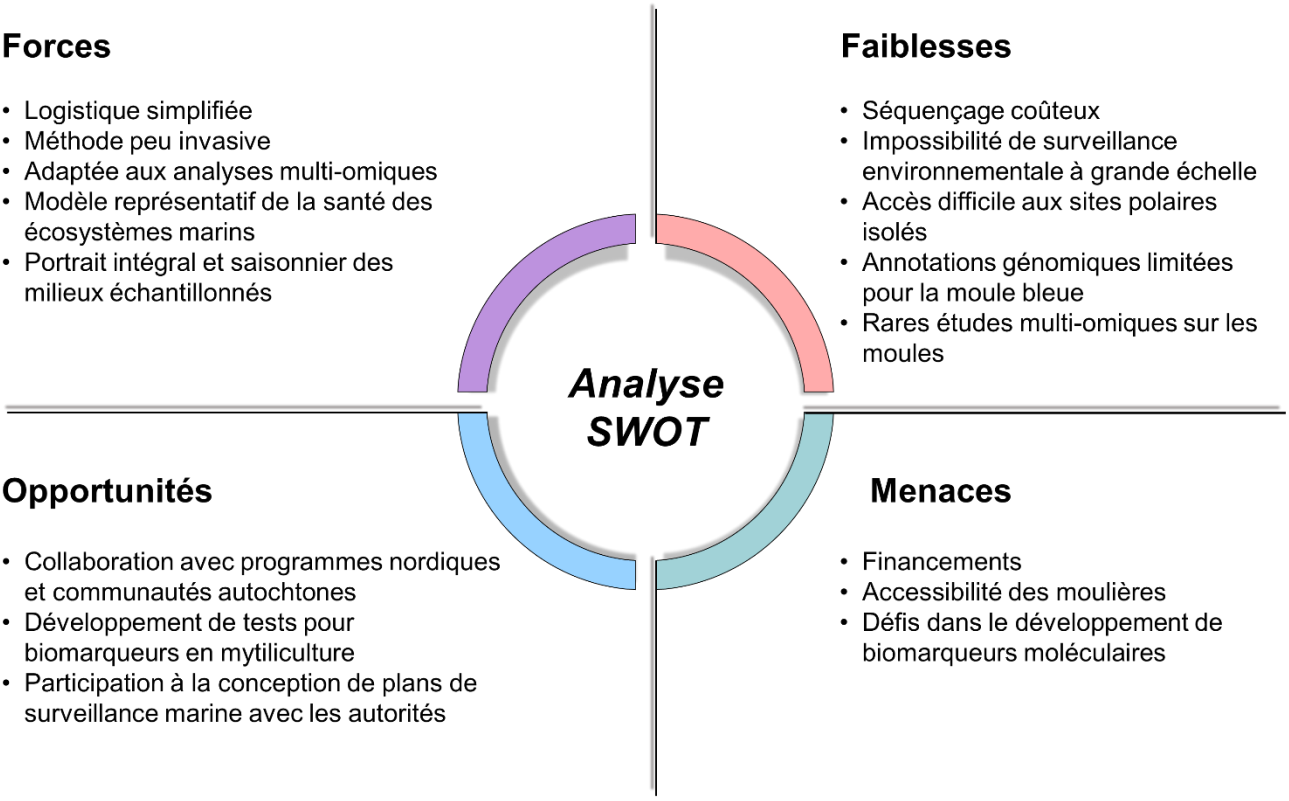

Figure 1. Analyse *SWOT* (*Strengths, Weaknesses, Opportunities, and Threats*) illustrant les principales forces, faiblesses, opportunités et menaces associées au projet de recherche.

Innovation et défis dans la surveillance des milieux marins

L'utilisation de la biopsie liquide en écologie marine (*eLBiom*, *environmental Liquid Biopsy in marine ecology*), mise en évidence par cette étude, se distingue comme une alternative intéressante pour le développement de biomarqueurs en écologie marine et la mise en place de programmes de surveillance à long terme, répondant ainsi aux défis posés par les changements climatiques et l'augmentation des températures océaniques. Ces progrès, bien que significatifs, rencontrent néanmoins des défis dans l'application pratique du eLBiom. Malgré les progrès technologiques qui facilitent l'accès au séquençage du ccfDNA, des obstacles demeurent concernant l'extraction, la préparation et l'analyse robuste et fiable du ccfDNA [167]. De plus, l'analyse de grandes quantités de données génomiques exige des ressources informatiques conséquentes et l'utilisation de

modèles statistiques sophistiqués pour une interprétation adéquate [202, 258]. Le manque de normes et de standardisation dans l'analyse du ccfDNA peut rendre difficile la comparaison et l'interprétation des résultats entre différentes études, ainsi que la validation des méthodes [158].

Pour surmonter ces défis, il est crucial de rester à l'avant-garde des innovations dans le domaine biomédical et d'explorer les applications potentielles de la biopsie liquide en écologie. Cela comprend l'élaboration de modèles prédictifs basés sur de nouveaux biomarqueurs, qui pourraient anticiper les changements dans les populations marines avant qu'ils ne deviennent irréversibles. De telles avancées pourraient transformer notre capacité à préserver la biodiversité marine et à mettre en œuvre des stratégies de gestion adaptative, assurant ainsi une utilisation durable des ressources marines et la résilience des écosystèmes marins face aux changements globaux. Cette intégration entre biotechnologie et gestion écologique favorise également une collaboration interdisciplinaire essentielle, intégrant les données biologiques à grande échelle avec les efforts de conservation et les politiques environnementales.

Chapitre 7

Conclusion générale

En conclusion, notre étude a permis d'établir les fondations de l'application du concept de la biopsie liquide en écologie marine (eLBiom), et ce dans un contexte multi-omique. Nous avons pu notamment explorer en détails le ccfDNA hémolymphatique de la moule bleue à travers différents écosystèmes marins, révélant que l'ADN du non-soi chez la moule est de 12 à 50 fois supérieur à celui de l'humain et qu'il est principalement composé d'ADN microbien. Ces découvertes soulignent aussi la nécessité de mieux comprendre l'influence des conditions environnementales sur le ccfDNA hémolymphatique. De plus, dans un contexte où l'intégration de multiples ensembles de données devient cruciale, la combinaison de la biopsie liquide avec une approche multi-omique chez la moule représente un avancement notable vers le développement de nouveaux biomarqueurs sensibles et prédictifs pour la surveillance des milieux marins et côtiers.

En perspectives, plusieurs axes de développement sont envisagés pour continuer ce projet à court et moyen terme. Premièrement, il est essentiel de réaliser des comparaisons entre les analyses de biodiversité obtenues par biopsie liquide et celles obtenues via l'ADNe au sein d'une même moulière. Cette comparaison nous permettrait d'évaluer l'efficacité et les spécificités de chaque méthode dans la surveillance des écosystèmes marins. Deuxièmement, il est nécessaire d'approfondir notre compréhension de l'impact des conditions physico-chimiques sur la dégradation du ccfDNA. Une meilleure compréhension de ces processus pourrait significativement augmenter la fiabilité des analyses génétiques dans des environnements variés. Enfin, il est clair que l'intégration de données multi-omiques combinées aux biomarqueurs traditionnels et physico-chimiques pourra bénéficier du *machine learning*. L'objectif serait de développer de nouveaux biomarqueurs prédictifs capables de faciliter le suivi de l'état de santé des milieux marins et côtiers. L'adoption de cette approche intégrée améliorerait la gestion de la surveillance des écosystèmes aquatiques face aux défis environnementaux et anthropiques. Ces orientations stratégiques renforceraient la portée et la précision des recherches futures, en optimisant les méthodes d'analyse et en exploitant les avancées technologiques pour une meilleure conservation et gestion des milieux marins et côtiers.

Références

1. Lee, H. and J. Romero. Summary for Policymakers. In: *Climate Change 2023: Synthesis Report. A Report of the Intergovernmental Panel on Climate Change. Contribution of Working Groups I, II and III to the Sixth Assessment Report of the Intergovernmental Panel on Climate Change.* IPCC, Geneva, Switzerland. Last accessed: 2024–05–20. https://doi.org/10.59327/IPCC/AR6-9789291691647
2. Stern, D.I. and R.K. Kaufmann (2014). Anthropogenic and natural causes of climate change. *Clim. change*. **122**, 257-269. https://doi.org/10.1007/s10584-013-1007-x
3. Kogan, F. (2023). Causes of Climate Warming. In: *Remote Sensing Land Surface Changes: The 1981-2020 Intensive Global Warming.* Springer: Cham, 149-179.
4. Von Schuckmann, K., A. Minère, F. Gues, F.J. Cuesta-Valero, G. Kirchengast, S. Adusumilli, F. Straneo, *et al.* (2022). Heat stored in the Earth system 1960–2020: where does the energy go? *Earth Syst. Sci. Data Discuss.* **15**, 1675-1709. https://doi.org/10.5194/essd-15-1675-2023
5. Yerlikaya, B.A., S. Ömezli, and N. Aydoğan. (2020). Climate change forecasting and modeling for the year of 2050. In *Environment, Climate, Plant and Vegetation Growth*. Springer: Cham, Switzerland, 109–122. https://doi.org/10.1007/978-3-030-49732-3_5
6. IPCC (2021). Climate change 2021: The physical science basis. In: *Contribution of Working Group I to the Sixth Assessment Report of the Intergovernmental Panel on Climate Change* (eds: Masson-Delmotte, V., *et al.*). Cambridge University Press, Cambridge, UK. https://doi.org/10.1017/9781009157896
7. IPCC. (2022). Contribution of Working Group II to the Sixth Assessment Report of the Intergovernmental Panel on Climate Change. In: *Climate Change 2022: Impacts, Adaptation and Vulnerability* (eds: Pörtner, H.-O., *et al.*). Cambridge University Press, Cambridge, UK.
8. Lannuzel, D., L. Tedesco, M. van Leeuwe, K. Campbell, H. Flores, B. Delille, *et al.* (2020). The future of Arctic sea-ice biogeochemistry and ice-associated ecosystems. *Nat. Clim. Change.* **10**, 983–992. https://doi.org/10.1038/s41558-020-00940-4
9. Cochrane, S.K.J., J.H. Andersen, T. Berg, H. Blanchet, A. Borja, J. Carstensen, *et al.* (2016). What is marine biodiversity? Towards common concepts and their implications for assessing biodiversity status. *Front. Mar. Sci.* **3**, 248. https://doi.org/10.3389/fmars.2016.00248
10. Tiedje, J.M., M.A. Bruns, A. Casadevall, C.S. Criddle, E. Eloe-Fadrosh, D.M. Karl, *et al.* (2022). Microbes and climate change: a research prospectus for the future. *mBio*. **13**, e00800-22. https://doi.org/10.1128/mbio.00800-22
11. Talukder, B., N. Ganguli, R. Matthew, K.W. Hipel, and J. Orbinski. (2022). Climate change-accelerated ocean biodiversity loss & associated planetary health impacts. *J. Clim. Change Health.* **6**, 100114.
12. Duchenne-Moutien, R.A. and H. Neetoo. (2021). Climate change and emerging food safety issues: a review. *J. Food Prot.* **84**, 1884-1897. https://doi.org/10.4315/JFP-21-141
13. Burge, C.A. and P.K. Hershberger. (2020). Climate change can drive marine diseases. In: *Marine disease ecology*. (eds: D.C. Behringer, B.R. Silliman, and K.D. Lafferty). Oxford University Press, Oxford, UK, 83-94.

14. Shi, Y. and Y. Li. (2024). Impacts of ocean acidification on physiology and ecology of marine invertebrates: a comprehensive review. *Aquat Ecol*. **58**, 207-226. https://doi.org/10.1007/s10452-023-10058-2
15. Findlay, H.S. and C. Turley. (2021). Ocean acidification and climate change. In: *Climate Change*. Elsevier, 251-279.
16. Buelow, C.A., R.M. Connolly, M.P. Turschwell, M.F. Adame, G.N. Ahmadia, D.A. Andradi-Brown, *et al.* (2022). Ambitious global targets for mangrove and seagrass recovery. *Curr. Biol.* **32**, 1641-1649. https://doi.org/10.1016/j.cub.2022.02.013
17. James, R.K., L.M. Keyzer, S.J. van de Velde, P.M. Herman, M.M. van Katwijk, and T.J. Bouma. (2023). Climate change mitigation by coral reefs and seagrass beds at risk: How global change compromises coastal ecosystem services. *Sci. Total Environ.* **857**, 159576. https://doi.org/10.1016/j.scitotenv.2022.159576
18. Messina, S., D. Costantini, and M. Eens. (2023). Impacts of rising temperatures and water acidification on the oxidative status and immune system of aquatic ectothermic vertebrates: A meta-analysis. *Sci. Total Environ.* **868**, 161580. https://doi.org/10.1016/j.scitotenv.2023.161580
19. Greenspan, S.E., G.H. Migliorini, M.L. Lyra, M.R. Pontes, T. Carvalho, L.P. Ribeiro, *et al.* (2020). Warming drives ecological community changes linked to host-associated microbiome dysbiosis. *Nat. Clim. Change.* **10**, 1057-1061. https://doi.org/10.1038/s41558-020-0899-5
20. Froelich, B.A. and D.A. Daines. (2020). In hot water: effects of climate change on Vibrio–human interactions. *Environ. Microbiol.* **22**, 4101–4111. https://doi.org/10.1111/1462-2920.14967
21. Lesser, M.P., M.M. Thompson, and C.W. Walker. (2019). Effects of thermal stress and ocean acidification on the expression of the retrotransposon steamer in the softshell Mya arenaria. *J. Shellfish Res.* **38**, 535-541. https://doi.org/10.2983/035.038.0304
22. Metzger, M.J., A. Villalba, M.J. Carballal, D. Iglesias, J. Sherry, C. Reinisch *et al.* (2016). Widespread transmission of independent cancer lineages within multiple bivalve species. *Nature.* **534**, 705-709. https://doi.org/10.1038/nature18599
23. Paynter, A.N., M.J. Metzger, J.A. Sessa, and M.E. Siddall. (2017). Evidence of horizontal transmission of the cancer-associated Steamer retrotransposon among ecological cohort bivalve species. *Dis. Aquat. Organ.* **124**, 165-168. https://doi.org/10.3354/dao03113
24. Verdier, A.G. (2020). Les Terres et mers australes françaises, sanctuaire de biodiversité au coeur de l'océan Austral. *Rev. Patrim. Mond.* **2020**, 24-29. https://doi.org/10.18356/27887146-2020-96-3
25. Féral, J.P., T. Saucède, E. Poulin, C. Marschal, G. Marty, J.C. Roca, *et al.* (2016). PROTEKER: implementation of a submarine observatory at the Kerguelen islands (Southern Ocean). *Underw. Technol.* **34**, 3-10. https://doi.org/10.3723/ut.34.003
26. Maltais, B. and E. Pelletier. (2018). Le parc marin du Saguenay–Saint-Laurent: création et gestion participative inédite au Canada. *Nat. Can.* **142**, 4-17. https://doi.org/10.7202/1047144ar
27. Brisson, C (2023). *Profil écotouristique de la clientèle des croisières d'observation des mammifères marins dans le parc marin du Saguenay-Saint-Laurent*. Unités départementales des sciences de la gestion. Rimouski, Canada.

28. Ballance, L.T., L.R. Benaka, S.U. Ellgen, S.M. Fitzgerald, A.E. Henry, M.A. Kim, *et al.* (2019). National Seabird Program Five-Year Strategic Plan: 2020-2024. *NOAA Tech. Memo. NMFS-F/SPO-202,* 190 p.
29. Goldberg, E.D. (1986). The mussel watch concept. *Environ. Monit. Assess.* **7**, 91-103. https://doi.org/10.1007/BF00398031
30. Pascher, K., V. Švara, and M. Jungmeier. (2022). Environmental DNA-based methods in biodiversity monitoring of protected areas: Application range, limitations, and needs. *Diversity.* **14**, 463. https://doi.org/10.3390/d14060463
31. Costello, M.J., Z. Basher, L. McLeod, I. Asaad, S. Claus, L. Vandepitte, *et al.* (2017). Methods for the study of marine biodiversity. In: *The GEO handbook on biodiversity observation networks*.(eds: Walters, M. and R.J. Scholes). 129-163. https://doi.org/10.1007/978-3-319-27288-7_6
32. Pawlowski, J., A. Bonin, F. Boyer, T. Cordier, and P. Taberlet. (2021). Environmental DNA for biomonitoring. *Mol. Ecol.* **30**, 2931. https://doi.org/10.1111/mec.16023
33. Ruppert, K.M., R.J. Kline, and M.S. Rahman. (2019). Past, present, and future perspectives of environmental DNA (eDNA) metabarcoding: A systematic review in methods, monitoring, and applications of global eDNA. *Glob. Ecol. Conserv.* **17**, e00547. https://doi.org/10.1016/j.gecco.2019.e00547
34. Sigsgaard, E.E., M.R. Jensen, I.E. Winkelmann, P.R. Møller, M.M. Hansen, and P.F. Thomsen. (2020). Population-level inferences from environmental DNA—Current status and future perspectives. *Evol. Appl.* **13**, 245-262. https://doi.org/10.1111/EVA.12882
35. Bernatchez, L., A.L. Ferchaud, C.S. Berger, C.J. Venney, and A. Xuereb. (2023). Genomics for monitoring and understanding species responses to global climate change. *Nat. Rev. Genet.* **25**, 165–183. https://doi.org/10.1038/s41576-023-00657-y
36. Zaiko, A., X. Pochon, E. Garcia-Vazquez, S. Olenin, and S.A. Wood. (2018). Advantages and limitations of environmental DNA/RNA tools for marine biosecurity: management and surveillance of non-indigenous species. *Front. Mar. Sci.* **5**, 322. https://doi.org/10.3389/fmars.2018.00322
37. Naef, T., A.L. Besnard, L. Lehnen, E.J. Petit, J. Van Schaik, and S.J. Puechmaille. (2023). How to quantify factors degrading DNA in the environment and predict degradation for effective sampling design. *Environ. DNA.* **5**, 403-416. https://doi.org/10.1002/edn3.414
38. Mauvisseau, Q., D. Halfmaerten, S. Neyrinck, A. Burian, and R. Brys. (2021). Effects of preservation strategies on environmental DNA detection and quantification using ddPCR. *Environ. DNA.* **3**, 815-822. https://doi.org/10.1002/edn3.188
39. Sepulveda, A.J., P.R. Hutchins, M. Forstchen, M.N. Mckeefry, and A.M. Swigris. (2020). The elephant in the lab (and field): Contamination in aquatic environmental DNA studies. *Front. Ecol. Evol.* **8**, 609973. https://doi.org/10.3389/fevo.2020.609973
40. Beng, K.C. and R.T. Corlett. (2020). Applications of environmental DNA (eDNA) in ecology and conservation: opportunities, challenges and prospects. *Biodivers. Conserv.* **29**, 2089-2121. https://doi.org/10.1007/s10531-020-01980-0

41. Schwacke, L.H., F.M. Gulland, and S. White. (2012). Sentinel species in oceans and human health. In: *Environmental toxicology: selected entries from the encyclopedia of sustainability Science and technology* (eds: Meyers, R.A.). Springer, New York, USA, 9156–9174. https://doi.org/10.1007/978-1-4419-0851-3_831
42. Berthet, B. (2013). Sentinel species. In: *Ecological biomarkers: indicators of ecotoxicological effects* (eds: Amiard-Triquet, C., J.C. Amiard, and P.S. Rainbow). CRC Press, Boca Raton, USA, 155–186. https://doi.org/10.1201/b13036-8
43. Hazen, E.L., B. Abrahms, S. Brodie, G. Carroll, M.G. Jacox, M.S. Savoca, *et al.* (2019). Marine top predators as climate and ecosystem sentinels. *Front. Ecol. Environ.* **17**, 565-574. https://doi.org/10.1002/fee.2125
44. Elliott, J.E., R. Kesic, S.L. Lee, and K.H. Elliott. (2023). Temporal trends (1968–2019) of legacy persistent organic pollutants (POPs) in seabird eggs from the northeast Pacific: Is it finally twilight for old POPs? *Sci. Total Environ.* **858**, 160084. https://doi.org/10.1016/j.scitotenv.2022.160084
45. Sonne, C., U. Siebert, K. Gonnsen, J.P. Desforges, I. Eulaers, S. Persson, *et al.* (2020). Health effects from contaminant exposure in Baltic Sea birds and marine mammals: A review. *Environ. Int.* **139**, 105725. https://doi.org/10.1016/j.envint.2020.105725
46. Beyer, J., N.W. Green, S. Brooks, I.J. Allan, A. Ruus, T. Gomes, *et al.* (2017). Blue mussels (Mytilus edulis spp.) as sentinel organisms in coastal pollution monitoring: A review. *Mar. Environ. Res.* **130**, 338-365. https://doi.org/10.1016/j.marenvres.2017.07.024
47. Sun, T., X. Tang, Y. Jiang, and Y. Wang. (2017). Seawater acidification induced immune function changes of haemocytes in Mytilus edulis: a comparative study of CO2 and HCl enrichment. *Sci. Rep.* **7**, 41488. https://doi.org/10.1038/srep41488
48. Sokolova, I. and G. Lannig. (2008). Interactive Effects of Metal Pollution and Temperature on Metabolism in Aquatic Ectotherms: Implications of Global Climate Change. *Clim. Res.* **37**, 181–201. https://doi.org/10.3354/cr00764
49. Linnaeus, C. (1758). *Systema Naturae per regna tria naturae, secundum classes, ordines, genera, species; cum characteribus, differentiis, synonymis, locis.* Laurentius Salvius, Stockholm, Sweeden.
50. de Lamarck, J.B.D.M. (1843). *Histoire naturelle des animaux sans vertèbres...: Histoire des mollusques.* Vol. 10, J.B. Baillière, Verdière, Paris.
51. Gould, A.A. (1850). Descriptions of shells from the United States exploring expedition. *Proc. Boston Soc. Nat. History.* **3**, 343–348..
52. Conrad, T.A. (1837). Description of new marine shells from Upper California, collected by Thomas Nuttal Esquire. *J. Acad. Nat. Sci.* **7**, 227-268.
53. Lamy, E. (1936). Révision des Mytilidae vivants du Museum national d'histoire naturelle de Paris. *J. Conchol.* **80**, 66-102.
54. Michalek, K., A. Ventura, and T. Sanders. (2016). Mytilus hybridisation and impact on aquaculture: A minireview. *Mar. Genom.* **27**, 3-7. https://doi.org/10.1016/j.margen.2016.04.008
55. Fraïsse, C., A. Haguenauer, K. Gérard, A.A.T. Weber, N. Bierne, and A. Chenuil. (2021). Fine-grained habitat-associated genetic connectivity in an admixed

population of mussels in the small isolated Kerguelen Islands. *Peer Community J.* **1**. https://doi.org/10.24072/pcjournal.18
56. Heinemann, A. (2011). *The suitability of Mytilus edulis as proxy archive and its response to ocean acidification.* Doctoral thesis, Christian-Albrechts-Universität, Kiel, Germany.
57. Eggermont, M., P. Cornillie, M. Dierick, D. Adriaens, N. Nevejan, P. Bossier, *et al.* (2020). The blue mussel inside: 3D visualization and description of the vascular-related anatomy of Mytilus edulis to unravel hemolymph extraction. *Sci. Rep.* **10**, 6773. https://doi.org/10.1038/s41598-020-62933-9
58. Yurchenko, O.V., O.I. Skiteva, E.E. Voronezhskaya, and V.A. Dyachuk. (2018). Nervous system development in the Pacific oyster, Crassostrea gigas (Mollusca: Bivalvia). *Front. Zool.* **15**, 10. https://doi.org/10.1186/s12983-018-0259-8
59. Wiegemann, M. (2005). Adhesion in blue mussels (Mytilus edulis) and barnacles (genus Balanus): Mechanisms and technical applications. *Aquat. Sci.* **67**, 166-176. https://doi.org/10.1007/s00027-005-0758-5
60. Freeman, A.S., J. Meszaros, and J.E. Byers. (2009). Poor phenotypic integration of blue mussel inducible defenses in environments with multiple predators. *Oikos.* **118**, 758-766. https://doi.org/10.1111/j.1600-0706.2008.17176.x
61. Wilson, J. (2016). *Introgression patterns in Scottish blue mussel (Mytilus edulis) populations.* Institute of Aquaculture, University of Stirling, Stirling, Scotland.
62. Breton, S., C. Capt, D. Guerra, and D. Stewart. (2018). Sex-determining mechanisms in bivalves. In: Transitions between sexual systems (eds: Leonard, J.) Springer: Cham, 165-192.
63. Rosa, M., J.E. Ward, and S.E. Shumway. (2018). Selective capture and ingestion of particles by suspension-feeding bivalve molluscs: a review. *J. Shellfish Res.* **37**, 727-746. https://doi.org/10.2983/035.037.0405
64. Riisgård, H.U. (1991). Filtration rate and growth in the blue mussel, Mytilus edulis Linneaus, 1758: dependence on algal concentration. *J. Shellfish Res.* **10**, 29-36.
65. Riisgård, H.U., P. Funch, and P.S. Larsen. (2015). The mussel filter–pump–present understanding, with a re-examination of gill preparations. *Acta Zool.* **96**, 273-282. https://doi.org/10.1111/azo.12110
66. Gianazza, E., I. Eberini, L. Palazzolo, and I. Miller. (2021). Hemolymph proteins: An overview across marine arthropods and molluscs. *J. Proteom.* **245**, 104294. https://doi.org/10.1016/j.jprot.2021.104294
67. Bouallegui, Y. (2019). Immunity in mussels: an overview of molecular components and mechanisms with a focus on the functional defenses. *Fish Shellfish Immunol.* **89**, 158-169. https://doi.org/10.1016/j.fsi.2019.03.057
68. De la Ballina, N.R., F. Maresca, A. Cao, and A. Villalba. (2022). Bivalve haemocyte subpopulations: a review. *Front. Immunol.* **13**, 826255. https://doi.org/10.3389/fimmu.2022.826255
69. Le Foll, F., D. Rioult, S. Boussa, J. Pasquier, Z. Dagher, and F. Leboulenger. (2010). Characterisation of Mytilus edulis hemocyte subpopulations by single cell time-lapse motility imaging. *Fish Shellfish Immunol.* **28**, 372-386. https://doi.org/10.1016/j.fsi.2009.11.011

70. Borthagaray, A.I. and A. Carranza. (2007). Mussels as ecosystem engineers: their contribution to species richness in a rocky littoral community. *Acta Oecol.* **31**, 243-250. https://doi.org/10.1016/j.actao.2006.10.008
71. Sousa, R., J.L. Gutiérrez, and D.C. Aldridge. (2009). Non-indigenous invasive bivalves as ecosystem engineers. *Biol. Invasions.* **11**, 2367-2385. https://doi.org/10.1007/s10530-009-9422-7
72. van Broekhoven, W., H. Jansen, M. Verdegem, E. Struyf, K. Troost, H. Lindeboom, *et al.* (2015). Nutrient regeneration from feces and pseudofeces of mussel Mytilus edulis spat. *Mar. Ecol. Prog.* **534**, 107-120. https://doi.org/10.3354/meps11402
73. Kobak, J., T. Kakareko, Ł. Jermacz, and M. Poznańska. (2013). The impact of zebra mussel (Dreissena polymorpha) periostracum and biofilm cues on habitat selection by a Ponto-Caspian amphipod Dikerogammarus haemobaphes. *Hydrobiologia.* **702**, 215-226. https://doi.org/10.1007/s10750-012-1322-1327
74. Lintas, C. and R. Seed. (1994). Spatial variation in the fauna associated with Mytilus edulis on a wave-exposed rocky shore. *J. Molluscan Stud.* **60**, 165-174. https://doi.org/10.1093/mollus/60.2.165
75. Llewellyn, L., A. Negri, and A. Robertson. (2006). Paralytic shellfish toxins in tropical oceans. *Toxin Rev.* **25**, 159-196. https://doi.org/10.1080/15569540600599217
76. Jacobs, P., R. Riegman, and J. van der Meer. (2015). Impact of the blue mussel Mytilus edulis on the microbial food web in the western Wadden Sea, The Netherlands. *Mar. Ecol. Prog.* **527**, 119-131. https://doi.org/10.3354/meps11227
77. FAO. (2022). *The state of world fisheries and aquaculture. Towards blue transformation.* FAO, Rome, Italia.
78. Rapinski, M., A. Cuerrier, C. Harris, E.O. Ivujivik, E.O. Kangiqsujuaq, and M. Lemire. (2018). Inuit perception of marine organisms: from folk classification to food harvest. *J. Ethnobiol.* **38**, 333-355. https://doi.org/10.2993/0278-0771-38.3.333
79. Finlayson-Trick, E., B. Barker, S. Manji, S.L. Harper, C.P. Yansouni, and D.M. Goldfarb. (2021). Climate Change and Enteric Infections in the Canadian Arctic: Do We Know What's on the Horizon? *Gastrointest. Disord.* **3**, 113-126. https://doi.org/10.3390/gidisord3030012
80. Benito, D., D. Paleček, X. Lekube, U. Izagirre, I. Marigómez, B. Zaldibar, *et al.* (2022). Variability and distribution of parasites, pathologies and their effect on wild mussels (Mytilus sp) in different environments along a wide latitudinal span in the Northern Atlantic and Arctic Oceans. *Mar. Environ. Res.* **176**, 105585. https://doi.org/10.1016/j.marenvres.2022.105585
81. Lévesque, B., C. Barthe, B.R. Dixon, L.J. Parrington, D. Martin, B. Doidge *et al.* (2010). Microbiological quality of blue mussels (Mytilus edulis) in Nunavik, Quebec: a pilot study. *Can. J. Microbiol.* **56**, 968-977. https://doi.org/10.1139/W10-078
82. Robledo, J.A.F., R. Yadavalli, B. Allam, E.P. Espinosa, M. Gerdol, S. Greco, *et al.* (2019). From the raw bar to the bench: Bivalves as models for human health. *Dev Comp. Immunol.* **92**, 260-282. https://doi.org/10.1016/j.dci.2018.11.020
83. Espinosa, E.P., A. Koller, and B. Allam. (2016). Proteomic characterization of mucosal secretions in the eastern oyster, Crassostrea virginica. *J. Proteom.* **132**, 63-76. https://doi.org/10.1016/j.jprot.2015.11.018

84. E.P. Espinosa and B. Allam. (2018). Reverse genetics demonstrate the role of mucosal C-type lectins in food particle selection in the oyster Crassostrea virginica. *J. Exp. Biol.* **221**, jeb174094. https://doi.org/10.1242/jeb.174094
85. Gerdol, M., M. Gomez-Chiarri, M.G. Castillo, A. Figueras, G. Fiorito, R. Moreira, *et al.* (2018). Immunity in molluscs: recognition and effector mechanisms, with a focus on bivalvia. In: *Advances in Comparative Immunology* (eds: Cooper, E.). Springer: Cham, 225-341. https://doi.org/10.1007/978-3-319-76768-0_11
86. Lau, Y.T., L. Gambino, B. Santos, E.P. Espinosa, and B. Allam. (2018). Transepithelial migration of mucosal hemocytes in Crassostrea virginica and potential role in Perkinsus marinus pathogenesis. *J. Invertebr. Pathol.* **153**, 122-129. https://doi.org/10.1016/j.jip.2018.03.004
87. Allam, B. and E.P. Espinosa. (2016). Bivalve immunity and response to infections: Are we looking at the right place? *Fish Shellfish Immunol.* **53**, 4-12. https://doi.org/10.1016/j.fsi.2016.03.037
88. Espinosa, E.P., M. Perrigault, and B. Allam. (2010). Identification and molecular characterization of a mucosal lectin (MeML) from the blue mussel Mytilus edulis and its potential role in particle capture. *Comp. Biochem. Physiol. A Mol. Integr. Physiol.* **156**, 495-501. https://doi.org/10.1016/j.cbpa.2010.04.004
89. Jing, X., E.P. Espinosa, M. Perrigault, and B. Allam. (2011). Identification, molecular characterization and expression analysis of a mucosal C-type lectin in the eastern oyster, Crassostrea virginica. *Fish Shellfish Immunol.* **30**, 851-858. https://doi.org/10.1016/j.fsi.2011.01.007
90. Galdiero, S., A. Falanga, R. Berisio, P. Grieco, G. Morelli, and M. Galdiero. (2015). Antimicrobial peptides as an opportunity against bacterial diseases. *Curr. Med. Chem.* **22**, 1665-1677. https://doi.org/10.2174/0929867322666150311145632
91. Giuliani, A., G. Pirri, and S. Nicoletto. (2007). Antimicrobial peptides: an overview of a promising class of therapeutics. *Open Life Sci.* **2**, 1-33. https://doi.org/10.2478/s11535-007-0010-5
92. Guryanova, S.V., S.V. Balandin, O.Y. Belogurova-Ovchinnikova, and T.V. Ovchinnikova. (2023). Marine invertebrate antimicrobial peptides and their potential as novel peptide antibiotics. *Mar. Drugs* **21**, 503. https://doi.org/10.3390/md21100503
93. Canesi, L., M. Auguste, T. Balbi, and P. Prochazkova. (2022). Soluble mediators of innate immunity in annelids and bivalve mollusks: A mini-review. *Front. Immunol.* **13**, 1051155. https://doi.org/10.3389/fimmu.2022.1051155
94. Mahlapuu, M., J. Håkansson, L. Ringstad, and C. Björn. (2016). Antimicrobial peptides: an emerging category of therapeutic agents. *Front. Cell. Infect. Microbiol.* **6**, 194. https://doi.org/10.3389/fcimb.2016.00194
95. Anjum, K., S.Q. Abbas, N. Akhter, B.I. Shagufta, S.A.A. Shah, and S.S.U. Hassan. (2017). Emerging biopharmaceuticals from bioactive peptides derived from marine organisms. *Chem. Biol. Drug Des.* **90**, 12-30. https://doi.org/10.1111/cbdd.12925
96. Terada, D., A.R. Voet, H. Noguchi, K. Kamata, M. Ohki, C. Addy, *et al.* (2017). Computational design of a symmetrical beta-trefoil lectin with cancer cell binding activity. *Sci. Rep.* **7**, 5943. https://doi.org/10.1038/s41598-017-06332-7

97. Barrett, D.G., G.G. Bushnell, and P.B. Messersmith. (2013). Mechanically robust, negative-swelling, mussel-inspired tissue adhesives. *Adv. Healthc. Mater.* **2**, 745-755. https://doi.org/10.1002/adhm.201200316
98. Petersen, J.M. and J. Osvatic. (2018). Microbiomes In Natura: Importance of Invertebrates in Understanding the Natural Variety of Animal-Microbe Interactions. *mSystems.* **3**, e00179-17. https://doi.org/10.1128/msystems.00179-17
99. Paillard, C., Y. Gueguen, K.M. Wegner, D. Bass, A. Pallavicini, L. Vezzulli, *et al.* (2022). Recent advances in bivalve-microbiota interactions for disease prevention in aquaculture. *Curr. Opin. Biotechnol.* **73**, 225-232. https://doi.org/10.1016/j.copbio.2021.07.026
100. Egan, S. and M. Gardiner. (2016). Microbial Dysbiosis: Rethinking Disease in Marine Ecosystems. *Front. Microbiol.* **7**, 991. https://doi.org/10.3389/fmicb.2016.00991
101. Burge, C.A., C.J. Closek, C.S. Friedman, M.L. Groner, C.M. Jenkins, A. Shore-Maggio, *et al.* (2016). The use of filter-feeders to manage disease in a changing world. *Integr. Comp. Biol.* **56**, 573-587. https://doi.org/10.1093/icb/icw048
102. Farabegoli, F., L. Blanco, L.P. Rodríguez, J.M. Vieites, and A.G. Cabado. (2018). Phycotoxins in marine shellfish: Origin, occurrence and effects on humans. *Mar. Drugs.* **16**, 188. https://doi.org/10.3390/md16060188
103. Hegaret, H., G.H. Wikfors, and S.E. Shumway. (2007). Diverse feeding responses of five species of bivalve mollusc when exposed to three species of harmful algae. *J. Shellfish Res.* **26**, 549-559. https://doi.org/10.2983/0730-8000(2007)26[549:DFROFS]2.0.CO;2
104. Hégaret, H. and G.H. Wikfors. (2005). Time-dependent changes in hemocytes of eastern oysters, Crassostrea virginica, and northern bay scallops, Argopecten irradians irradians, exposed to a cultured strain of Prorocentrum minimum. *Harmful Algae.* **4**, 187-199. https://doi.org/10.1016/j.hal.2003.12.004
105. Manfrin, C.H., G.I. De Moro, V. Torboli, P. Venier, A. Pallavicini, and M.A. Gerdol. (2012). Physiological and molecular responses of bivalves to toxic dinoflagellates. *Invertebrate Surviv. J.* **9**, 184-199.
106. Carballal, M.J., B.J. Barber, D. Iglesias, and A. Villalba. (2015). Neoplastic diseases of marine bivalves. *J. Invertebr. Pathol.* **131**, 83-106. https://doi.org/10.1016/j.jip.2015.06.004
107. Barber, B.J. (2004). Neoplastic diseases of commercially important marine bivalves. *Aquat. Living Resour.* **17**, 449-466. https://doi.org/10.1051/alr:2004052
108. Metzger, M.J., C. Reinisch, J. Sherry, and S.P. Goff. (2015). Horizontal transmission of clonal cancer cells causes leukemia in soft-shell clams. *Cell* **161**, 255-263. https://doi.org/10.1016/j.cell.2015.02.042
109. Hendricks, S.A., A. Storfer, and P.A. Hohenlohe. (2021).Population genomics of wildlife cancer. In: *Population Genomics: Wildlifeeds*. Springer: Cham, Switzerland, 385-416.
110. Caza F., E. Bernet, F.J. Veyrier, S. Betoulle, and Y. St-Pierre. (2020). Hemocytes released in seawater act as Trojan horses for spreading of bacterial infections in mussels. *Sci. Rep.* **10**, 19696. https://doi.org/10.1038/s41598-020-76677-z
111. Kocot, K.M., F. Aguilera, C. McDougall, D.J. Jackson, and B.M. Degnan. (2016). Sea shell diversity and rapidly evolving secretomes: insights into the evolution of

biomineralization. *Front. Zool.* **13**, 1-10. https://doi.org/10.1186/s12983-016-0155-z
112. Fossi, M.C. and C. Panti. (2017). Sentinel species of marine ecosystems. In: *Oxford Research Encyclopedia of Environmental Science*. University Press, Oxford, UK. https://doi.org/10.1093/acrefore/9780199389414.013.110
113. Multisanti, C.R., C. Merola, M. Perugini, V. Aliko, and C. Faggio. (2022). Sentinel species selection for monitoring microplastic pollution: A review on one health approach. *Ecol. Indic.* **145**, 109587. https://doi.org/10.1016/j.ecolind.2022.109587
114. Lomartire, S., J.C. Marques, and A.M. Gonçalves. (2021). Biomarkers based tools to assess environmental and chemical stressors in aquatic systems. *Ecol. Indic.* **122**, 107207. https://doi.org/10.1016/j.ecolind.2020.107207
115. Duarte, I.A., P. Reis-Santos, S. França, H. Cabral, and V.F. Fonseca. (2017). Biomarker responses to environmental contamination in estuaries: A comparative multi-taxa approach. *Aquat. Toxicol.* **189**, 31-41. https://doi.org/10.1016/j.aquatox.2017.05.010
116. Brucker, N., S.N. do Nascimento, L. Bernardini, M.F. Charão, and S.C. Garcia. (2020). Biomarkers of exposure, effect, and susceptibility in occupational exposure to traffic-related air pollution: A review. *J. Appl. Toxicol.* **40**, 722-736. https://doi.org/10.1002/jat.3940
117. Briant, N., T. Chouvelon, L. Martinez, C. Brach-Papa, J.F. Chiffoleau, N. Savoye, *et al.* (2017). Spatial and temporal distribution of mercury and methylmercury in bivalves from the French coastline. *Mar. Pollut. Bull.* **114**, 1096–1102. https://doi.org/10.1016/j.marpolbul.2016.10.018
118. Wu, H. and W.X. Wang. (2011). Tissue-specific toxicological effects of cadmium in green mussels (Perna viridis): Nuclear magnetic resonance-based metabolomics study. *Environ. Toxicol. Chem.* **30**, 806-812. https://doi.org/10.1002/etc.446
119. Solé, M., R. Freitas, L. Viñas, and G.A. Rivera-Ingraham. (2020). Biomarker considerations in monitoring petrogenic pollution using the mussel Mytilus galloprovincialis. *Environ. Sci. Pollut. Res.* **27**, 31854–31862. https://doi.org/10.1007/s11356-020-09427-3
120. Lushchak, V.I. (2011). Environmentally induced oxidative stress in aquatic animals. *Aquat. Toxicol.* **101**, 13-30. https://doi.org/10.1016/j.aquatox.2010.10.006
121. Serafim, A., B. Lopes, R. Company, A. Cravo, T. Gomes, V. Sousa, *et al.* (2011). A multi-biomarker approach in cross-transplanted mussels Mytilus galloprovincialis. *Ecotoxicol.* **20**, 1959-1974. https://doi.org/10.1007/s10646-011-0737-7
122. Brooks, S., B. Lyons, F. Goodsir, J. Bignell, and J. Thain. (2009). Biomarker responses in mussels, an integrated approach to biological effects measurements. *J. Toxicol. Environ. Health - A.* **72**, 196-208. https://doi.org/10.1080/15287390802539038
123. Yap, C.K., S.G. Tan, A. Ismail, and H. Omar. (2004). Allozyme polymorphisms and heavy metal levels in the green-lipped mussel Perna viridis (Linnaeus) collected from contaminated and uncontaminated sites in Malaysia. *Environ. Int.* **30**, 39-46. https://doi.org/10.1016/S0160-4120(03)00144-2
124. Yap, C.K., W.H. Cheng, C.C. Ong, and S.G. Tan. (2013). Heavy metal contamination and physical barrier are main causal agents for the genetic

differentiation of Perna viridis populations in Peninsular Malaysia. *Sains Malays.* **42**, 1557-1564.
125. Dos Santos, F.S., R.A. Neves, M.A.C. Crapez, V.L. Teixeira, and N. Krepsky. (2022). How does the brown mussel Perna perna respond to environmental pollution? A review on pollution biomarkers. *J. Environ. Sci.* **111**, 412-428. https://doi.org/10.1016/j.jes.2021.04.006
126. Tlili, S. and C. Mouneyrac. (2021). New challenges of marine ecotoxicology in a global change context. *Mar. Pollut. Bull.* **166**, 112242. https://doi.org/10.1016/j.marpolbul.2021.112242
127. Lemos, M.F., B. Duarte, V.F. Fonseca, and S.C. Novais. (2022). Effects on Biomarkers in Stress Ecology Studies. Well, So What? What Now? *Biol.* **11**, 1777. https://doi.org/10.3390/biology11121777
128. Babrak, L.M., J. Menetski, M. Rebhan, G. Nisato, M. Zinggeler, N. Brasier, *et al.* (2019). Traditional and digital biomarkers: two worlds apart? *Digit. Biomark.* **3**, 92-102. https://doi.org/10.1159/000502000
129. Rodrigues, N.M., J.E. Batista, P. Mariano, V. Fonseca, B. Duarte, and S. Silva. (2021). Artificial Intelligence Meets Marine Ecotoxicology: Applying Deep Learning to Bio-Optical Data from Marine Diatoms Exposed to Legacy and Emerging Contaminants. *Biol.* **10**, 932. https://doi.org/10.3390/biology10090932
130. Lionetto, M.G., R. Caricato, and M.E. Giordano. (2021). Pollution biomarkers in the framework of marine biodiversity conservation: State of art and perspectives. *Water.* **13**, 1847. https://doi.org/10.3390/w13131847
131. Kadim, M.K. and Y. Risjani. (2022). Biomarker for monitoring heavy metal pollution in aquatic environment: An overview toward molecular perspectives. *Emerg. Contam.* **8**, 195-205. https://doi.org/10.1016/j.emcon.2022.02.003
132. Li, S., A.C. Alfaro, T.V. Nguyen, T. Young, and R. Lulijwa. (2020). An integrated omics approach to investigate summer mortality of New Zealand Greenshell™ mussels. *Metabolomics.* **16**, 100. https://doi.org/10.1007/s11306-020-01722-x
133. Châtel, A., C. Lièvre, A. Barrick, M. Bruneau, and C. Mouneyrac. (2018). Transcriptomic approach: a promising tool for rapid screening nanomaterial-mediated toxicity in the marine bivalve Mytilus edulis—application to copper oxide nanoparticles. *Comp. Biochem. Physiol. C. Toxicol. Pharmacol.* **205**, 26-33. https://doi.org/10.1016/j.cbpc.2018.01.003
134. Yu, D., H. Wu, X. Peng, C. Ji, X. Zhang, J. Song, *et al.* (2020). Profiling of microRNAs and mRNAs in marine mussel Mytilus galloprovincialis. *Comp. Biochem. Physiol. C. Toxicol. Pharmacol.* **230**, 108697. https://doi.org/10.1016/j.cbpc.2019.108697
135. Yu, D., Z. Peng, H. Wu, X. Zhang, C. Ji, and X. Peng. (2021). Stress responses in expressions of microRNAs in mussel Mytilus galloprovincialis exposed to cadmium. *Ecotoxicol. Environ. Saf.* **212**, 111927. https://doi.org/10.1016/j.ecoenv.2021.111927
136. Šrut, M. (2021). Ecotoxicological epigenetics in invertebrates: Emerging tool for the evaluation of present and past pollution burden. *Chemosphere* **282**, 131026. https://doi.org/10.1016/j.chemosphere.2021.131026

137. Pham, K., L. Ho, C.P. D'Incal, A. De Cock, W.V. Berghe, and P. Goethals. (2023). Epigenetic analytical approaches in ecotoxicological aquatic research. *Environ. Pollut.* **330**, 121737. https://doi.org/10.1016/j.envpol.2023.121737
138. Laird, P. (2010). Principles and challenges of genome-wide DNA methylation analysis. *Nat. Rev. Genet.* **11**, 191-203. https://doi.org/10.1038/nrg2732
139. MacKenzie, M. and C. Argyropoulos. (2023). An introduction to nanopore sequencing: past, present, and future considerations. *Micromachines.* **14**, 459. https://doi.org/10.3390/mi14020459
140. Pérez-Cobas, A.E., L. Gomez-Valero, and C. Buchrieser. (2020). Metagenomic approaches in microbial ecology: an update on whole-genome and marker gene sequencing analyses. *Microb. Genom.* **6**, e000409. https://doi.org/10.1099/mgen.0.000409
141. Van de Sande, B., J.S. Lee, E. Mutasa-Gottgens, B. Naughton, W. Bacon, J. Manning, *et al.* (2023). Applications of single-cell RNA sequencing in drug discovery and development. *Nat. Rev. Drug. Discov.* **22**, 496-520. https://doi.org/10.1038/s41573-023-00688-4
142. Arya, S.S., S.B. Dias, H.F. Jelinek, L.J. Hadjileontiadis, and A.M. Pappa. (2023). The convergence of traditional and digital biomarkers through AI-assisted biosensing: A new era in translational diagnostics? *Biosens. Bioelectron.* **235**, 115387. https://doi.org/10.1016/j.bios.2023.115387
143. Fabbri, E., P. Valbonesi, and T.W. Moon. (2023). Pharmaceuticals in the marine environment: occurrence, fate, and biological effects. In: *Contaminants of Emerging Concern in the Marine Environment* (eds: León, V.M. and J. Bellas). Elsevier, Amsterdam, The Netherlands, 11-71. https://doi.org/10.1016/B978-0-323-90297-7.00008-1
144. Lupo, C., S. Bougeard, V. Le Bihan, J.L. Blin, G. Allain, P. Azema, *et al.* (2021). Mortality of marine mussels Mytilus edulis and M. galloprovincialis: systematic literature review of risk factors and recommendations for future research. *Rev. Aquac.* **13**, 504–536. https://doi.org/10.1111/raq.12484
145. Roland, H.B., J. Kohlhoff, K. Lanphier, S. Hoysala, E.G. Kennedy, J. Harley, *et al.* (2024). Perceived challenges to tribally led shellfish toxin testing in Southeast Alaska: Findings from key informant interviews. *GeoHealth.* **8**, e2023GH000988. https://doi.org/10.1029/2023GH000988
146. Heidrich, I., L. Ačkar, P. Mossahebi Mohammadi, and K. Pantel. (2021). Liquid biopsies: Potential and challenges. *Int. J. Cancer.* **148**, 528-545. https://doi.org/10.1002/ijc.33217
147. Lianidou, E. and K. Pantel. (2019). Liquid biopsies. *Genes Chromosomes Cancer.* **58**, 219-232. https://doi.org/10.1002/gcc.22695
148. Alix-Panabières, C. and K. Pantel. (2017). Clinical prospects of liquid biopsies. *Nat. Biomed. Eng.* **1**, 0065. https://doi.org/10.1038/s41551-017-0065
149. Connal, S., J.M. Cameron, A. Sala, P.M. Brennan, D.S. Palmer, J.D. Palmer, *et al.* (2023). Liquid biopsies: the future of cancer early detection. *J. Transl. Med.* **21**, 118. https://doi.org/10.1186/s12967-023-03960-8
150. Tsoneva, D.K., M.N. Ivanov, N.V. Conev, R. Manev, D.S. Stoyanov, and M. Vinciguerra. (2023). Circulating histones to detect and monitor the progression of cancer. *Int. J. Mol. Sci.* **24**, 942. https://doi.org/10.3390/ijms24020942

151. Praharaj, P.P., S.K. Bhutia, S. Nagrath, R.L. Bitting, and G. Deep. (2018). Circulating tumor cell-derived organoids: Current challenges and promises in medical research and precision medicine. . *Biochim. Biophys. Acta - Rev. Cancer.* **1869**, 117-127. https://doi.org/10.1016/j.bbcan.2017.12.005
152. Ashworth, T.R. (1869). A case of cancer in which cells similar to those in the tumors were seen in the blood after death. *Australas. Med. J.* **14**, 146-149.
153. Mandel, P. and P. Metais. (1948). Nuclear Acids In Human Blood Plasma. *C. R. Seances Soc. Biol. Fil.* **142**, 241-243.
154. Tan, E.M., P.H. Schur, R.I. Carr, and H. Kunkel. (1966). Deoxybonucleic acid (DNA) and antibodies to DNA in the serum of patients with systemic lupus erythematosus. *J. Clin. Invest.* **45**, 1732-1740.
155. Stroun, M., P. Anker, J. Lyautey, C. Lederrey, and P.A. Maurice. (1987). Isolation and characterization of DNA from the plasma of cancer patients. *Eur. J. Cancer. Clin. Oncol.* **23**, 707-712. https://doi.org/10.1016/0277-5379(87)90266-5
156. Sorenson, G.D., D.M. Pribish, F.H. Valone, V.A. Memoli, D.J. Bzik, and S.L. Yao. (1994). Soluble normal and mutated DNA sequences from single-copy genes in human blood. *Cancer Epidemiol. Biomarkers Prev.* **3**, 67-71.
157. Pantel, K. and C. Alix-Panabières. (2010). Circulating tumour cells in cancer patients: challenges and perspectives. *Trends Mol. Med.* **16**, 398-406. https://doi.org/10.1016/j.molmed.2010.07.001
158. Adhit, K.K., A. Wanjari, S. Menon, and K. Siddhaarth. (2023). Liquid Biopsy: An Evolving Paradigm for Non-invasive Disease Diagnosis and Monitoring in Medicine. *Cureus.* **15**, e50176. https://doi.org/10.7759/cureus.50176
159. Han, D., R. Li, J. Shi, P. Tan, R. Zhang, and J. Li. (2020). Liquid biopsy for infectious diseases: a focus on microbial cell-free DNA sequencing. *Theranostics.* **10**, 5501. https://doi.org/10.7150/thno.45554
160. Gaitsch, H., R.J. Franklin, and D.S. Reich. (2023). Cell-free DNA-based liquid biopsies in neurology. *Brain.* **146**, 1758–1774. https://doi.org/10.1093/brain/awac438
161. Ozturk, E.A. and A. Caner. (2022). Liquid biopsy for promising non-invasive diagnostic biomarkers in parasitic infections. *Acta Parasit.* **67**, 1-17. https://doi.org/10.1007/s11686-021-00444-x
162. Jackson, A.M., C. Amato-Menker, and M. Bettinotti. (2021). Cell-free DNA diagnostics in transplantation utilizing next generation sequencing. *Hum. Immunol.* **82**, 850-858. https://doi.org/10.1016/j.humimm.2021.07.006
163. Alix-Panabières, C. and K. Pantel. (2021). Liquid biopsy: from discovery to clinical application. *Cancer Discov.* **11**, 858-873. https://doi.org/10.1158/2159-8290.CD-20-1311
164. Pantel, K. and C. Alix-Panabières. (2019). Liquid biopsy and minimal residual disease — latest advances and implications for cure. *Nat. Rev. Clin. Oncol.* **16**, 409-424. https://doi.org/10.1038/s41571-019-0187-3
165. Pessoa, L.S., M. Heringer, and V.P. Ferrer. (2020). ctDNA as a cancer biomarker: A broad overview. *Crit. Rev. Oncol. Hematol.* **155**, 103109. https://doi.org/10.1016/j.critrevonc.2020.103109

166. Ponti, G., M. Maccaferri, A. Percesepe, A. Tomasi, and T. Ozben. (2021). Liquid biopsy with cell free DNA: new horizons for prostate cancer. *Crit. Rev. Clin. Lab. Sci.* **58**, 60-76. https://doi.org/10.1080/10408363.2020.1803789
167. Song, P., L.R. Wu, Y.H. Yan, J.X. Zhang, T. Chu, L.N. Kwong, *et al.* (2022). Limitations and opportunities of technologies for the analysis of cell-free DNA in cancer diagnostics. *Nat. Biomed. Eng.* **6**, 232-245. https://doi.org/10.1038/s41551-021-00837-3
168. Siljan, W.W., J.C. Holter, S.H. Nymo, C. Schjalm, F. Müller, P.A. Jenum, *et al.* (2016). Circulating cell-free DNA is elevated in community acquired bacterial pneumonia and predicts short-term outcome. *J. Infect.* **73**, 383–386. https://doi.org/10.1016/j.jinf.2016.07.011
169. Lindahl, T. (1993). Instability and decay of the primary structure of DNA. *Nature.* **362**, 709-715. https://doi.org/10.1038/362709a0
170. Richter, C., J.W. Park, and B.N. Ames. (1988). Normal oxidative damage to mitochondrial and nuclear DNA is extensive. *Proc. Natl Acad. Sci. USA.* **85**, 6465–6467. https://doi.org/10.1073/pnas.85.17.6465
171. Lau, B.T., A. Almeda, M. Schauer, M. McNamara, X. Bai, Q. Meng, *et al.* (2023). Single-molecule methylation profiles of cell-free DNA in cancer with nanopore sequencing. *Genome Med.* **15**, 33. https://doi.org/10.1186/s13073-023-01178-3
172. Katsman, E., S. Orlanski, F. Martignano, I. Fox-Fisher, R. Shemer, Y. Dor, *et al.* (2022). Detecting cell-of-origin and cancer-specific methylation features of cell-free DNA from Nanopore sequencing. *Genome Biol.* **23**, 158. https://doi.org/10.1186/s13059-022-02710-1
173. Rahikainen, A.L., J.U. Palo, W. de Leeuw, B. Budowle, and A. Sajantila. (2016). DNA quality and quantity from up to 16 years old post-mortem blood stored on FTA cards. *Forensic Sci. Int.* **261**, 148-153. https://doi.org/10.1016/j.forsciint.2016.02.014
174. Heider, K., J.C. Wan, J. Hall, J. Belic, S. Boyle, I. Hudecova, *et al.* (2020). Detection of ctDNA from dried blood spots after DNA size selection. *Clin. Chem.* **66**, 697–705. https://doi.org/10.1093/clinchem/hvaa050
175. Fouts, A.N., A. Romero, J. Nelson, M. Hogan, and S. Nasarabadi. (2020). Ambient Biobanking Solutions for Whole Blood Sampling, Transportation, and Extraction. In: *Biochemical Analysis Tools-Methods for Bio-Molecules Studies* (eds: Boldura, O.M., C. Balta, and N.S. Awwad). IntechOpen, London, UK.
176. Dobbs, L.J., M.N. Madigan, A.B. Carter, and L. Earls. (2002). Use of FTA gene guard filter paper for the storage and transportation of tumor cells for molecular testing. *Arch. Pathol. Lab. Med.* **126**, 56-63. https://doi.org/10.5858/2002-126-0056-UOFGGF
177. Cohen, J.D., L. Li, Y. Wang, C. Thoburn, B. Afsari, L. Danilova, *et al.* (2018). Detection and localization of surgically resectable cancers with a multi-analyte blood test. *Science.* **359**, 926-930. https://doi.org/http://doi.org/10.1126/science.aar3247
178. Li, Y., S. Sui, and A. Goel. (2024). Extracellular vesicles associated microRNAs: Their biology and clinical significance as biomarkers in gastrointestinal cancers. In: *Seminars in Cancer Biology*. Academic Press, 5-23. https://doi.org/10.1016/j.semcancer.2024.02.001

179. Armakolas, A., M. Kotsari, and J. Koskinas. (2023). Liquid biopsies, novel approaches and future directions. *Cancers.* **15**, 1579. https://doi.org/10.3390/cancers15051579
180. Boeri, M., C. Verri, D. Conte, L. Roz, P. Modena, F. Facchinetti, *et al.* (2011). MicroRNA signatures in tissues and plasma predict development and prognosis of computed tomography detected lung cancer. *Proc. Natl. Acad. Sci. USA.* **108**, 3713-3718. https://doi.org/10.1073/pnas.1100048108
181. Wang, J., J. Ni, J. Beretov, J. Thompson, P. Graham, and Y. Li. (2020). Exosomal microRNAs as liquid biopsy biomarkers in prostate cancer. *Crit. Rev. Oncol. Hematol.* **145**, 102860. https://doi.org/10.1016/j.critrevonc.2019.102860
182. Ozawa, P.M.M., T.S. Jucoski, E. Vieira, T.M. Carvalho, D. Malheiros, and E.M.D.S.F. Ribeiro. (2020). Liquid biopsy for breast cancer using extracellular vesicles and cell-free microRNAs as biomarkers. *Transl. Res.* **223**, 40-60. https://doi.org/10.1016/j.trsl.2020.04.002
183. Decker, B. and L.M. Sholl. (2020). Cell-Free DNA Testing. In: *Genomic Medicine: A Practical Guide*. Springer: Cham, Switzerland, 41-54.
184. Blauwkamp, T.A., S. Thair, M.J. Rosen, L. Blair, M.S. Lindner, I.D. Vilfan, *et al.* (2019). Analytical and clinical validation of a microbial cell-free DNA sequencing test for infectious disease. *Nat. Microbiol.* **4**, 663-674. https://doi.org/10.1038/s41564-018-0349-6
185. Di Renzo, G.C., J.L. Bartha, and C.M. Bilardo. (2019). Expanding the indications for cell-free DNA in the maternal circulation: clinical considerations and implications. *Am. J. Obstet. Gynecol.* **220**, 537-542. https://doi.org/10.1016/j.ajog.2019.01.009
186. Grati, F.R., F. Malvestiti, J.C. Ferreira, K. Bajaj, E. Gaetani, C. Agrati, *et al.* (2014). Fetoplacental mosaicism: potential implications for false-positive and false-negative noninvasive prenatal screening results. *Genet. Med.* **16**, 620-624. https://doi.org/10.1038/gim.2014.3
187. Yu, S.C., L.L. Choy, and Y.D. Lo. (2023). 'Longing' for the Next Generation of Liquid Biopsy: The Diagnostic Potential of Long Cell-Free DNA in Oncology and Prenatal Testing. *Mol. Diagn. Ther.* **27**, 563-571. https://doi.org/10.1007/s40291-023-00661-2
188. Grskovic, M., D.J. Hiller, L.A. Eubank, J.J. Sninsky, C. Christopherson, J.P. Collins, *et al.* (2016). Validation of a clinical-grade assay to measure donor-derived cell-free DNA in solid organ transplant recipients. *J. Mol. Diagn.* **18**, 890-902. https://doi.org/10.1016/j.jmoldx.2016.07.003
189. Dinakaran, V., A. Rathinavel, M. Pushpanathan, R. Sivakumar, P. Gunasekaran, and J. Rajendhran. (2014). Elevated levels of circulating DNA in cardiovascular disease patients: metagenomic profiling of microbiome in the circulation. *PLoS One.* **9**, e105221. https://doi.org/10.1371/journal.pone.0105221
190. Castillo, D.J., R.F. Rifkin, D.A. Cowan, and M. Potgieter. (2019). The healthy human blood microbiome: fact or fiction? *Front. Cell. Infect. Microbiol.* **9**, 449041. https://doi.org/10.3389/fcimb.2019.00148
191. Perez-Carrasco, V., A. Soriano-Lerma, M. Soriano, J. Gutiérrez-Fernández, and J.A. Garcia-Salcedo. (2021). Urinary microbiome: yin and yang of the urinary tract.

Front. Cell. Infect. Microbiol. **11**, 617002. https://doi.org/10.3389/fcimb.2021.617002
192. Gorski, A., E. Wazna, B.W. Dabrowska, K. Dabrowska, K. Switala-Jelen, and R. Miedzybrodzki. (2006). Bacteriophage translocation. *FEMS Immunol. Med. Microbiol.* **46**, 313-319. https://doi.org/10.1111/j.1574-695X.2006.00044.x
193. Nagpal, R. and H. Yadav. (2017). Bacterial translocation from the gut to the distant organs: an overview. *Ann. Nutr. Metab.* **71**, 11-16. https://doi.org/10.1159/000479918
194. Bomsel, M. and A. Alfsen. (2003). Entry of viruses through the epithelial barrier: pathogenic trickery. *Nat. Rev. Mol. Cell Biol.* **4**, 57-68. https://doi.org/10.1038/nrm1005
195. Hong, D.K., T.A. Blauwkamp, M. Kertesz, S. Bercovici, C. Truong, and N. Banaei. (2018). Liquid biopsy for infectious diseases: sequencing of cell-free plasma to detect pathogen DNA in patients with invasive fungal disease. *Diagn. Microbiol. Infect. Dis.* **92**, 210–213. https://doi.org/10.1016/j.diagmicrobio.2018.06.009
196. Fernández-Carballo, B.L., T. Broger, R. Wyss, N. Banaei, and C.M. Denkinger. (2019). Toward the development of a circulating free DNA-based in vitro diagnostic test for infectious diseases: a review of evidence for tuberculosis. *J. Clin. Microbiol.* **57**, 10-1128. https://doi.org/10.1128/jcm.01234-18
197. Liao, W., X. Zuo, G. Lin, Y. Zhou, Y. Fu, S. Cai, *et al.* (2020). Microbial cell-free DNA in plasma of patients with sepsis: a potential diagnostic methodology. *Discov. Med.* **29**, 129-137.
198. Kowarsky, M., J. Camunas-Soler, M. Kertesz, I. De Vlaminck, W. Koh, W. Pan, *et al.* (2017). Numerous uncharacterized and highly divergent microbes which colonize humans are revealed by circulating cell-free DNA. *Proc. Natl. Acad. Sci. USA.* **114**, 9623-9628. https://doi.org/10.1073/pnas.1707009114
199. Watts, G.S. and B.L. Hurwitz. (2020). Metagenomic next-generation sequencing in clinical microbiology. *Clin. Microbiol. Newsl.* **42**, 53-59. https://doi.org/10.1016/j.clinmicnews.2020.03.004
200. Langelier, C., M. Fung, S. Caldera, T. Deiss, A. Lyden, B.C. Prince, *et al.* (2020). Detection of pneumonia pathogens from plasma cell-free DNA. *Am. J. Respir. Crit. Care Med.* **201**, 491-495. https://doi.org/10.1164/rccm.201904-0905LE
201. Chen, F., J. Wang, Y. Wu, Q. Gao, and S. Zhang. (2022). Potential biomarkers for liver cancer diagnosis based on multi-omics strategy. *Front. Oncol.* **12**, 822449. https://doi.org/10.3389/fonc.2022.822449
202. Chen, G., J. Zhang, Q. Fu, V. Taly, and F. Tan. (2023). Integrative analysis of multi-omics data for liquid biopsy. *Br. J. Cancer.* **128**, 505-518. https://doi.org/10.1038/s41416-022-02048-2
203. Di Sario, G., V. Rossella, E.S. Famulari, A. Maurizio, D. Lazarevic, F. Giannese, *et al.* (2023). Enhancing clinical potential of liquid biopsy through a multi-omic approach: A systematic review. *Front. Genet.* **14**, 1152470. https://doi.org/10.3389/fgene.2023.1152470
204. Abou Daya, S. and R. Mahfouz. (2018). Circulating tumor DNA, liquid biopsy, and next generation sequencing: A comprehensive technical and clinical applications review. *Meta Gene.* **17**, 192-201. https://doi.org/10.1016/j.mgene.2018.06.013

205. Yu, C., Y. Lin, Y. Luo, Y. Guo, Z. Ye, R. Ou, *et al.* (2023). The fragmentomic property of plasma cell-free DNA enables the non-invasive detection of diabetic nephropathy in patients with diabetes mellitus. *Front. Endocrinol.* **14**, 1164822. https://doi.org/10.3389/fendo.2023.1164822
206. Cristiano, S., A. Leal, J. Phallen, J. Fiksel, V. Adleff, D.C. Bruhm, *et al.* (2019). Genome-wide cell-free DNA fragmentation in patients with cancer. *Nature.* **570**, 385-389. https://doi.org/10.1038/s41586-019-1272-6
207. Polina, I.A., D.V. Ilatovskaya, and K.Y. DeLeon-Pennell. (2020). Cell free DNA as a diagnostic and prognostic marker for cardiovascular diseases. *Clin. Chim. Acta.* **503**, 145-150. https://doi.org/10.1016/j.cca.2020.01.013
208. Drag, M.H. and T.O. Kilpeläinen. (2021). Cell-free DNA and RNA—measurement and applications in clinical diagnostics with focus on metabolic disorders. *Physiol. Genomics.* **53**, 33-46. https://doi.org/10.1152/physiolgenomics.00086.2020
209. Lo, Y.D., D.S. Han, P. Jiang, and R.W. Chiu. (2021). Epigenetics, fragmentomics, and topology of cell-free DNA in liquid biopsies. *Science.* **372**, eaaw3616. https://doi.org/10.1126/science.aaw3616
210. Han, X., J. Wang, and Y. Sun. (2017). Circulating tumor DNA as biomarkers for cancer detection. *Genom. Proteom. Bioinform.* **15**, 59-72. https://doi.org/10.1016/j.gpb.2016.12.004
211. Chaddha, M., H. Rai, R. Gupta, and D. Thakral. (2023). Integrated analysis of circulating cell free nucleic acids for cancer genotyping and immune phenotyping of tumor microenvironment. *Front. Genet.* **14**, 1138625. https://doi.org/10.3389/fgene.2023.1138625
212. Tkac, J., T. Bertok, M. Hires, E. Jane, L. Lorencova, and P. Kasak. (2019). Glycomics of prostate cancer: updates. *Expert Rev. Proteomics.* **16**, 65-76. https://doi.org/10.1080/14789450.2019.1549993
213. Joo, E.J., A. Weyers, G. Li, L. Gasimli, L. Li, W.J. Choi, *et al.* (2014). arbohydrate-containing molecules as potential biomarkers in colon cancer. *OMICS J. Integr. Biol.* **18**, 231-241. https://doi.org/10.1089/omi.2013.0128
214. Amon, R., E.M. Reuven, S.L. Ben-Arye, and V. Padler-Karavani. (2014). Glycans in immune recognition and response. *Carbohydr. Res.* **389**, 115-122. https://doi.org/10.1016/j.carres.2014.02.004
215. Varki, A. and P. Gagneux. (2015). Biological functions of glycans. In: *Essentials of Glycobiology* (eds: Varki, A., *et al.*). Cold Spring Harbor Laboratory Press, New York, USA, 77-88.
216. Zoldoš, V., M. Novokmet, I. Bečeheli, and G. Lauc. (2013). Genomics and epigenomics of the human glycome. *Glycoconj. J.* **30**, 41-50. https://doi.org/10.1007/s10719-012-9397-y
217. Wishart, D.S., Y.D. Feunang, A. Marcu, A.C. Guo, K. Liang, R. Vázquez-Fresno, T. Sajed, *et al.* (2018). HMDB 4.0: the human metabolome database for 2018. *Nucleic Acids Res.* **46**, D608–D617. https://doi.org/10.1093/nar/gkx1089
218. Schmidt, D.R., R. Patel, D.G. Kirsch, C.A. Lewis, M.G. Vander Heiden, and J.W. Locasale. (2021). Metabolomics in cancer research and emerging applications in clinical oncology. *CA Cancer J. Clin.* **71**, 333-358. https://doi.org/10.3322/caac.21670

219. Nannini, G., G. Meoni, A. Amedei, and L. Tenori. (2020). Metabolomics profile in gastrointestinal cancers: Update and future perspectives. *World J. Gastroenterol.* **26**, 2514. https://doi.org/10.3748/wjg.v26.i20.2514
220. Bronkhorst, A.J., V. Ungerer, A. Oberhofer, S. Gabriel, E. Polatoglou, H. Randeu, *et al.* (2022). New perspectives on the importance of cell-free DNA biology. *Diagnostics.* **12**, 2147. https://doi.org/10.3390/diagnostics12092147
221. Goggs, R., U. Jeffery, D.N. LeVine, and R.H. Li. (2020). Neutrophil-extracellular traps, cell-free DNA, and immunothrombosis in companion animals: a review. *Vet. Pathol.* **57**, 6-23. https://doi.org/10.1177/030098581986172
222. Bayless, R.L., B.L. Cooper, and M.K. Sheats. (2022). Investigation of plasma cell-free DNA as a potential biomarker in horses. *J. Vet. Diagn. Invest.* **34**, 402-406. https://doi.org/10.1177/10406387221078047
223. Kim, J., H. Bae, S. Ahn, S. Shin, A. Cho, K.W. Cho, *et al.* (2021). Cell-free DNA as a diagnostic and prognostic biomarker in dogs with tumors. *Front. Vet. Sci.* **8**, 735682. https://doi.org/ https://doi.org/10.3389/fvets.2021.735682
224. Flory, A., K.M. Kruglyak, J.A. Tynan, L.M. McLennan, J.M. Rafalko, P.C. Fiaux, *et al.* (2022). Clinical validation of a next-generation sequencing-based multi-cancer early detection "liquid biopsy" blood test in over 1,000 dogs using an independent testing set: The CANcer Detection in Dogs (CANDiD) study. *PLoS One.* **17**, e0266623. https://doi.org/10.1371/journal.pone.0266623
225. Aucamp, J., H. van der Zwan, Z. Geldenhuys, A. Abera, R. Louw, and R. van der Sluis. (2023). Diagnostic applications and limitations for the use of cell-free fetal DNA (cffDNA) in animal husbandry and wildlife management. *Res. J. Vet. Sci.* **158**, 106-116. https://doi.org/10.1016/j.rvsc.2023.03.013
226. Scarsella, E., M. Sandri, S.D. Monego, D. Licastro, and B. Stefanon. (2020). Blood Microbiome: A New Marker of Gut Microbial Population in Dogs? *Vet. Sci.* **7**, 198. https://doi.org/10.3390/vetsci7040198
227. Scarsella, E., A. Zecconi, M. Cintio, and B. Stefanon. (2021). Characterization of microbiome on feces, blood and milk in dairy cows with different milk leucocyte pattern. *Animals.* **11**, 1463. https://doi.org/10.3390/ani11051463
228. Vientós-Plotts, A.I., A.C. Ericsson, H. Rindt, and C.R. Reinero. (2021). Blood cultures and blood microbiota analysis as surrogates for bronchoalveolar lavage fluid analysis in dogs with bacterial pneumonia. *BMC Vet. Res.* **17**, 129. https://doi.org/10.1186/s12917-021-02841-w
229. Vientós-Plotts, A.I., A.C. Ericsson, H. Rindt, M.E. Grobman, A. Graham, K. Bishop, *et al.* (2017). Dynamic changes of the respiratory microbiota and its relationship to fecal and blood microbiota in healthy young cats. *PLoS One.* **12**, e0173818. https://doi.org/10.1371/journal.pone.0173818
230. Mandal, R.K., T. Jiang, A.A. Al-Rubaye, D.D. Rhoads, R.F. Wideman, J. Zhao, *et al.* (2016). An investigation into blood microbiota and its potential association with Bacterial Chondronecrosis with Osteomyelitis (BCO) in Broilers. *Sci. Rep.* **6**, 25882. https://doi.org/10.1038/srep25882
231. Potgieter, M., J. Bester, D.B. Kell, and E. Pretorius. (2015). The dormant blood microbiome in chronic, inflammatory diseases. *FEMS Microbiol. Rev.* **39**, 567-591. https://doi.org/10.1093/femsre/fuv013

232. Wani, A.K., N.M Hashem, N. Akhtar, R. Singh, M. Madkour, and A. Prakash. (2022). Understanding microbial networks of farm animals through genomics, metagenomics and other meta-omic approaches for livestock wellness and sustainability – A Review. *Ann. Anim. Sci.* **22**, 839-853. https://doi.org/10.2478/aoas-2022-0002
233. Auguste, M., M. Leonessi, T. L. D. Balbi, C. Oliveri, L. Vezzulli, and L. Canesi. (2024). Seasonal fluctuations of hemolymph microbiota and immune parameters in Mytilus galloprovincialis farmed at La Spezia, Italy. *Aquaculture.* **578**, 740028. https://doi.org/https://doi.org/10.1016/j.aquaculture.2023.740028
234. Vezzulli, L., L. Stagnaro, C. Grande, G. Tassistro, L. Canesi, and C. Pruzzo. (2018). Comparative 16SrDNA Gene-Based Microbiota Profiles of the Pacific Oyster (Crassostrea gigas) and the Mediterranean Mussel (Mytilus galloprovincialis) from a Shellfish Farm (Ligurian Sea, Italy). *Microb. Ecol.* **75**, 495-504. https://doi.org/10.1007/s00248-017-1051-6
235. Caza, F., P. G. Joly de Boissel, R. Villemur, S. Betoulle, and Y. St-Pierre. (2019). Liquid biopsies for omics-based analysis in sentinel mussels. *PLoS One* **14**, e0223525. https://doi.org/10.1371/journal.pone.0223525
236. Angeles, A.K., F. Janke, S. Bauer, P. Christopoulos, A.L. Riediger, and H. Sültmann. (2021). Liquid biopsies beyond mutation calling: genomic and epigenomic features of cell-free DNA in cancer. *Cancers.* **13**, 5615. https://doi.org/10.3390/cancers13225615
237. Maass, K.K., P.S. Schad, A.M. Finster, P. Puranachot, F. Rosing, T. Wedig, *et al.* (2021). From sampling to sequencing: a liquid biopsy pre-analytic workflow to maximize multi-layer genomic information from a single tube. *Cancers.* **13**, 3002. https://doi.org/10.3390/cancers13123002
238. da Cunha Santos, G. (2018). FTA cards for preservation of nucleic acids for molecular assays: a review on the use of cytologic/tissue samples. *Arch. Pathol. Lab. Med.* **142**, 308-312. https://doi.org/10.5858/arpa.2017-0303-RA
239. Vaquer-Sunyer, R. and C.M. Duarte. (2008). Thresholds of hypoxia for marine biodiversity. *Proc. Natl. Acad. Sci. USA.* **105**, 15452-15457. https://doi.org/10.1073/pnas.0803833105
240. Agbaje, O.B.A., I.B. Shir, D.B. Zax, A. Schmidt, and D.E. Jacob. (2018). Biomacromolecules within bivalve shells: Is chitin abundant? *Acta Biomater.* **80**, 176-187. https://doi.org/10.1016/j.actbio.2018.09.009
241. Rey-Campos, M., R. Moreira, M. Gerdol, A. Pallavicini, B. Novoa, and A. Figueras. (2019). Immune tolerance in Mytilus galloprovincialis hemocytes after repeated contact with Vibrio splendidus. *Front. Immunol.* **10**, 471443. https://doi.org/10.3389/fimmu.2019.01894
242. Feng, J., Y. Huang, M. Huang, J. Luo, L. Que, S. Yang, *et al.* (2023). A novel perlucin-like protein (PLP) protects Litopenaeus vannamei against Vibrio harveyi infection. *Fish Shellfish Immunol.* **139**, 108932. https://doi.org/10.1016/j.fsi.2023.108932
243. Salazar, M.L., J.M. Jiménez, J. Villar, M. Rivera, M. Báez, A. Manubens, *et al.* (2019). N-Glycosylation of mollusk hemocyanins contributes to their structural stability and immunomodulatory properties in mammals. *J. Biol. Chem.* **294**, 9546-19564. https://doi.org/10.1074/jbc.RA119.009525

244. Sforzini, S., M. Banni, C. Oliveri, M.N. Moore, and A. Viarengo. (2020). New insights into the possible multiple roles of histidine-rich glycoprotein in blue mussels. *Comp. Biochem. Physiol. B Biochem. Mol. Biol.* **245**, 110440. https://doi.org/10.1016/j.cbpb.2020.110440
245. Mueller, D. and B. Győrffy. (2022). DNA methylation-based diagnostic, prognostic, and predictive biomarkers in colorectal cancer. *Biochim. Biophys. Acta, Rev. Cancer.* **1877**, 188722. https://doi.org/10.1016/j.bbcan.2022.188722
246. Constâncio, V., S.P. Nunes, R. Henrique, and C. Jerónimo. (2020). DNA methylation-based testing in liquid biopsies as detection and prognostic biomarkers for the four major cancer types. *Cells.* **9**, 624. https://doi.org/10.3390/cells9030624
247. Goldsmith, C., J.R. Rodríguez-Aguilera, I. El-Rifai, A. Jarretier-Yuste, V. Hervieu, O. Raineteau, *et al.* (2021). Low biological fluctuation of mitochondrial CpG and non-CpG methylation at the single-molecule level. *Sci. Rep.* **11**, 8032. https://doi.org/10.1038/s41598-021-87457-8
248. Morris, M.J., L.B. Hesson, and N.A. Youngson. (2020). Non-CpG methylation biases bisulphite PCR towards low or unmethylated mitochondrial DNA: Recommendations for the field. *Environ. Epigenet.* **6**, dvaa001. https://doi.org/10.1093/eep/dvaa001
249. Patil, V., C. Cuenin, F. Chung, J.R.R. Aguilera, N. Fernandez-Jimenez, I. Romero-Garmendia, *et al.* (2019). Human mitochondrial DNA is extensively methylated in a non-CpG context. *Nucleic Acids Res.* **47**, 10072–10085. https://doi.org/10.1093/nar/gkz762
250. Bellizzi, D., P. D'Aquila, T. Scafone, M. Giordano, V. Riso, A. Riccio, *et al.* (2013). The control region of mitochondrial DNA shows an unusual CpG and non-CpG methylation pattern. *DNA Res.* **20**, 537-547. https://doi.org/10.1093/dnares/dst029
251. Devall, M., D.M. Soanes, A.R. Smith, E.L. Dempster, R.G. Smith, J. Burrage, *et al.* (2023). Genome-wide characterization of mitochondrial DNA methylation in human brain. *Front. Endocrinol.* **13**, 1059120. https://doi.org/10.3389/fendo.2022.1059120
252. Parreno, V., V. Loubiere, B. Schuettengruber, M. Erokhin, B. Győrffy, M. Di Stefano, *et al.* (2024). Transient loss of Polycomb components induces an epigenetic cancer fate. *Nature*. https://doi.org/10.1038/s41586-024-07328-w
253. Maceda-Veiga, A., J. Figuerola, A. Martínez-Silvestre, G. Viscor, N. Ferrari, and M. Pacheco. (2015). Inside the Redbox: Applications of haematology in wildlife monitoring and ecosystem health assessment. *Sci. Total Environ.* **514**, 322-332. https://doi.org/10.1016/j.scitotenv.2015.02.004
254. Bossdorf, O., C.L. Richards, and M. Pigliucci. (2008). Epigenetics for ecologists. *Ecol. Lett.* **11**, 106-115. https://doi.org/10.1111/j.1461-0248.2007.01130.x
255. Li, S., T.L. Nguyen, E.M. Wong, P.A. Dugué, G.S. Dite, N.J. Armstrong, *et al.* (2020). Genetic and environmental causes of variation in epigenetic aging across the lifespan. *Clin. Epigenet.* **12**, 158. https://doi.org/10.1186/s13148-020-00950-1
256. Zhang, L. and J. Li. (2023). Unlocking the secrets: the power of methylation-based cfDNA detection of tissue damage in organ systems. *Clin. Epigenet.* **15**, 168. https://doi.org/10.1186/s13148-023-01585-8

257. Sigurpalsdottir, B.D., O.A. Stefansson, G. Holley, D. Beyter, F. Zink, M.Þ. Hardarson, *et al.* (2024). A comparison of methods for detecting DNA methylation from long-read sequencing of human genomes. *Genome Biol.* **25**, 69. https://doi.org/10.1186/s13059-024-03207-9
258. Bohers, E., P.J. Viailly, and F. Jardin. (2021). cfDNA sequencing: technological approaches and bioinformatic issues. *Pharm.* **14**, 596. https://doi.org/10.3390/ph14060596

Annexes

Annexe I

Signatures microbiennes du mucus et du sang des truites (*Salmo trutta*) sédentaires et migratrices des îles de Kerguelen

fishes

MDPI

Article

Skin and Blood Microbial Signatures of Sedentary and Migratory Trout (*Salmo trutta*) of the Kerguelen Islands

Sophia Ferchiou [1,†], France Caza [1,†], Richard Villemur [1], Jacques Labonne [2] and Yves St-Pierre [1,*]

[1] INRS-Centre Armand-Frappier Santé Biotechnologie, Laval, QC H7V 1B7, Canada
[2] UMR INRAE-UPPA, ECOBIOP, Université de Pau et des Pays de l'Adour, 64310 Saint-Pée-sur-Nivelle, France
* Correspondence: yves.st-pierre@inrs.ca; Tel.: +33-450-686-5354; Fax: +33-450-686-5501
† These authors share the first authorship.

Abstract: Our understanding of how microbiome signatures are modulated in wild fish populations remains poorly developed and has, until now, mostly been inferred from studies in commercial and farmed fish populations. Here, for the first time, we have studied changes in the skin and blood microbiomes of the *Salmo trutta* population of the volcanic Kerguelen archipelago located at the northern limit of the Antarctic Ocean. The Kerguelen Islands present a natural framework of population expansion and reveal a likely situation representing further climate change in distribution areas. Our results showed that *S. trutta* of the Kerguelen Islands has a microbiome signature distinct from those of salmonids of the Northern Hemisphere. Our study also revealed that the skin and blood microbiomes differ between sedentary and migratory *S. trutta*. While 18 phyla were shared between both groups of trout, independent of the compartment, 6 phyla were unique to migratory trout. Further analyses showed that microbiome signatures undergo significant site-specific variations that correlate, in some cases, with the peculiarity of specific ecosystems. Our study also revealed the presence of potential pathogens at particular sites and the impact of abiotic factors on the microbiome, most notably due to the volcanic nature of the environment. This study contributes to a better understanding of the factors that modulate the microbiome signatures of migratory and sedentary fish populations. It will also help to better monitor the impacts of climate change on the colonization process in the sub-Antarctic region.

Keywords: blood microbiome; skin microbiome; fish; *Salmo trutta*; migration; Kerguelen Islands; 16S rRNA

Key Contribution: This work highlighted the compartment-specific microbial signatures and the environmental influence on the microbiome signatures between migratory and sedentary trout of Kerguelen.

Citation: Ferchiou, S.; Caza, F.; Villemur, R.; Labonne, J.; St-Pierre, Y. Skin and Blood Microbial Signatures of Sedentary and Migratory Trout (*Salmo trutta*) of the Kerguelen Islands. *Fishes* **2023**, *8*, 174. https://doi.org/10.3390/fishes8040174

Academic Editors: Jesús L. Romalde and Giacomo Zaccone

Received: 23 January 2023
Revised: 8 March 2023
Accepted: 21 March 2023
Published: 24 March 2023

1. Introduction

The microbiota is now recognized as a key player in health and disease progression. Defining the microbiome signature, which includes nucleic acid originating from microorganisms, has thus become an essential component of the biomarker schematic in medicine and ecology. In clinical settings, for example, specific signatures will determine if a cancer patient will respond to particular therapies [1,2]. This progress has been greatly facilitated by the development of next-generation sequencing (NGS) technologies for analyzing 16S ribosomal RNA (rRNA) gene amplicons, which allows for rapid evaluation of microbial biodiversity while overcoming the limitations of cultivation-based methods. Despite these technical developments, our understanding of the microbiome in wild animals is only in its infancy. This is particularly true in fish populations, notably those inhabiting environments sensitive to pollution and climate change. Moreover, until now, studies of the fish microbiome have mostly focused on the gut microbiota and, to a lesser extent, on the

skin (mucosal microbiota). In fish, in particular, the skin mucus represents the first barrier defense against infectious stressors in the environment. The nonpathogenic skin microbial flora helps the immune system protect itself against pathogens [3,4]. Its composition depends on several factors, including host genetics and their surrounding environment. Captivity, pollution, and habitat transition are other factors that affect the microbiome signature of animals [5–7]. However, most microbiome studies in fish have been conducted in fish farms or experimental settings simulating freshwater-to-seawater transitions [8,9]. We still need to learn more about how the skin microbiome differs between migratory and sedentary wild fish populations. Considering the importance of the microbiome as a biomarker and the need to adopt less costly and invasive procedures, the concept of "circulating microbiome DNA" (cmDNA) has been developed as an alternative to studying the microbiome in clinical settings [10]. Since the middle of the 20th century, we have known that DNA fragments are present in the blood [11], but it is only in recent years that the advent of NGS methods has allowed us to better understand the origin of these circulating DNA fragments. We now know that blood contains a vast array of self and non-self DNA fragments originating from multiple tissues, including infected tissues, and that a significant percentage of the DNA within the blood originates from microorganisms [12–14]. Combined with the 16S rRNA approach, cmDNA analysis has thus become a central tool for studying an individual's health status and measuring its ability to respond to treatment or environmental stressors [15–19]. Several recent studies have applied this concept to study the hemolymphatic microbiome of bivalves and its changes in response to environmental stressors [20–22]. The existence of a blood microbiome is a concept that is now widely accepted in humans and animals (including pigs, cows, goats, rodents, camels, and dogs [21,23–29]. A blood microbiome has also been reported in fish and discussed in reviews [5,30–32]. The existence of a circulating microbiome has also been reported in invertebrates. In many cases, this has been applied to facilitate the detection of pathogens. The Kerguelen Islands (also known as the Desolation Islands) are located in the Southern Ocean just north of the polar front. Long-term monitoring studies have shown that this archipelago, which comprises more than 300 islands that cover more than 7000 km^2 and has almost 3000 km of shoreline, is particularly sensitive to global warming [33,34]. Previously devoid of freshwater fish, the Kerguelen Islands were populated at multiple sites with various stocks of fish over three decades (1962–1993). Overall, 22 successful imports were conducted, with eggs collected from 8 salmonid species in the Northern Hemisphere [35]. *Salmo trutta* (*S. trutta*) is among the different species that successfully colonized the largest number of watersheds following the early occurrence of alternative anadromous (e.g., migratory) species to pursue its life cycle in seawater [36]. Given its remoteness and limited anthropogenic activities, Kerguelen's salmonid populations thus provide a unique subpolar environment to study the impact of the environment and migratory activity on microbiome compartments and to better understand how climate change can impact these populations [37].

The objective of the present work was to define and compare the phylogenetic structure of the skin (mucus) and circulating (blood) microbiomes of migratory and sedentary *S. trutta* populations collected at different sites in the Kerguelen Islands. First, we assessed the overall composition of both the skin and blood microbiota in resident and migrating trout. We then proceeded to compare both skin and blood samples, as well as resident and migratory traits. We also analyzed site-specific variations to establish whether the local environment could trigger substantial contrasts in microbiota. Our study also revealed the presence of potential pathogens at certain sites and the impact of abiotic factors on the microbiome, most notably due to the volcanic nature of the environment. Finally, we further showed that FTA® Cards-based sampling is perfectly adapted for establishing mucosal and circulating 16S rRNA microbiome signatures, an interesting avenue for long-term monitoring programs in remote and sensitive polar environments.

2. Materials and Methods

2.1. Sample Collection

A total of 83 skin and blood microbiomes collected from 52 trout samples were analyzed (Table S1). Sedentary trout were captured by electrofishing in freshwater rivers, and migratory trout were captured by trolling (fly fishing). Immediately after capture, the fish were anesthetized, as described by Marandel et al. (2018) [38]. Blood was immediately withdrawn from the caudal vein using sterile nonheparinized syringes and spotted on Whatman 903™ Flinders Technology Associates filter paper (FTA® Cards) (Sigma–Aldrich, Oakville, ON, Canada). To avoid cross-contamination between samples, all samples were allowed to air dry and were stored individually in a plastic bag with a desiccant, as previously described [39]. Mucus samples were collected using a sterile scalpel blade by scraping along the fish's lateral line and were immediately spotted to cover an entire disc of the FTA cards. The same preservation method was applied as above. The care and use of field-sampled animals complied with the Government of France's animal welfare laws, guidelines, and policies (Comité d'Ethique), as approved by the Terres Australes et Antarctiques Françaises administration. All methods are reported using ARRIVE guidelines.

2.2. DNA Extraction, Preprocessing, and Sequencing

All procedures were conducted in a white room where pressure, temperature, and humidity were controlled to eliminate contaminants. Individual discs were cut from the FTA® Cards using a sterile 5.0 mm single round hole punch. Total DNA was isolated using the QIAamp DNA Investigator Kit (Qiagen, Hilden, Germany), according to the manufacturer's protocol. DNA was quantified in duplicate using a Quant-iT™ PicoGreen® dsDNA detection kit (Molecular Probes, Eugene OR, USA). Amplification of the 16S ribosomal RNA (rRNA) genes and 16S gene amplicon sequencing for all DNA samples were performed at the Centre d'Expertise et de Services Génome Québec (Montréal, QC, Canada) using the universal primers 341F (5′-CCTACGGGNGGCWGCAG-3′) and 805R (5′-GACTACHVGGGTATCTAATCC-3′) targeting the V3–V4 hypervariable regions [40]. Sequence libraries were prepared by Génome Québec with the TruSeq® DNA Library Prep Kit (Illumina, San Diego, CA, USA) and quantified using the KAPA Library Quantification Kit for Illumina platforms (Kapa Biosystems, MA, USA). Paired-end sequences were generated on a MiSeq platform PE300 (Illumina Corporation, San Diego, CA, USA) with the MiSeq Reagent Kit v3 600 cycles (Illumina, San Diego, CA, USA). The raw data files are publicly available on the NCBI Sequence Read Archive (PRJNA772886).

2.3. 16S rRNA Data Processing

Illumina sequence data (FASTQ files) were trimmed using Cutadapt (version 2.8, Uppsala, Sweden). The amplicon sequence variants (ASVs) were generated with the DADA2 pipeline (version 1.16.0, Stanford, CA, USA) [41] and subsequently analyzed within the R environment (R version 4.0.3, Vienna, Austria) [42]. Forward and reverse reads were then trimmed, filtered, and truncated with the filterAndTrim function. The error model (maxEE) was calculated for forward and reverse reads, and low-quality reads were removed. After denoising and merging, chimeric sequences (bimeras) were removed from the datasets. The minimum and maximum lengths were set at 400 bp and 428 bp, respectively. All reads had an average quality score of $\geq$30. The RDP (Ribosomal Database Project) 16 classifier database was used for ASV taxonomy assignment [43]. The RDP contains 16S rRNA sequences available from the International Nucleotide Sequence Database Collaboration (INSDC) databases and can accurately classify bacterial 16S rRNA sequences [44,45]. Archaea and unclassified ASVs at the phylum level (representing 4.7% of the total ASVs) were removed. The phyloseq (version 1.34.0), microbiomeSeq (version 0.1), microbiomeMarker (version 1.3.3) and vegan (version 2.6.4) R packages were used to characterize the microbial communities [46–49].

2.4. Statistical Analysis

The alpha diversity index, was calculated using the phyloseq R package [46]. The average values of each group were compared using Wilcoxon rank sum tests. Microbiota composition differences among groups were determined using multivariate analysis of variance with permutation (PERMANOVA) with 9999 permutations followed by pairwise permutation tests. We studied the functional content of the blood and skin microbiomes predicted from the KEGG database using the Piphillin tool (Piphillin server. http://piphillin.secondgenome.com/ (accessed on 1 April 2021)) [50]. Heatmaps were generated based on the relative abundance and constructed with the 30 most abundant genera. Linear discriminant analysis (LDA) identified the effect size (LEfSe) that differentiates the samples among these taxa. The threshold on the logarithmic score of the LDA analysis was set to 3.0. Differences in the overall bacterial community composition among specimens were determined based on the UniFrac distance and visualized by principal coordinates analysis (PCoA). Permutation multivariate analysis of dispersion (PERMDISP) was also conducted with the betadisper function to test for the homogeneity of multivariate dispersions (i.e., deviations from centroids) among the specimens.

3. Results

3.1. General View of the Mucosal and Circulating Bacterial Microbiome

A total of 83 samples were collected from the blood (n = 45) and skin mucus (n = 38) of sedentary and migratory trout captured at different sites of the Kerguelen Islands (Figure 1). Each sample was immediately stored on-site on FTA cards (Table S1).

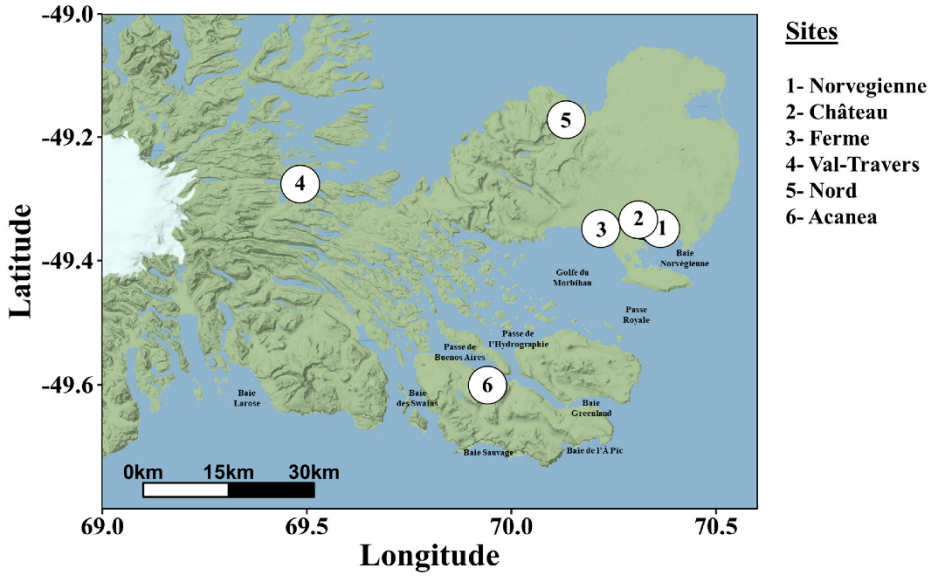

Figure 1. Map of the French subantarctic Kerguelen Islands showing the location of the rivers. Sedentary trout were collected from freshwater (FW), and migratory trout were collected from the mouth of the river (seawater (SW)).

For each sample, the cmDNA was determined by sequencing the V3-V4 hypervariable region of the 16S rRNA gene amplicons. A total of 1,976,043 paired-end sequences passed quality filtering (23,808 ± 14,925 per sample). Amplicon sequence variants (ASVs) were generated from 12,985 high-quality reads, and 89.2% of samples contained more than 10,000 reads. We first examined the overall skin and blood microbiomes at the phylum level, focusing on phyla representing at least 2% of all ASVs. Individual variations in

the circulating and mucosal microbiomes are shown in Figure S1. Our results showed that the microbiomes of *S. trutta* were dominated by *Pseudomonadota* (~45–75%) and *Bacteroidota* (~5–11%) and, to a lesser extent, *Parcubacteria* (~0.1–20%), *Bacillota* (~1–9%), *Actinomycetota* (~3–6%), and *Planctomycetota* (~2–5%) (Figure 2A). *Parcubacteria*, which has been described in the seawater of polar regions [51], was more abundant in the blood (17.1%) than in the mucus (0.3%) ($p = 0.014$ (LefSE)). *Bacillota* and *Chloroflexota* were also significantly more abundant in the blood of the migratory trout compared to the sedentary population ($p < 0.05$ linear discriminant analysis effect size (LEfSE)). At the genus level, we found a dominance of genera under *Pseudomonadota*, the most abundant being the *Aliivibrio* genus, and to a lesser extent, bacterial DNA derived from *Sphingomonas*, *Pseudoalteromonas*, *Yersinia*, and *Aquabacterium*, among others (Figure 2B). Concerning differences between the skin and blood microbiomes, we found that the *Corynebacterium*, *Streptococcus*, *Acidovorax*, and *Acinetobacter* genera were found only in the blood, but not in the skin mucus. In contrast, *Psychrobacter*, *Yersinia*, and *Aeromonas* were only found in the circulating microbiome. Discriminatory genera between the blood and mucus are shown in Figure S2 (LDA score). *Aliivibrio* had the highest LDA score in the mucus, and *Flavobacterium* dominated the blood microbiome. Overall, these results indicate that the bacterial microbiome signature differs between the skin and blood microbiomes.

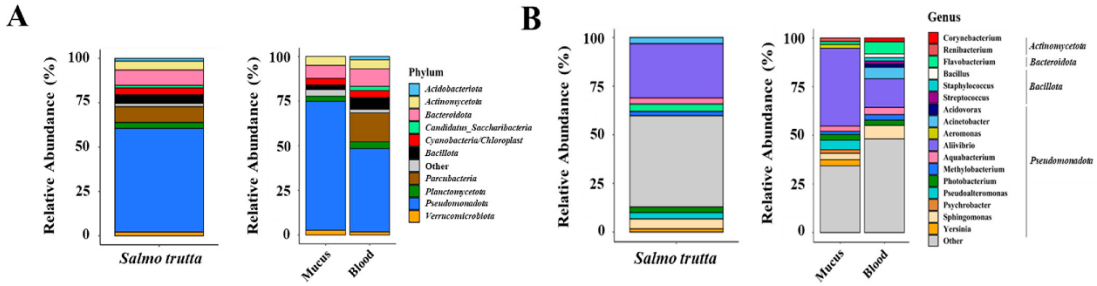

Figure 2. Phylum and genus level analysis of circulating and mucosal bacterial DNA. (**A**) Phylum and (**B**) genus levels were analyzed for all samples (**left**) and mucosal and circulating compartments (**right**) were analyzed in brown trout (*S. trutta*). Phylum and genus with a relative abundance of ≤1.5% are represented as "Other".

3.2. Comparative Analysis between Sedentary and Migratory S. trutta

We next examined whether the skin and blood microbiome signatures differ between sedentary and migratory trout. We first compared the alpha diversity between migratory and sedentary populations using three diversity indices: richness, the Shannon index, and Pielou's evenness. Globally, we found no significant differences in the alpha diversity between the two populations for either the skin or blood microbiome (Figure 3). Moreover, alpha diversity was also not dependent on sex differences (Figure S3). Further analyses, however, revealed significant differences at the phylum and genus levels in the composition of the microbiomes between the sedentary and migratory trout. The high abundance of rare ASVs in the blood of migratory trout was reflected by the Chao1 index (Figure 4A).

Focusing on unique and shared phyla, we found that 18 were shared between sedentary and migratory trout, independent of the compartment. A total of 7 phyla (*BRC1*, *Chlorobiota*, *Elusimicrobiota*, *Ignavibacteriota*, *Lentisphaerota*, *Poribacteria*, and *Mycoplasmatota)* were unique to migratory trout (Figure 4B). Another 2 phyla (*Spirochaetota* and *SR1*) were unique to the mucus of both populations, and 1 phylum (*Chlorobiota*) was uniquely found in the blood, but not in the mucus. A clear dominance of unique bacteria in the mucosal microbiome of migratory trout was also found at the genus level (Figure 4C). Overall, migratory trout had more than six times the number of unique genera in their compartments compared to sedentary trout (233 versus 39). This result is consistent with a multivariate analysis (PERMANOVA) showing that the global composition of the microbiome was

significantly different between the two populations (UniFrac PERMANOVA, F(1, 82) = 1.44, $p = 0.02$). Principal coordinate analysis (PCoA) based on the unweighted UniFrac distance was carried out for both migratory and sedentary trout (Figure S4).

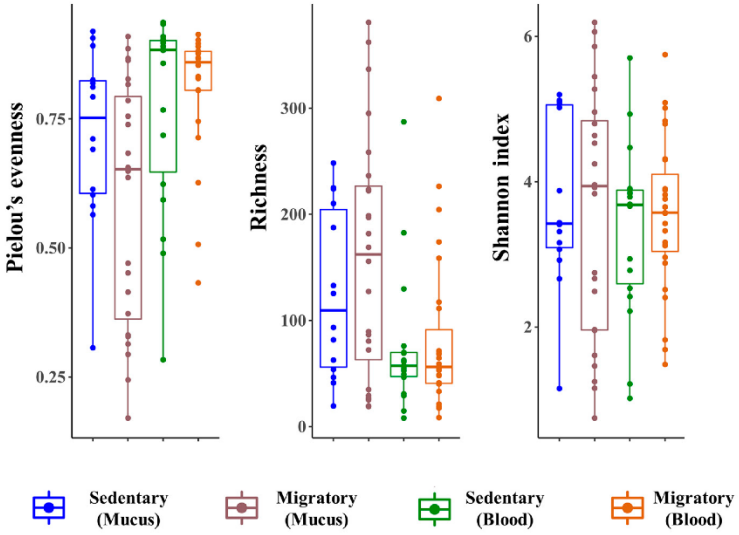

Figure 3. Alpha diversity analysis of both *S. trutta* phenotypes for circulating and mucosal microbiomes. Species evenness, observed richness and Shannon diversity indexes were calculated for each group. No significant differences between migratory and sedentary specimens for the same compartment were observed.

To further study the differences between migratory and sedentary trout, we examined the distribution of phyla and genera. At the phylum level, we found that the skin microbiome of sedentary trout contained significantly ($p < 0.05$) higher DNA fragments of *Cyanobacteria/chloroplasts* and *Verrucomicrobiota* than that of migratory trout (Figure 5). In contrast, the latter had higher levels of *Bacillota* in both the skin and blood microbiomes. At the genus level, sedentary trout had a higher abundance of *Aquabacterium* ($p < 0.05$), *Flavobacterium* ($p < 0.01$), *Luteolibacteria* ($p < 0.01$), and *Sphingomonas* ($p < 0.05$) than the skin microbiome of migratory trout (Figure 6). In contrast, the skin microbiome of migratory trout had higher levels of *Aeromonas* ($p < 0.05$) and *Yersinia* ($p < 0.05$) (Figure 6). Other differences in the skin microbiome that approached conventional levels of significance ($p < 0.10$) were also observed in the case of *Methylobacterium* and *Pseudoalteromonas*. Taken together, these results indicate that the skin microbiome signatures differed between migratory and sedentary trout.

3.3. Site-Specific Variations

A general overview of individual site-specific variations for phyla that constituted at least 1.5% of the total phylum is shown in Figure 7. Independent of the sampling site and the compartment, *Pseudomonadota* was the dominant phylum in the majority of samples, especially in the skin microbiome. This abundance of *Pseudomonadota* was almost absolute in samples collected at Rivière-du-Nord, independent of the population and the compartment. The presence of *Parcubacteria* was also omnipresent at all sites, except at Rivière-du-Nord. Focusing on the 30 most abundant genera at the genus level, we found that *Aliivibrio* was abundant in Rivière-du-Nord, in both sedentary and migratory trout, and in the skin microbiome of migratory trout in Val-Travers (Figure S5). Compared to other sites, at Rivière-du-Nord and other sites, the skin microbiome was particularly rich in psychrophilic genera in migratory trout (Figure S6). We also paid special attention

to bacterial genera associated with the degradation of hydrocarbons, such as polycyclic aromatic hydrocarbons (PAHs). We found that migratory trout sampled at Acaena were particularly rich in this regard compared to those at other sites (Figures S7 and S8) [52]. Migratory trout from this site also had skin and blood microbiome signatures that were abundant in potentially pathogenic genera compared to other migratory or sedentary trout (Figure S9). Taken together, these results showed that both skin and blood microbiome signatures are site-dependent and may reveal specific environmental conditions.

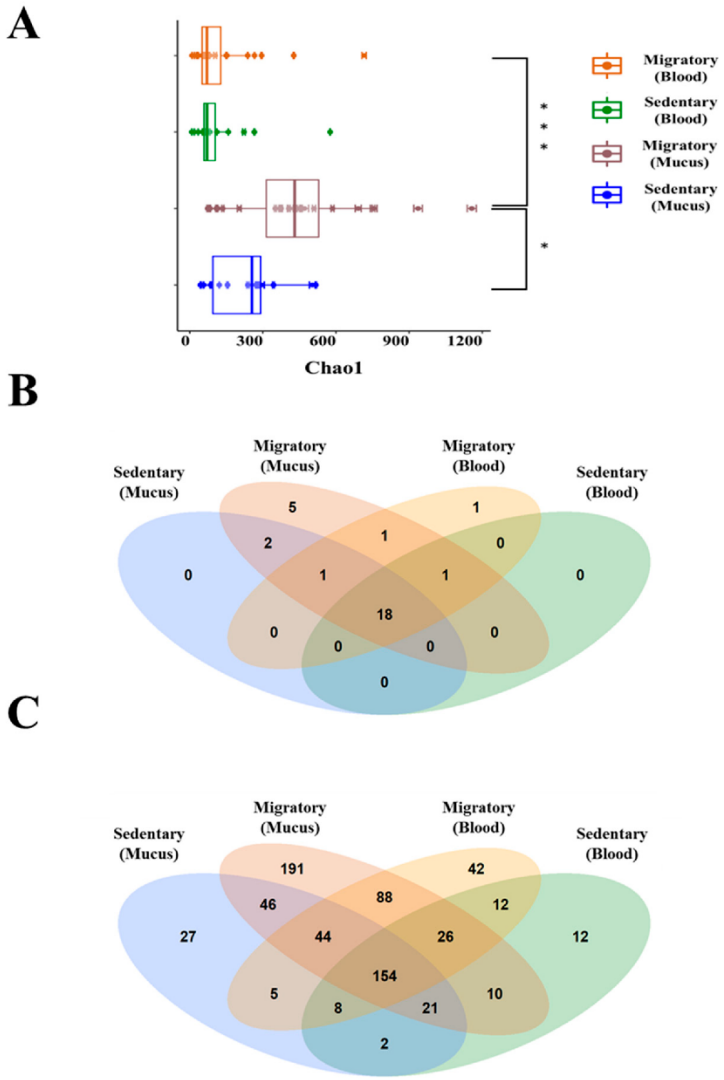

Figure 4. Comparisons between migratory and sedentary trout in both compartments. (**A**) The Chao1 index was calculated for each group. Venn diagrams showing the number of unique and shared (**B**) bacterial phyla and (**C**) genera in mucosal and circulating compartments in both sedentary and migratory brown trout (*S. trutta*). Note: * $0.01 < p \leq 0.05$; *** $p \leq 0.001$.

3.4. Functional Analysis of the CmDNA

Predictive functional analysis from 16S rRNA profiling of cmDNA is routinely used to link the abundance of specific taxa with metabolic profiles [50,53,54]. To further explore

the distinctive traits between sedentary and migratory *S. trutta*, we studied the predicted metabolic pathways based on 16S rRNA. This analysis revealed two major differences. The first is the distinct difference in the metabolic profiles of migratory versus sedentary trout (Figure 8). We found a clear lipid metabolism shift consistent with previous studies in the salmonids [55]. A similar shift has recently been observed in lipid metabolism in the skin microbiome of *S. salar* during experimental seawater acclimatization [8]. Among the other potential differences between the sedentary and migratory microbial communities in terms of metabolism, we found a generally higher amino metabolism and biosynthesis of beta-lactams in the latter form, consistent with previous findings by Dehler et al. [8].

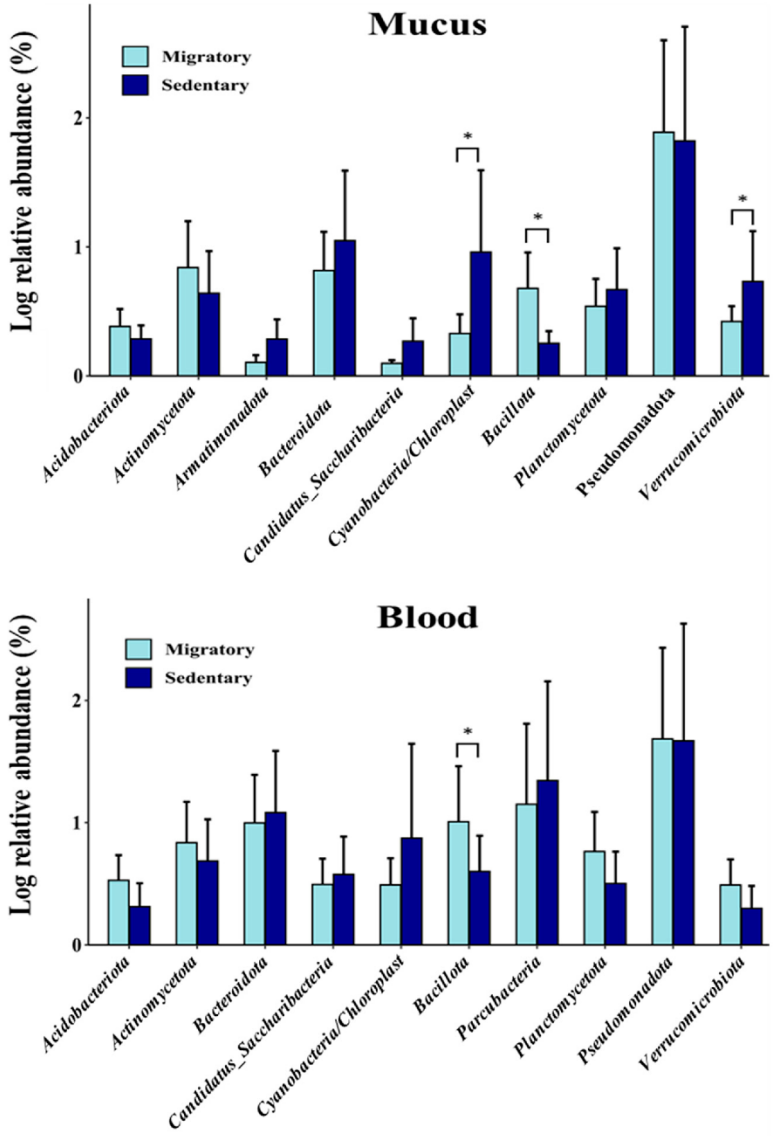

Figure 5. Relative abundance (%) of the top 10 bacterial phyla in circulating and mucosal microbiomes in *S. trutta*. Bar graph analysis displays the logarithm (base 10) of the relative abundance (mean ± SE). White and black colors represent migratory and sedentary brown trout, respectively. Note: * $0.01 < p \leq 0.05$.

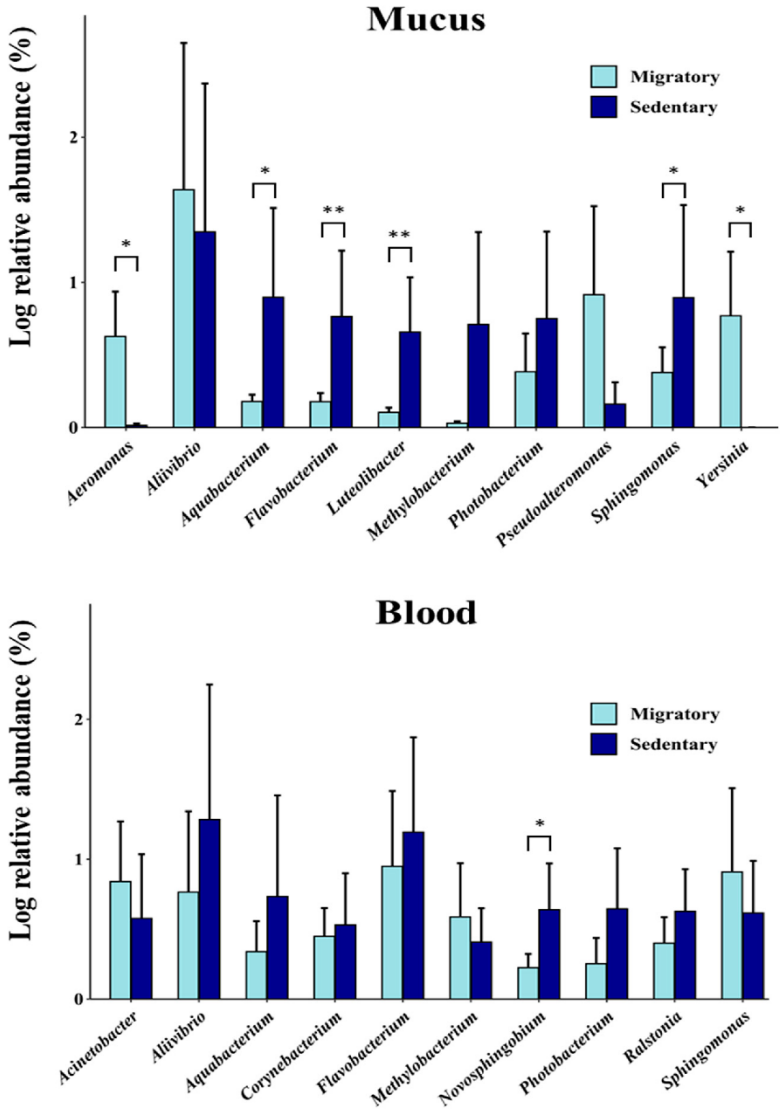

Figure 6. Relative abundance (%) of the top 10 bacterial genera in circulating and mucosal microbiomes in *S. trutta*. Bar graph analysis displays the logarithm (base 10) of the relative abundance (mean ± SE). White and black colors represent migratory and sedentary brown trout, respectively. Note: * $0.01 < p \leq 0.05$; ** $0.001 < p \leq 0.01$.

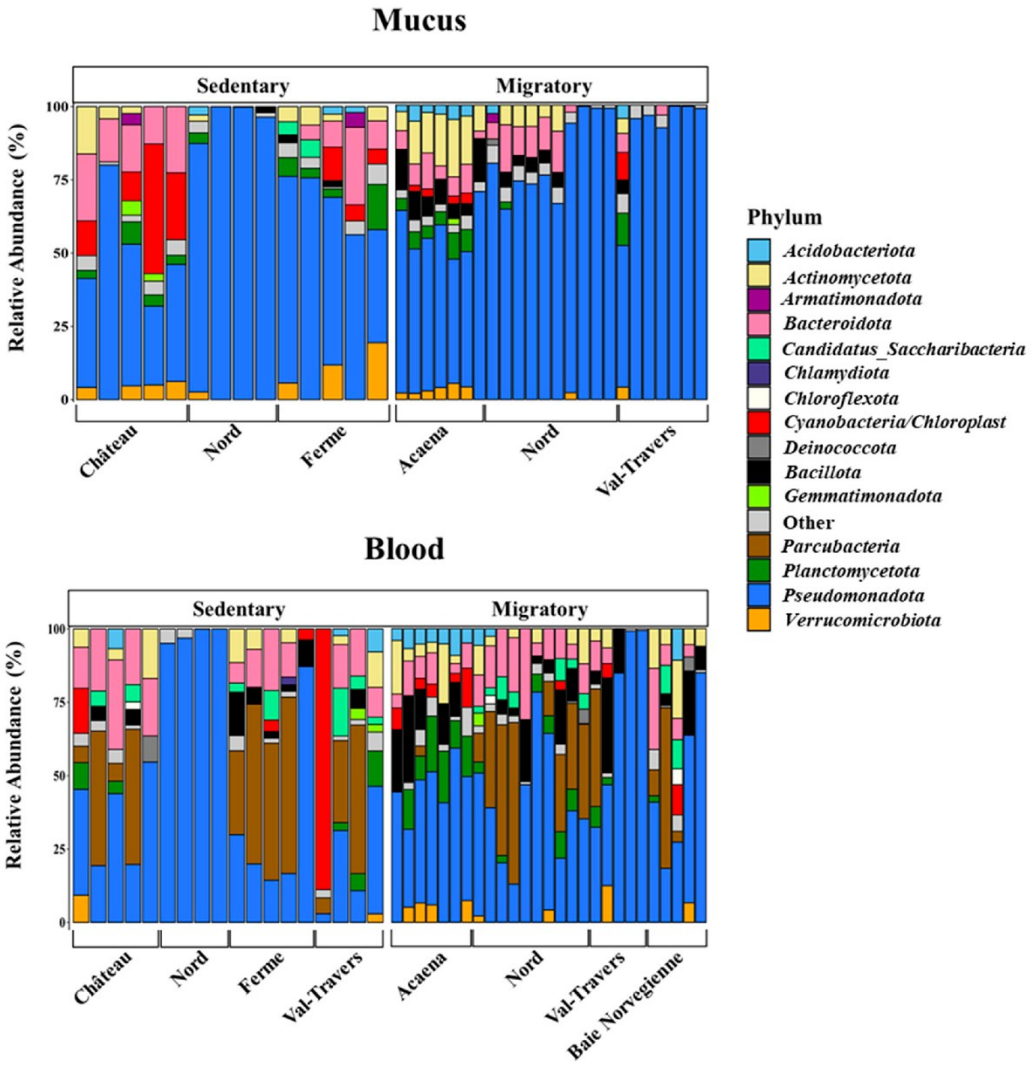

Figure 7. Inter-individual variability of circulating and mucosal microbiomes at the phylum level. Bar plots display the major phyla between sedentary (**left**) and migratory (**right**) brown trout (*S. trutta*) collected at different sites. Phyla with a relative abundance of ≤1.5% are represented as "Other".

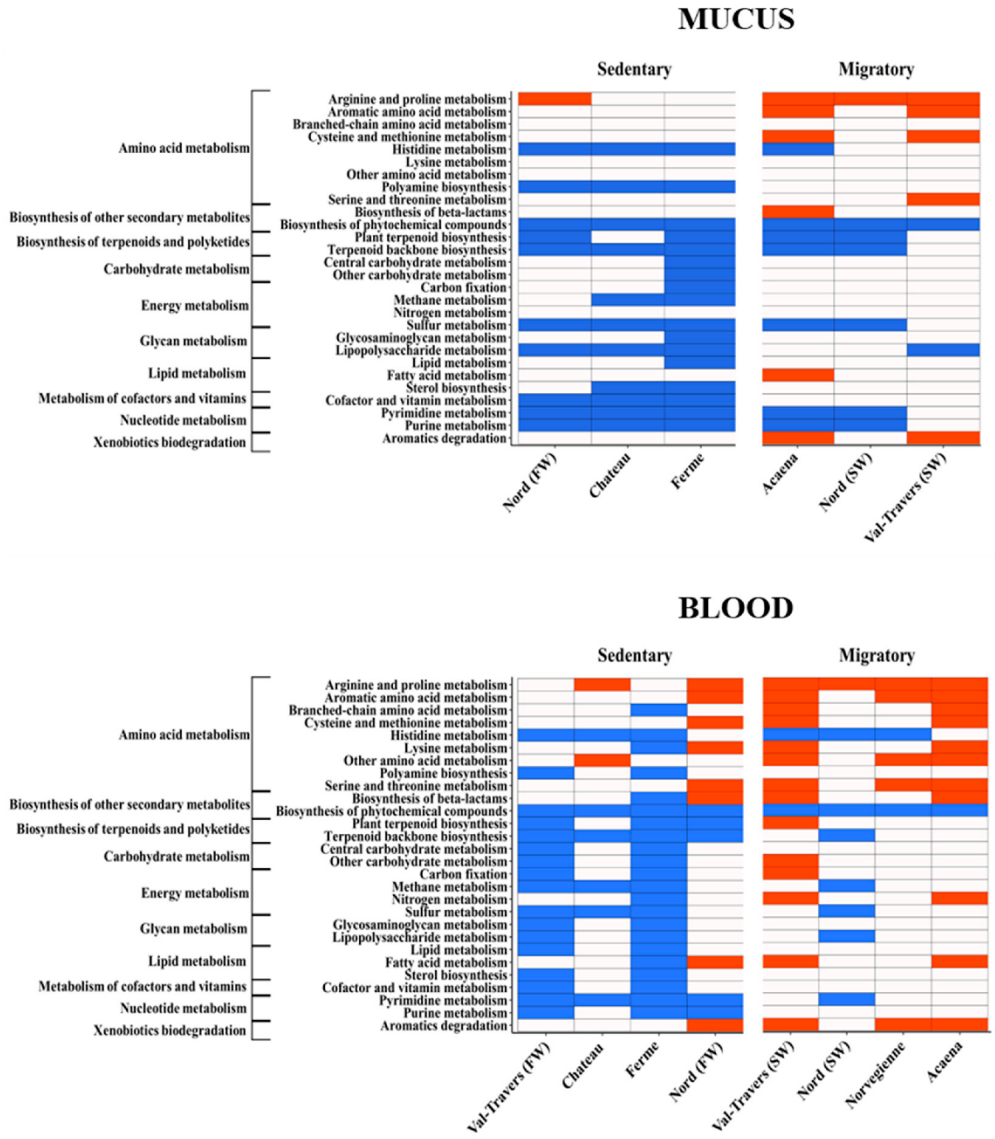

Figure 8. Heatmaps show the relative abundance (natural logarithm base) of metabolic pathways based on 16S rRNA data in migratory and resident trout collected from different sites.

4. Discussion

In the present work, we compared the skin and blood microbiomes of the Kerguelen Islands' sedentary and migratory S. trutta. We have shown that the skin and blood microbiome signatures (1) differ at both the phylum and genus levels, (2) differ between migratory and sedentary trout, and (3) are site-dependent. This is the first study comparing the skin and blood microbiomes of wild sedentary and migratory salmonids and the first characterization of the circulating blood microbiome in a fish species. Finally, from a methodological perspective, our logistically simple and minimally invasive sampling platform offers an alternative approach for the long-term monitoring of fish populations in sensitive and remotely polar ecosystems.

Defining microbiome signatures is now recognized as a key step toward identifying factors shaping animal-associated microbiomes, including genetic (species-specific) and environmental factors. In teleost, in particular, the gut, mucosal, or blood microbiome is increasingly recognized as an important biomarker to detect disturbances in ecosystems or aquacultures. However, studies on the microbiome composition of wild fish populations remain relatively scarce and have, until now, mostly focused on the gut- and skin-associated microbiomes in fish farms. In the case of salmonids, Lokesh and Kiron (2016) have shown that the skin-associated microbiome of Atlantic salmon (*S. salar*) in the transition from freshwater to seawater in Norway was dominated by *Pseudomonadota*, *Bacteroidota*, and *Bacillota* [56]. Our data also revealed an abundance of *Pseudomonadota* and *Bacteroidota* in the skin-associated microbiome of both migratory and sedentary *S. trutta* of the Kerguelen Islands. This dominance was also found in the blood microbiome. In our study, however, the dominance of *Pseudomonadota* was not related to the abundance of the *Oleispira* genus, as reported for *S. salar* [8]. In fact, we did not find a dominance (or even a detection, for that matter) of *Oleispira* in the skin mucus (or in the blood) of migratory trout.Another difference from the study reported for *S. salar* is that we did not find a dominance of *Bacillota* in the skin-associated microbiome of sedentary trout [8]. Instead, we found that *Bacillota* were more abundant in migratory *S. trutta*. This was true for both mucosal and blood microbiomes. This increase in *Bacillota* in migratory *S. trutta*, which was driven by the presence of *Aerococcus*, *Bacillus*, *Hathewaya*, and *Clostridium_sensu_stricto* genera, which differed from the *Bacillota* found in the sedentary trout, which mainly included *Staphylococcus* and *Lactobacillus* genera. We also found an increased abundance of *Verrucomicrobiota* and *Cyanobacteria* in the skin mucus of sedentary trout. This shift was not found in the blood microbiome. Other bacteria previously found in the skin mucus of *S. salar*, such as *Thalassomonas*, *Psychromonas*, *Agarivorans*, *Pseudoalteromonas*, *Marinomonas*, *Arcobacter*, *Perlucidibaca*, and *Octadecabacter*, were also absent in *S. trutta*. However, a clear difference at the phylum level was noted by the abundance of *Actinomycetota* and *Parcubacteria* in the blood microbiome, but not in the mucus, of both migratory and sedentary trout. This signature is, in fact, similar to a recent metagenomic study showing that bacteria enriched in seawater in polar regions were mostly *Pseudomonadota*, *Actinomycetota*, *Bacteroidota*, and *Parcubacteria* [50], the latter being one of the most abundant phyla in intestinal fish microbiota [57,58]. Interestingly, we also found a similar signature in the hemolymphatic (blood-like) microbiome of mussel species (Figure S10) that inhabit the coastal marine ecosystems of the Kerguelen Islands [59]. These results suggest the existence of a possible "Kerguelen signature," at least at the phylum level, driven by the environmental conditions of the Kerguelen Islands. Metagenomic profiling using the 16S rRNA microbiome signature is a cost-effective and rapid method to screen for candidate pathogens associated with infectious and noninfectious diseases in a given population [16,60–63]. Here, we paid particular attention to this aspect, given the history of salmonids in the Kerguelen Islands and their isolation from other salmonid populations. Our data revealed the presence of *Aliivibrio* and *Pseudomonas* within the skin mucus and blood microbiomes of all trout from the Kerguelen Islands. These genera include several pathogenic strains, such as *Aliivibrio salmonicida*, a common pathogen found in fish farms [64]. Our study also revealed the presence of *Renibacterium* in the skin microbiome of migratory trout at Acaena. This genus includes *Renibacterium salmoninarum*, the causative agent of bacterial kidney disease, a deadly disease affecting wild and cultured salmonids worldwide [65]. This pathogen was introduced in 1987 following the importation of Chinook salmon from the United States into the Armor basin. This was one of the reasons why the Aquasaumon Sea ranching project at Armor was abandoned [66]. There is a possibility that the bacteria have spread, since infected juveniles escaped from Armor in 1987. Moreover, Artic chars, kept in the Armor Hatchery, were released into the nearby Lac des Fougères in 1991 [35,67]. As of 2012, no signs of the disease have been observed [35]. We confirmed the presence of DNA derived from this bacterium by PCRs in mucosal and blood samples of brown trout collected in the Acaena river (Figure S11). Among the other sites that were distinguishable was

Rivière-du-Nord. The microbiome of either sedentary or migratory trout showed a unique signature. This was generally apparent in the blood microbiome of sedentary trout, which were dominated by two genera: *Aliivibrio* and *Photobacterium*. The dominance of *Aliivibrio* was also found in the skin microbiome. Whether such dominance of *Aliivibrio* reveals the presence of *Aliivibrio salmonicida*, a common pathogen known to cause cold-water vibriosis in salmonids [68], is certainly an issue that warrants further investigation. This pathogen, found mainly in estuaries, is usually found in high amounts in the blood of moribund fish. ASVs corresponding to *Aliivibrio salmonicida* were only found at Rivière-du-Nord, while all ASVs from other sites corresponded to *Aliivibrio logei*, a commonly found genus in the skin and gut microbiota [69]. Interestingly, the sedentary trout sampled at Rivière-du-Nord harbored an almost identical metabolic profile to that of migratory trout [70]. However, it is important to note that the 16S method does not allow for the identification of pathogens per se, but represents a rapid means to screen for potential pathogens and expression of virulence genes in subsequent analyses. Moreover, the presence of blood DNA fragments of bacterial pathogens does not necessarily reflect the onset of a disease. Rather, it provides a rapid, ethical, and sensitive means to signal their presence. The idea of a circulating microbiome is a concept increasingly studied in humans for identifying biomarkers in a clinical context. Despite all the precautions associated with the collection of samples, the fact remains that precautions are essential to minimize the impact of contaminants in the interpretation of the results [71–73]. These precautions are even more important when this concept is applied in environmental ecology, particularly in an inhospitable environment, such as the subantarctic islands such as those of Kerguelen. Despite the precautions we took during sampling, including proper aseptic cleaning methods, the use of sterile equipment, no template (water) controls, the use of FTA blank cards (and adjacent punches on the sampled cards), as well as the use of laboratories, materials, and equipment specifically dedicated to the preparation of DNA, it is necessary to remain critical in the interpretation of the results. This is particularly the case in studies that provide a snapshot of the microbiome, as in this case, and this is why it is important to carry out spatiotemporal analyzes and to carry out the validation of certain unexpected results, such as the presence of genera commonly associated with pathogenic species of interest, such as *Renibacterium salmoninarum*, which we found at specific sites in the Kerguelen Islands. Without a doubt, the use of logistically simple DNA sampling and preservation methods that minimize contamination in the field are useful tools for such future studies. Overall, our study may help better evaluate the impact of specific microbial structures on the fitness-related traits of specific populations, including their dispersal and reproductive abilities. Indeed, their presence in pathogenic strains would imply a higher energy expenditure on the immune system and a possible eco-evolutionary effect on MHC-related genes. For instance, MHC genes are highly homozygous in the Val Travers population, which is quite unusual compared to the data available in the literature. This could be partly related to inbreeding or the relaxation of selective pressures on pathogens [74].

Our data further revealed that another type of information that can be obtained from microbiome-based signatures is related to the physicochemical characteristics of the ecosystem. A clear example is the abundance of hydrocarbon degrader genera within the microbiomes of migratory trout sampled at Acaena. We hypothesize that their presence at the mouth of the Acaena River is possibly due to the nearby presence of multiple lignite deposits, also called "brown coal" at the Ravin du Charbon and the Ravin Jaune near the Acaena River [75].

To our knowledge, this is one of the rare studies of the blood microbiome of fish. Historically, most studies on the microbiome composition were carried out on the gut microbiome, with emphasis on their role in nutrition and related diseases, including inflammatory diseases. However, advances in sequencing NGS technologies have shown that plasma DNA fragments originate from multiple organs, providing an opportunity to obtain a systemic view of tissue damage. It is now possible to determine the exact tissue origin of plasma DNA fragments by examining footprints of consensus sequences

specific for transcription factors [76]. These findings have contributed to the emerging concept of the circulating microbiome and subsequent studies showing that the blood contains a rich source of microbial DNA to assess the host's health status [12,13,77]. As the blood microbiome originates from multiple tissues [78,79], the possibility of using a single drop of blood for monitoring a much broader microbial diversity within a host opens the door for easier monitoring and the understanding of factors that contribute to shaping the microbiome in aquatic species (as well as terrestrial species, for that matter), most notably in response to environmental stressors, including climate change.

Finally, we would like to briefly discuss the sampling approach used in our study. This study and our previous work on bivalves indicate that FTA® card-based sampling is perfectly adapted for establishing skin and blood (or hemolymphatic) 16S rRNA microbiome signatures. The efficacy of FTA® cards as a stable means to preserve DNA samples, even at room temperature, has been well documented [39]. Such a minimally invasive and ethical (nonlethal) sampling procedure is particularly well adapted for long-term monitoring programs in remote areas and for limiting the impact of large cohort studies on a given population inhabiting, for example, natural reserves (such as the Kerguelen Islands), for endangered species, or for storage and transport for fieldwork in areas where proper conditions for RNA preservation are challenging to achieve [80]. Sampling using FTA® cards is gaining momentum as it is compatible with basic nucleic acid-based detection methods. It has been used, for example, for molecular diagnosis, the detection of viruses, etc. [81,82]. It is particularly useful for safely transporting infectious material, which is rapidly inactivated upon binding the nucleic acid to the chemically modified paper [80]. This low-cost method is logistically simple (without the need to maintain a cold chain for sample integrity) and is ideally adapted for biobanking.

5. Conclusions

In conclusion, we have shown that migratory and sedentary trout of the Kerguelen Islands exhibit unique microbiome signatures compared to other salmonid populations reported in the Northern Hemisphere. It will be interesting to study the impacts of these microbial shifts on host physiology and how these signatures may change in response to climate change and the colonization process of salmonids in this unique ecosystem. This work also revealed the presence of potential pathogens at some sites and highlighted the impact of environmental factors on the microbiome. Finally, this study showed that FTA® Cards-based sampling is adapted for research in remote regions for establishing mucosal and circulating 16S rRNA microbiome signatures.

Supplementary Materials: The following supporting information can be downloaded at: https://www.mdpi.com/article/10.3390/fishes8040174/s1, Figure S1: Individual variations in the circulating and mucosal microbiomes at the phylum level; Figure S2: Discriminant genera between the circulating and mucosal compartments; Figure S3: Alpha diversity analysis of mucosal and circulating microbiomes in (A) sedentary and (B) migratory brown trout (*S. trutta*); Figure S4: Principal Coordinates Analysis (PCoA) of bacterial DNA bacterial communities in both sedentary and migratory brown trout (*S. trutta*); Figure S5: Heatmaps showing relative abundance (%) of the top 30 bacterial genera of mucosal and circulating microbiomes between sedentary and migratory brown trout (*S. trutta*); Figure S6: Presence of psychrophilic bacterial genera isolated from Kerguelen sites and compared to Poli et al. (2017) identification of psychrophilic bacteria; Figure S7: Presence of Kerguelen bacterial genera commonly associated to oil spills (cited more than four times in different scientific papers) based on Hedaoo et al. (2018); Figure S8: Presence of Kerguelen bacterial genera known to degrade alkanes, phenols and phenanthrene which can be used as biomarkers for PAHs detection, based on Kuchi et al. (2021); Figure S9: Presence of potentially pathogenic bacterial genera found at different sites in Kerguelen; Figure S10: Bacterial cmDNA profiles in blue mussels (*Mytilus platensis*) and brown trout (*S. trutta*) collected at the mouth of the Norvegienne river; Figure S11: Amplified fragments shown on 1.5% agarose gel electrophoresis; Table S1: Characteristics of brown trout (*S. trutta*) collected at different sites at Kerguelen Islands.

Author Contributions: F.C.: Conceptualization, data curation, formal analysis, investigation, methodology, validation, visualization, writing—original draft, writing—review and editing; S.F.: conceptualization, data curation, formal analysis, investigation, methodology, validation, visualization, writing—original draft, writing—review and editing; R.V.: conceptualization, research, methodology, validation, writing—review and editing; J.L.: conceptualization, data curation, investigation, methodology, resources, validation, writing—review and editing; Y.S.-P.: conceptualization, acquisition, analysis, methodology, project administration, resources, supervision, validation, visualization, writing—original draft, writing—review and editing. All authors have read and agreed to the published version of the manuscript.

Funding: This research was funded by the National Science and Engineering Research Council of Canada (RGIN-2019-06607) and the Institut Polaire Paul-Émile Victor. This study is part of the Zone Atelier et Terres Australes LTSER.

Institutional Review Board Statement: The care and use of experimental animals complied with the French environmental and animal welfare laws, guidelines, and policies, as approved by the ethical committee for birds and fishes in the French region Nouvelle Aquitaine (CEEA073, authorization APAFIS#16249-201807241223324v3, project name "Ecologie Evolutive de la Colonisation des Îles Kerguelen par les Salmonidés").

Data Availability Statement: The raw data files used in this study are publicly available on the NCBI Sequence Read Archive (PRJNA772886).

Acknowledgments: This research was performed in the Kerguelen Islands, with the logistic support of the French Polar Institute Paul-Emile-Victor (IPEV). The authors would like to thank all the personnel from the IPEV and the Terres Australes et Antarctiques Françaises (TAAF) for their help and hospitality during our stay. The authors would also like to thank Jean-Pierre Féral and Thomas Saucède and the PROTEKER team for their expert advice and technical support and Jep Lokesh for helpful discussions on the manuscript. The authors would also like to thank Marlène Fortier for her excellent technical support and Stéphane Betoulle for insightful discussions and helping in the organization of the project.

Conflicts of Interest: The authors declare that they have no known competing financial interest or personal relationships that could have appeared to influence the work reported in this paper.

References

1. Chen, H.; Ma, Y.; Liu, Z.; Li, J.; Li, X.; Yang, F.; Qiu, M. Circulating microbiome DNA: An emerging paradigm for cancer liquid biopsy. *Cancer Lett.* **2021**, *521*, 82–87. [CrossRef] [PubMed]
2. Ignatiadis, M.; Sledge, G.W.; Jeffrey, S.S. Liquid biopsy enters the clinic—Implementation issues and future challenges. *Nat. Rev. Clin. Oncol.* **2021**, *18*, 297–312. [CrossRef] [PubMed]
3. Cabillon, N.A.R.; Lazado, C.C. Mucosal barrier functions of fish under changing environmental conditions. *Fishes* **2019**, *4*, 2. [CrossRef]
4. Lowrey, L.; Woodhams, D.C.; Tacchi, L.; Salinas, I. Topographical mapping of the rainbow trout (*Oncorhynchus mykiss*) microbiome reveals a diverse bacterial community with antifungal properties in the skin. *Appl. Environ. Microbiol.* **2015**, *81*, 6915–6925. [CrossRef] [PubMed]
5. Tarnecki, A.M.; Brennan, N.P.; Schloesser, R.W.; Rhody, N.R. Shifts in the skin-associated microbiota of hatchery-reared common snook Centropomus undecimalis during acclimation to the wild. *Microb. Ecol.* **2019**, *77*, 770–781. [CrossRef]
6. Uren Webster, T.M.; Consuegra, S.; Hitchings, M.; Garcia de Leaniz, C. Interpopulation variation in the Atlantic Salmon microbiome reflects environmental and genetic diversity. *Appl. Environ. Microbiol.* **2018**, *84*, e00691-18. [CrossRef]
7. Uren Webster, T.M.; Rodriguez-Barreto, D.; Castaldo, G.; Gough, P.; Consuegra, S.; de Leaniz, C.G. Environmental plasticity and colonisation history in the Atlantic salmon microbiome: A translocation experiment. *Mol. Ecol.* **2020**, *29*, 886–898. [CrossRef]
8. Dehler, C.E.; Secombes, C.J.; Martin, S.A. Seawater transfer alters the intestinal microbiota profiles of Atlantic salmon (*Salmo salar* L.). *Sci. Rep.* **2017**, *7*, 13877. [CrossRef]
9. Rudi, K.; Angell, I.L.; Pope, P.B.; Vik, J.O.; Sandve, S.R.; Snipen, L.G. Stable core gut microbiota across the freshwater-to-saltwater transition for farmed Atlantic salmon. *Appl. Environ. Microbiol.* **2018**, *84*, e01974-17. [CrossRef]
10. Whittle, E.; Leonard, M.O.; Harrison, R.; Gant, T.W.; Tonge, D.P. Multi-method characterization of the human circulating microbiome. *Front. Microbiol.* **2019**, *9*, 3266. [CrossRef]
11. Mandel, P.; Metais, P. Nuclear Acids in Human Blood Plasma. *C. R. Seances Soc. Biol. Fil.* **1948**, *142*, 241–243. [PubMed]
12. Blauwkamp, T.A.; Thair, S.; Rosen, M.J.; Blair, L.; Lindner, M.S.; Vilfan, I.D.; Kawli, T.; Christians, F.C.; Venkatasubrahmanyam, S.; Wall, G.D.; et al. Analytical and clinical validation of a microbial cell-free DNA sequencing test for infectious disease. *Nat. Microbiol.* **2019**, *4*, 663–674. [CrossRef] [PubMed]

13. Hong, D.K.; Blauwkamp, T.A.; Kertesz, M.; Bercovici, S.; Truong, C.; Banaei, N. Liquid biopsy for infectious diseases: Sequencing of cell-free plasma to detect pathogen DNA in patients with invasive fungal disease. *Diagn. Microbiol. Infect. Dis.* **2018**, *92*, 210–213. [CrossRef]
14. Kowarsky, M.; Camunas-Soler, J.; Kertesz, M.; De Vlaminck, I.; Koh, W.; Pan, W.; Martin, L.; Neff, N.F.; Okamoto, J.; Wong, R.J.; et al. Numerous uncharacterized and highly divergent microbes which colonize humans are revealed by circulating cell-free DNA. *Proc. Natl. Acad. Sci. USA* **2017**, *114*, 9623–9628. [CrossRef] [PubMed]
15. Amar, J.; Lange, C.; Payros, G.; Garret, C.; Chabo, C.; Lantieri, O.; Courtney, M.; Marre, M.; Charles, M.A.; Balkau, B.; et al. Blood microbiota dysbiosis is associated with the onset of cardiovascular events in a large general population: The D.E.S.I.R. study. *PLoS ONE* **2013**, *8*, e54461. [CrossRef]
16. Cho, E.J.; Leem, S.; Kim, S.A.; Yang, J.; Lee, Y.B.; Kim, S.S.; Cheong, J.Y.; Cho, S.W.; Kim, J.W.; Kim, S.-M.; et al. Circulating microbiota-based metagenomic signature for detection of hepatocellular carcinoma. *Sci. Rep.* **2019**, *9*, 7536. [CrossRef]
17. Huang, C.C.; Du, M.; Wang, L. Bioinformatics analysis for circulating cell-free DNA in cancer. *Cancers* **2019**, *11*, 805. [CrossRef]
18. Paisse, S.; Valle, C.; Servant, F.; Courtney, M.; Burcelin, R.; Amar, J.; Lelouvier, B. Comprehensive description of blood microbiome from healthy donors assessed by 16S targeted metagenomic sequencing. *Transfusion* **2016**, *56*, 1138–1147. [CrossRef]
19. Potgieter, M.; Bester, J.; Kell, D.B.; Pretorius, E. The dormant blood microbiome in chronic, inflammatory diseases. *FEMS Microbiol. Rev.* **2015**, *39*, 567–591. [CrossRef]
20. Auguste, M.; Lasa, A.; Pallavicini, A.; Gualdi, S.; Vezzulli, L.; Canesi, L. Exposure to TiO2 nanoparticles induces shifts in the microbiota composition of Mytilus galloprovincialis hemolymph. *Sci. Total Environ.* **2019**, *670*, 129–137. [CrossRef]
21. Lokmer, A.; Wegner, M.K. Hemolymph microbiome of Pacific oysters in response to temperature, temperature stress and infection. *ISME J.* **2015**, *9*, 670–682. [CrossRef] [PubMed]
22. Wilkins, L.G.E.; Leray, M.; O'Dea, A.; Yuen, B.; Peixoto, R.S.; Pereira, T.J.; Bik, H.M.; Coil, D.A.; Duffy, J.E.; Herre, E.A.; et al. Host-associated microbiomes drive structure and function of marine ecosystems. *PLoS Biol.* **2019**, *17*, e3000533. [CrossRef] [PubMed]
23. Rynkiewicz, E.C.; Hemmerich, C.; Rusch, D.B.; Fuqua, C.; Clay, K. Concordance of 605 bacterial communities of two tick species and blood of their shared rodent host. *Mol. Ecol.* **2015**, *24*, 2566–2579. [CrossRef] [PubMed]
24. Jeon, S.J.; Cunha, F.; Vieira-Neto, A.; Bicalho, R.C.; Lima, S.; Bicalho, M.L.; Galvão, K.N. Blood as a route of transmission of uterine pathogens from the gut to the uterus in cows. *Microbiome* **2017**, *5*, 109. [CrossRef]
25. Scarsella, E.; Sandri, M.; Monego, S.D.; Licastro, D.; Stefanon, B. Blood Microbiome: A New Marker of Gut Microbial Population in Dogs? *Vet. Sci.* **2020**, *7*, 198. [CrossRef]
26. Hyun, H.; Lee, M.S.; Park, I.; Ko, H.S.; Yun, S.; Jang, D.H.; Kim, S.; Kim, H.; Kang, J.H.; Lee, J.H.; et al. Analysis of Porcine Model of Fecal-Induced Peritonitis Reveals the Tropism of Blood Microbiome. *Front. Cell. Infect. Microbiol.* **2021**, *11*, 676650. [CrossRef]
27. Scarsella, E.; Zecconi, A.; Cintio, M.; Stefanon, B. Characterization of microbiome on feces, blood and milk in dairy cows with different milk leucocyte pattern. *Animals* **2021**, *11*, 1463. [CrossRef] [PubMed]
28. Vientós-Plotts, A.I.; Ericsson, A.C.; Rindt, H.; Reinero, C.R. Blood cultures and blood microbiota analysis as surrogates for bronchoalveolar lavage fluid analysis in dogs with bacterial pneumonia. *BMC Vet. Res.* **2021**, *17*, 129. [CrossRef]
29. Tilahun, Y.; Pinango, J.Q.; Johnson, F.; Lett, C.; Smith, K.; Gipson, T.; McCallum, M.; Hoyt, P.; Tritt, A.; Yadav, A.; et al. Transcript and blood-microbiome analysis towards a blood diagnostic tool for goats affected by Haemonchus contortus. *Sci. Rep.* **2022**, *12*, 5362. [CrossRef]
30. Tarnecki, A.M.; Patterson, W.F.; Arias, C.R. Microbiota of wild-caught red snapper Lutjanus campechanus. *BMC Microbiol.* **2016**, *16*, 245. [CrossRef]
31. Kelly, C.; Salinas, I. Under pressure: Interactions between commensal microbiota and the teleost immune system. *Front. Immunol.* **2017**, *8*, 559. [CrossRef]
32. Pratte, Z.A.; Besson, M.; Hollman, R.D.; Stewart, F.J. The gills of reef fish support a distinct microbiome influenced by host-specific factors. *Appl. Environ. Microbiol.* **2018**, *84*, e00063-18. [CrossRef] [PubMed]
33. Féral, J.-P.; Saucède, T.; Poulin, E.; Marschal, C.; Marty, G.; Roca, J.C.; Motreuil, S.; Beurier, J.-P. PROTEKER: Implementation of a submarine observatory at the Kerguelen islands (Southern Ocean). *Underw. Technol.* **2016**, *34*, 3–10. [CrossRef]
34. Meredith, M.; Sommerkorn, M.; Cassotta, S.; Derksen, C.; Ekaykin, A.; Hollowed, A.; Kofinas, G.; Mackintosh, A.; Melbourne-Thomas, J.; Muelbert, M.M.C.; et al. Polar Regions. In *IPCC Special Report on the Ocean and Cryosphere in a Changing Climate*; Pörtner, H.-O., Roberts, D.C., Masson-Delmotte, V., Zhai, P., Eds.; Cambridge University Press: Cambridge, UK; New York, NY, USA, 2019; pp. 203–320.
35. Lecomte, F.; Beall, E.; Chat, J.; Davaine, P.; Gaudin, P. The complete history of salmonid introductions in the Kerguelen Islands, Southern Ocean. *Polar Biol.* **2013**, *36*, 457–475. [CrossRef]
36. Dodson, J.J.; Aubin-Horth, N.; Thériault, V.; Páez, D.J. The evolutionary ecology of alternative migratory tactics in salmonid fishes. *Biol. Rev.* **2013**, *88*, 602–625. [CrossRef]
37. Labonne, J.; Vignon, M.; Prévost, E.; Lecomte, F.; Dodson, J.J. Invasion Dynamics of a Fish-Free Landscape by Brown Trout (*Salmo trutta*). *PLoS ONE* **2013**, *8*, e71052. [CrossRef]
38. Marandel, L.; Gaudin, P.; Guéraud, F.; Glise, S.; Herman, A.; Plagues-Juan, E.; Véron, V.; Panserat, S.; Labonne, J. A reassessment of the carnivorous status of salmonids: Hepatic glucokinase is expressed in wild fish in Kerguelen Islands. *Sci. Total Environ.* **2018**, *612*, 276–285. [CrossRef] [PubMed]

39. Caza, F.; Joly de Boissel, P.G.; Villemur, R.; Betoulle, S.; St-Pierre, Y. Liquid biopsies for omics-based analysis in sentinel mussels. *PLoS ONE* **2019**, *14*, e0223525. [CrossRef]
40. Klindworth, A.; Pruesse, E.; Schweer, T.; Peplies, J.; Quast, C.; Horn, M.; Glöckner, F.O. Evaluation of general 16S ribosomal RNA gene PCR primers for classical and next-generation sequencing-based diversity studies. *Nucleic Acids Res.* **2013**, *41*, e1. [CrossRef]
41. Callahan, B.J.; McMurdie, P.J.; Rosen, M.J.; Han, A.W.; Johnson, A.J.; Holmes, S.P. DADA2: High-resolution sample inference from Illumina amplicon data. *Nat. Methods* **2016**, *13*, 581–583. [CrossRef]
42. Team, R.C. *R: A Language and Environment for Statistical Computing*; R Foundation for Statistical Computing: Vienna, Austria, 2021.
43. Wang, L.-Y.; Ke, W.J.; Sun, X.-B.; Liu, J.-F.; Gu, J.-D.; Mu, B.-Z. Comparison of bacterial community in aqueous and oil phases of water-flooded petroleum reservoirs using pyrosequencing and clone library approaches. *Appl. Microbiol. Biotechnol.* **2014**, *98*, 4209–4221. [CrossRef]
44. Vilo, C.; Dong, Q. Evaluation of the RDP classifier accuracy using 16S rRNA gene variable regions. *Metagenomics* **2012**, *1*, 104303. [CrossRef]
45. Hung, Y.M.; Lyu, W.N.; Tsai, M.L.; Liu, C.L.; Lai, L.C.; Tsai, M.H.; Chuang, E.Y. To compare the performance of prokaryotic taxonomy classifiers using curated 16S full-length rRNA sequences. *Comput. Biol. Med.* **2022**, *145*, 105416. [CrossRef] [PubMed]
46. McMurdie, P.J.; Holmes, S. phyloseq: An R package for reproducible interactive analysis and graphics of microbiome census data. *PLoS ONE* **2013**, *8*, e61217. [CrossRef] [PubMed]
47. Cao, Y.; MicrobiomeMarker: Microbiome Biomarker Analysis. R Package Version 0.0. 1.9000. Available online: https://github.com/yiluheihei/microbiomeMarker (accessed on 23 October 2022).
48. Ssekagiri, A.; Sloan, W.; Ijaz, U.Z.; MicrobiomeSeq: An R Package for Analysis of Microbial Communities in an Environmental Context. ISCB Africa ASBCB Conference. Available online: https://github.com/umerijaz/microbiomeSeq (accessed on 22 February 2019).
49. Oksanen, J.; Blanchet, F.G.; Friendly, M.; Kindt, R.; Legendre, P.; McGlinn, D.; Solymos, P.; Stevens, M.H.; Wagner, H.; Vegan: Community Ecology Package. R Package Version 2.5-7. Available online: https://cran.r-project.org/package=vegan (accessed on 11 October 2022).
50. Narayan, N.R.; Weinmaier, T.; Laserna-Mendieta, E.J.; Claesson, M.J.; Shanahan, F.; Dabbagh, K.; Iwai, S.; DeSantis, T.Z. Piphillin predicts metagenomic composition and dynamics from DADA2-corrected 16S rDNA sequences. *BMC Genom.* **2020**, *21*, 56.
51. Cao, S.; Zhang, W.; Ding, W.; Wang, M.; Fan, S.; Yang, B.; Mcminn, A.; Wang, M.; Xie, B.-B.; Qin, Q.L.; et al. Structure and function of the Arctic and Antarctic marine microbiota as revealed by metagenomics. *Microbiome* **2020**, *8*, 47. [CrossRef]
52. Hedaoo, M.; Gore, D.; Fadnavis, S.; Dange, M.; Soni, M.A.; Kopulwar, A.P. Bioinformatics approach in speciation of oil degrading uncultured bacterium and its frequency recording. *J. Pharm. Res.* **2018**, *12*, 628–635.
53. Koner, S.; Chen, J.S.; Hsu, B.M.; Tan, C.W.; Fan, C.W.; Chen, T.H.; Hussain, B.; Nagarajan, V. Assessment of Carbon Substrate Catabolism Pattern and Functional Metabolic Pathway for Microbiota of Limestone Caves. *Microorganisms* **2021**, *9*, 1789. [CrossRef]
54. Peng, W.; Huang, J.; Yang, J.; Zhang, Z.; Yu, R.; Fayyaz, S.; Zhang, S.; Qin, Y.-H. Integrated 16S rRNA sequencing, metagenomics, and metabolomics to characterize gut microbial composition, function, and fecal metabolic phenotype in non-obese type 2 diabetic Goto-Kakizaki rats. *Front. Microbiol.* **2020**, *10*, 3141. [CrossRef] [PubMed]
55. Sheridan, M.A. Alterations in lipid metabolism accompanying smoltification and seawater adaptation of salmonid fish. *Aquaculture* **1989**, *82*, 191–203. [CrossRef]
56. Lokesh, J.; Kiron, V. Transition from freshwater to seawater reshapes the skin-associated microbiota of Atlantic salmon. *Sci. Rep.* **2016**, *6*, 19707. [CrossRef] [PubMed]
57. Fogarty, C.; Burgess, C.M.; Cotter, P.D.; Cabrera-Rubio, R.; Whyte, P.; Smyth, C.; Bolton, D.J. Diversity and composition of the gut microbiota of Atlantic salmon (Salmo salar) farmed in Irish waters. *J. Appl. Microbiol.* **2019**, *127*, 648–657. [CrossRef] [PubMed]
58. Ferreira, M.; Abdelhafiz, Y.A.A.; Abreu, H.; Silva, J.; Valente, L.M.; Viswanath, K. Gracilaria gracilis and Nannochloropsis oceanica, singly or in combination, in diets alter the intestinal microbiota of European seabass (*Dicentrarchus labrax*). *Front. Mar. Sci.* **2022**, *9*, 1001942. [CrossRef]
59. Ferchiou, S.; Caza, F.; Villemur, R.; Betoulle, S.; St-Pierre, Y. Species- and site-specific circulating bacterial DNA in Subantarctic sentinel mussels Aulacomya atra and Mytilus platensis. *Sci. Rep.* **2022**, *12*, 9547. [CrossRef]
60. Chiu, C.Y.; Miller, S.A. Clinical metagenomics. *Nat. Rev. Genet.* **2019**, *20*, 341–355. [CrossRef] [PubMed]
61. Chiu, K.-P.; Yu, A.L. Application of cell-free DNA sequencing in characterization of bloodborne microbes and the study of microbe-disease interactions. *PeerJ* **2019**, *7*, e7426. [CrossRef]
62. Guo, W.; Zhang, Y.; Guo, S.; Mei, Z.; Liao, H.; Dong, H.; Wu, K.; Ye, H.; Zhang, Y.; Zhu, Y.; et al. Tumor microbiome contributes to an aggressive phenotype in the basal-like subtype of pancreatic cancer. *Commun. Biol.* **2021**, *4*, 1019. [CrossRef]
63. Velmurugan, G.; Dinakaran, V.; Rajendhran, J.; Swaminathan, K. Blood microbiota and circulating microbial metabolites in diabetes and cardiovascular disease. *Trends Endocrinol. Metab.* **2020**, *31*, 835–847. [CrossRef]
64. Onarheim, A.M.; Wiik, R.; Burghardt, J.; Stackebrandt, E. Characterization and identification of two Vibrio species indigenous to the intestine of fish in cold sea water; description of Vibrio iliopiscarius sp. nov. *Syst. Appl. Microbiol.* **1994**, *17*, 370–379. [CrossRef]
65. Delghandi, M.R.; El-Matbouli, M.; Menanteau-Ledouble, S. Renibacterium salmoninarum—The causative agent of bacterial kidney disease in salmonid fish. *Pathogens* **2020**, *9*, 845. [CrossRef]
66. Caraguel, J.M.; Guerri, O.; Davaine, P. Pacage marin du saumon à Kerguelen. In *Rapport de Campagne ARMOR 1992*; INRA: Paris, France, 1993.

67. Eldøy, S.H.; Davidsen, J.; Vignon, M.; Power, M. The biology and feeding ecology of Arctic charr in the Kerguelen Islands. *J. Fish Biol.* **2020**, *98*, 526–536. [CrossRef] [PubMed]
68. Austin, B.; Austin, D.A. Vibrionaceae representatives. In *Bacterial Fish Pathogens*; Austin, B., Austin, D.A., Eds.; Springer: Dordrecht, The Netherlands, 2012; pp. 357–411.
69. Klemetsen, T.; Karlsen, C.R.; Willassen, N.P. Phylogenetic revision of the genus Aliivibrio: Intra-and inter-species variance among clusters suggest a wider diversity of species. *Front. Microbiol.* **2021**, *12*, 626759. [CrossRef] [PubMed]
70. Davidsen, J.G.; Bordeleau, X.; Eldøy, S.H.; Whoriskey, F.; Power, M.; Crossin, G.T.; Buhariwalla, C.; Gaudin, P. Marine habitat use and feeding ecology of introduced anadromous brown trout at the colonization front of the sub-Antarctic Kerguelen archipelago. *Sci. Rep.* **2021**, *11*, 11917. [CrossRef]
71. Castillo, D.J.; Rifkin, R.F.; Cowan, D.A.; Potgieter, M. The healthy human blood microbiome: Fact or fiction? *Front. Cell. Infect. Microbiol.* **2019**, *9*, 148. [CrossRef] [PubMed]
72. Schierwagen, R.; Alvarez-Silva, C.; Madsen, M.S.A.; Kolbe, C.C.; Meyer, C.; Thomas, D.; Uschner, F.E.; Magdaleno, F.; Jansen, C.; Pohlmann, A.; et al. Circulating microbiome in blood of different circulatory compartments. *Gut* **2019**, *68*, 578–580. [CrossRef] [PubMed]
73. Schierwagen, R.; Alvarez-Silva, C.; Servant, F.; Trebicka, J.; Lelouvier, B.; Arumugam, M. Trust is good, control is better: Technical considerations in blood microbiome analysis. *Gut* **2020**, *69*, 1362–1363. [CrossRef] [PubMed]
74. Labonne, J.; Kaeuffer, R.; Gueraud, F.; Zhou, M.; Manicki, A.; Hendry, A.P. From the bare minimum: Genetics and selection in populations founded by only a few parents. *Evol. Ecol. Res.* **2016**, *17*, 21–34.
75. Frey, F.A.; Weis, D.; Yang, H.J.; Nicolaysen, K.; Leyrit, H.; Giret, A. Temporal geochemical trends in Kerguelen Archipelago basalts: Evidence of decreasing magma supply from the Kerguelen plume. *Chem. Geol.* **2000**, *164*, 61–80. [CrossRef]
76. Snyder, M.W.; Kircher, M.; Hill, A.J.; Daza, R.M.; Shendure, J. Cell-free DNA comprises an in vivo nucleosome footprint that informs its tissue origin. *Cell* **2016**, *164*, 57–68. [CrossRef]
77. Abril, M.K.; Barnett, A.S.; Wegermann, K.; Fountain, E.; Strand, A.; Heyman, B.M.; Blough, B.A.; Swaminathan, A.C.; Sharma-Kuinkel, B.; Ruffin, F.; et al. Diagnosis of Capnocytophaga canimorsus sepsis by next generation whole-genome sequencing. *Open Forum Infect. Dis.* **2016**, *3*, ofw144. [CrossRef]
78. Miller, R.R.; Montoya, V.; Gardy, J.L.; Patrick, D.M.; Tang, P. Metagenomics for pathogen detection in public health. *Genome Med.* **2013**, *5*, 81. [CrossRef] [PubMed]
79. Poore, G.D.; Kopylova, E.; Zhu, Q.; Carpenter, C.; Fraraccio, S.; Wandro, S.; Kosciolek, T.; Janssen, S.; Metcalf, J.; Song, S.J.; et al. Microbiome analyses of blood and tissues suggest cancer diagnostic approach. *Nature* **2020**, *579*, 567–574. [CrossRef] [PubMed]
80. Cardona-Ospina, J.A.; Villalba-Miranda, M.F.; Palechor-Ocampo, L.A.; Mancilla, L.I.; Sepúlveda-Arias, J.C. A systematic review of FTA cards® as a tool for viral RNA preservation in fieldwork: Are they safe and effective? *Prev. Vet. Med.* **2019**, *172*, 104772. [CrossRef] [PubMed]
81. Cortes, A.L.; Montiel, E.R.; Gimeno, I.M. Validation of Marek's disease diagnosis and monitoring of Marek's disease vaccines from samples collected in FTA® Cards. *Avian Dis.* **2009**, *54*, 510–516. [CrossRef]
82. Moscoso, H.; Raybon, E.O.; Thayer, S.G.; Hofacre, C.L. Molecular detection and serotyping of infectious bronchitis virus from FTA® filter paper. *Avian Dis.* **2005**, *49*, 24–29. [CrossRef]

Supplementary Materials: Skin and blood microbial signatures of sedentary and migratory trout (*Salmo trutta*) of Kerguelen Islands

Sophia Ferchiou[1] †, France Caza[1] †, Richard Villemur[1], Jacques Labonne[2] and Yves St-Pierre[1]*

† These authors share first authorship.
[1] INRS-Centre Armand-Frappier Santé Biotechnologie, Laval, QC, Canada
[2] Université de Pau et des pays de l'Ardour, UMR ONRAE-UPPA, ECOBIOP Saint-Pée-sur-Nivelle, France
* Correspondence: Yves St-Pierre ; E- mail: yves.st-pierre@inrs.ca; INRS-Centre Armand-Frappier Santé Technologie, 531 Boul. des Prairies, Laval, Québec, Canada, H7V 1B7 ; Phone: 450-686-5354; Fax: 450-686-5501.

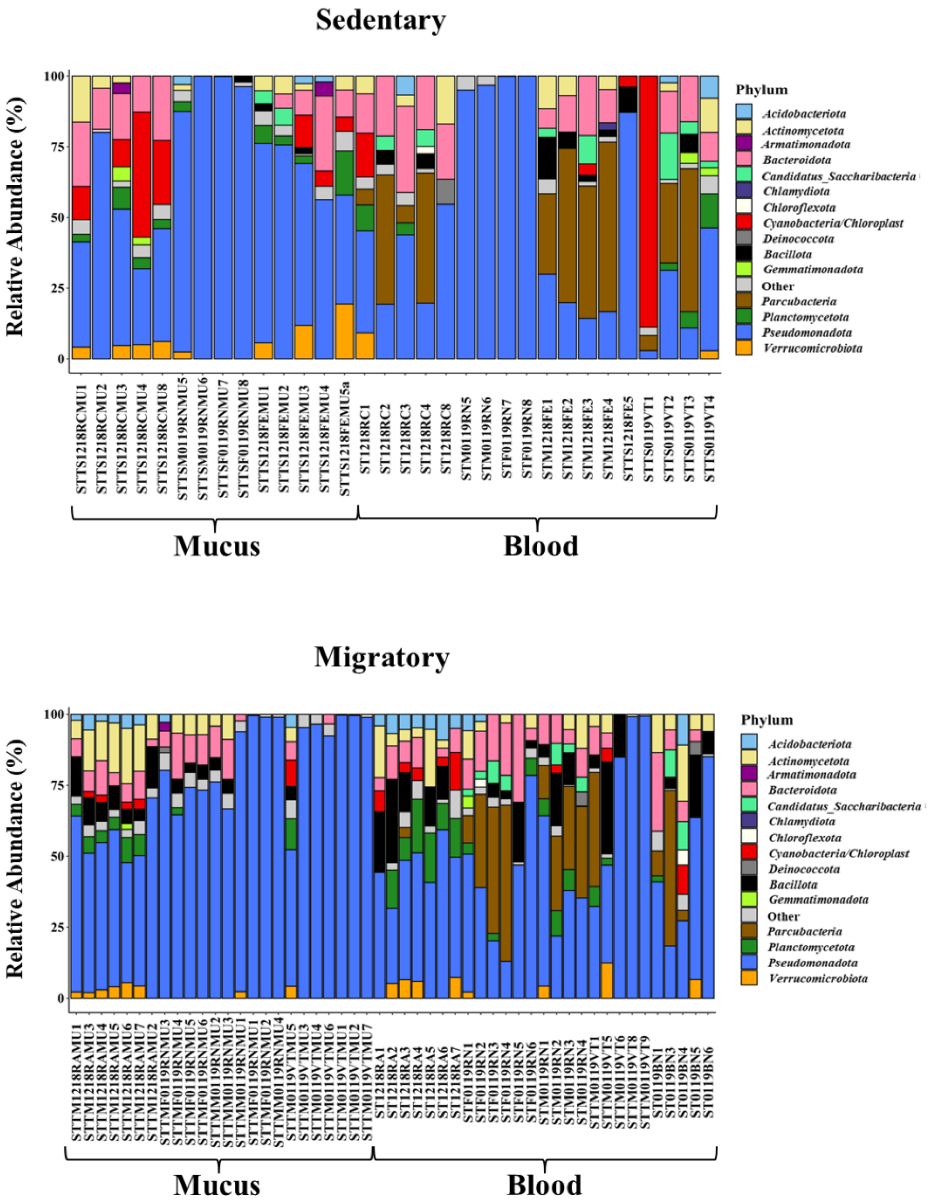

Figure. S1: Individual variations in the circulating and mucosal microbiomes at the phylum level. Bar plots display the main phyla between sedentary and migratory brown trout (*S. trutta*) for mucosal (left) and circulating (right) microbiomes. Phyla with a relative abundance of ≤ 1.5%are represented as "Other."

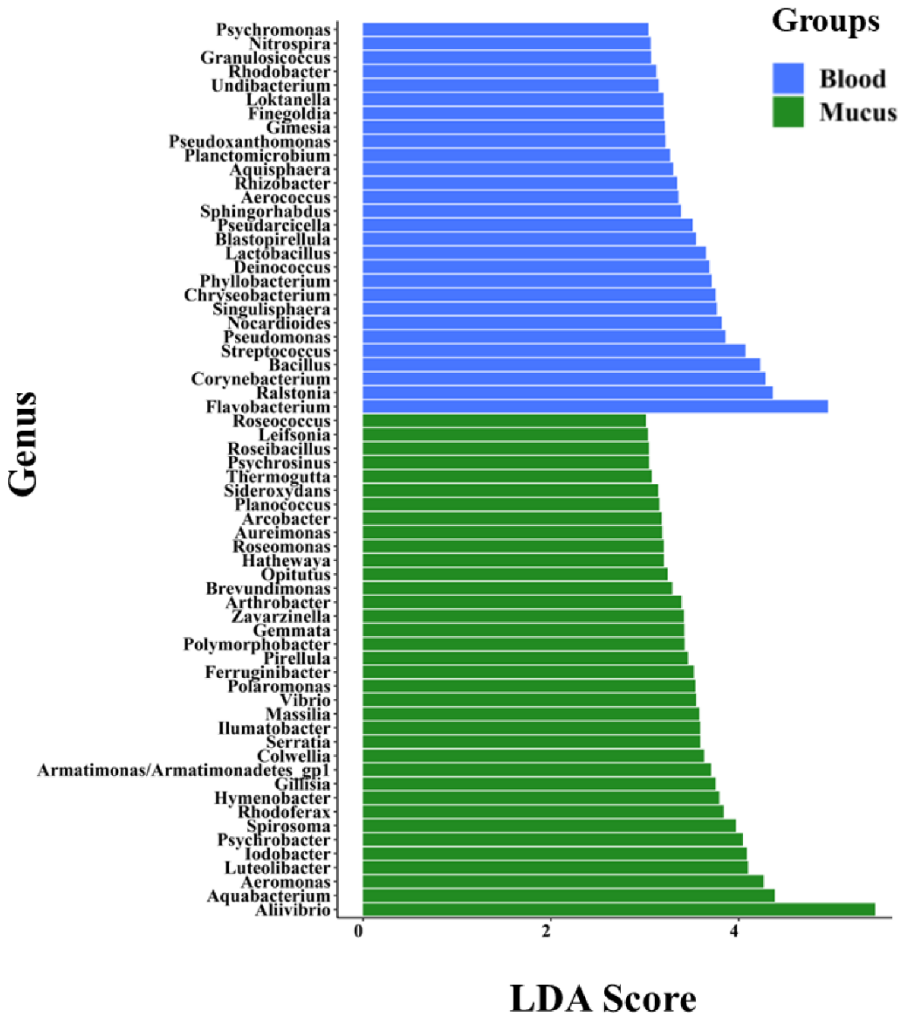

Figure. S2: Discriminant genera between the circulating and mucosal compartments. LEfSe analysis (log-transformed LDA > 3) showing the top genus-level biomarkers that distinguished both compartments in brown trout (*S. trutta*).

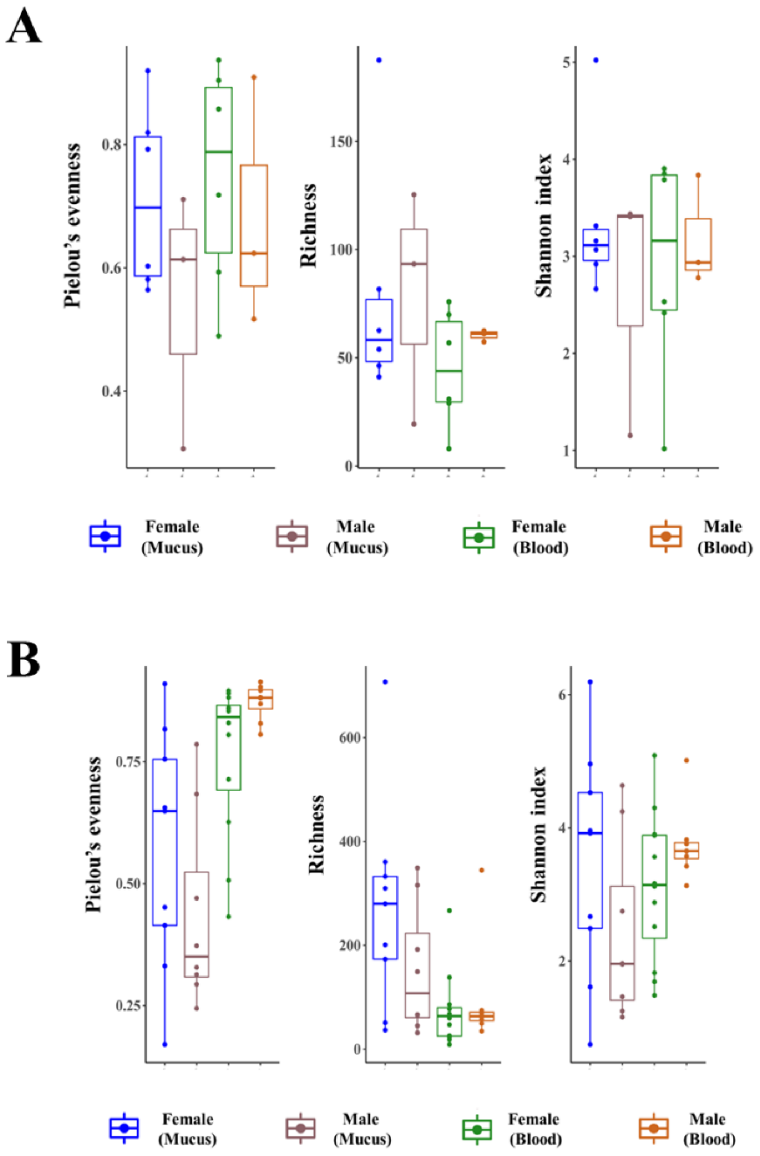

Figure. S3: Alpha diversity analysis of mucosal and circulating microbiomes in (A) sedentary and (B) migratory brown trout (*S. trutta*). Species evenness, observed richness and Shannon diversity indexes were calculated for both female and male samples. No significant differences were observed between specimens for the same compartment.

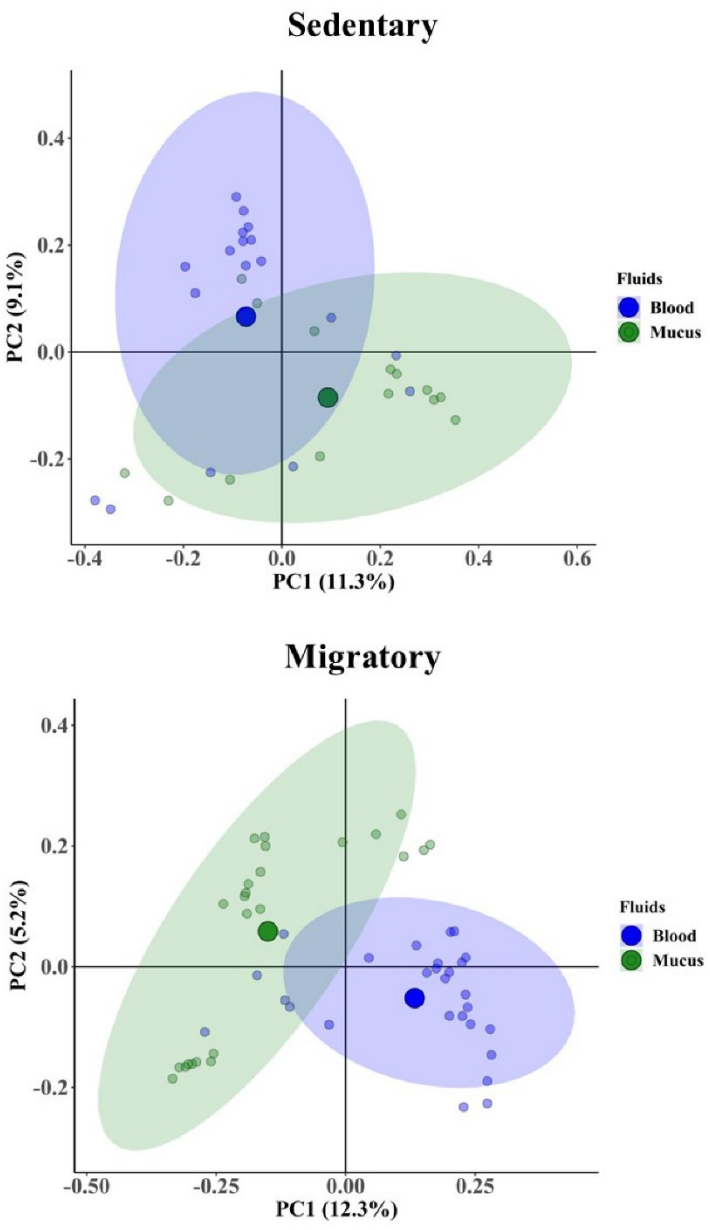

Figure. S4: Principal Coordinates Analysis (PCoA) of bacterial DNA bacterial communities in both sedentary and migratory brown trout (*S. trutta*). Unweighted UniFrac-based of blood (blue) and mucosa (red) samples. Centroids for each site are illustrated by larger circles. Ellipses represent 95% confidence interval.

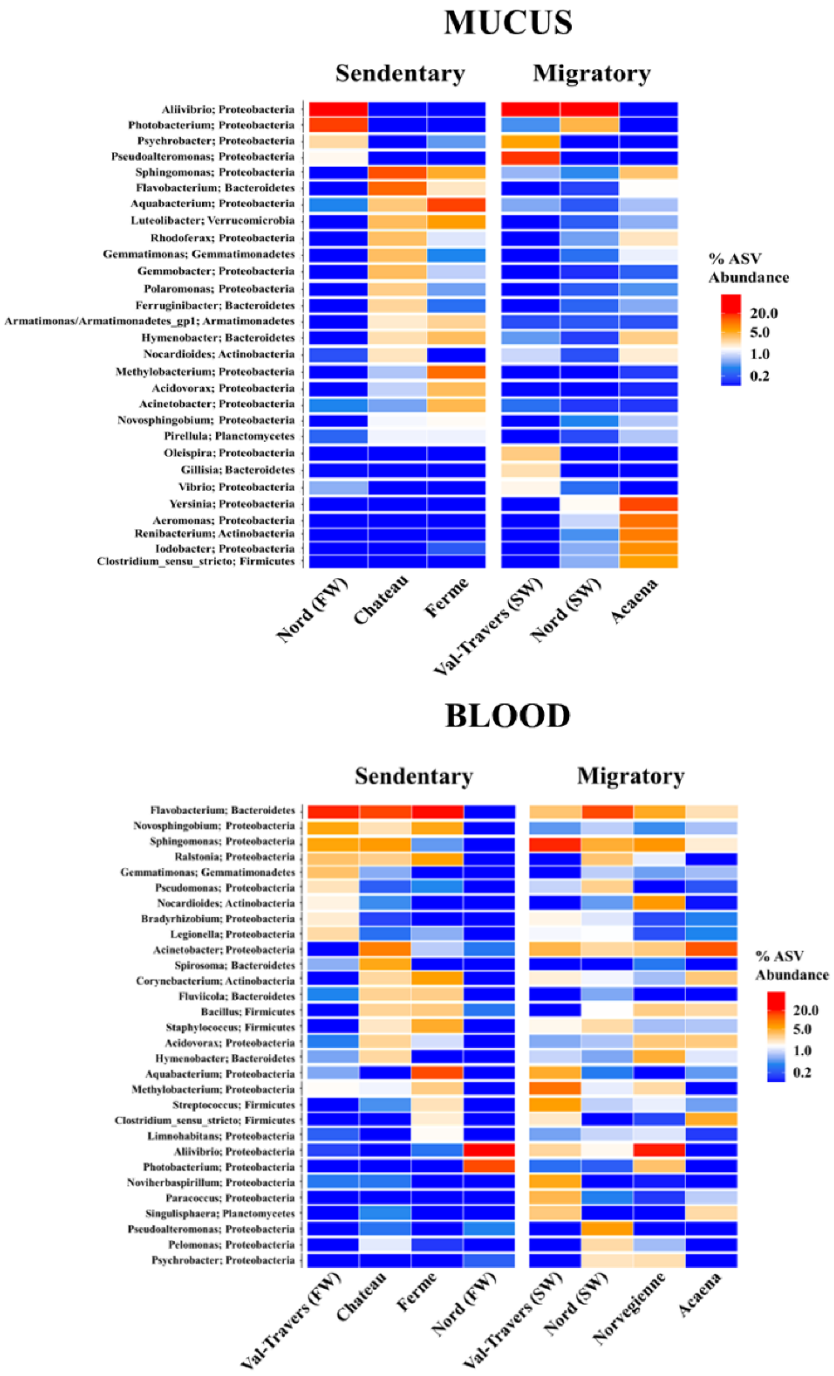

Figure. S5: Heatmaps showing relative abundance (%) of the top 30 bacterial genera of mucosal and circulating microbiomes between sedentary and migratory brown trout (*S. trutta*). Red colors indicate higher abundance and blue colors indicate lower abundances.

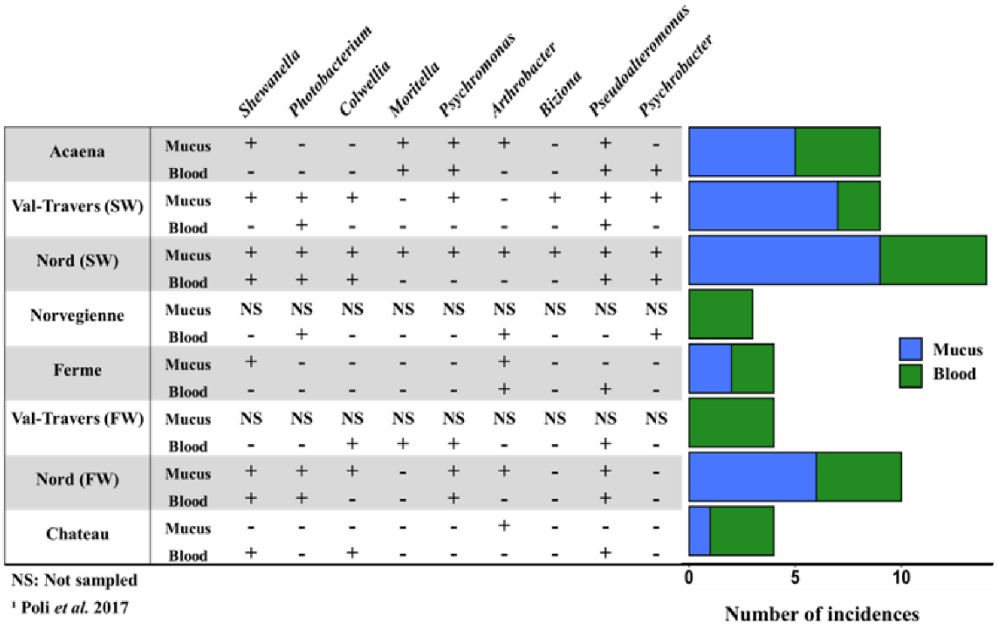

Figure. S6: Presence of psychrophilic bacterial genera isolated from Kerguelen sites and compared to Poli *et al.* (2017) identification of psychrophilic bacteria.

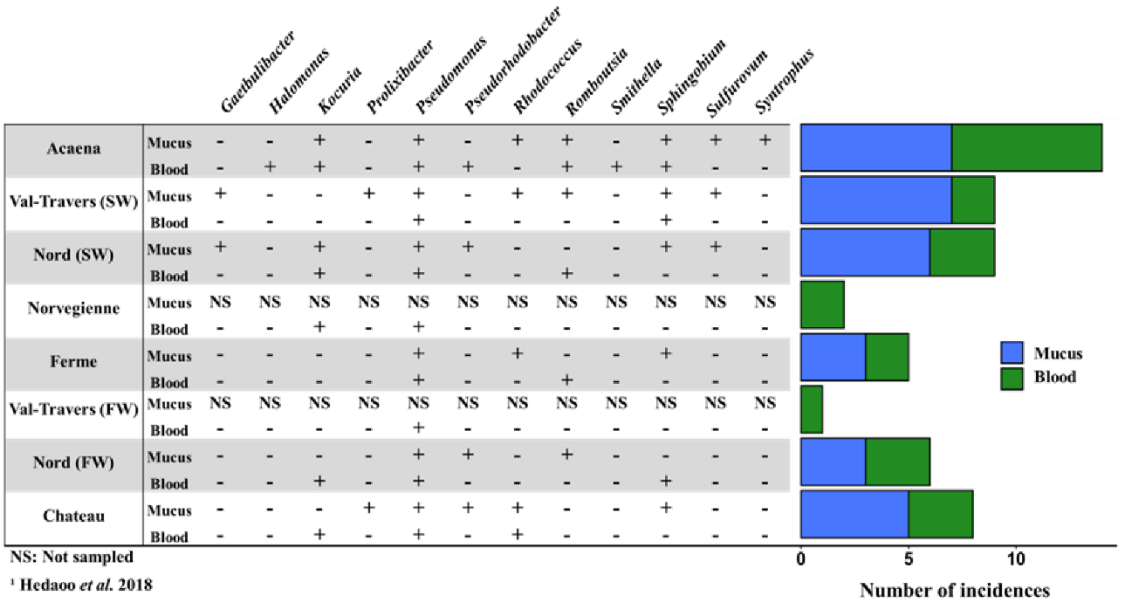

NS: Not sampled

[1] Hedaoo *et al.* 2018

Figure. S7: Presence of Kerguelen bacterial genera commonly associated to oil spills (cited more than four times in different scientific papers) based on Hedaoo *et al.* (2018).

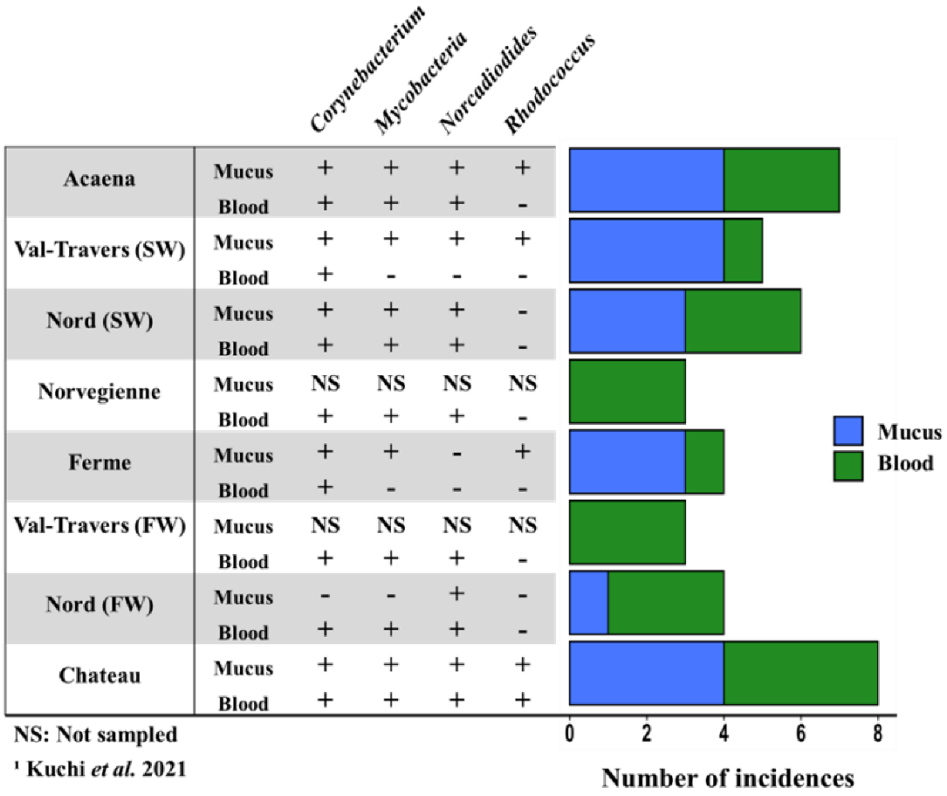

Figure. S8: Presence of Kerguelen bacterial genera known to degrade alkanes, phenols and phenanthrene which can be used as biomarkers for PAHs detection, based on Kuchi *et al.* (2021).

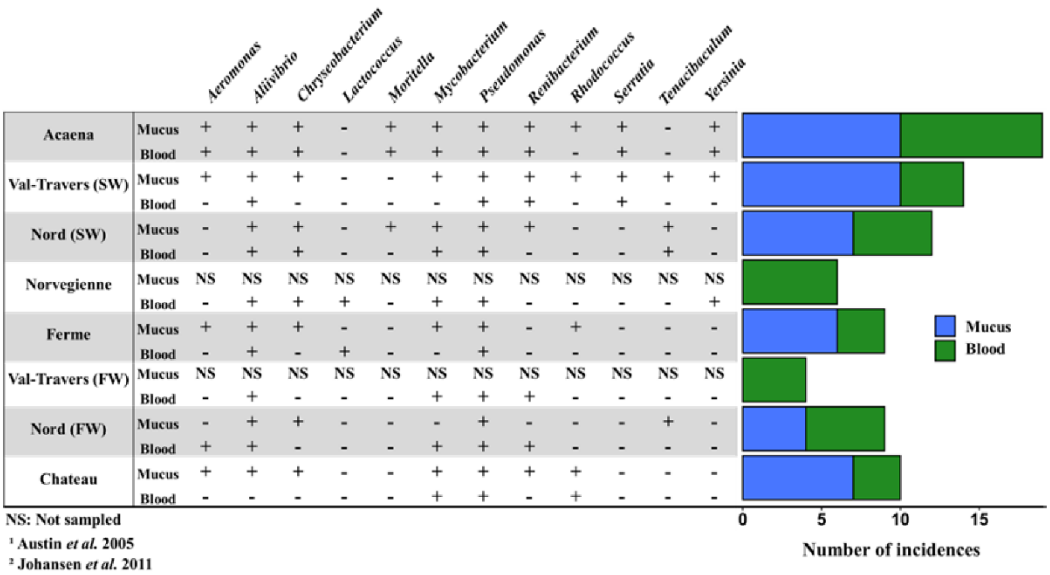

Figure. S9: Presence of potentially pathogenic bacterial genera found at different sites in Kerguelen.

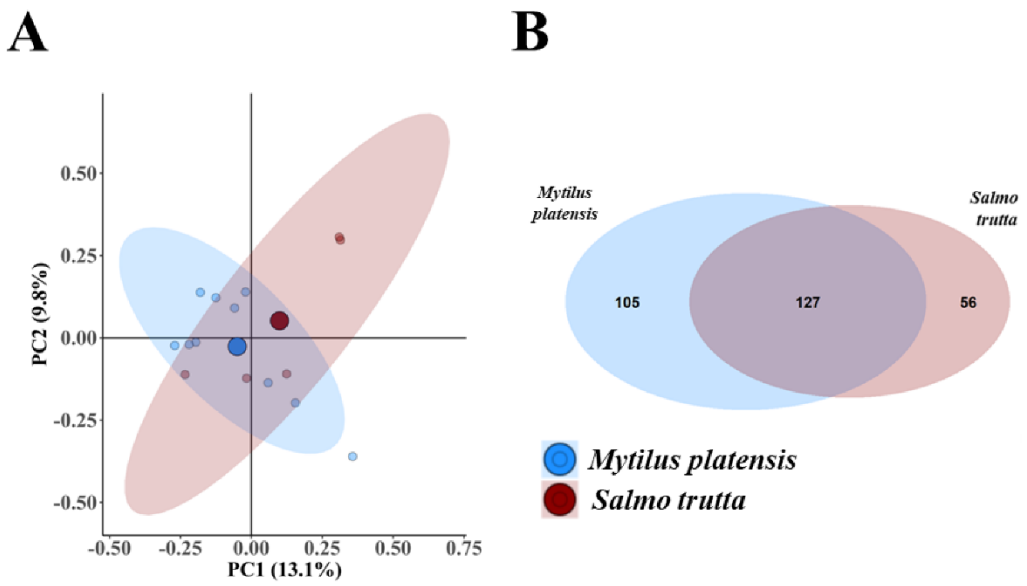

Figure. S10: Bacterial cmDNA profiles in blue mussels (*Mytilus platensis*) and brown trout (*S. trutta*) collected at the mouth of the Norvegienne river. (**A**) Principal Coordinates Analysis (PCoA) of bacterial DNA bacterial communities in both species. Unweighted UniFrac-based of blue mussels (blue) and brown trout (red) samples. Centroids for each site are illustrated by larger circles. Ellipses represent 95% confidence interval. (**C**) A Venn diagram showing the number of unique and shared bacterial genera in blue mussels (blue) and brown trout (red) samples.

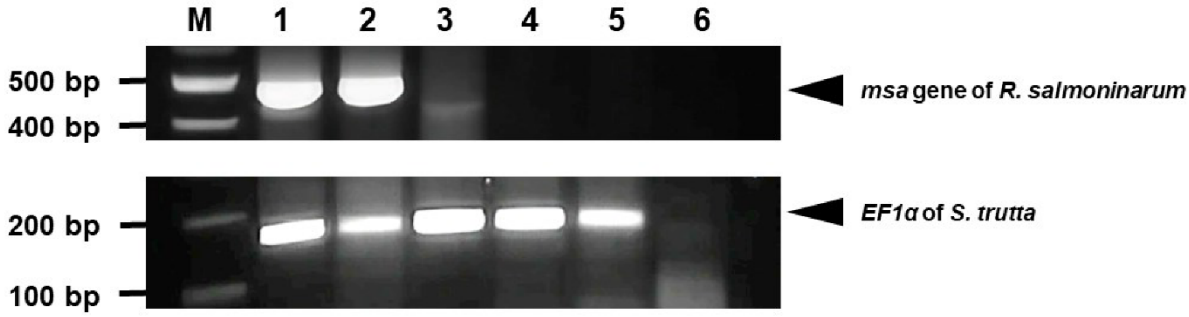

Figure. S11: Amplified fragments shown on 1.5% agarose gel electrophoresis. A. Amplicons generated from the *msa* gene of *R. salmoninarum* in positive mucosal and blood samples from Acaena river according to the protocol by Brown *et al.*(1994). No amplification occurred in samples from Baie Norvegienne river. The primer sequences are 5'-CAAGGTGAAGGGAATTCTTCCACT-3' and 5'-GACGGCAATGTCCGTTCCCGGTTT-3' for the forward and the reverse primers, respectively. **B.** Amplicons generated from the *EF1α* gene of *S. trutta* samples. The primer sequences are 5'-ATTGCCACACTGCTCACATC-3' and 5'-CTGGAAGCTCTCCACACACA-3' for the forward and the reverse primers, respectively. M: 100-base-pair DNA ladder; lanes 1–2: mucosal samples from Acaena river; lane 3: blood sample from Acaena river; lanes 4-5: blood samples from Baie Norvégienne river; lane 6: no DNA template.

Table S1. Characteristics of brown trout (*S. trutta*) collected at different sites at Kerguelen Islands.

Phenotype	Site	Compartment	*n*	Average weight (kg) ± SE
Sedentary	Chateau	Mucosal/Blood	5/5	0.9 ± 0.1
Sedentary	Nord	Mucosal/Blood	4/4	2.7 ± 0.4
Sedentary	Ferme	Mucosal/Blood	5/5	0.3 ± 0.06
Sedentary	Val-Travers	Blood	4	0.08 ± 0.01
Migratory	Acaena	Mucosal/Blood	7/7	1.7 ± 0.4
Migratory	Nord	Mucosal/Blood	10/10	2.2 ± 0.3
Migratory	Val-Travers	Mucosal/Blood	7/7	1.8 ± 0.2
Migratory	Norvegienne	Blood	5	3.2 ± 0.4

Annexe II

Aperçus du microbiome circulant des populations de flétan de l'Atlantique et du Groenland : le rôle des facteurs spécifiques aux espèces et des facteurs environnementaux

scientific reports

OPEN

Insights into the circulating microbiome of Atlantic and Greenland halibut populations: the role of species-specific and environmental factors

Fanny Fronton[1], Sophia Ferchiou[1], France Caza[1], Richard Villemur[1], Dominique Robert[2] & Yves St-Pierre[1]✉

Establishing long-term microbiome-based monitoring programs is critical for managing and conserving wild fish populations in response to climate change. In most cases, these studies have been conducted on gut and, to a lesser extent, skin (mucus) microbiomes. Here, we exploited the concept of liquid biopsy to study the circulating bacterial microbiome of two Northern halibut species of economic and ecological importance. Amplification and sequencing of the 16S rRNA gene were achieved using a single drop of blood fixed on FTA cards to identify the core blood microbiome of Atlantic and Greenland halibut populations inhabiting the Gulf of St. Lawrence, Canada. We provide evidence that the circulating microbiome DNA (cmDNA) is driven by genetic and environmental factors. More specifically, we found that the circulating microbiome signatures are species-specific and vary according to sex, size, temperature, condition factor, and geographical localization. Overall, our study provides a novel approach for detecting dysbiosis signatures and the risk of disease in wild fish populations for fisheries management, most notably in the context of climate change.

Abbreviations

R. hippoglossoides	*Reinhardtius hippoglossoides*
H. hippoglossus	*Hippoglossus hippoglossus*
cmDNA	Circulating microbiome DNA
PCoA	Principal coordinate analysis
ASV	Amplicon sequence variants
OTU	Operational taxon unit
PERMANOVA	Multivariate analysis of variance with permutation
LEfSe	Linear discriminant analysis effect size

The Atlantic halibut *Hippoglossus hippoglossus* (Linnaeus, 1758) *(H. hippoglossus)* and the Greenland halibut *Reinhardtius hippoglossoides* (Walbaum, 1792) *(R. hippoglossoides)* are two species of flatfish widely distributed in the Northwest Atlantic and characterized by distinct populations in the Gulf of St. Lawrence (GSL)[1,2]. These populations support the region's two most valuable groundfish fisheries and are biannually assessed to provide scientific advice for management[3,4]. The Atlantic halibut abundance has been steadily increasing, whereas the Greenland halibut stock has declined over the last two decades. Although the reasons for these fluctuations are not fully clear, the rapid warming of the deep channels of the GSL[3,5] and increased competition by redfish for Greenland halibut[6,7] are considered the primary factors driving these changes. Given the impact of such changes on the physiology of the fish, developing sensitive and predictive biomarkers is essential for a close follow-up of the health status of these stocks.

The microbiome, or the pool of nucleic acids from microbes found in/on a host species, has attracted considerable attention from scientists in recent years as a predictive biomarker to assess the health status of an

[1]INRS-Centre Armand-Frappier Santé Technologie, 531 Boul. des Prairies, Laval, QC H7V 1B7, Canada. [2]Institut des Sciences de la Mer, Université du Québec à Rimouski, 310, allée des Ursulines, C.P. 3300, Rimouski, QC G5L 3A1, Canada. ✉email: yves.st-pierre@inrs.ca

individual[8]. The microbiome is an important determinant of the health status of an organism, as it contributes to the regulation of several physiological processes, such as the immune response and host energy metabolism.

Although most studies on the use of microbiome signatures as a predictive tool were initially performed in clinical settings, the increased accessibility of next-generation sequencing (NGS) technologies for the analysis of 16S ribosomal RNA (rRNA) gene amplicons has facilitated its application in different research fields, including studies in fish populations[9]. Studies on fish's skin and gut bacterial microbiomes have shown that a balanced microbiome plays a critical role in the host's health, protecting against pathogens while bringing nutritional benefits[10]. Disruption of this balance, often called dysbiosis, changes the biodiversity and abundance of specific bacterial communities, often leading to health complications[11].

Considering their economic and ecological importance, an increasing number of studies have thus focused on defining the microbiome signatures of Teleost. These studies have shown that microbiome signature depends on several factors, including host genetics, morphometrics, and several environmental factors, including biotic and abiotic factors[12,13]. In most cases, however, these studies have been conducted in laboratory/experimental settings or fish farms and performed on the gut microbiome and, to a lesser extent, skin (mucus) microbiomes[13–15]. In recent years, however, the concept of a circulating microbiome has emerged as an interesting alternative to invasive, lethal, and logistically challenging tissue biopsies. Even if blood has historically been considered exempt from microbes in healthy individuals, it is now irrefutable that bacterial, viral, fungal and other microorganism genomes are present in the blood (blood-cell or plasma)[16–20]. This feature allows us to study the microbiota of an organism without the need for tissue biopsy. The concept of the circulating microbiome is particularly well adapted to the development of routine and predictive biomarkers. The utility of this approach has recently been demonstrated in clinical settings, offering a new perspective for the development of biomarkers in ecology[21–24] similar to those described for several diseases in humans[16,20,25]. In fact, the existence of a blood microbiome is a concept that is now widely accepted in humans and animals, including pigs, broiler chickens, camels, cows, goats, cats and dogs[21,23,24,26–29].

In the present work, we have characterized, for the first time, the blood 16S rRNA microbiome signatures of two wild fish populations of ecological and economic interest from the GSL, the Atlantic halibut and the Greenland halibut. These two species are characterized by opposite abundance trends. Our general hypothesis is that physiological and environmental factors impact their microbiome signature. By providing a reference for future studies to examine climate change's impact on halibut populations, we further hypothesize that our approach will help develop novel biomarkers for monitoring the condition and health of wild fish populations.

Material and methods

Sampling. Blood samples from Greenland halibut (n = 97; length: 316.2 ± 15.1 mm) and Atlantic halibut (n = 86; 762.0 ± 30.1 mm) were collected between August 15th and October 1st, 2019, during the annual bottom trawl surveys performed on the northern and southern sectors of the GSL (Canada) by the Department of Fisheries and Oceans (DFO) (Table 1). Scanmar hydroacoustic sensors attached to the trawl and a conductivity, temperature, and depth (CTD) probe were used to record the temperature. Blood samples were taken immediately upon trawl retrieval, and liquid biopsies were performed at 56 sites for at least one species (Fig. 1). The number of liquid biopsies performed per station (ranging from 1 to 14) was opportunistic and depended on the presence of either halibut species and workload at a given site. Blood samples were collected with a heparin-coated 3-mL sterile syringe and a 22-G needle following a dorsal incision using a sterilized knife. Drops of blood were collected and immediately stored on a Flinders Technology Associates (FTA) card (Sigma-Aldrich, Oakville, ON, Canada). Samples were allowed to air dry and kept in a plastic bag with a desiccant, as Caza et al. (2019) described. The sex of each sampled individual was determined by visual identification of the gonads following the dissection of specimens by the DFO science crew. The care and use of field-sampled animals complied with the Government of Canada's animal welfare laws, guidelines, and policies approved by Fisheries and Oceans Canada. All methods were conducted following ARRIVE guidelines (https://arriveguidelines.org/).

DNA extraction, amplification and sequencing. All DNA extraction and purification procedures were conducted in a white room where pressure, temperature, and humidity were controlled to minimize contamination. Individual discs were cut from the FTA cards using a sterile 5.0-mm single round hole punch, and

Species	Sex	N	Length (mm) mean ± SE	Weight (g) mean ± SE
Greenland halibut	Total	97	316.2 ± 15.1	518.4 ± 72.2[a]
	Male	19	341.2 ± 23.7	407.1 ± 67.5
	Female	32	433.0 ± 22.7	915.1 ± 125.8
	Unknown	46	224.5 ± 17.0	37.6 ± 1.6[b]
Atlantic halibut	Total	86	762.0 ± 30.1[c]	6 976.8 ± 879.7[c]
	Male	55	755.1 ± 36.4[d]	6 628.5 ± 871.0[d]
	Female	30	760.3 ± 54.6	7 167.8 ± 1935.6
	Unknown	1	1 190	20 060

Table 1. Summary of the fish samples used for cmDNA analysis. Number of samples for which the data were available: [a]n = 73, [b]n = 22, [c]n = 85 and [d]n = 54.

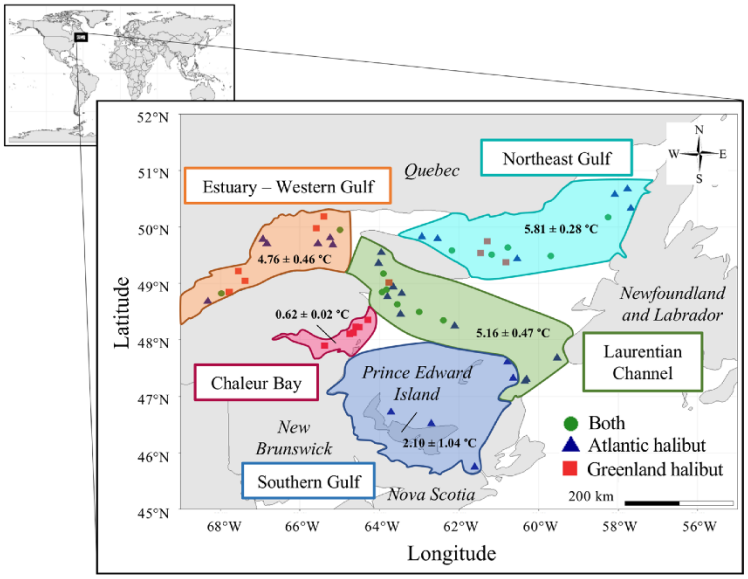

Figure 1. Map of the sample sites divided into five different areas. The regional temperature is given for each zone (mean ± SE).

total DNA was isolated using the QIAamp DNA Investigator Kit (Qiagen, Toronto, ON, Canada), according to the manufacturer's protocol. DNA was quantified in duplicate using a Quant-iT PicoGreen dsDNA detection kit (Molecular Probes, Eugene OR, USA). Amplification of the V3–V4 region of the 16S ribosomal RNA (rRNA) gene and 16S gene amplicon sequencing for all DNA samples were performed at Centre d'Expertise et de Services, Génome Québec (Montréal, QC, Canada). Amplification used the universal primers 341F (5′-CCTACG GGNGGCWGCAG-3′) and 805R (5′-GACTACHVGGGTATCTAATCC-3′). Sequence libraries were prepared by Genome Quebec with the TruSeq DNA Library Prep Kit (Illumina, San Diego, CA, USA) and quantified using the Kapa Library Quantification Kit for Illumina platforms (Kapa Biosystems). Paired-end sequences were generated on a MiSeq platform PE300 (Illumina Corporation, San Diego, CA, USA) with the MiSeq Reagent Kit v3 using 600 cycles (Illumina, San Diego, CA, USA). Raw data files are publicly available on the NCBI Sequence Read Archive (PRJNA853332).

16S rRNA data processing. Illumina sequence data (FASTQ files) were trimmed using *Cutadapt* (version 2.8). The 16S rRNA (V3-V4) amplicon sequence variants (ASVs) were generated with the DADA2 pipeline (version 1.16.0; Callahan et al. (2016)) and subsequently within the R environment (R version 4.0.3, Team (2021)). The Ribosomal Database Project (RDP)16 database was used for the ASV assignment. The software packages *phyloseq* (1.36.0)[30], *microbiomeSeq* (0.1)[31], *microbiomeMarker* (0.99.0)[32], and *vegan* (2.5.7)[33] were used to characterize the microbial communities. The maps were created with the packages *ggplot2* (3.3.6)[34] and *rnaturalearth* (0.1.0)[35]. An ASV was considered part of the core microbiome if it had a minimum prevalence (rate of presence in the group of samples) of 70% with a detection threshold of 0.01% relative abundance[36]. A similar decision tree was applied for the core genus (abundance of ASVs of the same genus were summed) but with 90% prevalence. A stringent threshold of 90% was chosen, as reported in previous studies[37–39]. The prevalence varies greatly between microbiome studies, ranging from > 10 to 100% [22,36,37,39–42]. Hence, we chose not to limit the core microbiome at 100% prevalence because the study was not under controlled conditions; instead, it was performed in wild populations where greater variation was expected, especially with sample sizes considered.

Classes based on environmental and morphometric data. Individual fish were classified to assess environmental and ontogenetic effects. They were assigned as mature or immature according to the known length at which 50% of males had reached reproductive size (L50), i.e., 360 mm for Greenland halibut[3,7] and 920 mm for Atlantic halibut[43]. Given that sex information was missing from many individuals, the male L50 was chosen, as it is lower, so the mature individuals would have less chance to be mislabeled as immature. Because diet composition is a likely factor influencing the microbiome, we split Greenland halibut specimens into four size classes based on body lengths where major shifts in diet composition have previously been described[44]. Briefly, four classes were defined for the Greenland halibut: (1) Class 1, individuals smaller than 200 mm feeding on small prey; (2) Class 2, individuals ranging from 200 to 400 mm feeding on intermediate prey; and (3) Class 3, individuals larger than 400 mm feeding on large prey. Defining length classes for the Atlantic halibut was impos-

sible, as the number of small and large individuals was too low. Classes were also defined according to the water temperature. Individuals occupying temperatures below than 5 °C were considered "cold water", and those occupying temperatures above 5 °C were considered "warm water"[7]. Given that Atlantic halibuts' range of temperature tolerance is wider than those measured, they were not included in temperature-based analyses[45,46]. Finally, the relative condition K factor, a broad health index for fish, was also calculated based on the length and weight of each individual[47,48]. A linear regression was performed between $\log_{10}$ (weight) and $\log_{10}$ (length) as follows:

$\log_{10}(W) = \log_{10}(a) + b * \log_{10}(L)$[49].where W is the weight, L is the length, and a and b are constant coefficients.

The coefficients a and b were calculated and used to estimate the expected weight W_e of each individual based on their length with the following equation:

$$W_e = aL^b$$

Finally, the K_{rel} of Le Cren was calculated as follows:

$$K_{rel} = \frac{W}{W_e}$$

The comparison between the individual's actual weight and their expected weight gives us the fish's plumpness, a glimpse of its health status. Basically, if an individual is skinnier than others of the same length within the same species, it is under stress, and K_{rel} will be under 1. On the contrary, a plump fish is associated with beneficial environmental influence, and K_{rel} will be over 1[50].

The autocorrelation, the homoscedasticity of the error terms and the normal distribution of the linear regression residuals were validated with statistical analysis (Durbin Watson, Breusch–Pagan and Shapiro–Wilk tests). Classes were created with $K_{rel} > 1$ corresponding to the "high condition" and $K_{rel} < 1$ corresponding to the "low condition"[47,50].

Spatial analysis. Overall, five geographical zones were defined. Spatial zones were created to separate different habitats in the Gulf based on sample sites with similar characteristics as follows (e.g., depth, temperature, and spatial closeness); The Estuary-Western Gulf area extends from 65°W to 69°W longitude and from 49.7°N to 51°N latitude, considered to be the primary nursery area for the Greenland halibut[51], the Northeast Gulf area, situated between 57°W and 63.7°W longitude and 49°N and 51°N latitude; the Lawrence Channel area is between longitudes 59°W and 65°W and latitudes 47°N and 49.7°N with sample sites deeper than 110 m (included); the Chaleur Bay area includes sampling sites between 64°W and 67°W longitude and 47.5°N and 48.5°N latitude, and finally, the Southern Gulf area is located between 60.5°W and 65.5°W longitude and 45.5°N and 48°N latitude with sampling sites less deep than 110 m (not included). For Greenland halibut, the number of fish per area was n = 22 for the Estuary-Western Gulf t, n = 19 for the Chaleur Bay, n = 22 for the Northeast Gulf and n = 34 in the Laurentian Channel. Regarding Atlantic halibut, the number of fish was n = 14 for the Estuary-Western Gulf, n = 11 for the Southern Gulf, n = 17 for the Northeast Gulf and n = 44 for the Laurentian Channel.

Statistical analysis. Bacterial taxonomic α-diversity (intrasample) was estimated using the richness and the Shannon and Simpson indices, as implemented in the R package *microbiome* (1.14.0)[52]. Variations in bacterial α-diversity and taxa abundances between the two species were assessed using either the Kruskal–Wallis test or Wilcoxon-Mann–Whitney test, given that none of the variables exhibited a normal distribution. In addition, α-diversity was also calculated among classes according to the length, temperature and condition factor K[48]. The Kruskal–Wallis test was followed by a pairwise Wilcoxon-Mann–Whitney test if the *p*-value (p) was significant ($p < 0.05$). The β-diversity (intersample) was estimated using phylogenetic weighted UNIFRAC dissimilarities assessed by principal coordinates analysis (PCoA). Differences in community composition were tested using permutational multivariate analysis of variance (PERMANOVA) for weighted UNIFRAC indices with 999 permutations, as implemented in the R *vegan* package (2.5.7) or the *pairwise Adonis* package (0.4). Detailed statistical analyses on variations with morphometric and environmental data are presented in Supplementary Information. Differences were considered statistically significant at alpha = 0.05. Linear discriminant analysis (LDA) effect size (LEfSe) was performed on the microbiome of each species and on the different classes to highlight discriminative taxa for each class. This analysis was performed using the *microbiomeMarker* package (0.99.0). The cutoff was chosen at an LDA score of $\log_{10}$ (LDA score) ≥ 4. All analyses were performed in R studio (v4.0.5)[53].

Results

Preliminary characterization of the cmDNA. A total of 183 Atlantic and Greenland halibut blood samples were collected at the end of summer and early fall of 2019 in the Gulf of St. Lawrence (Fig. 1). The cmDNA signatures were determined by sequencing the V3-V4 hypervariable regions of the 16S rRNA gene. Approximately 6 million raw reads were retrieved after filtering (2.5 and 3.5 million for Atlantic and Greenland halibut, respectively). The number of sequences per sample ranged between 3,985 and 55, 077. The mean numbers of reads per individual were 35,575 ± 971 and 29,296 ± 1 185 for Greenland halibut and Atlantic halibut, respectively. The number of ASVs per sample curve confirmed that the sequencing depth was sufficient to plateau the number of ASVs (Figure S1). A total of 7,105 unique ASVs were obtained, including 7,102 identified as having bacterial origins (3 of archaeal origin were removed from the analysis). A total of 6,450 ASVs were greater than or equal to 0.01% in relative abundance. Overall, 3,362 ASVs were present in Atlantic halibut (mean = 112 ± 7 per individual) and 5,023 in Greenland halibut (mean = 161 ± 9 per individual).

Differences in the circulating microbiome at the phylum level. Given both halibut species' genetic and behavioral differences, we first tested the hypothesis that the microbiome differs between the Atlantic and Greenland halibut. Overall, 30 different phyla were identified (23 and 29 in Atlantic halibut and Greenland halibut, respectively), 63 classes (44 and 59), 121 orders (88 and 112), 241 families (189 and 224) and 685 genera (473 and 587) (Table 2). At the phylum level, the blood microbiome signature was dominated by *Proteobacteria*, *Firmicutes*, *Bacteroidetes*, and *Actinobacteria* (Fig. 2). The mean relative abundance of *Proteobacteria* was, however, significantly higher in Greenland halibut (81.6 ± 1.5% versus 62.4 ± 2.3% in Atlantic halibut) (Wilcoxon-Mann–Whitney test; $p < 0.001$). Similarly, the other three main phyla were significantly higher in Atlantic halibut at 9.3 ± 0.9% versus 6.9 ± 0.8% for *Firmicutes* ($p = 0.032$), 6.6 ± 0.7% versus 4.4 ± 0.5% for *Bacteroidetes* ($p = 0.044$) and 4.0% ± 0.5% versus 2.6 ± 0.4% for *Actinobacteria* ($p = 0.0028$) (Fig. 2A). The mean relative abundance of uncharacterized bacteria was nonetheless important in Atlantic halibut, accounting for ~ 15% on average. This finding is even more apparent based on the individual relative abundance, with some individuals possessing 60% of uncharacterized bacteria (Fig. 2B). The microbiome structures with other taxa are provided in Supplementary Figures S2-S3.

The genus-level core circulating microbiome. To further test the hypothesis that the microbiome signature of both species differs, we carried out a detailed analysis at the genus level. Three genera, *Pseudoalteromonas, Psychrobacter* and *Acinetobacter,* were present in 90% of samples for both species (ASVs were aggregated together at the genus level). In Atlantic halibut, these genera were found to be the most abundant, accounting for 12.9%, 12.1% and 8.7% of the mean relative abundance, respectively. A fourth genus that was present in 90% of samples was *Staphylococcus,* with a mean relative abundance of 3.2% (Fig. 3A). In Greenland halibut, these three genera represented 23.6%, 16.6% and 3.4% of the average blood microbiome, respectively, whereas *Vibrio* was the fourth core genus with 6.9% mean relative abundance. In total, 685 genera were found, 375 of which were present in both halibut species (54.7%) (Fig. 3B). Although most of the genera found at 50% prevalence were shared by both species, some genera were unique in each species, such as *Enhydrobacter* in Atlantic halibut and *Oleispira* in Greenland halibut (Fig. 3C). This distribution of genera differed between the two species; major differences were the higher abundance of *Vibrio* and the lower abundance of *Acinetobacter* in Greenland halibut. The number of genera with a prevalence of 50% was also higher in Greenland halibut than in Atlantic halibut.

Comparative analysis of the bacterial diversity between species. We next compared the overall biodiversity of the cmDNA between both species using a UniFrac-based PCoA that showed that the microbiomes tended to cluster according to species, but with high variations within species composing the microbiome and a low percentage of variance explained by the two axes (32.8%) (Fig. 4A). PERMANOVA confirmed the significant difference between the two halibut species ($p < 0.001$), but the effect size was very low for the groups ($R^2 = 0.06$) compared to the residuals ($R^2 = 0.94$), suggesting that the species of the individual was not a strong determinant between these fish microbiomes. These findings support a recent study showing that the gut microbiome of flounders (*Pleuronectidae)* is similar among family members (Huang et al., 2020). Regarding α-diversity indicators, no significant differences in evenness or diversity were noted between the two species; the mean Simpson index (Atlantic halibut, 0.11; Greenland halibut, 0.13) and the mean Shannon diversity index (Atlantic halibut 3.36; Greenland halibut, 3.37) were equivalent (Fig. 4B). The richness index, however, was higher in the case of Greenland halibut, with an average of 161 ± 9 ASVs per individual compared to 112 ± 7 ASVs per individual for Atlantic halibut ($p < 0.001$).

LEfSe comparison of the two species. To further investigate the differences between the circulating microbiomes of the two halibut species, a Linear discriminant analysis Effect Size (LEfSe) was performed with a cutoff at $\log_{10}$ (LDA score) ≥ 4. This criterion allowed us to observe several differences in the structure of the two blood microbiomes at the phylum and genus levels (Fig. 4C and D). In particular, *Proteobacteria* were found in higher abundance in Greenland halibut, whereas *Actinobacteria*, *Firmicutes* and *Bacteroidetes* were more abundant in Atlantic halibut (Fig. 4C). At the genus level, more genera were discriminative for Greenland halibut (Fig. 4D). These genera included the core genera *Pseudoalteromonas* and *Psychrobacter* or *Vibrio* and other genera, such as *Photobacterium*, *Burkholderia* and *Escherichia/Shigella.* The core genera *Staphylococcus* and *Acinetobacter* were discriminative exclusively for Atlantic halibut.

Taxon	Atlantic halibut (n = 86)	Greenland halibut (n = 97)	Total
Phylum	23	29	30
Class	44	59	63
Order	88	112	121
Family	189	224	241
Genus	473	587	685

Table 2. Number of taxa in the cmDNA of the Atlantic halibut (*H. hippoglossus*) and the Greenland halibut (*R. hippoglossoides*).

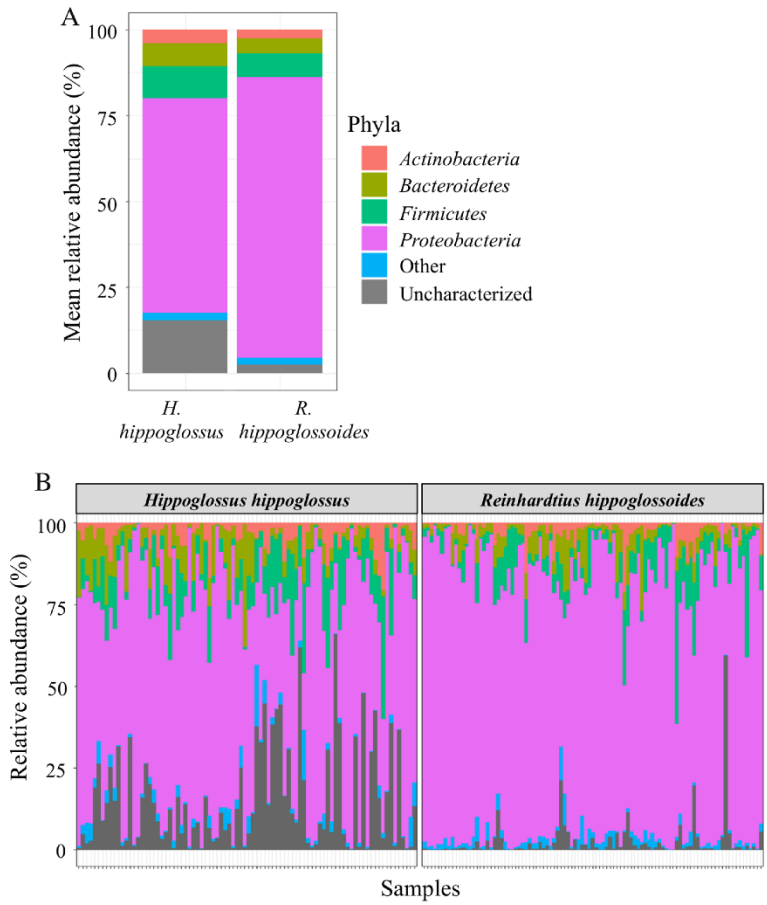

Figure 2. Microbiome structure at the phylum level. (**A**) Mean relative abundance (%) of the four main phyla present in the blood microbiome of Atlantic halibut (*H. hippoglossus*) and Greenland halibut (*R. hippoglossoides*). (**B**) Individual variation in the relative abundance (%) of the main phyla of Atlantic halibut (n = 86) and Greenland halibut (n = 97).

Correlations with biotic and abiotic factors. Given the influence of the environment and the physiology on the microbiome, we next tested the hypothesis that the blood microbiome signature within each fish species varies according to different variables, including maturity classes (length), water temperature (measured at the sampling depth of the trawl), sex, and Fulton's condition factor (K). We found that the blood microbiome structure varied depending on the maturity stage for both species at the phylum and genus levels. (Fig. 5A) In the case of Greenland halibut, significant differences in the abundance of *Corynebacterium*, *Staphylococcus*, *Burkholderia*, *Pseudoalteromonas*, *Psychrobacter* and *Vibrio* were noted (Fig. 5A, Figure S4). At the genus level, the most important difference between the mature and immature classes was in the case of *Vibrio*, which decreased by almost threefold in the mature class (from 9.7% to 3.3%; $p < 0.001$) (Table 3). The difference in *Burkholderia* between mature (0.7%) and immature (4.5%) Greenland halibut was also significant ($p < 0.001$). In the case of Atlantic halibut, the only two discriminative genera between both classes were *Psychrobacter* and *Escherichia/Shigella* (Fig. 5B, Figure S5). As for the α and β-diversity, some significant differences between the blood microbiome of mature and immature individuals were noted. In the case of Greenland halibut, we found a significant difference in the richness index (Fig. 5C), but no differences were noted for the Atlantic halibut (Figure S9). Significant differences in the β diversity between mature and immature individuals were found for both halibut species (Figures S6 and S7).

We next assessed whether temperature had an impact on the circulating microbiome signatures. Given the limited temperature tolerance of Greenland halibut[54], we divided the populations into two groups based on whether they were sampled at temperatures below or above 5 °C. Atlantic halibuts have a wider temperature tolerance than the Greenland halibuts[45,46], higher than the temperature recorded in this study. This is why no

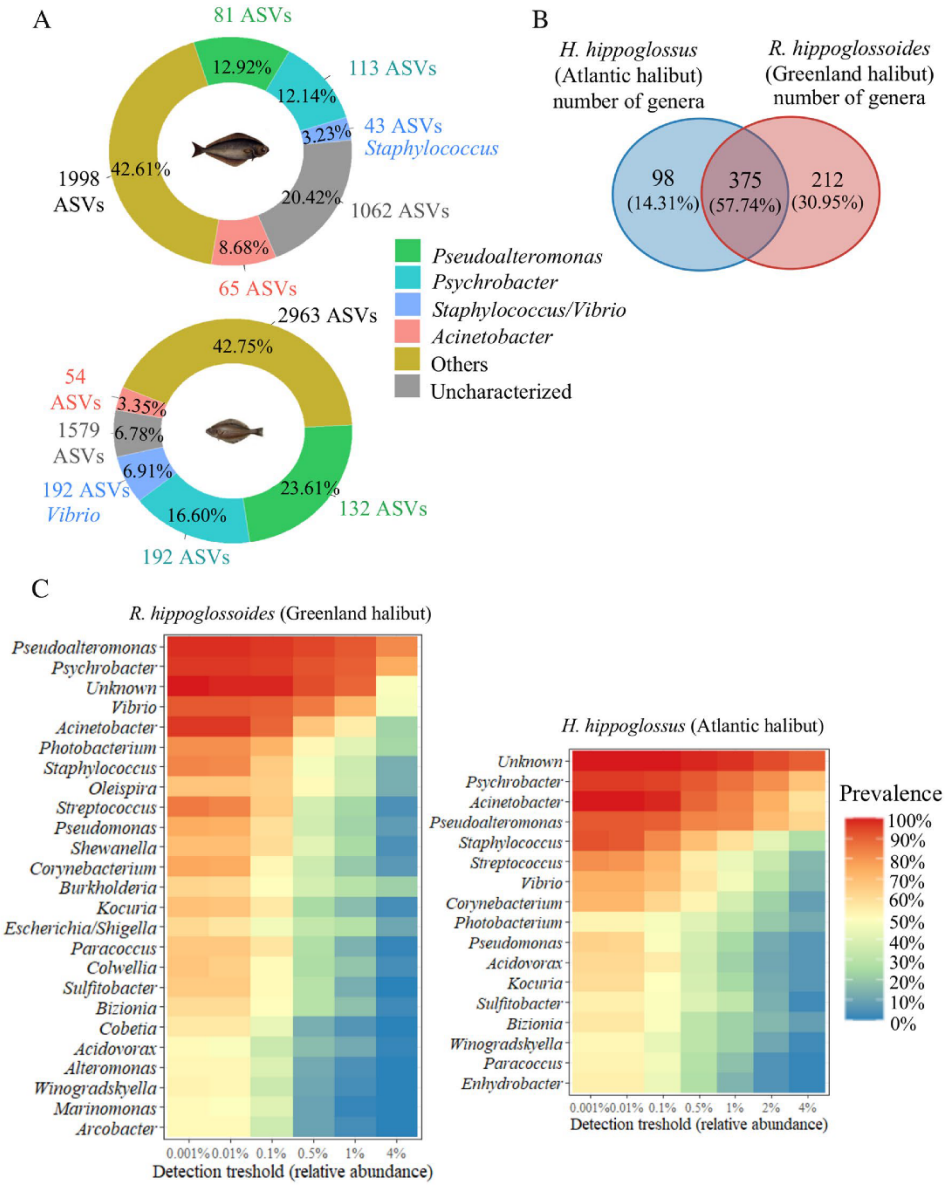

Figure 3. Core blood microbiome analysis. (**A**) Mean relative abundance (%) of the core genera aggregated (90% prevalence) in the cmDNA of the blood microbiome of the Atlantic halibut (*H. hippoglossus*) (top) and the Greenland halibut (*R. hippoglossoides*) (bottom). The mean relative abundance is given in each pie chart, and the number of aggregated ASVs is indicated next to each pie chart. (**B**) Venn diagram showing common and distinctive genera in the blood microbiome. (**C**) Heatmaps of the core microbiome. These heatmaps identify the most prevalent bacteria in both halibut species. Atlantic halibut, n = 86, Greenland halibut, n = 97.

temperature analysis was carried out on this species. Our results showed significant temperature-related differences in Greenland halibut at both the phylum and genus levels (Fig. 6A, Figure S6). The relative abundance of *Pseudoalteromonas* was 34.4% in specimens distributed in relatively cold waters, compared to 19.9% in relatively warm water ($p = 0.005$) (Table 4). The relative abundance of *Vibrio* was also lower in Greenland halibut, distributed in warmer water (9.8%) than in cold water (5.9%) ($p = 0.001$). Similar findings were observed in the

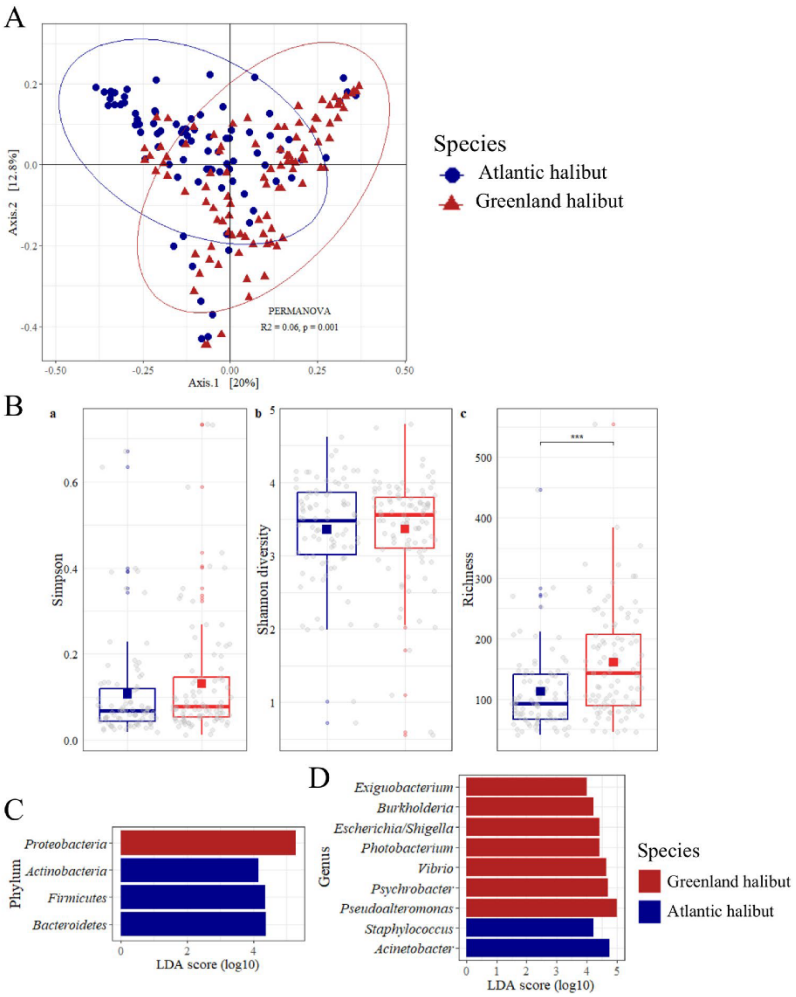

Figure 4. Biodiversity analysis. (**A**) PCoA plot of the β-diversity of the blood microbiome based on weighted UniFrac distances. (**B**) α-Diversity metrics for the cmDNA of Atlantic halibut (blue) and Greenland halibut (red). ***: $p < 0.001$. (**C** and **D**). Discriminative taxa at the phylum and genus levels in the cmDNA of both halibut populations ($p < 0.05$). Atlantic halibut, n = 86, Greenland halibut, n = 97.

case of *Pseudoalteromonas* (Figure S8). Again, we found significant variations in the α and β diversity between temperature classes for Greenland halibut (Figures S6 and S9).

We next determined whether the circulating microbiome varied in association with the size class of the Greenland halibut. Discriminative taxa included *Psychrobacter*, which was more abundant in fish-eating small prey (Fig. 6B), with the highest mean relative abundance of 27.9% in this group (Kruskal–Wallis; $p < 0.001$) (Table 5). The two other core genera were identified as discriminative in intermediate-sized prey-eating fish, with a mean relative abundance of 10.4% for *Vibrio* ($p < 0.001$) and 37.2% for *Pseudoalteromonas* ($p < 0.001$). *Corynebacterium*, *Staphylococcus*, *Acinetobacter* and *Burkholderia* were discriminative for large prey-eating fish (Figure S10). All these genera were previously documented in teleost fishes' gut or skin microbiome, and *Acinetobacter* was identified as a biomarker of carnivorous fish (Huang et al. 2020).

Concerning differences between males and females, we found only a few statistically significant differences (Figure S11). *Shewanella* and *Psychrobacter* were more abundant in Greenland and Atlantic male halibut, respectively, whereas the relative abundance of *Acinetobacter* was more abundant in Atlantic halibut females. This abundance of *Shewanella* in female versus male Greenland halibut was significant (0.4% in females compared to 3.2% in males). We did not observe any variations in the α and β diversity between males and females for either species (Figures S6, S7, and S9).

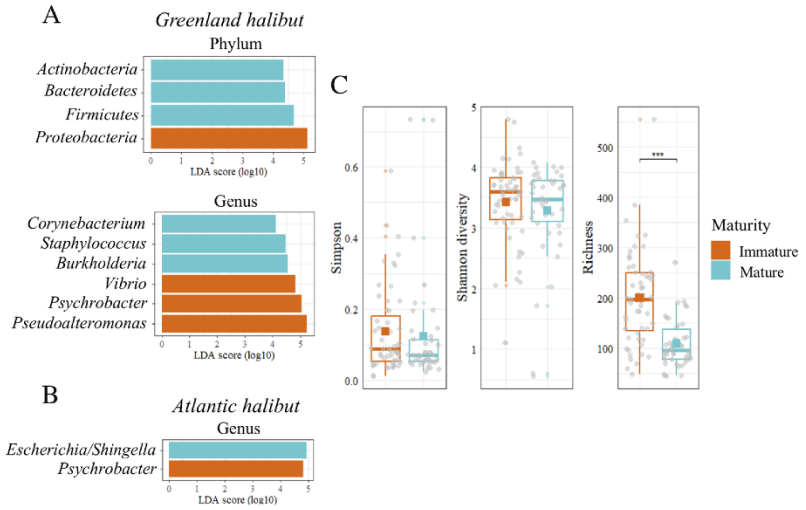

Figure 5. Maturity analysis. LEfSe analysis of the blood microbiome showing the significantly different taxa in mature (blue) and immature (red) fish in (**A**) Greenland halibut (Immature, n = 55, mature, n = 42) and (**B**) Atlantic halibut (Immature, n = 56, mature, n = 25). (**C**).α-Diversity metrics for immature and mature Greenland halibut. ***: $p < 0.001$.

Species	Taxa	Immature mean ± SE (n = 56)	Mature mean ± SE (n = 25)	*P* values	Test Statistics W
Greenland halibut	*Proteobacteria*	87.3 ± 1.1[a]	74.3 ± 2.8	< 0.001	620
	Firmicutes	5.1 ± 0.7	< 0.001	< 0.01	1543
	Actinobacteria	1.6 ± 0.4	3.8 ± 0.7	< 0.001	1615
	Bacteroidetes	3.3 ± 0.4	5.9 ± 0.9	< 0.05	1433
	Vibrio	9.7 ± 1.2	3.3 ± 0.9	< 0.001	438
	Burkholderia	0.7 ± 0.3	4.5 ± 0.9	< 0.001	1833
	Corynebacterium	0.4 ± 0.1	1.7 ± 0.5	< 0.001	1765
	Psychrobacter	21.1 ± 2.3	10.8 ± 2.0	< 0.001	670
	Pseudoalteromonas	31.5 ± 2.9	13.2 ± 2.2	< 0.001	521
	Staphylococcus	0.6 ± 0.2	3.6 ± 1.1	< 0.001	1676
Atlantic halibut	*Psychrobacter*	13.8 ± 2.0	7.9 ± 2.3	< 0.05	533
	Escherichia/Shingella	1.7 ± 1.5	9.5 ± 5.0	< 0.005	1008

Table 3. Mean relative abundance of discriminative taxa found in the cmDNA in mature and immature halibuts. [a]Values are expressed as percentages.

Finally, according to the factor K_{rel} conditions, a health index based on the individual's plumpness, only *Photobacterium* was highlighted as a discriminative genus for low-condition Atlantic halibut. In contrast, Streptococcus was a marker of high-condition individuals (Figure S12). In Greenland halibut, the only significant difference was the lower abundance of *Escherichia/Shigella* in the Greenland halibut with a low relative condition factor (K).

Spatial variation. We next tested the hypothesis that variations in the circulating microbiome could be attributed to geographic distribution. LEfSe analyses showed several variations at the genus level in both halibut species that were dependent on the collection site (Fig. 7A,B). More specifically, in the case of Greenland halibut, *Photobacterium* and *Burkholderia* were significantly more abundant in the Laurentian Channel than in the other areas with mean relative abundances of 13.2 ± 2.8% ($p < 0.001$) and 5.2 ± 1.0% ($p < 0.001$), respectively (Fig. 7C). *Exiguobacterium* and *Oleispira* were also more abundant in the Northeast Gulf ($p < 0.001$), whereas *Oleispira* was especially abundant in the Estuary and Western Gulf ($p < 0.001$). This finding contrasted with that noted for *Psychrobacter*, which was equally abundant in the Northeast gulf and the Estuary–Western gulf but less abundant in the Chaleur Bay and the Laurentian channel. Among other notable differences in Greenland halibut, we found a higher abundance of *Vibrio* in the Chaleur Bay and Northeast Gulf ($p < 0.001$). In the case of the Atlantic halibut, the Southern Gulf was characterized by a higher abundance of *Bizionia* ($p = 0.009$) and *Neorickettsia* ($p = 0.015$)

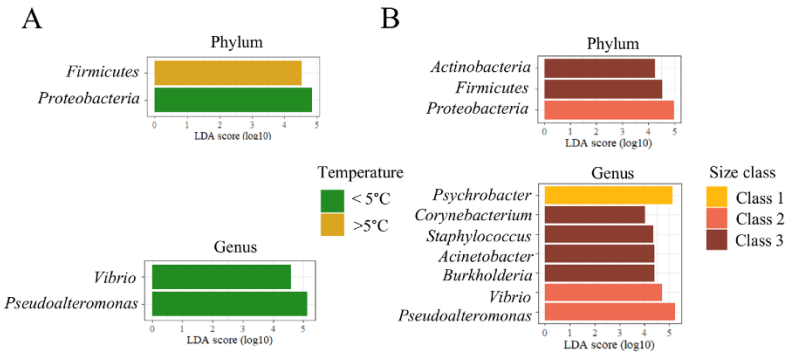

Figure 6. Discriminant taxa associated with seawater temperature and size classes. (**A**) LEfSe analysis of the blood microbiome showing the significantly different taxa in Greenland halibut (**A**) inhabiting cold (n = 25) and warm (n = 72) seawater and (**B**) according to their size class (Class 1, n = 36, Class 2, n = 22, Class 3, n = 39).

Taxa	Cold mean ± SE (n = 25)	Warm mean ± SE (n = 72)	*P* values	Test Statistics W
Proteobacteria	87.2 ± 2.0[a]	79.7 ± 1.9	< 0.05	626
Firmicutes	4.2 ± 0.8	7.9 ± 1.0	< 0.05	1166
Pseudoalteromonas	34.4 ± 4.9	19.9 ± 2.1	< 0.01	562
Vibrio	9.8 ± 1.4	5.9 ± 1.0	< 0.005	505.5

Table 4. Mean relative abundance (%) of discriminative taxa found in the cmDNA of Greenland halibuts inhabiting cold and warm water. [a]Values are expressed as percentages.

Taxa	Class 1 mean ± SE (n = 36)	Class 2 mean ± SE (n = 22)	Class 3 mean ± SE (n = 39)	*P* values[b]	Test Statistics Kruskal–Wallis χ^2
Proteobacteria	86.4 ± 1.4	87.5 ± 2.0	73.9 ± 3.0	< 0.005	13.24
Actinobacteria	1.8 ± 0.5	1.6 ± 0.4	3.9 ± 0.7	< 0.01	10.252
Firmicutes	5.8 ± 1.0	4.5 ± 1.0	9.3 ± 1.6	< 0.05	6.5906
Vibrio	8.8 ± 1.6	10.4 ± 1.6	3.2 ± 1.0	< 0.001	26.687
Psychrobacter	27.9 ± 2.9	8.3 ± 1.4	10.8 ± 2.1	< 0.001	26.643
Acinetobacter	2.8 ± 0.7	1.4 ± 0.4	5.0 ± 1.2	< 0.05	6.7541
Pseudolalteromonas	27.0 ± 2.9	37.2 ± 5.7	12.9 ± 2.2	< 0.001	21.364
Burkholderia	0.8 ± 0.4	1.8 ± 0.9	4.1 ± 0.9	< 0.001	20.681
Alcaligenes	0.1 ± 0.1	1.4 ± 1.1	0.02 ± 0.01	< 0.001	21.464
Corynebacterium	0.4 ± 0.2	0.3 ± 0.1	1.7 ± 0.5	< 0.001	18.396
Staphylococcus	0.7 ± 0.2	0.8 ± 0.3	3.7 ± 1.2	< 0.001	14.658

Table 5. Mean relative abundance (%) of the discriminative taxa found in the cmDNA of Greenland halibuts (*R. hippoglossoides*) according to the size classes. [a]Values are expressed as percentages.

relative to that in the Northeast Gulf and a lower abundance of *Staphylococcus* compared to the Estuary and Western Gulf ($p = 0.039$) (Fig. 7D). In terms of biodiversity, we did not find notable differences among areas except for a lower richness in the Laurentian Channel compared to Chaleur Bay (Figure S9).

Discussion

The circulating microbiome is an emerging concept that has drawn a high level of interest in the biomedical field, given its potential to generate predictive biomarkers and the means to screen for potential pathogens. In the present work, we applied this concept to characterize the circulating microbiome signature to two wild halibut populations of economic and ecological importance. We further studied how the microbiome signature composition and structure correlate with physiological and environmental factors.

Typically, in humans and other species, including fish, most microbiome studies have focused on the gut microbiome. In this study, even though the fish were euthanized during the DFO bottom survey and sex was

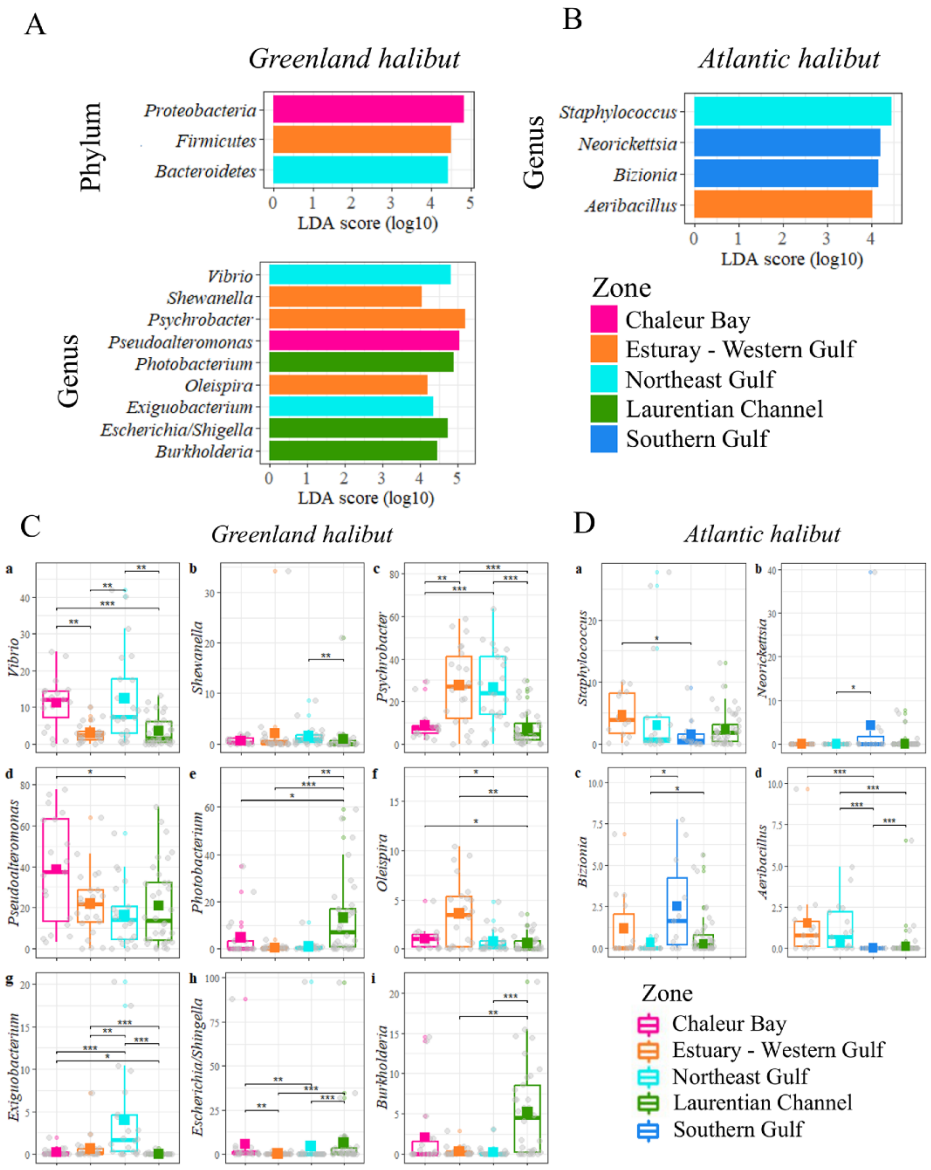

Figure 7. Spatial analysis. LEfSe analysis of the blood microbiome showing the significantly different taxa in (**A**) Greenland and (**B**) Atlantic halibut according to their localization. (**C** and **D**). Relative abundance of the discriminative genera in Greenland and Atlantic halibut. (*) $p < 0.05$; (**) $p < 0.01$; (***) $p < 0.00$. Greenland halibut: Estuary–Western Gulf, n = 22, Chaleur Bay, n = 19, Northeast Gulf, n = 22, Laurentian Channel, n = 34. Atlantic halibut: Estuary–Western Gulf, n = 14, Southern Gulf, n = 11, Northeast Gulf, n = 17, Laurentian Channel, n = 44.

assessed by visual characterization, the individual's sex could have been genetically determined with the blood samples[55,56]. In addition to ethical and logistical considerations, recent studies in humans and other species have shown that defining the core blood microbiome using a single drop of blood exhibits considerable potential as a disease biomarker[16,20]. The circulating microbiome can be used to facilitate the detection of pathogens, given that pathogenic (and symbiotic) bacteria are not exclusively found in the gut but also in other tissues. It is important to note, however, that the presence of bacteria in the blood is not de facto associated with a disease state, as

the existence of a healthy blood microbiome is increasingly recognized[16]. Indeed, the paradigm that the blood is a sterile compartment has shifted radically since the development of 16S rRNA next-generation sequencing methods. However, it is not clear at present whether the blood microbiome reflects bacteria that inhabit the blood in dormancy[16] or bacteria that translocate from one niche to another via blood circulation, a process referred to as "atopobiosis"[57]. According to this hypothesis, not only do bacteria use blood vessels to migrate from one tissue to another, but they can also do so by protecting themselves by infecting erythrocytes or white blood cells. Notwithstanding these fundamental questions, defining a dysbiotic blood microbiome has become a promising avenue for developing clinical biomarkers[58,59]. Combined with a logistically simple method based on a single drop of blood that can be stored at room temperature on cellulose paper, our study thus opens the door to developing a new type of biomarker that could be easily integrated into long-term monitoring programs.

From a fundamental point of view, our study has revealed that the blood microbiome of Greenland halibut and Atlantic halibut is unexpectedly richer than that reported to date in the blood of other endotherm animals[21–24], as well as in the gut or skin microbiome of other fish and marine species[38,40,41,60–68]. In addition, we found close similarities with core blood microbiomes, from other species and organs, such as skin and gut microbiomes, in terms of phyla (*Proteobacteria*, *Firmicutes*, *Bacteroidetes* and *Actinobacteria*) and genera[12,41,69]. However, a first glimpse at the blood microbiome of these two species revealed that their core blood microbiomes share many features, most notably at the phylum and genus levels. Overall, 30 different phyla, 63 classes, and 685 genera were identified within the cmDNA of both species. At the phylum level, the microbiome signatures of the cmDNA were dominated by *Proteobacteria*, *Firmicutes*, *Bacteroidetes* and *Actinobacteria*, although both species showed significantly different relative abundances in their phyla. At the genus level, the aggregated core genera were dominated by *Pseudoalteromonas*, *Psychrobacter* and *Acinetobacter* for both fish. The core ASV analysis provides more information on the core bacteria found with the aggregated genera. While the core genera were based on hundreds of ASVs (ASVs that belong to the same genera were aggregated together), those ASV were genetically different from each other. A closer analysis of each ASV, approximately 30% (on average) of the microbiome was represented by only five ASVs for Atlantic halibut and nine for Greenland halibut out of 3362 and 5023 ASVs in total, respectively (Figure S13). For example, *Pseudoalteromonas* represented an average of 23.6% of the Greenland halibut circulating microbiome when considering all 132 ASVs characterized as *Pseudoalteromonas*. However, the mean relative abundance is unequal among those ASVs, given that one represents 18.2% on average and the other only 5.4%. Moreover, no *Vibrio* nor *Staphylococcus* ASV stood out in the ASV analysis, even though the prevalence was lower. This finding indicates that *Vibrio* and *Staphylococcus* vary considerably more among individuals than *Pseudoalteromonas*, *Psychrobacter* and *Acinetobacter*.

Another notable difference between fish circulating microbiomes was the α- and β-diversity, and the richness per individual was higher in Greenland halibut. This microbiome was also more diverse in terms of the number of ASVs (5023 ASVs against 3362 ASVs in Atlantic halibut). We also found distinct genera in each species (*Enhydrobacter* for the Atlantic halibut and *Oleispira*, *Burkholderia* or *Shewanella,* among others for the Greenland halibut). All these differences could reflect genetic factors and coevolution history, as confirmed in the case of the gut microbiome[12,13,41]. Some genera have been found in the microbiome of other fish. For example, *Enhydrobacter* was identified in the mucus microbiome of three freshwater species[67] and present in at least 50% of the circulating microbiome of Atlantic halibut in the current study. *Shewanella* is another example found in high abundance in the gut microbiome of Atlantic mackerel[12] and previously described as an indicator of piscivorous behavior[41]. The environment is another factor that plays a role in the structure of the circulating microbiome. Greenland halibut is a cold-water (1–4 °C) species, whereas Atlantic Halibut is characterized by a higher temperature tolerance (1–13 °C). Our study also revealed that the relative abundance of the core genera and phyla varied according to size and temperature for Greenland halibut. *Vibrio* and *Pseudoalteromonas* were identified as discriminative taxa for each environmental factor studied. *Vibrio* and *Pseudoalteromonas* were abundant in cold water and immature individuals, particularly for fish-eating intermediate-sized prey. Additionally, *Psychrobacter* was significantly more abundant in immature fish for both species, especially in Greenland halibut eating small prey and male Atlantic halibut. Finally, *Acinetobacter* varied according to sex in Atlantic halibut and with the size class in Greenland halibut. It is, however, important to consider confounding factors before drawing conclusions. For example, in our case, sexual dimorphism implies that males are smaller than females at the same age in both species. Overall, our results indicate that biotic and abiotic factors, similar to the fish gut microbiome, impact the core blood microbiome[12,13,69].

An interesting finding was the difference in the blood core microbiota between males and females. Their microbiome did not differ in α- or β-diversity. However, LEfSe analysis pointed to a genus that discriminated between males and females in Greenland halibut. Specifically, *Shewanella* was more prevalent in male Greenland halibut, as confirmed by the change in relative abundance. This genus did not appear in any other LEfSe for other classes. In humans and animals, sex is among the most important factors that shape the gut microbiome[70]. In fish, such differences between males and females have been reported for the gut microbiome. Indeed, a study in three-spined stickleback and Eurasian perch showed that the diet-associated microbiota is sex-dependent[71].

Our LEfSe analysis comparing the blood microbiome between condition classes showed that fish with high condition levels presented significantly more Streptococcus than those with low-condition individuals in Atlantic halibut. In contrast, *Photobacterium* and *Vibrionaceae* were highlighted as discriminative taxa for low-condition Atlantic halibut. Although both genera have been identified in symbionts of other flatfish gut microbiomes[72,73], they also comprise well-known pathogenic species[74,75]. One must consider, however, that Fulton's K varies with multiple factors, including age, sex, and seasons.

Finally, our results highlighted spatial differences in the circulating microbiome signatures, particularly evident at the genus level (Figures S14 and S15). Several factors could explain such variations, including the location of nurseries for Greenland halibuts in some of these areas[51]. The genera correlated with the nurseries area corresponded to those correlated with the immature individuals, i.e., *Psychrobacter* and *Vibrio*. However, it is

important to consider potential confounding effects that may play a role in these variations, most notably for *Burkholderia*, which was also found in the large fish that are more common in the Laurentian Channel. Although the reasons behind these variations remain unclear, our data provide the basis for further investigation into the role of specific biotic and abiotic factors and how changes in these factors impact the circulating microbiome of these species.

In conclusion, our study provides answers to critical research questions about (1) fundamental differences between both halibut species and (2) the identification of factors that impact their circulating microbiome signatures. Our manuscript further provides a logistically-friendly sampling method for future longitudinal studies of dysbiosis in response to environmental stress factors. Based on the use of a single drop of blood fixed on cellulose paper, we hypothesize that the logistically friendly method we used is particularly well adapted for long-term monitoring of fish populations, most notably in response to climate change and the increase in ocean temperatures. It is important to note, however, that precautions, such as proper aseptic method, the use of sterile equipment, and controls (including no template controls and blank FTA cards) are essential to minimize the impact of contaminants in the interpretation of the results. Proper aseptic cleaning methods, the use of sterile equipment, no template controls (including control FTA cards and adjacent punches on the sampled cards), as well as the use of laboratories, materials and equipment specifically dedicated to the preparation of DNA needed, are necessary to remain critical in the interpretation of the results With such measures, given the stability of blood DNA on cellulose papers, this approach is perfectly adapted for biobanking purposes, facilitating future spatiotemporal retrospective studies. This study brings a first glimpse of what a circulating microbiome in fish looks like, but many questions remain unanswered. The similarities with the gut microbiome were striking and should be investigated. Furthermore, sex, maturity, diet and health indicators influenced the microbiome, especially the core microbiome. However, studies in a more controlled environment with finer maturity assessments, health and diet are needed to confirm these observations. Such studies would also reveal the impact of the environment on the relationship between physiological factors and the circulating microbiome. Future studies at a finer taxonomic level combined with multi-omics analysis, including transcriptomics and metabolomics, are also needed to determine the major driving factors that shape the blood microbiome in these two species.

Data availability

The sequence data supporting this study's findings are available on the NCBI website at https://www.ncbi.nlm.nih.gov/bioproject/PRJNA853332. The full dataset is available at https://doi.org/10.6084/m9.figshare.21482325, and the Rstudio code is available at https://doi.org/10.6084/m9.figshare.21482355.

Received: 22 November 2022; Accepted: 31 March 2023
Published online: 12 April 2023

References

1. Carrier, E., Ferchaud, A., Normandeau, E., Sirois, P. & Bernatchez, L. Estimating the contribution of Greenland Halibut (*Reinhardtius hippoglossoides*) stocks to nurseries by means of genotyping-by-sequencing: Sex and time matter. *Evol. Appl.* **13**, 2155–2167 (2020).
2. Kess, T. *et al.* A putative structural variant and environmental variation associated with genomic divergence across the Northwest Atlantic in Atlantic Halibut. *ICES J. Mar. Sci.* **78**(7), 2371–2384 (2021).
3. DFO. Assessment of the Gulf of St. Lawrence (4RST) Greenland halibut stock in 2020. *DFO Can. Sci. Advis. Sec.* Sci. Advis. Rep. 2021/017. (2021).
4. DFO. Stock Assessment of Gulf of St. Lawrence (4RST) Atlantic Halibut in 2020. *DFO Can. Sci. Advis. Sec.* Sci. Advis. Rep. 2021/034. (2021).
5. Shackell, N. L. *et al.* Spatial ecology of Atlantic Halibut across the Northwest Atlantic: A recovering species in an era of climate change. *Rev. Fisheries Sci. Aquac.* **30**(3), 281–305 (2022).
6. Brown-Vuillemin, S. *et al.* Diet composition of redfish (Sebastes sp) during periods of population collapse and massive resurgence in the Gulf of St. Lawrence. *Front. Mar. Sci.* **9**, 963039 (2022).
7. Gauthier, J., Marquis, M.-C., Bourdages, H., Ouellette-Plante, J. & Nozères, C. Gulf of St. Lawrence (4RST) Greenland Halibut Stock Status in 2018: Commercial Fishery and Research Survey Data. *DFO Can. Sci. Advis. Sec.* **Res. Doc. 2020/016**, v +130 (2020).
8. Gilbert, J. A. *et al.* Microbiome-wide association studies link dynamic microbial consortia to disease. *Nature* **535**, 94–103 (2016).
9. Ghanbari, M., Kneifel, W. & Domig, K. J. A new view of the fish gut microbiome: Advances from next-generation sequencing. *Aquaculture* **448**, 464–475 (2015).
10. Suchodolski, J. S. Diagnosis and interpretation of intestinal dysbiosis in dogs and cats. *Vet. J.* **215**, 30–37 (2016).
11. Bozzi, D. *et al.* Salmon gut microbiota correlates with disease infection status: potential for monitoring health in farmed animals. *Anim. Microbiome* **3**, 30 (2021).
12. Egerton, S., Culloty, S., Whooley, J., Stanton, C. & Ross, R. P. The gut microbiota of marine fish. *Front. Microbiol.* **9**, 873 (2018).
13. Legrand, T. P. R. A., Wynne, J. W., Weyrich, L. S. & Oxley, A. P. A. A microbial sea of possibilities: Current knowledge and prospects for an improved understanding of the fish microbiome. *Rev. Aquacult.* **12**, 1101–1134 (2020).
14. Perry, W. B., Lindsay, E., Payne, C. J., Brodie, C. & Kazlauskaite, R. The role of the gut microbiome in sustainable teleost aquaculture. *Proc. R. Soc. B.* **287**, 20200184 (2020).
15. Reverter, M., Tapissier-Bontemps, N., Lecchini, D., Banaigs, B. & Sasal, P. Biological and ecological roles of external fish mucus: A review. *Fishes* **3**, 41 (2018).
16. Castillo, D. J., Rifkin, R. F., Cowan, D. A. & Potgieter, M. The healthy human blood microbiome: Fact or fiction?. *Front. Cell. Infect. Microbiol.* **9**, 148 (2019).
17. Kowarsky, M. *et al.* Numerous uncharacterized and highly divergent microbes which colonize humans are revealed by circulating cell-free DNA. *Proc. Natl. Acad. Sci. USA* **114**, 9623–9628 (2017).
18. Panaiotov, S., Filevski, G., Equestre, M., Nikolova, E. & Kalfin, R. Cultural isolation and characteristics of the blood microbiome of healthy individuals. *AIDS Patient Care STDs* **8**, 406–421 (2018).
19. Poore, G. D. *et al.* Microbiome analyses of blood and tissues suggest cancer diagnostic approach. *Nature* **579**, 567–574 (2020).
20. Whittle, E., Leonard, M. O., Harrison, R., Gant, T. W. & Tonge, D. P. Multi-method characterization of the human circulating microbiome. *Front. Microbiol.* **9**, 3266 (2019).

21. Mandal, R. K. *et al.* An investigation into blood microbiota and its potential association with Bacterial Chondronecrosis with Osteomyelitis (BCO) in Broilers. *Sci. Rep.* **6**, 25882 (2016).
22. Scarsella, E., Sandri, M., Monego, S. D., Licastro, D. & Stefanon, B. Blood microbiome: A new marker of gut microbial population in dogs?. *Vet. Sci.* **13**, 198 (2020).
23. Scarsella, E., Zecconi, A., Cintio, M. & Stefanon, B. Characterization of microbiome on feces, blood and milk in dairy cows with different milk leucocyte pattern. *Animals* **11**, 1463 (2021).
24. Vientós-Plotts, A. I. *et al.* Dynamic changes of the respiratory microbiota and its relationship to fecal and blood microbiota in healthy young cats. *PLoS ONE* **12**, e0173818 (2017).
25. Amar, J. *et al.* Blood microbiota dysbiosis is associated with the onset of cardiovascular events in a large general population: The D.E.S.I.R. study. *PLoS ONE* **8**, e54461 (2013).
26. Hyun, H. *et al.* Analysis of porcine model of fecal-induced peritonitis reveals the tropism of blood microbiome. *Front. Cell. Infect. Microbiol.* **11**, 676650 (2021).
27. Mohamed, W. M. A. *et al.* Exploring prokaryotic and eukaryotic microbiomes helps in detecting tick-borne infectious agents in the blood of camels. *Pathogens* **10**, 351 (2021).
28. Tilahun, Y. *et al.* Transcript and blood-microbiome analysis towards a blood diagnostic tool for goats affected by *Haemonchus contortus*. *Sci. Rep.* **12**, 5362 (2022).
29. Vientós-Plotts, A. I., Ericsson, A. C., Rindt, H. & Reinero, C. R. Blood cultures and blood microbiota analysis as surrogates for bronchoalveolar lavage fluid analysis in dogs with bacterial pneumonia. *BMC Vet. Res.* **17**, 129 (2021).
30. McMurdie, P. J. & Holmes, S. phyloseq: An R package for reproducible interactive analysis and graphics of microbiome census data. *PLoS ONE* **8**, e61217 (2013).
31. Ssekagiri, A., Ijaz, D. U. Z. & Sloan, W. T. MicrobiomeSeq: An R package for analysis of microbial communities in an environmental context. In *ISCB Africa ASBCB Conference* (Kumasi, Ghana, 2017).
32. Cao, Y. *MicrobiomeMarker: Microbiome Biomarker Analysis. R Package Version 0.0. 1.9000*. Available online: https://github.com/yiluheihei/microbiomeMarker.
33. Oksanen, J. *et al.* Community Ecology Package. *R package version* **2**, 321 (2020).
34. Wickham, H. *ggplot2: Elegant Graphics for Data Analysis* (Springer, 2016).
35. South, A. *Rnaturalearth: World Map Data from Natural Earth. R package version 0.1.0*. https://CRAN.R-project.org/package=rnaturalearth (2017).
36. Palanisamy, V., Gajendiran, V. & Mani, K. Meta-analysis to identify the core microbiome in diverse wastewater. *Int. J. Environ. Sci. Technol.* **19**, 5079–5096 (2022).
37. Jing, H. *et al.* Composition and ecological roles of the core microbiome along the Abyssal-Hadal transition zone sediments of the Mariana trench. *Microbiol. Spectr.* **10**, e01988-e2021 (2022).
38. Lokesh, J. & Kiron, V. Transition from freshwater to seawater reshapes the skin-associated microbiota of Atlantic salmon. *Sci. Rep.* **6**, 19707 (2016).
39. Wang, Y. *et al.* Insights into bacterial diversity in compost: Core microbiome and prevalence of potential pathogenic bacteria. *Sci. Total Environ.* **718**, 137304 (2020).
40. Gatesoupe, F.-J., Zambonino Infante, J.-L., Cahu, C. & Quazuguel, P. The highly variable microbiota associated to intestinal mucosa correlates with growth and hypoxia resistance of sea bass, *Dicentrarchus labrax*, submitted to different nutritional histories. *BMC Microbiol.* **16**, 1–13 (2016).
41. Huang, Q. *et al.* Diversity of gut microbiomes in marine fishes is shaped by host-related factors. *Mol. Ecol.* **29**, 5019–5034 (2020).
42. Huse, S. M., Ye, Y., Zhou, Y. & Fodor, A. A. A core human microbiome as viewed through 16S rRNA sequence clusters. *PLoS ONE* **7**, e34242 (2012).
43. DFO. Stock assessment of Gulf of St. Lawrence (4RST) Atlantic halibut in 2018. *DFO Can. Sci. Advis. Sec.* Sci. Advis. Rep. 2019/038 (2019).
44. DFO. Assessment of the Gulf of St. Lawrence (4RST) Greenland Halibut stock in 2018. *DFO Can. Sci. Advis. Sec.* Sci. Advis. Rep. 2019/023 (2019).
45. Jonassen, T. M., Imsland, A. K., Kadowaki, S. & Stefansson, S. O. Interaction of temperature and photoperiod on growth of Atlantic halibut *Hippoglossus hippoglossus* L. *Aquac. Res.* **31**, 219–227 (2000).
46. Björnsson, B. & Tryggvadóttir, S. V. Effects of size on optimal temperature for growth and growth efficiency of immature Atlantic halibut (*Hippoglossus hippoglossus* L.). *Aquaculture* **142**, 33–42 (1996).
47. Le Cren, E. D. The length-weight relationship and seasonal cycle in gonad weight and condition in the perch (*Perca fluviatilis*). *J. Anim. Ecol.* **20**, 201 (1951).
48. Froese, R. Cube law, condition factor and weight-length relationships: History, meta-analysis and recommendations. *J. Appl. Ichthyol.* **22**, 241–253 (2006).
49. Keys, A. B. The weight-length relation in fishes. *Proc. Natl. Acad. Sci. U.S.A.* **14**, 922–925 (1928).
50. Blackwell, B. G., Brown, M. L. & Willis, D. W. Relative weight (Wr) status and current use in fisheries assessment and management. *Rev. Fish. Sci.* **8**, 1–44 (2000).
51. Youcef, W. A., Lambert, Y. & Audet, C. Spatial distribution of Greenland halibut Reinhardtius hippoglossoides in relation to abundance and hypoxia in the estuary and Gulf of St. Lawrence: *Greenland halibut distribution in estuary and Gulf of St Lawrence*. *Fish. Oceanogr.* **22**, 41–60 (2013).
52. Lahti, L., *et al. Microbiome R Package*. https://github.com/microbiome/microbiome/ (2018).
53. Rstudio Team. RStudio: Integrated Development Environment for R. (2021).
54. Morgan, M. J. *et al.* Changes in distribution of Greenland halibut in a varying environment. *ICES J. Mar. Sci.* **70**, 352–361 (2013).
55. Ferchaud, A.-L. *et al.* Chromosome-level assembly reveals a putative Y-autosomal fusion in the sex determination system of the Greenland Halibut (*Reinhardtius hippoglossoides*). *G3 Genes Genomes Genet.* **12**, jkab376 (2022).
56. Edvardsen, R. B. *et al.* Heterochiasmy and the establishment of gsdf as a novel sex determining gene in Atlantic halibut. *PLoS Genet* **18**, e1010011 (2022).
57. Potgieter, M., Bester, J., Kell, D. B. & Pretorius, E. The dormant blood microbiome in chronic, inflammatory diseases. *FEMS Microbiol. Rev.* **39**, 567–591 (2015).
58. Chen, H. *et al.* Circulating microbiome DNA: An emerging paradigm for cancer liquid biopsy. *Cancer Lett.* **521**, 82–87 (2021).
59. Wang, C. *et al.* Characterization of the blood and neutrophil-specific microbiomes and exploration of potential bacterial biomarkers for sepsis in surgical patients. *Immun. Inflamm. Dis.* **9**, 1343–1357 (2021).
60. Bhute, S. S. *et al.* The gut microbiome and its potential role in paradoxical anaerobism in pupfishes of the Mojave Desert. *Anim. Microbiome* **2**, 20 (2020).
61. Eryemez, M. & Balcázar, J. L. Bacterial community structure in the intestinal ecosystem of rainbow trout (*Oncorhynchus mykiss*) as revealed by pyrosequencing-based analysis of 16S rRNA genes. *Res. Vet. Sci.* **100**, 8–11 (2015).
62. Lowrey, L., Woodhams, D. C., Tacchi, L. & Salinas, I. Topographical mapping of the rainbow trout (*Oncorhynchus mykiss*) microbiome reveals a diverse bacterial community with antifungal properties in the skin. *Appl. Environ. Microbiol.* **81**, 6915–6925 (2015).
63. Lyons, P. P., Turnbull, J. F., Dawson, K. A. & Crumlish, M. Phylogenetic and functional characterization of the distal intestinal microbiome of rainbow trout *Oncorhynchus mykiss* from both farm and aquarium settings. *J. Appl. Microbiol.* **122**, 347–363 (2017).

64. Nielsen, S., Walburn, J. W., Vergés, A., Thomas, T. & Egan, S. Microbiome patterns across the gastrointestinal tract of the rabbitfish *Siganus fuscescens*. *PeerJ.* **5**, e3317 (2017).
65. Reinhart, E. M., Korry, B. J., Rowan-Nash, A. D. & Belenky, P. Defining the distinct skin and gut microbiomes of the northern pike (*Esox lucius*). *Front. Microbiol.* **10**, 2118 (2019).
66. Rosado, D., Pérez-Losada, M., Severino, R., Cable, J. & Xavier, R. Characterization of the skin and gill microbiomes of the farmed seabass (*Dicentrarchus labrax*) and seabream (*Sparus aurata*). *Aquaculture* **500**, 57–64 (2019).
67. Sylvain, F. -É. *et al.* Fish skin and gut microbiomes show contrasting signatures of host species and habitat. *Appl. Environ. Microbiol.* **86**, e00789 (2020).
68. Walter, J. M., Bagi, A. & Pampanin, D. M. Insights into the potential of the atlantic cod gut microbiome as biomarker of oil contamination in the marine environment. *Microorganisms* **7**, 209 (2019).
69. Clements, K. D., Angert, E. R., Montgomery, L. & Choat, J. H. Intestinal microbiota in fishes: What's known and what's not. *Mol. Ecol.* **23**, 1891–1898 (2014).
70. Kim, Y. S., Unno, T., Kim, B.-Y. & Park, M.-S. Sex differences in gut microbiota. *World J. Mens. Health* **38**, 48 (2020).
71. Bolnick, D. I. *et al.* Individual diet has sex-dependent effects on vertebrate gut microbiota. *Nat. Commun.* **5**, 4500 (2014).
72. Cerdà-Cuéllar, M. & Blanch, A. R. Determination of *Vibrio scophthalmi* and its phenotypic diversity in turbot larvae. *Environ. Microbiol.* **6**, 209–217 (2004).
73. Sugita, H. & Ito, Y. Identification of intestinal bacteria from Japanese flounder (*Paralichthys olivaceus*) and their ability to digest chitin. *Lett. Appl. Microbiol.* **43**, 336–342 (2006).
74. Thyssen, A. & Ollevier, F. *Photobacterium*. In *Bergey's Manual of Systematics of Archaea and Bacteria* (eds Whitman, W. B. *et al.*) 1–11 (Wiley, New York, 2015).
75. Yeung, P. S. M. & Boor, K. J. Epidemiology, Pathogenesis, and Prevention of Foodborne *Vibrio parahaemolyticus* Infections. *Foodborne Pathog. Dis.* **1**, 74–88 (2004).

Acknowledgements
This research was performed with the logistic support of Fisheries and Oceans Canada (DFO). The authors would like to thank all of the personnel from the DFO for their help and hospitality during the survey of the Northern and Southern Gulf of St. Lawrence. The authors would also like to thank Dr. Claire Plissonneau for their expert advice and technical support. The author would also like to thank Marlène Fortier and Clémence Del Valle for their excellent technical help. This work was funded by the Fonds de Recherche du Québec-Nature et Technologie (YSP, RV and DR) and is supported by the Canada Research Chair Program.

Author contributions
D.R., R.V., F.F. and Y.S.P. conceived the study. All authors were responsible for the interpretation of data and critical appraisal. All authors executed the experiments and/or contributed to the experimental design and/or analyses of the results. F.F. and Y.S.P. drafted the manuscript with input from all authors at all stages.

Competing interests
The authors declare no competing interests.

Additional information
Supplementary Information The online version contains supplementary material available at https://doi.org/10.1038/s41598-023-32690-6.

Correspondence and requests for materials should be addressed to Y.S.-P.

Reprints and permissions information is available at www.nature.com/reprints.

Publisher's note Springer Nature remains neutral with regard to jurisdictional claims in published maps and institutional affiliations.

SUPPLEMENTARY MATERIAL

Defining the circulating microbiome of wild-fish halibut populations using a single drop of blood: a novel approach to monitoring the health status of wild fish populations.

Fanny Fronton[1], Sophia Ferchiou[1], France Caza[1], Richard Villemur[1], Dominique Robert[2], and Yves St-Pierre[1].

1) INRS-Centre Armand-Frappier Santé Technologie, 531 Boul. des Prairies, Laval, QC, Canada, H7V 1B7

2) Institut des Sciences de la Mer, Université du Québec à Rimouski, 310, allée des Ursulines, C.P. 3300 Rimouski (Québec)

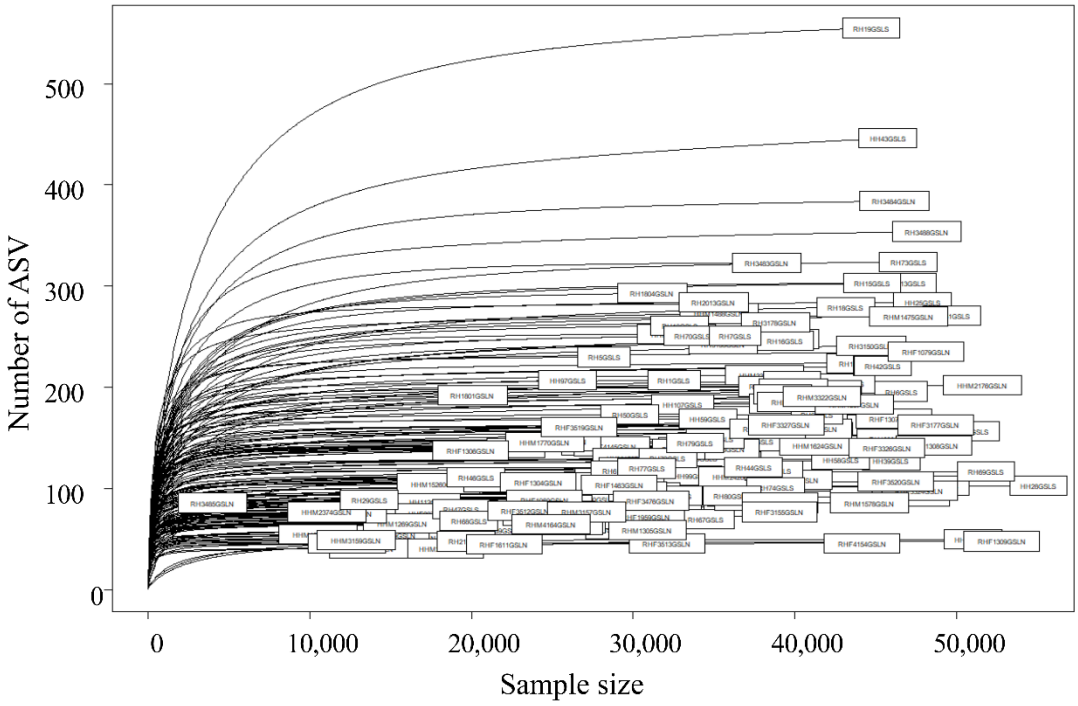

Figure S1: Sequencing depth curves based on the number of reads (sample size) and the number of ASVs for each sample. Each line represents one sample.

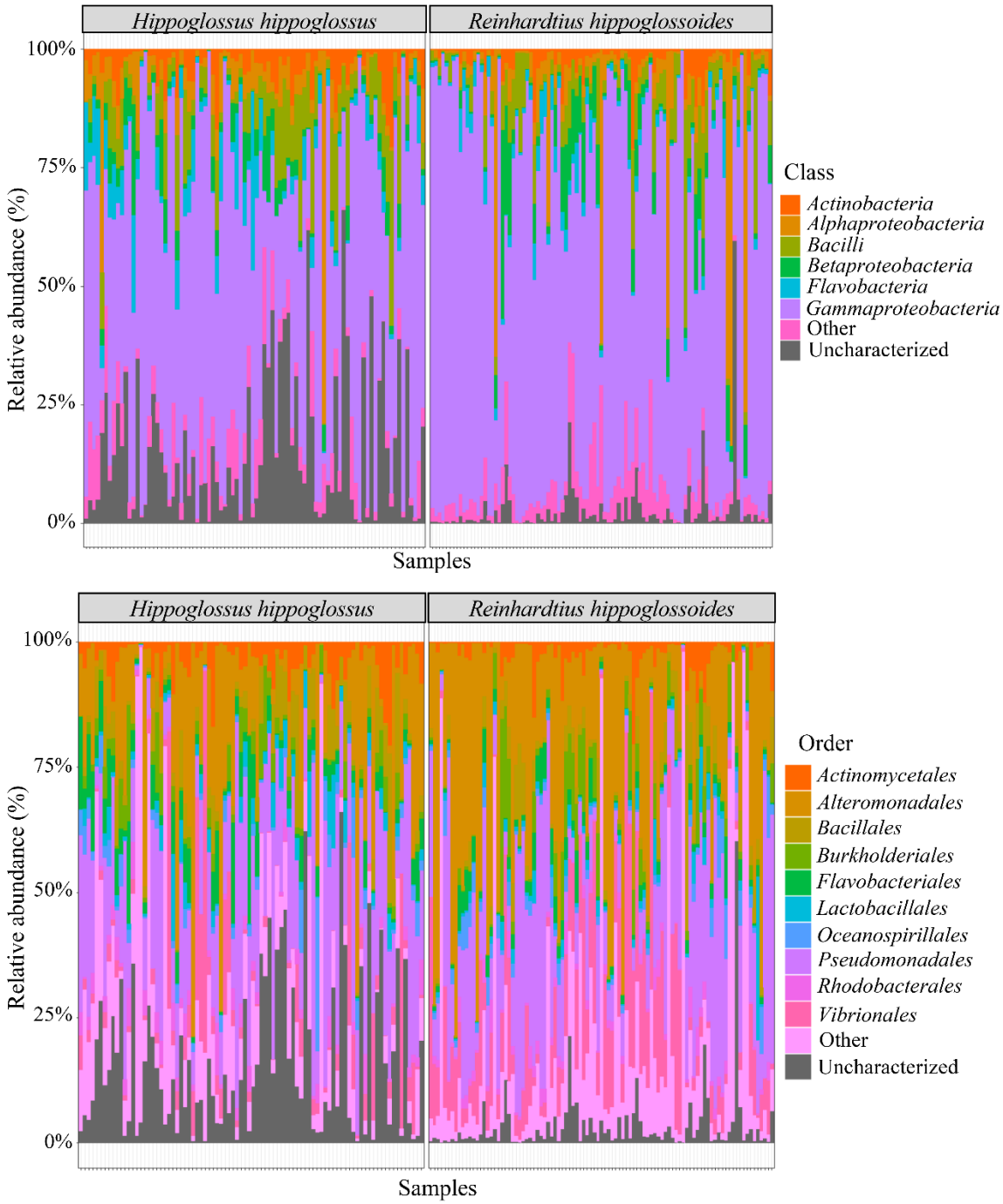

Figure S2: Relative abundance at the class and order levels of the halibuts' circulating microbiome. Relative abundance of the main classes (top) and orders (bottom) present the blood microbiome of the Atlantic halibut (left) and the Greenland halibut (right). Atlantic halibut, n = 86, Greenland halibut, n = 97.

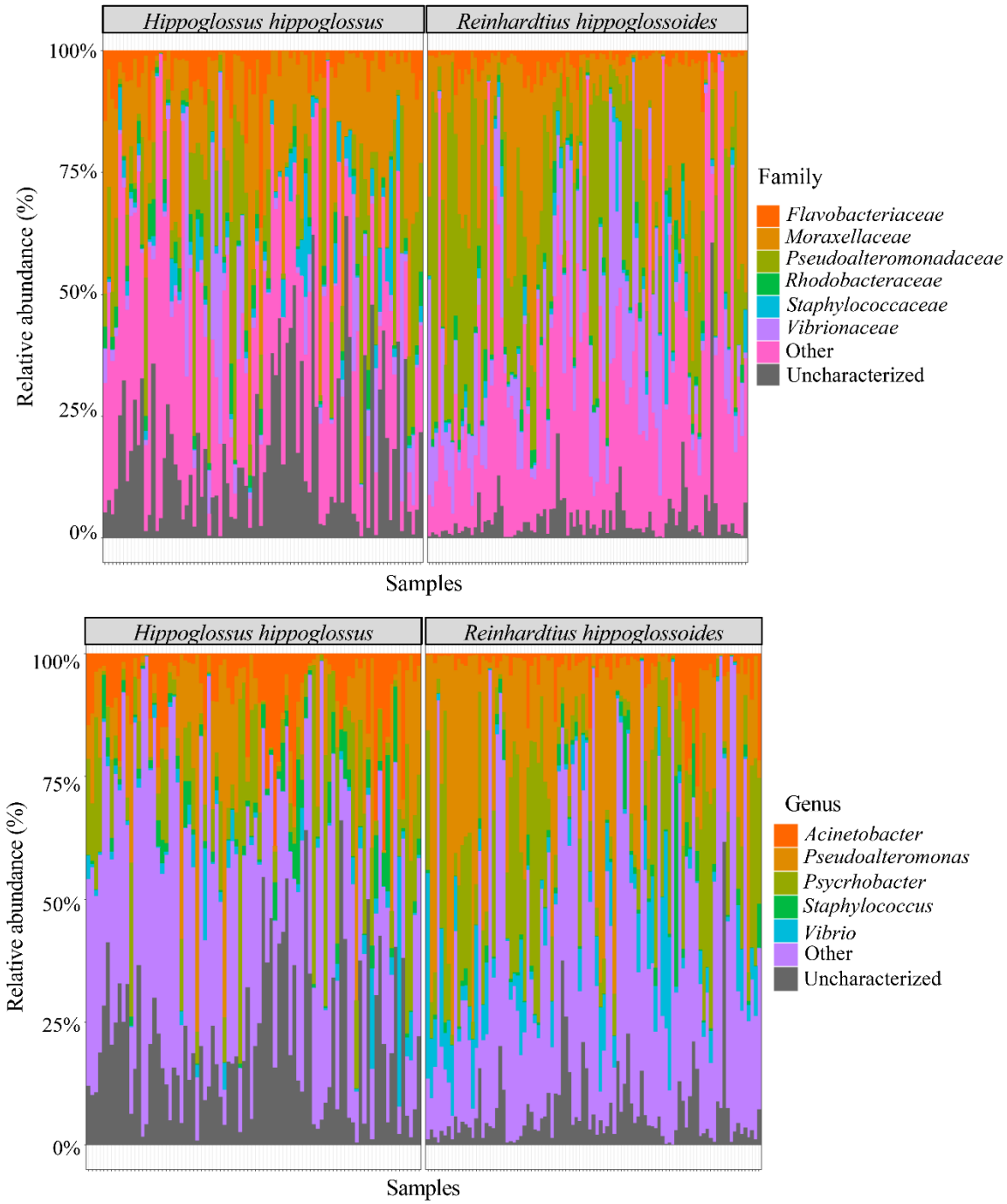

Figure S3: Relative abundance at the family and genus levels of the halibuts' circulating microbiome. Relative abundance of the main family (top) and genus (bottom) present the blood microbiome of the Atlantic halibut (left) and the Greenland halibut (right). Atlantic halibut, n = 86, Greenland halibut, n = 97.

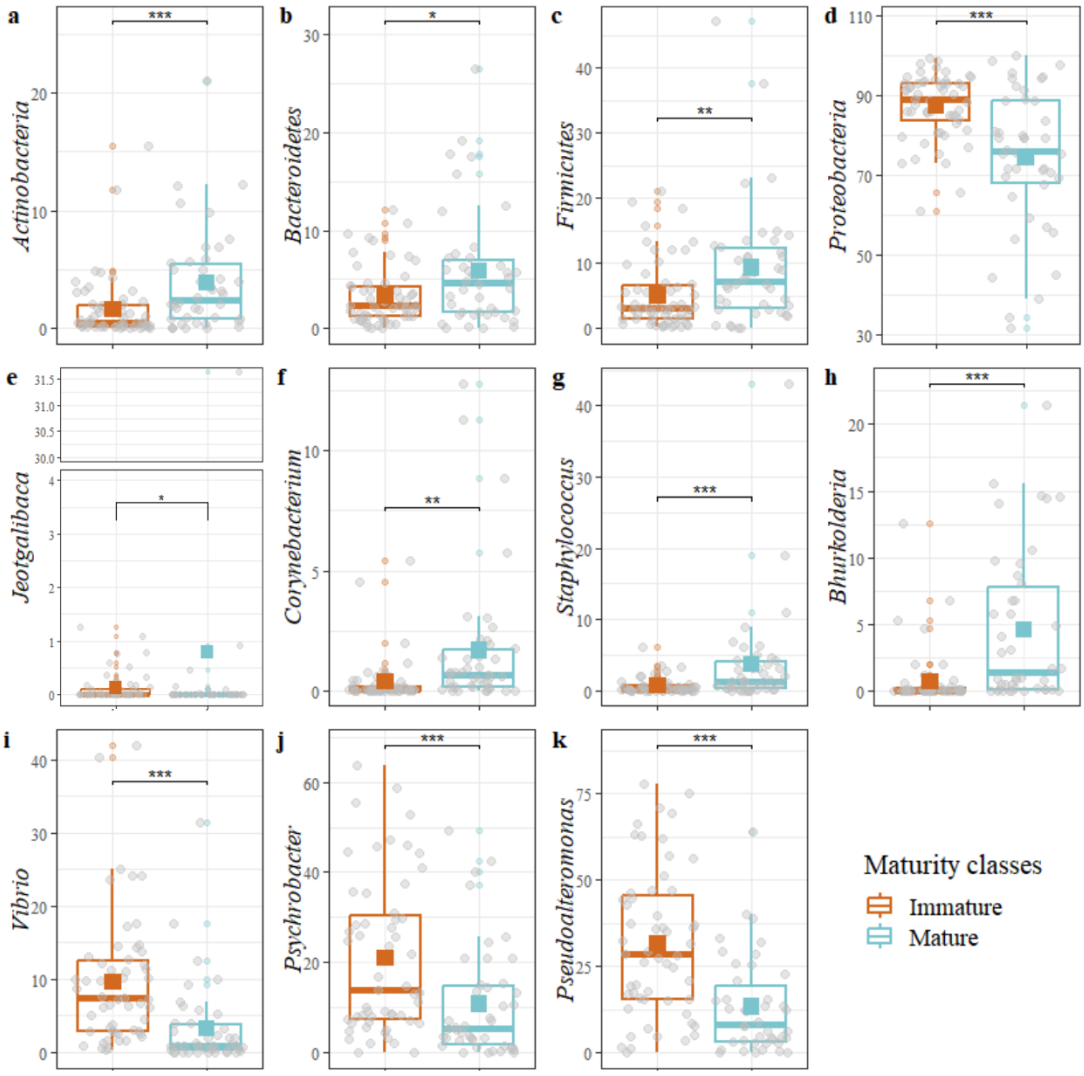

Figure S4: Relative abundance (%) of the discriminative phylum or genera found in the blood microbiome of immature (n = 55) and mature (n = 42) Greenland halibuts. (*) $p < 0.05$; (**) $p < 0.01$; (***) $p < 0.001$.

Hippoglossus hippoglossus

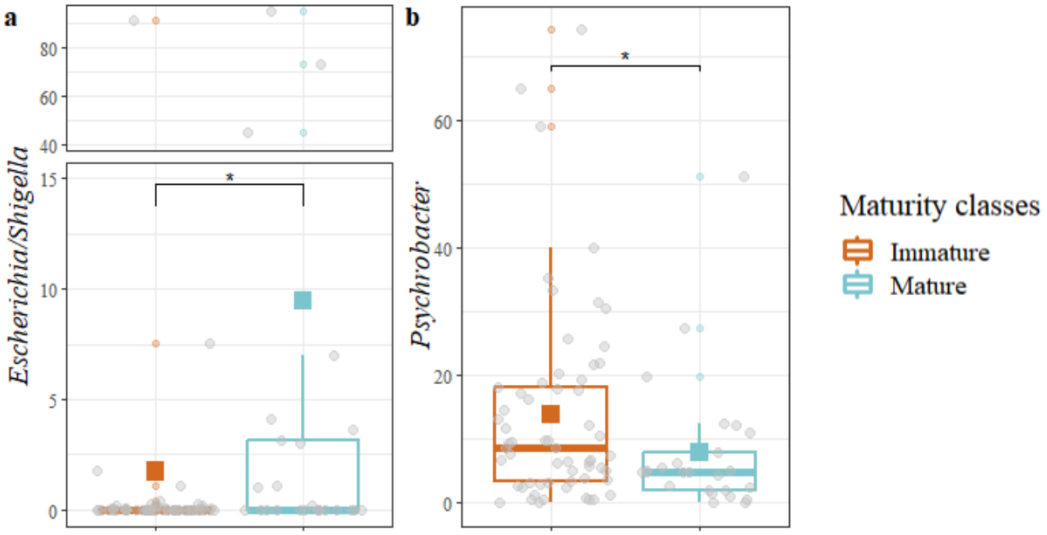

Figure S5: Relative abundance (%) of the discriminative phylum or genera found in the blood microbiome of immature (n = 56) and mature (n = 25) Atlantic halibut. (*) $p < 0.05$; (**) $p < 0.01$; (***) $p < 0.001$.

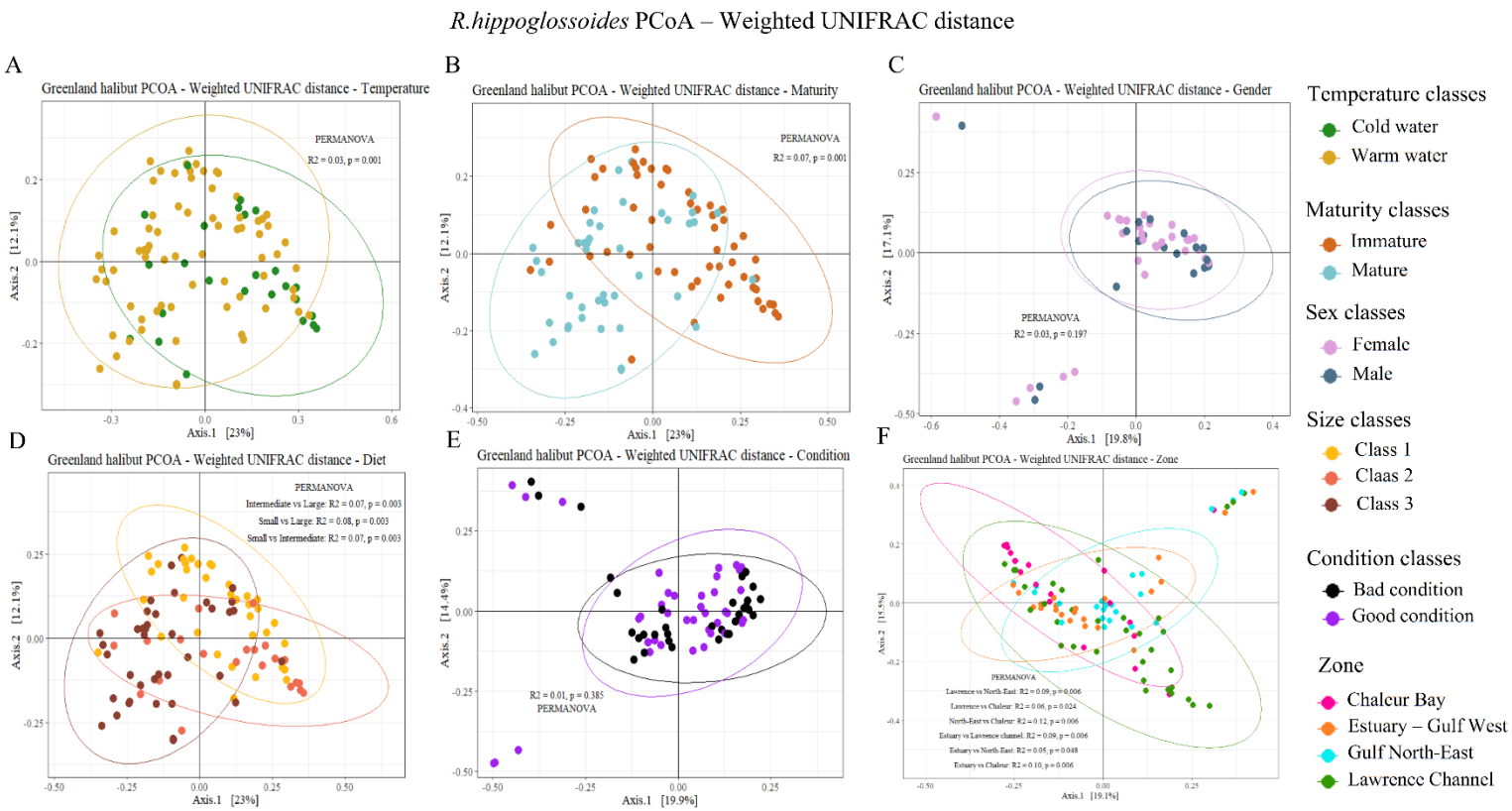

Figure S6: **PCoA (β-diversity) of the blood microbiome of the Greenland halibut (*R. hippoglossoides*).** The β-diversity was compared between temperature, diet, condition and maturity classes, sex, and zones.

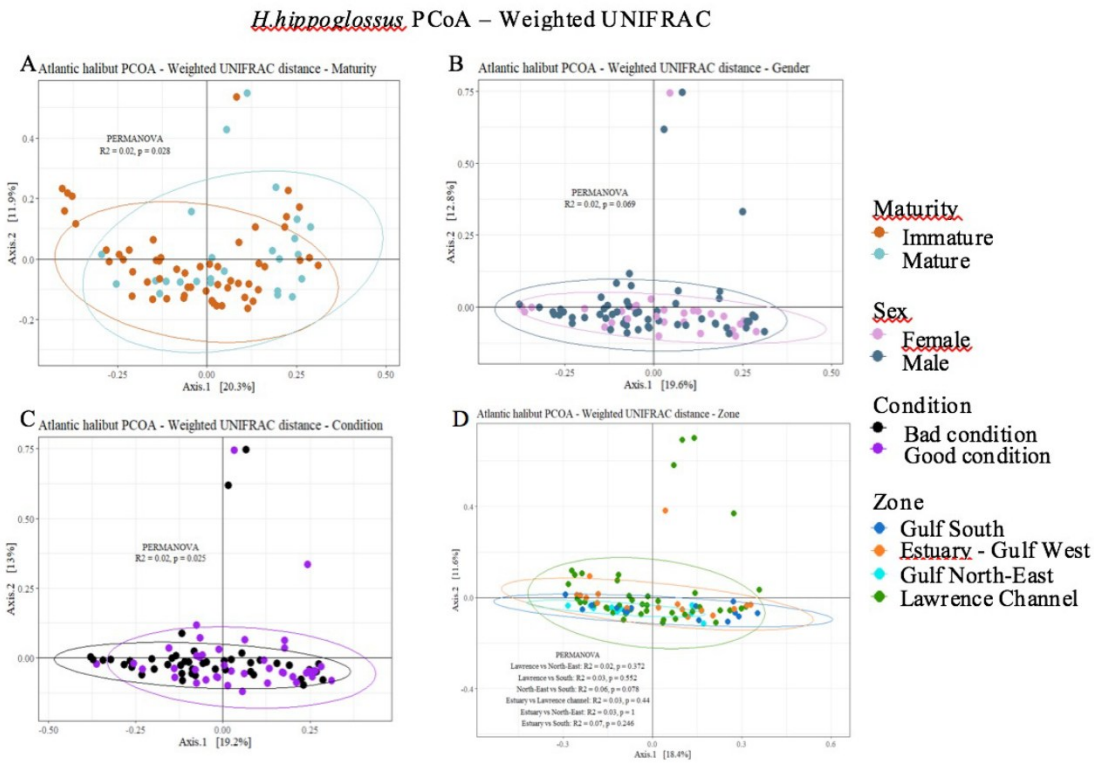

Figure S7: **PCoA (β-diversity) of the blood microbiome of the Atlantic halibut (*R. hippoglossus*).** The β-diversity was compared between condition and maturity classes, sex, and zones.

Reinhardtius hippoglossoides

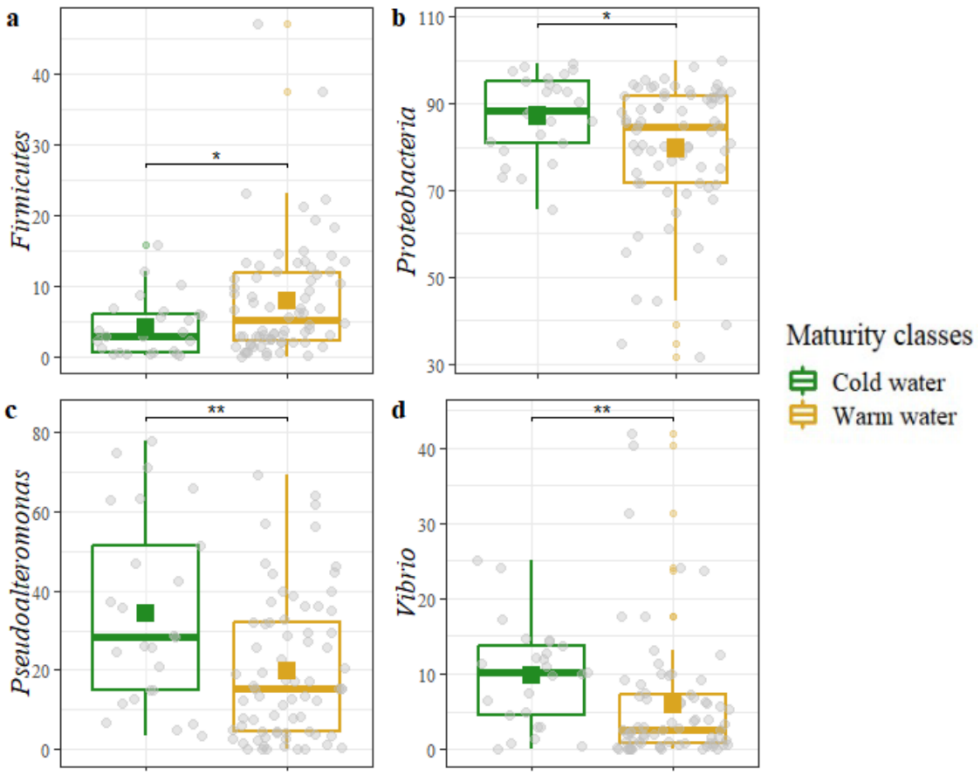

Figure S8: Relative abundance (%) of the discriminative phylum or genera in the blood of individuals inhabiting cold (<5°C) or warm (>5°C) water. Cold water, n = 25, warm water, n = 72. Significant differences between temperature classes were measured using the Wilcoxon-Mann-Whitney test. (*) $p < 0.05$; (**) $p < 0.01$; (***) $p < 0.001$.

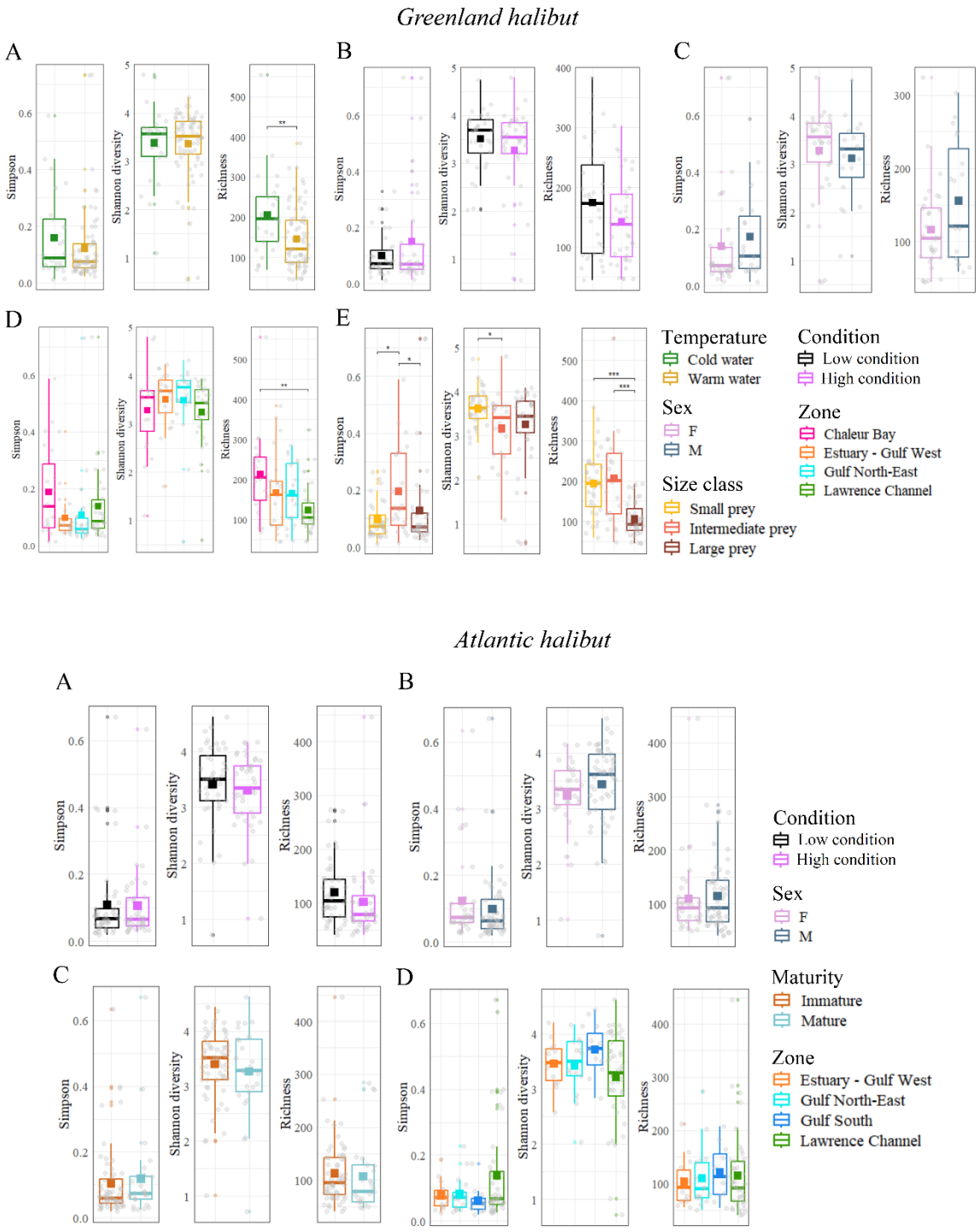

Figure S9: **Variations of α-diversity analysis of the blood microbiome of the Greenland and Atlantic halibut.**

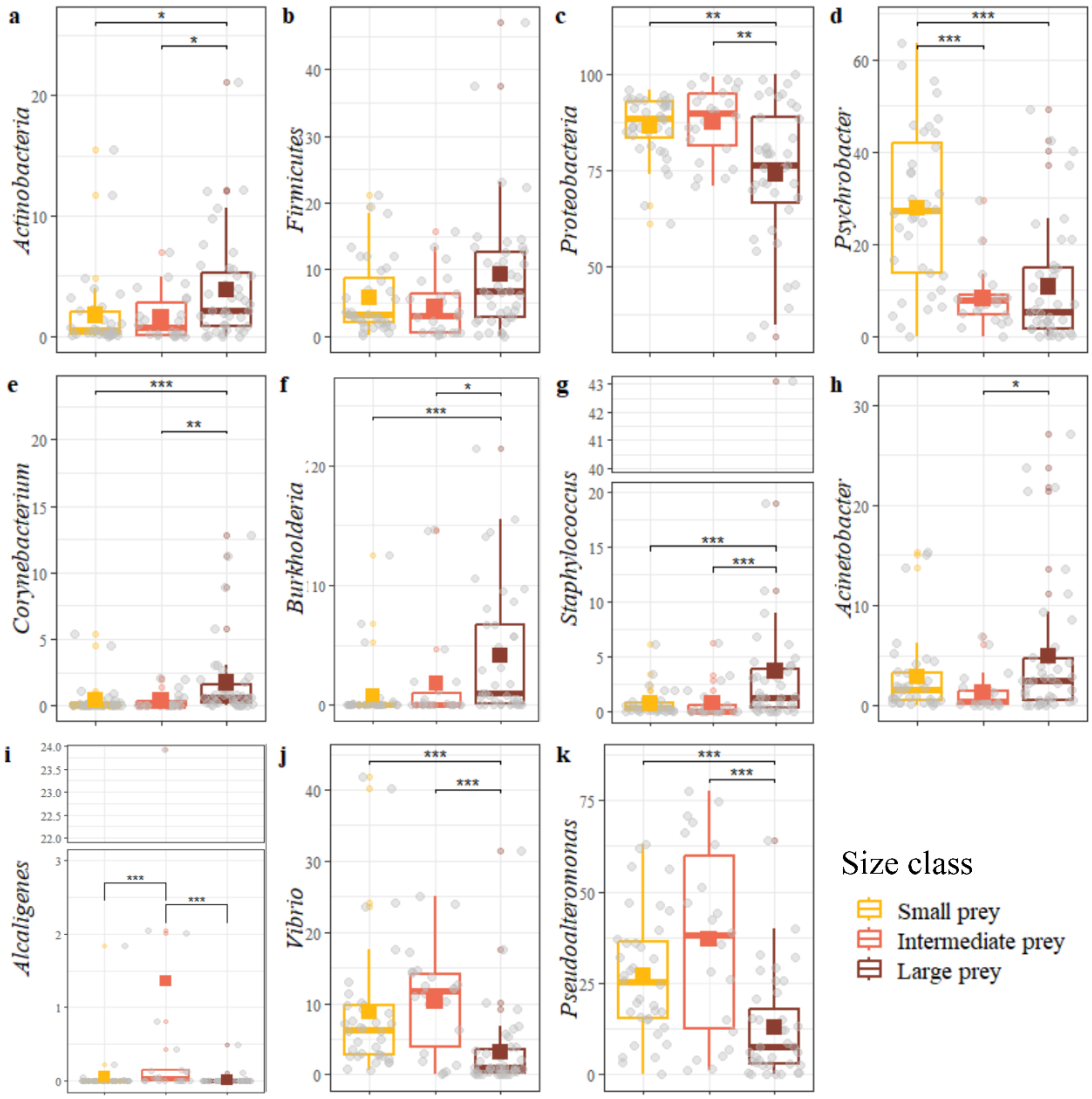

Figure S10: Relative abundance (%) of the discriminative phylum or genera in the blood of individuals according to diet classes. Small, n = 36, intermediate, n = 22, large, n = 39. Significant differences between temperature classes were measured using the Wilcoxon-Mann-Whitney test. (*) $p < 0.05$; (**) $p < 0.01$; (***) $p < 0.001$.

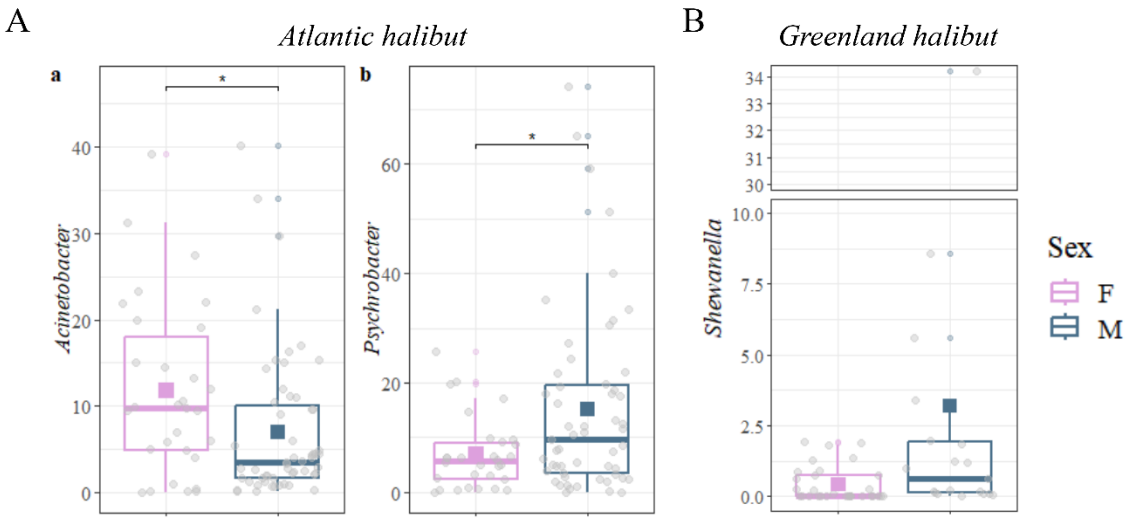

Figure S11: Relative abundance (%) of the discriminative taxa in the blood of male and female Atlantic (A) and Greenland (B) halibuts. Significant differences between sex were measured using the Wilcoxon-Mann-Whitney test. (*) $p < 0.05$; (**) $p < 0.01$; (***) $p < 0.001$.

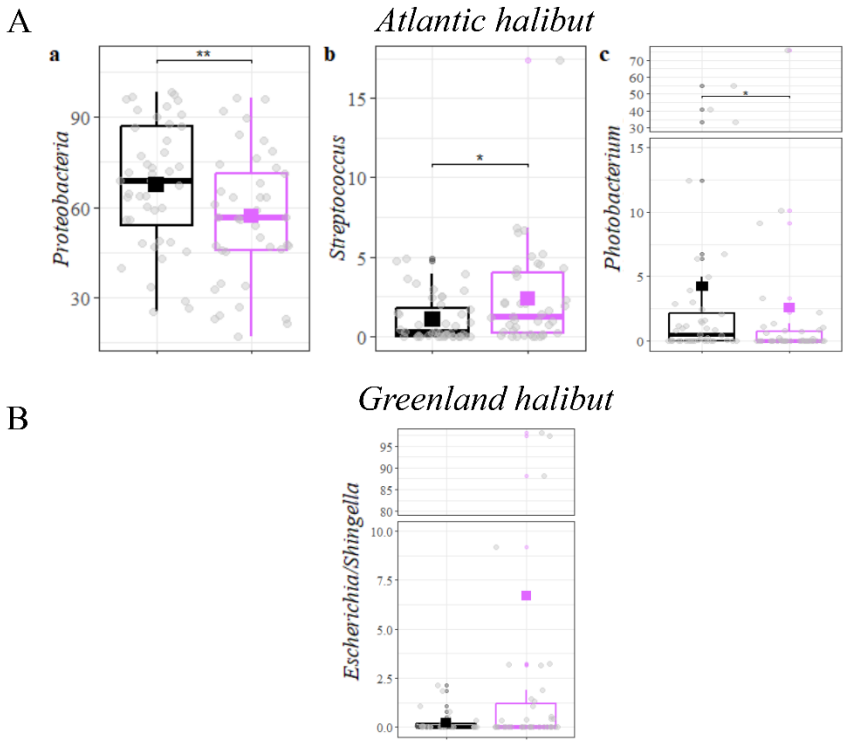

Figure S12: Relative abundance (%) of the discriminative taxa in the blood microbiome of according to condition classes. Discriminative taxa for (**A**) Atlantic and Greenland (**B**) halibut in bad (K>1) (black boxes) and good (K>1) (purple boxes) conditions. Significant differences between condition classes were tested with the Wilcoxon-Mann-Whitney test. (*) $p < 0.05$; (***) $p < 0.001$

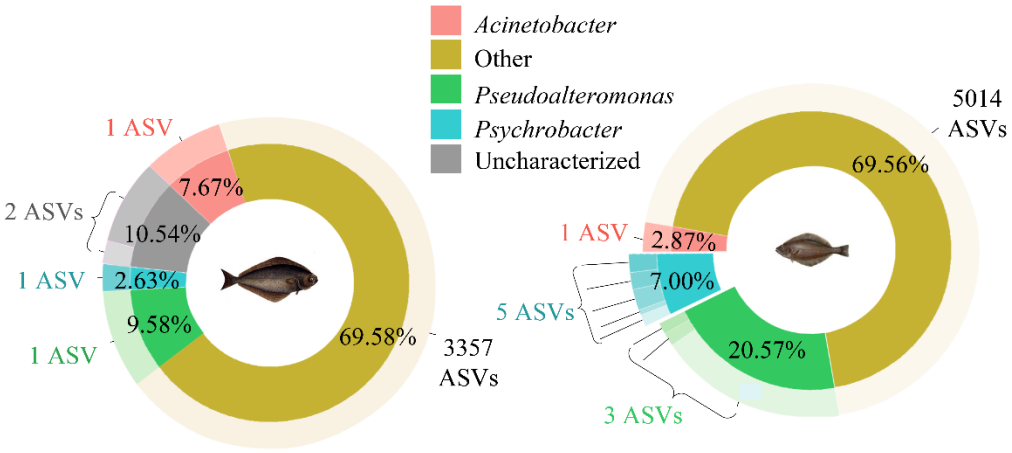

Figure S13: **Mean relative abundance of the core ASVs of the halibuts' circulating microbiome.** Mean relative abundance (%) of the core ASVs (70% prevalence) present the circulating microbiome of the Atlantic halibut (*H. hippoglossus*) and the Greenland halibut (*R. hippoglossoides*). The mean relative abundance is given in each pie. Atlantic halibut, n = 86, Greenland halibut, n = 97.

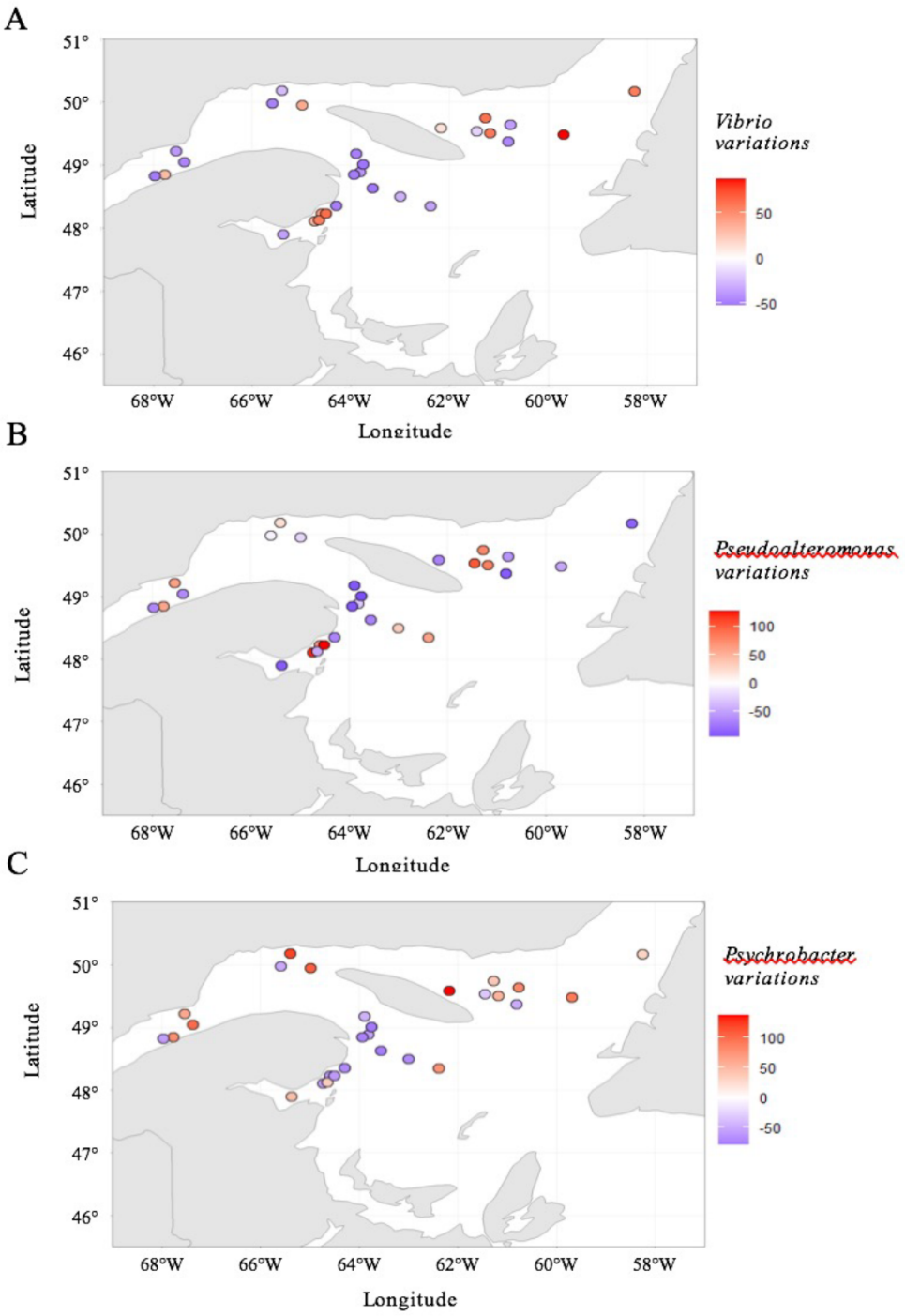

Figure S14: Maps of the variations around the mean flatted by a squared root in the Greenland halibut (*R. hippoglossoides*) blood microbiome core genera. A. *Vibrio* B. *Pseudoalteromonas*. C. *Psychrobacter.*

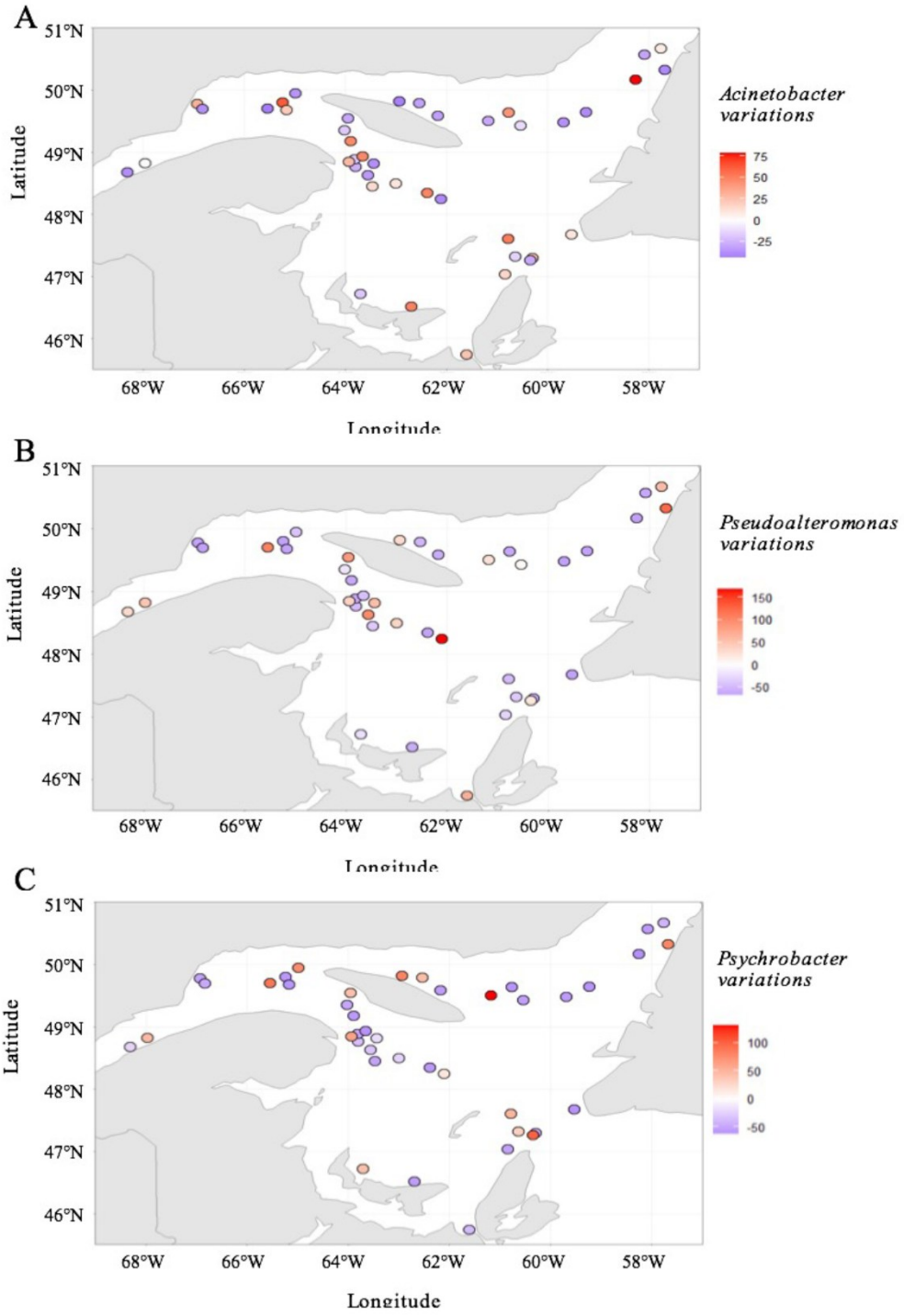

Figure S15: Maps of the variations around the mean flatted by a squared root in the Atlantic halibut (*H. hippoglossus*) blood microbiome core genera. A. *Acinetobacter* B. *Pseudoalteromonas*. C. *Psychrobacter*.

Annexe III

Effets du tébuconazole sur le microbiome de la truite arc-en-ciel (*Oncorhynchus mykiss*) : Implications pour la santé des poissons et les conséquences écologiques

Effects of Tebuconazole on the Microbiome of Rainbow Trout (Oncorhynchus mykiss): Implications for Fish Health and Ecological Consequences.

France Caza[1], Sophia Ferchiou[1], Morgane Danion[2], Sévérine Paris[3], Iris Barjhoux[3], Élise David[3], Jérôme Lambert[4], Patrick Kestemont[4], Claudia Cosio[3], Yves St-Pierre[1]

1) INRS-Centre Armand-Frappier Santé Technologie, 531 Boul. des Prairies, Laval, QC, Canada, H7V 1B7

2) Agence Nationale de Sécurité Sanitaire de l'Alimentation, de l'Environnement et du Travail, Laboratoire de Ploufragan-Plouzané-Niort, Technopôle Brest-Iroise, 29280 Plouzané, France

3) Université Reims Champagne-Ardenne, UMR-I 02 SEBIO Stress environnementaux et Biosurveillance des milieux aquatiques, Campus Moulin de la Housse, 51687 Reims, France.

4) Research Unit in Environmental and Evolutionary Biology, University of Namur, Namur, Belgium

Keywords: Tebuconazole, fungicide, microbiome, trout, 16SrRNA,

Abbreviations: TBZ, tebuconazole; RT, rainbow trout, EDCs, endocrine disruptors; IHNV, infectious hematopoietic necrosis virus; PICRUSt2, Phylogenetic Investigation of communities by Reconstruction of Unobserved States; PCoA, principal coordinate analysis; ASVs, amplicon sequence variants; LEfSe, Linear discriminant analysis Effect Size.

Corresponding author: Yves St-Pierre, INRS-Centre Armand-Frappier Santé Technologie, 531 Boul. des Prairies, Laval, Québec, Canada, H7V 1B7. Phone: 450-686-5354; Fax: 450-686-5501; E-mail: yves.st-pierre@inrs.ca

HIGHLIGHTS

- TBZ exposure impacts rainbow trout microbiome diversity.
- Shifts in bacterial composition due to TBZ exposure.
- Altered functional profiles in TBZ-exposed rainbow trout.
- Complex interactions between TBZ, virus, and fish microbiome.
- Ecological implications of TBZ exposure in aquatic organisms.

Declaration of interests

☒The authors declare that they have no known competing financial interests or personal relationships that could have appeared to influence the work reported in this paper.

☐The authors declare the following financial interests/personal relationships which may be considered as potential competing interests:

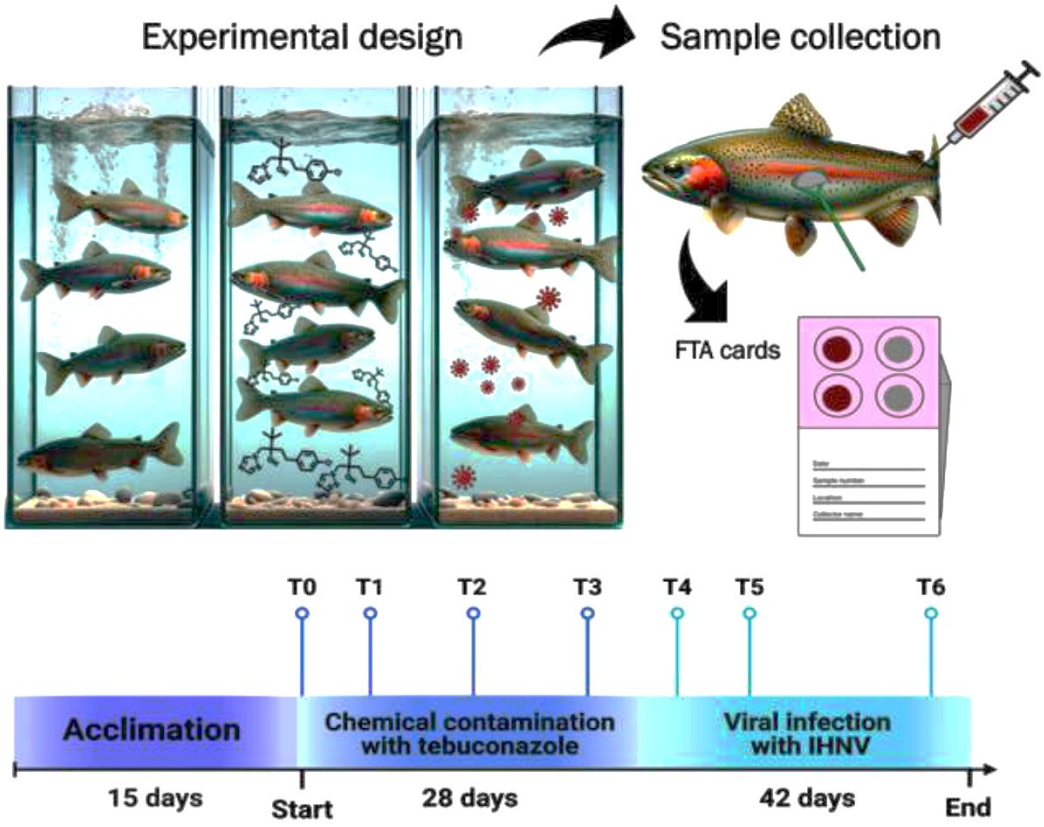
Experimental design
Sample collection
FTA cards
T0
T1
T2
T3
T4
T5
T6
Acclimation
Chemical contamination with tebuconazole
Viral infection with IHNV
15 days
Start
28 days
42 days
End

ABSTRACT

Tebuconazole (TBZ) is a commonly used fungicide in agriculture to treat plant pathogenic fungi. Understanding the effects of TBZ on the microbiome of fish, such as rainbow trout (RT), is crucial for assessing fish health and well-being and the ecological consequences in aquatic ecosystems. The present study investigated the impact of TBZ exposure in the context of experimental infection with the infectious hematopoietic necrosis virus (IHNV) on the RT microbiome in controlled laboratory conditions. Blood samples were collected from TBZ-exposed RT and control groups at various time points, and the microbiome composition was analyzed using 16S rRNA gene sequencing. The study found significant changes in the beta diversity of the RT microbiome following 24 days of TBZ exposure. At the genus level, TBZ exposure led to a decline in Actinomycetota abundance and an increase in low-abundance genera. Principal coordinate analysis and PERMANOVA analysis demonstrated significant differences in microbiome composition between the control and TBZ-treated groups. Furthermore, alpha diversity analysis revealed higher Shannon and Simpson diversity indices in RT exposed to TBZ for 24 days. This suggests that TBZ exposure alters the composition and diversity of the microbiome in RT. Functional profiling using PICRUSt analysis predicted significant functional changes, particularly in endocrine function and other metabolic pathways, indicating potential impacts on fish health. Additionally, the study found that pre-exposure to TBZ modulates the mucosal microbiome of IHNV-infected RT, highlighting the complex interactions between chemical exposure, viral infection, and the fish skin microbiome. The study's findings suggest that TBZ exposure can alter the microbiome's composition, diversity, and functional profiles in RT. These results provide valuable insights into the potential ecological implications of TBZ exposure on aquatic organisms.

1. Introduction

Fungicides like tebuconazole (TBZ) are commonly employed in various agricultural and horticultural practices. TBZ belongs to a class of fungicides called triazoles, which are widely used to control fungal diseases in crops such as cereals, fruits, vegetables, and ornamental plants. TBZ can be applied through various methods, including foliar sprays, seed treatments, and soil drenches, depending on the target crop and disease, and can enter non-target aquatic habitats through spray drift and run-off. While these chemicals effectively combat harmful fungi, they can also have unintended consequences on non-target organisms. TBZ, for example, has been shown to alter the activity and structure of soil microbial communities (El Azhari et al., 2018; Han et al., 2021; Bacmaga et al., 2022). More recently, it has also been shown to alter the microbiome's structure of the brown planthopper (*Nilaparva lugens*) (Ren et al., 2023), the Zebrafish *Danio rerio* (Jiang et al., 2021), and mice (Meng et al., 2022; Ku et al., 2023). Understanding how fungicides impact the microbiomes of organisms is of great significance due to the vital roles these microbiomes play in the overall health and well-being of the host.

RT is an important component of aquatic ecosystems and is crucial in maintaining their balance. The health and welfare of RT are vital for the sustainability of their populations, fisheries, and aquaculture industries. Moreover, RT populations are often used as indicators of the overall health of aquatic ecosystems and are frequently used as a biological model in ecotoxicology. Fish's circulating and skin microbiomes are essential for maintaining normal physiological functions, including immune system regulation, nutrient metabolism, and defense against pathogens.

In the present work, we investigated the effects of TBZ on RT's circulating and skin microbiomes under controlled conditions and during experimental infection with the IHNV.

2. Materials and Methods

2.1.Experimental Animals

Our study used specific pathogen-free RT (*Oncorhynchus mykiss*) sourced from the protected and monitored facilities at the ANSES Plouzané laboratory site in France (Dupuy et al., 2019). A total of 975 RT, comprising a mixture of males and females, with an average weight of 26 ± 4g, were acclimated for 15 days before the experiment. Some individuals underwent thorough examinations and bacteriological and virological analyses to ensure their optimal health condition. Throughout the acclimation period and the experiment, the fish were provided with a daily feeding regimen consisting of commercial dry pellets (Neo prima 4 pellets, Le Gouessant Aquaculture, Lamballe-Armor, France). This standardized feeding approach ensured consistent nutritional intake for the RT throughout the study.

2.2.Tebuconazole

Tebuconazole (TBZ; 1-p-chrlorophenyl-4,4-dimethyl-3-(1H-1,2,4-triazol-1-ylmethyl)pentan-3-o1, chemical formula C16H22ClN3O; CAS107534-96-3) is a triazole fungicide. Detailed information about its chemical and physical characteristics can be found on the PubChem website at https://pubchem.ncbi.nlm.nih.gov/compound/Tebuconazole. The TBZ used in this study was obtained as a powder (from Sigma-Aldrich, Germany). A 1g/L stock solution was prepared weekly by dissolving TBZ in methanol to ensure better dispersion of the toxicant. This stock solution was stored in the dark at 4°C until use. For experimental exposure, the stock solution was diluted in fresh water to achieve concentrations of 0.23 or 10 µg/L of TBZ, representing chronic or acute

environmental pollution levels, respectively (De Sousa et al., 2020; Kang et al., 2020). Notably, the methanol concentration in the exposure units remained below 0.0001%, which is well below the No Observed Effect Concentration (NOEC).

2.3. Virus Production and Titration

For our experiments, we used the IHNV strain N61 (genotype E), which was isolated from RT fry exhibiting typical signs of IHN. A 100 ml stock of the virus was produced at 14°C using an epithelioma papulosum cyprini cell line (Fijan et al., 1983) in Tris-buffered Stoker's medium (pH 7.6), supplemented with 10% fetal bovine serum (FBS). Once the cytopathic effect was observed, the cell culture supernatant was centrifuged for 15 min at 2,000 x g and subsequently stored at -80°C. An aliquot of the stock was titrated using the 50% tissue culture infective dose (TCID50) endpoint method in 96-well plates, following the calculation method described by Karber (1931). The infectious titer of the viral production was determined to be 5.10^7 $TCID_{50}$/ml.

2.4. Experimental Design

The study was conducted under controlled laboratory conditions at the ANSES laboratories, authorized by the MSRI (Ministry of Scientific Research and Innovation), with the study protocol approved by the APAFIS (Animal Protection Committee) under reference number #29714-2021020817172290 v6. The care and treatment of the animals adhered to the animal welfare laws, guidelines, and policies established by the Government of France, as overseen by the Ethics Committee (Ethics Committee No. 16). The experiment was conducted under a natural light/dark cycle (approximately 14 h of light and 10 h of darkness in spring) in a room with hourly air volume changes. The water temperature was continuously maintained at 11 ± 2°C and monitored using a

92 wireless probe (Cobalt, Oceasoft®) connected to an acquisition system (ThermoClient 4.1.0.24).
93 Weekly measurements of oxygen saturation, nitrate, and nitrite concentrations were performed
94 using an Oxymeter (WTW-OXI315I) and the JBL® colorimetric test. The RT were randomly
95 distributed among three conditions, with four tanks assigned to each condition. These conditions
96 included a control group and two groups exposed to different concentrations of TBZ. For 24 days,
97 the exposure tanks were continuously supplied with fresh water and a volume of TBZ stock
98 solution to maintain optimal water conditions for the fish. The water was renewed every 3 h to
99 ensure oxygen saturation above 80%, pH close to 8, and absence of nitrates and nitrites. The fish
100 in the exposure tanks were exposed to either a low concentration (0.23 µg/L) or a high
101 concentration (10 µg/L) of TBZ. Subsequently, a subset of RT from the TBZ-exposed groups and
102 the control group were further exposed to IHNV through bath balneation to investigate the stress
103 on stress effects of TBZ exposure and viral infection on RT microbiomes. The remaining RT
104 served as uninfected controls. The bath balneation involved immersing the fish in static freshwater
105 with high oxygenation containing 10^5 $TCID_{50}$/mL of IHNV (or non-infected EPC cell supernatant
106 for negative controls). After 4 h, the water inlet was adjusted to a flow rate of 0.3 m3/h. During
107 the viral challenge, the fish's general behavior, clinical signs of rhabdovirosis, and mortality were
108 recorded twice daily. Any deceased individuals were stored at -20°C for viral examination, and
109 the presence and concentration of the virus were assessed in a pool of organs (spleen, kidneys,
110 heart, and brain) following the protocol described by Louboutin et al. (2021). At six weeks post-
111 infection, all surviving fish were sampled, and 2 mL of blood was withdrawn from the caudal vein
112 using a lithium heparinized vacutainer (BD Vacutainer LH 85 IU) to measure neutralizing
113 antibodies in RT plasma.

114 *2.5. Sampling*

115 Throughout the exposure period, triplicate samples of 500 mL of water were collected from the
116 middle of the water column in each exposure tank to assess the concentration of TBZ. Fish samples
117 were obtained from each exposure tank at three-time points: 24 h (T1), 7 days (T2), and 24 days
118 (T3) into the TBZ exposure period. Additionally, fish were sampled after 24 h (T4), 72 h (T5), and
119 46 days (T6) following IHNV infection. Blood and mucosal samples were collected following
120 established protocols (Caza et al., 2019). Blood was withdrawn from the caudal vein with a lithium
121 heparinized vacutainer (BD Vacutainer LH 85 IU). Drops of blood were promptly deposited onto
122 FTA® cards (Sigma–Aldrich, Oakville, ON, Canada). Subsequently, the samples were allowed to
123 air dry and then stored in a plastic bag with a desiccant to maintain their integrity. A sterile cell
124 scraper was employed to gently scrape along the fish's lateral line for mucosal sampling. The
125 collected mucus was immediately transferred onto FTA® cards, ensuring complete coverage of
126 the designated disc area. The same preservation method described above was applied to the
127 mucosal samples, ensuring proper drying and storage conditions. Lastly, at the conclusion of the
128 24-day TBZ exposure period, muscle samples were obtained from the fish and promptly frozen at
129 -80°C for subsequent analysis of TBZ bioconcentration.
130
131 *2.6. Chemical Analysis*
132 The determination of TBZ concentrations in water and fish flesh was conducted using a validated
133 method (n° MIOE-MO-0040) accredited by the French Accreditation Committee (Cofrac). The
134 analysis involved a two-step process: solid-phase extraction (SPE) followed by liquid
135 chromatography-tandem mass spectrometry (LC-MS/MS).
136 *2.7. DNA Extraction, Preprocessing, and Sequencing Microbiome*

All DNA extraction and purification procedures were performed in a controlled, clean room environment, maintaining precise control over pressure, temperature, and humidity to minimize contamination risks. Individual discs were carefully excised from the FTA® cards using a sterile 5.0 mm single round hole punch. Total DNA extraction was conducted using the QIAamp DNA Investigator Kit (Qiagen, Toronto, ON, Canada) following the manufacturer's protocol. The concentration of extracted DNA was quantified using the Qubit dsDNA Quantification, High Sensitivity kit (ThermoFisher, Waltham, MA, USA). Amplification of the V3-V4 region of the 16S rRNA gene and subsequent amplicon sequencing were performed at the Centre d'Expertise et de Services Génome Québec (Montréal, QC, Canada). Universal primers 341F (5'-CCTACGGGNGGCWGCAG-3') and 805R (5'-GACTACHVGGGTATCTAATCC-3') were used to amplify (Klindworth et al., 2013). To prepare the sequence libraries, the TruSeq® DNA Library Prep Kit (Illumina, San Diego, CA, USA) was employed, and library quantification was performed using the KAPA Library Quantification Kit designed for Illumina platforms (Kapa Biosystems). Paired-end sequencing was conducted on the MiSeq platform PE300 (Illumina Corporation, San Diego, CA, USA) using the MiSeq Reagent Kit v3 600 cycles (Illumina, San Diego, CA, USA). The raw sequencing data files have been deposited in the NCBI Sequence Read Archive (SRA) under the project accession number PRJNA1026604. These data are publicly available for further analysis and investigation.

2.8. 16S rRNA Data Processing.

The Illumina sequence data in FASTQ format were processed using Cutadapt (version 2.8) for trimming. To generate the amplicon sequence variants (ASVs) of the 16S rRNA gene (V3-V4 region), we employed the DADA2 pipeline (version 1.16.0, CA, USA) as described by Callahan et al. (2016). Subsequent analysis of the ASVs was conducted within the R environment (R version

160 4.0.3, VIEN, AT). The forward and reverse reads were trimmed, filtered, and truncated using the
161 filterAndTrim function in the DADA2 pipeline. The error model (maxEE) was calculated for both
162 the forward and reverse reads, and low-quality reads were eliminated. After denoising and
163 merging, any chimeric sequences (bimeras) were removed from the datasets. All retained reads
164 had an average quality score of ≥30. For the taxonomic assignment of the ASVs, we utilized the
165 RDP (Ribosomal Database Project) 16 classifier database, as outlined by Vilo et al. (2014). To
166 characterize the microbial communities, we employed several R packages, including phyloseq
167 v.1.34.0 (McMurdie & Holmes, 2013), microbiomeSeq (version 0.1) (Ssekagiri et al., 2019),
168 microbiomeMarker (version 1.3.3) (Cao 2022), and vegan (version 2.6.4) (Oksanen et al., 2022).
169 These packages provided the necessary tools for comprehensive analysis and characterization of
170 the microbial communities in our study.

171 *2.9. Statistical Analysis*

172 To assess the alpha diversity index, we used the phyloseq R package (McMurdie & Holmes, 2013).
173 Wilcoxon rank sum tests were performed to compare the average value of each group. To
174 determine the differences in microbiota composition among the groups, we employed multivariate
175 analysis of variance with permutations (PERMANOVA), using 9999 permutations. Pairwise
176 permutation tests were subsequently conducted to compare specific group differences. For the
177 functional analysis of the blood and skin microbiomes, we predicted the functional content using
178 the KEGG database through the Phylogenetic Investigation of Communities by Reconstruction of
179 Unobserved States (PICRUSt2) software (Douglas et al., 2020). Linear discriminant analysis
180 (LDA) effect size (LEfSe) analysis was performed to identify taxa that significantly differentiated
181 the samples. The logarithmic score threshold for the LDA analysis was set at 3.0. Principal

coordinate analysis (PCoA) based on the UniFrac distance was conducted to visualize the differences in overall bacterial community composition among the specimens. Additionally, permutation multivariate analysis of dispersion (PERMDISP) was carried out using the betadisper function to test for the homogeneity of multivariate dispersion, which assesses deviations from centroids among the specimens. This analysis provided insights into the variation in bacterial community composition among the studied samples.

3. Results

3.1.TBZ Bioconcentration

To investigate the impact of TBZ exposure on the RT microbiome, we conducted a well-controlled study using separate groups of RT housed in tanks. The first experimental group was exposed to a concentration of 230 ng/L (referred to as the "low TBZ" group), while the second experimental group was exposed to a concentration of 10 µg/L (referred to as the "high TBZ" group). In the control tanks, both water and fish flesh samples exhibited TBZ concentrations below the detection limit of the analytical methods. Throughout the experiment, the mean TBZ concentrations measured in the exposure tanks closely aligned with the nominal concentrations. Specifically, in the low-concentration units, the measured concentrations averaged between 0.2 ± 0.1 and 0.3 µg/L, while in the high-concentration units, the measured concentrations ranged from 3.2 ± 0.2 to 5.8 ± 0.1 µg/L. Following a 24-day exposure period, the TBZ fish TBZ concentration in muscle tissue was 5.0 ± 2.0 µg/kg. In contrast, fish exposed to the high TBZ concentration displayed a higher bioconcentration, reaching 261.7 ± 137.7 µg/kg in their muscle tissue. Throughout the study, no mortality was observed in any groups, indicating the absence of acute toxic effects caused by TBZ

exposure. Furthermore, we found no significant differences in the RT's weight, length, or general condition between the control group and those exposed to TBZ (**Supplementary Figure 1a**).

3.2.The Impact of TBZ on the Blood Microbiome at the Phylum Level.

A total of 101 blood samples were collected, including samples taken before exposure (Day 0) and at different time points post-exposure (on days 1, 7, and 24). To compare the composition of the circulating microbiome in blood samples from TBZ-exposed and control RT, we performed standard sequencing analysis targeting the V3-V4 region of the 16S rRNA gene, commonly found in the genomes of bacteria and archaea. On average, we obtained 15,003 ± 8,270 reads per individual after cleaning the data. The DNA reads obtained from the sequencing were computationally assigned to taxonomic groups, allowing us to compare the microbial composition. At the phylum level, the dominant phyla observed in the blood microbiome signature were *Bacillota, Actinomycetota, Pseudomonadota*, and, to a lesser extent, *Bacteroidota* and *Cyanobacteria* (**Figure 1**). After 24 days of exposure to both low and high concentrations of TBZ, significant increases in the abundance of the phyla *Bacteroidota* ($p = 0.018$ and $p = 0.008$, respectively) and *Pseudomonadota* ($p = 0.048$ and $p = 0.011$, respectively) were observed, compared to the non-exposed control group. Additionally, a Linear Discriminant Analysis (LDA) effect size (LEfSe) analysis revealed a higher abundance of *Bacteroidota* at day 24 (LDA score: 4.829, $p = 0.02$). These findings suggest that exposure to TBZ can lead to distinct changes in the

223 composition of the blood microbiome, particularly an increase in *Bacteroidota*, following
224 prolonged exposure.

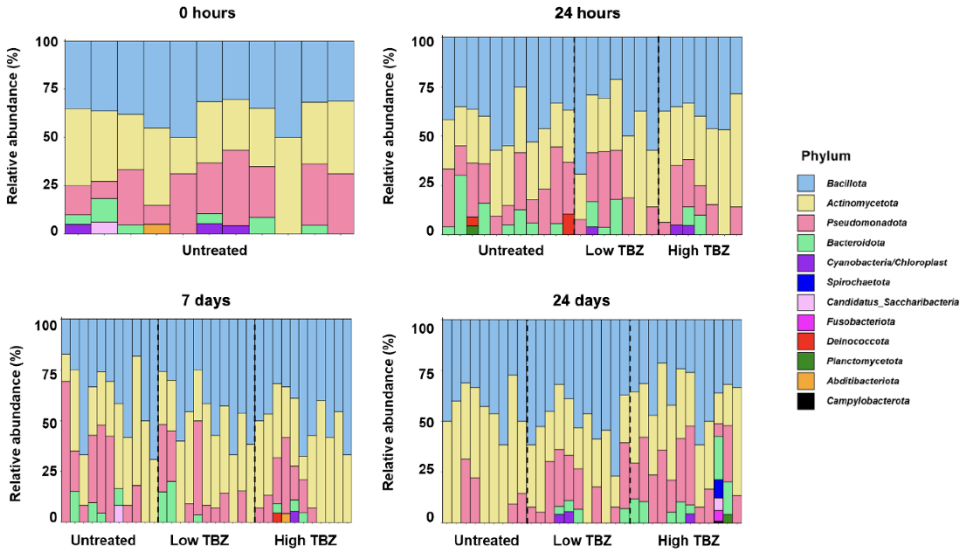

Figure 1: Phylum-level circulating microbiome. Relative abundance of the taxa in individual trout for each group at different times during exposure to TBZ.

225

226 *3.3.Genus-Level Alterations in the Microbiome Following Tebuconazole Exposure.*

227 At the genus level, the core circulating microbiome consisted primarily of three genera:
228 *Prauserella* (*Actinomycetota* phylum), *Alteribacillus* (*Bacillota*), and *Rubrobacter*
229 (*Actinomycetota*), which were found in more than 90% of the samples (**Figure 2A**). When
230 investigating the impact of TBZ exposure at the genus level, we observed significant differences.
231 For example, the genus *Allosalinactinospora* (LDA 4.695, p = 0.009) was found to be discriminant
232 (lower abundance) for the low TBZ group on Day 24. Examining the 'others' category, representing
233 genera with a frequency of less than 5% of ASVs, we found a notably higher number of low-

234 abundance genera in RT exposed to either low or high concentrations of TBZ (**Figure 2B**).

235 Together, these results demonstrate that exposure to TBZ changed the composition of the

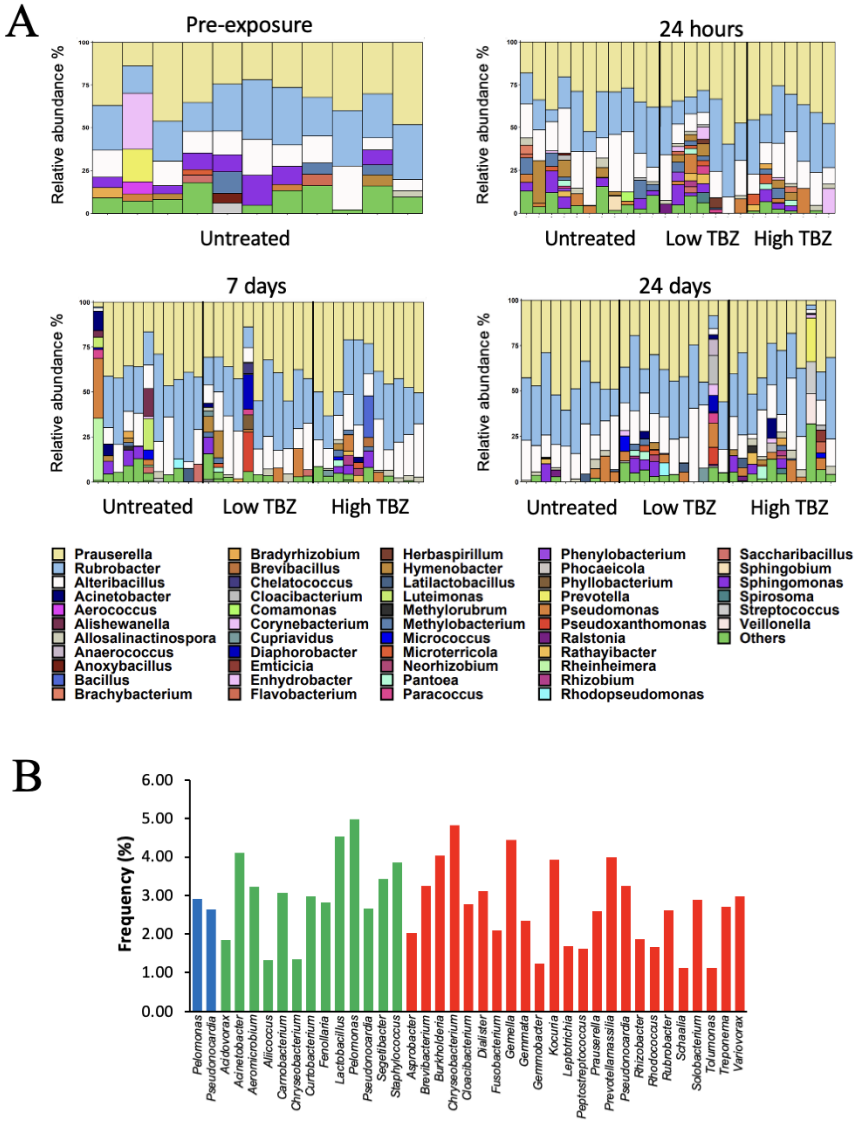

Figure 2: Genus-level circulating microbiome. (**A**) Relative abundance of the taxa in individual trout for each group at different times during exposure to TBZ. (**B**) Genera identified as "others" (< 5%) in (A) for each group on Day 24. Control group (*Blue*), Low TBZ (*Green*), High TBZ (*Red*).

236 circulating microbiome of the RT.

237

238 *3.4.Effect of TBZ on Trout Circulating Microbiome: Insights into Microbial Changes and*
239 *Diversity.*

240 To further examine the effect of TBZ on the microbiome, we performed a pCOA (Principal
241 Coordinate Analysis) Weighted-Unifrac analysis, a multivariate statistical method commonly used
242 in microbiome research to examine the dissimilarity or similarity between microbial communities
243 based on their overall phylogenetic composition. Our results revealed a significant change in
244 microbiome composition between the control group and the TBZ-treated groups ($p = 0.008$)
245 (**Figure 3**). Similarly, a PERMANOVA analysis demonstrated significant differences between the
246 control group and the low TBZ group ($p = 0.023$) and between the control group and the high TBZ
247 group ($p = 0.009$) (**Table 1**). Regarding the alpha diversity, our data showed a higher Shannon
248 diversity index for RT exposed for 24 days at low or high TBZ concentrations (low TBZ: $p =$
249 0.022; high TBZ, $p = 0.005$) (**Figure 4**). A statistically significant increase was also found in the
250 Simpson index for RT exposed for 24 days at low or high TBZ concentrations (Low TBZ: $p =$

Table 1: Comparison of TBZ-exposed groups to control group using Unifrac distance weighted p values.

	TBZ^{Low} vs Control	TBZ^{High} vs Control	TBZ^{Low} vs TBZ^{High}
Day 1	0.521	0.528	0.528
Day 7	0.830	0.386	0.830
Day 24	0.023	0.009	0.691

251 0.021; high TBZ, p = 0.004). Taken together, these results further validate that exposure to TBZ

252 alters the circulating microbiome of RT.

253

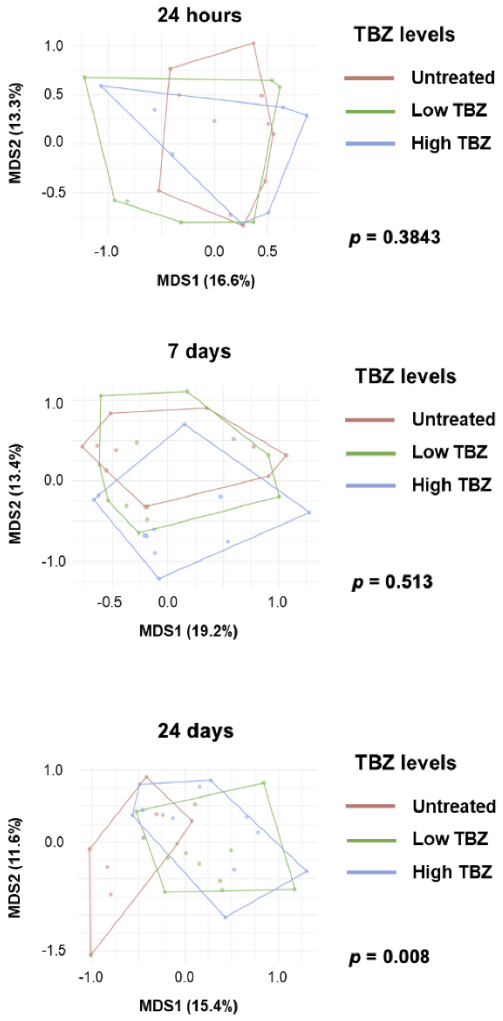

Figure 3. Non-metric multidimensional scaling (MDS1 and MDS2) ordination plot. Convex hull polygons show differences in microbial sequence assemblage compositions among the control group (Untreated) and trout exposed to low and high concentrations of TBZ.

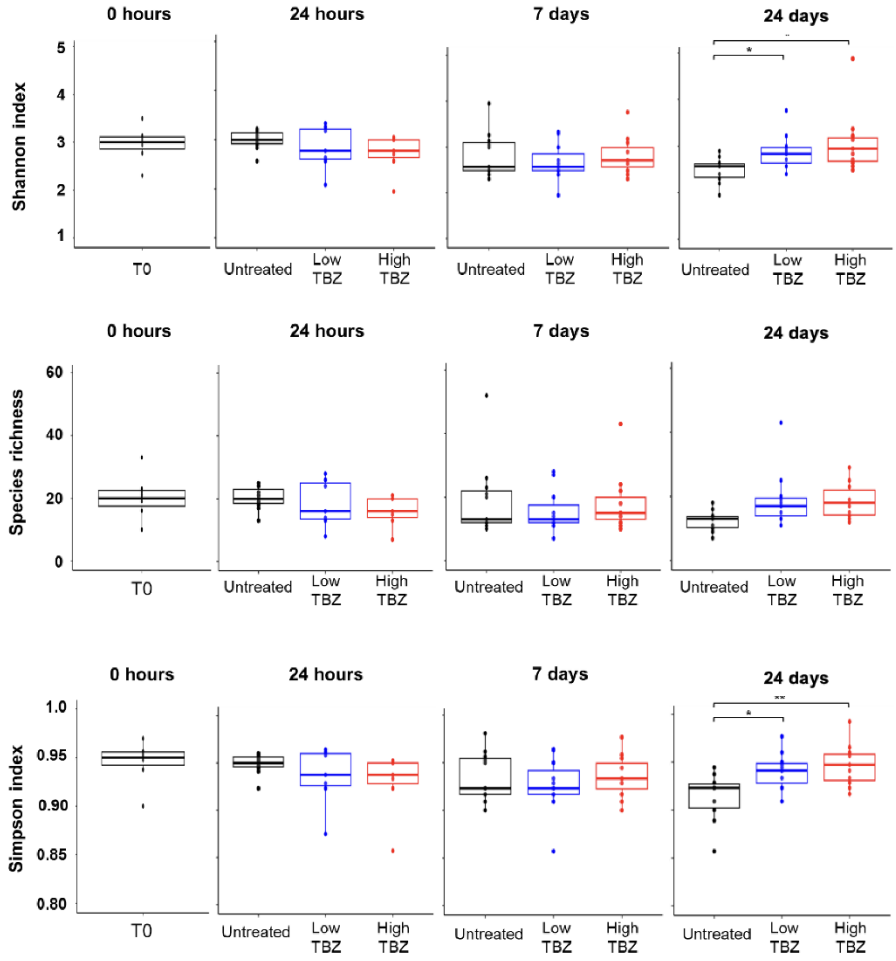

Figure 4. Alpha diversity metrics. Shannon, Richness and Simpson diversity indices for each group. P-values represent pairwise comparisons. * $p < 0.05$, *** $p < 0.001$.

254

255 *3.5.Prediction of the Functional Profile of Bacterial Communities*

256 Next, we carried out a PICRUSt analysis (Phylogenetic Investigation of Communities by

257 Reconstruction of Unobserved States) to gain functional insights into the microbial community

based on its composition. PICRUSt is a bioinformatics tool that predicts functional impacts on the interaction between the blood microbiome based on 16S rRNA gene sequencing data (Langille et al., 2013). Our analysis revealed several statistically significant functional changes induced upon exposure to low and high TBZ concentrations compared to the control group (**Figure 5**). The LDA score obtained from the PICRUSt analysis revealed negative and positive associations when comparing the group exposed to low and high concentrations of TBZ to the control group, most notably regarding the endocrine function, consistent with previous studies showing that TBZ should be considered an endocrine disruptor (Taxvig et al., 2007; Li et al., 2019; Draqskau et al., 2022). We also found significant changes in cellular processes related to growth, cell death, and vulnerability to infectious and parasitic agents ($p = 0.002$). The analysis also predicted changes in lipid metabolism, xenobiotic degradation, and cellular membrane function, suggesting a comprehensive alteration in metabolic and cellular processes in the high TBZ group compared to the control group. These findings highlight more pronounced changes in the functional profiles of bacterial communities following exposure to TBZ.

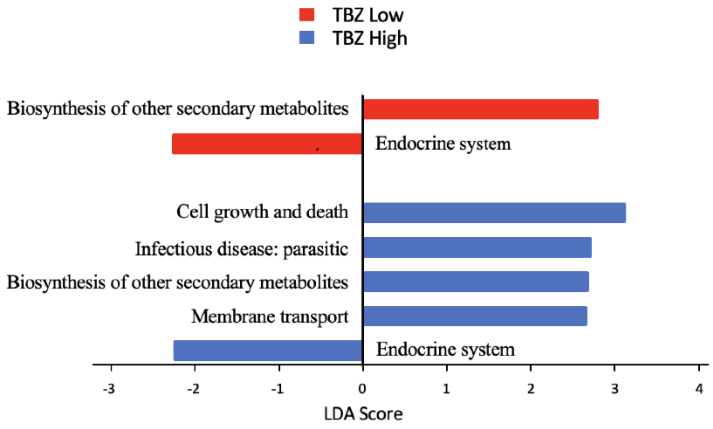

Figure 5. LEfSe analysis of microbial functions predicted by PICRUSt in different groups. LDA, linear discriminant analysis; LEfSe, linear discriminant analysis effect size; PICRUSt, Phylogenetic Investigation of Communities by Reconstruction of Unobserved States.

3.6.Alterations of the Circulating Microbiome in RT Pre-Exposed to TBZ and IHNV.

Recent studies have demonstrated that exposure to pesticides can modulate trout's immune response to viral infections, particularly infectious hematopoietic necrosis viruses, a well-studied virus of salmonid fishes (Eder et al., 2008; Danion et al., 2012; Dupuy et al., 2019). Considering the close functional relationships between the immune response and the microbiome, we investigated whether a 28-day pre-exposure to TBZ could modulate the circulating microbiome of RT infected with IHNV. To test this hypothesis, a subset of RT from the TBZ-exposed and the control groups were further exposed to IHNV through bath balneation to investigate the combined stress effects of TBZ exposure and viral infection on RT microbiomes. In the infected groups, classical signs of IHN disease were evident, including darkening of the skin, petechial hemorrhage in the visceral fatty tissues and around the eye pupil, swollen abdomen, and pallor of the internal organs. No mortality, clinical symptoms, or lesions were observed in the negative control group (non-infected). The distribution of cumulative mortality did not show significant differences among the infected groups. Mortality began at 6 days post-infection (dpi) and stabilized after 17 dpi, with approximately 90% survival regardless of the TBZ exposure condition (**Supplementary Figure 2b**). Viral examination confirmed that the mortality observed during the challenges was associated with the virus. For our study, we paid particular attention to the early phase of the immune response, characterized by significant changes in the immune parameters (Purcell et al., 2004). When comparing the IHNV-infected groups that had been exposed to low and high concentrations of TBZ to the non-exposed infected group, no significant differences in phylum and genus levels were found at 24 (T4) and 72 (T5) h post-infection (**Figure 6A**). However, after 46 days (T6), we observed a slight but statistically significant change in the abundance of *Actinomyceta* ($p = 0.052$) between the IHNV-infected group pre-exposed to TBZ and the control

infected group. Further analysis at the genus level revealed no discernible taxa above an LDA score of 4. These findings were supported by PERMANOVA and weighted UniFrac analyses. No significant dissimilarity was observed at 1 and 3 days after infection. However, at 46 days, the

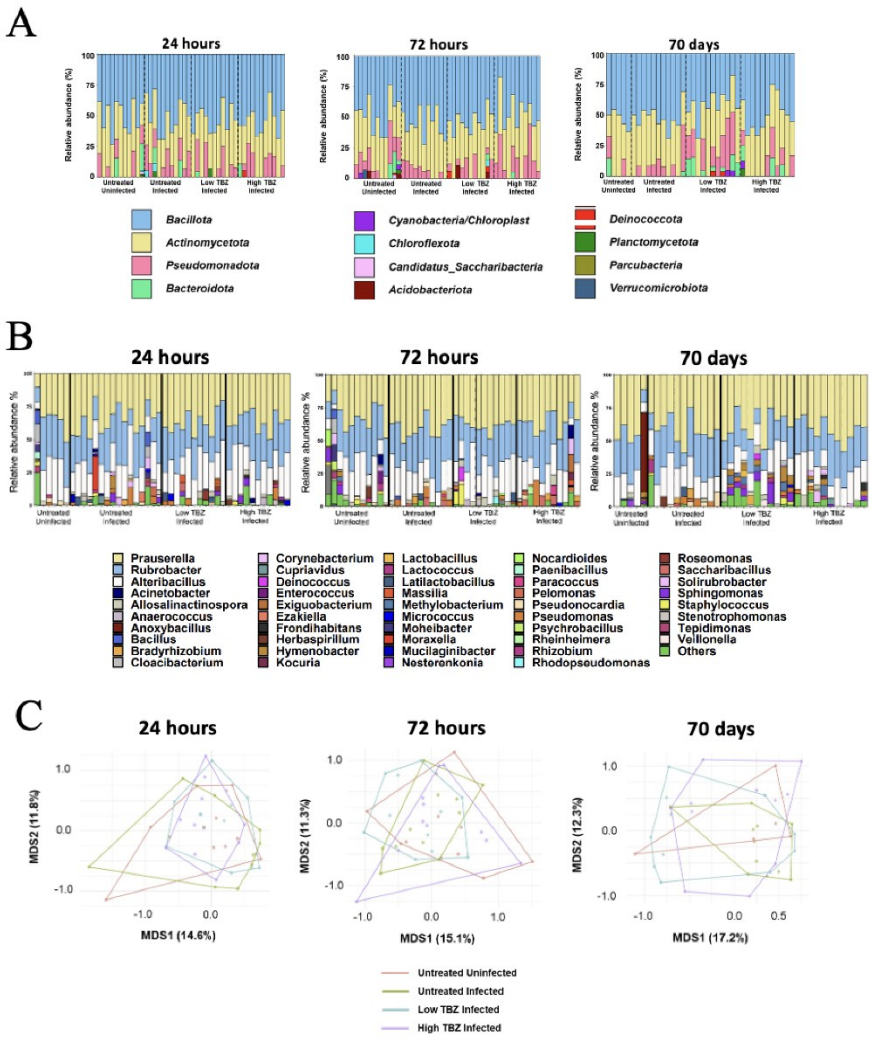

Figure 6: Circulating Microbiome Analysis in IHNV-Infected Trout following Pre-Exposure to Low and High Concentrations of TBX. (A) and (**B**) Phylum (> 0.5%) and Genus-level Microbiome Compositions: Bar chart depicting the relative abundance of microbial taxa at the genus level in the different experimental groups. (**C**) Non-metric multidimensional scaling (MDS1 and MDS2) ordination plots. No significant changes were observed at 24 ($p = 0.898$) and 72 ($p = 0.760$) hours post-infection for any of the four groups. A statistically significant difference ($p = 0.039$) was observed at day 70 between infected trout exposed to low doses of TBZ and the non-exposed, infected group.

IHNV-infected group pre-exposed to low concentrations of TBZ demonstrated a difference compared to the control-infected group ($p = 0.0388$) (**Figures 6B and C**). These differences did not, however, impact the alpha diversity (**Figure 7**). In summary, the viral infection did not change the composition of the circulating microbiome or alpha-diversity indices compared to the uninfected group. However, a specific phylum was potentially influenced by prior exposure to low TBZ, indicating persistent microbiome modulation even after the cessation of TBZ treatment.

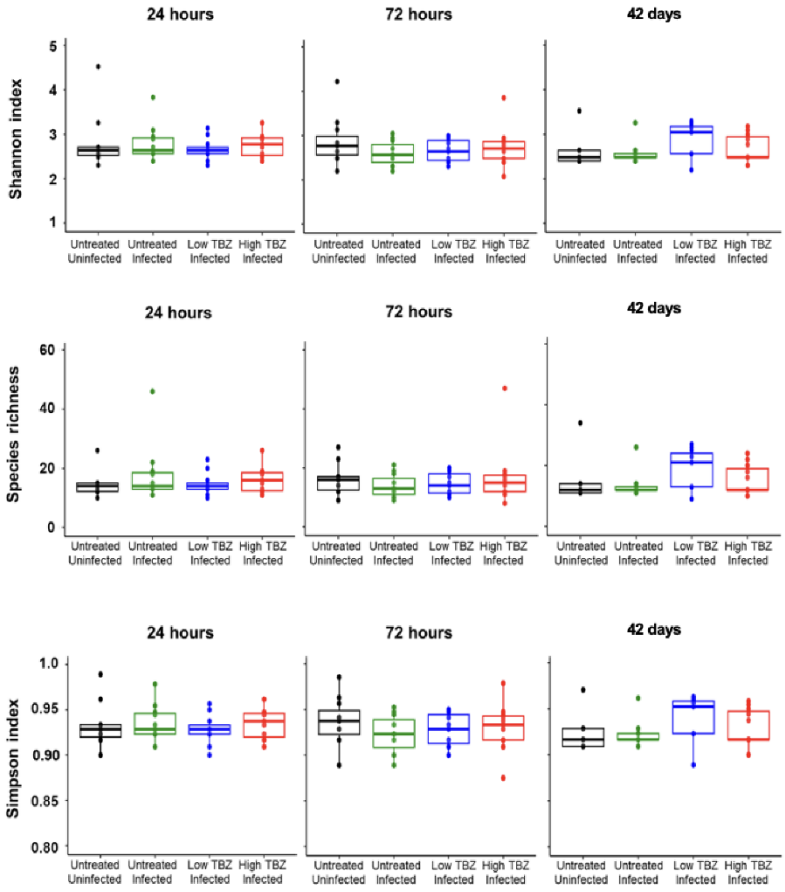

Figure 7. Alpha diversity metrics of the skin microbiome of IHNV-infected RT pre-exposed to TBZ. Shannon, Richness and Simpson diversity indices for each group.

306 *3.7.Does Pre-Exposure to TBZ and IHNV Infection Induce Alterations of the Skin*
307 *Microbiome?*

308 The skin microbiome of fish plays a crucial role in their overall health and well-being by acting as
309 a barrier against potential pathogens and aiding in environmental adaptation. To investigate the
310 impact of TBZ and IHNV infection on the skin microbiome, mucus samples were collected 24 and
311 72 h after IHNV infection and the cessation of TBZ exposure. These time points were chosen to
312 comprehensively understand the host-virus interaction, infection progression, and associated
313 changes in the host immune response and skin microbiome (Eder et al., 2008; Danion et al., 2012;
314 Dupuy et al., 2019). Our data first revealed distinct differences in the composition of the mucosal
315 microbiome compared to the circulating microbiome. The dominant phyla in the mucosal
316 microbiomes were primarily *Pseudomonodata*, *Bacteriodata*, and, to a lesser extent,
317 *Planctomycetota* and *Verrucomicrobiota* (**Figure 8A**). At the genus level, we observed a diverse
318 repertoire of bacteria in the mucus compartment compared to the blood microbiome (**Figure 9A**
319 **and Supplementary Figure 3**). The number of genera in the mucus compartment was
320 significantly higher, ranging from 10 to 40 times more than in the blood (**Figure 9B**).
321 Discriminative genera, such as *Flavobacterium* (LDA 4.5) and *Rheinheimera* (LDA 4.4), were
322 identified in the group pre-exposed to high concentrations of TBZ. At 72 h, no discriminative phyla
323 or genera with an LDA value greater than four were observed. In our PERMANOVA analysis, we
324 found that IHNV infection significantly affected the mucosal microbiome at 24 and 72 h in the
325 untreated (not pre-exposed to TBZ) group ($p = 0.046$ and $p = 0.003$, respectively) (**Figure 8B**).
326 Additionally, in RT infected with IHNV, we observed a significant difference at 24 h between
327 untreated RT and those pre-exposed to either low or high TBZ concentrations ($p = 0.004$ and $p =$
328 0.001, respectively). A similar effect of low or high TBZ concentrations was observed at 72 h (p

= 0.0002 and p = 0.0003, respectively). Pre-exposure to TBZ also significantly altered alpha diversity for both groups at 72 h post-infection, as indicated by all three diversity indexes (**Figure 8C**). These findings demonstrate that pre-exposure to TBZ modulates the mucosal microbiome of

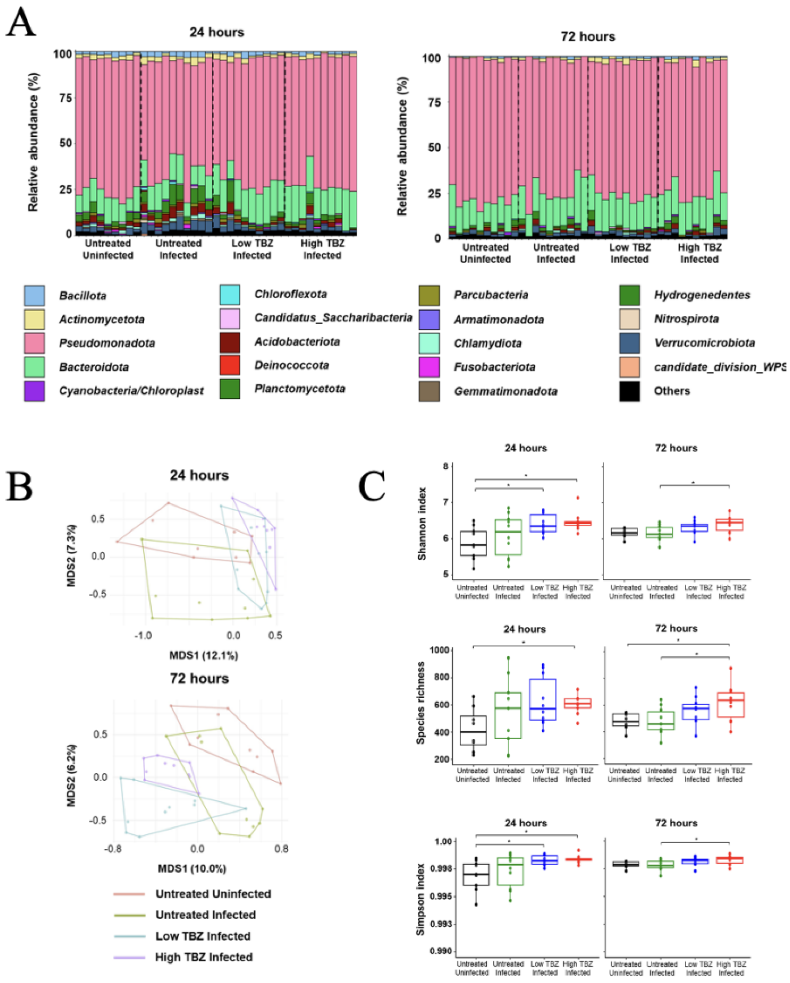

Figure 8: Composition and diversity of mucosal microbiome. (A) Phylum-level mucosal microbiome. Relative abundance of the taxa in individual trout for each group at 24 and 72 hours post-infection. **(B)** Non-metric multidimensional scaling (MDS1 and MDS2) ordination plots. Convex hull polygons show differences in microbial sequence assemblage compositions among the control groups and trout exposed to low and high concentrations of TBZ. **(C)** Alpha diversity metrics showing Shannon, Richness and Simpson diversity indices for each group. * $p < 0.05$.

IHNV-infected RT, highlighting the intricate interactions between chemical exposure, viral infection, and the fish skin microbiome.

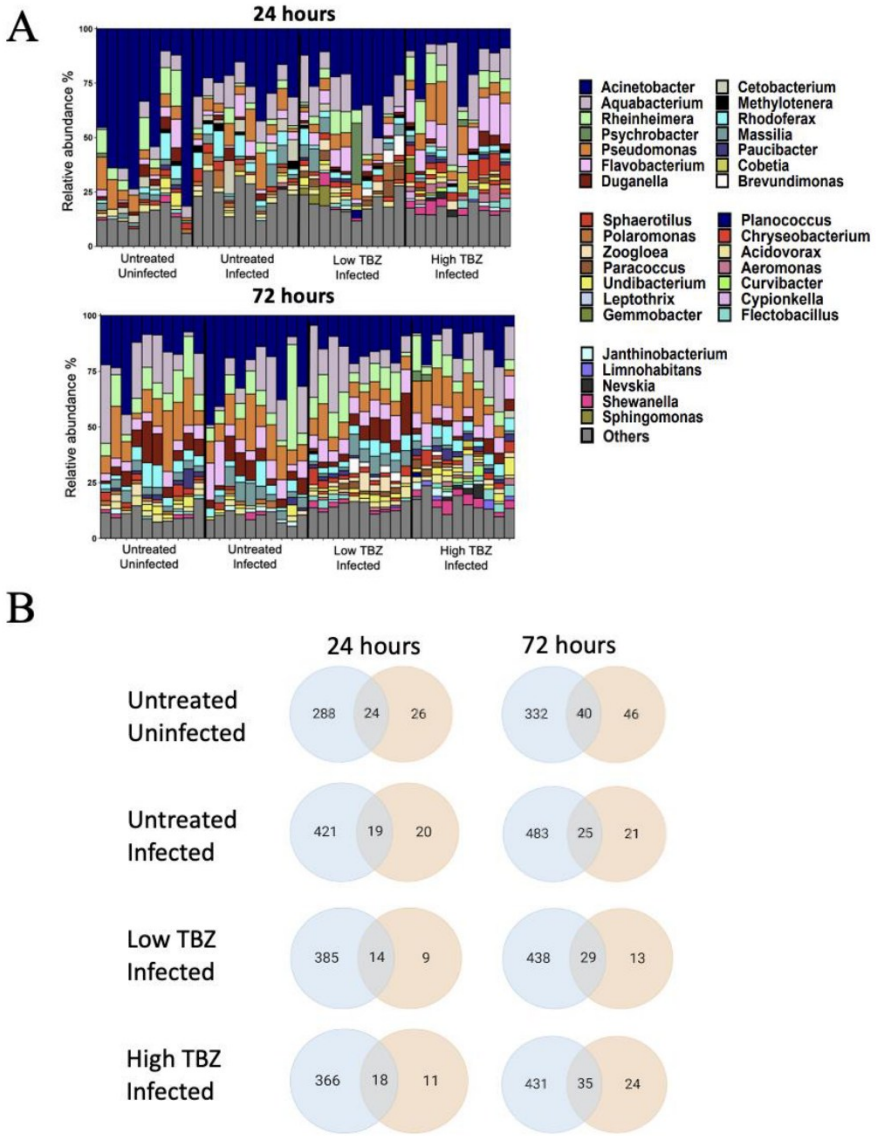

Figure 9: Genus-level mucosal microbiome. **(A)** Relative abundance of the taxa in individual trout for each group at different times post-infection. **(B)** Comparative analysis showing unique and common genera between mucosal (blue) and blood (beige) microbiomes.

4. Discussion

The bacterial microbiome is crucial in maintaining individual homeostasis and overall health. In humans, dysbiosis in the intestinal microbiome has been linked to various autoimmune diseases (Wu et al., 2012; Lin and Zhang, 2017; Mousa et al., 2022), as well as metabolic disorders such as diabetes and obesity (Hou et al., 2022; Cox et al., 2022). Additionally, the microbiome protects against pathogenic infections (Afzaal et al., 2022). In this work, we demonstrated that exposure to TBZ disrupts the RT microbiome. More specifically, our study indicates that 1) exposure of juvenile RT for 24 days to TBZ disrupts the circulating microbiome of RT, particularly at environmental doses or at doses from accidental spills; 2) Following 24 days of exposure to low and high concentrations of TBZ, the phylum *Bacteroidota* and *Pseudomonodota* exhibited significant increases in the circulating microbiome compared to the non-exposed control group; 3) at the genus level, we observed a higher number of low-abundance genera in RT exposed to either low or high concentrations of TBZ; 4) these changes in the circulating microbiome predicted functional changes in lipid metabolism, xenobiotic degradation, and cellular membrane function, suggesting a comprehensive alteration in metabolic and cellular processes following exposure to TBZ, and 5) pre-exposure to TBZ altered the circulating and mucosal microbiomes of RT exposed to IHNV.

Our study makes a significant contribution by being the first to demonstrate the impact of TBZ on the microbiome of an aquatic species, thus expanding our understanding of the ecological effects of this compound in aquatic environments. Moreover, it is one of the few studies that specifically aims to investigate the effects of TBZ on an animal's microbiome. Previous research on TBZ has predominantly focused on its effects on the microbiome of soil, plants, or insects (Pesce et al.,

356 2026; Han et al., 2021; Bacmaga et al., 2022; Li et al., 2019; Ren et al., 2023; Yu et al., 2023;
357 Zhang et al., 2023). There have been a limited number of studies conducted in mice where TBZ-
358 induced disruption of the microbiome over similar timeframes to our experimental model has been
359 associated with the promotion of inflammatory processes and alterations of synaptic integrity (Ku
360 et al., 2023; Meng et al., 2023). Our findings also offer valuable insights into the functional
361 consequences of TBZ exposure on the metagenome. Our functional analysis revealed potential
362 alterations in several metabolic pathways, even at environmentally relevant doses. The observed
363 changes in endocrine functions are of particular concern, which aligns with prior research
364 identifying TBZ and other pesticides as endocrine-disrupting chemicals (EDCs) (Duh-Leong et
365 al., 2023). Our findings are consistent with Li et al.'s study, which demonstrated the endocrine-
366 disrupting effects of TBZ through laboratory exposure on zebrafish (Li et al., 2019). Thus, our
367 study contributes to the growing body of research on the impact of EDCs on the microbiome
368 (Rosenfeld, 2017; Velmurugan et al., 2017; Calero-Medina et al., 2023; and Vacca et al., 2024).

369 Our study revealed significant alterations in the alpha diversity indices of the microbiome
370 following 24 days of TBZ exposure. Increases in the Shannon and Simpson indices, commonly
371 employed to assess microbial community diversity in response to chemical exposure, have been
372 reported in various organisms, including invertebrates and humans (Castelli et al., 2021; Ma et al.,
373 2020; Bai et al., 2019; Lei et al., 2019; Wang et al., 2019). However, it is crucial to acknowledge
374 that the effects of pesticides on the microbiome can vary depending on several factors, such as the
375 specific pesticide, dosage, duration of exposure, and the species involved. In some instances,
376 chemical substances may have the opposite effect, reducing biodiversity or the proliferation of
377 specific pathogens or bacteria. This observation is consistent with the Anna Karenina principle,

which posits that perturbations in the microbiome can result in either a decrease or an increase in diversity and stability (Zaneveld et al., 2017).

To the best of our knowledge, our study represents the first evidence that exposure to fungicides disrupts the skin microbiome in fish. We have observed significant alterations in the beta biodiversity of the skin microbiome, while no changes were observed in alpha diversity. The skin microbiome plays a crucial role as the first line of defence against opportunistic environmental pathogens for fish. It competes for resources, produces antimicrobial compounds, facilitates adaptation to different environmental conditions, and aids in wound healing by preventing the colonization of harmful bacteria while promoting the growth of beneficial bacteria that contribute to tissue regeneration. Our results also raise the possibility that changes in the microbiome may favor the emergence of pathogen bacteria. These findings will guide our future investigations into the effects of TBZ on mucosal functions. Understanding these dysbioses will help us assess the long-term impacts on the health status of aquatic species, such as RT, in ecosystems where TBZ and other EDCs may be present.

Our study focused specifically on analyzing circulating microbial DNA to identify potential changes associated with TBZ exposure. The circulating microbiome concept has emerged as a powerful alternative to invasive, lethal, and logistically challenging tissue biopsies (Whittle et al., 2019; Sciarra et al., 2023). In medicine, the characterization of the peripheral blood-derived microbiome signature is increasingly utilized by clinicians to assess an individual's health status, detect dysbiosis and potential pathogens, and inform disease severity and progression. This concept is also gaining momentum in ecology, as studies on the circulating microbiome of dog, bovine, wild bird, and wild fish populations have revealed that the genetic structure of the blood

microbiome, similar to humans, is influenced by genetic and environmental factors (Mtshali, 2022; Herder et al., 2023; Ferchiou et al., 2023; Fronton et al., 2023; Fronton et al., 2024; Mani et al., 2023; Muñoz-Baquero et al., 2023). It is also a logistically friendly, non-invasive approach that could guide future studies on pathogens' emergence following TBZ exposure or any other environmental stressor. While sequencing the V3-V4 region of the 16S rRNA gene can be a valuable tool in microbial identification and community analysis, it is generally not sufficient for definitively identifying specific pathogens on its own because it does not provide enough unique sequence information to distinguish between closely related species, particularly within the same genus, where pathogens often reside. Thus, confirmatory methods like whole genome sequencing or targeted sequencing are needed for identifying pathogens.

5. Conclusion.

This study illustrates the importance of better understanding the effects of endocrine disruptors on aquatic species. Based on our findings, it would be beneficial to investigate their impact on various aquatic species to better understand the potential ecological consequences and identify any species-specific responses. Here, we focused on a 24-day exposure period, but examining the effects of prolonged or chronic exposure to fungicides and EDCs would be informative. Long-term studies can reveal cumulative effects, potential recovery, or adaptation mechanisms and provide insights into the persistence of microbiome alterations over time. Understanding the underlying mechanisms by which TBZ and other EDCs impact the microbiome will also be important. This can involve exploring the direct effects of these chemicals on microbial communities and investigating potential indirect effects through changes in host physiology, immune responses, or other factors. Future research should also consider that aquatic ecosystems

often face multiple stressors simultaneously. Investigating the interactive effects of fungicides and EDCs with other environmental stressors, such as pollutants or climate change-related factors, can provide insights into the combined effects and potential synergistic or antagonistic interactions. Such future research programs will contribute to risk assessment and management efforts and ultimately support the conservation and sustainable management of these vital environments.

Declaration of Competing Interest

The authors declare that they have no known competing financial interests or personal relationships that could have appeared to influence the work reported in this paper.

Data Accessibility

Metagenome sequencing data have been deposited in the NCBI Sequence Read Archive under the Bioproject PRJNA1026604.

Declaration of generative AI and AI-assisted technologies in the writing process

During the preparation of this work, the author(s) used ChatGPT3.5 to improve the language and readability. After using this tool/service, the author(s) reviewed and edited the content as needed and took (s) full responsibility for the publication's content.

References

441 Afzaal M, Saeed F, Shah YA, Hussain M, Rabail R, Socol CT, Hassoun A, Pateiro M, Lorenzo
442 JM, Rusu AV, Aadil RM. Human gut microbiota in health and disease: Unveiling the relationship.
443 Frontiers in microbiology. 2022 Sep 26;13:999001.
444
445 Baćmaga M, Wyszkowska J, Borowik A, Kucharski J. Effects of Tebuconazole Application on
446 Soil Microbiota and Enzymes. Molecules. 2022 Nov 3;27(21):7501.
447
448 Bai YF, Wang SW, Wang XX, Weng YY, Fan XY, Sheng H, Zhu XT, Lou LJ, Zhang F. The
449 flavonoid-rich Quzhou Fructus Aurantii extract modulates gut microbiota and prevents obesity in
450 high-fat diet-fed mice. Nutrition & diabetes. 2019 Oct 23;9(1):30.
451
452 Callahan BJ, McMurdie PJ, Holmes SP. Exact sequence variants should replace operational
453 taxonomic units in marker-gene data analysis. ISME J. 2017;11:2639–43.
454
455 Calero-Medina L, Jimenez-Casquet MJ, Heras-Gonzalez L, Conde-Pipo J, Lopez-Moro A, Olea-
456 Serrano F, Mariscal-Arcas M. Dietary exposure to endocrine disruptors in gut microbiota: A
457 systematic review. Science of the Total Environment. 2023 May 9:163991.
458
459 Cao Y. microbiomeMarker: microbiome biomarker analysis. R package version 0.0. 1.9000.
460
461 Castelli L, Balbuena S, Branchiccela B, Zunino P, Liberti J, Engel P, Antúnez K. Impact of chronic
462 exposure to sublethal doses of glyphosate on honey bee immunity, gut microbiota and infection
463 by pathogens. Microorganisms. 2021 Apr 15;9(4):845.

464

465 Caza F, Joly de Boissel PG, Villemur R, Betoulle S, St-Pierre Y. Liquid biopsies for omics-based
466 analysis in sentinel mussels. PLoS One. 2019 Oct 3;14(10):e0223525.

467

468 Cox TO, Lundgren P, Nath K, Thaiss CA. Metabolic control by the microbiome. Genome
469 Medicine. 2022 Dec;14(1):1-3.

470

471 Danion M, Le Floch S, Castric J, Lamour F, Cabon J, Quentel C. Effect of chronic exposure to
472 pendimethalin on the susceptibility of rainbow trout, Oncorhynchus mykiss L., to viral
473 hemorrhagic septicemia virus (VHSV). Ecotoxicology and environmental safety. 2012 May
474 1;79:28-34.

475

476 Defois C, Ratel J, Garrait G, Denis S, Le Goff O, Talvas J, Mosoni P, Engel E, Peyret P. Food
477 chemicals disrupt human gut microbiota activity and impact intestinal homeostasis as revealed by
478 in vitro systems. Scientific reports. 2018 Jul 20;8(1):11006.

479

480 De Souza R, Seibert D, Quesada H, de Jesus Bassetti F, Fagundes-Klen M, Bergamasco, R.
481 Occurrence, impacts and general aspects of pesticides in surface water : A review. 2020. Process
482 Safety and Environmental Protection, 135, 22-37.

483

484 Douglas GM, Maffei VJ, Zaneveld JR, Yurgel SN, Brown JR, Taylor CM, Huttenhower C,
485 Langille MG. PICRUSt2 for prediction of metagenome functions. Nature biotechnology. 2020
486 Jun;38(6):685-8.

487

488 Draskau MK, Svingen T. Azole fungicides and their endocrine disrupting properties: perspectives
489 on sex hormone-dependent reproductive development. Frontiers in Toxicology. 2022 Apr
490 28;4:883254.

491

492 Duh-Leong C, Maffini MV, Kassotis CD, Vandenberg LN, Trasande L. The regulation of
493 endocrine-disrupting chemicals to minimize their impact on health. Nature Reviews
494 Endocrinology. 2023 Oct;19(10):600-14.

495

496 Dupuy C, Cabon J, Louboutin L, Le Floch S, Morin T, Danion M. Cellular, humoral and molecular
497 responses in rainbow trout (Oncorhynchus mykiss) exposed to a herbicide and subsequently
498 infected with infectious hematopoietic necrosis virus. Aquatic Toxicology. 2019 Oct
499 1;215:105282.

500

501 Eder KJ, Clifford MA, Hedrick RP, Köhler HR, Werner I. Expression of immune-regulatory genes
502 in juvenile Chinook salmon following exposure to pesticides and infectious hematopoietic necrosis
503 virus (IHNV). Fish & shellfish immunology. 2008 Nov 1;25(5):508-16.

504

505 El Azhari N, Dermou E, Barnard RL, Storck V, Tourna M, Beguet J, Karas PA, Lucini L, Rouard
506 N, Botteri L, Ferrari F. The dissipation and microbial ecotoxicity of tebuconazole and its
507 transformation products in soil under standard laboratory and simulated winter conditions. Science
508 of the Total Environment. 2018 Oct 1;637:892-906.

509

510 Ferchiou S, Caza F, Villemur R, Labonne J, St-Pierre Y. Skin and Blood Microbial Signatures of
511 Sedentary and Migratory Trout (*Salmo trutta*) of the Kerguelen Islands. Fishes. 2023;8:174.
512
513 Fijan N, Sulimanović D, Bearzotti M, Muzinić D, Zwillenberg LO, Chilmonczyk S, Vautherot JF,
514 De Kinkelin P. Some properties of the Epithelioma papulosum cyprini (EPC) cell line from carp
515 Cyprinus carpio. InAnnales de l'Institut pasteur/Virologie 1983 Apr 1 (Vol. 134, No. 2, pp. 207-
516 220). Elsevier Masson.
517
518 Fronton F, Ferchiou S, Caza F, Villemur R, Robert D, St-Pierre Y. Insights into the circulating
519 microbiome of Atlantic and Greenland halibut populations: the role of species-specific and
520 environmental factors. Sci Rep. 2023;13:5971
521
522 Fronton F, Villemur R, Robert D, St-Pierre Y. Divergent bacterial landscapes: unraveling
523 geographically driven microbiomes in Atlantic cod. Scientific Reports. 2024 Mar 13;14(1):6088.
524
525 Han L, Kong X, Xu M, Nie J. Repeated exposure to fungicide tebuconazole alters the degradation
526 characteristics, soil microbial community and functional profiles. Environmental Pollution. 2021
527 Oct 15;287:117660.
528
529 Herder EA, Skeen HR, Lutz HL, Hird SM. Body Size Poorly Predicts Host-Associated Microbial
530 Diversity in Wild Birds. Microbiol Spectr. 2023;11:e03749-22.
531

Hou K, Wu ZX, Chen XY, Wang JQ, Zhang D, Xiao C, Zhu D, Koya JB, Wei L, Li J, Chen ZS. Microbiota in health and diseases. Signal transduction and targeted therapy. 2022 Apr 23;7(1):135.

Jiang J, Chen L, Liu X, Wang L, Wu S, Zhao X. Histology and multi-omic profiling reveal the mixture toxicity of tebuconazole and difenoconazole in adult zebrafish. Science of The Total Environment. 2021 Nov 15;795:148777.

Kang D, Doudrick K, Park N, Choi Y, Kim K, Jeon J. Identification of transformation products to characterize the ability of a natural wetland to degrade synthetic organic pollutants. 2020. Water Research
Volume 187, 15 December 2020, 116425.

Karber G. 50% end point calculation. Archiv fur Experimentelle Pathologie und Pharmakologie. 1931;162:480-3.

Klindworth A, Pruesse E, Schweer T, Peplies J, Quast C, Horn M, Glöckner FO. Evaluation of general 16S ribosomal RNA gene PCR primers for classical and next-generation sequencing-based diversity studies. Nucleic acids research. 2013 Jan 1;41(1):e1-.

Ku T, Liu Y, Xie Y, Hu J, Hou Y, Tan X, Ning X, Li G, Sang N. Tebuconazole mediates cognitive impairment via the microbe-gut-brain axis (MGBA) in mice. Environment International. 2023 Mar 1;173:107821.

555 Langille MG, Zaneveld J, Caporaso JG, McDonald D, Knights D, Reyes JA, Clemente JC,
556 Burkepile DE, Vega Thurber RL, Knight R, Beiko RG. Predictive functional profiling of microbial
557 communities using 16S rRNA marker gene sequences. Nature biotechnology. 2013 Sep;31(9):814-
558 21.
559
560 Lei M, Menon R, Manteiga S, Alden N, Hunt C, Alaniz RC, Lee K, Jayaraman A. Environmental
561 chemical diethylhexyl phthalate alters intestinal microbiota community structure and metabolite
562 profile in mice. Msystems. 2019 Dec 17;4(6):10-128.
563
564 Li S, Sun Q, Wu Q, Gui W, Zhu G, Schlenk D. Endocrine disrupting effects of tebuconazole on
565 different life stages of zebrafish (Danio rerio). Environmental Pollution. 2019 Jun 1;249:1049-59.
566
567 Lin L, Zhang J. Role of intestinal microbiota and metabolites on gut homeostasis and human
568 diseases. BMC immunology. 2017 Dec;18:1-25.
569
570 Louboutin L, Cabon J, Vigouroux E, Morin T, Danion M. Comparative analysis of the course of
571 infection and the immune response in rainbow trout (*Oncorhynchus mykiss*) infected with the 5
572 genotypes of infectious hematopoietic necrosis virus. Virology. 2021 Jan 2:552:20-31.
573
574 Ma J, Chen QL, O'Connor P, Sheng GD. Does soil CuO nanoparticles pollution alter the gut
575 microbiota and resistome of Enchytraeus crypticus?. Environmental Pollution. 2020 Jan
576 1;256:113463.
577

578 Mani A, Henn C, Couch C, Patel S, Korytar T, Salinas I. A niche-adapted brain microbiome in
579 salmonids at homeostasis. bioRxiv. 2023:2023-12.
580
581 McMurdie PJ, Holmes S. phyloseq: an R package for reproducible interactive analysis and
582 graphics of microbiome census data. PloS one. 2013 Apr 22;8(4):e61217.
583
584 Meng Z, Sun W, Liu W, Wang Y, Jia M, Tian S, Chen X, Zhu W, Zhou Z. A common fungicide
585 tebuconazole promotes colitis in mice via regulating gut microbiota. Environmental Pollution.
586 2022 Jan 1;292:118477.
587
588 Mousa WK, Chehadeh F, Husband S. Microbial dysbiosis in the gut drives systemic autoimmune
589 diseases. Frontiers in Immunology. 2022 Oct 20;13:906258.
590
591 Mtshali K. Exploration and comparison of bacterial communities present in bovine milk, faeces
592 and blood using 16S rRNA metagenomic sequencing. North-West University; 2022.
593
594 Muñoz-Baquero M, Lorenzo-Rebenaque L, García-Vázquez FA, García-Párraga D, Martínez-
595 Priego L, De Marco-Romero G, Galán-Vendrell I, D'Auria G, Marco-Jimenez F. Unveiling
596 microbiome signature in inner body fluids: comparison between wild and aquarium small-spotted
597 catshark (Scyliorhinus canicula). Frontiers in Marine Science. 2023 Jun 29.
598
599 Oksanen J, Blanchet FG, Kindt R, Legendre P, Minchin PR, O'hara RB, Simpson GL, Solymos P,
600 Stevens MH, Wagner H. Community ecology package. R package version 2.0-2.

601

602 Pesce S, Zoghlami O, Margoum C, Artigas J, Chaumot A, Foulquier A. Combined effects of
603 drought and the fungicide tebuconazole on aquatic leaf litter decomposition. Aquatic Toxicology.
604 2016 Apr 1;173:120-31.

605

606 Purcell MK, Kurath G, Garver KA, Herwig RP, Winton JR. Quantitative expression profiling of
607 immune response genes in rainbow trout following infectious haematopoietic necrosis virus
608 (IHNV) infection or DNA vaccination. Fish & shellfish immunology. 2004 Nov 1;17(5):447-62.

609

610 Ren Z, Cai T, Wan Y, Zeng Q, Li C, Zhang J, Ma K, He S, Li J, Wan H. Unintended consequences:
611 Disrupting microbial communities of *Nilaparvata lugens* with non-target pesticides. Pesticide
612 Biochemistry and Physiology. 2023 Aug 1;194:105522.

613

614 Rosenfeld CS. Gut dysbiosis in animals due to environmental chemical exposures. Frontiers in
615 cellular and infection microbiology. 2017 Sep 8;7:396.

616

617 Scarsella E, Meineri G, Sandri M, Ganz HH, Stefanon B. Characterization of the Blood
618 Microbiome and Comparison with the Fecal Microbiome in Healthy Dogs and Dogs with
619 Gastrointestinal Disease. Veterinary Sciences. 2023;10:277.

620

621 Sciarra F, Franceschini E, Campolo F, Venneri MA. The Diagnostic Potential of the Human Blood
622 Microbiome: Are We Dreaming or Awake?. International Journal of Molecular Sciences. 2023
623 Jun 21;24(13):10422.

624

625 Ssekagiri AT, Sloan W, Ijaz UZ. microbiomeSeq: An R package for analysis of microbial
626 communities in an environmental context. InISCB Africa ASBCB Conference 2017 Aug 21.
627 Kumasi: ISCB.

628

629 Taxvig C, Hass U, Axelstad M, Dalgaard M, Boberg J, Andeasen HR, Vinggaard AM. Endocrine-
630 disrupting activities in vivo of the fungicides tebuconazole and epoxiconazole. Toxicological
631 Sciences. 2007 Dec 1;100(2):464-73.

632

633 Vacca M, Calabrese FM, Loperfido F, Maccarini B, Cerbo RM, Sommella E, Salviati E, Voto L,
634 De Angelis M, Ceccarelli G, Di Napoli I. Maternal Exposure to Endocrine-Disrupting Chemicals:
635 Analysis of Their Impact on Infant Gut Microbiota Composition. Biomedicines. 2024 Jan
636 19;12(1):234.

637

638 Velmurugan G, Ramprasath T, Gilles M, Swaminathan K, Ramasamy S. Gut microbiota,
639 endocrine-disrupting chemicals, and the diabetes epidemic. Trends in Endocrinology &
640 Metabolism. 2017 Aug 1;28(8):612-25.

641

642 Vilo C, Dong Q. Evaluation of the RDP classifier accuracy using 16S rRNA gene variable regions.
643 Metagenomics. 2012 May 1;1(235551):104303.

644

Wang R, Li S, Jin L, Zhang W, Liu N, Wang H, Wang Z, Wei P, Li F, Yu J, Lu S. Four-week administration of nicotinemoderately impacts blood metabolic profile and gut microbiota in a diet-dependent manner. Biomedicine & Pharmacotherapy. 2019 Jul 1;115:108945.

Whittle E, Leonard MO, Harrison R, Gant TW, Tonge DP. Multi-Method Characterization of the Human Circulating Microbiome. Front Microbiol. 2019;9:3266.

Wu HJ, Wu E. The role of gut microbiota in immune homeostasis and autoimmunity. Gut microbes. 2012 Jan 1;3(1):4-14.

Yu Y, Zhang Q, Kang J, Xu N, Zhang Z, Deng Y, Gillings M, Lu T, Qian H. Effects of organic fertilizers on plant growth and the rhizosphere microbiome. Applied and Environmental Microbiology. 2024 Jan 9:e01719-23.

Zaneveld JR, McMinds R, Vega Thurber R. Stress and stability: applying the Anna Karenina principle to animal microbiomes. Nature microbiology. 2017 Aug 24;2(9):1-8.

Zhang W, Di S, Yan J. Chiral pesticides levels in peri-urban area near Yangtze River and their correlations with water quality and microbial communities. Environmental Geochemistry and Health. 2023 Jun;45(6):3817-31.

Supplementary Material

Evaluating the Disruptive Effect of Experimental Tebuconazole Exposure on the Circulating and Mucosal Microbiome of Trout.

A

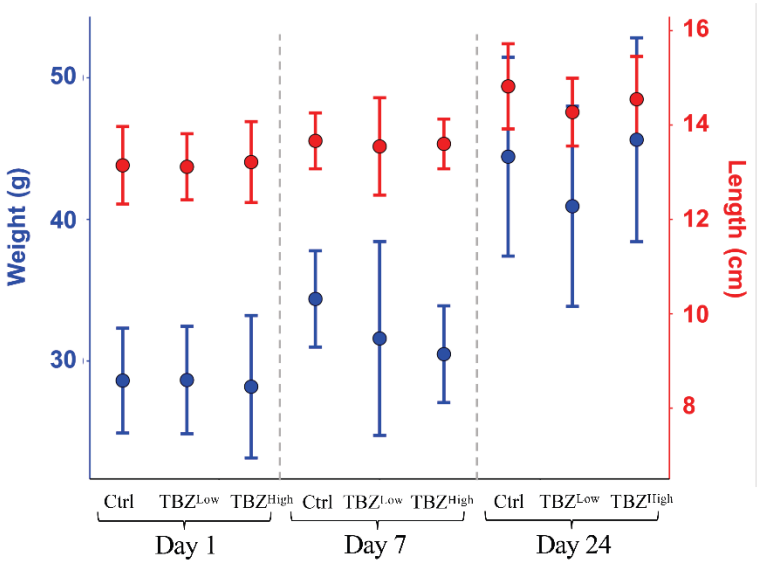

Supplementary Figure 1: General conditions of trout exposed to TBZ. **(A)** Changes of total length (cm) and weight (g).

B

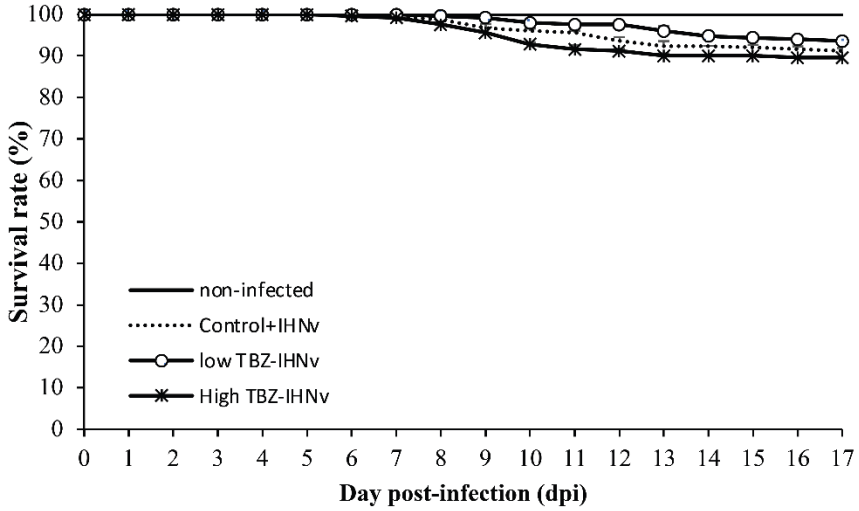

Supplementary Figure 2: Kinetics of cumulative mortality (%) in negative control fish (black line), infected fish with IHNV previously not exposed to TBZ (dotted line), exposed to low TBZ (white circle) or exposed to high TBZ (black cross). Data are expressed as a function of time in days post-infection (dpi). Error bars represent standard errors. Each challenge was performed with 250 fish distributed in four tanks.

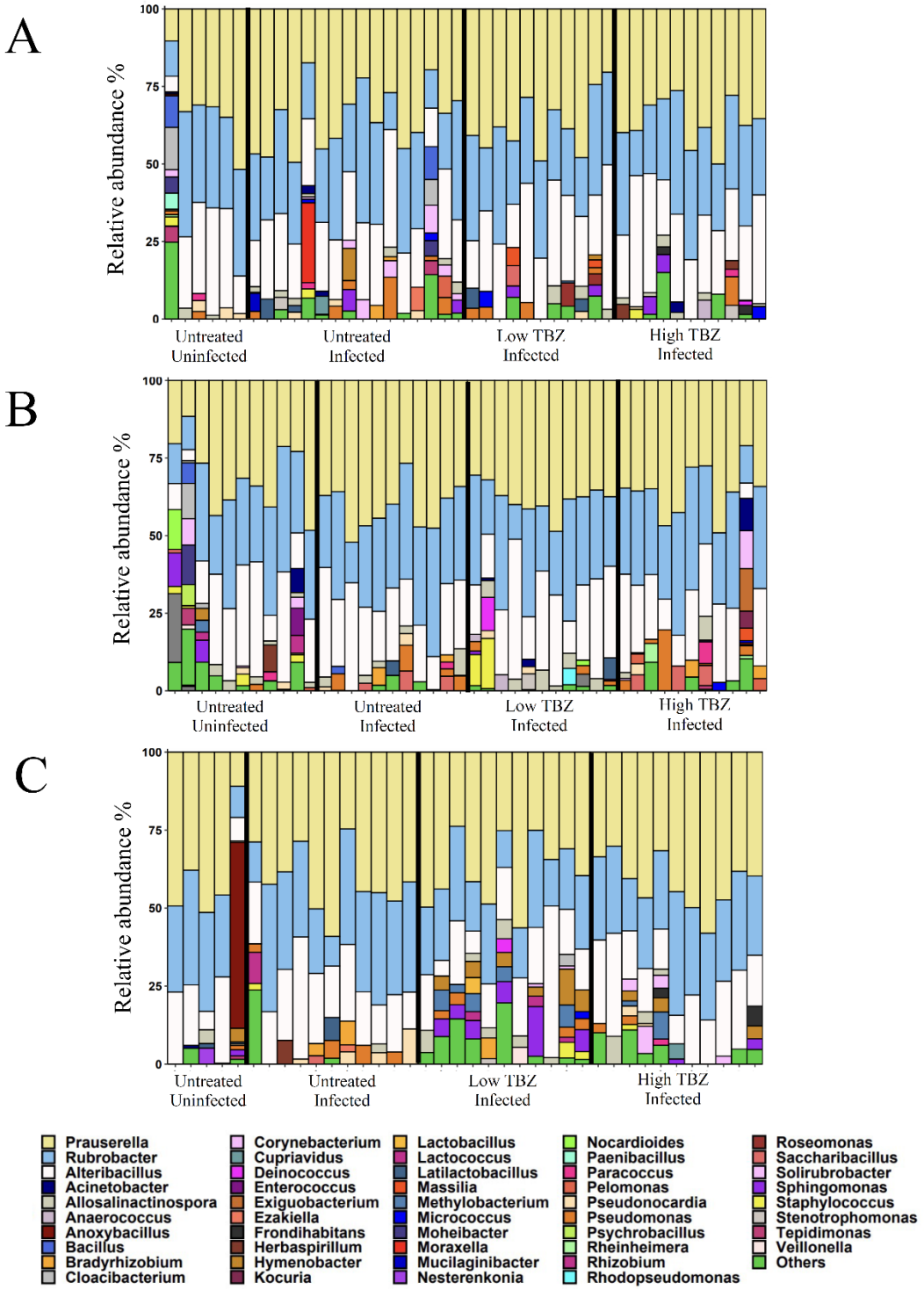

Supplementary Figure 3: Relative genus-level abundance (>1%) of the blood microbiome at (**A**) 24 hours, (**B**) 72 hours, and (**C**)46 days post-infection.

Table S1. Nominal and measured concentration of TBZ in freshwater (µg/L) and in fish flesh (µg/kg). Values are means ± standard deviation (SD). (*n* = 7 and 9 for measurement of water concentration and n = 3 for flesh.

Nominal [TBZ] exposure (µg/L)	Measured [TBZ] in freshwater (µg/L)	Measured [TBZ] in flesh (µg/kg)
0	Blq*	blq
0.23	0.25 ± 0.05	5.00 ± 2.00
10	4.69 ± 1.27	261.70 ± 137.68

*: Below limit of detection (<1 ng/L).

Annexe IV

Comparaison des profils de taille du ccfDNA entre les organismes à système circulatoire fermé et ceux à système circulatoire semi-ouvert

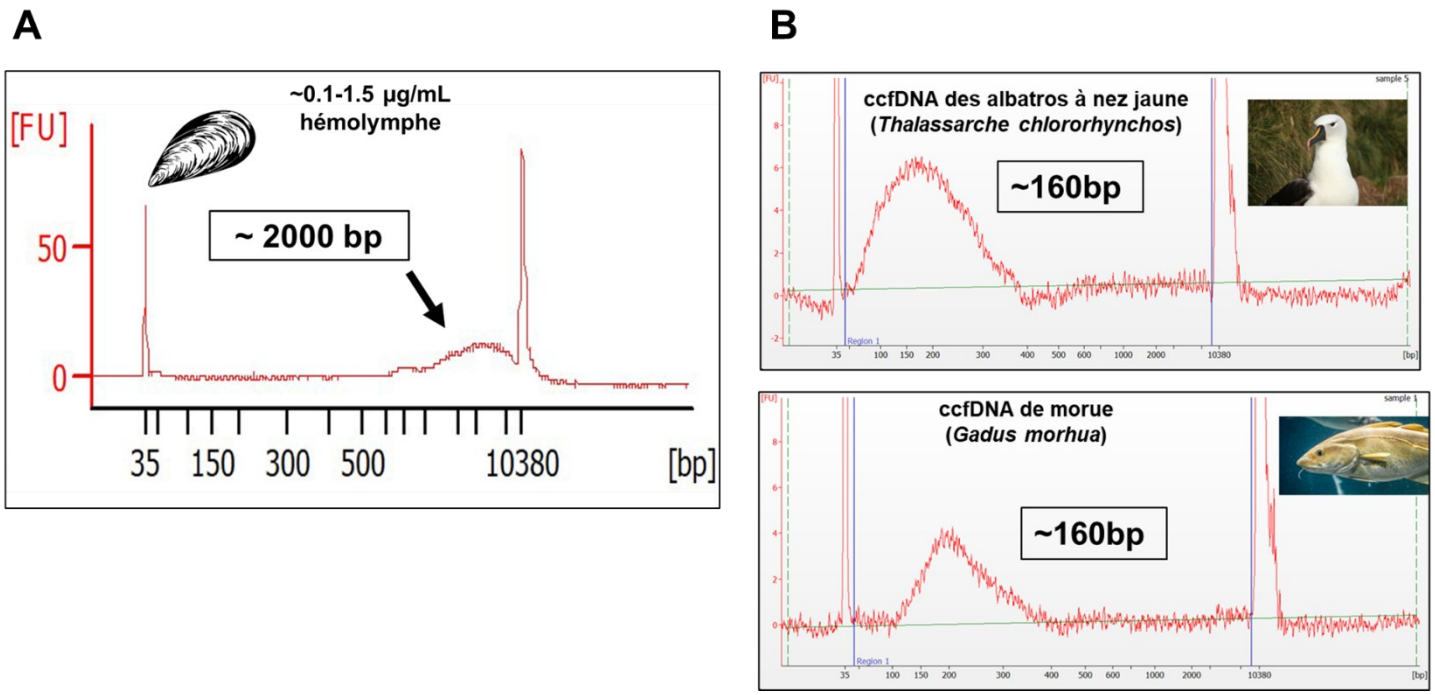

Figure AIV.1. Comparaison des profils d'électrophérogrammes représentatifs de la taille du ccfDNA entre les organismes à A) système circulatoire semi-ouvert, comme la moule bleue, et B) système circulatoire fermé, tels que les oiseaux marins et les poissons téléostéens.